New Methods for Isolation, Characterisation and Modification of Natural Colorants

Muhammad Hizbul Wathon

Submitted in accordance with the requirements for the degree of
Doctor of Philosophy

The University of Leeds
School of Chemistry

May 2021

The candidate confirms that the work submitted is his own, except where work which has formed part of jointly-authored publications has been included. The contribution of the candidate and the other authors to this work has been explicitly indicated below. The candidate confirms that appropriate credit has been given within the thesis where reference has been made to the work of others.

Chapter 2 in this thesis based on:

Wathon, M.H., Beaumont, N., Benohoud, M., Blackburn, R.S., Rayner, C.M., 2019. Extraction of anthocyanins from *Aronia melanocarpa* skin waste as a sustainable source of natural colorants. *Color. Technol*., **135**, 5-16.

The candidate conducted the experimental design, laboratory work, data analysis, data interpretation, wrote a draft of publication and answered the reviewer's comments. The co-authors reviewed the draft of the publication, supervised, guided and provided valuable feedback to the candidate, and also contributed to answering the reviewer's comments.

Acknowledgements

Foremost, all praise be to Allah SWT, Lord of all the worlds who taught man the whole science and the names of all things. I would like to take this opportunity to express my gratitude to everyone who helped and supported me throughout my PhD studies at the School of Chemistry, University of Leeds.

I am deeply thankful to my supervisors Professor Chris Rayner and Professor Richard Blackburn, for the opportunity to do this research, for the guidance through each stage of my study, and for the continuous support and invaluable advice during my study. The encouragement I received from them is very much appreciated.

I would also like to express my deepest gratitude to Indonesia Endowment Fund for Education (LPDP), Ministry of Finance, The Republic of Indonesia for the provision of financial support within the framework of Beasiswa Pendidikan Indonesia, allowing me to conduct my PhD studies.

I would like to thank Martin Huscroft, Dr Jeanine Williams, Dr Mark Howard, and Dr Stuart Warriner for their technical support, assistance, and advice during my practical work. I would also like to thank all members of staff at Chemistry stores for their support and efforts.

I would like to thank Dr Meryem Benohoud, Dr Nikitia Mexia and Dr Sannia Farooque for their guidance and nice discussion. I would also like to extend my thanks to the rest of those associated with the Rayner and Blackburn research group, present and past members, for their help and good company during my time in Leeds.

Finally, I would like to express my special thanks to my beloved wife, drh. Tuti Tri Sedya Renaning Tyas, for her patience, encouragement, and moral support. I must thank my late father, Moh. Sholeh, who passed away a few months before the thesis submission and my mother, Johariyah, both of whom have been a constant source of inspiration for me. I would also like to extend my thank you to my parents in law and the rest of my family members for their love, encouragement and support throughout my PhD studies and my entire life.

Abstract

Aronia skin waste contains anthocyanins in high concentrations and has a simpler anthocyanin profile than other anthocyanin-containing berries. Their instability towards pH, heat, hydrolysis *etc*., limits their application as natural colorants and antioxidants. Anthocyanins were extracted in a simple batch process and a new extraction method, which integrates both extraction and separation in a single process. The new method showed better anthocyanin yield and purity compared to the batch method. Anthocyanins from *Aronia* skin waste were identified as Cy3gal, Cy3glc, Cy3ara, Cy3xyl alongside its aglycone, contributing up to 44.7% w/w of RASE (Refined *Aronia* Skin Waste Extract). Neutral polyphenols such as DHBA (3,4-dihydroxybenzoic acid), nCA (neochlorogenic acid), CA (chlorogenic acid), and Q (quercetin) contributed up to 14.2 % w/w of RASE. Polymeric proanthocyanidins contributed up to 39.4% w/w of RASE. Inorganic salts and other harder to observe compounds contributed up to 1.7% w/w of RASE. Anthocyanin salts with carboxylate anions were prepared by applying various milder organic acids during the extraction-purification process. RASE with carboxylate anions were relatively more stable than RASE-chloride. Preserving anthocyanins at milder pH with a more hydrophobic counterion is suggested, especially if used for a longer period (months). The characterisation of flavylium-hemiketal forms mixture for Cy3gal, Cy3glc, Cy3ara and Cy3xyl was obtained by dissolving these anthocyanins in methanol-d_4 and analysed by NMR spectroscopy. Hemiketal forms of Cy3gal have been characterised as a single compound through slow evaporation, while nucleophilic addition occurred at the carbon position 2 of anthocyanin by hydration. Overall, a proper structural modification of anthocyanins could increase the physio-chemical properties of anthocyanins with fair antioxidant activity. Mono- and diacylated anthocyanins could maintain the original colour of their precursor. Due to their lipophilic property, acylated derivatives of anthocyanins from *Aronia* skin waste have a higher potential to be incorporated in lipid-based foods, textiles, cosmetic formulations, and pharmaceutical products than its precursor.

Table of Contents

Acknowledgements ..... **iii**

Abstract ..... **iv**

Table of Contents ..... **v**

List of Tables ..... **xiii**

List of Figures ..... **xviii**

List of Schemes ..... **xxiv**

List of Abbreviations ..... **xxvi**

Chapter 1 General Introduction **1**

1.1. Overview of Anthocyanins 1

1.1.1. Anthocyanins 1

1.1.2. Classification of Anthocyanins and Resultant Colours 2

1.1.3. Biosynthesis of Anthocyanins 4

1.1.4. Reactivity of Anthocyanins 6

1.1.4.1. Nucleophilic Additions 7

1.1.4.1.1. Nucleophilic Addition at C-2 7

1.1.4.1.2. Nucleophilic Addition at C-4 8

1.1.4.2. Antioxidant Activity 9

1.1.4.3. Anthocyanin Complexes 10

1.1.4.3.1. Self-Association and Co-Pigmentation 10

1.1.4.3.2. Metal complexes 11

1.1.5. Colour and Stability of Anthocyanins 11

1.1.6. Health Benefits of Anthocyanins 14

1.1.7. Utilisation of Anthocyanins as Natural Colorants 16

1.2. *Aronia melanocarpa* (Black Chokeberry) as Natural Sources of Anthocyanins 16

1.3. Methods for the Extraction of Anthocyanins from Natural Resources (Solid-Liquid Extraction) 21

1.4. Purification of Anthocyanins through Solid-Phase Extraction (SPE) 23

1.5. Aims of this project 25

Chapter 2 Development of New Extraction-Adsorption Methods for Anthocyanins from *Aronia* skin waste **27**

2.1 Preliminary Studies for Optimisation of Extraction-Adsorption of Anthocyanins from *Aronia* Skin Waste 28

2.1.1. Batch Extraction Approach. 29

2.1.1.1. The effect of extraction temperature on the extraction yield and anthocyanin content 30

2.1.1.2. The effect of extraction time on the extraction yield and anthocyanin content 33

2.1.1.3. The effect of pH on the extraction yield and anthocyanin content 34

2.1.1.4. The effect of the biomass-to-solvent ratio on the extraction yield and anthocyanin content 35

2.1.1.5. The effect of biomass to SPE resin ratio on the extraction yield and anthocyanin content 36

2.1.2. An Integrated Extraction-adsorption Method for Anthocyanin production. 37

2.1.2.1. The effect of an applied cooling process during SPE sample loading on the extraction yield and anthocyanin content 39

2.1.2.2. The effect of sample loading flow rate on the extraction yield and anthocyanin content 40

2.2. Identification and Evaluation of Refined *Aronia* Skin Waste Extract (RASE) 40

2.2.1. UV-Vis Studies 41

2.2.1.1. The Absorbance of RASE at Various pHs 41

2.2.2. HPLC studies 42

2.2.2.1. Development of an HPLC Method to Identify Anthocyanins from RASE 42

2.2.2.2. HPLC studies to Investigate the Deglycosylation of Anthocyanins during the Extraction-Purification Process 45

2.2.3. LC-MS studies 51

2.2.4. ^{1}H-NMR studies 51

2.3. Comparison between the Batch Extraction Method and the New Integrated Process. 54

2.3.1. Comparison of Anthocyanin Profiles in RASE from the Batch and Integrated Methods. 54

2.3.2. Effect of Acid Concentration on Anthocyanin Deglycosylation 58

2.3.3. Net Efficiency for Extracting Anthocyanins from *Aronia* skin waste 59

2.4. Conclusion 60

Chapter 3 Further Purification, Characterisation and Total Chemical Composition of RASE 62

3.1. Further Purification of RASE 63

3.1.1. Semi-preparative HPLC-DAD 65
3.1.1.1. Isolation of Individual Polyphenols in RASE 65
3.1.1.2. Characterisation of Anthocyanidin and Individual Anthocyanins..... 66
3.1.1.2.1. Cyanidin (Cy) 68
3.1.1.2.2. Cyanidin-3-*O*-β-galactoside (Cy3gal)..... 71
3.1.1.2.3. Cyanidin-3-*O*-β-glucoside (Cy3glc)..... 76
3.1.1.2.4. Cyanidin-3-*O*-β-arabinoside (Cy3ara)..... 78
3.1.1.2.5. Cyanidin-3-*O*-β-xyloside (Cy3xyl) 81
3.1.1.2.6. Characterisation of Polymeric Species 83
3.1.2. Purification of RASE by Liquid-liquid Extraction (LLE) 84
3.1.2.1. Isolation of Neutral Polyphenols from RASE 84
3.1.2.2. Characterisation of Isolated Neutral Polyphenols from RASE 85
3.1.2.2.1. Characterisation of polyphenols from *i*propyl acetate extraction. 86
3.1.2.2.2. Characterisation of Polyphenols from Ethyl Acetate Extraction87
3.1.3. Biotage Flash Purification Studies 90
3.1.4. Summary: Efficient Separation and Purification of Anthocyanins from *Aronia* Skin Waste 92
3.2. Quantification of Total Components Present in RASE 94
3.2.1. Determination of molar absorptivity (Ɛ) of Cy3gal 94
3.2.1.1. Molar Absorptivity of Cy3gal in Buffer Solution pH 1 95
3.2.1.1. Stability of Cy3gal in Buffer Solution pH 1 for 4 days..... 96
3.2.2. Determination of pK'_a of Cy3gal 97
3.2.3. Total Chemical Composition of RASE..... 98
3.3. Conclusion 99
Chapter 4 Preparation, Characterisation and Properties of Anthocyanins with Organic Counterions..... 101
4.1. Preparation of Anthocyanins with Carboxylate Anions..... 102
4.1.1. Anthocyanin salts with carboxylate anions..... 103
4.1.2. Yield of anthocyanins using alternative counterions..... 104
4.2. Characterisation of RASE with Organic Counterions 107
4.2.1. UV-Vis studies 107
4.2.2. HPLC studies..... 110

4.2.3. NMR studies 113

4.2.3.1. NMR studies of RASE in acidified methanol (CD_3OD/CF_3COOD 95:5) 113

4.2.3.2. NMR studies of RASE in neutral methanol (CD_3OD) 120

4.3. Effect of Counterions on Deglycosylation of RASE. 125

4.4. Evaluation of the physico-chemical properties of RASE with Organic Counterions 130

4.4.1. Total Phenolic Content (TPC) of RASE 130

4.4.2. DPPH Radical Scavenging Activity (%RScA) of RASE 131

4.4.3. Lipophilicity (Log P) 134

4.5. Conclusion 136

Chapter 5 New Methods for Preparation and Characterisation of Hemiketal Forms of Anthocyanins from *Aronia* Skin Waste 138

5.1. New Methods for Preparation and Characterisation of Hemiketal Forms of Cy3gal. 138

5.1.1. Selective Formation of hemiketals of Cy3gal. 141

5.1.2. Characterisation of Hemiketal Forms of Cy3gal 143

5.2. Preparation and Characterisation of Flavylium-Hemiketal mixture of Individual Anthocyanins from RASE 147

5.2.1. NMR Studies to Produce Flavylium-Hemiketal Mixtures 147

5.2.2. Characterisation of Flavylium-Hemiketal Forms of Cy3gal 147

5.2.3. Characterisation of Flavylium-Hemiketal Forms of Cy3glc, Cy3ara and Cy3xyl 149

5.3. Extraction-Purification of Anthocyanins to Produce RASE in Hemiketal Forms 151

5.4. pH jump to Alkaline pH 153

5.5. Conclusion 156

Chapter 6 Chemical Modification of Anthocyanins from *Aronia* Skin Waste, Structural Characterisation and Determination of Physico-chemical Properties 158

6.1. Preliminary Studies on the Acylation of Selected Polyphenols 160

6.1.1. Synthesis of *trans*-3,4',5-triacetyl resveratrol 161

6.1.2. Synthesis of 3,3',4',5,7-pentaacetyl quercetin 162

6.2. Chemical Modification of Anthocyanins from *Aronia* Skin Waste to Produce Novel Lipophilic Derivatives 165

6.2.1. Method Development for Lipophilisation of Anthocyanins 165

6.2.1.1. Effect of Solvent 165

6.2.1.2. Effect of a Biphasic Solvent System 167

6.2.1.3. Effect of RASE counterions on acylation efficiency. ... 169
6.2.1.4. Effect of Reaction Temperature ... 170
6.2.1.5. Effect of Reaction Time ... 171
6.2.2. Synthesis and Chemical Characterisation of Novel Acylated Anthocyanins ... 172
6.2.2.1. Acylation of anthocyanins with Acetyl Chloride (C_2) ... 174
6.2.2.1.1. Cy3gal monoacetate (Cyanidin-3-β-*O*-(6”-acetylgalactoside)) trifluoroacetate ... 174
6.2.2.1.2. Cy3gal diacetate (Cyanidin-3-β-*O*-(3”,6”-diacetylgalactoside)) trifluoroacetate ... 175
6.2.2.1.3. Cy3gal triacetate (Cyanidin-3-β-*O*-(3”,4”,6”-triacetylgalactoside)) trifluoroacetate ... 176
6.2.2.1.4. Cy3gal tetraacetate (Cyanidin-3-β-*O*-(2”,3”,4”,6”-tetraacetylgalactoside)) ... 177
6.2.2.1.5. Cy3gal pentaacetate (Cyanidin-3-β-*O*-(4’,2”,3”,4”,6”-pentaacetylgalactoside)) trifluoroacetate ... 178
6.2.2.1.6. Cy3gal hexaacetate (Cyanidin-3-β-*O*-(4’,7,2”,3”,4”,6”-hexaacetylgalactoside)) trifluoroacetate ... 179
6.2.2.2. Acylation of anthocyanins with Butanoyl Chloride (C_4) 181
6.2.2.2.1. Cy3gal monobutanoate (Cyanidin-3-β-*O*-(6”-butyrylgalactoside)) trifluoroacetate ... 181
6.2.2.2.2. Cy3gal dibutanoate (Cyanidin-3-β-*O*-(3”,6”-dibutyrylgalactoside)) trifluoroacetate ... 182
6.2.2.3. Acylation of anthocyanins with Octanoyl Chloride (C_8) 183
6.2.2.3.1. Cy3gal monooctanoate (Cyanidin-3-β-O-(6”-caprylylgalactoside)) trifluoroacetate ... 183
6.2.2.3.2. Cy3gal dioctanoate (Cyanidin-3-β-O-(3”,6”-dicaprylylgalactoside)) trifluoroacetate ... 184
6.2.3. Determination of Physico-chemical Properties of Novel Acylated Anthocyanins ... 185
6.2.3.1. Lipophilicity ... 185
6.2.3.2. UV-Vis Absorbance ... 187
6.2.3.3. Thermostability in Lipophilic Medium ... 188
6.2.3.4. DPPH Antioxidant Activity (IC_{50}) ... 189
6.3. New Potential Approach for Anthocyanin Modification ... 190

6.4. Conclusion and Future Work 196
6.4.1. Conclusion 196
6.4.2. Future Work 197
Chapter 7 Experimental 199
7.1. General Methods 199
7.2. Chemical and Materials 200
7.3. Sequential Batch Extraction – adsorption Method 201
7.3.1. Effect of extraction temperature on the extraction yield 202
7.3.2. Effect of extraction time on the extraction yield 203
7.3.3. Effect of extraction pH on the extraction yield 203
7.3.4. Effect of the biomass-solvent ratio on the extraction yield 203
7.3.5. Effect of the biomass-SPE resin ratio on the extraction yield ... 204
7.4. Integrated Extraction – adsorption Method 204
7.4.1. Effect of the cooling process during sample loading on the extraction yield 205
7.4.2. Effect of flow rate of sample loading on the extraction yield 205
7.5. Determination of UV-Vis Properties 205
7.5.1. Determination of λ_{max} 205
7.5.2. Determination of Molar Absorptivity of Cy3gal 206
7.5.3. Determination of pK'_a of Cy3gal 207
7.6. Purification of anthocyanins and acylated anthocyanins by semi-preparative HPLC-DAD 208
7.7. Purification of Anthocyanins by Liquid-liquid Extraction (LLE) 209
7.8. Purification of Anthocyanins by Biotage Flash Purification 209
7.9. Total monomeric anthocyanin content (TMAC) Assay 209
7.10. Total Phenolic Content (TPC) Assay 218
7.11. Lipophilicity (Log P) Assay 219
7.12. Radical Scavenging Activity (RScA) Assay 221
7.13. Thermal Stability Assay 226
7.15. Chemical Characterisation of anthocyanins extracted from *Aronia* skin waste 231
7.15.1. Flavylium cationic form (AH^+) 231
Cyanidin-3-*O*-β-galactoside (Cy3gal), 27 231
Cyanidin-3-*O*-β-glucoside (Cy3glc), 21 232
Cyanidin-3-*O*-β-arabinoside (Cy3ara), 28 232
Cyanidin-3-*O*-β-xyloside (Cy3xyl), 29 233

Cyanidin (Cy), 2 233
7.15.2. Hemiketal form (B) 234
Cyanidin-3-*O*-β-galactoside (Cy3gal) 234
Cyanidin-3-*O*-β-glucoside 235
Cyanidin-3-*O*-β-arabinoside (Cy3ara) 235
Cyanidin-3-*O*-β-xyloside (Cy3xyl) 236
7.16. Characterisation of Neutral Polyphenols in RASE 237
3,4-Dihydroxybenzoic acid (DHBA), 39 237
Quercetin (Q), 40 237
Neochlorogenic acid (nCA), 31 237
Chlorogenic acid (CA), 32 238
7.19. Synthesis of ester derivatives of selected polyphenols 238
7.19.1. *trans*-3,4',5'-Triacetyl resveratrol, 42 238
7.19.2. 3,3',4',5,7-Pentaacetyl quercetin, 43 239
7.20. Lipophilisation of anthocyanins from *Aronia* skin waste 240
7.21. Characterisation of acylated anthocyanins 240
Cy3gal monoacetate (Cyanidin-3-β-*O*-(6"-acetylgalactoside)), 44 240
Cy3gal diacetate (Cyanidin-3-β-*O*-(3",6"-diacetylgalactoside)), 45 241
Cy3gal triacetate (Cyanidin-3-β-*O*-(3",4",6"-triacetylgalactoside)), 46 241
Cy3gal tetraacetate (Cyanidin-3-β-*O*-(2",3",4",6"-tetraacetylgalactoside)), 47 242
Cy3gal pentaacetate (Cyanidin-3-β-*O*-(4',2",3",4",6"-pentaacetylgalactoside)), 48 242
Cy3gal hexaacetate (Cyanidin-3-β-*O*-(4',7,2",3",4",6"-hexaacetylgalactoside)), 49 243
Cy3gal monobutanoate (Cyanidin-3-β-*O*-(6"-butyrylgalactoside)), 50 243
Cy3gal dibutanoate (Cyanidin-3-β-*O*-(3",6"- dibutyrylgalactoside)), 51 244
Cy3gal monooctanoate (Cyanidin-3-β-*O*-(6"- caprylylgalactoside)), 52 244
Cy3gal dioctanoate (Cyanidin-3-β-*O*-(3",6"- dibutyrylgalactoside)), 53 245
7.22. Acetonation of Anthocyanins 245
List of References 247
Appendix A 256
A.1 Chapter 4 256

A.1.1 HPLC Chromatograms of the Octanol Layers after partitioning from Log P Experiment for RASE 256

A.1.2 HPLC Chromatograms of the water Layers after partitioning from Log P Experiment for RASE..... 257

A.2 Chapter 5..... 258

A.3 Chapter 6..... 259

A.3.1 *trans*-3,4',5-triacetyl resveratrol, 42 259

A.3.2 3,3',4',5,7-pentaacetyl quercetin, 43..... 260

A.3.3 Cyanidin-3-β-*O*-(6"-acetylgalactoside) trifluoroacetate, 44..... 262

A.3.4 Cyanidin-3-β-*O*-(3",6"-diacetylgalactoside), 45 263

A.3.5 Cyanidin-3-β-*O*-(3",4",6"-triacetylgalactoside), 46..... 264

A.3.6 Cyanidin-3-β-*O*-(2",3",4",6"-tetraacetylgalactoside), 47..... 265

A.3.7 Cyanidin-3-β-*O*-(4',2",3",4",6"-pentaacetyl galactoside), 48 266

A.3.8 Cyanidin-3-β-*O*-(4',7,2",3",4",6"-hexaacetylgalactoside), 49 267

A.3.9 Cyanidin-3-β-*O*-(6"-butyrylgalactoside), 50..... 268

A.3.10 Cyanidin-3-β-*O*-(3",6"-dibutyrylgalactoside), 51 269

A.3.11 Cyanidin-3-β-O-(6"-caprylylgalactoside), 52 270

A.3.12 Cyanidin-3-β-O-(3",6"-dicaprylylgalactoside), 53..... 271

List of Tables

Table 1.1 Six major anthocyanidins present in nature with their respective colours at pH < 3 and also its maximum wavelength.[8,13,15] 3

Table 1.2 Reports of different health benefits of anthocyanins from *Aronia melanocarpa* (black chokeberry) 15

Table 1.3 Composition of anthocyanins in *Aronia* fruit, pomace and juice.[4,65–68] 18

Table 1.4 The contents of anthocyanins in various *Aronia* chokeberries.[67] 19

Table 1.5 General extraction parameters used for the solid-liquid extraction of anthocyanins from various sources. 22

Table 1.6 Physicochemical properties of Amberlite XAD-7 resin.[85] 24

Table 2.1 Extraction yield of anthocyanins (mg g^{-1} DW) under various conditions for solid-liquid extraction of *Aronia* skin waste (pomace) using a batch method. TMAC is given as % w/w DW of RASE. 30

Table 2.2 Extraction yield of anthocyanins under various conditions for solid-liquid extraction of *Aronia* skin waste using an integrated extraction-adsorption method. All extractions were carried out at 60 °C, pH 2.4, biomass-to-solvent ratio 1:16, and biomass-to-SPE resin ratio 1:1. TMAC is given as % DW of RASE. 38

Table 2.3 The chromatogram of anthocyanins and its aglycone present in RASE obtained by using LC-MS-ESI in positive mode. 51

Table 2.4 The yield of anthocyanins recovered from *Aronia* skin waste (mg g^{-1} DW pomace). The extraction was conducted at 60 °C for 3 h. 60

Table 3.1 The fractions collected from a Semi-preparative HPLC-DAD at 520 nm. The purity was determined at 285 nm. 66

Table 3.2 Chemical shift (H-4, ppm) of individual anthocyanins isolated from RASE. 68

Table 3.3 ^{1}H (500 MHz) and ^{13}C (125 MHz) NMR Data for cyanidin in CD_3OD/CF_3COOD (95:5, v/v) at 25 °C. 70

Table 3.4 Summary of the long-range correlations observed in the ^{1}H-^{13}C HMBC spectrum of cyanidin. 70

Table 3.5 ^{1}H (500 MHz) and ^{13}C (125 MHz) NMR Data for Cy3gal in CD_3OD/CF_3COOD (95:5, v/v) recorded at 25 °C. 72

Table 3.6 Summary of the long-range correlations observed in the ^{1}H-^{13}C HMBC spectrum of Cy3gal. 75

Table 3.7 ^{1}H (500 MHz) and ^{13}C (125 MHz) NMR Data for Cy3glc in CD_3OD/CF_3COOD (95:5, v/v) at 25 °C. 78

Table 3.8 ^{1}H (500 MHz) and ^{13}C (125 MHz) NMR Data for Cy3ara in CD_3OD/CF_3COOD (95:5, v/v) at 25 °C. 80

Table 3.9 ^{1}H (500 MHz) and ^{13}C (125 MHz) NMR Data for Cy3xyl in CD_3OD/CF_3COOD (95:5, v/v) at 25 °C. 83

Table 3.10 ^{1}H-NMR spectra (500 MHz) of DHBA from *i*propyl acetate layer in CD_3OD at 25 °C. 87

Table 3.11 ^{1}H-NMR spectra (500 MHz) of quercetin from *i*propyl acetate layer in CD_3OD at 25 °C. 87

Table 3.12 ^{1}H-NMR spectra (500 MHz) of nCA and CA from ethyl acetate layer in CD_3OD at 25 °C. 89

Table 3.13 Comparison of purification methods for the production of anthocyanins from *Aronia* skin waste. 93

Table 3.14 Calculation of the TMAC of RASE by using a measured molar absorptivity of Cy3gal. The literature molar absorptivity of Cy3glc is also given. ANC: anthocyanin. 96

Table 3.15 The molar absorptivity of Cy3gal in buffer solution pH 1 measured for 4 consecutive days. Detected at 520 nm. Mr of Cy3gal. CF_3COO^- is 562.2 g/mol. 97

Table 4.1 The yield of anthocyanins recovered from *Aronia* skin waste was obtained after solid-phase extraction (SPE). 105

Table 4.2 $\lambda_{vis\text{-}max}$ of RASE measured in methanol and water. 109

Table 4.3 The ratio of Cy3gal/Cy3ara based on HPLC chromatograms (520 nm). 112

Table 4.4 Comparison of integration of H-4 of anthocyanins with the integration of acid's proton. Solvent: CD_3OD at 25 ºC. 115

Table 4.5 ^{1}H-NMR spectrum of Cyanidin (Cy, 2) in CD_3OD/CF_3COOD (95:5, v/v). Recorded at 500 MHz (25 °C). 117

Table 4.6 ^{1}H-NMR spectra of Cyanidin-3-*O*-galactoside (Cy3gal, 27) and Cyanidin-3-*O*-glucoside (Cy3glc, 21) in CD_3OD/CF_3COOD (95:5, v/v). Recorded at 500 MHz (25 °C). 118

Table 4.7 ^{1}H-NMR spectra of Cyanidin-3-*O*-arabinoside (Cy3ara, 28) and Cyanidin-3-*O*-xyloside (Cy3xyl, 29) in CD_3OD/CF_3COOD (95:5, v/v). Recorded at 500 MHz (25 °C). 119

Table 4.8 ^{1}H-NMR spectra of Cyanidin-3-*O*-galactoside (Cy3gal, 25) and Cyanidin-3-*O*-glucoside (Cy3glc, 21) in CD_3OD. Recorded at 500 MHz (25 °C). 122

Table 4.9 ^{1}H NMR spectra of Cyanidin-3-*O*-arabinoside (Cy3ara, 26) and Cyanidin-3-*O*-xyloside (Cy3xyl, 27) in CD_3OD. Recorded at 500 MHz (25 °C). 123

Table 4.10 Total Phenolic Content (TPC) of RASE with various counterions. 130

Table 4.11 IC_{50} of RASE with various counterions 133

Table 5.1 ^{1}H (500 MHz) and ^{13}C (125 MHz) NMR Data for Cy3gal in CD_3OD at 25 °C (hemiketal a, major) 146

Table 5.2 ^{1}H (500 MHz) and ^{13}C (125 MHz) NMR Data for Cy3gal in CD_3OD at 25 °C (hemiketal b, minor) 146

Table 5.3 ^{1}H (500 MHz) and ^{13}C (125 MHz) NMR data for Cy3glc in CD_3OD at 25 °C as the hemiketal forms a (major) and b (minor). *under solvent peak 150

Table 5.4 ^{1}H (500 MHz) and ^{13}C (125 MHz) NMR data for Cy3ara in CD_3OD at 25 °C as the hemiketal a (major) and hemiketal b (minor). 150

Table 5.5 ^{1}H (500 MHz) and ^{13}C (125 MHz) NMR Data for Cy3xyl in CD_3OD at 25 °C as the hemiketal a (major) and hemiketal b (minor). 151

Table 6.1 Complete assignments of the NMR data of 42 measured in $CDCl_3$. ^{1}H NMR was recorded at 400 MHz. Concentration: 6.3 x 10^{-2} M. 161

Table 6.2 Complete assignments of the NMR data of 43 measured in $CDCl_3$. ^{1}H-NMR was recorded at 400 MHz. Concentration: 4.2 x 10^{-2} M. 163

Table 6.3 Effect of solvent on the formation of acylated anthocyanins. 166

Table 6.4 Comparison of biphasic (acetonitrile/hexane, 1:1) and monophasic approaches for the formation of acylated anthocyanins. 168

Table 6.5 The effect of RASE counterion on the formation of acylated anthocyanins. 169

Table 6.6 The effect of reaction temperature on the formation of acylated anthocyanins. 171

Table 6.7 List of possible acylated anthocyanins with different acylating agents and number of acylation (C_2, acetate; C_4, butanoate; and C_8, octanoate).* 173

Table 6.8 ^{1}H (500 MHz) and ^{13}C (125 MHz) NMR Data for 44 in $(CD_3)_2SO$ /CF_3COOD (95:5, v/v) at 25 °C. 174

Table 6.9 ^{1}H (500 MHz) and ^{13}C (125 MHz) NMR Data for 45 in $(CD_3)_2SO$ /CF_3COOD (95:5, v/v) at 25 °C. 175

Table 6.10 ^{1}H (500 MHz) and ^{13}C (125 MHz) NMR Data for 46 in $(CD_3)_2SO$ /CF_3COOD (95:5, v/v) at 25 °C. 176

Table 6.11 ^{1}H (500 MHz) and ^{13}C (125 MHz) NMR Data for 48 in $(CD_3)_2SO$ /CF_3COOD (95:5, v/v) at 25 °C. 177

Table 6.12 ^{1}H (500 MHz) and ^{13}C (125 MHz) NMR Data for 48 in $(CD_3)_2SO$ /CF_3COOD (95:5, v/v) at 25 °C. 178

Table 6.13 ^{1}H (500 MHz) and ^{13}C (125 MHz) NMR Data for 49 in $(CD_3)_2SO$ /CF_3COOD (95:5, v/v) at 25 °C. 179

Table 6.14 Summary of the order of acylation site on Cy3gal. 180

Table 6.15 ^{1}H (500 MHz) and ^{13}C (125 MHz) NMR Data for 50 in $(CD_3)_2SO$ /CF_3COOD (95:5, v/v) at 25 °C. 181

Table 6.16 ^{1}H (500 MHz) and ^{13}C (125 MHz) NMR Data for 51 in $(CD_3)_2SO$ /CF_3COOD (95:5, v/v) at 25 °C. 182

Table 6.17 ^{1}H (500 MHz) and ^{13}C (125 MHz) NMR Data for 52 in $(CD_3)_2SO$ /CF_3COOD (95:5, v/v) at 25 °C. 183

Table 6.18 ^{1}H (500 MHz) and ^{13}C (125 MHz) NMR Data for 53 in $(CD_3)_2SO$ /CF_3COOD (95:5, v/v) at 25 °C. 184

Table 6.19 Log P of Cy3gal and its derivatives. 186

Table 6.20 Kinetic parameters of thermal degradation at different temperatures. 189

Table 6.21 DPPH antioxidant activity (IC_{50}) of Cy3gal and its derivatives. 190

Table 6.22 ^{1}H (500 MHz) NMR Data for Cy3gal, 27, and Cyanidin-3-*O*-4,6-*O*-isopropylidene-β-galactoside, 56, in CD_3COCD_3/CF_3COOD (95:5, v/v) at 25 °C 196

Table 7.1 Concentration of acid used in the extraction-purification 0.1% v/v 201

Table 7.2 The extraction yields of *Aronia* skin waste after SPE and evaporation. 203

Table 7.3 The extraction yields of *Aronia* skin waste after SPE and evaporation. 203

Table 7.4 The extraction yields of *Aronia* skin waste after SPE and evaporation. 203

Table 7.5 The extraction yields of *Aronia* skin waste after SPE and evaporation. 204

Table 7.6 The extraction yields of *Aronia* skin waste after SPE and evaporation. 204

Table 7.7 The extraction yields of *Aronia* skin waste after SPE and evaporation. 205

Table 7.8 The extraction yields of *Aronia* skin waste after SPE and evaporation. 205

Table 7.9 Solvent proportions (v/v) of the 11 different buffer solutions applied in the pH region of 1-12.[35,92] 206

Table 7.10 ε of Cy3gal in Buffer Solution pH 1 for 4 consecutive days 207

Table 7.11 Absorbance of Cy3gal at various pH (511 nm). 208

Table 7.12 TMAC of RASE obtained from the effect of extraction temperature on the anthocyanin content experiments 211

Table 7.13 TMAC of RASE obtained from the effect of extraction time on the anthocyanin content experiments 211

Table 7.14 TMAC of RASE obtained from the effect of pH on the anthocyanin content experiments 212

Table 7.15 TMAC of RASE obtained from the effect of biomass-solvent ratio on the anthocyanin content experiments 213

Table 7.16 TMAC of RASE obtained from the effect of biomass-SPE resin ratio on the anthocyanin content experiments 213

Table 7.17 TMAC of RASE obtained from the effect of a cooling process during sample loading on the anthocyanin content experiments 214

Table 7.18 TMAC of RASE obtained from the effect of sample loading flow rate on the anthocyanin content experiments 214

Table 7.19 Comparison of Batch and Integrated method 215

Table 7.20 Comparison of Extraction-Purification in A Batch Method with Various Acids 215

Table 7.21 Comparison of Extraction-Purification in A Batch Method with Various Acids 216

Table 7.22 Gallic acid standard. 218

Table 7.23 TPC of RASE with different counterions 218

Table 7.24 Log P of RASE with different counterions 220

Table 7.25 Log P of Cy3gal and its ester derivatives 220

Table 7.26 %RScA of RASE with different counterions 222

Table 7.27 %RScA of Cy3gal and its ester derivatives 223

Table 7.28 Thermostability of Cy3gal and its ester derivatives 227

List of Figures

Figure 1.1 A flavylium cationic form of anthocyanins, R^1, R^2 = H, OH, or OCH_3; R^3 = glycosyl or H; and R^4 = OH or O-glycosyl.[8] 2

Figure 1.2 The composition of an acylated anthocyanin (cyanidin-3-O-β-(6"-acetyl)glucoside, 1) anthocyanidin, 2) glycoside, 3) acyl group. 2

Figure 1.3 Chemical structures of the 6 major (most common) anthocyanidins found in nature. 3

Figure 1.4 Likely reactive positions of anthocyanins in a flavylium cationic form toward nucleophiles and electrophiles. Cy3gal is presented as an example. 7

Figure 1.5 Model of the intramolecular co-pigmentation in polyacylated anthocyanins. 11

Figure 1.6 *Aronia melanocarpa* berries with glossy black colour.[60] 17

Figure 1.7 The four major anthocyanins found in the berries of *Aronia Melanocarpa.*[4] 18

Figure 1.8 Phenolic acids present in *Aronia* berries.[4,69] 19

Figure 1.9 Flavonols present in *Aronia* berries.[4,69] 20

Figure 1.10 (-)-Epicatechin and polymeric procyanidins present in *Aronia* berries.[53] 20

Figure 1.11 Chemical structure of Amberlite XAD-7 resin. R= polyfunctional aliphatic residues.[85] 23

Figure 1.12 Typical four-step in an SPE procedure.[88] 24

Figure 2.1 General procedure for the extraction-purification of anthocyanins from *Aronia* skin waste. 27

Figure 2.2 Extraction profiles during a batch extraction of *Aronia* skin waste at various temperatures. The absorbance was monitored using UV-Vis spectrophotometer at 520 nm. 31

Figure 2.3 Extraction profiles during a batch extraction of *Aronia* skin waste at different pH (2.4 and 5.2). The absorbance was monitored using UV-Vis spectrophotometer at 520 nm. 34

Figure 2.4 Extraction profiles during a batch extraction of *Aronia* skin waste using different biomass-solvent ratios. The absorbance was monitored using UV-Vis spectrophotometer at 520 nm. The red box shows a saturation of *Aronia*'s extract. 35

Figure 2.5 Illustration of experimental set-up for integrated extraction-adsorption process. 38

Figure 2.6 Effect of pH on UV-Vis absorbance of anthocyanins extracted from *Aronia* skin waste. The measurement was carried out on RASE. The resultant colours of aqueous solutions tested are shown at the top. 41

Figure 2.7 HPLC chromatograms of anthocyanins/ anthocyanidins present in RASE. Peaks are labelled as follows: (25) Cy3gal, (21) Cy3glc (26) Cy3ara (27) Cy3xyl (2) Cyanidin (28) Polymeric proanthocyanidins. The HPLC system is the same for all samples besides the additive, which is the acid written in bold on each sub-image. Detected by DAD at 520 nm. This experiment was run at different times. The samples from the same RASE were freshly prepared prior to injection. 43

Figure 2.8 HPLC chromatograms of anthocyanins/ anthocyanidins in each process (a) crude extract from solid-liquid extraction (b) solution exiting SPE column during sample loading (c) acidified water eluate (d) acidified ethanol eluate (e) dried RASE. Detected by DAD at 520 nm. 46

Figure 2.9 HPLC chromatograms of anthocyanins/ anthocyanidins which are present in RASE from an integrated method. (a) initial RASE (b) RASE after 1-month (c) RASE after 2 years. Detected by DAD at 520 nm. 48

Figure 2.10 ^{1}H-NMR spectra of crude extract without purification by SPE, post-SPE residues of ethyl acetate wash and RASE. The ^{1}H-NMR spectra were recorded at 500 MHz. Solvent: CD_3OD/CF_3COOD, 95:5. 52

Figure 2.11 The ^{1}H-^{1}H COSY spectrum of RASE showing the aromatic region. Recorded at 500 MHz (25 °C). (●) 3,4-dihydroxybenzoic acid. 53

Figure 2.12 The ^{1}H-^{1}H COSY spectrum of RASE showing the sugar region. Recorded at 500 MHz (25 °C). 54

Figure 2.13 Profile of anthocyanins shown in HPLC chromatograms of (a) the batch and (b) the integrated method. Solvent A: H_2O/TFA (99.5:0.5); Solvent B: acetonitrile. Detected at 520 nm. 55

Figure 2.14 Total anthocyanins calculated according to relative % shown in HPLC chromatograms of the batch method and the integrated method. Solvent A: H_2O/TFA (99.5:0.5); Solvent B: acetonitrile. Detected at 520 nm. 56

Figure 2.15 ^{1}H-NMR spectra of RASE for the batch method and the integrated method. The ^{1}H-NMR spectra were recorded at 500 MHz. Anthocyanins and anthocyanidin are labelled correspond to their H-4 proton. 57

Figure 2.16 The effect of acid concentration on total anthocyanins calculated according to relative % shown in HPLC chromatograms of (a) the batch and (b) the integrated method. Solvent A: H_2O/TFA (99.5:0.5); Solvent B: acetonitrile. Detected at 520 nm. 58

Figure 2.17 The comparison between a batch method (left) and an integrated extraction-adsorption method (right). 59

Figure 3.1 The general procedure to purify and quantify the total chemical composition of RASE. 62

Figure 3.2 HPLC chromatogram of RASE detected at 285, 350 and 520 nm. Column: Eclipse XDB C18, 5 µm, 150 x 2.1 mm column. Solvent A: H_2O/TFA (99.5:0.5); Solvent B: acetonitrile. New peaks at 350 nm belong to neutral polyphenols (blue squares) 63

Figure 3.3 Proposed co-pigmentation interaction of anthocyanins (Cy3gal) with polyphenols (quercetin and 2,4-dihydrobenzoic acid) or amongst anthocyanins present in RASE. 64

Figure 3.4 The Semi-preparative HPLC chromatogram of polyphenols present in RASE. Column: XBridge™ Prep C18, 10 x 50 mm, 5 µm, Solvent A: H_2O/TFA (99.5:0.5); Solvent B: acetonitrile, 40 min run. Detected at 520 nm. Fractions from the first 10 min were discarded as these come from the column. 65

Figure 3.5 ^{1}H-NMR spectrum (500 MHz) of RASE, isolated individual anthocyanins and polymeric species. Solvent: CD_3OD/CF_3COOD (95:5). Recorded at 25 °C. 67

Figure 3.6 ^{1}H NMR spectrum (500 MHz) of cyanidin in CD_3OD/CF_3COOD (95:5, v/v) recorded at 25 °C. Concentration of 8.34 x10^{-3} M. 68

Figure 3.7 Expanded region of a ^{1}H-^{1}H COSY and ^{1}H-^{13}C HSQC spectrum (500 MHz) of cyanidin in CD_3OD/CF_3COOD (95:5) at 25 °C. 69

Figure 3.8 Expanded region of a ^{1}H-^{13}C HMBC and ^{1}H-^{1}H NOESY spectrum (500 MHz) of cyanidin in CD_3OD/CF_3COOD (95:5) at 25 °C. 71

Figure 3.9 ^{1}H NMR spectrum (500 MHz) of cy3gal in CD_3OD/CF_3COOD (95:5, v/v) recorded at 25 °C. Concentration of 7.11x10^{-3} M. 72

Figure 3.10 Expanded region of a ^{1}H-^{1}H COSY and ^{1}H-^{13}C HSQC spectrum (500 MHz) of Cy3gal at 25 °C in CD_3OD/CF_3COOD (95:5). The line shows a correlation of a proton with its correlated proton. 73

Figure 3.11 Expanded region of a ^{1}H-^{13}C HMBC (left) and ^{1}H-^{1}H NOESY (right) spectrum (500 MHz) of Cy3gal in CD_3OD/CF_3COOD (95:5) at 25 °C. 74

Figure 3.12 ^{1}H-NMR spectrum (500 MHz) of Cy3glc in CD_3OD/CF_3COOD (95:5, v/v) recorded at 25 °C. Concentration of 5.3 x10^{-3} M. 76

Figure 3.13 Expanded region of a ^{1}H-^{1}H COSY (left) and ^{1}H-^{13}C HSQC spectrum (right) (500 MHz) of Cy3glc in CD_3OD/CF_3COOD (95:5) at 25 °C. 77

Figure 3.14 ^{1}H NMR spectrum (500 MHz) of Cy3ara in CD_3OD/CF_3COOD (95:5, v/v) recorded at 25 °C. Concentration of 6.26 x10^{-3} M. 78

Figure 3.15 Expanded region of a ^{1}H-^{1}H COSY, ^{1}H-^{13}C HSQC and ^{1}H-^{1}H NOESY spectrum (500 MHz) of Cy3ara in CD_3OD/CF_3COOD (95:5) at 25 °C. 79

Figure 3.16 ^{1}H-NMR spectrum (500 MHz) of Cy3xyl in CD_3OD/CF_3COOD (95:5, v/v) recorded at 25 °C. Concentration of 6.26 x10^{-3} mM. 81

Figure 3.17 Expanded region of a ^{1}H-^{1}H COSY and ^{1}H-^{13}C HSQC spectrum (500 MHz) of Cy3xyl in CD_3OD/CF_3COOD (95:5) at 25 °C. 82

Figure 3.18 ^{1}H NMR spectrum (500 MHz) of polymeric proanthocyanidins in CD_3OD/CF_3COOD (95:5, v/v) recorded at 25 °C. 83

Figure 3.19 ^{1}H-NMR spectrum (500 MHz) of ^{i}propyl acetate layer in CD_3OD at 25 °C. DHBA: 3,4-dihydroxybenzoic acid. Q: quercetin. 85

Figure 3.20 ^{1}H-NMR spectra (500 MHz) ethyl acetate layer in CD_3OD at 25 °C. DHBA: 3,4-dihydroxybenzoic acid. CA: chlorogenic acid. nCA: neochlorogenic acid. 86

Figure 3.21 ^{1}H-NMR spectra (500 MHz) of original RASE, ^{i}propyl acetate and ethyl acetate layers, insoluble solid and RASE after LLE from water layer in CD_3OD at 25 °C. H-4a belongs to Cy3gal and Cy3glc, H-4b belongs to Cy3ara and Cy3xyl, and H-4c belongs to Cyanidin. (●) 3,4-dihydroxybenzoic acid (DHBA). (♦) Quercetin. (▲) Chlorogenic acid and neochlorogenic acid; 90

Figure 3.22 The elution profile of a Biotage flash purification. Collection at 520 nm (– red line) and monitor at 280 nm (– black line). F1: Fraction 1; F2: Fraction 2; F3: Fraction 3. 91

Figure 3.23 Elution profile of all fractions from Biotage flash purification by HPLC-DAD. Detected at 520 nm. 92

Figure 3.24 ^{1}H-NMR spectrum of Fraction 3 of Biotage purification showing the presence of cyanidin and polymeric proanthocyanidins. Solvent: CD_3OD. 92

Figure 3.25 Molar absorptivity (ε) of Cy3gal in buffer solution pH 1 included its counter ion (CF_3COO^-), Mr of Cy3gal.CF_3COO^- is 562.41 g/mol. 95

Figure 3.26 The stability of Cy3gal in buffer solution pH 1 with various concentrations for 4 days. Monitored at 520 nm. 97

Figure 3.27 Absorption spectra of equilibrated solutions of Cy3gal as a function of pH. Concentration: 6.3 x 10^{-5} M (Mr of Cy3gal. CF_3COO^- is 562.2 g/mol); inset – determination of pK'_a using the absorbance at 511 nm.[132] 98

Figure 3.28 Total chemical composition of RASE (% w/w). 99

Figure 4.1 General scheme for the preparation, characterisation, and evaluation of RASE from *Aronia* skin waste with various organic counterions. 101

Figure 4.2 Anthocyanins in flavylium cationic forms with carboxylate, sulfinate and chloride as its counter anions, R^1, R^2 = H, OH, or OCH_3; R^3 = glycosyl or H; and R^4 = OH or O-glycosyl.[133] 102

Figure 4.3 Various acids used in the extraction-purification of anthocyanins from *Aronia* skin waste.[139–142] 103

Figure 4.4 Effect of various acids on the absorbance of anthocyanins extracted from *Aronia* skin waste measured in methanol and water 108

Figure 4.5 Anthocyanin profiles of RASE shown in HPLC chromatograms. Solvent A: H_2O/TFA (99.5:0.5); solvent B: acetonitrile. Detected by DAD at 520 nm. 110

Figure 4.6 Relative percentage (%) of anthocyanins and its aglycone in RASE with various counterions. 112

Figure 4.7 ^{1}H-NMR spectrum of RASE from different extractions using various acids in the extraction. 1) HCl, 2) FA, 3) AA, 4) OA, 5) TFA. Recorded at 500 MHz (25 °C). Solvent: CD_3OD/ CF_3COOD (95:5). Circles indicate protons from acid counterion where relevant. 114

Figure 4.8 Expanded ^{1}H-NMR spectrum of RASE using various acids in the extraction (aromatic region). 1) HCl, 2) FA, 3) AA, 4) OA, 5) TFA. Recorded at 500 MHz (25 °C). Solvent: CD_3OD/ CF_3COOD (95:5). (●) DHBA (♦) Q (▲) CA and nCA. 116

Figure 4.9 ^{1}H-NMR spectra of RASE from different extraction-purifications using HCl and TFA. Recorded at 500 MHz, 25 °C. Solvent: CD_3OD (no TFA added). 120

Figure 4.10 Extended ^{1}H-NMR spectra of RASE from different extraction-purifications using various acids 1) FA, 2) AA, 3) OA. Recorded at 500 MHz, 25 °C. Solvent: CD_3OD (no TFA added). 121

Figure 4.11 HPLC-DAD chromatogram of crude extract from HCl, TFA, FA and AA. Solvent A: H_2O/TFA (99.5:0.5); Solvent B: acetonitrile. Detected by DAD at 285 nm. The injection volume for all samples was same and all parameters were equivalent. 126

Figure 4.12 HPLC-DAD chromatogram of crude extract from HCl, TFA, FA and AA. Solvent A: H_2O/TFA (99.5:0.5); Solvent B: acetonitrile. Detected by DAD at 350 nm. The injection volume for all samples was same and all parameters were equivalent. 127

Figure 4.13 HPLC-DAD chromatogram of crude extract from HCl, TFA, FA and AA. Solvent A: H_2O/TFA (99.5:0.5); Solvent B: acetonitrile. Detected by DAD at 520 nm. The injection volume for all samples was same and all parameters were equivalent. 127

Figure 4.14 HPLC-DAD chromatogram of RASE from HCl, FA, AA and OA with the storage time of over 17 months in the dark at room temperature. The red circle shows the peak of cyanidin (Cy). Solvent A: H_2O/TFA (99.5:0.5); Solvent B: acetonitrile. Detected by DAD at 520 nm..... 129

Figure 4.15 Colour development of the mixture solution of DPPH radical reaction with Cy3gal. Solvent: methanol..... 133

Figure 4.16 Antioxidant activity (%RScA) vs TPC of RASE with various counterions. 134

Figure 4.17 Lipophilicity assay of RASE in an octanol-water system. *Stored for 7 months. 135

Figure 5.1 General scheme for preparing and characterising hemiketal forms of anthocyanins from RASE as an individual compound and mixture. 138

Figure 5.2 General preparation to produce hemiketal forms of anthocyanins. N_2 is passed through a vial containing water, and it goes to a vial containing anthocyanins in CD_3OD to dry the solvent out slowly. 141

Figure 5.3 ^{1}H-NMR spectra (500 MHz, 25 °C) of Cy3gal showing the formation of hemiketal forms by nucleophilic addition of water experiment. f = flavylium cation; a = hemiketal a (major); b = hemiketal b (minor). 142

Figure 5.4 ^{1}H-NMR spectrum of Cy3gal hemiketals dissolved in neutral CD_3OD. Recorded at 500 MHz (25 ºC). 143

Figure 5.5 Expanded region of a COSY spectrum (500 MHz) of Cy3gal in CD_3OD at 25 °C. a = hemiketal a (major); b = hemiketal b (minor). 144

Figure 5.6 Expanded region of an HSQC spectrum (500 MHz) of Cy3gal in CD_3OD at 25 °C. a = hemiketal a (major); b = hemiketal b (minor). 145

Figure 5.7 ^{1}H-NMR spectra (500 MHz) of Cy3gal in different conditions at 25 °C. Flavylium (top), a mixture of flavylium-hemiketal (middle) and hemiketal (bottom). f = flavylium; a = hemiketal a (major); b = hemiketal b (minor). 147

Figure 5.8 Expanded region of a NOESY spectrum (500 MHz) of Cy3gal in CD_3OD at 25 °C. f = flavylium; a = hemiketal a (major); b = hemiketal b (minor). 148

Figure 5.9 The appearance of Amberlite XAD-7HP resin on the left after elution with acidified wash (red) and on the right after elution with a copious amount of water (bluish-red). 152

Figure 5.10 ^{1}H-NMR spectra of RASE from different SPE elution experiments (HCl) recorded at 500 MHz (25 °C). Solvent: CD_3OD. 153

Figure 5.11 ^{1}H-NMR spectra of Cy3gal after addition of NaOD 5%. The ^{1}H-NMR spectra were recorded at 500 MHz (25 °C). Solvent: CD_3OD. (▲) Flavylium catanionic form, (●) Hemiketal form, (♦) quinonoid base..... 154

Figure 5.12 The ^{1}H-NMR spectra were recorded at 500 MHz (25 °C). Solvent: CD_3OD. AH^+: Flavylium cationic form, B: Hemiketal form, A: Quinonoid form. 155

Figure 6.1 UV spectra of 41 (blue) and 42 (red). The UV spectra were measured in DMSO..... 162

Figure 6.2 The UV spectra of 40 (blue) and 43 (red). The UV spectra were measured in DMSO..... 164

Figure 6.3 Acylation reaction in a biphasic solvent system..... 168

Figure 6.4 Distribution of Cy3gal and its ester derivatives (%) in acetonitrile at room temperature for 24 h. The starting material was obtained from the Biotage experiment. The acylating agent was 4 equivalents relative to Cy3gal..... 172

Figure 6.5 UV-Vis spectra of Cy3gal and its derivatives in methanol..... 187

Figure 6.6 HRMS chromatogram of isopropylidene derivatives of Cy3gal (m/z 489.1391) and Cy3ara (m/z 459.1284)..... 193

Figure 6.7 HRMS chromatogram of deuterated isopropylidene derivatives of Cy3gal (m/z 495.1787) and Cy3ara (m/z 465.1676). 194

Figure 6.8 ^{1}H-NMR spectra of Cy3gal and crude isopropylidene derivatives of anthocyanins from RASE-trifluoroacetate in CD_3COCD_3/CF_3COOD, 95:5. Protons labelled with a: Cy3gal, b: Cyanidin-3-*O*-4,6-*O*-isopropylidene-β-galactoside, 56..... 195

Figure 7.1. Thermal stability of Cy3gal and its derivatives at 25 °C 228

Figure 7.2. Thermal stability of Cy3gal and its derivatives at 40 °C 229

Figure 7.3. Thermal stability of Cy3gal and its derivatives at 60 °C 230

List of Schemes

Scheme 1.1 The general scheme of the anthocyanin biosynthesis pathway. 5

Scheme 1.2 Methylation of the hydroxyl groups on the B-ring of anthocyanins. OMT, *O*-methyltransferase. 6

Scheme 1.3 Resonance structures through delocalisation of the flavylium cationic form.[24] 7

Scheme 1.4 Addition of water to C-2 of the flavylium cationic form, to give the colourless hemiketal. 8

Scheme 1.5 S-centred bisulphite addition at C-4 on an anthocyanin, forming a colourless bisulphite-adduct.[26] 8

Scheme 1.6 Formation of pyranoanthocyanin from malvidin-3-*O*-glucoside and acetone.[27] 9

Scheme 1.7 Stabilisation of the radical of cyanidin-based anthocyanin via resonance.[5] 9

Scheme 1.8 Types of co-pigmentation for anthocyanins. (A) Intermolecular co-pigmentation with phenols, (B) self-association.[29] 10

Scheme 1.9 Metal-complexed anthocyanins.[30] 11

Scheme 1.10 Effect of pH on the structure of anthocyanins and resultant colours.[37,38] 12

Scheme 2.1 Formation of cyanidin-tannin (A-T) adduct through direct condensation reactions.[109] 47

Scheme 2.2 General deglycosylation reaction of anthocyanins forming its aglycone via a flavylium cationic form resulting in two positive charges in one molecule. 48

Scheme 2.3 Proposed deglycosylation mechanism of Cy3gal. R = Anthocyanidin core in hemiketal form or quinonoid base. Protonation occurs at an oxygen atom connecting an aglycone and a sugar moiety. The products are an aglycone (cyanidin) in a flavylium cationic form and galactose. 49

Scheme 2.4 Proposed deglycosylation mechanism of Cy3gal. R = Anthocyanidin core in hemiketal form or quinonoid base. Protonation occurs at an oxygen atom in a sugar moiety resulting in a ring-opening. The products are an aglycone (cyanidin) in a flavylium cationic form and galactose. 50

Scheme 4.1 The equilibrium of a flavylium cationic form and hemiketal forms of cyanidin-based anthocyanins (a, major and b, minor).[112] 121

Scheme 4.2 Mechanism reaction of antioxidant activity of DHBA as one of neutral polyphenols found in RASE. 132

Scheme 4.3 DPPH and antioxidant reaction.[165] 132

Scheme 5.1 An equilibrium between flavylium cation and hemiketal forms of cyanidin glycoside.[147] 140

Scheme 5.2 Proposed mechanism of nucleophilic addition of water at carbon position 2 of a flavylium cationic form in general.[147] 143

Scheme 6.1 Synthesis of malvidin-3-*O*-glucoside-stearic acid conjugates from malvidin-3-glucoside and stearoyl chloride.[179] 159

Scheme 6.2 Synthesis of malvidin-3-*O*-glucoside-oleic acid conjugates from malvidin-3-glucoside and oleic acid under enzymatic catalysis acylation.[145] 160

Scheme 6.3 Synthesis of *trans*-3,4',5-triacetyl resveratrol (42). 161

Scheme 6.4 Synthesis of 3,3',4',5,7-pentaacetyl quercetin (43). 163

Scheme 6.5 Transformation of D-glucose to β-D-glucopyranose triacetate via isopropylidene intermediate.[201] 191

Scheme 6.6 Proposed reaction mechanism of acetonation of anthocyanins. Galactoside structure is used as an example. R = Cyanidin aglycone. 192

Scheme 6.7 Proposed acetonation reaction of Cy3gal and Cy3ara as the major anthocyanins in *Aronia* skin waste. 193

Scheme 6.8 Proposed acetonation reaction of Cy3gal and Cy3ara using deuterated reagents. 194

List of Abbreviations

AA acetic acid

ANS anthocyanidin synthase

CA chlorogenic acid

CGE cyanidin-3-*O*-galactoside equivalent

CHI chalcone isomerase

CHS chalcone synthase

COSY correlation spectroscopy

Cy cyanidin

Cy3gal cyanidin-3-*O*-galactoside

Cy3glc cyanidin-3-*O*-glucoside

Cy3ara cyanidin-3-*O*-arabinoside

Cy3xyl cyanidin-3-*O*-xyloside

DAD diode array detector

DEPT distortionless enhancement by polarization transfer

DFR dihydroflavonol 4-reductase

DHBA 3,4-dihydroxybenzoic acid

Dp delphinidin

DPPH 2,2-diphenyl-1-picrylhydrazyl

DW dry weight

EI electrophilic

ESI electron spray ionisation

FA formic acid

F3H flavanone-3-hydroxylase

F3'H flavonoid 3'-hydroxylase

F3'5'H flavonoid 3'5'-hydroxylase

F-C folin ciocalteu

FW fresh weight

GAE gallic acid equivalent

Gly glycoside

HPLC high performance liquid chromatography

HMBC heteronuclear multiple-bond correlation spectroscopy

HSQC heteronuclear single-quantum correlation spectroscopy

LC-MS liquid chromatography-mass spectrometry

LDOX leucoanthocyanidin oxidase

LLE liquid-liquid extraction

Mv malvidin

nCA neochlorogenic acid

NMR nuclear magnetic resonance

NOESY nuclear overhauser effect spectroscopy

Nu nucleophilic

OA octanoic acid

OMT *O*-methyltransferase

PA phosphoric acid

PI positive ionisation

Pg pelargonidin

Pn peonidin

Pt petunidin

PUFAs polyunsaturated fatty acids

Q quercetin

RASE refined *Aronia* skin waste extract

ROS radical oxygen species

RScA radical scavenging activity

SPE solid phase extraction

TFA trifluoroacetic acid

TMAC total monomeric anthocyanin content

TPC total phenolic content

UFGT flavonoid glucosyltransferase

UHPLC ultra-high performance liquid chromatography

UV-Vis ultraviolet-visible

Chapter 1
General Introduction

The valorisation of food industry-related wastes to produce bioactive compounds for various applications is increasing.[1] Approximately 30% of dry solids produced from juice-processing press-berries are discharged as waste.[2] Such waste can cause new environmental problems if it is not properly treated. Additionally, the waste still contains valuable bioactive and functional compounds such as polyphenols which are well known as antioxidants, vitamins, and other compounds.[2] Therefore, unavoidable wastes such as pomaces, which consist of the skin of berries (epicarp), seeds, and some residues of twigs, from winery or juice industries can be utilised as a source of a wide range of valuable bioactive and functional compounds without competing with the food chain.[2,3] This food waste valorisation is necessary to encourage an ideal 'zero-waste' objective and to add value to the waste itself. The raw material used in this study is *Aronia melanocarpa* (black chokeberry) skin waste (pomace) generated as a by-product from the production of *Aronia* berry juice. These *Aronia* skin wastes are rich in polyphenols, especially anthocyanins which are the second-highest polyphenol component after polymeric proanthocyanidins.[4] Anthocyanins display bright and attractive colours, which suggest the potential application of these compounds as natural colorants. This study has focused on the development of new methods for the isolation, derivatisation and utilisation of anthocyanins extracted from *Aronia* skin waste as natural colorants and antioxidants. Some related literature studies are discussed in this chapter.

1.1. Overview of Anthocyanins

1.1.1. Anthocyanins

In Greek, the word anthocyanin (also anthocyan) derives from *anthos,* which means flower and *kyanos,* which means dark blue.[5] Anthocyanins are natural, non-toxic, water-soluble, highly coloured molecules, and are responsible for most red, blue, orange and purple colours in fruits (especially berries), flowers, stems, roots, and leaves of some plants.[6–8] These compounds are phenolic secondary metabolites which belong to the flavonoid group. In general, the structure of anthocyanins consists of two main components which are the core structure of the anthocyanin and at least one sugar moiety. The core structure of the anthocyanin, usually represented in its flavylium cationic form (**Figure 1.1)**, can be described as a C_6–C_3–C_6 skeleton. This skeleton contains a phenolic ring (the A-ring) fused to a pyran with an additional phenolic ring (the B-ring) connected at the 2 position of the pyran, providing

conjugated double bonds in the anthocyanin core.[9] This extensive π-system is responsible for the absorption of light at visible wavelengths resulting in bright colours in anthocyanins. This structure is referred to as an aglycone or anthocyanidin, the non-glycosylated anthocyanin.[10] However, it is rare to find anthocyanidins in plants due to its instability.[11] Anthocyanidins are usually found during the isolation process as a deglycosylation product. The second component of anthocyanins is the sugar moiety which can occur through a glycosidation at position 3, 5 and/or 7 in the anthocyanidin. Monosaccharides such as glucose, galactose, arabinose and rhamnose are the most common sugars attached to the anthocyanidin core. The sugar moieties of anthocyanins can also be further acylated with organic acids such as cinnamic acids as well as aliphatic acids (**Figure 1.2**). Acylated anthocyanins are commonly found in nature.[12]

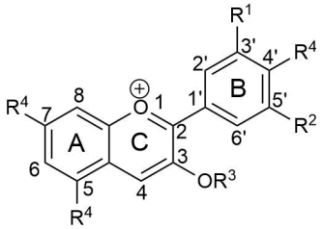

Figure 1.1 A flavylium cationic form of anthocyanins, R^1, R^2 = H, OH, or OCH_3; R^3 = glycosyl or H; and R^4 = OH or O-glycosyl.[5]

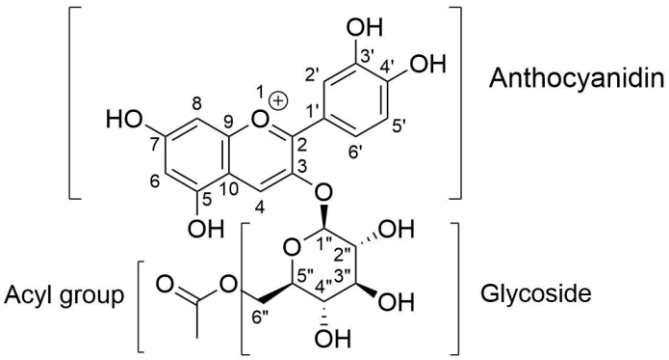

Figure 1.2 The composition of an acylated anthocyanin (cyanidin-3-O-β-(6”-acetyl)glucoside, 1) anthocyanidin, 2) glycoside, 3) acyl group.

1.1.2. Classification of Anthocyanins and Resultant Colours

In 2018, there are more than 700 different anthocyanins found in nature, but approximately 90% of all anthocyanins are based on the six major (most common) anthocyanidins shown in **Table 1.1**.[5,13] The differences between individual anthocyanins relate to the number of hydroxyl groups on the B-ring (**Figure 1.3**), the nature and number of sugars attached to the molecule, the position of this attachment, and the nature and number of aliphatic (acetic, malonic or succinic) or aromatic (hydroxycinnamic or hydroxybenzoic) acids attached to sugar moiety(s).[5,12]

The larger the number of hydroxyl groups, the bluer the colour of anthocyanins. Meanwhile, a slight reddening effect can be caused by *O*-methylation of anthocyanins. The glycoside moiety can also cause a slight reddening effect. Furthermore, aromatic acylation of the hydroxyl groups of the sugar moiety can cause a blue shift and stabilise anthocyanins. In contrast, aliphatic acylation does not change the colour but can increase the stability, and affect the solubility of anthocyanins.[14]

Table 1.1 Six major anthocyanidins present in nature with their respective colours at pH < 3 and also its maximum wavelength.[5,13,15]

Name	Abbreviation	Colour (pH < 3)	λ_{max} (nm)*
Pelargonidin	Pg	Orange	504
Cyanidin	Cy	Orange-red	517
Delphinidin	Dp	Bluish-red	518
Peonidin	Pn	Orange-red	525
Petunidin	Pt	Bluish-red	525
Malvidin	Mv	Bluish-red	528

*λ_{max} values shown are for the corresponding 3-*O*-glucoside at pH 3.1

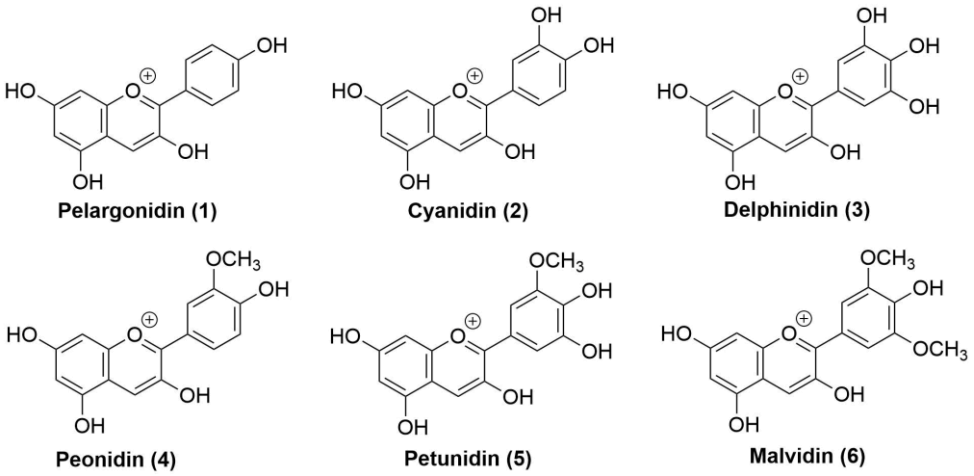

Figure 1.3 Chemical structures of the 6 major (most common) anthocyanidins found in nature.

The glycosides of the three non-methylated anthocyanidins (cyanidin, pelargonidin and delphinidin) are the most common anthocyanidins found in nature. They are present in 80% of pigmented leaves, 69% of fruits and 50% of flowers.[5] Amongst other anthocyanidins, cyanidin is the most abundant at around 50% followed by pelargonidin (12%), peonidin (12%), delphinidin (12%), petunidin (7%) and malvidin (7%).[5]

1.1.3. Biosynthesis of Anthocyanins

Anthocyanins play an important role in plants; in most cases, these bright compounds attract animals involved in pollination and seed dispersal for their reproduction, repel harmful insects, and prevent tissue damage caused by UV light due to their ability to absorb blue-green and ultraviolet light.[16] Anthocyanins are synthesised through a flavonoid pathway in the cytosol and then stored in the vacuole.[14] The biosynthesis of anthocyanins is presented in **Scheme 1.1**.[14,17–19] The typical colour of each anthocyanin is also presented, but the actual colour depends on various factors, as discussed in **Section 1.1.2**. The A-, B- and C-rings with the carbon numbers are as marked for naringenin (**11**). Naringenin is flavanone which has a single chiral centre at the position 2 of the C-ring.

One molecule of *p*-coumaroyl-CoA (**7**) condenses with three molecules of malonyl-CoA (**8**) by the action of chalcone synthase (CHS), forming a tetrahydroxychalcone (**9**) which is the basic structure of flavonoids. Chalcone acts as the precursor for all groups of flavonoids, including flavones, flavonols, isoflavones, proanthocyanidins and anthocyanins.[17] The C-ring is closed by chalcone isomerase (CHI), resulting in the formation of flavanones (e.g. naringenin). Colourless naringenin (**11**) is then converted to dihydroflavonol (**14**) by the action of flavanone 3-hydroxylase (F3H). Hydroxyl groups can be introduced at the 3’ or 3’, 5’ positions of the B-ring by the flavonoid 3’-hydroxylase (F3’H) or the flavonoid 3’,5’-hydroxylase (F3’5’H) to produce dihydroquercetin (**15**) and dihydromyricetin (**13**), respectively. Dihydroflavonol 4-reductase (DFR) reduces dihydroflavonols forming 3,4-*cis*-leucoanthocyanidins (**16**, **17**, **18**). DFR is a specific enzyme for the anthocyanin synthesis. The colourless leucoanthocyanidins are subsequently converted to anthocyanidins (pelargonidin **1**, cyanidin **2**, delphinidin **3**) by the action of leucoanthocyanidin oxidase/ anthocyanidin synthase (LDOX/ANS). Anthocyanidins are then converted to anthocyanins (**19**, **20**, **21**) through glycosylation by the action of flavonoid glucosyltransferase (UFGT). As anthocyanidins are unstable under physiological conditions, glycosylation is important because it can increase their hydrophilicity and stability.[18]

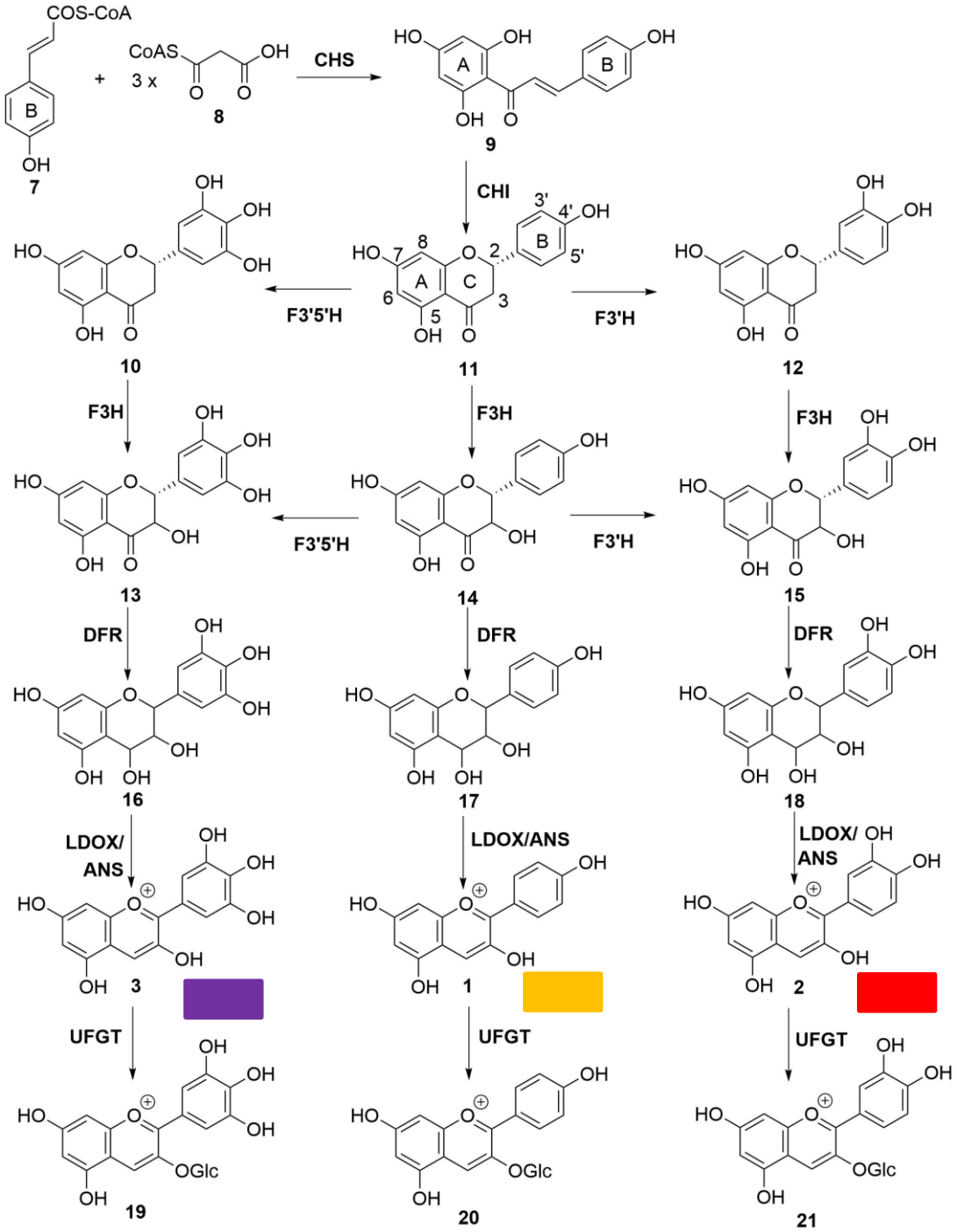

Scheme 1.1 The general scheme of the anthocyanin biosynthesis pathway.

Methylation of the hydroxyl groups can also occur at the C3' position or both at the C3' or C5' positions on the B-ring of anthocyanins by the action of *O*-methyltransferase (OMT). Methylation of the hydroxyl group at the C3' position of cyanidin-3-*O*-glucoside (**21**) forms peonidin-3-*O*-glucoside (**24**), while, petunidin-3-*O*-glucoside (**22**) and malvidin-3-*O*-glucoside (**23**) are formed from delphinidin-3-*O*-glucoside (**19**) (**Scheme 1.2**).[18,19]

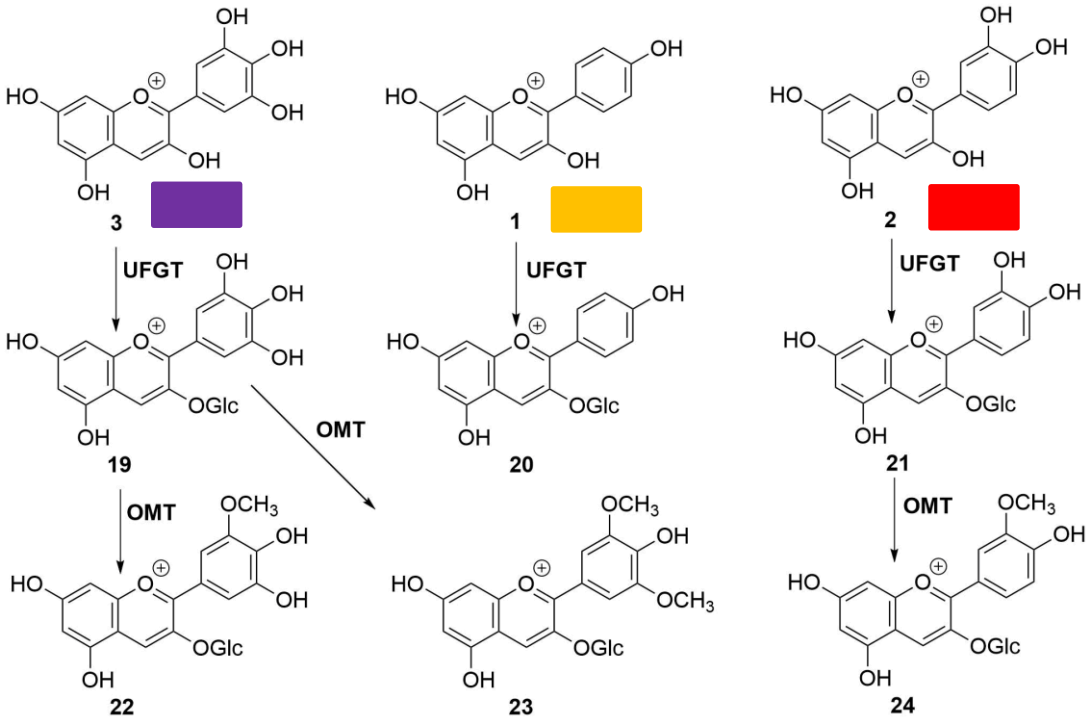

Scheme 1.2 Methylation of the hydroxyl groups on the B-ring of anthocyanins. OMT, *O*-methyltransferase.

1.1.4. Reactivity of Anthocyanins

Anthocyanins are relatively reactive compounds compared to other flavonoids, and require careful handling; otherwise, degradation may occur during processing. The natural chemical composition of anthocyanins such as aglycones which has specific pyrylium nucleus (the C-ring), sugar moiety and acyl moiety affect the reactivity and stability of anthocyanins.[20] Additionally, Farr *et al.* reported that the stereochemical properties or location of glycosidic linkages within the sugar moiety affect the reactivity of mono-, di- and tri-substituted cyanidin-3-*O*-glycosylates.[21]

Anthocyanins have the potential to react with different nucleophilic and electrophilic sources at a variety of positions (**Figure 1.4**).[22] Nucleophilic attack on anthocyanins can occur at the 2 and 4 positions of the C-ring. In contrast, an electrophilic attack can occur at the hydroxyl groups and also the 6 and 8 positions of the A-ring. Chemical modification of anthocyanins can be done through the esterification of hydroxyl groups, including those of the glycosyl groups and anthocyanidins with aliphatic or aromatic acids.[23]

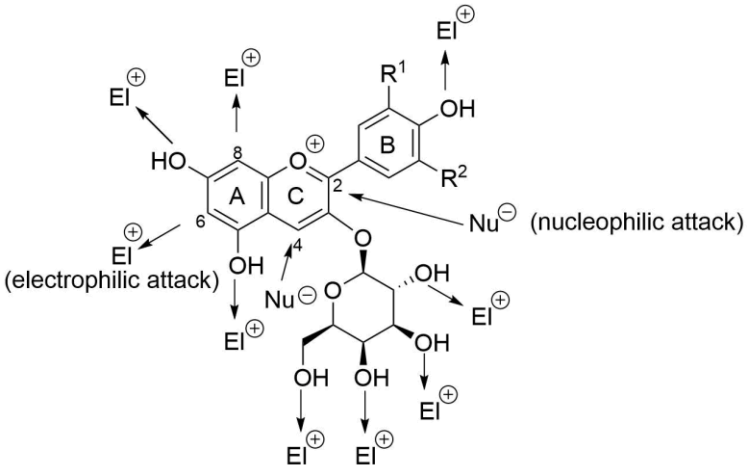

Figure 1.4 Likely reactive positions of anthocyanins in a flavylium cationic form toward nucleophiles and electrophiles. Cy3gal is presented as an example.

1.1.4.1. Nucleophilic Additions

The sensitivity of anthocyanins towards nucleophilic addition, which leads to the destruction of the visible chromophore, limits their application as natural colorants. The absence of conjugated double bonds connecting the A-, B-, and C-rings causes this decolourisation. The positively charged oxygen of a flavylium cationic form can be delocalised over position 2 and 4 (**Scheme 1.3**), allowing nucleophilic addition at either of these positions. However, the tertiary carbocation (3°, C-2) is more stable (and hence is likely to contribute most to the overall resonance structure) and therefore is preferable than secondary carbocation (2°, C-4) for the nucleophilic addition. The C-2 position is also known to be the most electron deficient.[24]

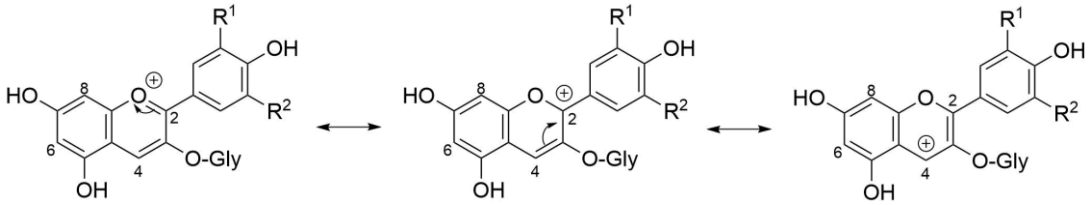

Scheme 1.3 Resonance structures through delocalisation of the flavylium cationic form.[24]

1.1.4.1.1. Nucleophilic Addition at C-2

The most common example for the nucleophilic addition of anthocyanins at position C-2 is the formation of a colourless hemiketal (2 epimers) by the addition of water (**Scheme 1.4**).[25] This process is known as hydration and can be characterised by the thermodynamic hydration constant (K_h). It is discussed more detail in the equilibrium of anthocyanins at different pHs (**Section 1.1.5)**.

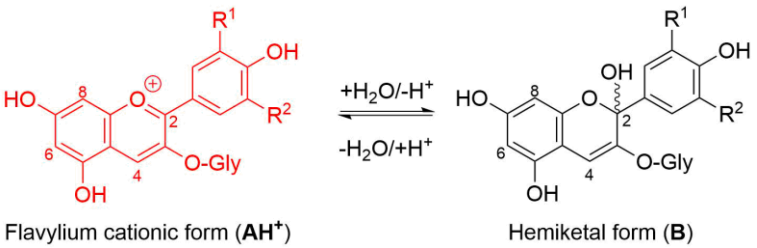

Scheme 1.4 Addition of water to C-2 of the flavylium cationic form, to give the colourless hemiketal.

1.1.4.1.2. Nucleophilic Addition at C-4

Nucleophilic addition at C-4 is potentially more likely than C-2 because of reduced steric hindrance. Sodium bisulphite addition to malvidin-3-*O*-glucoside (**23**) is known to form the colourless bisulphite-adduct (**25**) through its sulphur atom (**Scheme 1.5**).[26] The application of this reaction is mainly in the food industries as bisulphite acts as an antimicrobial and anti-browning agent.[20]

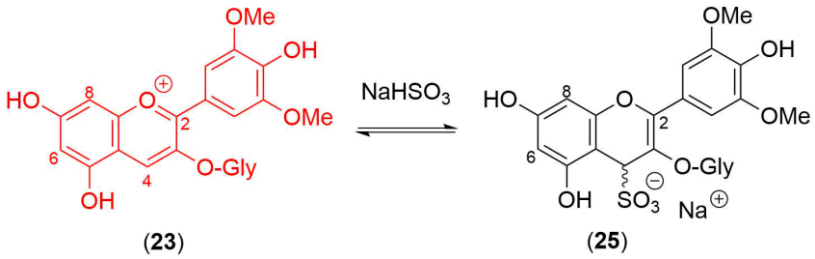

Scheme 1.5 S-centred bisulphite addition at C-4 on an anthocyanin, forming a colourless bisulphite-adduct.[26]

Nucleophilic addition at C-4 can also take place during the condensation reaction between anthocyanins (**23**) and acetone to produce pyranoanthocyanins (**26**), which have been reported to be more stable than their anthocyanin precursors (**Scheme 1.6**).[27] This reaction also requires electrophilic addition by a hydroxyl group attached to C-5 forming a new ring. Pyranoanthocyanins are produced during the maturation and ageing of wine, and have been reported to show chromatic shades with a wide range of colours from yellow, orange, red, purple, and blue at various pHs.[28] Therefore, these molecules may have the potential to be used as dyes in a wide range of potential applications.

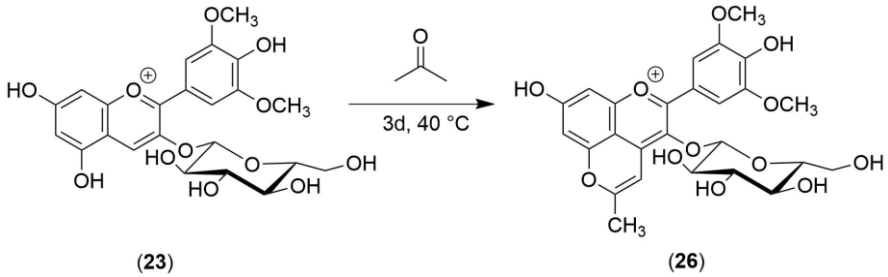

Scheme 1.6 Formation of pyranoanthocyanin from malvidin-3-*O*-glucoside and acetone.[27]

1.1.4.2. Antioxidant Activity

Antioxidants are molecules that can donate a free electron (radical) or hydrogen atoms to reactive free radicals. The chain reactions caused by free radicals from oxidation can jeopardise organisms' cells, resulting in tumours or cancers (*vide infra*). The mechanism of action for antioxidant activity of anthocyanins is presented in **Scheme 1.7**.[6] Anthocyanins possess hydrogen donating capabilities to act as antioxidants and therefore can protect oxidisable biomolecules such as polyunsaturated fatty acids (PUFAs), proteins and DNA.[20] The anthocyanin radicals formed are stabilised through delocalisation and resonance, and less likely to result in damage to neighbouring biomolecules.[6]

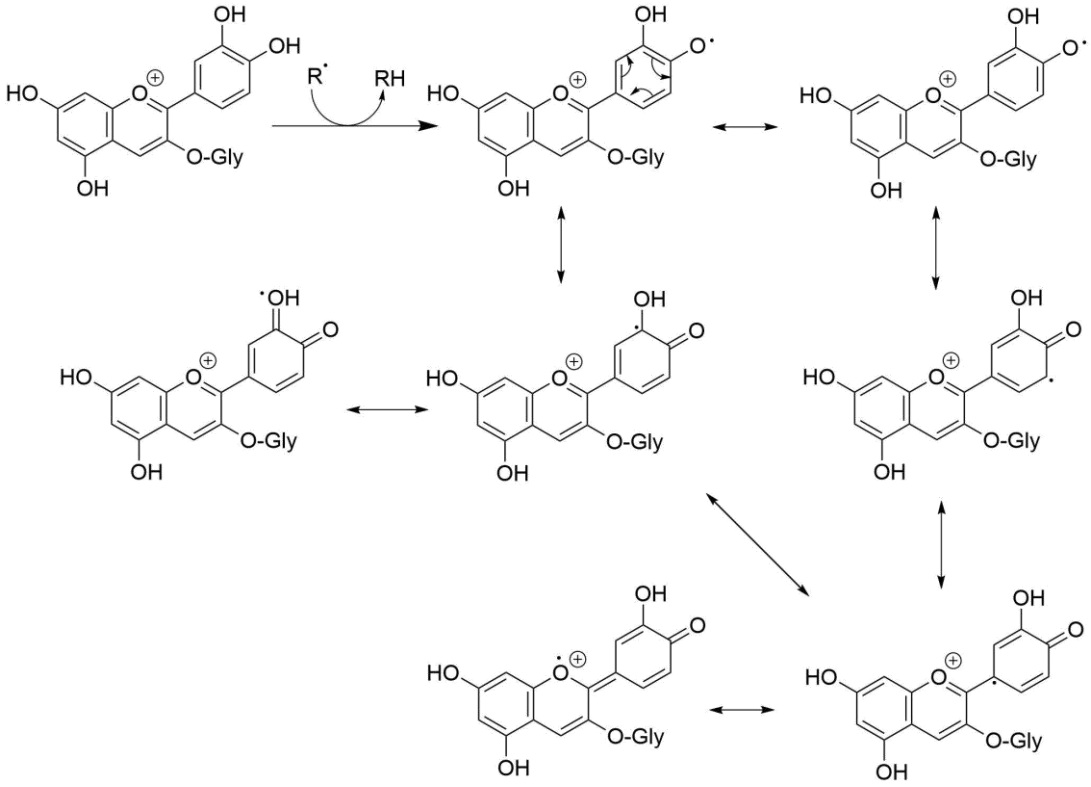

Scheme 1.7 Stabilisation of the radical of cyanidin-based anthocyanin via resonance.[6]

1.1.4.3. Anthocyanin Complexes

In nature, anthocyanins can undergo self-association, co-pigmentation and/or metal complex formation.[29,30] These anthocyanin complexes result in bathochromic shift (an increase of visible absorption band) and hyperchromic shift (an increase of absorption intensity) compared to the precursors.[31] Additionally, these complexes contribute to the stabilisation of anthocyanins. The aromatic nuclei are flat polarisable non-polar surfaces and contribute to strong dispersion interactions amongst anthocyanins or with other polyphenols. In addition, polar OH groups of anthocyanins, especially in the B-ring, can act as metal chelators.[20]

1.1.4.3.1. Self-Association and Co-Pigmentation

The π-stacking interactions of anthocyanins with other anthocyanins are known as self-association, while co-pigmentation is when anthocyanins bind with other polyphenols (**Scheme 1.8**).[29] These interactions are mostly driven by dispersion forces interactions. A self-association is stronger for a neutral quinonoid base than the corresponding flavylium cationic form or anionic quinonoid base, as the latter two cases are destabilised by charge repulsion.[20] An addition of hydroxyl group at the position C-3' weakens self-association whereas addition of hydroxyl group at the position C-5' facilitates self-association.[32] Co-pigmentation can occur through intra- and intermolecular interactions. The intramolecular co-pigmentation occurs when anthocyanins bind with aromatic groups attached in a sugar moiety(s) (**Figure 1.5**), while the intermolecular co-pigmentation occurs when anthocyanins bind with uncoloured compounds such as flavanols or flavones.[29]

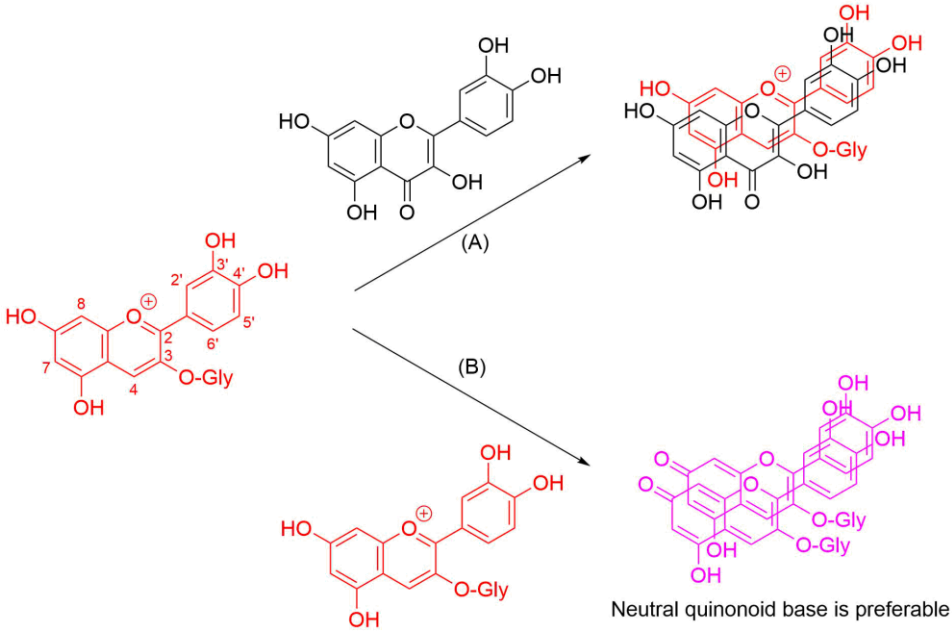

Scheme 1.8 Types of co-pigmentation for anthocyanins. (A) Intermolecular co-pigmentation with phenols, (B) self-association.[29]

Figure 1.5 Model of the intramolecular co-pigmentation in polyacylated anthocyanins.

1.1.4.3.2. Metal complexes

Metal complex formation with anthocyanins is associated with blue colour development. Metal-complexed anthocyanins form through the complexation of a quinonoid base with additional proton loss from C3'-OH and positively charged metal ions. The interactions are caused by the hydroxyl groups of anthocyanins (cyanidin, delphinidin, and petunidin derivatives) in the B-ring with metal ions in mildly acidic to neutral solution (**Scheme 1.9**).[20,30] The most common metals associated with anthocyanin complex formation are tin, copper, iron, aluminium, magnesium and potassium.[30,33] Metal-complexed anthocyanins are mostly stabilised by ion-dipole electrostatic interactions than by electron pair sharing.[34]

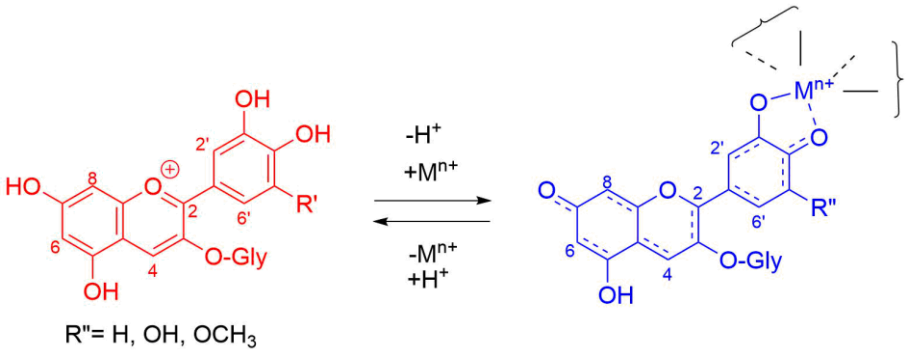

Scheme 1.9 Metal-complexed anthocyanins.[30]

1.1.5. Colour and Stability of Anthocyanins

The colour and stability of pure anthocyanins are influenced by pH, and covers the whole of the pH scale. Fossen *et al*. studied the stability of cyanidin-3-*O*-glucoside (Cy3glc) at various pHs ranging from 1-9 during 60 days of storage at 10 and 23 °C.[35] The most stable form of anthocyanins is the flavylium cationic form (**AH^+**) which is predominantly present in an acidic solution (pH <3). The stability of anthocyanins decreased drastically with an increasing of pH. At higher pH, anthocyanins can also be found as a quinonoid base (**A**), hemiketal (**B**) and chalcone forms (**C_E/C_Z**) through a kinetic and thermodynamic competition of two reaction pathways. The quinonoid base is a kinetic product formed by deprotonation of the flavylium cationic form (**AH^+**). A neutral quinonoid base (**A**) is in equilibrium with an anionic quinonoid base (**A^-**). A

transformation of a flavylium cationic form (**AH**$^+$) to a neutral quinonoid typically causes the shift of the maximum visible wavelength absorption by 20-30 nm (**AH**$^+$ → **A**) and by 50-60 nm for a neutral quinonoid to an anionic quinonoid (**A** → **A**$^-$). These shifts correspond to the colour changes of anthocyanins from red to purple-blue.[36]

The quinonoid form (**A**) is slowly converted into the hemiketal form (**B**) via a flavylium cationic form (**AH**$^+$).[36] Meanwhile, the hemiketal (**B**) as a thermodynamic product can be formed through a nucleophilic attack by water at carbon position 2, losing a proton to give the colourless or pale-yellow hemiketal (sometimes referred to as hemiacetal) form. This species can then undergo ring-opening tautomerism to form the *cis*/*trans* chalcone (**C$_E$**/**C$_Z$**). The flavylium cationic form can usually be regenerated through reacidification as most of the processes are reversible. The equilibrium of anthocyanins in aqueous solutions is presented in **Scheme 1.10**.[37,38]

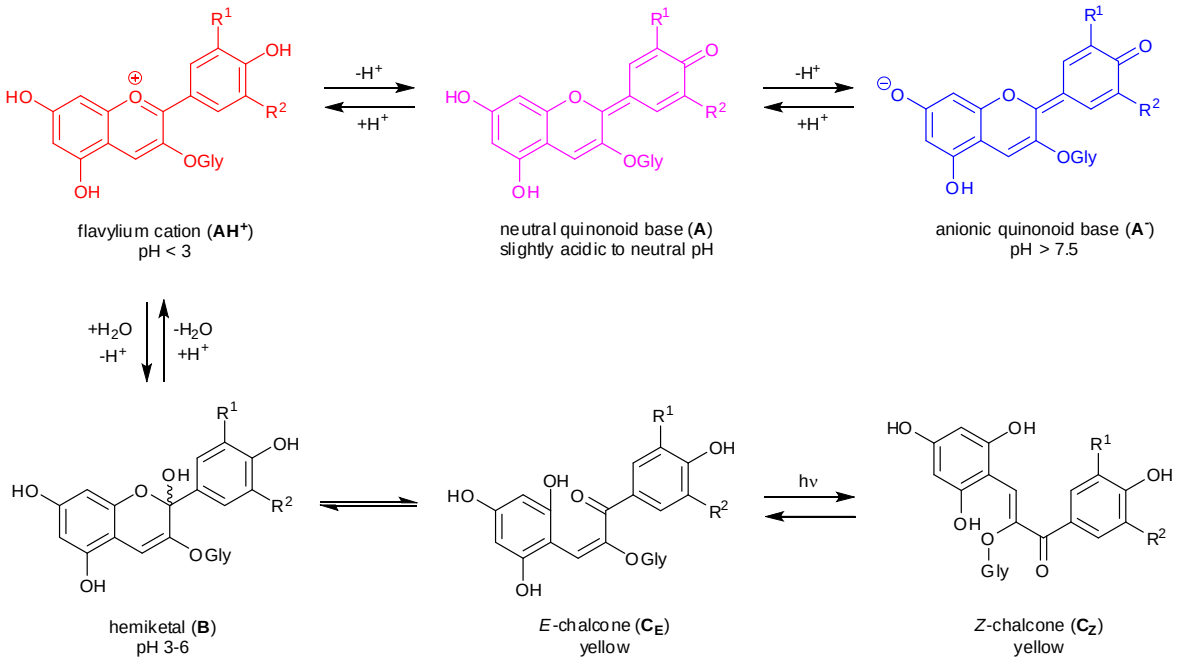

Scheme 1.10 Effect of pH on the structure of anthocyanins and resultant colours.[37,38]

The pK_a value of anthocyanins indicates the strength of anthocyanins as an acid in water. pK_a itself is the negative log of the anthocyanin dissociation constant of K_a value. The lower the pK_a value implies anthocyanins more fully dissociate one or more acidic protons in water. The phenolic OH groups of the flavylium cationic form at C-4', C-5 and C-7 are fairly acidic, where hydroxyl at C-7 is the most acidic group with a pK_{a1} of *ca*. 4.0 and at higher pH, the second proton loss at C-4'-OH results in the anionic base with maximised electron delocalisation over the rings of a pyrylium

ion with pK_{a2} of 7. It is quite acidic compared to pK_a of phenols which is 10. The most stable tautomer is a neutral quinonoid base (**A**) where carbonyl group found at C-7.[20]

Additionally, according to **Scheme 1.10**, the equilibriums of the flavylium structural transformations under acidic aqueous solutions can be explained by the following equations:

$$\mathbf{AH^+} \overset{K_a}{\rightleftharpoons} \mathbf{A} + \mathbf{H^+}$$; K_a proton transfer **Equation 1.1**

$$\mathbf{AH^+} \overset{K_h}{\rightleftharpoons} \mathbf{B} + \mathbf{H^+}$$; K_h hydration **Equation 1.2**

$$\mathbf{B} \overset{K_t}{\rightleftharpoons} \mathbf{C_E}$$; K_t tautomerisation **Equation 1.3**

$$\mathbf{C_E} \overset{K_i}{\rightleftharpoons} \mathbf{C_Z}$$; K_i isomerisation **Equation 1.4**

The equations above (**Equation 1.1-1.4**) can be simplified in one single acid-base equilibrium with K'_a constant (**Equation 1.5** and **1.6**) where the **A**, **B**, $\mathbf{C_E}$ and $\mathbf{C_Z}$ species are represented as one generic conjugate base **CB**, which is in equilibrium with the flavylium cationic form (**AH^+**):

$$\boldsymbol{K'_a = K_a + K_h + K_hK_t + K_hK_tK_i}$$ **Equation 1.5**

$$\boldsymbol{K'_a = \frac{[CB][H^+]}{[AH^+]}; [CB] = [A] + [B] + [C_E] + [C_Z]}$$ **Equation 1.6**

The value of pK'_a indicates the pH where at thermal equilibrium, half of the flavylium cationic form (**AH^+**) has been transformed into its conjugate base (**CB**). It explains the direct correlation between the colour stability of a flavylium cationic form (red-coloured species) with pH. The higher the pK'_a value, the higher stability of a flavylium cationic form of anthocyanins toward the deprotonation (K_a) and hydration (K_h) processes.[39]

The stability of anthocyanidins is influenced by the B-ring substituents and the presence of additional hydroxyl or methoxyl groups, which decrease the aglycon stability in neutral media.[40] Amongst anthocyanins with respect to the aglycone, pelargonidin is the most stable, followed by cyanidin, peonidin, petunidin, malvidin and delphinidin. The hydroxyl radical at the 3' position can stabilise more than the methoxyl radical in the same position. The substituents at the 5' position can

decrease the stability of anthocyanins with the exception of petunidin-3-*O*-glucoside, which is more stable than delphinidin-3-*O*-glucoside (see **Figure 1.3** in **Section 1.1.2**). In general, *O*-glycosylation can stabilise anthocyanins. For glycosylated derivatives, the most stable are glucosides, followed by galactosides and arabinosides. The sugar moieties prevent the degradation of the highly unstable α-diketone intermediates that can be formed on opening of the C-ring. Sugar moieties can also prevent dimerisation of anthocyanins because of its steric hindrance.[40,41] Further acylation on sugar moiety(s) of anthocyanins can increase its colour stability through an intramolecular co-pigmentation, reducing the possibility for a nucleophilic addition with water at the position C-2.[42]

1.1.6. Health Benefits of Anthocyanins

Berries and red fruits are good dietary sources of polyphenols as they are rich in anthocyanins.[43,44] Anthocyanins as phenolic compounds have been reported to possess a wide range of health benefits for humans mostly act as antioxidants (see **Section 1.1.5**). In our body, anthocyanin-containing foods are digested in the gut. Anthocyanins from *Aronia* chokeberry juice were reported to be stable in the gastric digestion-like condition *(in vitro*), which is a mixture of pepsin-HCl for 2h.[45] Meanwhile, approximately 40% of anthocyanins were degraded during pancreatic digestion. It mimics the condition in the small intestine, which is a slightly alkaline.[45]

In the following section, the discussion is focused on anthocyanins extracted from *Aronia melanocarpa* (black chokeberries); see **Section 1.2**. The potential health benefits reported in this section were obtained *in vitro,* which might be different from those results reported from *in vivo* studies, as, amongst other possible reasons, anthocyanins are sensitive to alkaline pancreatic digestion. These berries have been reported to show many human health beneficial effects, including anti-inflammatory,[46–48] antioxidant (which is the highest amongst other berries such as blueberry, blackcurrant and elderberry),[43,49,50] antitumor,[50] antimutagenic and anticancer activities.[51,52] Moreover, amongst other berries, anthocyanins from *Aronia* chokeberries can also reduce blood glucose levels.[53] The reports of different health benefits of the extracts of *Aronia* chokeberries are summarised in **Table 1.2**.

Table 1.2 Reports of different health benefits of anthocyanins from *Aronia melanocarpa* (black chokeberry)

Anthocyanin source	Health benefit	Conclusion	Ref.
A. melanocarpa fruit extract	Anti-inflammatory	*A. melanocarpa* extract can exhibit anti-inflammatory effects in HAECs by inhibiting the expression on endothelial CAMs, activation of NF-$_{\kappa}$B and production of reactive oxygen species (ROS).	46
Aronia berry extract	Anti-inflammatory	*Aronia* berry extracts inhibit LPS-induced IL-6 secretion (Cy3ara and quercetin) and induce IL-10 excretion (quercetin) in unstimulated splenocytes.	47
Chokeberry juice concentrate	Anti-inflammatory	Chokeberry juice concentrate inhibited both the release of TNFα, IL-6 and IL-8 in human peripheral monocytes and the activation of the NF-$_{\kappa}$B pathway in RAW 264.7 macrophage cells. The addition of selenium (sodium selenite) to chokeberry juice increases its anti-inflammatory activity significantly by inhibiting NF-$_{\kappa}$B activation, cytokine release and PGE_2 synthesis.	48
Chokeberry and blueberry extract	Antioxidant	Black chokeberry extract exhibited higher free radical-scavenging activity than blueberry extract based on the results from the *in vitro* assays such as DPPH, ABTS, radical-scavenging activity, FRAP and reducing powder.	49
Chokeberry extract	Antioxidant and antitumor	The positive correlations between antioxidant assays and the polyphenolic content suggest that the antioxidant capacity of chokeberries would derive more from anthocyanins (53-56%) and proanthocyanidins (35%) than from the other phenolic compound's contribution (9%). Cyanidin glycosides have potential antitumor because it can inhibit HeLa human cervical tumour cells and the production of ROS.	50
Chokeberry fruit juice	Antioxidant	Chokeberry was rich in anthocyanin content and showed strong antioxidant activity compared to other berries. It suggested that total anthocyanin content correlates strongly to its antioxidant activity.	43
Aronia melanocarpa fruit extract	Antimutagenic and anticancer	Anthocyanins isolated from *A. melanocarpa* fruits exert a marked antioxidative influence and exhibit strong antimutagenic activity against the standard mutagens' action.	51
Aronia melanocarpa fruit extract	Anticancer	Chokeberry crude extracts exhibit significant anticancer potential.	52
Aronia *melanocarpa* berries	Antidiabetic	Extracts from *A. melanocarpa* can inhibit α-glucosidase *in vitro.*	53

HAECs: Hirschsprung-associated enterocolitis, CAMs: Cytokine-induced adhesion molecules, NF-$_{\kappa}$B: Nuclear factor-$_{\kappa}$B, LPS: lipopolysaccharide, IL: Interleukin, TNFα: Tumour Necrosis Factor-alpha, PGE_2 synthesis: Prostaglandin E2, DPPH: 2,2-diphenyl-1-picrylhydrazyl, ABTS: 2,2'-azino-bis(3-ethylbenzothiazoline-6-sulfonic acid), FRAP: Ferric reducing antioxidant power.

1.1.7. Utilisation of Anthocyanins as Natural Colorants

The annual demand for natural colorants is about 10,000 tonnes worldwide, and it is equivalent to 1% of the global synthetic colorant consumption.[54] Because of the growing awareness of sustainable or environmentally friendly colorants, the demand for natural colorants is increasing rapidly.[55] The bright colours displayed by anthocyanins suggest potential applications as natural colorants in the textile, food, and cosmetic industries as alternatives to petroleum-derived colorants. Velmurugan *et al*. reported that natural colorants extracted from purple sweet potato displayed an effective, eco-friendly, and cleaner alternative to commercially available synthetic colorants in the textile dyeing industries (leather, silk, and cotton fabrics). This natural colorant can also be combined with silver nanoparticles to give an additional antibacterial property to fabrics.[55] In food industries, the use of anthocyanins as natural colouring agents are attractive to consumers, not only for their colours but also the health benefits they have. Andean red sweet potato and purple corn are inexpensive crop products which can be utilised as sources of anthocyanins.[56] Acylated anthocyanins from red sweet potato and purple carrot showed higher stability than non-acylated anthocyanins from purple corn.[56] The application of anthocyanins is limited by low solubility and stability in lipophilic solution as anthocyanins are water-soluble compounds. Chemical or enzymatic lipophilisation of an anthocyanin skeleton can alleviate this problem. Fernandez-Aulis *et al*. reported that acylated anthocyanins which were enzymatically synthesised from cyanidin-3-glucoside show higher antioxidant activity and thermostability than its precursors.[57] Additionally, acylation on anthocyanins can increase its lipophilicity and also inhibit lipid peroxidation in a lipophilic media.[58]

1.2. *Aronia melanocarpa* (Black Chokeberry) as Natural Sources of Anthocyanins

Aronia melanocarpa or also known as black chokeberry is native to North America and contains high amounts of antioxidant polyphenolic compounds, specifically anthocyanins. The berries have been used by Native Americans for medicinal purposes such as treatment of colds by making tea from the berries.[59] These berries can be visually identified as dark berries and have similarity to blackcurrants in size and colour (**Figure 1.6**).[60] Red chokeberries (*Aronia arbutifolia*) are also present in nature during winter but have lower anthocyanin content compared to black chokeberries. In this study, black chokeberry will be referred to as *Aronia* chokeberry(s). The plants of *Aronia* chokeberry tend to be small (90-180 cm high) and gather in clusters of 8 to 14 fruits on red pedicels[59] which can also be cultivated

on cut-over peatlands for small fruit production and show tolerance towards weeds.[61] *Aronia* chokeberries were firstly introduced to Europe more than 200 years ago.[62] They became popular amongst other berries and has been cultivated especially in Eastern Europe since then.[63] These berries can be harvested in July to August and are commonly utilised in producing wines, jams, syrups, juices, teas or as anthocyanin-based food colorants.[62,64] They can also be consumed raw, but their astringent taste creates a sensation making the mouth pucker which is the origin of the name chokeberry.[62]

Figure 1.6 *Aronia melanocarpa* berries with glossy black colour.[60]

During the production of *Aronia* chokeberry juices, the berries are pressed to release its juice, leaving the skins. The skins are usually left untreated and considered as by-products. The most common use of by-products from *Aronia* chokeberries is as fertilisers and animal feed, or is otherwise discarded. However, its skin wastes remain rich in anthocyanins and other polyphenols. Moreover, the polyphenolics content in the pomace itself is much higher than in the juice and fruits.[4] The high content of anthocyanins in the pomace has been proposed as a plant strategy to protect its seeds from the harmful effects of UV radiation. Such a high content of anthocyanins in *Aronia* chokeberry skin wastes represents a substantial opportunity for use in various applications, and this raw material is one of the most promising sources of anthocyanins from both an environmental (sustainable and renewable) and an economic point of view if it can be shown that useful products can be efficiently obtained.

Anthocyanins are responsible for the black colour of *Aronia* chokeberries and are found to be one of the richest plant sources of anthocyanins present.[43] About 25% of the total polyphenols in *Aronia* chokeberry fruits are anthocyanins, and the anthocyanins in pomace represent about 17% of the total polyphenols.[4] The total concentrations of anthocyanins were 1.9% and 1.8% (w/w DW) in fruit and pomace respectively, making it the second-largest group of phenolic compounds after the polymeric proanthocyanins (5.2% and 8.2% w/w DW) which contribute to 66% and 77% of the total polyphenols in fruits and pomaces respectively.[4] The major anthocyanins found in the *Aronia* chokeberries are a mixture of derivatives of cyanidin with four different monosaccharides (**Figure 1.7**), namely cyanidin-3-*O*-galactoside (Cy3gal), cyanidin-3-*O*-glucoside (Cy3glc), cyanidin-3-*O*-arabinoside (Cy3ara), and cyanidin-3-*O*-xyloside (Cy3xyl).[4,43] The composition of anthocyanins in *Aronia* fruit, pomace and juice is presented in **Table 1.3**.[4]

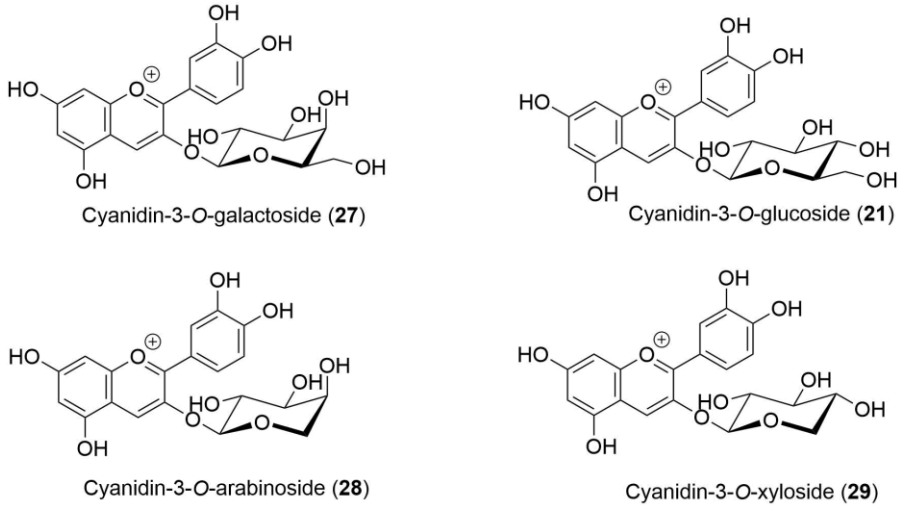

Figure 1.7 The four major anthocyanins found in the berries of *Aronia Melanocarpa.*[4]

Table 1.3 Composition of anthocyanins in *Aronia* fruit, pomace and juice.[4,65–68]

	Fruit	**Pomace**	**Juice**
Cyanidin 3-galactoside	64.5-65.5	60.3-61.0	67.1-69.9
Cyanidin 3-glucoside	2.2-2.4	3.4-4.3	2.4-3.2
Cyanidin 3-arabinoside	28.9-29.7	29.0-31.9	23.5-27.6
Cyanidin 3-xyloside	2.7-4.2	4.3-5.7	2.9-3.4

Similar compositions for *Aronia* chokeberry juices have been described by Jakobek *et al.*, for cyanidin-3-*O*-galactoside (68.9%), cyanidin-3-*O*-arabinoside (24.5%), cyanidin-3-*O*-xyloside (3.8%) and cyanidin-3-*O*-glucoside (2.8%).[43] It is notable that

cyanidin is the only aglycon (anthocyanidin) present in the berries. Cy3gal and Cy3ara are the major anthocyanins.[4,43] Jakobek *et al*. also compared the contents of anthocyanins in four different chokeberry cultivars, namely wild chokeberries, Viking, Nero and Galicianka which are summarised in **Table 1.4**.[43,67] The quantity of polyphenols in some berries may vary due to seasonal differences and geographic origin including the amount of rainfall, number of sunny days, soil nutrients *etc*.[67]

Table 1.4 The contents of anthocyanins in various *Aronia* chokeberries.[67]

Anthocyanins	Content (% w/w FW)			
	Wild	**Viking**	**Nero**	**Galicianka**
Cyanidin-3-O-galactoside	68.0-68.9	66.9-68.9	66.0-67.7	67.6-70.3
Cyanidin-3-*O*-glucoside	2.43-2.44	2.0-2.6	1.8-2.2	2.3-2.5
Cyanidin-3-*O*-arabinoside	25.8-26.0	25.5-27.2	27.2-27.9	24.5-26.5
Cyanidin-3-*O*-xyloside	2.9-3.5	3.3-3.6	3.0-4.2	3.0-3.4

Other phenolic compounds in *Aronia* chokeberries have been reported, including hydroxycinnamic acids (**Figure 1.8**) such as neochlorogenic acid (5-caffeoylquinic acid) and chlorogenic acid (3-caffeoylquinic acid); and flavonols (**Figure 1.9**) such as quercetin-3-*O*-galactoside (Q3gal), quercetin-3-*O*-glucoside (Q3glc) and quercetin-3-*O*-rutinoside (Q3rut).[4,69] Total neochlorogenic (nCA) and chlorogenic acids (CA) in fruits of *Aronia* chokeberries was 0.6% w/w DW and represented 7.5% of *Aronia* fruit's polyphenols. Total quercetin-3-*O*-galactoside, quercetin-3-*O*-glucoside and quercetin-3-*O*-rutinoside were 0.04%, 0.02% and 0.01% w/w DW, respectively and represent 0.9% of total *Aronia* fruit's polyphenols.[4]

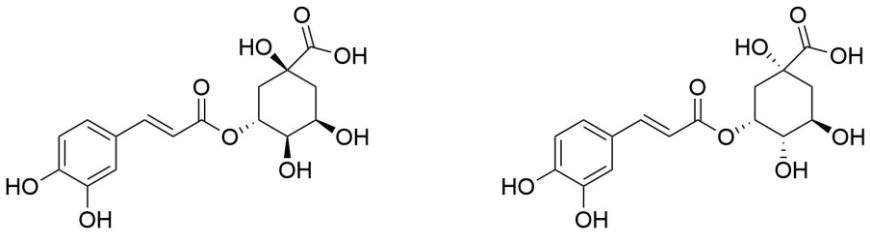

Figure 1.8 Phenolic acids present in *Aronia* berries.[4,69]

The total neochlorogenic and chlorogenic acids in pomaces of *Aronia* chokeberries was 0.4% w/w DW and represented 3.5% of total polyphenols. Total quercetin-3-*O*-galactoside, quercetin-3-*O*-glucoside and quercetin-3-*O*-rutinoside were 0.05%, 0.03% and 0.01% w/w DW, respectively and represent 0.8% of total polyphenols in *Aronia* pomaces.[4]

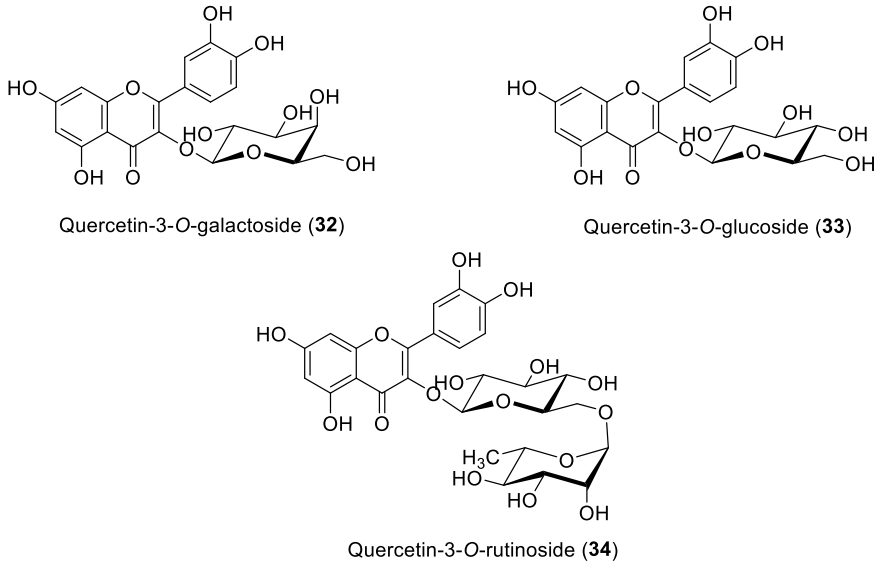

Figure 1.9 Flavonols present in *Aronia* berries.[4,69]

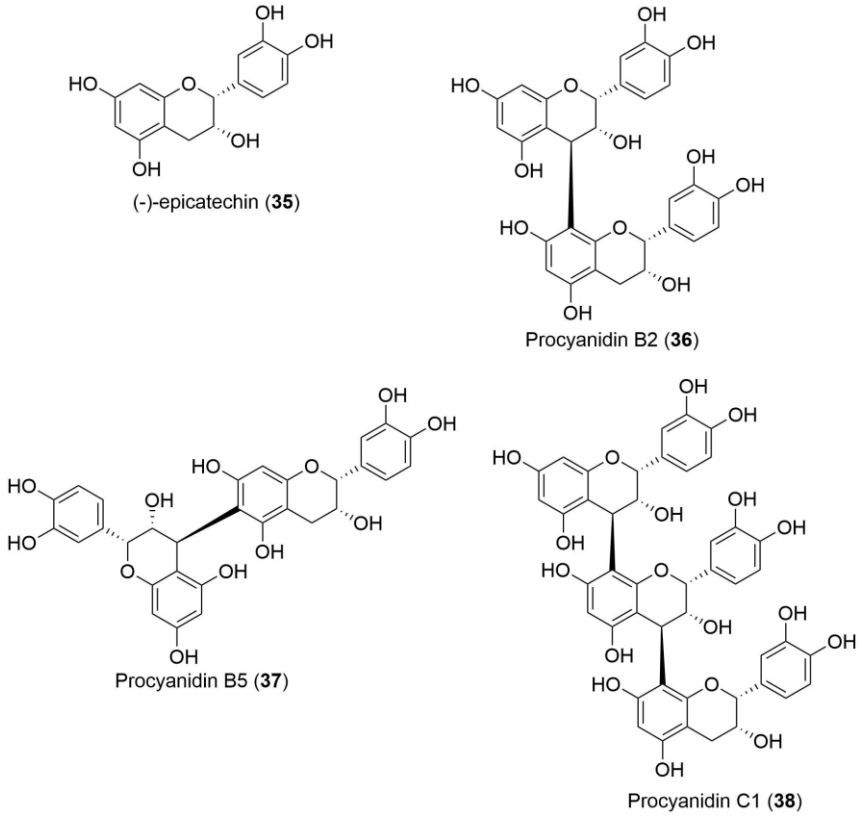

Figure 1.10 (-)-Epicatechin and polymeric procyanidins present in *Aronia* berries.[53]

Polymeric proanthocyanidins are also common and are predominantly composed of (-)-epicatechin (**35**) as the repeating unit (**Figure 1.10**). The degrees of polymerisation of proanthocyanidins were 23 and 34 in fruits and pomaces,

respectively. Although free (-)-epicatechin is also found in *Aronia* chokeberries, its concentration is much lower in comparison with the polymeric species (only 0.2% w/w DW of fruit's polyphenols and 0.1% w/w DW of pomace's polyphenols).[4] Taheri *et al*. reported that proanthocyanidins were dominated by polymers >10 whereas monomer to oligomers ranged from 0.02% to 0.38% w/w DW based on the normal phase HPLC chromatogram.[69]

Due to the high content of polyphenols, especially anthocyanins found in pomaces of *Aronia* chokeberries (skin waste), the valorisation of these materials to produce more sustainable, valuable and environmentally friendly products is worthy of detailed investigation. It can also promote the use of not only the juice of *Aronia* chokeberries but also its pomace as sources of natural colorants and antioxidants.[70]

1.3. Methods for the Extraction of Anthocyanins from Natural Resources (Solid-Liquid Extraction)

Extraction is a well-established method to separate the soluble compounds of interest from non-soluble matrices (residues).[71] It is the key first step in the analysis of natural products because this gives an initial crude extract which can then undergo further separation and isolation to get pure compounds. There are several things that need to be considered during the extraction, such as pre-washing, drying of plant materials and homogenising the samples through grinding to increase the surface area or contact of starting material and the selected solvent. Different solvents are often used for different purposes depending on the chemical properties of expected analytes that will be extracted.[72] Some parameters of extraction solvent such as polarity, stability, toxicity, volatility, viscosity and purity affect the efficiency of the extraction.[71]

The main principle of solid-liquid extraction is that when solid materials mix with a solvent, the soluble components of the solid materials move into the solvents. Consequently, the mass transfer of soluble compounds to the solvent will take place. It is important to keep in mind that the target compound should be exhaustively removed from the solid materials during extraction and as free as possible from interfering or unwanted compounds extracted from the same source. The equilibrium concentration between the original phase that the extract (E) was in (phase A) and the phase which it is being extracted into (phase B) can be calculated using a partition coefficient (**Equation 1.7**).[73] Extraction efficiency is known to be a function of process conditions. The higher K_d value, the more exhaustive extraction of the extract can be achieved.

$$K_d = \frac{[E_B]}{[E_A]}$$ **Equation 1.7**

Anthocyanins are commonly found in many plants, and their extraction can be influenced by many variables (**Table 1.5**) such as their chemical and physical properties, the extraction method employed, sample particle size, extraction time, extraction temperature, liquid-solid ratio, as well as the presence of interfering substances.[7,74] Maceration is a conventional technique to extract natural products, that has been widely used for many years because this is the simplest method of natural product extraction.[71] This technique involves soaking plant materials with a solvent and extracting at a certain temperature for a certain period with continuous agitation. However, this technique of extraction requires a large amount of solvent, long extraction times and can give low extraction yields.[71] Nowadays, alternative methods, which are considered to be more sustainable, have been developed, including the use of ultrasound extraction.[75–77] The methods of anthocyanin extraction summarised in **Table 1.5** are general methods for the extraction of anthocyanins from various sources and not limited to *Aronia* chokeberries only.

Table 1.5 General extraction parameters used for the solid-liquid extraction of anthocyanins from various sources.

Variables		Substrate	Ref.
Temperature (method)	1. 48 °C (ultrasound-assisted extract.)	Mulberry pulp	78
	2. 70 °C (ultrasound-assisted extract.)	Chokeberry by-product	76
	3. 25 °C (maceration, 170 rpm)	Chokeberry dried fruit	79
	4. 80-100 °C (pressurised liquid extraction)	Dried red grape skin	16
Time (method)	1. 0.7 s (ultrasonic irradiation)	Mulberry pulp	78
	2. 20 min (sonication)	Chokeberry pomace	70
	3. 45-90 min (ultrasound-assisted extract.)	Chokeberry by-product	76
	4. 60 min	Chokeberry dried fruit	79
	5. 6 h	Purple-fleshed potato	80
Solvent	1. Acidified methanol or mixture with water	Grape & *Aronia* pomace	70,78
	2. Acidified ethanol or mixture with water	Aronia pomace	76,79
	3. Acidified water	Chokeberry, elderberry, black currant, blackberry and blueberry	81
Solid-solvent ratio	1. 1:20	Chokeberry dried fruit	79
	2. 1.5:12	Mulberry pulp	78
pH adjustment by acidification	1. 1% HCl	Red cabbage	82
	2. 1% citric acid	Chokeberry, elderberry, black currant, blackberry and blueberry	81
		Blueberry	10
	3. 1% TFA	Dried red grape skin	16
	4. 0.1% HCl		
Particle size	0.75 mm	Chokeberry dried fruit	79

Solid-liquid extraction is a classical technique to recover anthocyanins from natural resources. This method is nevertheless not very selective because many other unwanted compounds are also typically co-extracted.[71] To alleviate this problem, solid-phase extraction (SPE) can be employed as a further step, to purify and separate selected analytes from co-extracted compounds.

1.4. Purification of Anthocyanins through Solid-Phase Extraction (SPE)

Solid-phase extraction (SPE) is widely used to clean-up and separate the target analytes from other analytes which may also be extracted during extraction. Their presence can accelerate the degradation of anthocyanins which could cause problems in further application, especially in characterising the extracts or derivatives of extracts. For this reason, a selective adsorbent is typically employed depending on the nature of desired compounds.[71] For anthocyanin purification, Amberlite XAD-7 (**Figure 1.11**) has been found to be the best adsorbent used for SPE in comparison with other adsorbents such as Amberlite XAD-2, Amberlite XAD-4, Amberlite XAD-16, Amberlite IRC-50 and Amberlite CG-50.[83,84] This resin could recover about 95% of anthocyanins in the SPE column with strongly acidic ethanol.[83]

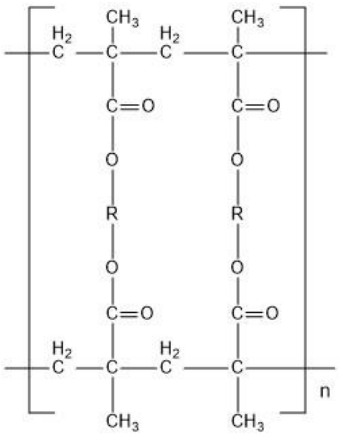

Figure 1.11 Chemical structure of Amberlite XAD-7 resin. R= polyfunctional aliphatic residues.[85]

Amberlite XAD-7 is a non-ionic polyacrylic ester resin that adsorbs and releases ionic species through hydrophobic and polar interactions. The resin has a porous structure with a high surface area (**Table 1.6**). The structure of the polyacrylic ester resin, which is weakly polar, can interact with anthocyanins through H-bonding. In addition, the hydrophobic part of anthocyanins interacts through van der Waals forces. Therefore, anthocyanins are able to bind strongly to this adsorbent, but they can still be separated from more polar components by using various of solvents with

increasing polarity.[5] Thus, it allows separation of anthocyanins from the unwanted polar components such as free sugars, phenolic acids and other phenolics with high recovery of anthocyanins and colour.[81,83]

Table 1.6 Physicochemical properties of Amberlite XAD-7 resin.[85]

Properties	
Particle size (mm)	0.3-1.2
Surface area (m^2 g^{-1})	≥ 380
Porosity (mL g^{-1})	≥ 0.50
Average pore diameter (Å)	90
Polarity	Weakly polar
Maximum adsorption capacity (q_m) (mg g^{-1} adsorbent)	TP: 139.3; TA: 2.5
Langmuir constant (k_L) (L g^{-1} adsorbent)	TP: 0.004; TA: 0.595

TP: total phenolics, TA: total anthocyanins

There are four typical steps in an SPE procedure for the purification of crude extracts extracted from natural sources (**Figure 1.12**).[86,87] These steps include conditioning, loading sample, washing and finally eluting the SPE column. Each step has its own purpose in eliminating impurities and purifying the desired compounds.

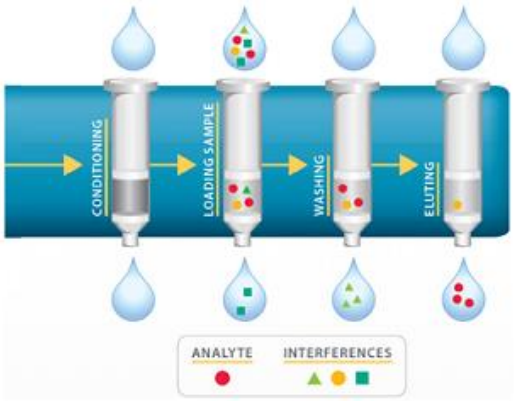

Figure 1.12 Typical four-step in an SPE procedure.[88]

1. Conditioning

The solid sorbent is conditioned using an appropriate solvent. It is followed by rinsing with the same solvent used for the sample. This procedure eliminates impurities present in the adsorbent or packaging and removes the air present in the SPE column. The SPE column is now filled and wetted with the solvent.

2. Loading sample

The sample can be loaded carefully into an SPE column by gravity. In this step, analytes will be retained on the sorbent and possibly some matrix components such as free sugars, phenolic acids *etc*. are also retained. However, some impurities that

have no interaction with the sorbent will pass through the SPE column, especially free sugars.

3. Washing

This step is done to eliminate matrix components that have been retained by the sorbent without removing selected analytes. In this study, acidified water was performed to remove free sugars.

4. Eluting

Different solvents of increasing polarity can be used to separate several components. In the first elution step using a solvent such as ethyl acetate, non-anthocyanin polyphenols are removed from the SPE column and anthocyanins remain on the sorbent.[71] For the final elution, the desired anthocyanins will be desorbed using acidified ethanol.

Generally, acidification of the water washing step and also the ethanolic eluent leads to a better anthocyanin recovery as a flavylium cationic form dominates at this pH. The absence of acidification on the SPE washing and eluting caused the colour changes on the SPE column from red to violet, which was caused by the formation of quinoidal form. Consequently, the anthocyanin recovery is incomplete, with slightly acidic to neutral solvents.[83] Kraemer-Schafhalter *et al*. reported that Amberlite XAD-7 resin could be applied in up to a 36-litre-scale column with no changes on the elution profile but higher pigment concentrations.[83]

1.5. Aims of this project

The present work aims to propose a new method for the isolation, characterisation, and utilisation of anthocyanins from *Aronia* skin waste as natural colorants and antioxidants. In order to achieve the aims, five research objectives are developed:

1. To develop a new method which is an integrated extraction-adsorption method for selective recovery of anthocyanins from *Aronia* skin wastes. Extraction parameters for both methods such as extraction temperature, time, pH, the ratio of biomass: solvent, the ratio of biomass: SPE resin for batch method; and cooling process during loading sample and flow rate of loading sample for an integrated method are optimised to get the higher extraction yield and anthocyanin content. The results from this new method are then compared to the results from the conventional batch method.
2. To characterise and quantify polyphenols present in refined *Aronia* skin waste extracts (RASEs). The characterisation of anthocyanins and other polyphenols

present in RASE is done after further purification to eliminate the complexity of the mixture. Further purifications such as a semi-preparative HPLC, liquid-liquid extraction (LLE) and Biotage purification are developed to obtain purer samples.

3. To prepare anthocyanin salts with anionic counterions derived from organic acids. Anthocyanin salts are prepared with the use of various organic acids in the extraction-purification process. The chemical characterisation of RASEs is performed. The physical and chemical properties of these RASEs are also investigated.
4. To develop methods to prepare hemiketal forms of anthocyanins either as a mixture with a flavylium cationic form, or as a pure hemiketal form.
5. To investigate the chemical modification of anthocyanins to improve stability and in order to increase solubility in lipophilic media. The initial work focuses on simple esterification with a variety of acylating agents to make anthocyanins more lipophilic, and to investigate the physical and chemical properties of modified anthocyanins. Alternative methods to improve lipophilicity are also to be developed.

Chapter 2
Development of New Extraction-Adsorption Methods for Anthocyanins from *Aronia* skin waste

This chapter discusses the development of new methods to isolate anthocyanins from *Aronia* skin waste, the identification and evaluation of refined *Aronia* skin waste extract (RASE) by UV-Vis, HPLC-DAD, LC-MS and NMR, and a comparison between a simple batch process, and a new extraction method, which integrates both extraction and separation in a single process. **Section 2.1** describes preliminary studies to optimise the extraction-adsorption parameters for a batch method and the new integrated method. **Section 2.2** describes the identification and evaluation of post-SPE residues referred to as refined *Aronia* skin waste extracts (RASEs). Finally, **Section 2.3** describes the comparison of RASE produced from the batch method and the integrated method. The deglycosylation of anthocyanins during the extraction-purification process was investigated to determine the origin of the formation of aglycone. Various concentration of acid was also used during the extraction-purification process to investigate the deglycosylation of anthocyanins. In general, the procedure for the extraction-adsorption of anthocyanins from *Aronia* skin waste is presented in **Figure 2.1**.

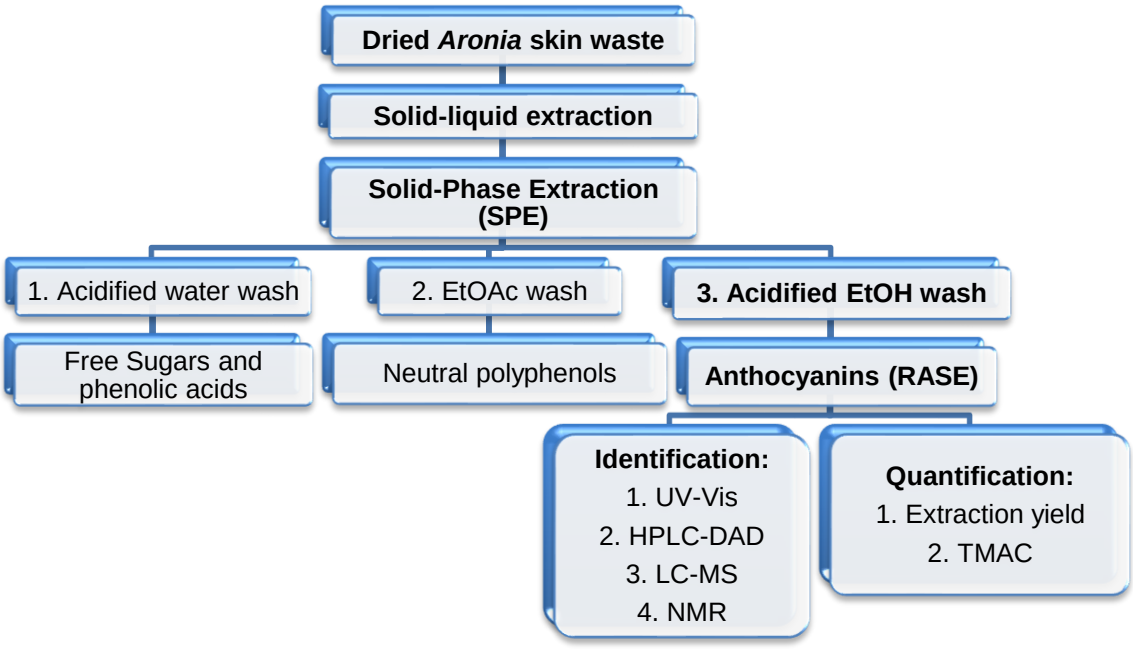

Figure 2.1 General procedure for the extraction-purification of anthocyanins from *Aronia* skin waste.

2.1 Preliminary Studies for Optimisation of Extraction-Adsorption of Anthocyanins from *Aronia* Skin Waste

Anthocyanins are soluble in water and stable to acidic pH, hence acidified water is commonly used as the extraction solvent for such solutes. Additionally, water is also an inexpensive, non-toxic, and environmentally friendly solvent. Dried *Aronia* skin waste was extracted using acidified water (0.1% v/v, HCl) followed by purification using SPE and sequential organic solvent elution. Amberlite XAD-7 resin was used to refine the crude extract, selectively removing impurities such as free sugars and phenolic acids by washing the loaded SPE resin with acidified water.[82,83,85] Ethyl acetate was employed to remove less polar non-anthocyanin phenolics from the SPE column.[89,90]

Acidified ethanol is then employed to recover the anthocyanins remaining on the SPE column.[82,83,85] The resulting ethanol solution was subsequently evaporated to dryness under reduced pressure on a rotary evaporator without neutralisation. The dried ethanolic extract is later referred as refined *Aronia* skin waste extract or RASE. Barnes *et al.* suggested that the alcohol provides strong hydrogen bonding with anthocyanins to enable desorption by considering the TMAC assay of the extracts.[10] However, a 100% desorption of the adsorbed anthocyanins from Amberlite XAD-7 HP resin could not be obtained with any of the acidic ethanol eluents. This remaining polyphenol was visually confirmed through the SPE resin retaining a faint pink colour after elution. Gao *et al.* reported that a residual purple colour on the SPE resin could still be visually observed after attempted desorption.[91] Chandrasekhar *et al.* also reported that even using 100% ethanol, only 91.7% of anthocyanins could be recovered with the addition of 1% HCl v/v. They suggested that using a higher concentration of ethanol is advantageous as removing residual water is more difficult.[82] D'Alessandro *et al.* also reported that Amberlite XAD-7HP resin could only recover anthocyanins up to 92% from the desorption.[85] These results were close to those reported by Denev *et al.* where 91.2% of total anthocyanins was recovered from black chokeberry extracts using Amberlite XAD-7 resin and 96% ethanol (v/v) as eluent.[81]

Our initial work was to understand the influence of the main extraction parameters on the extraction yield and anthocyanin content using the batch method. The best extraction parameters for extraction and adsorption were then performed continuously as part of the integrated extraction-adsorption method. The extraction

yield and Total Monomeric Anthocyanin Content (TMAC) for both methods were then compared to determine the best conditions.

The extraction yield was calculated after purification by SPE and is a measure of how efficient an extraction has been at recovering anthocyanins after SPE. The extraction yield was obtained from the SPE desorption using acidified ethanol and expressed as mg/g DW (dry weight) pomace. The concentration of anthocyanins in RASE was determined by performing a TMAC assay.[92] This is based on the pH-differential method, which exploits the fact that anthocyanins change colour with pH. The absorption of the sample was measured at pH 1 and pH 4.5 using buffer solutions. Monomeric anthocyanins undergo reversible structural transformations with a change in pH, from the coloured oxonium form at pH 1 to the colourless hemiketal form at pH 4.5 (see **Chapter 1**, **Scheme 1.10**). The difference in absorbance at $\lambda_{vis\text{-}max}$ (*ca*. 520 nm) is then proportional to the anthocyanin content. Degraded anthocyanins in the polymeric form are resistant to colour change regardless of pH and therefore are not included in the measurements because they absorb at pH 4.5 as well as pH 1.[92] The results were calculated as cyanidin-3-*O*-glucoside equivalents (Mr = 484.8 g/mol, including Cl^- as a counterion of anthocyanin in a flavylium cationic form) because it is the most common anthocyanin in nature (**Table 2.1**). The extinction coefficient is reported with values ranging from 18,800 to 34,300 L/mol.cm, depending on the solvent, wavelength of maximum absorbance, and purity. For this work, the extinction coefficient value of 26,900 L/mol.cm was used as it was obtained with similar aqueous systems.[92] The anthocyanin content is expressed as % w/w dry weight (DW) RASE. The overall yield of anthocyanins (mg/g DW pomace) was calculated by multiplying extraction yield (mg g^{-1} DW pomace) times TMAC (% w/w DW extract). The efficiency of the extraction-adsorption process in recovering anthocyanins from *Aronia* skin waste could then be understood from the anthocyanin yield.

2.1.1. Batch Extraction Approach.

Initially, extraction and adsorption of anthocyanins from *Aronia* skin waste were carried out sequentially in a batch method with stirrer bar agitation. In order to improve the efficiency, yield and extract quality, various extraction parameters including extraction temperature (25 °C, 40 °C, 60 °C and 70 °C), extraction time (3 h, 6 h, 24 h and 48 h), pH (acidified water with 0.1% v/v, HCl; and the absence of acid during solid-liquid extraction), the ratio of biomass-solvent (1:8 and 1:16) and

the ratio of biomass-SPE resin (1:1 and 1:2) were studied. The entries of these extraction parameters with their extraction yield and TMAC were summarised in **Table 2.1**. Each extraction parameter for the batch method is discussed in **Sections 2.1.1.1** to **Section 2.1.1.5**. To monitor the extraction, the UV-Vis absorbance of diluted samples of the extraction liquor was measured periodically at 520 nm as this is the maximum absorbance of the anthocyanins. This represents an approximate measurement for extraction monitoring.[93] It should be noted here that at this wavelength, both glycosylated derivatives of cyanidin and cyanidin itself and some other polyphenolics may also contribute to absorption.

Table 2.1 Extraction yield of anthocyanins (mg g^{-1} DW) under various conditions for solid-liquid extraction of *Aronia* skin waste (pomace) using a batch method. TMAC is given as % w/w DW of RASE.

Entry	T, °C	Time, h	pH	Extraction yield, mg g^{-1} DW pomace	TMAC, % w/w DW RASE	Anthocyanin yield, mg g^{-1} DW pomace
1	25	24	2.4	3.4	21.8	0.7
2	40	24	2.4	4.3	24.1	1.0
3	60	24	2.4	10.0	10.2	1.0
4	70	24	2.4	4.5	0.8	0.04
5	60	3	2.4	5.3	19.9	1.0
6	60	6	2.4	7.0	17.8	1.2
7	60	48	2.4	3.8	10.3	0.4
8	60	24	5.2[a]	6.8	12.8	0.9
9	60	6	2.4	4.3[b]	15.5	0.7
10	60	6	2.4	7.8[c]	18.7	1.4

[a] Deionised water without the addition of acid during solid-liquid extraction. [b] 1:8 ratio of biomass-to-solvent. [c] 1:2 ratio of biomass-to-resin

2.1.1.1. The effect of extraction temperature on the extraction yield and anthocyanin content

Extraction temperature is one of the most important parameters for extraction of anthocyanins. Despite the positive effect given by an increase of temperature on the extraction of phenolic compounds, the optimum temperature should be determined as anthocyanins are labile compounds which can degrade at high temperature.[94] This optimisation is intended to minimise energy cost and energy consumption during the process and to maximise extraction yield and anthocyanin content in RASE.

Anthocyanins and other phenolic compounds were extracted from dried *Aronia* skin waste in a batch extraction at varying temperatures (25, 40, 60 and 70 °C) using acidified water as an extraction solvent (pH 2.4), a biomass-to-solvent ratio of 1:16 (w/v), a biomass-to-SPE resin ratio of 1:1 (w/w) and the extractions were conducted for 24 h (**Table 2.1**, entries 1-4). The absorbance of anthocyanin and phenolic compounds in the extract was monitored using UV-Vis spectrophotometer at 520 nm **Figure 2.2**).

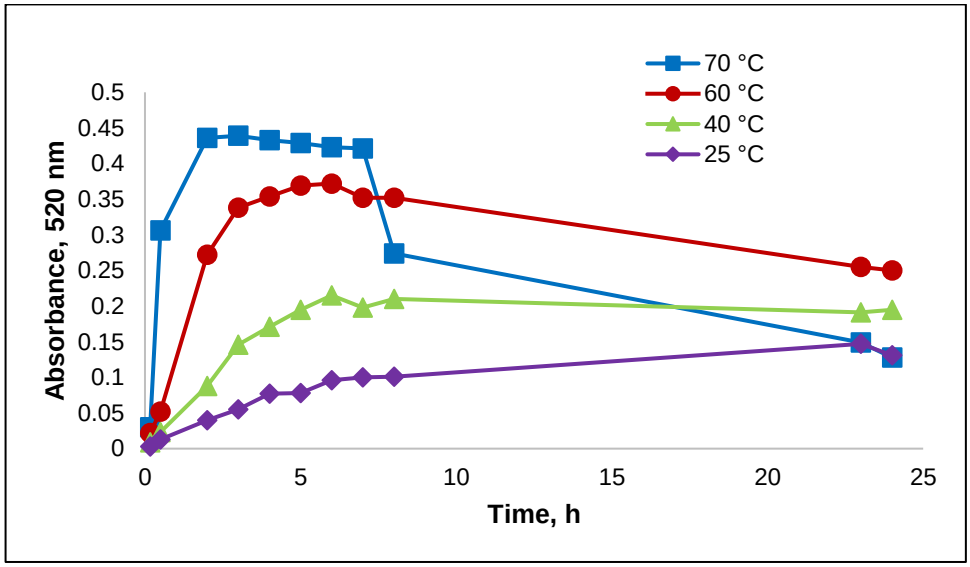

Figure 2.2 Extraction profiles during a batch extraction of *Aronia* skin waste at various temperatures. The absorbance was monitored using UV-Vis spectrophotometer at 520 nm.

Figure 2.2 shows that extraction at 40 and 60 °C reached the highest absorbance within 6 h but then decreased gradually over the following 24 h. The extraction conducted at 25 °C continually increased with time up to 24 h. The highest absorbance was observed when the extraction was run at 70 °C for 3 h, but it decreased markedly after 6 h and which continued over the following 24 h. This suggests that the deglycosylation of anthocyanins was accelerated at this temperature during extraction using an acidified aqueous solvent. Ekici *et al*. reported that anthocyanins degraded more rapidly at the higher temperature.[94] In buffer systems at pH 3, grape skin, black carrot, and red cabbage anthocyanins after treatment at 70 °C for 2 h degraded by up to 12, 9, and 3 % respectively.[94] Acylated anthocyanins in those plant materials clearly could increase the stability of anthocyanins at such conditions compared to anthocyanins extracted from *Aronia* skin waste which were found as non-acylated anthocyanis.[94,95] The thermal instability of anthocyanins at temperature of 70 °C during the extraction of *Aronia melanocarpa*

wastes for 4 h was also reported by D'Alessandro *et al*. with a decrease in the extraction yield and anthocyanin content.[96] For our work, the highest absorbance of polyphenols after extraction for 24 h was observed in a batch extraction conducted at 60 °C. This finding suggested that at this temperature, the extraction efficiency and anthocyanin deglycosylation are reasonably balanced.

It should be noted that the extract obtained may contain non-anthocyanin polyphenols which might not absorb at 520 nm, however most of these would be expected to be removed by the initial ethyl acetate wash of the SPE prior to using acidified ethanol. The extraction yield of RASE after 24h, post-SPE processing ranged from 3.4 to 10.0 mg g^{-1} DW of *Aronia* skin waste (pomace), and decreased in the following order: 60 °C >> 70 °C > 40 °C > 25 °C.

In general, an increase in extraction temperature gave a positive impact on the extraction yield. The higher the temperature, the higher the yield of ethanol wash fraction (RASE). D'Alessandro *et al*. reported a similar result where the extraction conducted at 60 °C gave three times the yield obtained at 20 °C.[75] This was reported to be because an increase in temperature will lead to a higher solubility and diffusion coefficients of polyphenols. A rise in extraction temperature can break the phenolic-matrix bonds and influence the membrane structure of plant cells, making them less selective by coagulation of lipoproteins. Furthermore, the dielectric constant of water decreases and solvent property and capacity change at the higher temperature.[97] However, the yield of extracted polyphenols at 70 °C was less than half of the comparative yield at 60 °C, suggesting that a further increase in extraction temperature may degrade phenolic compounds. Thus, an extraction temperature of 60 °C was chosen for further studies based on the combined effects of the high extraction yield of phenolic compounds and its stability during extraction as shown in **Table 2.1,** entries 1-4.

Higher extraction yield does not necessarily relate to the higher production of anthocyanins, and it was also necessary to consider the total monomeric anthocyanin content of RASE. Interestingly, extraction conducted at 60 °C showed the highest yield but contained lower levels of anthocyanins (10.2% w/w DW of RASE) compared to the extractions conducted at 40 and 25 °C (24.1 and 21.8% w/w DW of RASE, respectively). **Table 2.1**, entries 1-4 shows that an extraction temperature of 40 and 60 °C gives the highest yield of anthocyanins. However, according to the extraction

profiles presented in **Figure 2.2**, the absorption of anthocyanins in solution at 60 °C were much higher than at 40 °C, and the extraction time clearly affected the anthocyanin yield. The effect of extraction time at 60 °C is studied further in **Section 2.1.1.2.**

2.1.1.2. The effect of extraction time on the extraction yield and anthocyanin content

Both the duration and the temperature are particularly important parameters that need to be optimised in order to increase the efficiency of an extraction. The longer the extraction time, the higher the energy consumption during the extraction. Ćujić *et al*. reported that at longer extraction periods, the highest total phenolics (TP) and total anthocyanins (TA) were observed.[79] However, longer extraction periods, especially in the acidic solution (pH < 2.5) and high temperature (60 °C) may also give adverse effects. To investigate further, batch extractions at 60 °C were carried out using acidified water (pH 2.4), a biomass to solvent ratio of 1:16 (w/v), a biomass to SPE resin ratio of 1:1 (w/w) and the extraction was conducted for various extraction times (3, 6, 24 and 48 h) (see **Table 2.1**, entries 3, 5-7).

Generally, the longer the extraction time, the higher the extraction yields, with a range of 3.8-10.0 (mg/g DW of pomace). The highest extraction yield was found when the extraction was run for 24 h and decreased significantly when the extraction was run for 48 h (approximately 60% reduction of extraction yield), suggesting that longer extraction periods contribute significantly to the deglycosylation of anthocyanins especially when the extraction performed at high temperatures and in acidic aqueous solution. D'Alessandro *et al*. also reported that anthocyanin yield decreased with time, especially the extraction of anthocyanins conducted at high temperatures.[96] Approximately 50% of anthocyanins and other polyphenols were extracted from *Aronia* skin waste during the first 3 h while another 20% were extracted during the second 3 h (6 h of extraction time).

Even though extraction conducted for 3 h has the lower yield compared to 6 h and 24 h of extraction time, it gives the highest anthocyanin content, suggesting that shorter extraction times can quickly extract anthocyanins before it reaches saturation (see **Figure 2.2**). It can be concluded that 3 h extraction time is most effective and most convenient as a compromise, so has been chosen for further extraction studies.

2.1.1.3. The effect of pH on the extraction yield and anthocyanin content

Controlling the pH of the extraction solvent is also an important factor in providing a suitable environment for anthocyanin extraction. In order to understand the effect of pH on the extraction yield and anthocyanin content, two different conditions of extraction solvent were performed (**Table 2.1**, entries 3 and 8). One batch extraction used acidified water as an extraction solvent by adding 0.1% v/v, HCl (pH 2.4) whereas another batch extraction used only water with the absence of acid (pH 5.2). The extractions were conducted for 24 h, and the *Aronia* skin waste extract was periodically monitored by UV-Vis spectrophotometer at 520 nm, and the extraction profiles are presented in **Figure 2.3**. They show that acidified water (pH 2.4) gave much higher yields compared to when carried out in the absence of acid (pH 5.2), confirming that the extraction with the pH adjustment by acidification can increase the extraction yield. However, hydrochloric acid as a strong acid may also lead to deglycosylation of anthocyanin via hydrolysis. This is suggested by a decrease in absorbance over 24 h of extraction. Interestingly, even though lower overall, the absorbances of extraction at pH 5.2 increased progressively with time until it reached 24 h.

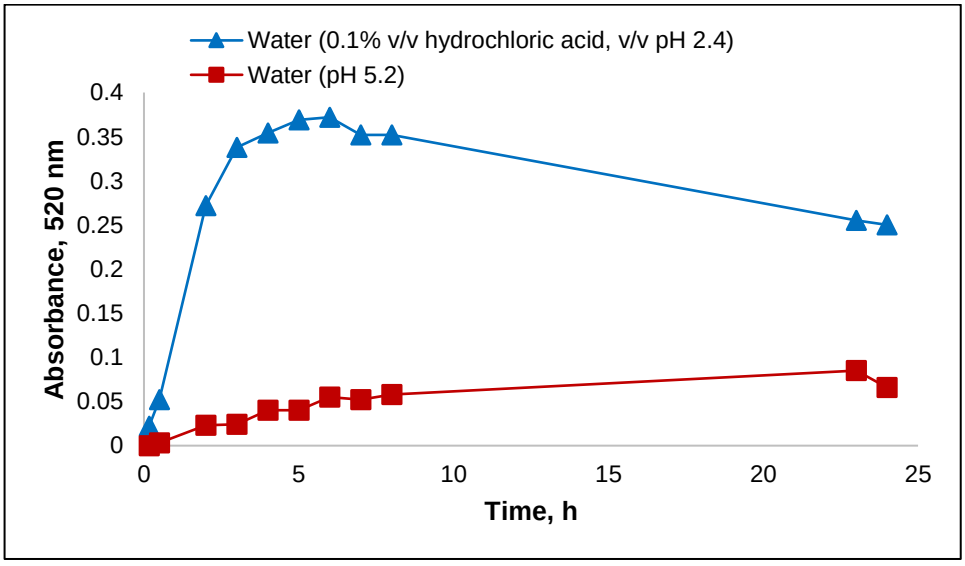

Figure 2.3 Extraction profiles during a batch extraction of *Aronia* skin waste at different pH (2.4 and 5.2). The absorbance was monitored using UV-Vis spectrophotometer at 520 nm.

The RASE extraction yields were 6.81 and 10.04 mg/g DW at pH of 5.2 and 2.4, respectively, suggesting that anthocyanins are more stable and solubilised in acidic pH solution (see anthocyanin equilibrium in **Section 1.1.5**) which can increase the extraction yield. This is in agreement with the work of Ju *et al*. that also showed a high yield.[16] **Table 2.1,** entries 3 and 8 shows that the yield of anthocyanins in RASE

produced by extraction with acidified water (pH 2.4) for 24 h at 60 °C was lower than the extraction conducted by using only water (approximately 20% lower). It suggests that the use of acid is good in terms of extraction yield, but the application is, however, limited by the extraction time (see **Section 2.1.1.2**). Acidified water with an addition of 0.1% of HCl (v/v) will be used as an extraction solvent for the further extractions but with a shorter time of extraction.

2.1.1.4. The effect of the biomass-to-solvent ratio on the extraction yield and anthocyanin content

The solubility of the solute in the extraction solvent potentially limits the extraction yield of anthocyanins. Changing the biomass-to-solvent ratio can lead to saturation of anthocyanins in the solvent, and this may occur when adding too much biomass. The effect of biomass-to-solvent ratio on the extraction yield and anthocyanin content from *Aronia* skin waste was studied at 60 °C with acidified water (pH 2.4) as a solvent as these parameters previously gave the highest yield of anthocyanins. The batch extraction was performed for 6 h with various biomass-solvent ratios and periodically monitored using UV-Vis spectrophotometer at 520 nm (**Figure 2.4**).

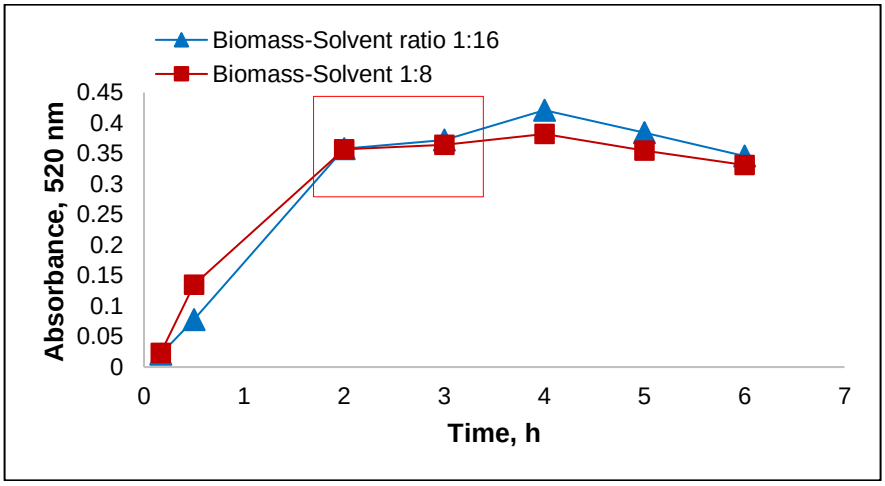

Figure 2.4 Extraction profiles during a batch extraction of *Aronia* skin waste using different biomass-solvent ratios. The absorbance was monitored using UV-Vis spectrophotometer at 520 nm. The red box shows a saturation of *Aronia*'s extract.

Figure 2.4 shows that the pattern of extraction profiles is similar at the two biomass-to-solvent ratios used. Similar absorbance shown by both parameters suggests that both parameters have a similar concentration of anthocyanins extracted in solution. However, absorbances of *Aronia* skin waste extracts in an extraction using the biomass-to-solvent ratio of 1:16 were slightly higher when the extraction was run over 3 h, suggesting the saturation started at this point. A larger volume of extraction liquor (twice the volume of extraction solvent) gives higher yield. TMAC of the biomass-to-

solvent ratio of 1:16 (17.8 % w/w DW of RASE) was slightly higher than the biomass-to-solvent ratio of 1:8 (15.5 % w/w DW of RASE). RASEs were 4.3 and 7.0 mg/g DW of pomace for the biomass-to-solvent ratio of 1:8 and 1:16, respectively (see **Table 2.1**, entries 6 and 9). This finding suggests that the use of more solvent volume can increase the interaction between biomass and solvent. Therefore, saturation during the extraction using lower solvent volume can be overcome, resulting in higher extraction yield.

The cost of extraction and the consumption of biomass can be reduced by using higher biomass-to-solvent ratio (1:16).[79] A higher biomass-to-solvent ratio allows greater dissolution of phenolic compounds by the solvent and reduces solubility limitations. Therefore, for the efficiency, the studies of the extraction of anthocyanins from *Aronia* skin waste at different parameters were carried out using this ratio (1:16). This ratio is in agreement with the ratio performed by Liu *et al*., which yielded the highest anthocyanin yield.[98] Additionally, Galvan d'Alessandro *et al*. reported that increasing the solid-to-solvent ratio from 1:20 to 1:40 did not significantly change the extraction yields, from 57.5% to 56.9% respectively.[75] Although the biomass to liquid ratio is useful for increasing the extraction yield, a further increase in the biomass-to-solvent ratio did not improve the extraction yield greatly.[75]

2.1.1.5. The effect of biomass to SPE resin ratio on the extraction yield and anthocyanin content

The effect of biomass-to-SPE resin ratio on the extraction yield and anthocyanin content from *Aronia* skin waste was studied at 60 °C by conducting extractions using acidified water as an extraction solvent. A constant biomass-to-solvent ratio of 1:16 was used in this study based on earlier optimisation results. There were two biomass-SPE resin ratios used in this study, 1:1 and 1:2. Amberlite XAD-7 resin was used as it has been used extensively within the group, and has been reported to give the highest extraction efficiency of phenolic compounds[99] amongst other resins such as Amberlite XAD-2, Amberlite XAD-4, Amberlite XAD-16, Amberlite IRC-50 and Amberlite CG-50 (see **Section 1.5**).

The purpose of increasing the ratio of biomass-SPE resin was to increase the amount of anthocyanins adsorbed in the SPE resin and to understand the saturation that may occur during sample loading. It is expected that the higher the amount of SPE resin, the more active sites there are that can interact with anthocyanins and other phenolics through the hydrogen bonding and Van der Waals forces which then can maximise the extraction yield. However, the adsorption efficiency was investigated to

seek the better ratio of biomass-SPE resin. The extraction liquor from the previously optimised extraction was loaded into an SPE column which had been packed with Amberlite XAD-7 resin at two different biomass-to-SPE resin ratios (1:1 and 1:2). The extraction yields of RASEs were 7.0 and 7.8 mg/g DW of pomace in the biomass-to-SPE resin ratio of 1:1 and 1:2, respectively (see **Table 2.1**, entries 6 and 10). Doubling the amount of resin only gave a 10% increase in yield. In addition to that, anthocyanins content by TMAC was found to be higher in the biomass-SPE resin ratio of 1:2, which was 18.7% (w/w DW of RASE) while the biomass-SPE resin ratio of 1:1 gave 17.8% of anthocyanins (w/w DW of RASE). It suggests that about 95% of anthocyanins were adsorbed in the ratio of 1:1 and further addition of Amberlite XAD-7 resin was not significantly increasing the anthocyanins content. Hence, the ratio of *Aronia* skin waste: Amberlite XAD-7 (1:1) was used in the next experiments with different variables. This ratio (1:1) is in agreement with the ratio performed by Galvan d'Alessandro *et al*. which shows a high value of anthocyanin content for both adsorption and desorption.[85]

2.1.2. An Integrated Extraction-adsorption Method for Anthocyanin production.

An integrated extraction-adsorption method was developed to improve the extraction efficiency, yield, and extract quality through a simple eco-friendly process with minimum consumption of time and energy. Deglycosylation of anthocyanins during batch extraction at relatively high temperature and acidic pH can potentially be minimised through an integrated extraction-adsorption method. This method offers a continuous process of extraction and adsorption which means that as soon as anthocyanins are extracted from *Aronia* skin waste, the solution containing anthocyanins is continuously circulated for adsorption onto the SPE resin, thus, integrating both extraction and adsorption stages and minimising the exposure of anthocyanins to a hot acidic solution. This method has the potential to be scaled up on an industrial scale. Our group and Galvan d'Alessandro *et al*. had previously investigated this method under a limited range of conditions, and a more detailed study was warranted.[85,100] The batch extraction using optimum extraction parameters as already discussed earlier in **Section 2.1.1** to **Section 2.1.5** were used: extraction temperature of 60 °C, extraction time of 3 h, extraction solvent of acidified water 0.1% v/v, HCl pH 2.4, the biomass-to-solvent ratio of 1:16 and the biomass-to-SPE resin ratio of 1:1. The extraction vessel was connected to an SPE column with a peristaltic pump employed to enable a continuous cycling process in a closed-loop (**Figure 2.5**). In this configuration, the extraction and adsorption take place at the same time. This method was optimised and then compared to the batch method.

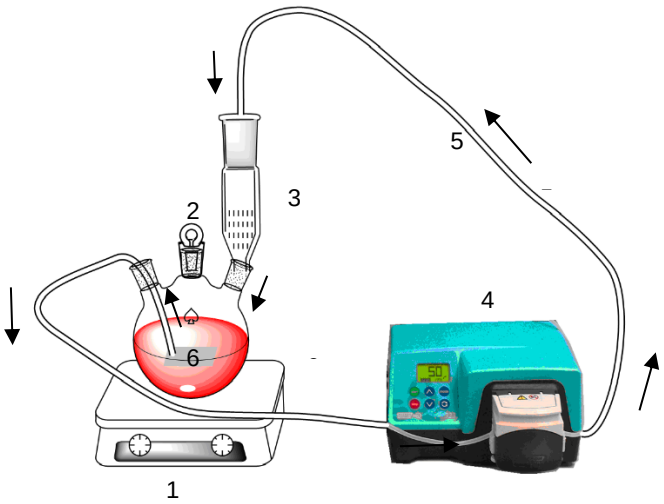

1. Hotplate and magnetic stirrer
2. Three neck round bottom flask
3. SPE column
4. Peristlatic pump
5. Tube
6. Polyester bag

Figure 2.5 Illustration of experimental set-up for integrated extraction-adsorption process.

The effect of the cooling process during sample loading and loading flow rate on the extraction yield and anthocyanin content were investigated. The absorbance of the liquors in the extraction vessel was monitored at 520 nm throughout the extraction process. It was observed that absorbance of the extraction liquor decreased until equilibrium was attained, where no further reduction in absorbance occurred. During the extraction-adsorption process, the colour of extraction liquor exiting the SPE column was not always colourless, with some evidence of colour leaching through in most cases. The entries of these extraction parameters with their extraction yield and TMAC were summarised in **Table 2.2**. Each extraction parameter is discussed in **Section 2.1.2.1** to **Section 2.1.1.2**.

Table 2.2 Extraction yield of anthocyanins under various conditions for solid-liquid extraction of *Aronia* skin waste using an integrated extraction-adsorption method. All extractions were carried out at 60 °C, pH 2.4, biomass-to-solvent ratio 1:16, and biomass-to-SPE resin ratio 1:1. TMAC is given as % DW of RASE.

Entry	Time, h	Cooling prior to resin loading?	Resin loading flow rate, ml s^{-1}	Extraction yield, mg g^{-1} DW Pomace	TMAC, % w/w DW RASE	Anthocyanin yield, mg g^{-1} DW pomace
1	3	Yes	1.0	8.1	20.9	1.7
2	3	No	1.0	9.1	19.7	1.8
3	24	Yes	1.0	10.7	9.1	1.0
4	24	No	1.0	20.0	6.1	1.2
5	3	No	0.6	7.8	16.8	1.3
6	3	No	1.3	14.4	15.7	2.3

2.1.2.1. The effect of an applied cooling process during SPE sample loading on the extraction yield and anthocyanin content

In the original batch process, after the extraction was completed, the extraction liquor was cooled down and then loaded into an SPE column. In the new integrated method, this is not feasible, and it was observed that the SPE adsorption was occurring within the range of 56-58 °C, just slightly lower than the actual extraction temperature. Different temperatures during sample loading onto an SPE column may affect the adsorption capacity of Amberlite XAD-7 resin. Therefore, the effect of an applied cooling process during sample loading onto the SPE resin on the extraction yield and anthocyanin content was studied. An ice bath cooler was added to the system between the extractor and the SPE column in order to maintain the temperature of extraction liquor between 23-24 °C prior to resin loading. The experiments were conducted at two different extraction times (3 h and 24 h) and the results of both different temperatures (with and without cooling) and times were compared. The extraction yields of RASEs were in the range of 8.1-20.0 mg/g DW of Pomace (see **Table 2.2**, entries 1-4).

In general, the extraction yields of RASEs were higher when the integrated extraction-adsorption processes were performed without the addition of the cooling process regardless of the extraction-adsorption time performed (3 h and 24 h). The highest yield was found when the extraction-adsorption was run without cooling for 24 h. It was also observed that during the extraction-adsorption attached with cooling process prior to resin loading, the effluent exiting the SPE column was slowed down. This finding suggested that the cooling process is not necessarily required for the future extraction-adsorption process. A higher adsorption temperature may lead to a higher extraction yield. However, the anthocyanin content of RASEs with an additional cooling process was slightly higher (20.9 and 9.1 % w/w DW RASE for 3 h and 24 h, respectively) than without the cooling process higher (19.7 and 6.1 % w/w DW RASE for 3 h and 24 h, respectively) regardless of the extraction-adsorption time performed. *Qiu et al*. also investigated the effect of temperature on adsorption of phenols, and showed that varying adsorption temperatures at 25, 30, 35, 40 °C gave little effect on the adsorption capacity of an acrylic ester-based resin.[101] Fundamental thermodynamic theory applying Gibbs free energy changes states that sorption energy (-ΔG) is directly proportional to temperature (T) (**Equation 2.1**).[102]

$$-\Delta G = R.T.\ln K \qquad \textbf{Equation 2.1}$$

This equation is always balanced with the solubility of the sorbate in the solvent. We observed that the sorption of anthocyanins onto the SPE resin at 60 °C was higher than at 25 °C, and this can be rationalised by assuming that the binding is so strong that there is less subsequent desorption back into solution in the extraction vessel. This finding is in agreement with Liu *et al*.[103]

2.1.2.2. The effect of sample loading flow rate on the extraction yield and anthocyanin content

As a continuous-flow system is used in the integrated extraction-adsorption method, the influence of solvent flow rate on the extraction yield and anthocyanin content were also investigated. At higher flow rates, the dissolved anthocyanins in the extraction vessel are quickly transferred into the SPE column. As such, it can minimise the effect of deglycosylation because of relatively high temperature and acidic solution. Additionally, a greater extract liquor volume loaded onto an SPE column allows the extracted anthocyanins interact to the SPE resin intensively compared to a lower extract liquor volume with the same SPE column size. In order to investigate its effect on the loading of anthocyanins into the column of Amberlite XAD-7 resin, 3 different loading flow rates were performed by varying from 0.6, 1.0, and 1.3 mL/s. The extraction-adsorption process was performed at 60 °C for 3 h. The extraction yields of RASEs were in the range of 7.8-14.4 mg/g DW (**Table 2.2**, entries 2, 5 and 6).

In general, the higher the flow rate of sample loading, the higher the extraction yield. The extraction yield of RASEs can be concluded in the following order: 1.3 mL/s > 1.0 mL/s > 0.6 mL/s. However, the flow rate was limited up to 1.3 mL/s as loading flows above 1.3 mL/s resulted in overflowing of the SPE column and subsequent overpressure, which stopped the SPE system from working effectively in adsorbing anthocyanins.

2.2. Identification and Evaluation of Refined *Aronia* Skin Waste Extract (RASE)

Anthocyanins are expected to be found in the post-SPE residues of ethanol wash (RASE) whereas non-anthocyanin phenolic compounds are expected to be found in the post-SPE residues of ethyl acetate wash. As already mentioned in the initial study (**Section 2.1**), the identification was done for RASE as this project focuses on anthocyanins by using UV-Vis, HPLC, LC-MS and ^{1}H-NMR. Deglycosylation of anthocyanins was investigated to help understand the origin of deglycosylation, mechanism of deglycosylation and the products of deglycosylation.

2.2.1. UV-Vis Studies

Anthocyanins are generally considered to be highly coloured compounds. The actual absorption wavelength is very dependent on pH due to the reversible equilibrium structures of anthocyanins. UV-Vis studies were performed to understand the colour profile of anthocyanins extracted from *Aronia* skin waste. The UV-Vis absorption spectra of anthocyanins from RASE (1 mg/mL) at various pHs ranging from 1 to 12 were recorded between 200 and 800 nm with an Agilent double beam scanning UV-Vis spectrophotometer.

2.2.1.1. The Absorbance of RASE at Various pHs

Extract stock solution was prepared by dissolving RASE (1 mg) in acidified water (0.1% v/v HCl, 1 mL). This forms the anthocyanin as a relatively stable flavylium cation. The extracted stock solution was then transferred into a variety of buffer solutions, and the colour changes were observed (**Figure 2.6**). The structural transformations of anthocyanins (see **Chapter 1**, **Section 1.1.5, Scheme 1.10**) are characterised by a shift in shade from red to purple to blue as the pH changes from acidic to basic. In strongly acidic aqueous media (at pH 3 and below), the red-coloured flavylium cationic form (**AH**$^+$) is predominant as expected with $\lambda_{max\text{-}vis}$ of 513-519 nm which is in agreement with Jakobek *et al.* for typical wavelengths of anthocyanins found in *Aronia* chokeberries.[67] Pedro *et al*. reported a slightly different maximum absorption which was 524 nm, most likely due to 50% ethanol which was also added into the aqueous solvent in this case.[104]

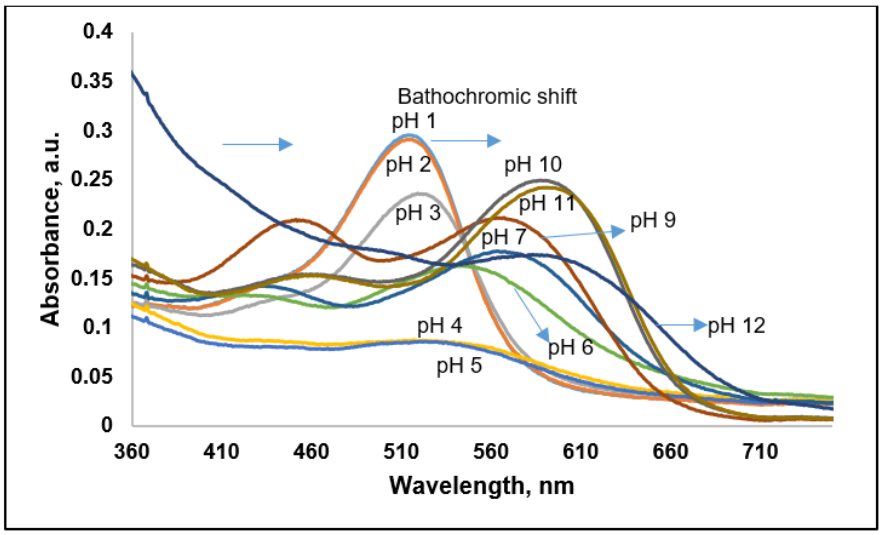

Figure 2.6 Effect of pH on UV-Vis absorbance of anthocyanins extracted from *Aronia* skin waste. The measurement was carried out on RASE. The resultant colours of aqueous solutions tested are shown at the top.

A wavelength of 520 nm is often used to identify anthocyanins, although in this case the maximum wavelength was at 514 nm (pH 1), which was ca. 1% higher intensity

than at 520nm. Increasing pH leads to kinetic and thermodynamic competition between two reactions (**Scheme 1.10**). Deprotonation occurs above pH 3 to form a kinetic product, a purple quinonoid base (**A**) with $\lambda_{max\text{-}vis}$ of 564 nm. Above pH 7, further deprotonation forms the anionic quinonoid base ($\mathbf{A}^-$) with $\lambda_{max\text{-}vis}$ of 590 nm and displays characteristic blue colour. It is noted that the intensities of the colours at pH 4 and pH 5 are lower than at pH 6 and pH 7, and that this is most likely because of more rapid formation of the colourless hemiketal (**B**). A colourless hemiketal form (**B**) is a thermodynamic product which is mainly transformed from a flavylium cationic form ($\mathbf{AH^+}$) through hydration. At pH 12, a yellow chalcone ($\mathbf{C_E}/\mathbf{C_Z}$) is mainly observed with $\lambda_{max\text{-}vis}$ of 450. In general, the maximum visible adsorption of RASE underwent a bathochromic shift on an increase of pH from 1 to 12 ($\mathbf{AH^+}$ 514 nm → **A** 564 nm → $\mathbf{A}^-$ 590 nm). The observed blue-shift of visible $\lambda_{max\text{-}vis}$ of anthocyanins with respect to pH increase, is in agreement with the results reported by Fossen *et al*., however, their analysis was conducted for a single compound, namely cyanidin-3-*O*-glucoside.[35]

2.2.2. HPLC studies

HPLC analysis gives information on the anthocyanin profile and is very useful in compound identification. Anthocyanins are usually detected at 520 nm using HPLC-UV analysis.[43,105] The maximum absorbance of other phenolic compounds can also be detected at different wavelengths as follows: phenolic acids such as neochlorogenic acid and chlorogenic acid (315 nm), proanthocyanins (271-275 nm), and flavonols such as quercetin-3-*O*-rutinoside and quercetin (250 and 340-353 nm).[67] This section discusses the method development of HPLC to identify anthocyanins from RASE, determination of individual anthocyanins and relative percentage of them in RASE, and finally investigation of anthocyanin deglycosylation during the extraction-purification process using HPLC.

2.2.2.1. Development of an HPLC Method to Identify Anthocyanins from RASE

Anthocyanins are sensitive to pH and can exist in different equilibrium forms depending on the pH of its environment, and it is crucial to maintain the pH below 3 (acidic) for the red flavylium cationic form to dominate during HPLC separation. Various acids as eluent additives were employed in order to find the best separation of anthocyanins present in RASE. Those additives, namely 0.1% formic acid (**FA**), 0.1% phosphoric acid (**PA**), 0.1% and 0.5% of trifluoroacetic acid (**TFA**) were added in solvent **A** during HPLC analysis separately. To achieve this, RASE (1 mg) was dissolved in acidified water/ethanol mixture (9:1, 0.1% v/v HCl, 1 mL) and analysed immediately. Samples were loaded on an Eclipse XDB C18 5-µm particle size, 150

x 2.1 mm inner diameter column. Two solvents were used: solvent **A**: water with the acid additive (HPLC grade); and solvent **B**: acetonitrile (HPLC grade). The chromatograms were run for 30 minutes at 520 nm and those for different acids used as additives are presented in **Figure 2.7**. The initial identification of individual anthocyanins present in RASE was based on comparison with data from the literature.[65,106] This identification was later confirmed using other techniques such as LC-MS and NMR, and by comparison with existing literature on anthocyanins from *Aronia* berries.

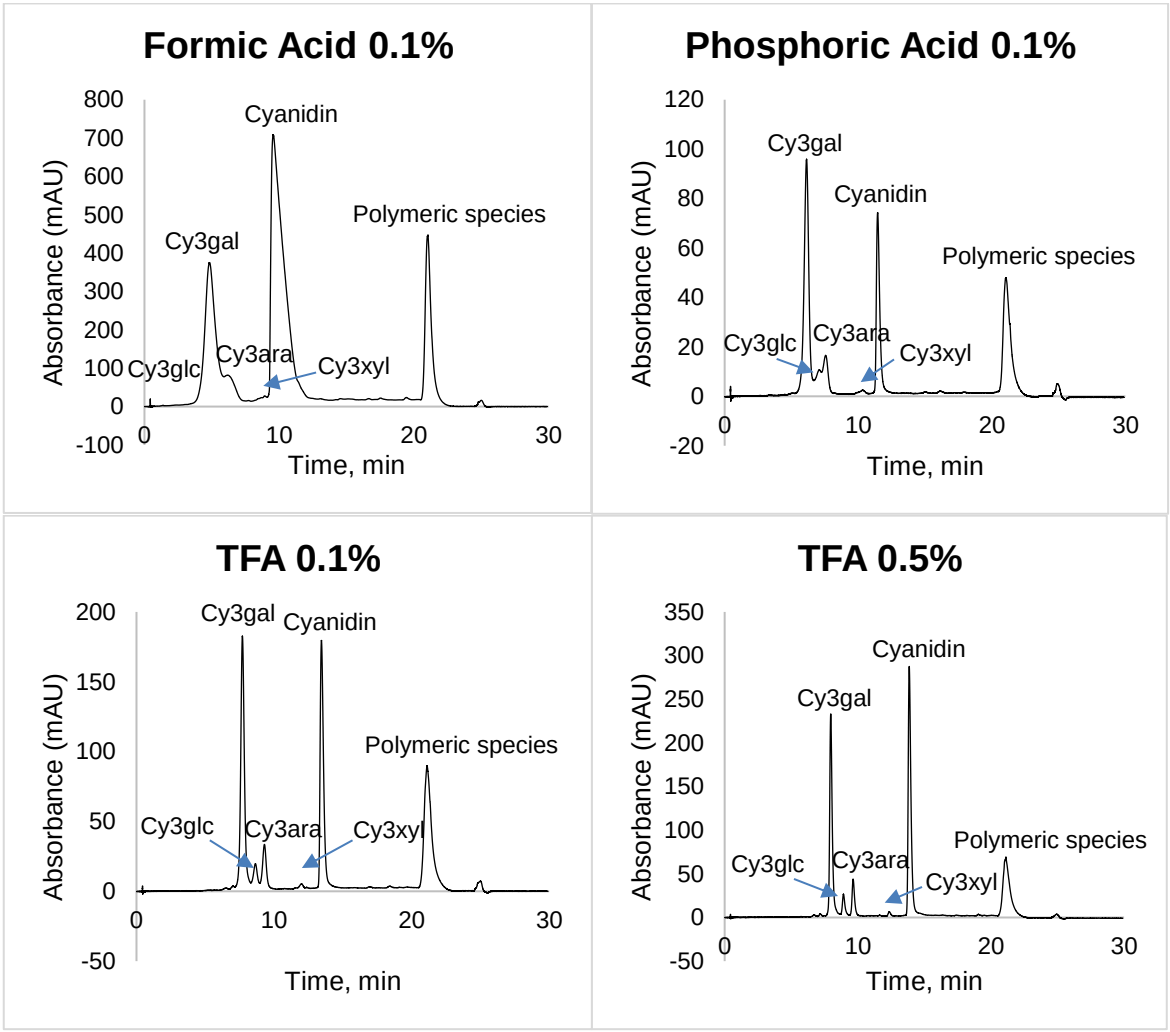

Figure 2.7 HPLC chromatograms of anthocyanins/ anthocyanidins present in RASE. Peaks are labelled as follows: (**25**) Cy3gal, (**21**) Cy3glc (**26**) Cy3ara (**27**) Cy3xyl (**2**) Cyanidin (**28**) Polymeric proanthocyanidins. The HPLC system is the same for all samples besides the additive, which is the acid written in bold on each sub-image. Detected by DAD at 520 nm. This experiment was run at different times. The samples from the same RASE were freshly prepared prior to injection.

The HPLC column used was reverse-phase where separation is based on the polarity of individual anthocyanins and other polyphenols in RASE through hydrogen bonding

and van der Waals forces. Anthocyanins in RASE all share the same aglycone, but with different sugars moiety attached. Galactoside (**27**) and glucoside (**21**) based cyanidin eluted first due to the extra of CH_2OH groups which make them most polar of the anthocyanins; these were then followed by arabinoside (**28**) and xyloside (**29**), which are less polar.

Galactose and glucose are epimers. The difference between galactose and glucose is the position of the hydroxyl group at carbon position 4. The position of a hydroxyl group (-OH) in the 4^{th} carbon is equatorial in the chair conformation of glucose while it is axial in the chair conformation of galactose. Additionally, arabinose and xylose are also epimers. The position of a hydroxyl group in the 4^{th} carbon is equatorial in the chair conformation of xylose whereas it is axial in the chair conformation of arabinose. The axial hydroxyl group at carbon position 4 has more affinity towards polar solvents resulting in an elution earlier than the equatorial hydroxyl group.

Edelman *et al.* reported that the hydration number of galactose (8.7) was higher than glucose (8.4) in liquid aqueous solution at 25 °C. They also reported that the hydrogen bonds between the hydroxyl group of sugars and water are stronger (shorter) than water-water hydrogen bonds.[107] Hydrogen bonds between equatorial-equatorial hydroxyl groups involve two hydrogens bonds (intramolecular and water) which might decrease the polarity of glucose and xylose.

In acidic aqueous solution, anthocyanins are mostly existing as flavylium cationic forms, however, the use of acidified water can also deglycosylate anthocyanins forming cyanidin (aglycone), which appeared as a new peak with shorter retention time than polymeric anthocyanidins. With 0.1% formic acid in the eluent, the anthocyanin separation was not successful and relatively broad peaks were observed. The pK_a of formic acid (3.75) is the highest amongst the acids used in this study which means it is the weakest acid used in this study whereas the pK_a of phosphoric acid is 2.12 and that of TFA is -0.23, The stronger acid is required to obtain a flavylium cationic from which leads to better anthocyanin separation. Phosphoric acid 0.1% showed better separation compared to chromatograms shown in the HPLC chromatogram of formic acid. The presence of cyanidin was found in the peak with the retention time of 11-12 minutes, however, the separation of Cy3glc and Cy3ara was still not completely successful.

Finally, the use of TFA as an eluent additive during an HPLC analysis showed the best separation for anthocyanins. This suggests that as trifluoracetic acid is a stronger acid than formic acid and phosphoric acid, the flavylium cationic form of the anthocyanin was maintained during the runs, giving superior resolution. Two different concentrations were used in this study; 0.1% and 0.5% TFA. Both methods showed a good separation for anthocyanins obtained from RASE. However, 0.5% of TFA showed a better separation for Cy3ara. Also, the retention times became longer and the resulting peaks started appearing at 10 minutes, with cyanidin aglycone at 17-18 minutes, although polymeric anthocyanidins showed little change. This suggests that the interaction of anthocyanins with a stationary phase was stronger than when the milder acids were applied. Therefore, for subsequent HPLC analysis, solvent **A** in the HPLC system will be using water with an addition of 0.5% TFA. The concentration of acid is limited to a maximum 0.5% as higher concentrations may lead to decomposition of the anthocyanins during HPLC separation and also could potentially damage the HPLC column itself. The optimum HPLC separation method was then applied to identify individual anthocyanins from RASE. The relative intensity of the peaks may vary depending on the quantity of acid in the extract, which could change the proportion of anthocyanins via deglycosylation. The deglycosylation of anthocyanins is further discussed in **Section 2.2.2.2**.

2.2.2.2. HPLC studies to Investigate the Deglycosylation of Anthocyanins during the Extraction-Purification Process

Anthocyanins extracted from *Aronia* skin waste may degrade during extraction-purification or concentration. This study was carried out to investigate the origin of anthocyanin deglycosylation. Deglycosylation can potentially be identified by the increasing intensity of aglycone (cyanidin) peak as the main product of deglycosylation while anthocyanin peaks decreased. Chandra *et al*. reported the presence of cyanidin in the *Aronia*'s extract where they carried out the extraction in 2% HCl/ MeOH solution by sonication for 15 min with occasional shaking.[105] The origin of cyanidin was further investigated whether it is derived from extraction-purification or concentration via deglycosylation as it is unusual to find free aglycones in nature. An aliquot of each extraction-purification step including concentration of SPE ethanol eluate to dryness (RASE) were collected and analysed immediately by HPLC-DAD (520 nm). Those steps include collecting crude extract from solid-liquid extraction, solution exiting the SPE column during sample loading, acidified water eluate, acidified ethanol eluate and concentration of acidified ethanol by rotary evaporator. The HPLC chromatograms show the anthocyanin profiles at each step in the process (**Figure 2.8**).

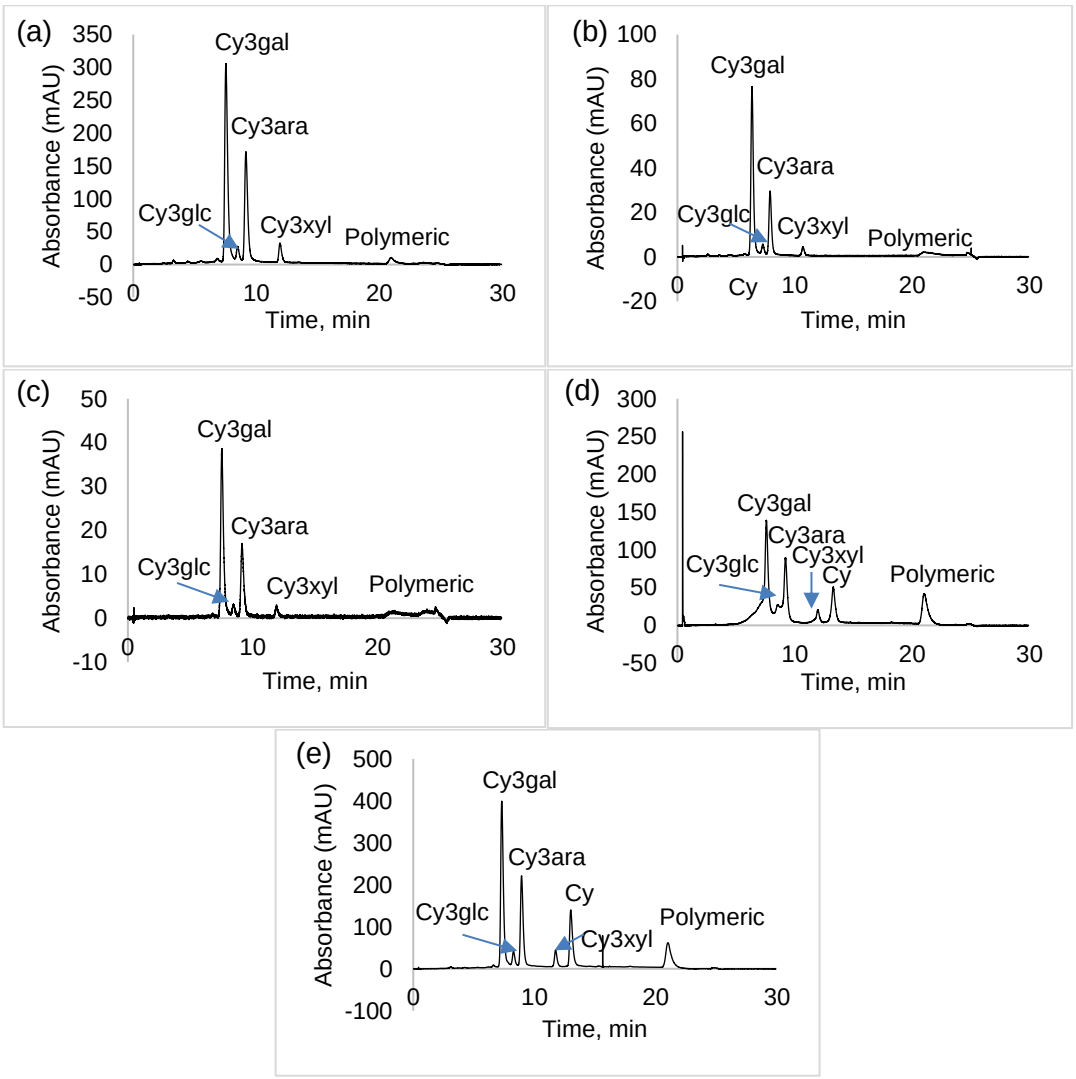

Figure 2.8 HPLC chromatograms of anthocyanins/ anthocyanidins in each process (a) crude extract from solid-liquid extraction (b) solution exiting SPE column during sample loading (c) acidified water eluate (d) acidified ethanol eluate (e) dried RASE. Detected by DAD at 520 nm.

The anthocyanin profile in the crude extract and acidified water wash were similar, suggesting that there were no significant changes that occurred during these processes. The first substantial appearance of the aglycone was observed in the acidified ethanol eluate. This suggests that the origin of aglycone is not from nature, but it is a product of deglycosylation of anthocyanins instead.[11] It was observed that after the SPE elution with ethyl acetate, the SPE resin turned purplish red, suggesting the transformation of anthocyanins to quinonoid base forms. At this form, anthocyanins are more susceptible to hydrolysis as it does not involve dication. The deglycosylation of anthocyanins is further discussed later.

The presence of strong acid (HCl, pKa -6.3) in the SPE column during desorption of anthocyanins is necessary to convert anthocyanins into positively charged flavylium cationic forms. Anthocyanins in this form have a weaker affinity toward Amberlite XAD-7HP resin than at higher pH thus it can be recovered from the SPE resin through an SPE elution with acidified solvent.[108] It was observed that the colour of the SPE resin turned red. However, for a longer time, an excess of acid can hydrolyse anthocyanins. The intensity of polymeric species also increases in this stage. It suggests that the formation of cyanidin aglycone correlated to the increasing intensity of polymeric species while the intensity of original anthocyanins decreased. Monagas *et al*. reported direct condensation reactions of anthocyanins and tannin (**Scheme 2.1**).[109] Takahama *et al*. reported the formation of cyanidin-catechin adduct where the 5-OH and C-4 of cyanidin were substituted by the addition of 5-OH and C-6 of (+)-catechin.[110] Aglycones from the deglycosylation of anthocyanins may also react with each other forming the polymeric species. This result is in agreement with Ichiyanagi *et al*., who reported that at higher TFA concentrations, the formed aglycones reacted successively with each other forming polymeric products.[111] The deglycosylation of anthocyanins was accelerated when the acidified ethanol eluate was concentrated to dryness in the rotary evaporator.

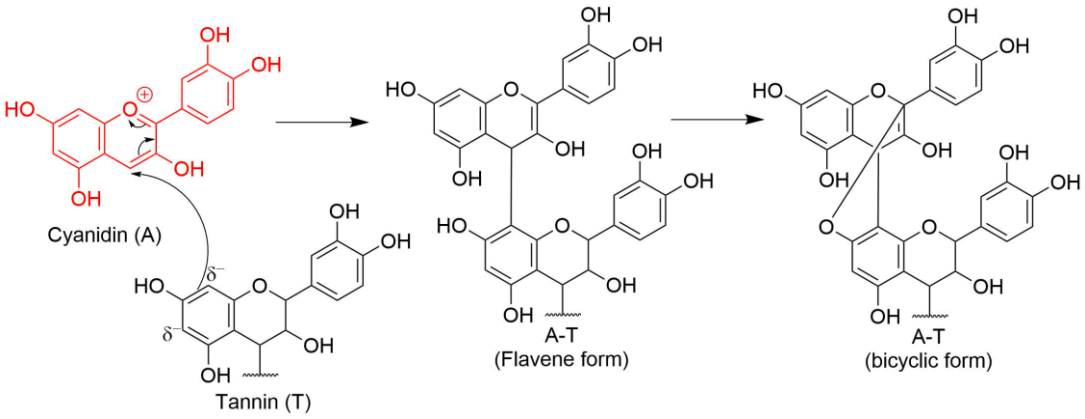

Scheme 2.1 Formation of cyanidin-tannin (A-T) adduct through direct condensation reactions.[109]

It has also been noted that anthocyanins in RASE degrade during the storage based on their HPLC chromatogram, which is shown by the increasing intensity of cyanidin peak (**Figure 2.9**). This study was done by comparing the HPLC chromatograms of the same sample after different times. The presence of hydrochloric acid in RASE (3.0-4.3%) which in this case was derived from the extraction-purification may be able to hydrolyse anthocyanins even though the dried extracts were stored at room temperature in a dark place and kept from open air. The effect of acid concentration used during extraction-purification is discussed more detail in **Section 2.3.2**.

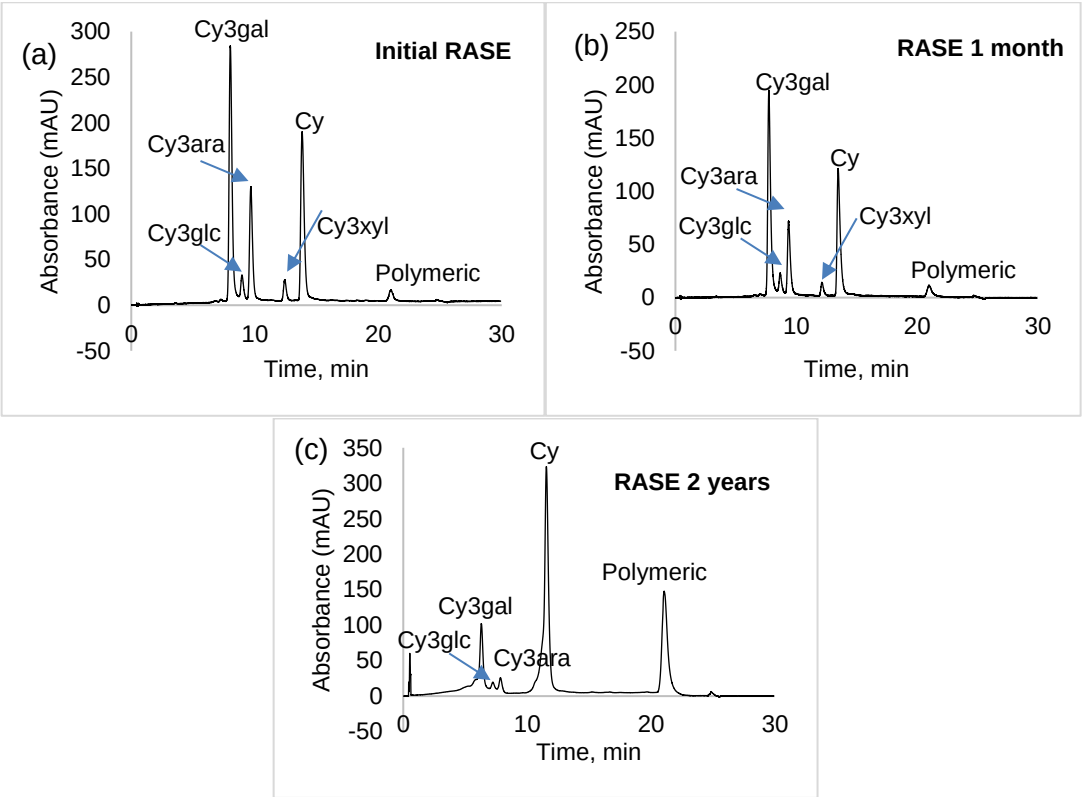

Figure 2.9 HPLC chromatograms of anthocyanins/ anthocyanidins which are present in RASE from an integrated method. (a) initial RASE (b) RASE after 1-month (c) RASE after 2 years. Detected by DAD at 520 nm.

The deglycosylation of anthocyanins via a flavylium cationic form is not practical as it is unlikely to have two positively charged oxygen atoms in one molecule (**Scheme 2.2**). Alternatively, the deglycosylation can occur via different forms such as the hemiketal form or quinonoid base form (see **Chapter 1**, **Section 1.1.6** for the transformation of anthocyanins). The deglycosylation can also occur through two different routes, one is through protonation an oxygen atom connecting an aglycone and a sugar moiety, and the other is through protonation an oxygen atom of sugar ring moiety resulting in a ring-opening in a sugar molecule (**Scheme 2.3** and **Scheme 2.4**). However, at the end of the reaction, the sugar will close the ring back.

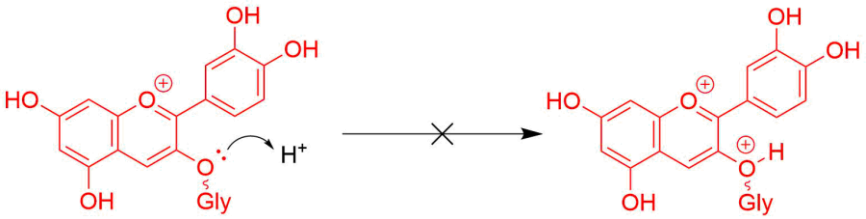

Scheme 2.2 General deglycosylation reaction of anthocyanins forming its aglycone via a flavylium cationic form resulting in two positive charges in one molecule.

The proposed mechanisms are presented for Cy3gal as an example, as this compound is the major product present in RASE, however, these mechanisms apply for deglycosylation of all anthocyanins in general. The products of deglycosylation of

anthocyanins are its aglycones and free sugars. The presence of free sugars in the extracts could promote the deglycosylation of anthocyanins as the hygroscopicity of the sugars is enough to attract water which reacts with anthocyanins forming a hemiketal. A hemiketal can then transform into a chalcone, and that is where anthocyanins start degrading. Lee *at al*. reported that the hygroscopicity of anthocyanin standards ranged from 10-22%.[92]

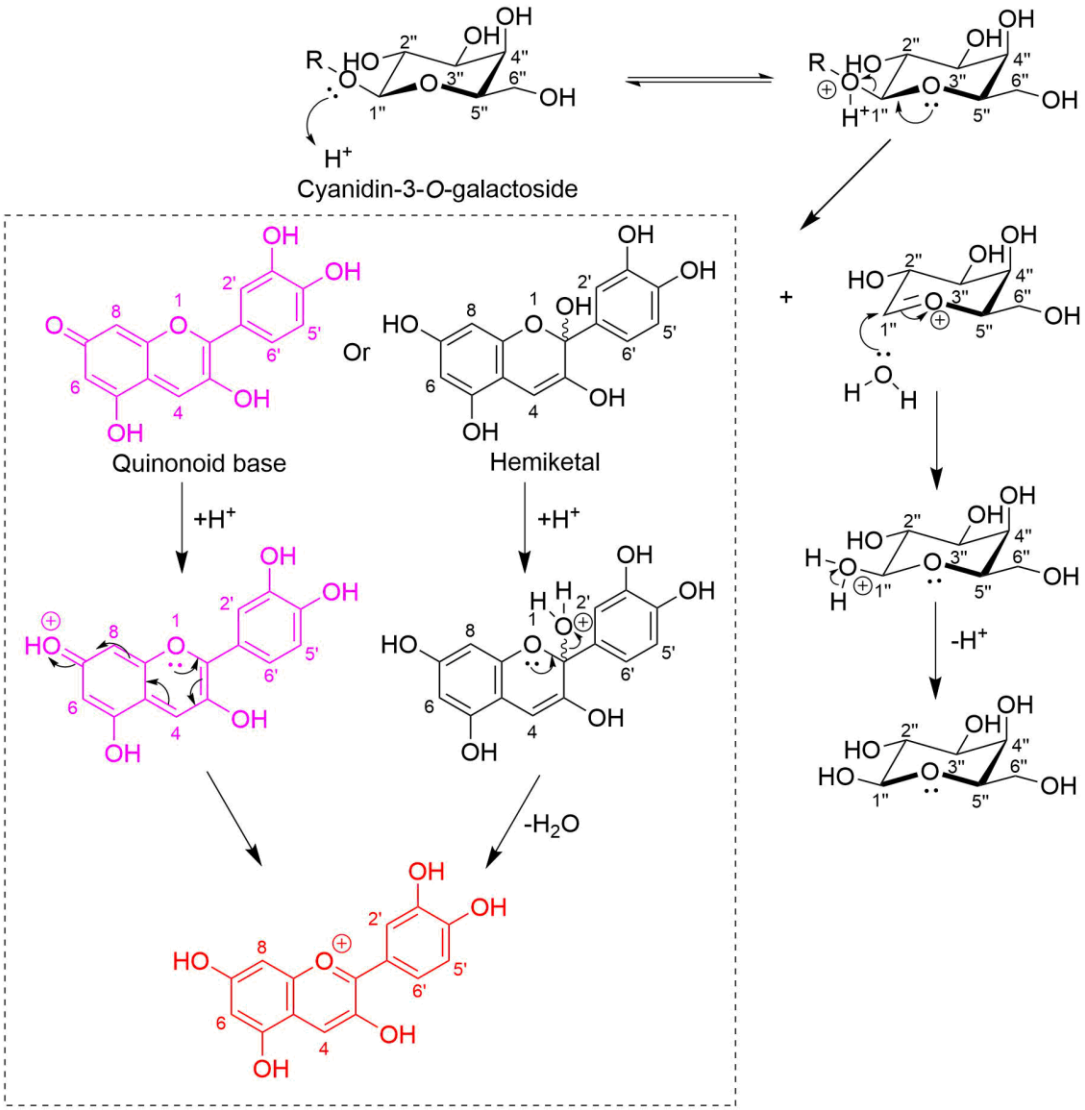

Scheme 2.3 Proposed deglycosylation mechanism of Cy3gal. R = Anthocyanidin core in hemiketal form or quinonoid base. Protonation occurs at an oxygen atom connecting an aglycone and a sugar moiety. The products are an aglycone (cyanidin) in a flavylium cationic form and galactose.

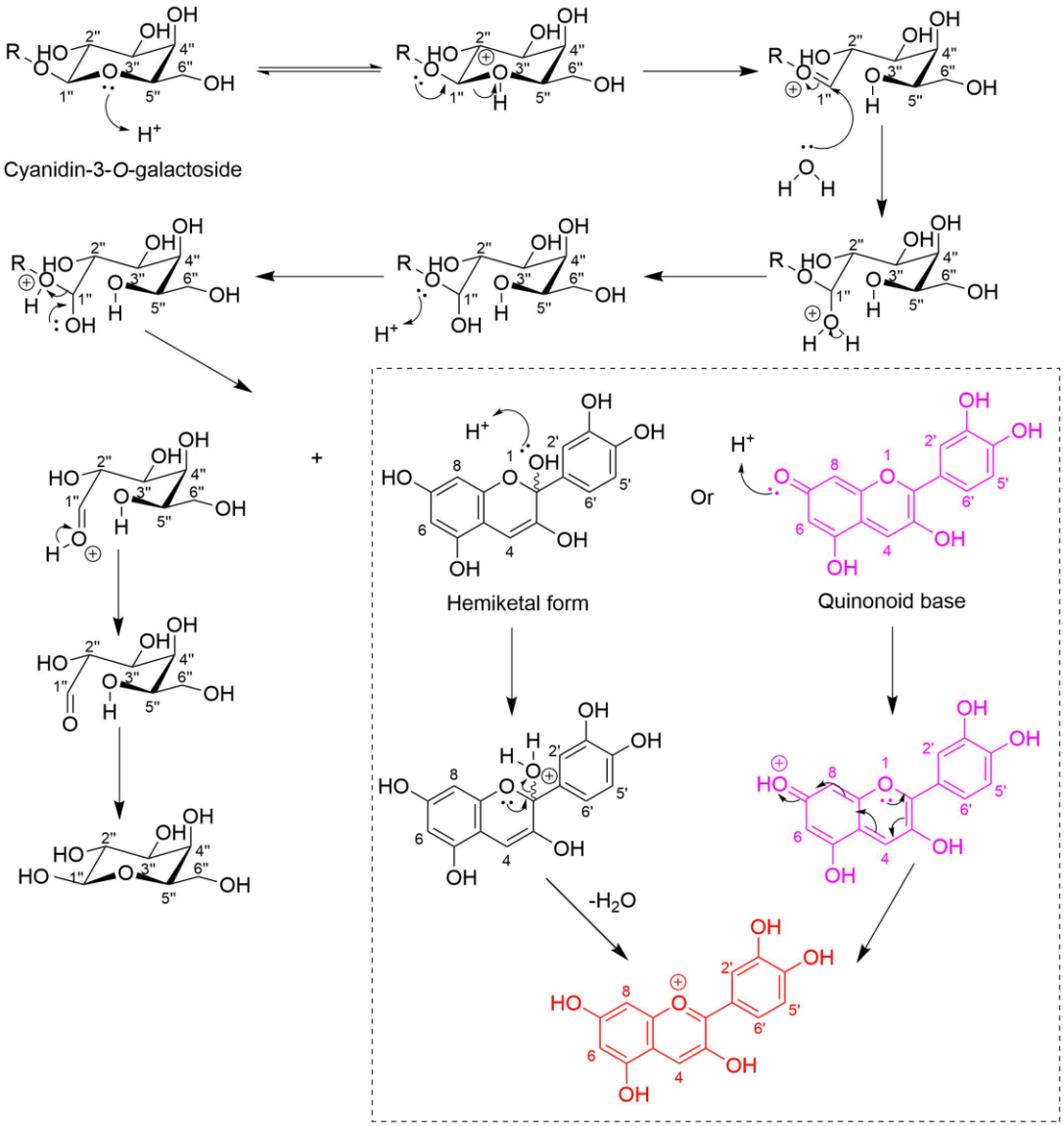

Scheme 2.4 Proposed deglycosylation mechanism of Cy3gal. R = Anthocyanidin core in hemiketal form or quinonoid base. Protonation occurs at an oxygen atom in a sugar moiety resulting in a ring-opening. The products are an aglycone (cyanidin) in a flavylium cationic form and galactose.

2.2.3. LC-MS studies

LC-MS was used to resolve further which anthocyanins were present in RASE. As a reverse-phase column was also used in this method, the principle of separation is similar, as described in **Section 2.2.2**. A full separation of the peaks was done by using this technique; it can differentiate between the glycosides of cyanidin with hexose sugars (Cy3gal and Cy3glc) and pentose sugars (Cy3ara and Cy3xyl). Anthocyanins and its anthocyanidin are mostly found in the positive mode and expressed as molecular ion $[M]^+$ (**Table 2.3**). Cy3gal and Cy3glc were identified with a mass to charge ratio (m/z) of 449.39. Cy3ara and Cy3xyl were identified with an m/z of 419.28. Finally, cyanidin was identified with an m/z of 287.33. The ESI-MS fragmentation pathway of anthocyanins is identified by losing -162 m/z to produce its aglycone, which makes the intensity of cyanidin higher. These peaks were consistent with the results reported in the literature.[69,105] For complete elucidation of anthocyanins present in RASE, NMR experiments were also carried out (**Section 2.2.4**).

Table 2.3 The chromatogram of anthocyanins and its aglycone present in RASE obtained by using LC-MS-ESI in positive mode.

Compound	$[M]^+$ m/z (reference)[69,105]	$[M]^+$ m/z (experimental)	Characterisation
25	449	449.39	Cy3gal
21	449	449.39	Cy3glc
26	419	419.28	Cy3ara
27	419	419.28	Cy3xyl
2	287	287.33	Cyanidin

2.2.4. ^{1}H-NMR studies

^{1}H-NMR studies were conducted to characterise anthocyanins and other polyphenols extracted from *Aronia* skin waste. In order to maximise the formation of a flavylium cationic form of the anthocyanins, RASE was dissolved in acidified deuterated methanol (CD_3OD/CF_3COOD, 95:5).[112] The samples were then homogenised to avoid any spectroscopic noise due to undissolved solid. The proton chemical shifts were assigned using 1D and 2D NMR techniques. The ^{1}H-NMR spectra of crude extract without SPE, post-SPE residues of ethyl acetate wash and RASE are compared in **Figure 2.10**.

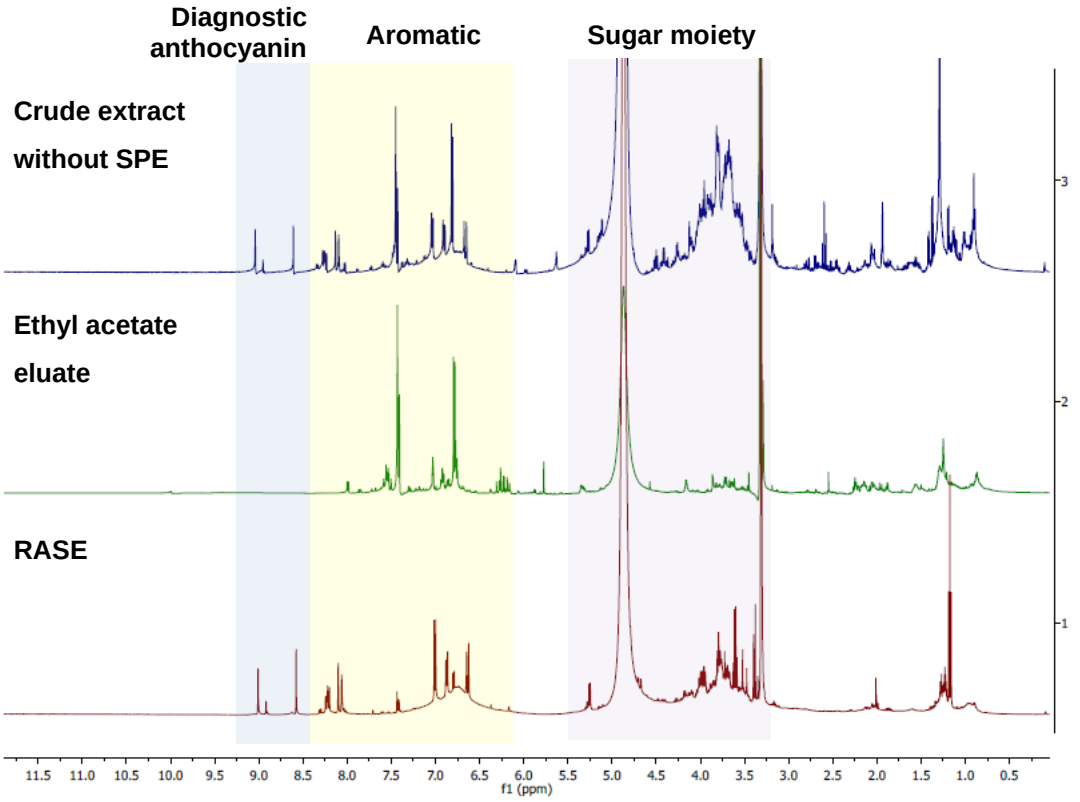

Figure 2.10 ^{1}H-NMR spectra of crude extract without purification by SPE, post-SPE residues of ethyl acetate wash and RASE. The ^{1}H-NMR spectra were recorded at 500 MHz. Solvent: CD_3OD/CF_3COOD, 95:5.

It can be seen in **Figure 2.10** that an SPE could mostly separate anthocyanins from other major polyphenols present in *Aronia* skin waste. The region of 8.5-9.02 ppm is particularly diagnostic for anthocyanin and anthocyanidin regions (H-4). These regions are mainly found in RASE but notably absent in the post-SPE of ethyl acetate wash, confirming the effectiveness of ethanol for desorption of anthocyanins. The ratio of anthocyanins in the ethanolic residues is consistent with the results obtained from HPLC experiments (see **Section 2.2.2**) as determined by integration of the anthocyanin (H-4) diagnostic chemical shifts which appear as singlets. H-6' and H-2' appear as a doublet of doublets, and doublets respectively at 8.0-8.3 ppm. H-5', H-8 and H-6 appear as doublets at 6.5-7.0 ppm. The 2D NMR such as ^{1}H-^{1}H COSY is a good technique to assign the protons which correlate to their neighbour protons (**Figure 2.11**). It shows that H-6' has a weak correlation with H-2' but strongly correlates with H-5', and H-8 and H-6 correlate to each other.

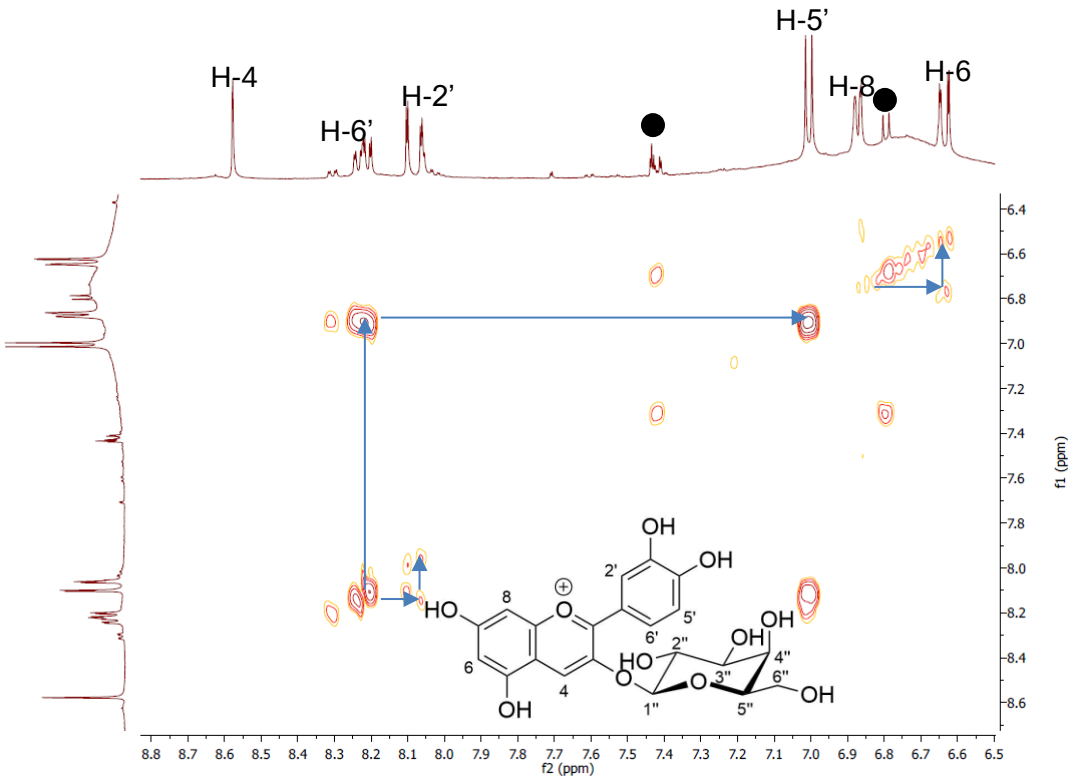

Figure 2.11 The ^{1}H-^{1}H COSY spectrum of RASE showing the aromatic region. Recorded at 500 MHz (25 °C). (●) 3,4-dihydroxybenzoic acid.

Evidence of the glycosyl moieties is from the signals in the region of 3.2-4.3 ppm alongside the anomeric protons (H-1") in the region of 5.0-5.5 ppm (**Figure 2.12**). The ^{1}H-^{1}H COSY spectrum shows the strong correlation of H-1" and H-2". Then, H-3", H-4", H-5", H-6"A/B can be assigned accordingly. An SPE column can remove the impurities such as free sugars in the extract as the broad peaks in the sugar region were significantly reduced in the spectra of the post-SPE of ethyl acetate wash and RASE. Polymeric species is identified as broad peaks at 6.5-7.3 ppm and mostly found in RASE compared to the post-SPE of ethyl acetate wash. However, because of the complexity of the mixture, the peaks of anthocyanins and anthocyanidin, especially the aromatic protons and sugar moiety protons overlap to each other which made unambiguous assignment difficult. Therefore, further purification to obtain individual anthocyanins and anthocyanidin from RASE was required. The full characterisation of individual anthocyanins and anthocyanidin, as well as other minor polyphenols present in RASE, is discussed later in **Chapter 3**.

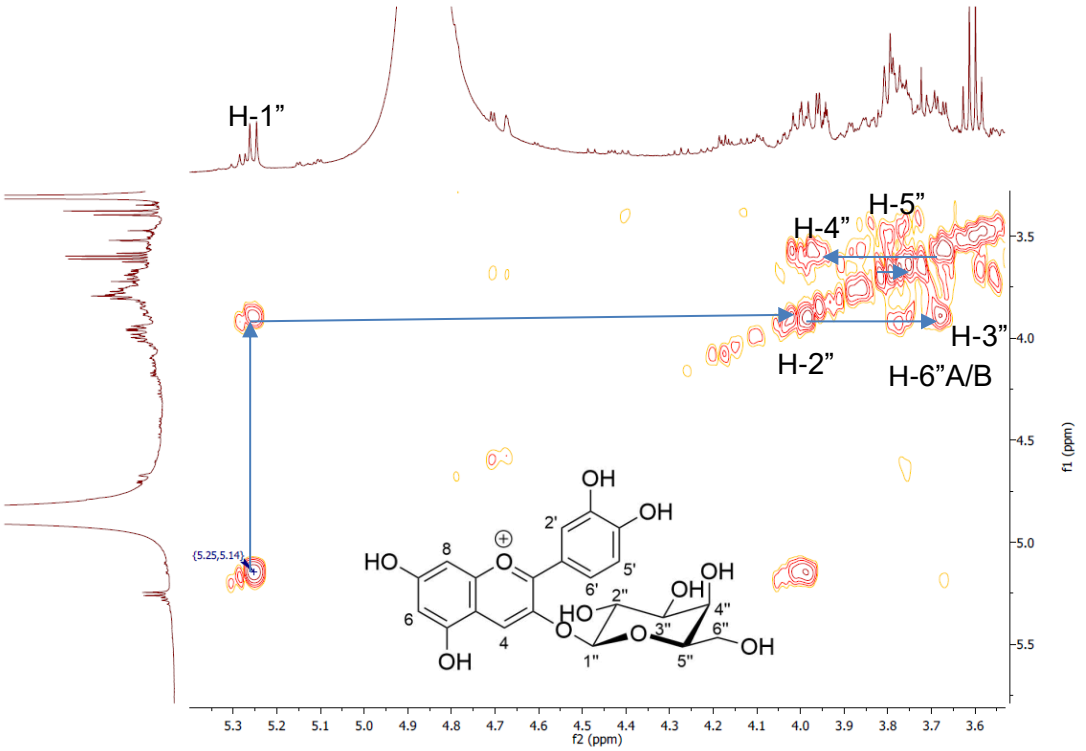

Figure 2.12 The ^{1}H-^{1}H COSY spectrum of RASE showing the sugar region. Recorded at 500 MHz (25 °C).

2.3. Comparison between the Batch Extraction Method and the New Integrated Process.

Anthocyanin profiles of RASE from both the batch method and the integrated method were compared according to their HPLC chromatograms and NMR spectra. In order to investigate the effect of acid on the anthocyanin profiles, various concentrations of acid were used during extraction-purification for both methods, and analysed by HPLC. Finally, the efficiency of extraction-adsorption for both methods were compared based on their extraction yield, total monomeric anthocyanin content and the quality of anthocyanins in RASE.

2.3.1. Comparison of Anthocyanin Profiles in RASE from the Batch and Integrated Methods.

Anthocyanin profiles (%) of individual anthocyanins present in RASE from both methods were compared using HPLC and NMR. For HPLC analysis, the detection was carried out at 520 nm. The elution profile of anthocyanins present in RASE for both methods is presented in **Figure 2.13**. The peaks were assigned in accordance with the literature.[43,90,105] Both methods show similar anthocyanin profiles, however

the levels of cyanidin are higher in the batch method compared to the integrated method.

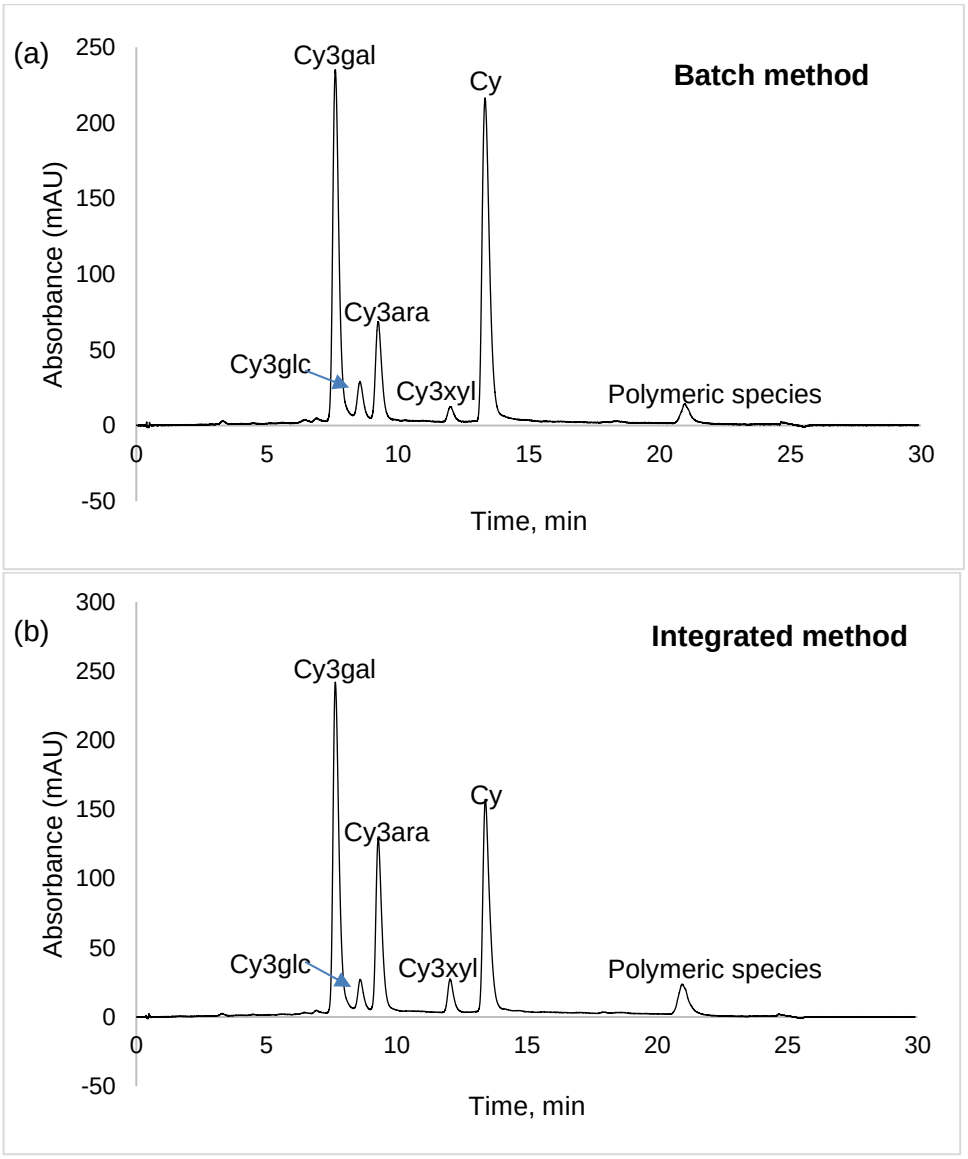

Figure 2.13 Profile of anthocyanins shown in HPLC chromatograms of (a) the batch and (b) the integrated method. Solvent A: H_2O/TFA (99.5:0.5); Solvent B: acetonitrile. Detected at 520 nm.

The relative percentage of individual anthocyanins as obtained from the HPLC chromatogram by comparing the Area (mAU*min) of each anthocyanin shown in the chromatogram (**Figure 2.14**). In the batch method sample, anthocyanins present in RASE were identified as Cy3gal (44%), Cy3glc (3.7%), Cy3ara (12.2%), Cy3xyl (1.4%) and the cyanidin aglycon (38.7%), whereas using the integrated method, content was Cy3gal (44.7%), Cy3glc (4.2%), Cy3ara (26.3%), Cy3xyl (4.5%) and the cyanidin aglycon (20.3%). Cy3gal and Cy3ara were the major anthocyanins found in

RASE for both methods. It can be concluded that Cy3gal is the most abundant anthocyanin followed by Cy3ara > Cy3glc > Cy3xyl using the batch method. Using the integrated method, Cy3xyl was slightly higher than Cy3glc, although both are at low levels.

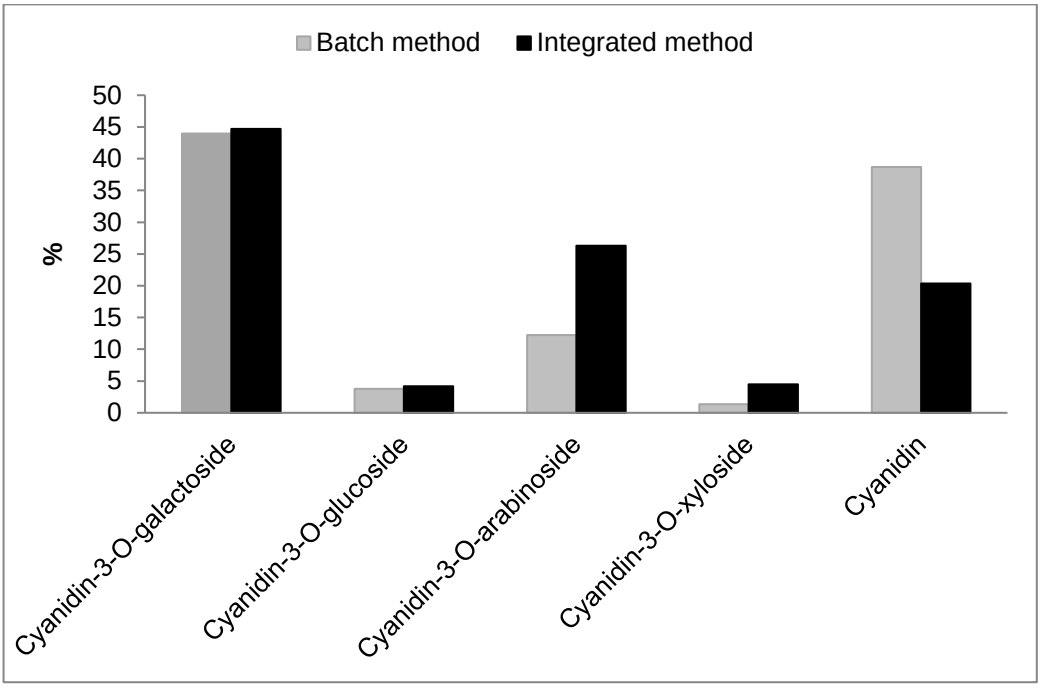

Figure 2.14 Total anthocyanins calculated according to relative % shown in HPLC chromatograms of the batch method and the integrated method. Solvent A: H_2O/TFA (99.5:0.5); Solvent B: acetonitrile. Detected at 520 nm.

As already discussed in **Section 2.2.2.3**, deglycosylation of anthocyanins can occur during the SPE elution, concentration and storage due to the presence of strong acid. The concentration of Cy3ara was doubled while Cy3xyl was tripled in samples using the integrated method compared to the batch method. The decreased concentration of Cy3ara and Cy3xyl from the batch samples correlated with the increasing concentration of cyanidin, suggesting they may be hydrolysed in preference to Cy3gal and Cy3glc (**Figure 2.14**). Ichiyanagi *et al*. reported that the hydrolysis rate of anthocyanins depends on the sugar moiety not on the aglycone structure.[111] The effect of concentration of acid on the deglycosylation of anthocyanins in both methods is further discussed in **Section 2.3.2**.

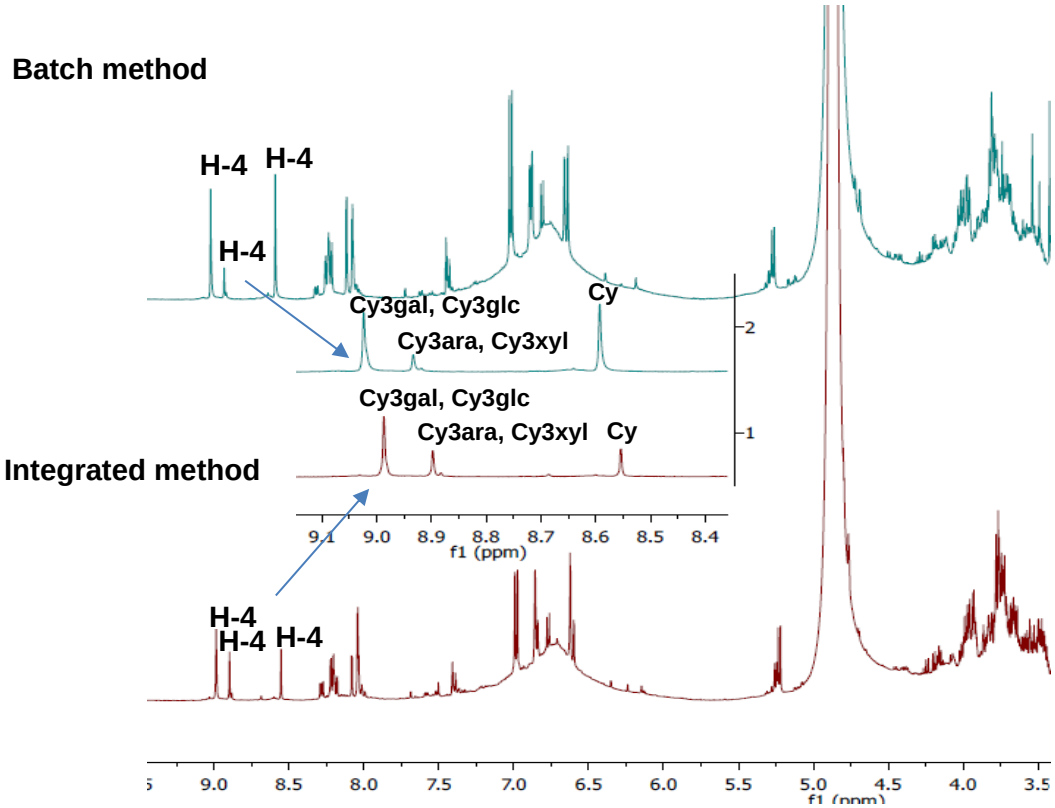

Figure 2.15 ^{1}H-NMR spectra of RASE for the batch method and the integrated method. The ^{1}H-NMR spectra were recorded at 500 MHz. Anthocyanins and anthocyanidin are labelled correspond to their H-4 proton.

^{1}H-NMR provides further relevant information for comparing the two extraction methods (**Figure 2.15**). The characteristic peak of anthocyanins is shown by a singlet of H-4 at the region of 8.5-9.0 ppm. It is noted that the ratio of the H-4 proton signals for Cy3gal + Cy3glc and Cy3ara + Cy3xyl for both the batch and integrated methods were consistent with the results by HPLC analysis. The broad peaks of polymeric proanthocyanins obscured the peaks of aromatics in these regions. In the region of 6.5-7.5 ppm, the peaks of neutral polyphenolic ring protons, such as those on the anthocyanins and any other polyphenols present in RASE are present alongside polymeric proanthocyanidins peaks. However, peaks of neutral polyphenols in this region for the batch method are more intense, suggesting that more neutral polyphenols are present in RASE. It was later confirmed that neutral polyphenols at 6.5-7.5 ppm were 3,4-dihydroxybenzoic acid (DHBA), quercetin (Q), chlorogenic acid (CA) and neochlorogenic acid (nCA). Full characterisation of these neutral polyphenols is discussed in **Chapter 3**.

2.3.2. Effect of Acid Concentration on Anthocyanin Deglycosylation

The effect of the concentration of hydrochloric acid was studied with respect to deglycosylation of anthocyanins. The acid concentration used in the extraction-purification ranged from 0.01 to 0.5 % v/v. Both extraction and SPE desorption used the same concentration of acid. RASEs from each concentration was analysed by HPLC-DAD at 520 nm. The relative percentage (%) of individual anthocyanins was then determined and compared (**Figure 2.16**).

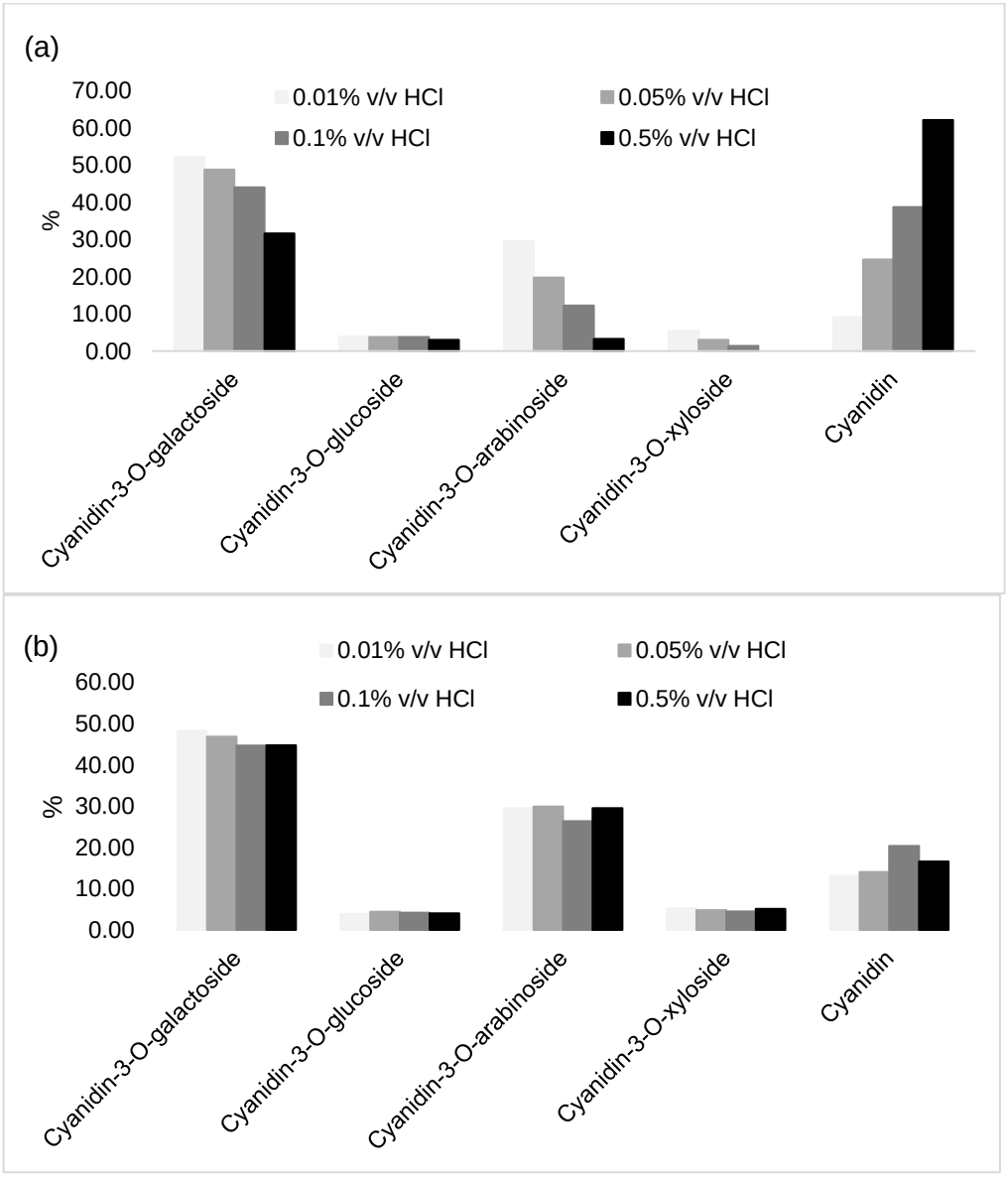

Figure 2.16 The effect of acid concentration on total anthocyanins calculated according to relative % shown in HPLC chromatograms of (a) the batch and (b) the integrated method. Solvent A: H_2O/TFA (99.5:0.5); Solvent B: acetonitrile. Detected at 520 nm.

Figure 2.16 shows that an increase in acid concentration for the batch method correlates to the level of deglycosylation of anthocyanins forming the aglycon cyanidin. Cy3ara suffers greater deglycosylation compared to Cy3gal, suggesting that pentose sugars are more prone to hydrolysis than hexose sugars. This finding is in agreement with Ichiyanagi *et al*., who reported that the rate constant of anthocyanin hydrolysis follows this order arabinoside > galactoside > glucoside regardless of their aglycone.[111] Additionally, they also reported that the rate constants of anthocyanin hydrolysis increased with the increase of acid (TFA) concentrations.[111] Interestingly, using the integrated method, the formation of cyanidin is only slightly increased by an increase in acid concentration.

2.3.3. Net Efficiency for Extracting Anthocyanins from *Aronia* skin waste

This section discusses the overall efficiency for extracting anthocyanins from *Aronia* skin waste for both the batch and integrated methods. **Figure 2.17** shows that the flow sheets of two different methods. Using the batch method, the first three steps did not contribute to any purification of anthocyanins extracted from *Aronia* skin waste but did provide the sample for the SPE. However, the integrated method replaced the first three steps in a batch method (cooling down process, filtration and SPE adsorption) which eventually simplified the process and reduced the energy and time consumption during the process. This process is potentially suitable to be scaled up on an industrial scale and also gives a more consistent product quality.

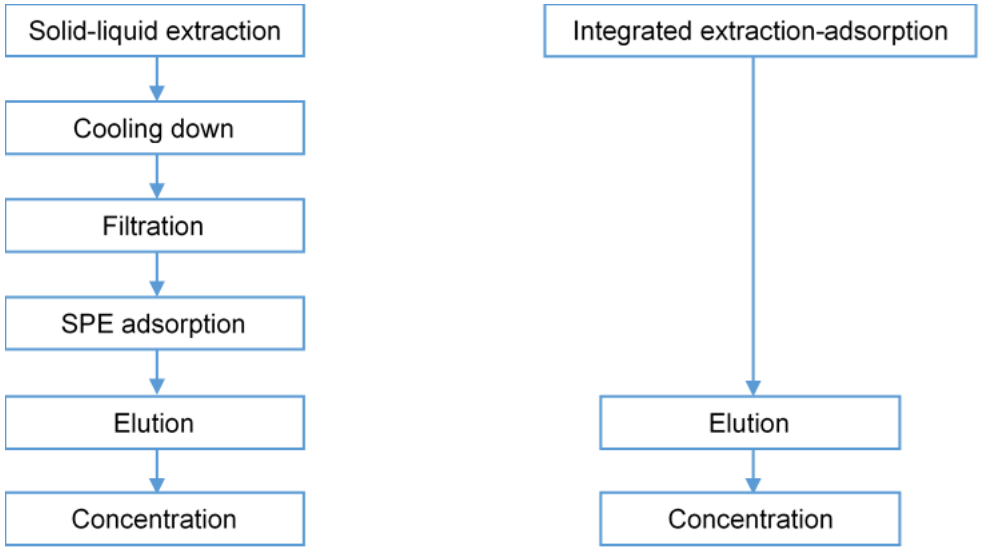

Figure 2.17 The comparison between a batch method (left) and an integrated extraction-adsorption method (right).

Although extraction yields are important, the quality of RASE, particularly with regard to anthocyanin content, is of primary importance in this study as further chemical modification of the anthocyanins was planned. Hence, the extraction yield and anthocyanin content of both methods were also compared to find the best method overall that will be used for further experiments. The comparison study was done for the experiment run at 60 °C for 3 h using the other optimum parameters. The result is presented in **Table 2.4**.

Table 2.4 The yield of anthocyanins recovered from *Aronia* skin waste (mg g^{-1} DW pomace). The extraction was conducted at 60 °C for 3 h.

Extraction-Adsorption method	Extraction yield, mg g^{-1} DW pomace	TMAC, % w/w DW RASE	Yield of anthocyanins, mg g^{-1} DW pomace
Batch	5.3*	19.9	1.05
Integrated	6.3**	28.4	1.79

Standard Deviation (SD), *SD= 0.10, **SD= 0.43, n = 3 replicates

Table 2.4 shows that the highest yield of anthocyanins was found using an integrated extraction-adsorption method. This could increase the extraction yield by up to about 20% and anthocyanin content up to 40%. This observation can be explained by the fact that in the continuous circulating process enriches the adsorption of anthocyanins on the SPE resin. It also avoids further deglycosylation during extraction under the acidic, high-temperature aqueous environment as extracted anthocyanins were circulated directly and rapidly absorbed onto the SPE resin. Additionally, the circulating process prevents saturation of the solvent in the extraction vessel allowing more anthocyanins to be extracted. Based on these results, it can be concluded that the new proposed method, namely the integrated extraction-adsorption method, showed an improvement in terms of yield of anthocyanins compared to a batch method, and this method is best for obtaining good quality anthocyanin samples from *Aronia* skin waste.

2.4. Conclusion

Extraction parameters have been optimised in order to produce RASE which contains anthocyanins in higher quality and to reduce losses during extraction-purification processes due to deglycosylation. This study compared a conventional batch method and a new integrated method for recovering anthocyanins from *Aronia* skin wastes. These methods consist of two main processes, namely extraction and adsorption. While extraction and adsorption are performed separately in a batch method, the new method offers an integrated extraction-adsorption process. The optimum conditions

used for the batch method are as follows: extraction temperature of 60 °C, extraction time of 3 h, acid additive (0.1% v/v HCl), biomass-solvent ratio of 1:16 and the biomass-SPE resin ratio of 1:1. The new method was investigated to obtain higher anthocyanin yields. The effect of the cooling process during sample loading and flow rate of sample loading were investigated. Higher anthocyanin yields are obtained when the process was performed for 3 h without cooling of the flow to the SPE column, and the best flow rate was 1.3 mL/s. Overall, the new proposed method showed a better anthocyanin yield and purity compared to the batch method. This method also simplified the process as three steps were eliminated during the process, which eventually saves time and energy. The continuous extraction-adsorption process enriches the anthocyanins adsorbed on the SPE resin resulting in a higher extraction yield as once anthocyanins were extracted from biomass, they were adsorbed onto the SPE resin. Additionally, the formation of cyanidin as a product of deglycosylation was minimised in the continuous extraction-adsorption process.

Anthocyanins and its aglycone present in *Aronia* skin wastes were identified as follows: Cyanidin-3-*O*-galactoside, Cyanidin-3-*O*-glucoside, Cyanidin-3-*O*-arabinoside, Cyanidin-3-*O*-xyloside and cyanidin according to literature. The confirmation of this finding is then further discussed in **Chapter 3**. Cyanidin-3-*O*-galactoside and cyanidin-3-*O*-arabinoside are the major anthocyanins found in *Aronia* berries. Using the batch method, Cyanidin-3-*O*-arabinoside suffers the deglycosylation more compared to Cyanidin-3-*O*-galactoside during the ethanol elution with an increase of acid concentration. Meanwhile, further hydrolysis can be avoided using the integrated method. Furthermore, the new proposed method is potentially industrial scalable and could be used to produce large quantities of anthocyanins. The presence of strong acid such as HCl in RASE could accelerate the deglycosylation of anthocyanins, and milder acids might also be used to produce RASE with higher stability.

Chapter 3
Further Purification, Characterisation and Total Chemical Composition of RASE

This chapter discusses the further purification, characterisation, and quantification of polyphenols in refined *Aronia* skin waste extract (RASE). **Section 3.1** discusses a further purification for RASE using three different techniques, namely semi-preparative HPLC-DAD, liquid-liquid extraction (LLE) and Biotage flash purification. Individual anthocyanins, cyanidin aglycone, polymeric proanthocyanidins and other neutral polyphenols separated and isolated from RASE by those techniques were then characterised by 1D and 2D NMR spectroscopy. The three techniques produced RASE with improved anthocyanin purity, in high quantity for further application. The use of simpler mixtures helps to better understand reactions, and aids separation and characterisation of final products. **Section 3.2** discusses the quantification of the total chemical composition of RASE. All polyphenols present in RASE, which have been identified individually, were then quantified and summarised in percentage (%). In general, the further purification of RASE, chemical characterisation and determination of the total composition of RASE is summarised in **Figure 3.1**.

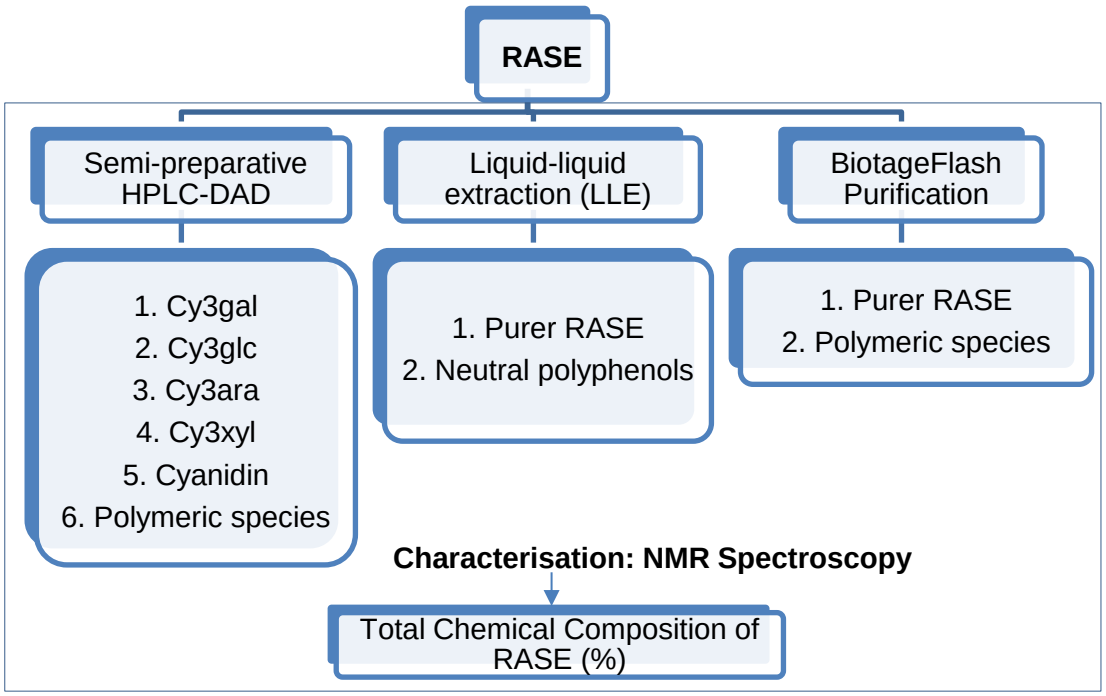

Figure 3.1 The general procedure to purify and quantify the total chemical composition of RASE.

3.1. Further Purification of RASE

Aronia skin waste was extracted and selectively purified through an SPE column to produce RASE. RASE in this study was obtained from a batch extraction with an extraction time of 3h, extraction temperature of 60 ºC, acid addition of 0.01% v/v HCl, the ratio of biomass-to-solvent of 1:16 and ratio of biomass-to-SPE resin ratio of 1:1 (see **Chapter 2**). Anthocyanins found in RASE have been identified according to the reported data in literature.[65] However, other polyphenols with similar retention affinity to anthocyanins on the SPE column could also be co-eluted. These non-anthocyanin polyphenols are present in RASE according to its HPLC chromatogram at 285 nm and 350 nm, which are characteristic of phenolic acids and flavonols, respectively (**Figure 3.2**).[7] The presence of these polyphenols could also be identified by NMR spectroscopy (see **Chapter 2**, **Section 2.2.4**).

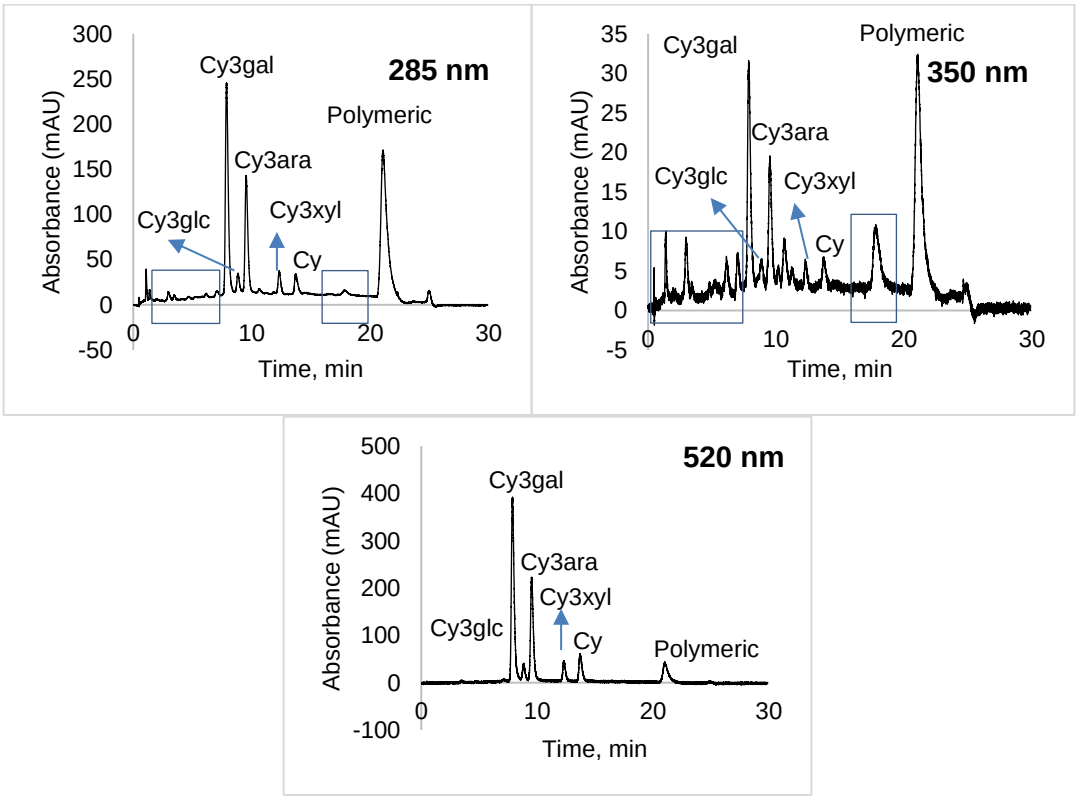

Figure 3.2 HPLC chromatogram of RASE detected at 285, 350 and 520 nm. Column: Eclipse XDB C18, 5 µm, 150 x 2.1 mm column. Solvent A: H_2O/TFA (99.5:0.5); Solvent B: acetonitrile. New peaks at 350 nm belong to neutral polyphenols (blue squares).

Non-anthocyanin polyphenols in *Aronia* berries have been well documented in literature[4,69] and might undergo co-pigmentation with anthocyanins (**Figure 3.3**), affecting their stability and colour properties.[42,113] The co-pigmentation of anthocyanins can occur through intra- or intermolecular interactions. A co-

pigmentation includes the stacking of the organic co-pigment molecule (electron-rich) on the planar polarisable core of the coloured anthocyanin forms such as a flavylium cationic form or a quinonoid form.[37,42] Hydrogen bonding interactions are also possible and may promote co-pigmentation. This may be the reason some polyphenols are still present in RASE even though the *Aronia* crude extract has been selectively purified in the SPE column using polar organic solvents. Therefore, further purification is still required to obtain purer samples for further chemical modification on anthocyanins.

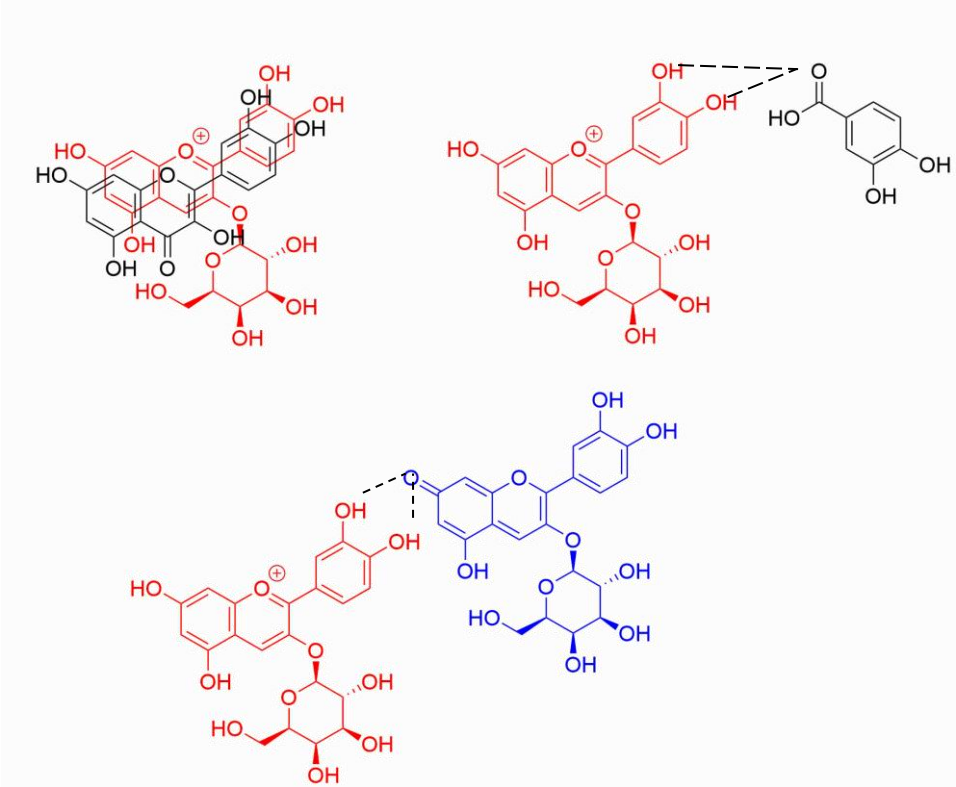

Figure 3.3 Proposed co-pigmentation interaction of anthocyanins (Cy3gal) with polyphenols (quercetin and 2,4-dihydrobenzoic acid) or amongst anthocyanins present in RASE.

This study performed three different techniques to further purify anthocyanins present in RASE from other neutral polyphenols. The first technique was a semi-preparative HPLC-DAD where individual anthocyanins can be separated and isolated from the mixture. Its aglycone and polymeric proanthocyanidins were also able to be isolated and characterised. The second technique was through a liquid-liquid extraction (LLE), an acidified aqueous solution containing anthocyanins was partitioned with selected organic solvents. This technique could isolate non-anthocyanin polyphenols. Finally, the last technique to separate anthocyanins from the polymeric proanthocyanidins was Biotage flash purification.

3.1.1. Semi-preparative HPLC-DAD

3.1.1.1. Isolation of Individual Polyphenols in RASE

The main objective of using semi-preparative HPLC was to isolate the desired products with high purity from other RASE components.[114,115] This isolation will ease the characterisation of individual anthocyanins and study on their properties. Even though this technique was not desirable for the purification and isolation of anthocyanins on a large scale, it was still good to obtain relatively pure anthocyanins from the mixture.[116] The chemical characterisation of these relatively pure compounds (> 90% pure) can be done using small quantities (mg scale).

The method used in the semi-preparative HPLC purification followed the optimum condition for separating anthocyanins from RASE in an analytical HPLC-DAD method with a slight modification (see **Chapter 2**, **Section 2.2.2**). The modification included the volume of sample injection, the column's size, run time and flow rate. The mobile phase used was the same, Solvent **A** was water, and Solvent **B** was acetonitrile. The separation was carried out under acidic conditions using TFA (0.5%) in the mobile phase.[117] The detection and collection of fractions were using 520 nm absorption.[69] Other compounds which have no absorption at this wavelength were discarded. The elution profile of anthocyanins shown in **Figure 3.4,** similar to the chromatogram shown in the analytical HPLC chromatogram (see **Figure 3.2** at 520 nm).

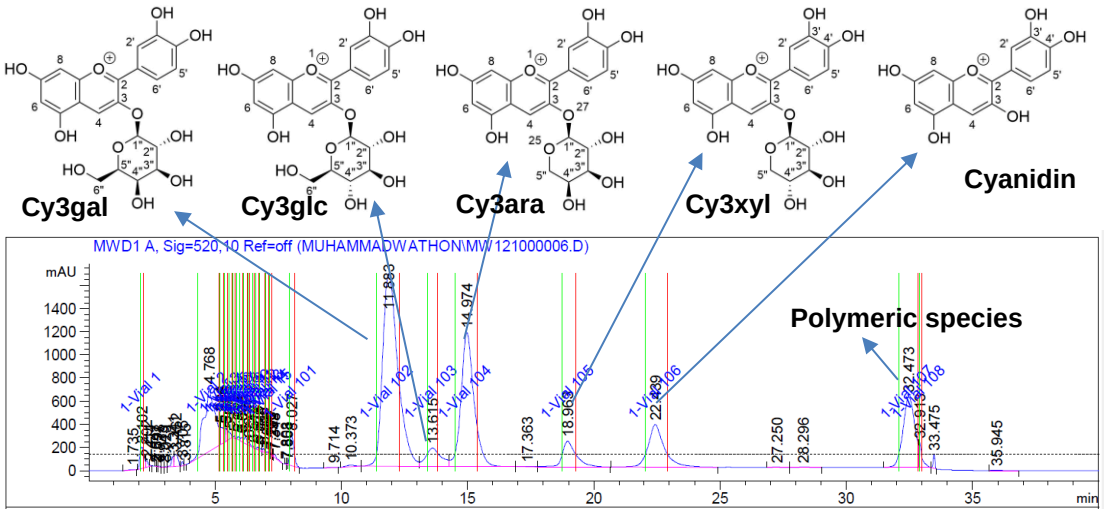

Figure 3.4 The Semi-preparative HPLC chromatogram of polyphenols present in RASE. Column: XBridge™ Prep C18, 10 x 50 mm, 5 µm, Solvent A: H_2O/TFA (99.5:0.5); Solvent B: acetonitrile, 40 min run. Detected at 520 nm. Fractions from the first 10 min were discarded as these come from the column.

The separation of anthocyanins from other components follows the polarity interaction principle in the analytic HPLC (see **Chapter 2**, **Section 2.2.2**). The semi-preparative HPLC experiment was repeated several times to get sufficient pure anthocyanins. LC-MS then analysed all collected fractions from one experiment to determine the molecular mass of each fraction. Once all the fractions have been identified based on their molecular mass (m/z), the fractions with the same retention time were then combined and labelled as the respective compounds. The fractions from RASE are summarised in **Table 3.1**. Each collected fraction was freeze-dried and stored in the freezer for further use. The purities of individual anthocyanins were determined by an analytical HPLC with the detection at 520 nm and monitored at 285 nm. The purity of anthocyanins was determined by the per cent (%) area of the isolated anthocyanins in the HPLC chromatogram at 285 nm.

Table 3.1 The fractions collected from a Semi-preparative HPLC-DAD at 520 nm. The purity was determined at 285 nm.

Fraction	Retention time (min)	$[M^+]$ m/z	Purity (%)
Cy3gal	11.88	449.1076	97
Cy3glc	13.61	449.1072	97
Cy3ara	14.97	419.0972	97
Cy3xyl	18.96	419.0968	91
Cyanidin	22.44	287.0470	93
Polymeric species	32.47	-	100

3.1.1.2. Characterisation of Anthocyanidin and Individual Anthocyanins.

The *Aronia* skin waste in this study contains only cyanidin-based anthocyanin with 4 different monosaccharide moieties. The characterisation of cyanidin aglycone and individual anthocyanins, which have been separated and isolated from RASE, was performed with 1D and 2D NMR techniques. This included ^{1}H, ^{13}C, ^{13}C-DEPT, ^{1}H-^{1}H COSY, ^{1}H-^{13}C HSQC, ^{1}H-^{13}C HMBC and ^{1}H-^{1}H NOESY NMR spectroscopy. All the NMR analysis were carried out in CD_3OD/CF_3COOD (95:5 v/v) solution.[118] The characterisation was then compared to data reported in literature.[106]

The proton H-4 of a flavylium cationic form of cyanidin and cyanidin-based anthocyanins have a diagnostic chemical shift of 8.5-9.5 ppm, which appears as a singlet. As such, it can easily distinguish one anthocyanin from the others present in

RASE. **Figure 3.5** shows the NMR spectra's comparison for RASE and individual components present in RASE after purification using a semi-preparative HPLC. It shows that RASE has more than one anthocyanin, and each anthocyanin has a diagnostic chemical shift (H-4).

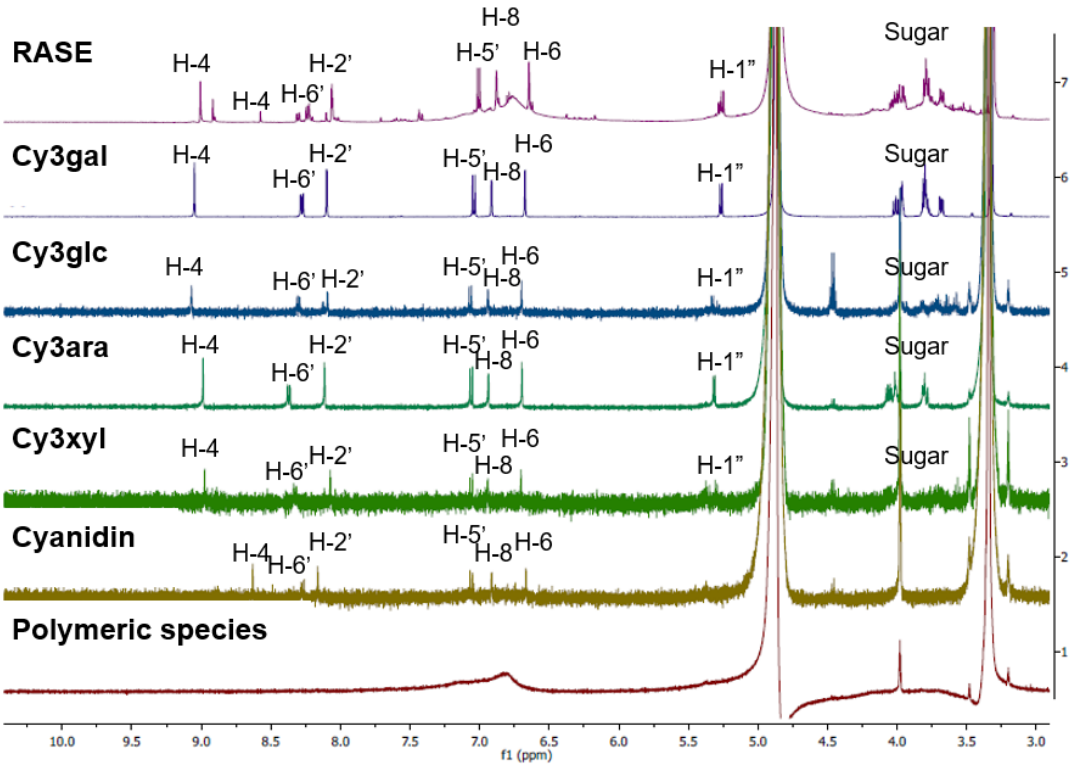

Figure 3.5 ^{1}H-NMR spectrum (500 MHz) of RASE, isolated individual anthocyanins and polymeric species. Solvent: CD_3OD/CF_3COOD (95:5). Recorded at 25 °C.

However, the quantity of samples was quite low, which gave poor quality NMR spectra. Therefore, the semi-preparative HPLC experiment was repeated until a reasonable amount of pure anthocyanins have been collected for the characterisation and evaluation of physico-chemical properties of these individual anthocyanins. Once a certain quantity of pure anthocyanins and anthocyanidin was achieved (*ca*. 2 mg), the full characterisation could be performed.[106] Characterisation on the individual fraction is discussed in **Section 3.1.1.2.1** to **3.1.1.2.6**.

The NMR data obtained confirmed the anthocyanin profile obtained in the HPLC chromatogram (see **Figure 3.2**). The ratio of anthocyanins (H-4) in the NMR spectrum shows similar pattern shown in the HPLC chromatogram, Cy3gal (52.2%) > Cy3ara (29.5%) > Cy (9.1%) > Cy3xyl (5.4%) > Cy3glc (3.9%). The chemical shifts of H-4 of anthocyanins with hexose sugar moieties are more deshielded than

anthocyanins with pentose sugar moieties. The chemical shift of H-4 of aglycone is the lowest and shifts to the upfield region (**Table 3.2**). Polymeric proanthocyanidins appear as broad peaks at 6.1-7.3 ppm and 3.3-4.3 ppm, which can overshadow the peaks of anthocyanins in the aromatic and sugar regions. Hence the removal of polymeric species from RASE should alleviate the complexity in characterising anthocyanins.

Table 3.2 Chemical shift (H-4, ppm) of individual anthocyanins isolated from RASE.

	Cy3gal	Cy3glc	Cy3ara	Cy3xyl	Cyanidin
H-4 (ppm)	9.03	9.02	8.84	8.92	8.59

3.1.1.2.1. Cyanidin (Cy)

Cyanidin was the fifth fraction collected from the semi-preparative HPLC with a retention time of 22.44 min. This anthocyanidin is the backbone of anthocyanins from *Aronia* skin waste. Therefore, cyanidin's chemical characterisation can be a reference in assigning protons of the 2-phenyl-1-benzopyrilium backbone of individual anthocyanins collected in this study. The collected fractions that contained cyanidin was confirmed by the molecular mass [M^+] m/z of 287.0549, calculated for [M^+]: 287.0550 (mass error of 0.3 ppm). The purity of isolated cyanidin was 93%. The ^{1}H-NMR spectrum of cyanidin is presented in **Figure 3.6**.

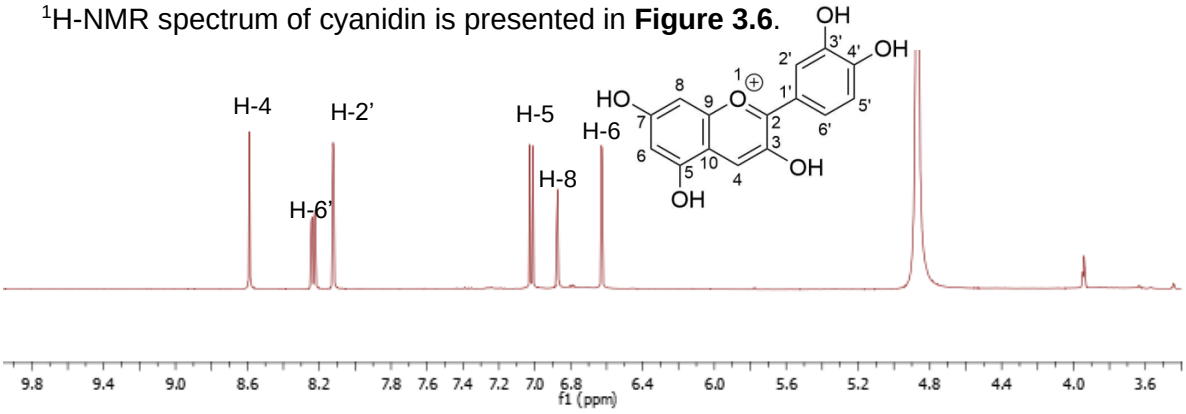

Figure 3.6 ^{1}H NMR spectrum (500 MHz) of cyanidin in CD_3OD/CF_3COOD (95:5, v/v) recorded at 25 °C. Concentration of 8.34 x10^{-3} M.

The proton at position 4, in a flavylium cationic form, has a diagnostic chemical shift (8.59 ppm) and appears as a singlet. The doublet of doublets at 8.23 ppm with coupling constants of 8.5 Hz and 2.0 Hz is assigned to H-6', which has *ortho* and *meta* coupling with H-5' and H-2', respectively. H-2' and H-5' are assigned as doublets at 8.12 and 7.02 ppm with the coupling constants of 2.0 Hz and 9.0 Hz, respectively. In the ^{1}H-^{1}H COSY spectrum (**Figure 3.7**), H-6' has a strong correlation

with H-5' (*ortho* coupling) and a weaker correlation with H-2' (*meta* coupling). Two doublets at 6.87 and 6.63 ppm are assigned to H-8 and H-6 with a coupling constant of 2.0 Hz for both peaks. H-8 and H-6 have a correlation shown in the COSY spectrum. Once all the protons have been assigned, the corresponding carbon peaks could be deduced from a ^{1}H-^{13}C HSQC experiment (**Figure 3.7**). The correlation of anthocyanin protons with corresponding carbons is summarised in **Table 3.3**.

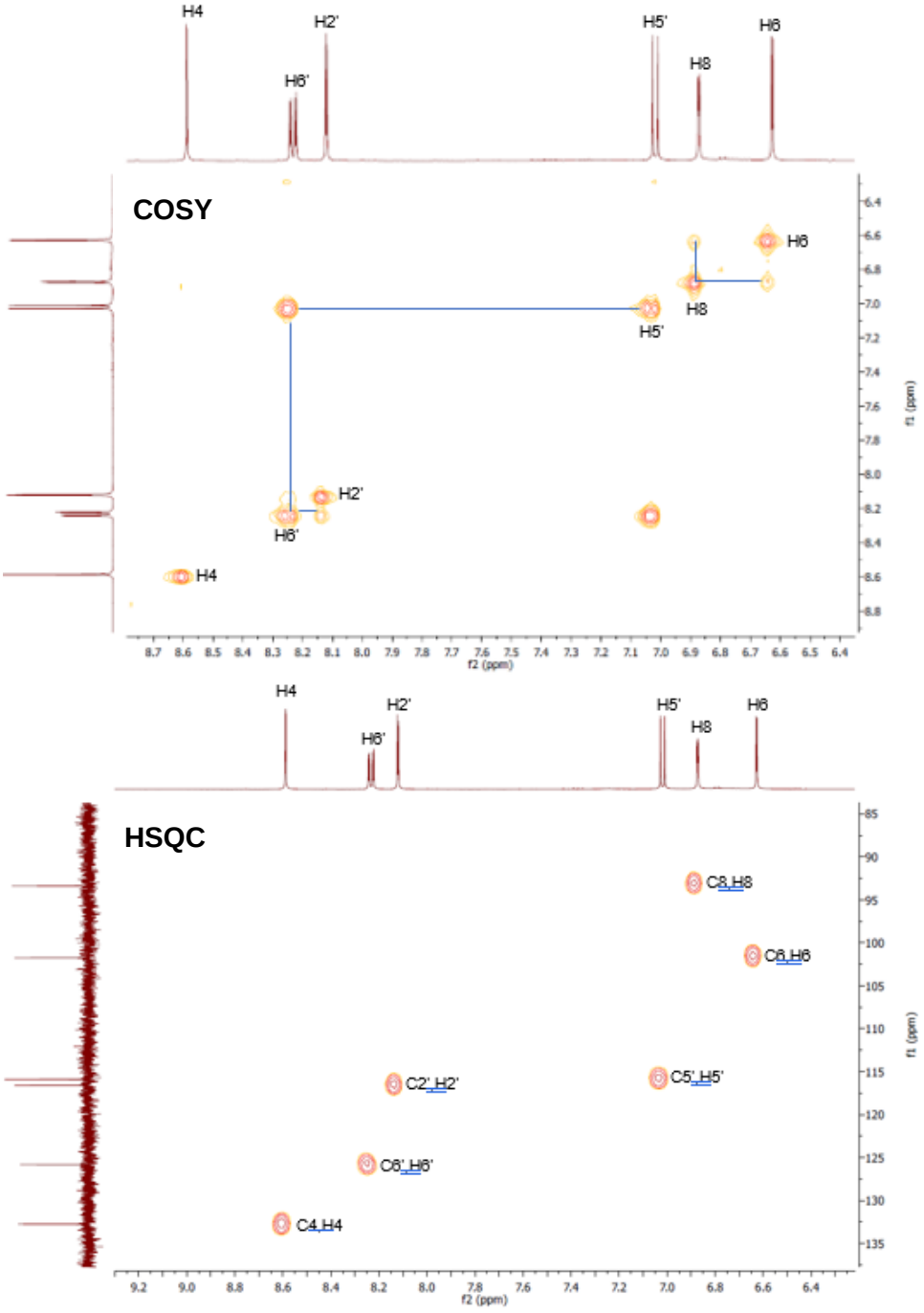

Figure 3.7 Expanded region of a ^{1}H-^{1}H COSY and ^{1}H-^{13}C HSQC spectrum (500 MHz) of cyanidin in CD_3OD/CF_3COOD (95:5) at 25 °C.

Table 3.3 ^{1}H (500 MHz) and ^{13}C (125 MHz) NMR Data for cyanidin in CD_3OD/CF_3COOD (95:5, v/v) at 25 °C.

Aglycone	Cy (experimental)		
	$\delta^{1}H$ (ppm)	J (Hz)	$\delta^{13}C$(ppm)
H-4	8.59	s	132.7
H-6'	8.23	dd, 8.5, 2.5	125.8
H-2'	8.12	d, 2.5	116.6
H-5'	7.02	d, 8.5	115.9
H-8	6.87	d, 2.0	101.7
H-6	6.63	d, 2.0	93.4

The 2D-NMR HMBC experiments (**Figure 3.8**) were performed to resolve the remaining carbons that are not attached to any protons. This technique shows the cross-peaks correlation of ^{1}H-^{13}C separated from each other with two or more chemical bonds away. A flavylium cationic form of cyanidin has three rings as a skeleton *i.e*. ring A, C and B, following the C_6-C_3-C_6 formula for general flavonoids. The cross-peaks at δ 8.59/160.8 (H-4/C2), 8.59/155.7 (H-4/C-5) and 8.59/145.3 (H-4/C-3) in the HMBC spectrum of cyanidin as the flavylium cationic form were used to assign C-2, C-5 and C-3, respectively. Similarly, the carbons belonging to the B-ring of cyanidin form were assigned from the cross-peaks at δ 8.23/160.8 (H-6'/C2), δ 8.23/153.8 (H-6'/C4'), δ 8.23/116.6 (H-6'/C2'), δ 8.12/153.8 (H-2'/C4'), δ 8.12/146.0 (H-2'/C3'), δ 8.12/125.8 (H-2'/C6'), δ 7.02/153.8 (H-5'/C4'), δ 7.02/146.0 (H-5'/C3'), δ 7.02/120.6 (H-5'/C1'). The rest of the A-ring of the cyanidin form were assigned from the cross-peaks at δ 6.87/167.6 (H-8/C7), 6.87/155.7 (H-8/C5), 6.87/112.3 (H-8/C10), 6.87/101.7 (H-8/C6), 6.63/167.6 (H-6/C7), 6.63/156.7 (H-6/C9), 6.63/112.3 (H-6/C10), 6.63/93.4 (H-6/C8). A summary of the long-range correlations observed in the HMBC spectrum is presented in **Table 3.4**. Additionally, a NOESY spectrum (**Figure 3.8**) shows the correlation in the space of H-6' and H-5'/H-2'/H-8, whereas H-2' correlates to H-6'/H-5'/H-8.

Table 3.4 Summary of the long-range correlations observed in the ^{1}H-^{13}C HMBC spectrum of cyanidin.

Proton	Correlated Carbon
4	2, 9, 5, 3
6'	2, 4', 2'
2'	4', 3', 6'
5'	4', 3', 1'
8	7, 9, 10, 6
6	7, 5, 10, 8

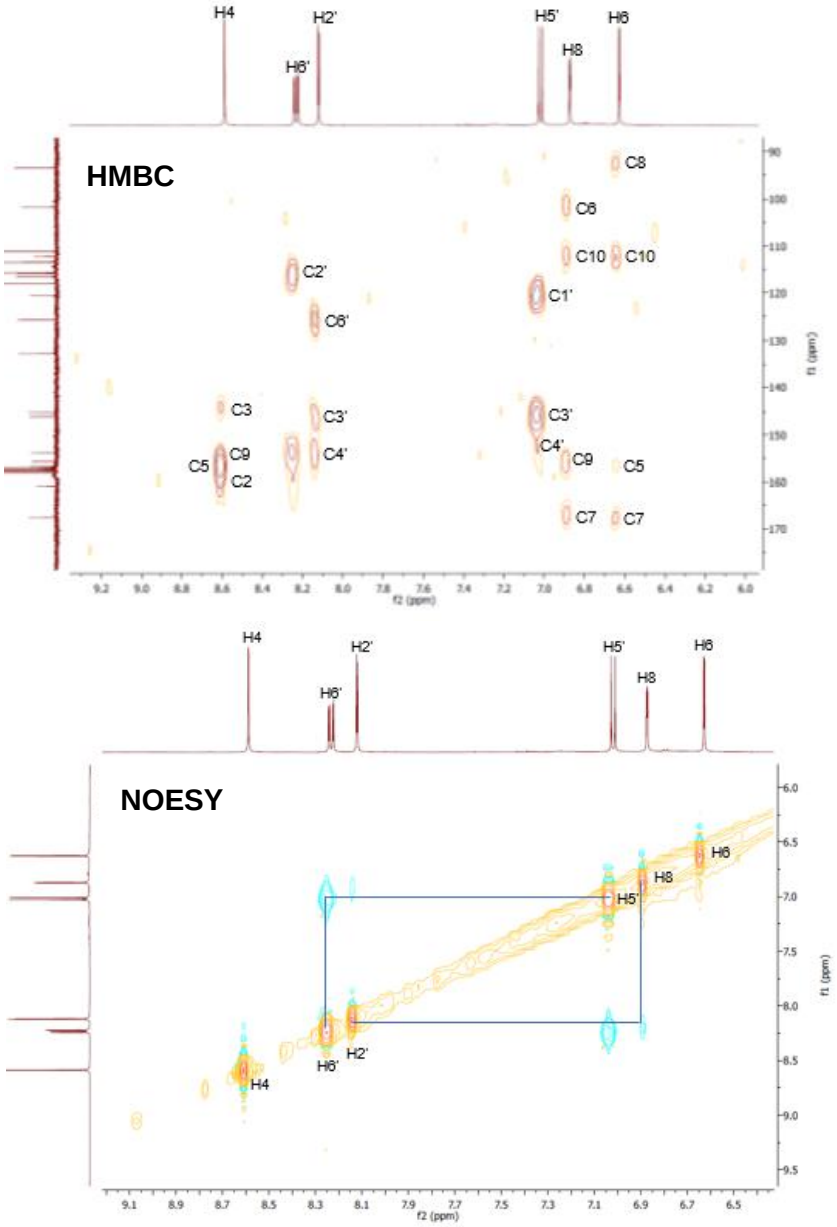

Figure 3.8 Expanded region of a ^{1}H-^{13}C HMBC and ^{1}H-^{1}H NOESY spectrum (500 MHz) of cyanidin in CD_3OD/CF_3COOD (95:5) at 25 °C.

3.1.1.2.2. Cyanidin-3-*O*-β-galactoside (Cy3gal)

Cy3gal is the major anthocyanin found in RASE and the first fraction collected from a semi-preparative HPLC with a retention time of 11.88 min. The collected fractions that contained Cy3gal was confirmed by the molecular mass [M^+] m/z of 449.1076, calculated for [M^+]: 449.1078 (mass error of 0.4 ppm) with a purity of 97%. The ^{1}H-NMR spectrum of Cy3gal is presented in **Figure 3.9**. The characterisation of this compound (^{1}H and ^{13}C) is summarised in **Table 3.5** and is in agreement with the characterisation conducted by Esatbeyoglu *et al*.[106]

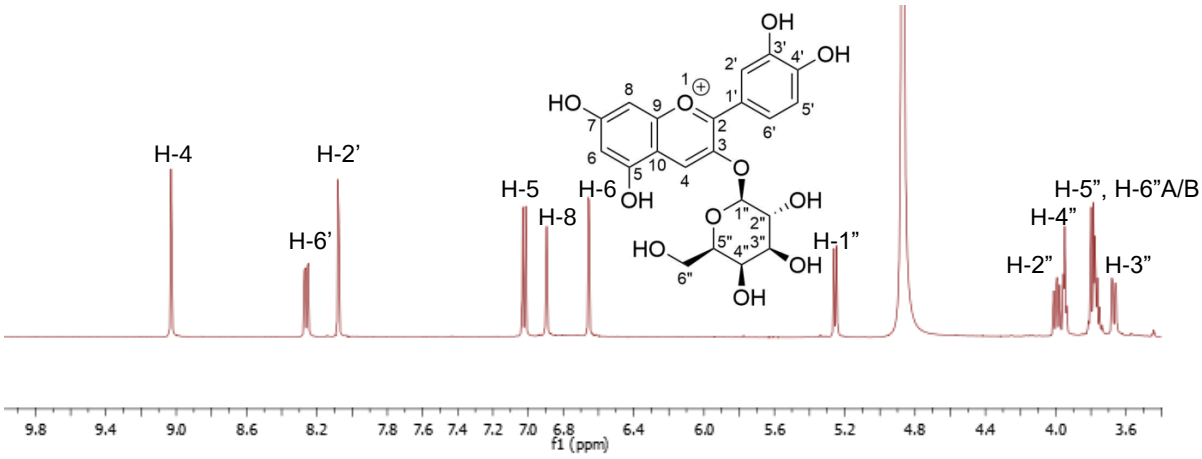

Figure 3.9 ^{1}H NMR spectrum (500 MHz) of cy3gal in CD_3OD/CF_3COOD (95:5, v/v) recorded at 25 °C. Concentration of $7.11x10^{-3}$ M.

Table 3.5 ^{1}H (500 MHz) and ^{13}C (125 MHz) NMR Data for Cy3gal in CD_3OD/CF_3COOD (95:5, v/v) recorded at 25 °C.

Aglycone	**Cy3gal (experimental)**			**Cy3gal (literature)**[106]		
	δ^{1}H (ppm)	J (Hz)	δ^{13}C(ppm)	δ^{1}H (ppm)	J (Hz)	δ^{13}C(ppm)
H-4	9.03	s	135.6	9.05	s	137.0
H-6'	8.26	dd, 8.5, 2.5	126.8	8.29	dd, 8.7, 2.2	128.3
H-2'	8.08	d, 2.5	117.1	8.09	d, 2.2	118.5
H-5'	7.02	d, 8.5	116.0	7.04	d, 8.7	117.4
H-8	6.90	d, 1.5	93.7	6.92	d, 1.8	95.2
H-6	6.66	d, 1.5	101.9	6.68	d, 1.7	103.4
Sugar						
H-1"	5.25	d, 7.5	103.0	5.29	d, 7.5	104.5
H-2"	3.99	dd, 9.5, 7.5	70.7	4.04	dd, 8.1, 8.9	72.1
H-3"	3.67	dd, 9.5, 3.5	73.5	3.72	dd, 3.2, 9.6	75.0
H-4"	3.94	d, 3.5	68.7	4.00	d, 3.1	70.1
H-5"	(3.82-3.73)	m	76.4	(3.80-3.85)	m	77.8
H-6"A/B			60.9			62.4

Data from literature was also recorded in the same solvent system, CD_3OD/CF_3COOD (95:5, v/v)

A COSY spectrum (**Figure 3.10**) is useful in assigning sugar peaks as they sometimes appear overlapping to each other peaks. The ^{1}H-^{1}H coupling constants for the anomeric protons are 7.5 Hz ($J_{ax\text{-}ax}$) and 1.5 Hz ($J_{ax\text{-}eq}$) for the β and α protons, respectively. The coupling constant of H-1" at 5.25 ppm, which appears as doublet was 7.5 Hz, thus this peak is assigned as β anomeric sugar.[27] H-2" has a strong correlation with H-1", therefore a doublet of doublet at 3.99 ppm with coupling constants of 7.5 Hz and 9.5 Hz is assigned as H-2". The same technique is used to distinguish H-3", H-4", H-5" and H-6"A/B. H-3" is assigned because of a strong correlation with H-2" shown in the COSY spectrum. It appears as a doublet of doublets at 3.67 ppm with coupling constants of 9.5 Hz and 3.5 Hz. H-4" also shows a strong correlation with H-3" as they are a neighbour proton to each other and can

be found at 3.94 ppm as a doublet with a coupling constant of 3.5 Hz. Meanwhile, H-5", H-6"A and H-6"B are found as multiplets at 3.73-3.82 ppm. This assignment has been confirmed with the reported literature.[106]

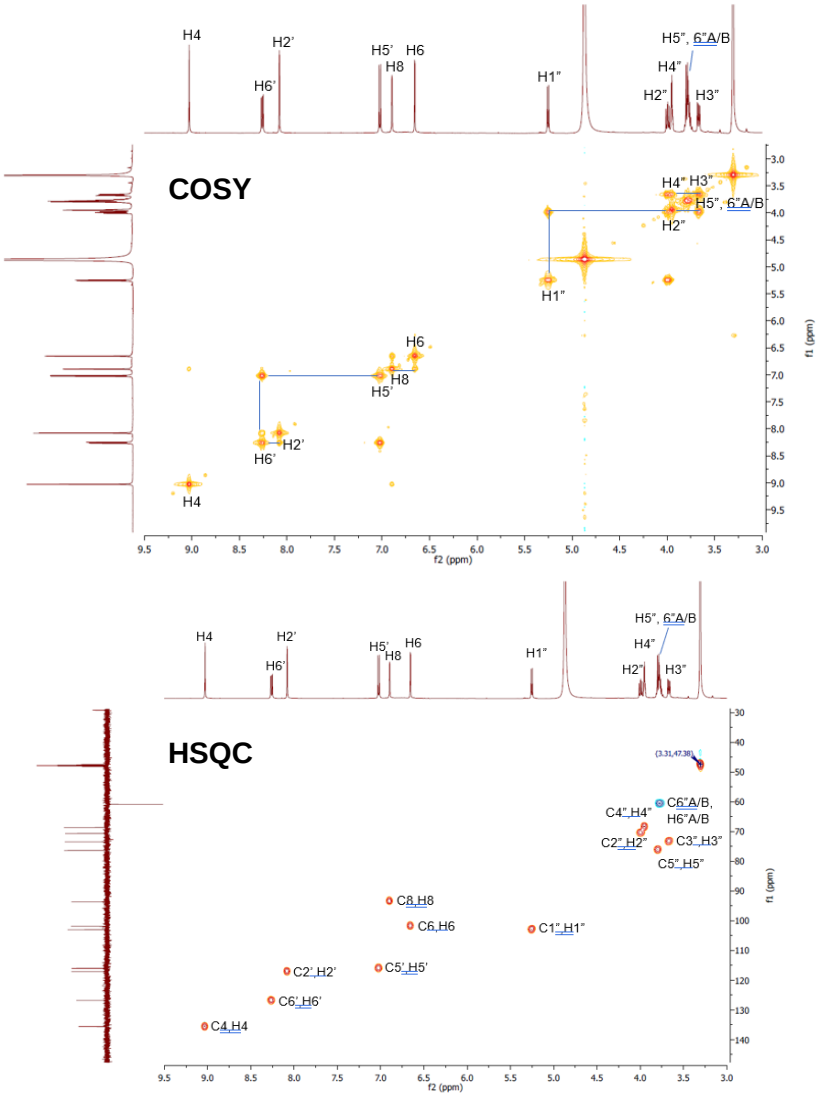

Figure 3.10 Expanded region of a ^{1}H-^{1}H COSY and ^{1}H-^{13}C HSQC spectrum (500 MHz) of Cy3gal at 25 °C in CD_3OD/CF_3COOD (95:5). The line shows a correlation of a proton with its correlated proton.

Once all the protons of cyanidin-3-*O*-β-galactoside were assigned, the corresponding carbon peaks could be deduced from ^{1}H-^{13}C HSQC experiments. In the HSQC spectrum (**Figure 3.10**), a ^{1}H-NMR spectrum was correlated to ^{13}C DEPT-135 spectrum and could differentiate methine (CH) from methylene (CH_2) correlations. Distortionless Enhancement by Polarisation Transfer (DEPT-135) was used to distinguish between the methylene group (-CH_2-) and the methyl (-CH_3) or methine (CH-) as this mode shows the negative peak for methylene and positive peak for

others. Previously, H-6”A/B (CH_2-) peaks at δ 3.73-3.82 ppm were assigned as a multiplet together with H-5”. Furthermore, in the HSQC spectrum, carbon of H-5” and H-6”A/B can be distinguished from each other as H-6”A/B peaks show negative peaks (blue) while H-5” shows a positive peak (red).

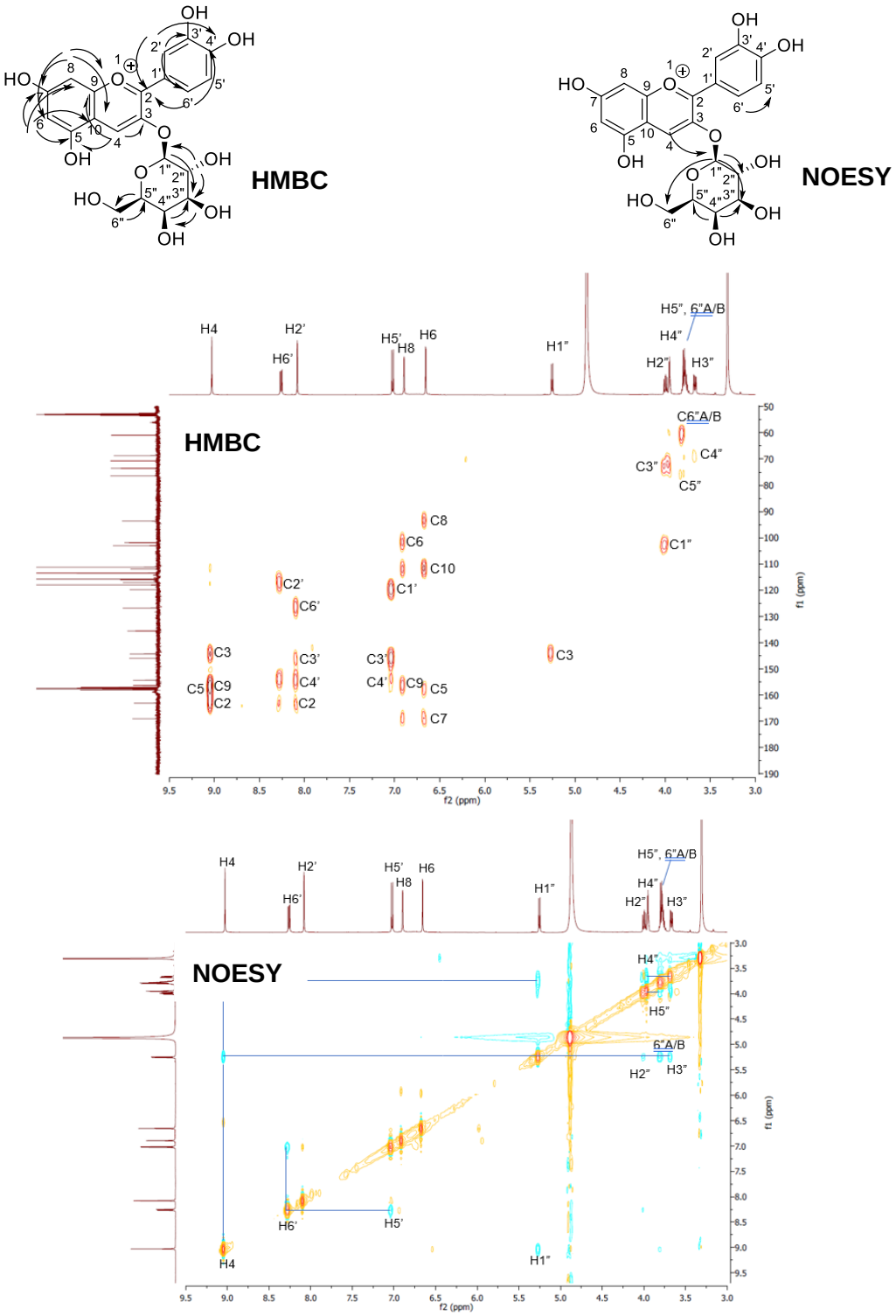

Figure 3.11 Expanded region of a ^{1}H-^{13}C HMBC (left) and ^{1}H-^{1}H NOESY (right) spectrum (500 MHz) of Cy3gal in CD_3OD/CF_3COOD (95:5) at 25 °C.

The cross-peaks at δ 9.03/163.1 (H-4/C2), 9.03/157.9 (H-4/C-5), 9.03/156.3 (H-4/C-9) and 9.03/144.3 (H-4/C-3) in the HMBC spectrum of cyanidin-3-*O*-galactoside as the flavylium cationic form were used to assign C-2, C-5, C-9 and C-3 (**Figure 3.11**). Similarly, the carbons belonging to the B-ring of anthocyanidin form were assigned from the cross-peaks at δ 8.26/163.1 (H-6'/C2), δ 8.26/154.4 (H-6'/C4'), δ 8.26/117.1 (H-6'/C2'), δ 8.08/163.1 (H-2'/C2), δ 8.08/154.4 (H-2'/C4'), δ 8.08/146.0 (H-2'/C3'), δ 8.08/126.8 (H-2'/C6'), δ 7.02/154.4 (H-5'/C4'), δ 7.02/146.0 (H-5'/C3'), δ 7.02/119.8 (H-5'/C1'). While the rest of the A-ring of anthocyanidin form were assigned from the cross-peaks at δ 6.90/169.0 (H-8/C7), 6.90/156.3 (H-8/C9), 6.90/112.0 (H-8/C10), 6.90/102.0 (H-8/C6), 6.66/169.0 (H-6/C7), 6.66/157.9 (H-6/C5), 6.66/112.0 (H-6/C10), 6.66/93.7 (H-6/C8). The cross-peaks at δ 5.25/144.3 (H-1"/C-3) confirm that the sugar moiety is connected to the aglycone at position 3. The other cross-peaks found in the upfield region were δ 3.99/103.0 (H-2"/C-1"), 3.99/73.5 (H-2"/C-3"), 3.94/73.5 (H-4"/C-3"), 3.73-3.82/62.4 (H-5"/C-6"A/B), 3.73-3.82/76.4 (H-6"A/B/C-5"), 3.67/68.7 (H-3"/C-4"). Summary of the long-range correlations observed in the ^{1}H-^{13}C HMBC spectrum of Cy3gal is presented in **Table 3.6**.

A Nuclear Overhauser Effect Spectroscopy (NOESY) experiment was the last technique to confirm the protons that are close to each other in space even if they are not bonded. This technique is useful when proton signals have not been assigned. As all protons of Cyanidin-3-*O*-β-galactoside have been assigned, a NOESY spectrum (**Figure 3.11**) was used to confirm the previous assignment. H-4 peak at 9.03 ppm has a strong correlation to H-1" and H-6"A/B. H-6' has a strong correlation with H-5'. H-1" has a strong correlation with H-2", H-3" and H-6"A/B. H-4" has strong correlations with H-3" and H-5".

Table 3.6 Summary of the long-range correlations observed in the ^{1}H-^{13}C HMBC spectrum of Cy3gal.

Proton	Correlated Carbon
4	2, 5, 9, 3
6'	2, 4', 2'
2'	2, 4', 3', 6'
5'	4', 3', 1'
8	7, 9, 10, 6
6	7, 5, 10, 8
1"	3
2"	1", 3"
4"	3"
5"	6"A/B
6"A/B	5"
3"	4"

3.1.1.2.3. Cyanidin-3-*O*-β-glucoside (Cy3glc)

The second fraction collected from the semi-preparative HPLC was Cy3glc. Cy3glc is the C-4'' epimer of Cy3gal, with the -OH group now equatorial. The collected fractions that contained Cy3glc was confirmed by the molecular mass [M^+] m/z of 449.1072, calculated for [M^+]: 449.1078 (mass error of 1.3 ppm). The purity of isolated Cy3glc was 97%. The ^{1}H-NMR spectrum of Cy3glc is presented in **Figure 3.12**.

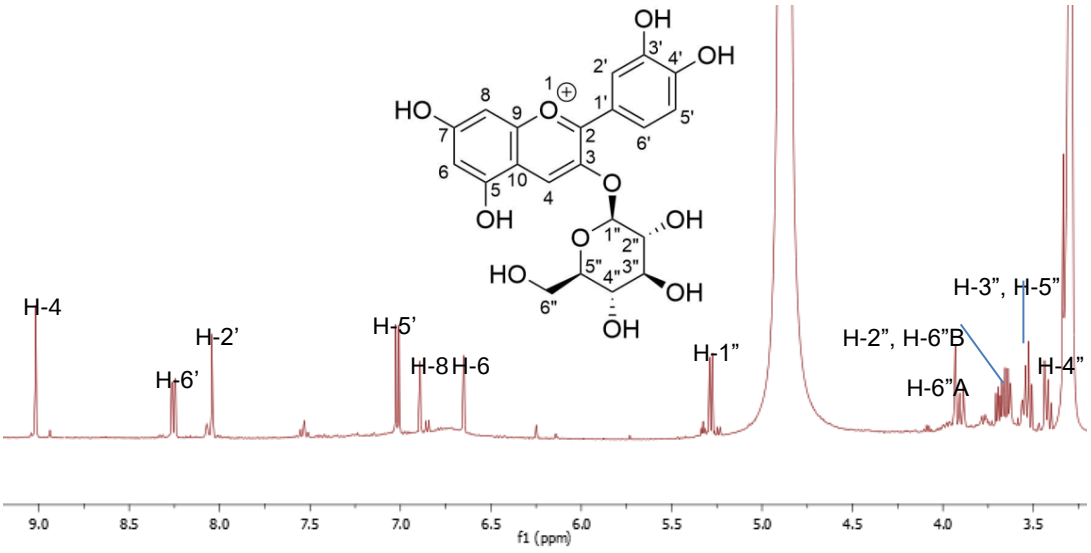

Figure 3.12 ^{1}H-NMR spectrum (500 MHz) of Cy3glc in CD_3OD/CF_3COOD (95:5, v/v) recorded at 25 °C. Concentration of 5.3 x10^{-3} M.

The coupling constant of H-1" at 5.28 ppm, which appears as doublet was 7.5 Hz, thus this is assigned as β anomeric sugar. H-2" has a strong correlation with H-1", therefore a doublet of doublet at 3.67 ppm with coupling constants of 9.5 Hz and 8.0 Hz was assigned as H-2". The same technique is used to distinguish H-3", H-4", H-5" and H6"A/B. H-3" peak is assigned because of a strong correlation with H-2" shown in the COSY spectrum. It appears as a doublet of doublets at 3.55 ppm with coupling constants of 9.5 Hz and 9.0 Hz. This proton is reported as a doublet in literature.[106] H-4" is assigned as doublet of doublets at 3.42 ppm with coupling constants of 9.5 Hz and 9.0 Hz. H-4" is assigned as double of doublet of doublets at 3.53 ppm with coupling constants of 9.5 Hz, 6.0 Hz and 2.0 Hz. Meanwhile, H-6"A is found as a doublet of doublets at 3.90 ppm with coupling constants of 2.5 Hz and 12.0 Hz. Additionally, H-6"B is assigned as a doublet of doublet at 3.69 with coupling constants of 6.0 Hz and 12.0 Hz. The corresponding carbon peaks could be deduced from ^{1}H-^{13}C HSQC experiments (**Figure 3.13**). The characterisation of this compound (^{1}H and

^{13}C) is summarised in **Table 3.7** and is in agreement with the characterisation conducted by Esatbeyoglu *et al*.[106]

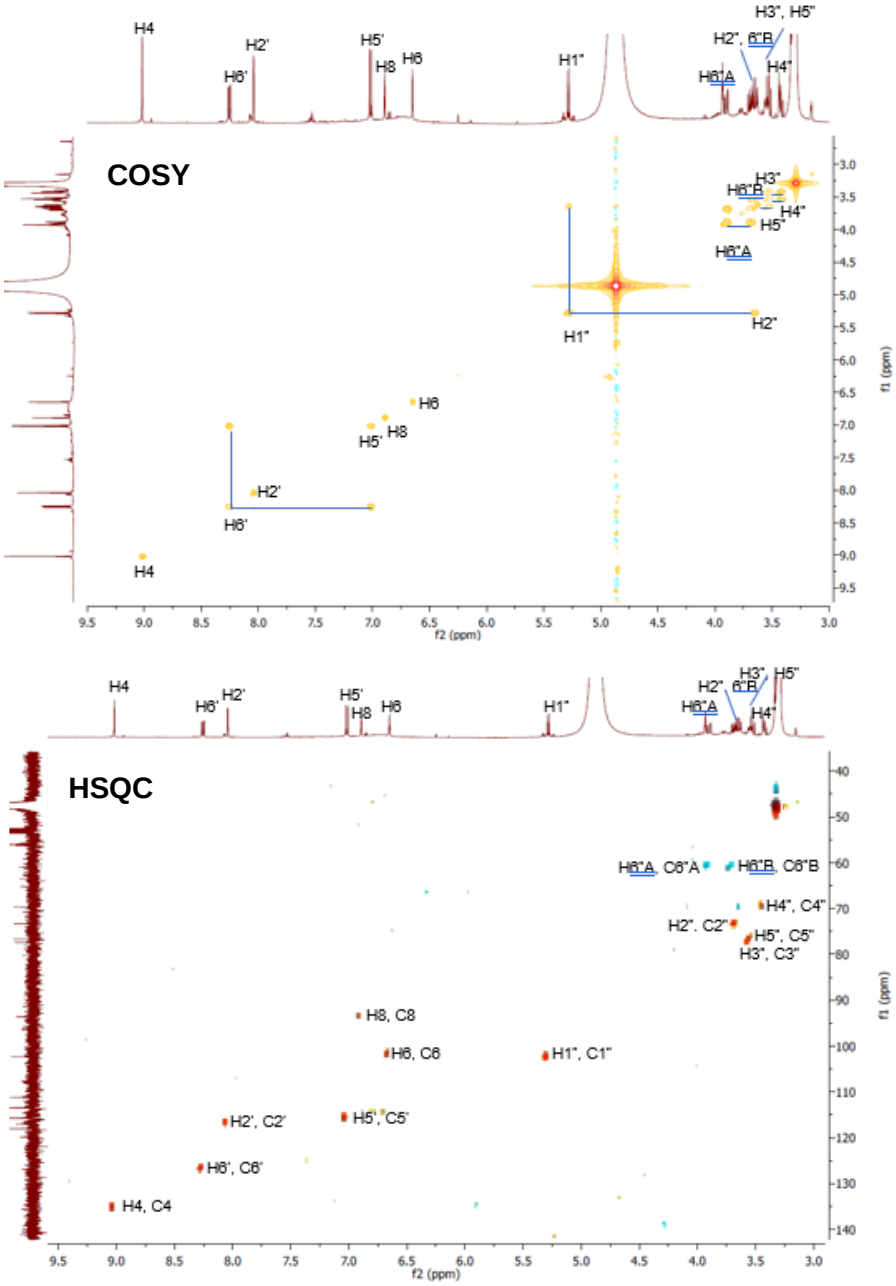

Figure 3.13 Expanded region of a ^{1}H-^{1}H COSY (left) and ^{1}H-^{13}C HSQC spectrum (right) (500 MHz) of Cy3glc in CD_3OD/CF_3COOD (95:5) at 25 °C.

Table 3.7 ^{1}H (500 MHz) and ^{13}C (125 MHz) NMR Data for Cy3glc in CD_3OD/CF_3COOD (95:5, v/v) at 25 °C.

Aglycone	Cy3glc (experimental)			Cy3glc (literature)[106]		
	$\delta^{1}H$ (ppm)	J (Hz)	$\delta^{13}C$(ppm)	$\delta^{1}H$ (ppm)	J (Hz)	$\delta^{13}C$(ppm)
H-4	9.02	s	135.8	9.06	s	137.1
H-6'	8.25	dd, 8.5, 2.5	126.9	8.29	dd, 8.7, 2.3	128.3
H-2'	8.04	d, 2.5	116.9	8.08	d, 2.3	118.5
H-5'	7.02	d, 8.5	115.8	7.05	d, 8.7	117.5
H-8	6.89	d, 1.5	93.6	6.93	dd, 0.8, 2.0	95.4
H-6	6.65	d, 1.5	101.7	6.69	d, 2.0	103.5
Sugar						
H-1"	5.28	d, 8.0	102.3	5.33	d, 7.8	103.9
H-2"	3.67	dd, 9.5, 8.0	73.3	3.71	dd, 7.9, 9.1	74.9
H-3"	3.55	dd, 9.5, 9.0	76.7	3.57	d, 9.1	78.2
H-4"	3.42	dd, 9.5, 9.0	69.6	3.48	dd, 9.3, 9.4	71.2
H-5"	3.53	ddd, 9.5, 6.0, 2.5	77.5	3.59	ddd, 2.3, 6.1, 8.9	78.9
H-6"A	3.90	dd, 12.0, 2.5	60.6	3.96	dd, 2.2, 12.1	62.5
H-6"B	3.69	dd, 12.0, 6.0	60.6	3.76	dd, 6.1, 12.1	62.5

Data from literature was also recorded in the same solvent system, CD_3OD/CF_3COOD (95:5, v/v)

3.1.1.2.4. Cyanidin-3-*O*-β-arabinoside (Cy3ara)

The third fraction collected from the semi-preparative HPLC was Cy3ara with a retention time of 14.97 min. This was confirmed by the molecular mass [M^+] m/z of 419.0967, calculated for [M^+]: 419.0973 (mass error of 1.4 ppm), and the purity of isolated Cy3ara was 97%. The ^{1}H-NMR spectrum of Cy3ara is presented in **Figure 3.14**.

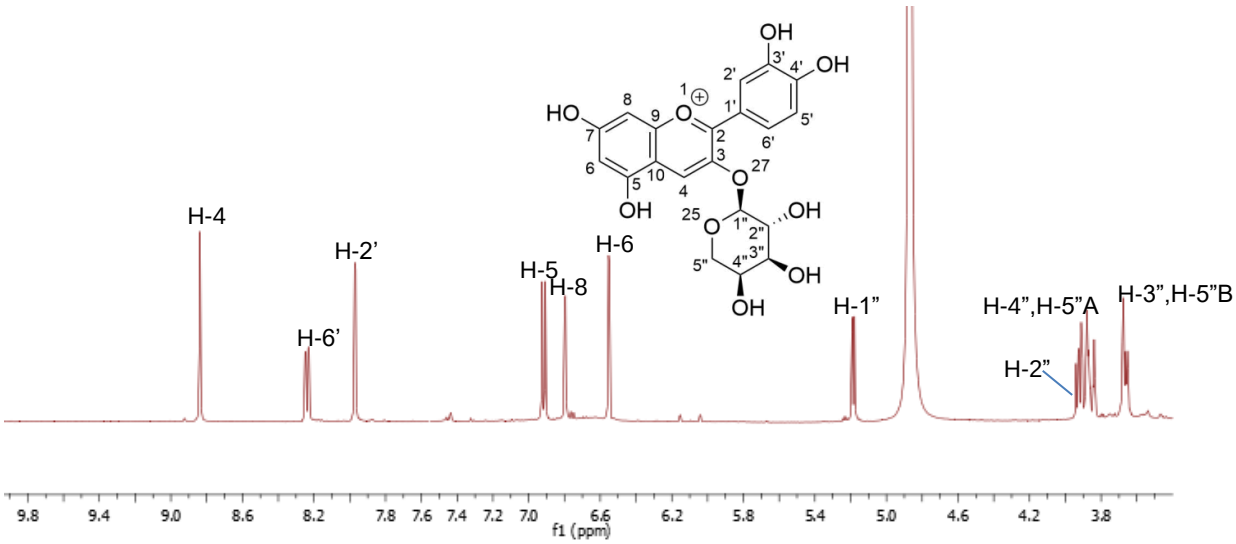

Figure 3.14 ^{1}H NMR spectrum (500 MHz) of Cy3ara in CD_3OD/CF_3COOD (95:5, v/v) recorded at 25 °C. Concentration of 6.26 x10^{-3} M.

The coupling constant of H-1" at 5.19 ppm, which appears as doublet was 6.0, thus this is assigned as β anomeric sugar. H-2" has a strong correlation with H-1",

therefore a doublet of doublets at 3.93 ppm with coupling constants of 6.0 Hz and 8.0 Hz was assigned as H-2”. The same technique is used to distinguish H-3”, H-4”, H-5”A and H5”B. H-3” peak is assigned because of a strong correlation with H-2” shown in the COSY spectrum (**Figure 3.15**). It appears as multiplets at 3.65-3.68 ppm together with H-5”B. H-4” also shows a strong correlation with H-3” as they are a neighbour proton to each other and can be found at 3.86-3.91 ppm as a multiplet together with H-5”A.

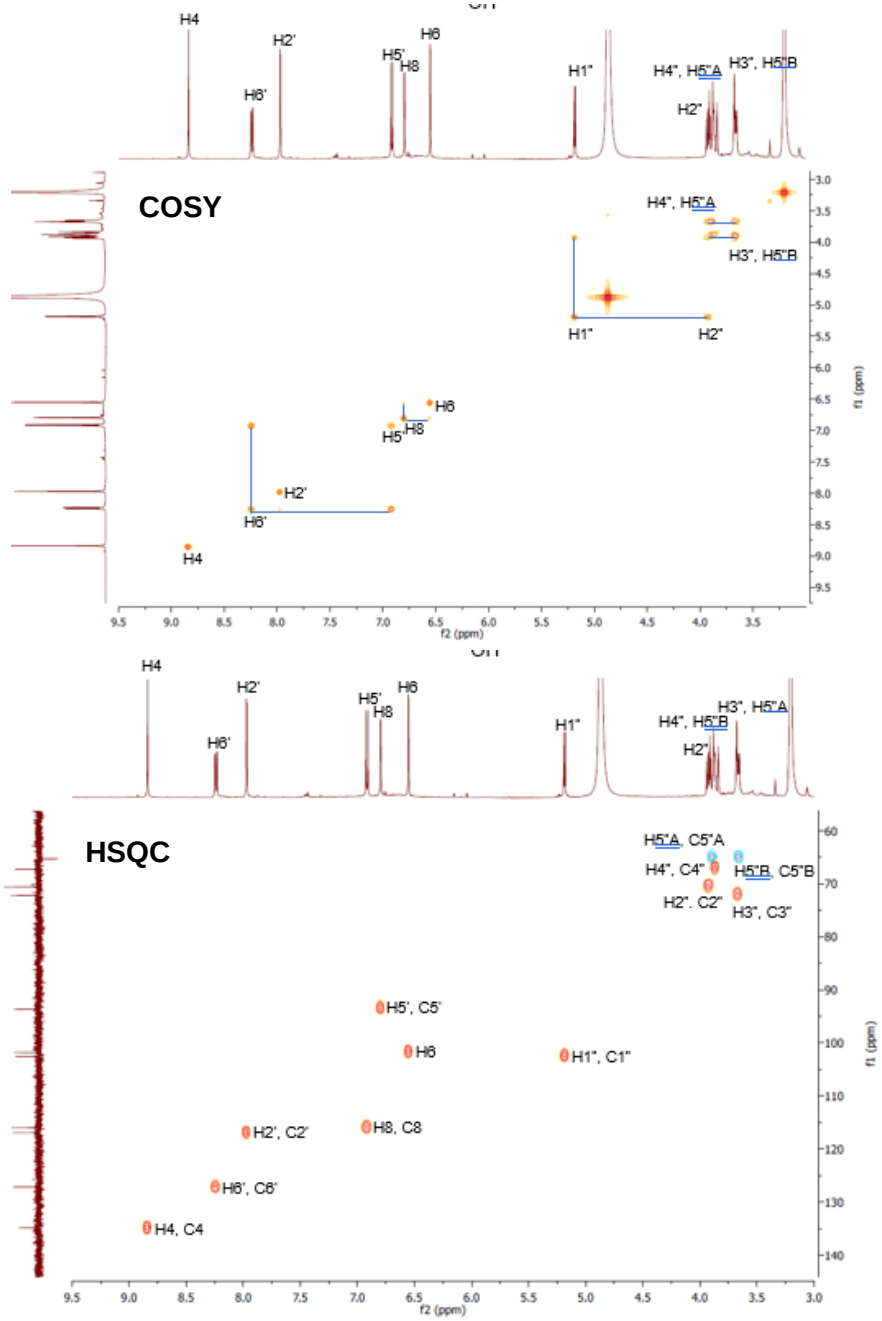

Figure 3.15 Expanded region of a ^{1}H-^{1}H COSY, ^{1}H-^{13}C HSQC and ^{1}H-^{1}H NOESY spectrum (500 MHz) of Cy3ara in CD_3OD/CF_3COOD (95:5) at 25 °C.

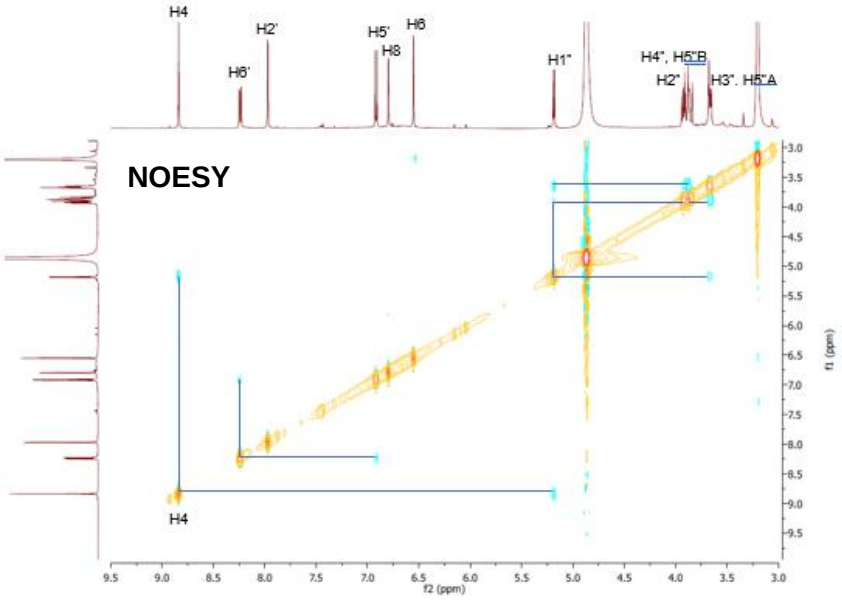

Figure 3.15. (continued).

Previously, H-5"A/B (CH_2-) peaks at δ 3.86-3.91 ppm and 3.65-3.68 ppm are assigned as multiplets together with H-4" and H-3". Furthermore, in the HSQC spectrum, carbon of H-3" and H-4" can be distinguished from H-5"A/B as H-5"A/B peaks show negative peak (singlet). In contrast, H-3" and H-4" show positive peaks (singlet). A NOESY spectrum (**Figure 3.15**) shows that H-4 peak at 8.84 ppm has a strong correlation to H-1" at 5.19 ppm. Additionally, H-1" correlates with H-5"A/B peaks which appear as multiplets at 3.86-3.91 and 3.65-3.68 ppm. The correlation of anthocyanin protons with corresponding carbons have been summarised in **Table 3.8**. This assignment has been confirmed with the reported literature.[106]

Table 3.8 ^{1}H (500 MHz) and ^{13}C (125 MHz) NMR Data for Cy3ara in CD_3OD/CF_3COOD (95:5, v/v) at 25 °C.

Aglycone	**Cy3ara (experimental)**			**Cy3ara (literature)**[106]		
	δ^{1}H (ppm)	J (Hz)	δ^{13}C(ppm)	δ^{1}H (ppm)	J (Hz)	δ^{13}C(ppm)
H-4	8.84	s	134.8	8.91	s	128.7
H-6'	8.24	dd, 9.0, 2.0	127.2	8.29	dd, 8.8, 2.3	121.3
H-2'	7.97	d, 2.0	116.9	8.03	d, 2.2	117.7
H-5'	6.92	d, 9.0	116.0	6.99	d, 8.8	117.5
H-8	6.80	d, 1.0	93.7	6.87	dd, 0.7, 1.7	95.2
H-6	6.55	d, 1.5	101.8	6.64	d, 1.7	103.5
Sugar						
H-1"	5.19	d, 6.0	102.6	5.27	d, 6.1	104.1
H-2"	3.93	dd, 8.0, 6.0	70.6	(3.97-3.99)	m	72.1
H-4"	(3.86-3.91)	m	67.3	3.57	ddd, 1.5, 6.3, 7.0	68.7
H-5"A	(3.86-3.91)	m	65.3	(3.97-3.99)	m	66.7
H-3"	(3.65-3.68)	m	72.2	3.79	dd, 2.2, 5.5	73.7
H-5"B	(3.65-3.68)	m	65.3	3.76	d, 5.4	66.7

Data from literature was also recorded in the same solvent system, CD_3OD/CF_3COOD (95:5, v/v)

3.1.1.2.5. Cyanidin-3-*O*-β-xyloside (Cy3xyl)

The fourth fraction collected from the semi-preparative HPLC was Cy3xyl with a retention time of 18.96 min. The collected fractions that contained Cy3xyl was confirmed by the molecular mass [M^+] m/z of 419.0967, calculated for [M^+]: 419.0973 (mass error of 1.4 ppm). The purity of isolated Cy3xyl was 91%. The ^{1}H-NMR spectrum of Cy3xyl is presented in **Figure 3.16**.

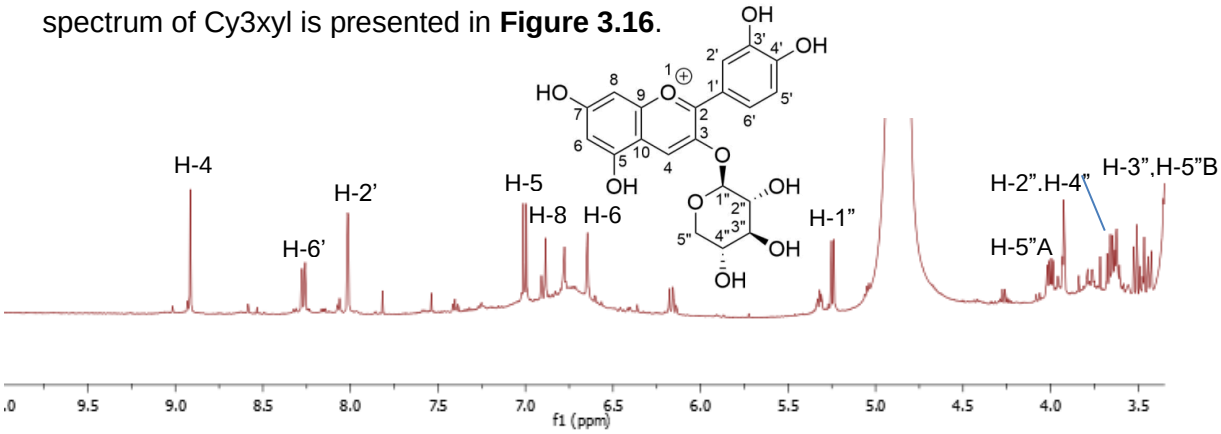

Figure 3.16 ^{1}H-NMR spectrum (500 MHz) of Cy3xyl in CD_3OD/CF_3COOD (95:5, v/v) recorded at 25 °C. Concentration of 6.26 x10^{-3} mM.

The coupling constant of H-1" at 5.25 ppm, which appears as doublet was 7.0, thus this is assigned as β anomeric sugar. H-2" has a strong correlation with H-1", therefore a doublet of doublets at 3.66 ppm with coupling constants of 7.5 Hz and 9.0 Hz is assigned as H-2". The same technique is used to distinguish H-3", H-4", H-5"A and H5"B. H-3" peak is assigned because of a strong correlation with H-2" shown in the COSY spectrum (**Figure 3.17**). It appears as multiplets at 3.44-3.53 ppm together with H-5"B. H-4" also shows a strong correlation with H-3" as they are a neighbour proton to each other and can be found at 3.98-4.02 ppm as a multiplet together with H-5"A.

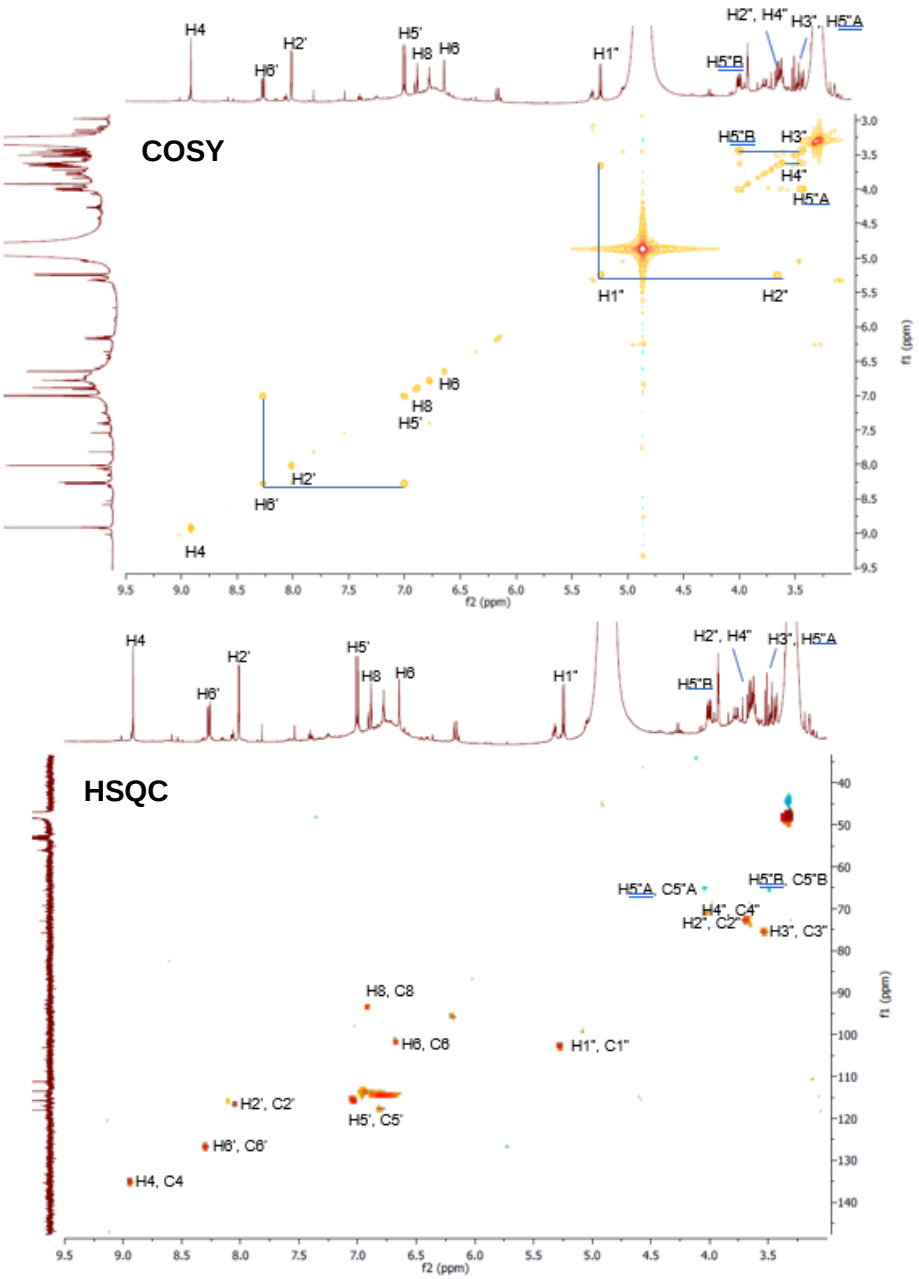

Figure 3.17 Expanded region of a ^{1}H-^{1}H COSY and ^{1}H-^{13}C HSQC spectrum (500 MHz) of Cy3xyl in CD_3OD/CF_3COOD (95:5) at 25 °C.

Previously, H-5”A/B (CH2-) peaks at δ 3.98-4.02 ppm and 3.44-3.53 ppm are assigned as multiplets together with H-4” and H-3”. Furthermore, in the HSQC spectrum (**Figure 3.17**), carbon of H-3” and H-4” can be distinguished from H-5”A/B as H-5”A/B peaks show negative peak (singlet). In contrast, H-3” and H-4” show positive peaks (singlet). The correlation of anthocyanin protons with corresponding carbons have been summarised in **Table 3.9**. This assignment has been confirmed with the reported literature.[106]

Table 3.9 ^{1}H (500 MHz) and ^{13}C (125 MHz) NMR Data for Cy3xyl in CD_3OD/CF_3COOD (95:5, v/v) at 25 °C.

Aglycone	Cy3xyl (experimental)			Cy3xyl (literature)[106]		
	$\delta^{1}H$ (ppm)	J (Hz)	$\delta^{13}C$(ppm)	$\delta^{1}H$ (ppm)	J (Hz)	$\delta^{13}C$(ppm)
H-4	8.92	s	135.4	8.97	s	137.0
H-6'	8.27	dd, 9.0, 2.5	127.1	8.29	dd, 8.7, 2.3	128.5
H-2'	8.01	d, 2.5	117.1	8.07	d, 2.3	118.0
H-5'	7.00	d, 9.0	116.1	7.06	d, 8.7	117.5
H-8	6.89	d, 1.0	93.5	6.93	d, 1.0	95.3
H-6	6.65	d, 1.0	101.8	6.69	d, 1.1	103.5
Sugar						
H-1"	5.24	d, 7.0	103.3	5.30	d, 7.1	104.7
H-2"	3.66	dd, 9.0, 7.0	72.8	3.72	dd, 7.2, 8.7	74.4
H-4"	3.63	ddd, 9.5, 8.5, 5.0	73.7	3.68	ddd, 5.0, 8.8, 9.2	70.8
H-5"A	4.00	dd, 11.5, 5.0	65.6	4.07	dd, 5.0, 11.5	67.1
H-3"	3.51	dd, 9.0, 8.5	75.5	3.57	dd, 8.3, 8.5	77.2
H-5"B	3.44	dd, 11.5, 9.5	65.6	3.51	dd, 9.5, 11.5	67.1

Data from literature was also recorded in the same solvent system, CD_3OD/CF_3COOD (95:5, v/v)

3.1.1.2.6. Characterisation of Polymeric Species

The last fraction collected from the semi-preparative HPLC was polymeric species with a retention time of 32.47. For polymeric species isolated from RASE, the resonance signals from repeating units appear as broad peaks, especially in the aromatic region, which could obscure other polyphenols' aromatic protons, even with high-field NMR spectrometers (600 MHz). Polymeric species are large molecules that lead to slow tumbling and poor molecular rotation of the backbone and the sidechain or groups of the polymers, resulting in invariably broad signals. In the literature, polymeric species in *Aronia* berries were reported to be polymeric proanthocyanidins in which (-)-epicatechins are the constitutive units, including extension unit and terminal unit (see **Section 1.2**, **Figure 1.10**).[4,68,119] The ^{1}H-NMR spectrum of polymeric species is presented in **Figure, 3.18**.

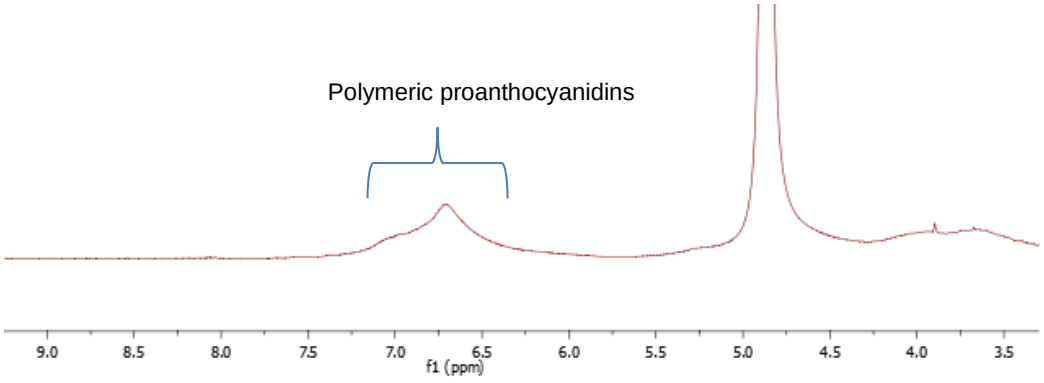

Figure 3.18 ^{1}H NMR spectrum (500 MHz) of polymeric proanthocyanidins in CD_3OD/CF_3COOD (95:5, v/v) recorded at 25 °C.

3.1.2. Purification of RASE by Liquid-liquid Extraction (LLE)

3.1.2.1. Isolation of Neutral Polyphenols from RASE

Liquid-liquid extraction (LLE) is a simple method to partition between liquid phases, usually an organic solvent and water. This method allows solubility based competition between two immiscible solvents to further purify the anthocyanins present in RASE from other non-anthocyanin polyphenols, which might be co-extracted or co-eluted during the extraction-purification process.[120] Organic solvents with different polarities such as ethyl acetate and isopropyl acetate were used in this study. Those organic solvents were selected as anthocyanins are much more soluble in water than the polar organic solvents. On the other hand, neutral polyphenols are more soluble in polar organic solvents than water.

LLE was carried out by dissolving RASE in acidified water (0.1% v/v HCl) to transform anthocyanins into a flavylium cationic form. Some of RASE did not dissolve completely and were removed by filtration. This insoluble material was confirmed as polymeric proanthocyanidins by ^{1}H-NMR spectroscopy (see **Section 3.1.1.2.6**). A sequential LLE of the acidified aqueous solution containing anthocyanins was then carried out using *i*propyl acetate followed by ethyl acetate. *i*propyl acetate and ethyl acetate were selected due to their polarity and immiscibility with water. The polarity index (P) of ethyl acetate is 4.4, and *i*propyl acetate is 4.2. The higher the polarity index, the higher polarity of this organic solvent.[121,122] Lipophilicity of *i*propyl acetate (1.02) is significantly greater than ethyl acetate (0.73), hence these two solvents can selectively extract non-anthocyanin polyphenols depending on the affinity of those polyphenols towards which organic solvents.[123]

The general rule of this separation is “Like Dissolves Like”. It means that polar solvents will dissolve ionic compounds and covalent compounds, which ionise, while nonpolar solvents will dissolve nonpolar covalent compounds. It indicates that the interaction between a solute(s) and solvent depends on the similarity of polarity amongst them.[121] The two organic layers can be distinguished visually from the aqueous layer, where the *i*propyl acetate layer was yellowish while the ethyl acetate layer was reddish. Each organic layer was evaporated to dryness. The neutral polyphenols isolated represented typically 14.2 % w/w of RASE. Meanwhile, the aqueous layer from LLE was freeze-dried and stored in the freezer. LLE is considered an appropriate technique for the semi-purification of anthocyanins extracted from the *Aronia* skin waste and can be scaled up relatively easily.[124]

3.1.2.2. Characterisation of Isolated Neutral Polyphenols from RASE

The dried organic residues of *i*propyl acetate and ethyl acetate extracts were dissolved in CD_3OD and analysed by ^{1}H-NMR spectroscopy. 2D NMR was carried out to assist the assignment of these compounds. *i*Propyl acetate could selectively extract less polar neutral polyphenols such as quercetin (Q) alongside 3,4-dihydroxybenzoic acid (DHBA). The ^{1}H-NMR spectrum of these polyphenols is presented in **Figure 3.19**. Meanwhile, ethyl acetate could isolate the remaining DHBA. It could also isolate more polar neutral polyphenols such as chlorogenic acid (CA) and neochlorogenic acid (nCA). The percentage of each component of non-anthocyanin polyphenols in RASE is quantified later. The ^{1}H-NMR spectrum of these polyphenols is presented in **Figure 3.20**.

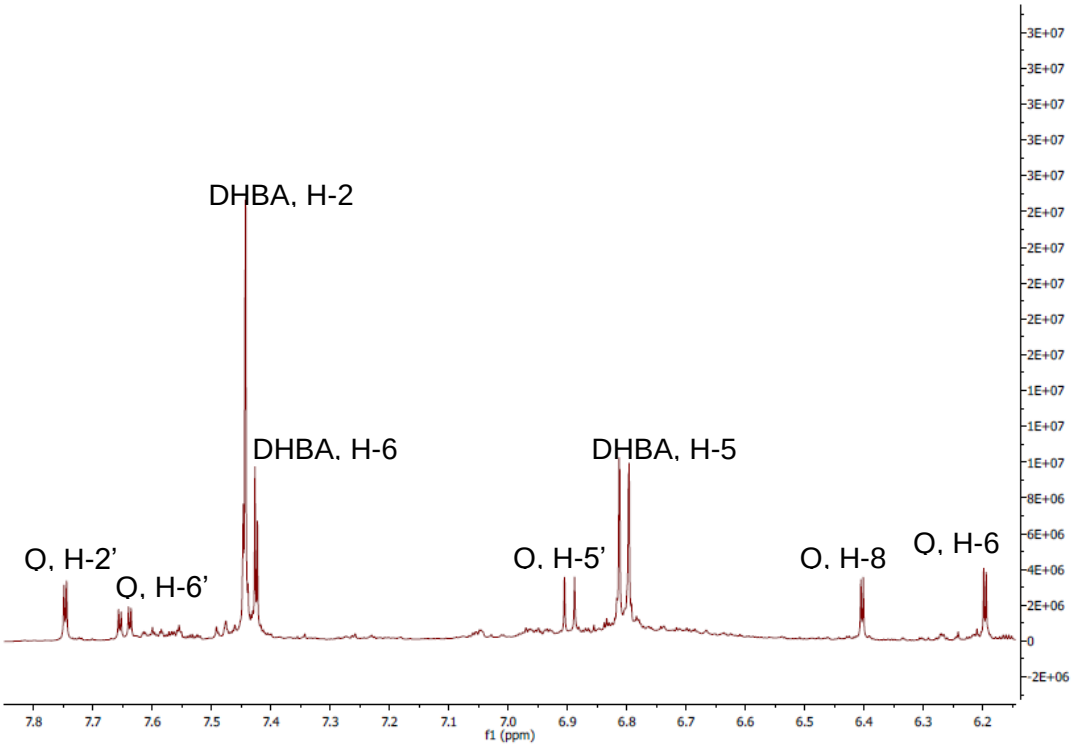

Figure 3.19 ^{1}H-NMR spectrum (500 MHz) of *i*propyl acetate layer in CD_3OD at 25 °C. DHBA: 3,4-dihydroxybenzoic acid. Q: quercetin.

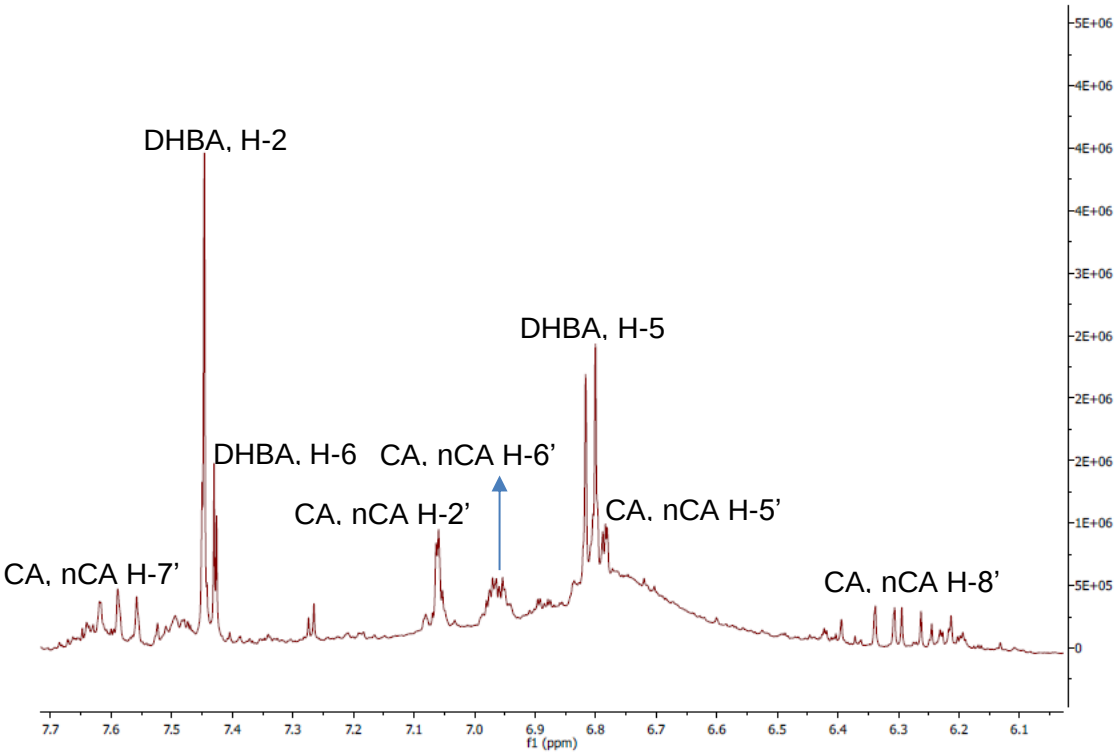

Figure 3.20 ^{1}H-NMR spectra (500 MHz) ethyl acetate layer in CD_3OD at 25 °C. DHBA: 3,4-dihydroxybenzoic acid. CA: chlorogenic acid. nCA: neochlorogenic acid.

3.1.2.2.1. Characterisation of polyphenols from *i*propyl acetate extraction.

3,4-Dihydroxybenzoic acid (DHBA, 39)

A doublet with a coupling constant of 2.0 at 7.46 ppm shows that it belongs to a proton that is *meta* coupled and is assigned as H-2. A doublet of doublets at 7.45 ppm with coupling constants of 2.0 and 8.5 shows that this proton is *ortho* and *meta* coupled with other protons. This proton is assigned as H-6. Finally, a proton that appears as a doublet at 6.82 ppm with a coupling constant of 8.5 is assigned as H-5. 2D NMR spectroscopy is carried out to assist the assignment of this compound. ^{1}H-^{1}H COSY shows a strong correlation between H-6 and H-5. Therefore, this compound was assigned as 3,4-dihydroxybenzoic acid (DHBA) or also known as protocatechuic acid (PCA), which has m/z of 153.0186 $[M-H]^+$, calculated for $[M-H]^-$: 153.0193 (mass error of 4.6 ppm); fragment m/z of 109.0283 $[M-H-CO_2]^-$ by HRMS. The assignment is summarised in **Table 3.10** and agreement with the results reported by Esatbeyoglu *et al*.[106]

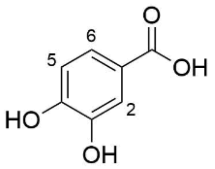

Table 3.10 ^{1}H-NMR spectra (500 MHz) of DHBA from *i*propyl acetate layer in CD_3OD at 25 °C.

	3,4-dihydroxybenzoic acid		Literature[106]	
	δ (ppm)	***J* (Hz)**	**δ (ppm)**	***J* (Hz)**
H-2	7.46	d, 2.0	7.44	s
H-6	7.45	dd, 2.0, 8.5	7.43	dd, 2.0, 8.5
H-5	6.82	d, 8.5	6.80	d, 8.5

Data from literature was also recorded in the same solvent system, CD_3OD

Quercetin (Q, 40)

A doublet at 7.75 with a coupling constant of 2.0 is assigned as H-2'. A doublet of doublet at 7.65 ppm with coupling constants of 2.0 and 8.5 shows that this proton was *ortho* and *meta* coupled with other protons, is assigned as H-6'. A doublet at 6.90 ppm with a coupling constant of 8.5 is assigned as H-5'. 2D NMR spectroscopy (^{1}H-^{1}H COSY) shows the strong correlation of H-6' and H-5' (*ortho* coupled). *Meta* coupling is shown by H-6' and H-2'. The neutral polyphenol is assigned as quercetin with m/z of 301.0352 $[M-H]^-$ by HRMS, calculated for $[M-H]^-$: 301.0354 (mass error of 0.7 ppm). The assignment is summarised in **Table 3.11** and agreement with the results reported by Penso *et al*.[125]

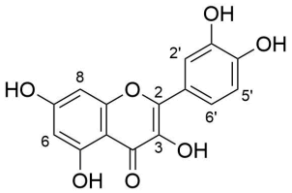

Table 3.11 ^{1}H-NMR spectra (500 MHz) of quercetin from *i*propyl acetate layer in CD_3OD at 25 °C.

	Quercetin		Literature[125]	
	δ (ppm)	***J* (Hz)**	**δ (ppm)**	***J* (Hz)**
H-2'	7.75	d, 2.0	7.67	d, 2.3
H-6'	7.65	dd, 2.0, 8.5	7.54	dd, 2.3, 8.4
H-5'	6.90	d, 8.5	6.88	d, 8.4
H-8	6.40	d, 2.0	6.40	d, 2.3
H-6	6.20	d, 2.0	6.18	d, 2.0

Data from literature is also recorded in the same solvent system, CD_3OD

3.1.2.2.2. Characterisation of Polyphenols from Ethyl Acetate Extraction

Neochlorogenic Acid (nCA, 31)

A doublet at 7.60 ppm with a coupling constant of 16.0 Hz is assigned as H-7'. The high coupling constant shows that this proton is *trans* coupled with another proton. H-2' signal is found at 7.06 ppm as a doublet with a coupling constant of 2.0. H-6' is

found at 6.96 ppm as a doublet of doublet with coupling constants of 8.0 and 2.0. A doublet at 6.80 ppm with a coupling constant of 8.0 is assigned as H-5'. 2D NMR spectroscopy (^{1}H-^{1}H COSY) shows the strong correlation of H-6' and H-5' (ortho coupled). *Meta* coupling is shown by H-6' and H-2'. A doublet at 6.32 ppm with a coupling constant of 16.0 belongs to H-8' and correlates strongly to H-7'. The remaining protons that belong to quinic acid appear as multiplets. This compound is assigned as neochlorogenic acid or 3-caffeoyl-(-)-quinic acid with m/z of 353.0872 $(M-H)^{-\cdot}$; calculated for $[M-H]^{-\cdot}$: 353.0878 (mass error of 1.7 ppm); fragment m/z of 191.0552, which belongs to a neutral loss of glucose (fragment loss of 162.032 amu) by ESI-MS/MS.[126] The assignment is summarised in **Table 3.12** and agreement with the results reported by Esatbeyoglu *et al*.[106]

Chlorogenic Acid (CA, 30)

A doublet at 7.57 ppm with a coupling constant of 15.5 Hz is assigned as H-7'. The high coupling constant shows that this proton is *trans* coupled with another proton. H-2' signal is found at 7.06 ppm as a doublet with a coupling constant of 2.0. H-6' is found at 6.97 ppm as a doublet of doublet with coupling constants of 8.0 and 2.5. A doublet at 6.79 ppm with a coupling constant of 8.0 is assigned as H-5'. 2D NMR spectroscopy (^{1}H-^{1}H COSY) shows the strong correlation of H-6' and H-5' (*ortho* coupled). *Meta* coupling is shown by H-6' and H-2'. A doublet at 6.28 ppm with a coupling constant of 15.5 belongs to H-8' and correlates strongly to H-7'. The remaining protons that belong to quinic acid appear as multiplets. This compound is assigned as chlorogenic acid or 5-caffeoyl-(-)-quinic acid with m/z of 353.0872 $[M-H]^-$; calculated for $[M-H]^{-\cdot}$: 353.0878 (mass error of 1.7 ppm); fragment m/z of 191.0552, which belongs to a neutral loss of glucose (fragment loss of 162.032 amu) by ESI-MS/MS.[126] The assignment is summarised in **Table 3.12** and agreement with the results reported by Esatbeyoglu *et al*.[106]

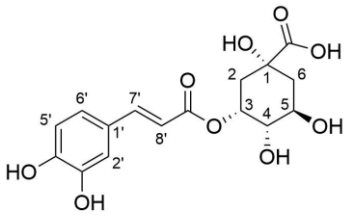

Neochlorogenic acid (**nCA**)

3-Caffeoyl-(-)-quinic acid

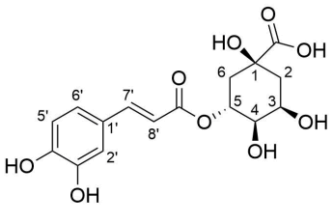

Chlorogenic acid (**CA**)

5-Caffeoyl-(-)-quinic acid

Table 3.12 ^{1}H-NMR spectra (500 MHz) of nCA and CA from ethyl acetate layer in CD_3OD at 25 °C.

	nCA		**Literature**[106]		**CA**		**Literature**[106]	
	δ (ppm)	***J* (Hz)**	**δ (ppm)**	***J* (Hz)**	**δ (ppm)**	***J* (Hz)**	**δ (ppm)**	***J* (Hz)**
H-7'	7.60	d, 16.0	7.59	d, 15.9	7.57	d, 15.5	7.56	d, 15.9
H-2'	7.06	d, 2.0	7.05	d, 1.7	7.06	d, 2.5	7.05	d, 2.0
H-6'	6.96	dd, 8.0, 2.0	6.94	dd, 8.2, 1.6	6.97	dd, 8.0, 2.5	6.95	dd, 8.2, 2.0
H-5'	6.80	d, 8.0	6.78	d, 8.1	6.79	d, 8.0	6.78	d, 8.2
H-8'	6.32	d, 16.0	6.30	d, 15.9	6.28	d, 15.5	6.26	d, 15.9
H-3	5.34-5.37	m	5.36	d, 2.6	4.10-4.16	m	4.17	dd, 7.0, 4.0
H-4	3.73-3.76	m	3.66	dd, 8.0, 2.5	3.73-3.76	m	3.72	dd, 8.6, 3.1
H-5	4.10-4.16	m	4.14	dt, 8.5, 3.2	5.26-5.29	m	5.34	dt, 9.1, 4.3
H-2A/B	2.11-2.23	m	1.90-2.28	m	2.06-2.19	m	2.03-2.13	m
H-6A/B	2.11-2.23	m	1.90-2.28	m	2.06-2.19	m	2.07-2.23	m

Data from literature was also recorded in the same solvent system, CD_3OD

The ^{1}H-NMR spectrum of the original RASE was compared to the ^{1}H-NMR spectrum of aqueous phase residues after further purified by LLE against ^{i}propyl acetate, followed by ethyl acetate (**Figure 3.21**). Both ^{i}propyl acetate and ethyl acetate layers alongside the insoluble solid spectra were also compared. The percentage of each isolated polyphenol by LLE was estimated based on the integration in the ^{1}H-NMR spectra. The further purification of RASE by LLE enriched the anthocyanin content. It removed most of the non-anthocyanin polyphenols such as 3,4-dihydroxybenzoic acid (DHBA, 7.1%), quercetin (Q, 2.4%), chlorogenic acid (CA, 2.4%) and neochlorogenic acid (nCA, 2.4%). Polymeric proanthocyanidins could also be partially removed by filtration during the dissolution of RASE in acidified water at the first LLE stage. The intensity of cyanidin as the anthocyanins' deglycosylation product was observed increasing compared to the initial cyanidin in the original RASE. As already discussed in **Chapter 2**, **Section 2.2.2.3**, cyanidin formation could occur during the evaporation of acidified aqueous layer in the freeze dryer as at this stage, the remaining acid was concentrated and could hydrolysis anthocyanins. This relatively pure RASE gives advantages for synthetic studies and characterisation of chemically modified anthocyanins products due to the low complexity of polyphenol profile in this RASE.

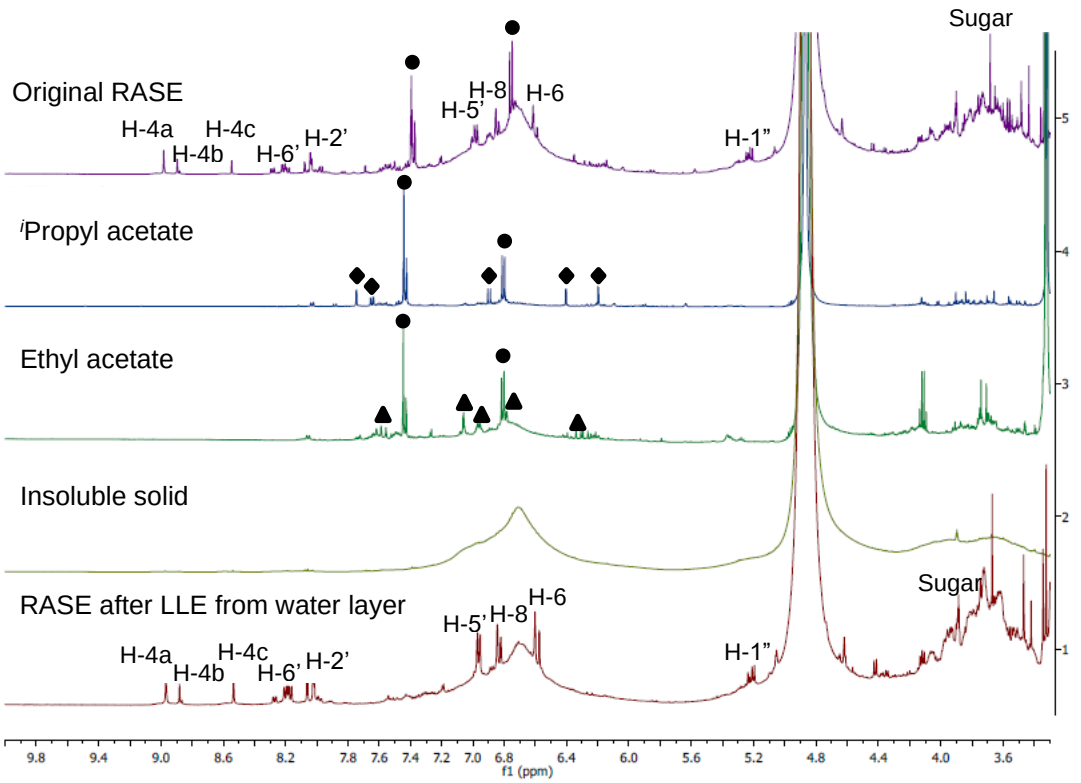

Figure 3.21 ^{1}H-NMR spectra (500 MHz) of original RASE, ^{i}propyl acetate and ethyl acetate layers, insoluble solid and RASE after LLE from water layer in CD_3OD at 25 °C. H-4a belongs to Cy3gal and Cy3glc, H-4b belongs to Cy3ara and Cy3xyl, and H-4c belongs to Cyanidin. (●) 3,4-dihydroxybenzoic acid (DHBA). (♦) Quercetin. (▲) Chlorogenic acid and neochlorogenic acid;

3.1.3. Biotage Flash Purification Studies

Another technique to purify RASE was through Biotage flash purification. Polymeric proanthocyanidins were reported to be the predominant polyphenols found in *Aronia* berries.[4] The presence of these compounds may adversely affect the chemical reaction on anthocyanins, and also complicate characterisation. The Biotage system cannot isolate single anthocyanins, but it can separate most anthocyanins from the polymeric species in the column. This separation takes a shorter separation time compared to other techniques and can also be scaled up. The method used in Biotage flash purification followed the optimum condition for separating anthocyanins from RASE in an analytical HPLC-DAD method with some modification. The mobile phase consisted of Solvent **A,** which was acidified water (an additive of TFA: 0.5%) and Solvent **B,** which was acetonitrile. This purification used a reversed-phase C18-Aq cartridge. The detection for the collection of fractions was monitored at 520 nm.[69] Other compounds which have no absorption at this wavelength were discarded. The elution profile of anthocyanins is shown in **Figure 3.22.** There were three fractions collected which were then freeze-dried and stored in the freezer for further use. Each fraction was analysed by LC-MS/HRMS, HPLC-DAD and ^{1}H-NMR.

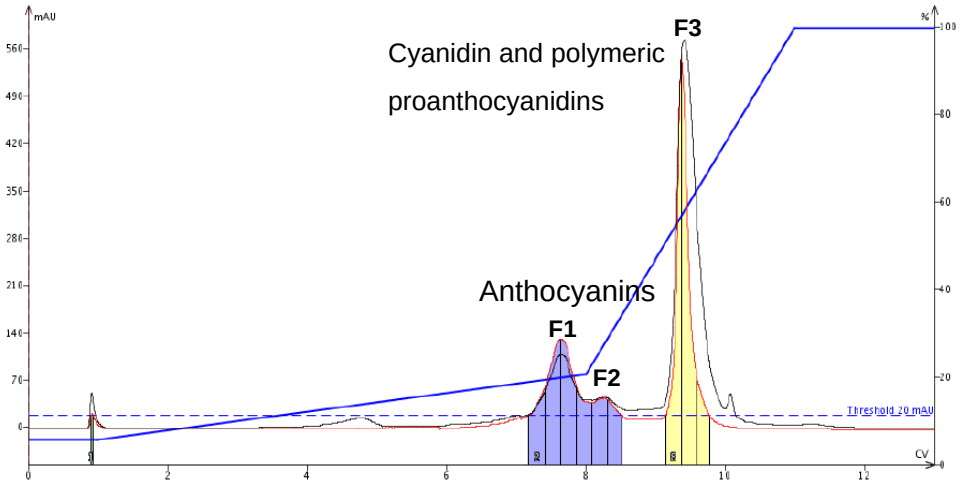

Figure 3.22 The elution profile of a Biotage flash purification. Collection at 520 nm (– red line) and monitor at 280 nm (– black line). F1: Fraction 1; F2: Fraction 2; F3: Fraction 3.

The HPLC chromatograms of dried Biotage fractions are presented in **Figure 3.23.** Cy3gal eluted first, followed by Cy3glc, Cy3ara, Cy3xyl, cyanidin and polymeric species. The separation of anthocyanins from other components follows the polarity interaction principle as in the analytic HPLC (see **Chapter 2**, **Section 2.2.2**). Fraction 1 mostly contained Cy3gal (89.6%), Cy3glc (4.9%) and Cy3ara (5.5%). Polymeric proanthocyanidins were not detected in this fraction. This finding was confirmed by HRMS, which shows that Fraction 1 has m/z of 449.1087 $[M]^{+\cdot}$ which belongs to Cy3gal and Cy3glc, whereas m/z of 419.0978 $[M]^{+}$ belongs to Cy3ara. A fragment was also found with m/z of 287.0548 $[M]^{+\cdot}$ which belong to cyanidin aglycone.

Fraction 2 mostly contained Cy3ara (97.2%) and a small quantity of Cy3xyl (2.8%). Polymeric proanthocyanidins were also not found in this fraction. Fraction 2 has m/z of 419.0986, with a fragment that has m/z of 287.0551. This m/z belongs to Cy3ara and Cy3xyl.

Fraction 3 contained cyanidin and polymeric proanthocyanidins. Polymeric species were only found in this fraction, suggesting that Biotage flash purification successfully separate and purify anthocyanins from polymeric proanthocyanidins. Fraction 3 has m/z of 287.87, which belongs to cyanidin by LC-MS. However, polymeric proanthocyanidins could not be characterised by this technique. To confirm this finding, NMR experiments were run (**Figure 3.24**). The assignment of polyphenols from RASE, which have absorbance at 520 nm, has been discussed in **Section**

3.1.1.2. It can be concluded that this technique is suitable for the removal of polymeric species from RASE to get purer samples for further application.

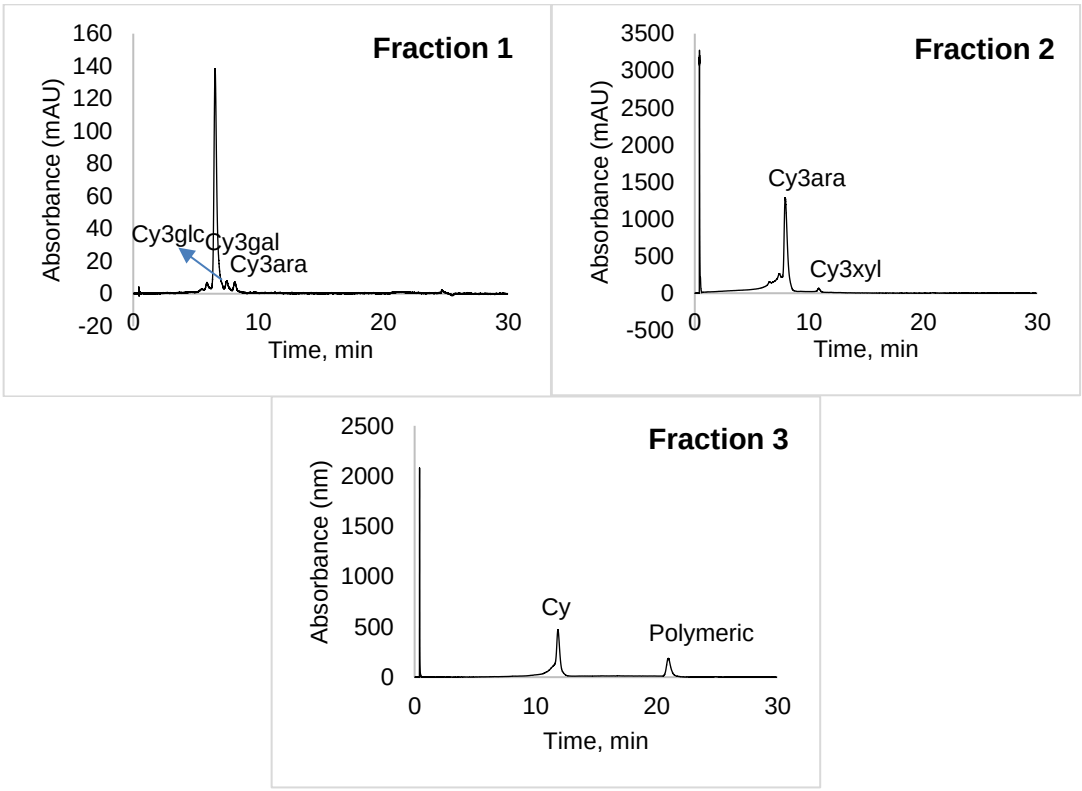

Figure 3.23 Elution profile of all fractions from Biotage flash purification by HPLC-DAD. Detected at 520 nm.

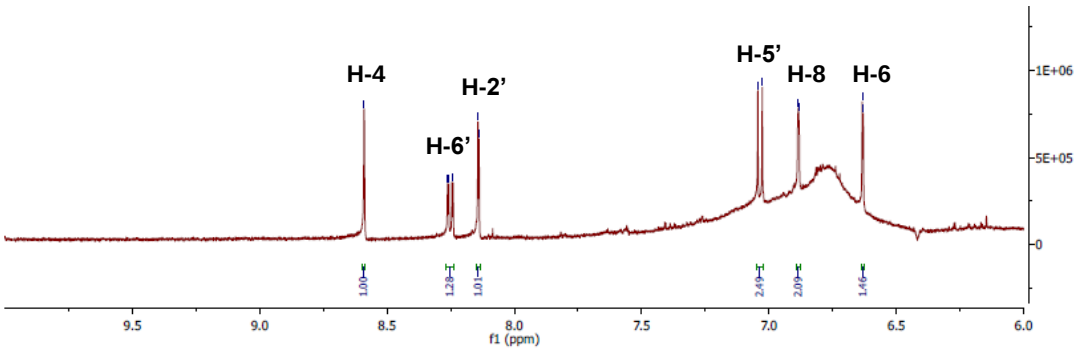

Figure 3.24 ^{1}H-NMR spectrum of Fraction 3 of Biotage purification showing the presence of cyanidin and polymeric proanthocyanidins. Solvent: CD_3OD.

3.1.4. Summary: Efficient Separation and Purification of Anthocyanins from *Aronia* Skin Waste

According to the results for the separation and purification of anthocyanins from *Aronia* skin waste, each method's efficiency can be summarised in **Table 3.13**.

Table 3.13 Comparison of purification methods for the production of anthocyanins from *Aronia* skin waste.

	Semi-preparative HPLC-DAD	**Liquid-liquid Extraction (LLE)**	**Biotage Flash Purification**
Selectivity	Very good. It can isolate the desired Individual anthocyanins and aglycone with high purity	Fair. It can isolate neutral non-anthocyanins polyphenols. It cannot separate anthocyanins from polymeric proanthocyanidins	Good. It can separate anthocyanins from polymeric proanthocyanidins. Fraction 1 mostly contained Cy3gal (89.6%), and Fraction 2 mostly contained Cy3ara (92.7%).
Scale-up	No and expensive	Yes and cheap	Yes and moderately cheap
Sample quantity for injection	mg scale (10 mg/mL) for XBridge Prep C18, 10 x 50, 5 µm in 900 µL injections	It depends on the size of the separating funnel. Up to 2 g for a 2 L separating funnel.	It depends on the column size. Up to 1 g for Redisep RF Gold® C18 Reversed Phase Column, 50 mg
Solvent	Solvent A: Water (0.5% TFA)	Aqueous solvent: Water (0.1% HCl)	Solvent A: Water (0.5% TFA)
	Solvent B: Acetonitrile.	Organic solvent: Ethyl acetate and ipropyl acetate	Solvent B: Acetonitrile.
Time	30-40 min	*Ca*. 30 min. If it forms an emulsion, then it takes longer to separate the two immiscible layers.	20 min
Equipment	HPLC-DAD equip.	Separating funnel	Biotage-DAD equip.
	HPLC Column	Conical flasks	Biotage Column
	Fraction collector		Fraction collector

Individual anthocyanins can be isolated through a semi-preparative HPLC-DAD with high purity. However, the purification through this method results in mg scale yield and is quite expensive to scale up. This method is suitable to obtain individual compounds for identification and characterisation purposes. A Biotage flash purification could separate anthocyanins from polymeric species. This purification method can be scaled up to produce higher purity anthocyanins relatively easily and is moderately cheap to carry out. Even though LLE could not separate anthocyanins from polymeric species, most neutral polyphenols such as DHBA, Q, CA, and nCA could be extracted, resulting in higher purity starting material. This method can also be scaled up relatively easy, and it is cheap.

3.2. Quantification of Total Components Present in RASE

Once all polyphenols from RASE had been identified, the quantity of these components could be determined. LLE determined the quantity of neutral polyphenols. Anthocyanins in RASE were calculated by Total Monomeric Anthocyanin Content (TMAC) assay, which used a pH differential method. Conventionally, the extinction coefficient or molar absorptivity (ε) of Cy3glc (26,900 L mol^{-1} cm^{-1}) has been used to determine anthocyanin content and is stated as Cy3glc equivalents.[92] Lee *et al*. reported that only 60% of anthocyanin (Cy3glc, purity 97%) could be detected using this method.[127] However, as Cy3glc is the minor anthocyanin in RASE, a new molar absorptivity of a major product, *i.e*. Cy3gal, was determined and applied in the calculation instead. Finally, the quantity of polymeric proanthocyanidins was calculated based on the relative percentage of this species compared to Cy3gal peak in an HPLC chromatogram. Overall, the total chemical components in RASE were determined and summarised as a percentage (%).

3.2.1. Determination of molar absorptivity (Ɛ) of Cy3gal

The molar absorptivity of anthocyanins (ε) measures these compounds' ability to absorb light at a given wavelength in a specific solvent and pH.[128] The higher the molar absorptivity, the higher the absorbance, following Lambert-Beer's law (**Equation 3.1**).

$$A = \varepsilon.c.l \qquad \textbf{Equation 3.1}$$

Where A is absorbance, ε is molar absorptivity (L x mol^{-1} x cm^{-1}), c is concentration (mol/L), l is pathlength (cm). The accuracy of the molar absorptivity value for individual anthocyanins depends on the quality of compound purity or sample concentration. The molar absorptivity of wide ranges of anthocyanins in specific solvents has been reported in the literature. However, the data reported is usually from the 1970s or before, which have inconsistencies and inaccuracies because of the limitation in preparing crystalline anthocyanins in a pure form.[114,128]

An underestimation of anthocyanins' molar absorptivity can also be explained by the presence of impurities that contribute to the total weight of the sample but not to the colour absorption. Additionally, some reported ε values in the literature are hampered by the lack of anthocyanin counterion information or water molecule of hydration in the calculations. The type of counterions for anthocyanins are also never considered in the calculations.[114] In this study, those factors will be considered in calculating molar absorptivity. Cy3gal was selected as this individual anthocyanin present in

large quantity (*ca*. 52.2% of anthocyanins in RASE see **Figure 3.2**) and therefore can give a more precise calculation. Cy3gal was obtained from a semi-preparative HPLC.

3.2.1.1. Molar Absorptivity of Cy3gal in Buffer Solution pH 1

Cy3gal (97% pure) was dissolved in 2 mL of pH 1 buffer solution (KCl/HCl) to make a stock solution with a concentration of 6.5 x 10^{-1} g/L. An exact aliquot of the stock solution was diluted in buffer solution pH 1 to give concentrations of 1.3-13.0 x 10^{-3} g/L. Each concentration was then measured its absorbance at 520 nm. Following Lambert-Beer's Law, the concentration and absorbance can be plotted and presented in **Figure 3.25**.[129] The slope of the equation determined the molar absorptivity. The calculation of molar absorptivity in this study was carried out including the contribution of a trifluoroacetate counterion (CF_3COO^-). This anthocyanin counterion was generated from a semi-preparative HPLC. The molar absorptivity of Cy3gal was then applied to calculate the TMAC of RASE. The result was compared with standard ε used to determine TMAC of a sample (ε of Cy3glc, 26,900 L mol^{-1} cm^{-1}).

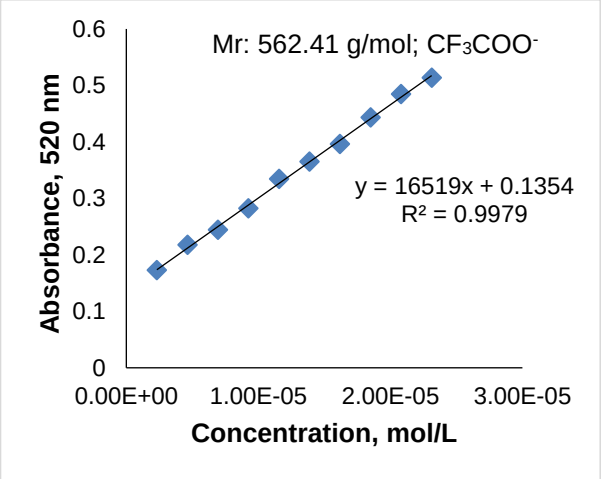

Figure 3.25 Molar absorptivity (ε) of Cy3gal in buffer solution pH 1 included its counter ion (CF_3COO^-), Mr of Cy3gal.CF_3COO^- is 562.41 g/mol.

The molar absorptivity of Cy3gal in buffer solution pH 1 was 16,519 L mol^{-1} cm^{-1}. To the best of our knowledge, the molar absorptivity of Cy3gal in buffer solution pH 1 has not been reported in the literature. Most of the literature was done in methanolic or ethanolic solution, which gave the molar absorptivity ranged from 30,200 to 44,900 L mol^{-1} cm^{-1}.[114] **Table 3.14** shows the anthocyanin content in RASE by applying molar absorptivity of Cy3gal.

Table 3.14 Calculation of the TMAC of RASE by using a measured molar absorptivity of Cy3gal. The literature molar absorptivity of Cy3glc is also given. ANC: anthocyanin.

	Cy3gal $ANC^+.CF_3COO^-$	**Cy3glc**[114] $ANC^+.Cl^-$
ε (L mol^{-1} cm^{-1})	16,519	26,900
Mr (g/mol)	562.2	484.8
TMAC (% w/w of RASE)	**44.7**	**23.6**

The calculation of TMAC of RASE using the molar absorptivity of Cy3gal resulted twice as high in the anthocyanin content (44.7% w/w of RASE) compared to the standard molar absorptivity of Cy3glc (22.6% w/w of RASE). However, other recent values of molar absorptivity of Cy3glc were also reported in the literature, and the values varied significantly.[114] Fossen *et al*. reported different molar absorptivity of Cy3glc, which was 20,000 L mol^{-1} cm^{-1} at a concentration of 0.21 mmol/L.[15] Meanwhile, Cy3glc at a concentration of 0.05 mmol/L had a molar absorptivity of 16,520 L mol^{-1} cm^{-1}.[130] The measurement of anthocyanin content in RASE at 520 nm rather than at the actual $\lambda_{max\text{-}vis}$ (513-519 nm) at pH 1-3 could also contribute to the inaccuracy of the calculation even though it only slightly affects the results (<1.5%).

3.2.1.1. Stability of Cy3gal in Buffer Solution pH 1 for 4 days

Cy3gal (97% pure) in buffer solution pH 1 (KCl/HCl) with various concentrations were monitored its absorbance at 520 nm for 4 consecutive days to study the stability of this compound (**Figure 3.26**). The solutions were kept in the dark at the refrigerator's temperature (4 ºC) for the next absorption measurement. Overall, the absorbance of Cy3gal in buffer solution pH 1 at various concentrations only slightly changed. The molar absorptivity of Cy3gal also did not change significantly over 4 days (**Table 3.15**). This finding agrees with the previous results for anthocyanins in RASE as a mixture at pH < 3. At this pH, anthocyanins are known to be in the flavylium cationic form which is the most stable form amongst other anthocyanin forms.[6,25,37,38] This finding suggests that the measurement of the molar absorptivity of Cy3gal can be performed up to 4 days after the preparation on conditions such as kept it in the dark and low temperature (4 ºC).

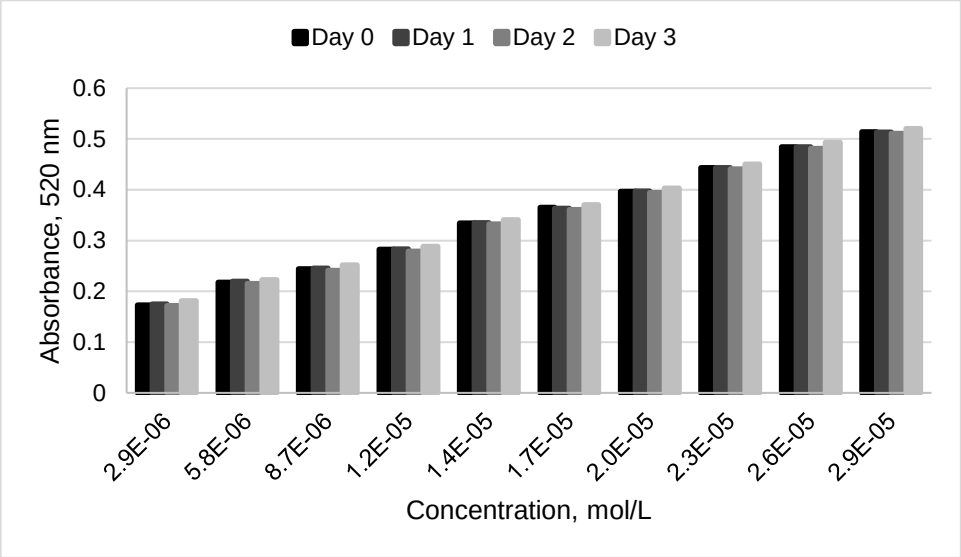

Figure 3.26 The stability of Cy3gal in buffer solution pH 1 with various concentrations for 4 days. Monitored at 520 nm.

Table 3.15 The molar absorptivity of Cy3gal in buffer solution pH 1 measured for 4 consecutive days. Detected at 520 nm. Mr of Cy3gal. CF_3COO^- is 562.2 g/mol.

	Day-0	**Day-1**	**Day-2**	**Day-3**
ε (L mol^{-1} cm^{-1})	16,519	16,410	16,479	16,544

3.2.2. Determination of p*K'*$_a$ of Cy3gal

The p*K'*$_a$ of Cy3gal, one of the major anthocyanins found in *Aronia* skin waste, could be used to help understand the equilibrium of anthocyanins in RASE due to the common cyanidin core. Spectrophotometry has been widely used to determine the p*K'*$_a$ of many indicators.[117,131,132] The decrease of the absorbance of a flavylium cationic form allows the calculation of p*K*'$_a$ of Cy3gal. The equilibrium of anthocyanins and their equilibrium constants can be seen in **Section 1.1.5**. The value of p*K*'$_a$ shows the pH where, at thermal equilibrium, half of the flavylium cationic form (**AH$^+$**) has been transformed into its conjugated base (**CB**).[39,131] It helps us understand the variation in stability of a flavylium cationic form with pH. The absorption band is measured at 511 nm as this is the maximum wavelength for Cy3gal in a flavylium cationic form. The absorption spectra of the thermally equilibrated solution of Cy3gal is presented in **Figure 3.27**.

The p*K*'$_a$ of Cy3gal in this study was 3.4 at a concentration of 4.1 x 10^{-4} M. To the best of our knowledge, p*K*'$_a$ of Cy3gal has not been reported in the literature.

However, Fernandes *et al*. reported the p*K*'$_a$ of Cy3glc was 2.8 at a concentration of 6 x 10^{-5} M.[117] Leydet *et al*. also reported the p*K*'$_a$ of Cy3glc were 2.9 and 3.2 at a concentration of 4 x 10^{-4} M and 8 x 10^{-4} M, respectively, showing an interesting variation with concentration.[132]

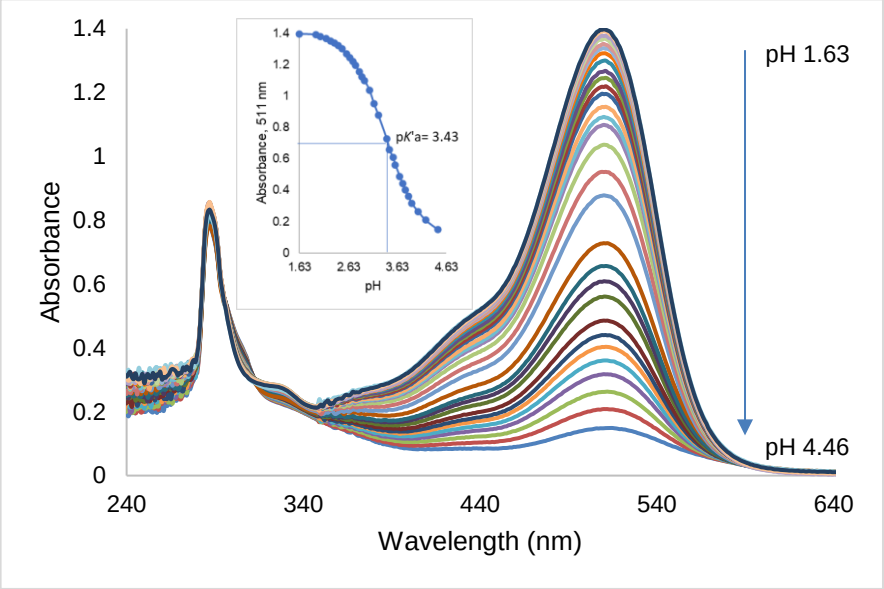

Figure 3.27 Absorption spectra of equilibrated solutions of Cy3gal as a function of pH. Concentration: 6.3 x 10^{-5} M (Mr of Cy3gal. CF_3COO^- is 562.2 g/mol); inset – determination of p*K*'$_a$ using the absorbance at 511 nm.[132]

3.2.3. Total Chemical Composition of RASE

The quantity of neutral polyphenols present in RASE has been determined based on their isolated yields through LLE. Meanwhile, anthocyanin content was calculated by a pH differential method using the observed molar absorptivity of Cy3gal. Although the polymeric anthocyanidins have not been fully characterised in this study, their quantity could be determined. The polymeric proanthocyanidins were quantified based on the relative percentage of this compound to anthocyanins on the HPLC-DAD chromatogram at 285 nm (**Figure 3.2**) and presented about 39.4% (%w/w of RASE). Polymeric proanthocyanidins were present as the major polyphenols in fruits, pomace, and juice of *Aronia* berries, representing 66%, 77% and 42% (%w/w of dried weight) of fruits polyphenols, respectively.[4]

All components in RASE which have been identified and quantified are summarised in **Figure 3.28**. Anthocyanins, alongside the aglycone, were the major components found in RASE (44.7% w/w of polyphenols in RASE). The percentage of individual

anthocyanins and anthocyanidin in RASE (% w/w of polyphenols in RASE) was found to be Cy3gal (23.3%) > Cy3ara (13.2%) > Cy (4.1%) > Cy3xyl (2.4%) > Cy3glc (1.7%). Neutral polyphenols such as 3,4-dihydroxybenzoic acid (DHBA, 7.1%), neochlorogenic acid (nCA, 2.4%), chlorogenic acid (CA, 2.4%), quercetin (Q, 2.4%) together constituted 14.2% w/w of polyphenols in RASE. About 1.7% w/w of RASE components are as yet unknown and may be inorganic salts or other compounds which are more difficult to observe and quantify.

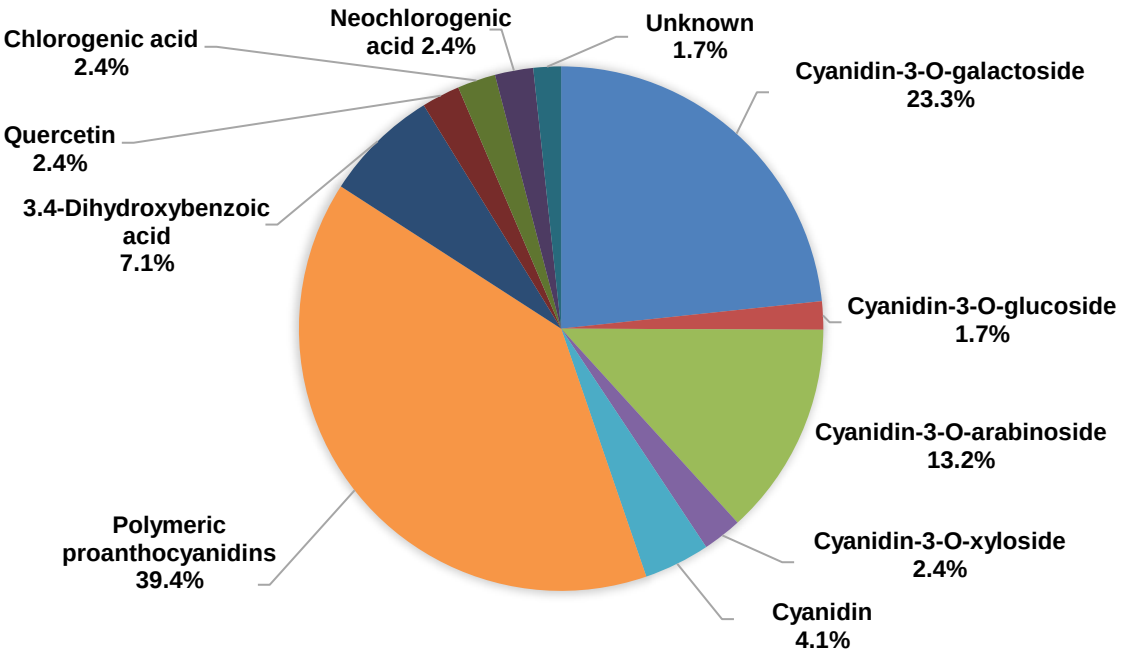

Figure 3.28 Total chemical composition of RASE (% w/w).

It should be noted that the total percentage of polyphenols in this study was calculated for RASE, which was produced from the extraction-purification using 0.01% v/v HCl. The polyphenol profiles should also apply to other RASE produced from the extraction-purification using different concentrations of HCl. However, the percentage of each polyphenol class might differ from what is reported in this study.

3.3. Conclusion

Aronia skin waste was generated from the pressed juice industry and known to have high polyphenols content. The extraction-purification method has successfully extracted anthocyanins from *Aronia* skin waste and removed major neutral polyphenols from the crude extracts. However, some of the neutral polyphenols were still present in RASE. Cy3gal, Cy3glc, Cy3ara, and Cy3xyl, and the aglycone, have been isolated, identified and characterised from other polyphenols through a semi-

preparative HPLC-DAD. Molar absorptivity (ε) and pK'_a of Cy3gal were 16,519 L mol^{-1} cm^{-1} and 3.4, respectively. To the best of our knowledge, this finding has not been reported in literature. For the total chemical composition of RASE, anthocyanins and its aglycone contributed up to 44.7% w/w of RASE. LLE could isolate neutral polyphenols present in RASE, such as DHBA, nCA, CA, and Q, against *i*propyl acetate followed by ethyl acetate. These neutral polyphenols from LLE contributed up to 14.2 % w/w of RASE.

Polymeric proanthocyanidins, constituted by (-)-epicatechin, could be isolated by either a semi-preparative HPLC or Biotage purification. They contributed up to 39.4% w/w of RASE. Inorganic salts and other harder to observe compounds contributed up to 1.7% w/w of RASE. Each purification method has pros and cons, depending on the purpose of the purification. A semi-preparative HPLC-DAD is suitable to isolate individual anthocyanins with high purity for identification and characterisation purposes. However, this method can only produce a small quantity of isolates (mg scale) and is expensive to scale up. Even though it is not as selective as a semi-preparative HPLC-DAD, a Biotage flash purification can separate anthocyanins from polymeric species, which is beneficial for the chemical modification of anthocyanins. This method can be scaled up depending on the column size. LLE is the cheapest and easiest method to purify anthocyanins, but it has the lowest selectivity than other purification methods. This method can also be scaled up depending on the separating funnel size. The organic solvents from this separation can be recycled and reused.

Chapter 4
Preparation, Characterisation and Properties of Anthocyanins with Organic Counterions

This chapter discusses the preparation of anthocyanins with organic counterions, characterisation on refined *Aronia* skin waste (RASE) with various counterions, and determination of their physico-chemical properties (**Figure 4.1**). **Section 4.1** discusses the preparation of anthocyanin salts with carboxylate anions by applying various acids such as trifluoracetic acid (TFA), formic acid (FA), acetic acid (AA) and octanoic acid (OA) during the extraction-purification process. These anthocyanin salts were compared to the more conventional RASE with chloride as a counterion. This study's extraction-purification methods followed the extraction parameters in a batch method reported in **Chapter 2**. Anthocyanin salts with different counter anions, the extraction yield, and their anthocyanin content are now discussed in this chapter. **Section 4.2** discusses the characterisation of RASE using different techniques such as UV-Vis spectrophotometer, HPLC-DAD and NMR spectroscopy. **Section 4.3** discusses the determination of the properties such as total phenolic content (TPC), antioxidant activity (%RScA) and lipophilicity (Log P) of various RASE with different counterions. The correlation of TPC with %RScA is discussed to study the effect of organic acids as anthocyanin counterions on RASE properties.

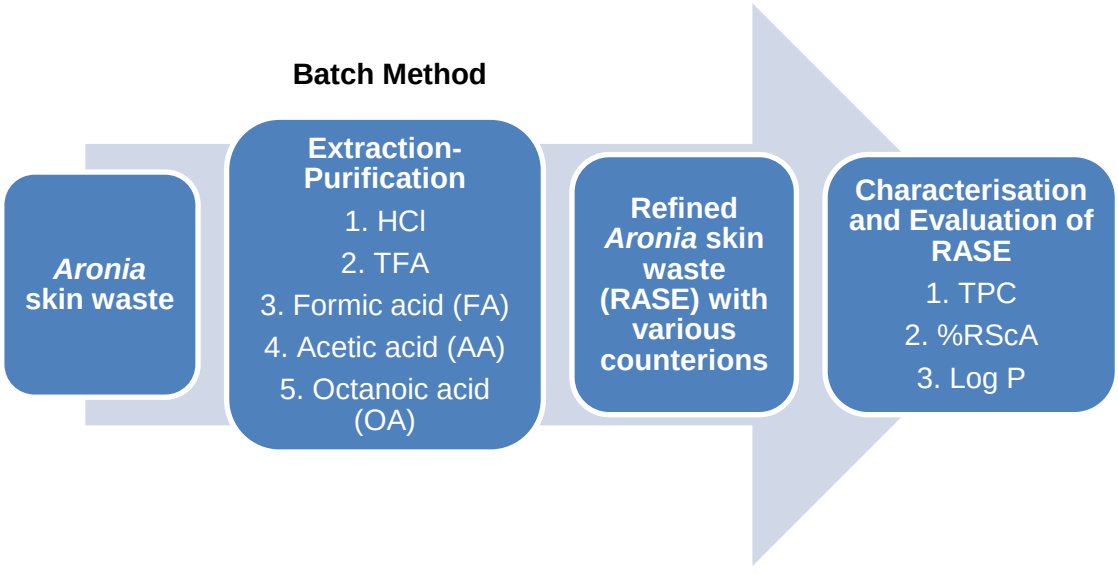

Figure 4.1 General scheme for the preparation, characterisation, and evaluation of RASE from *Aronia* skin waste with various organic counterions.

4.1. Preparation of Anthocyanins with Carboxylate Anions

Chloride is the most common counterion for anthocyanins in a flavylium cationic form (**Figure 4.2**).[5,133] Chloride is generated from the extraction-purification of anthocyanins using HCl. HCl has been commonly used in the extraction as an additive because it gives high yields.[16,134] Additionally, other anions such as sulfinate and carboxylate can also behave the same as chloride. Carboxylic acids in water produce carboxylates which can act as counterions for positively charged anthocyanins. Hence, milder acids and more hydrophobic acids, such as carboxylic acids, can be applied in the extraction-purification process to produce alternative counterions for anthocyanins.

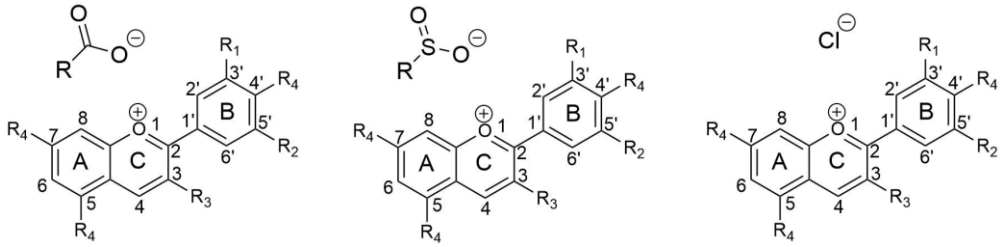

Figure 4.2 Anthocyanins in flavylium cationic forms with carboxylate, sulfinate and chloride as its counter anions, R^1, R^2 = H, OH, or OCH_3; R^3 = glycosyl or H; and R^4 = OH or O-glycosyl.[133]

The extraction-purification of anthocyanins from *Aronia* skin waste has so far been carried out in acidic solutions with concentrations of 0.01-0.5% v/v HCl (see **Chapter 2**, **Section 2.2.2.1**). However, the excessive of strong acid could result in hydrolysis of labile anthocyanins during the SPE elution and evaporation steps, producing its aglycone (see **Chapter 2**, **Section 2.2.2.3**). The presence of HCl in RASE could also accelerate the deglycosylation of anthocyanins over time during storage. Therefore, milder organic acids, such as formic acid, acetic acid, citric acid, and strong acid, such as trifluoroacetic acid with a low concentration (TFA, <3%), can be alternatively used.[53,135] TFA has previously been reported to be added to the extraction solvent to increase the yield.[10,136,137] In this study, the extractions using milder organic acids such as some carboxylic acids with different properties (**Figure 4.3**) were carried out to understand the effect of different counter anions for the flavylium cationic forms on its physico-chemical properties.[80,138] An increase in chain length of aliphatic carboxylic acids was expected to enhance the lipophilicity of anthocyanins, and hence formic acid (FA), acetic acid (AA) and octanoic acid (OA) were applied in the extraction and purification steps for comparative purposes.

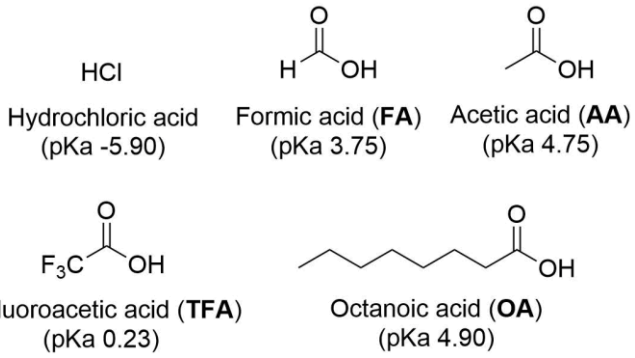

Figure 4.3 Various acids used in the extraction-purification of anthocyanins from *Aronia* skin waste.[139–142]

Modifying counterions for the flavylium cationic forms was expected to increase stability and the physico-chemical properties of anthocyanins itself, particularly in lipophilic media. This modification may enhance solubility in organic solvents, which can facilitate chemical modification. It is also important to ensure the chemical stability of anthocyanins to maximise their industrial applications.[143–145] Chemical modification can also increase dyeing performance on polyester or other hydrophobic fabrics and improve its stability towards pH, which is beneficial in a formulation. Lipophilic anthocyanins could also improve biological properties for other applications such as food, cosmetic and pharmaceutical applications.[143] The most important is that deglycosylation of anthocyanins in RASE could be avoided by using milder acids, as the hydrolysis is acid catalysed.[146] As such, it provides a good starting material for further chemical modification of anthocyanins.

4.1.1. Anthocyanin salts with carboxylate anions

The extraction of anthocyanins from *Aronia* skin waste was carried out by adaptation of previously developed methods (see **Chapter 2**, **Section 2.1**). The extraction was conducted in a batch process with the extraction parameters as follows: extraction temperature (60 °C), extraction time (3 h), solvent (acidified water, 0.1% v/v), ratio of biomass-solvent (1:16), and the ratio of biomass-SPE resin (1:1).[108] The concentration of acids used was kept to $6.3x10^{-3}$-$3.3x10^{-2}$ M (0.1% v/v of solvent), giving the pH < 3.7 (**Table 4.1**). The higher pH can lead to the higher proportion of hemiketal and quinoidal species in the solution, depending on the pK'_a of anthocyanins. In **Chapter 3**, pK'_a of Cy3gal (4.1×10^{-4} M) has been determined and was 3.4. Therefore, in the extraction solution with a pH below the pK'_a value of Cy3gal, anthocyanins will present predominantly as a flavylium cationic form (**AH^+**), and its conjugate bases (**CB**) are minor, [**CB**] = [**A**] + [**B**] + [**C_{trans}**] + [**C_{cis}**].[147] In the

extraction-purification using octanoic acid (**Table 4.1**, **Entry 5**), the pH of the extraction solution is slightly higher than the pK'_a value of Cy3gal. It is suggested that the proportion of (**AH$^+$**) in the solution decreased while its conjugate bases (**CB**) increased compared to the extraction solution, where the pH is lower than the pK'_a.

The crude extract was further purified using solid phase extraction (SPE). The loaded resin was washed with acidified water, eluted by ethyl acetate, and the desired anthocyanins were recovered by elution with acidified ethanol (see **Chapter 2**). The same carboxylic acid was used for both the extraction and purification process, including the acidified water wash and acidified ethanol wash during the SPE elution. The ethanolic eluate was then concentrated in *vacuo* to dryness. The obtained RASE contained a flavylium cationic form (**AH$^+$**) and its counter anion, which was the conjugate base of a carboxylic acid used during the extraction-purification.

In general, anthocyanin salts with organic counterions show a similar appearance as in RASE-chloride. The solid RASE from those acids have a dark red colour except RASE-trifluoroacetate, which was bright red. Solubility tests in organic solvents such as ethyl acetate, ^{i}propyl acetate, chloroform, DCM, and TBME were carried out. Unfortunately, all RASE salts were insoluble in those organic solvents even with heating (up to 60 ºC). The organic solvents remained colourless. This suggests that even though the lipophilicity of counterions of anthocyanins was increased, the anthocyanins were still very polar,[148] most likely as a result of the hydroxyl groups on both anthocyanin core (the A- and B-rings) and the sugar moiety.

4.1.2. Yield of anthocyanins using alternative counterions.

Anthocyanin concentration in RASE was quantified using the standard assay following a pH differential method (see **Chapter 2**, **Section 2.1**) and expressed as cyanidin-3-*O*-glucoside (Cy3glc, Mr 449.2 g/mol) equivalents.[92] For this study, the molar absorptivity value (ε) of 26,900 L/mol.cm from literature was applied as it was obtained with similar aqueous systems and kept the consistency in calculating anthocyanin content.[114] Molar absorptivity value (ε) of Cy3gal has been determined (see **Chapter 3**, **Section 3.3**) and is also included for comparison.

The nature of the counterions is often neglected in such calculations, leading to a less accurate result.[118] Only limited literature reports have included counter ions in

their calculation.[133] However, such counterions contribute to the weight of solid material, and therefore should not be ignored, particularly when calculating molarity. The molecular mass of anthocyanins in this study was calculated with its counter anion depending on acids used during the extraction-purification process, for instance, Mr $Cy3glc^+.Cl^-$, 484.8 g/mol, $Cy3glc^+.CF_3COO^-$, 562.2 g/mol, Mr $Cy3glc^+.HCOO^-$, 494.4 g/mol, Mr $Cy3glc^+.CH_3COO^-$, 508.4 g/mol, Mr $Cy3glc^+.CH_3(CH_2)_6COO^-$, 593.4 g/mol for HCl, TFA, FA, AA, OA respectively.

The anthocyanin content is expressed as % w/w of RASE. The yield of anthocyanins was then calculated by multiplying the extraction yield (mg/g of pomace) by the TMAC (w/w % of RASE) and summarised in **Table 4.1**. The differences of TMAC, including the molecular mass of anions, were as follows: 7.9, 25.2, 10.1, 13.2, 31.7% for HCl, TFA, FA, AA and OA compared to the results without considering counterions. The compounds which have higher molecular mass gave significant differences. Further research to investigate the effect of counterions in the calculation should be performed.

Table 4.1 The yield of anthocyanins recovered from *Aronia* skin waste was obtained after solid-phase extraction (SPE).

Entry	Acid	pH of extraction	Extraction yield (mg/g DW)	TMAC (w/w % RASE)*	TMAC (w/w % RASE)**	TMAC (w/w % RASE)***	Yield of anthocyanins (mg/g DW)
1	HCl	2.3	7.00	20.3	21.9	35.7	1.53
2	TFA	2.2	5.32	33.7	42.2	68.7	2.24
3	FA	2.7	5.01	23.8	26.2	42.7	1.31
4	AA	3.3	6.14	25.0	28.3	46.1	1.74
5	OA	3.7	7.18	18.9	24.9	40.6	1.79

* Mr 449.2 g/mol excluding the counterions. ε = 26,900 L/mol.cm from literature.[114]
**including the molecular mass of respective counterions. Mr $Cy3glc^+.Cl^-$, 484.8 g/mol, $Cy3glc^+.CF_3COO^-$, 562.2 g/mol, Mr $Cy3glc^+.HCOO^-$, 494.4 g/mol, Mr $Cy3glc^+.CH_3COO^-$, 508.4 g/mol, Mr $Cy3glc^+.CH_3(CH_2)_6COO^-$, 593.4 g/mol. ε = 26,900 L/mol.cm from literature.[114] This TMAC was used to calculate the yield of anthocyanins.
***including the molecular mass of respective counterions. ε = 16,519 L/mol.cm from an experiment reported in **Chapter 3**.

The excess of volatile acids such as TFA, FA and AA could be eliminated from RASE through high vacuum evaporation overnight. The yields ranged from 5.01 to 6.14 mg/g DW (**Table 4.1**, **Entries 2-4**). However, excess OA is not sufficiently volatile and is quite challenging to remove. For example, it cannot be removed from the acidified ethanolic eluate through the rotary evaporator, so an alternative procedure

was developed. After an SPE elution using acidified ethanol (0.1% v/v of OA), the ethanolic solution was evaporated. The remaining liquid RASE, which contained an excess of OA, was added with methanol and then washed several times with hexane. As the highly coloured anthocyanin does not dissolve in a non-polar solvent such as n-hexane, which remained colourless during the extraction process, it remains in methanol fraction while the excess of OA is extracted into the hexane fraction. The methanol fraction was then evaporated to dryness under reduced pressure on a rotary evaporator followed by evaporation under a high vacuum overnight to produce RASE octanoate (7.18 mg/g DW, **Table 4.1**, **Entry 5**). The purity of RASE-octanoate is discussed in the NMR section.

HCl and TFA (**Table 4.1**, **Entries 1** and **2**) as strong acids were expected to give higher yields than other organic acids because they can penetrate and break the cellular membranes more to extract anthocyanins and other neutral polyphenols. According to the HPLC chromatogram (see **Section 4.2**, **Figure 4.5**), HCl could extract more polyphenols than other acids. Consequently, the extraction yield of HCl was higher compared to other acids. Hong *et al*. also reported that extraction using 0.1 M HCl resulted in higher anthocyanin concentration than 1% v/v of FA and 5% v/v of AA with the same solvent system (methanol/water 8:2).[149] However, the anthocyanin proportion from HCl extraction-purification was lower than other acids. It suggested that the lower proportion of anthocyanins in this RASE is because HCl could also extract more other polyphenols, which changed the proportion of anthocyanins. The higher content of polyphenols in RASE-chloride is later discussed in **Section 4.4.1**. Some of RASE-chloride did not dissolve completely in aqueous pH 1 buffer solution during the TMAC assay. The insoluble solid was analysed by ^{1}H-NMR and confirmed as polymeric proanthocyanidins. The same finding was also reported by Hosseini *et al*., who found that the anthocyanin proportion from eggplant peel extracts was higher when using AA instead of HCl, however total phenols from the extraction was higher using HCl than AA.[150]

Interestingly, the yield for the extraction-purification by using TFA was lower than AA and OA (**Table 4.1**, **Entries 2-4**). The extraction pH of TFA, which was the most acidic amongst the carboxylic acids used in this study, could cause any further deglycosylation, resulting in a lower extraction yield. However, the highest anthocyanin content was found in RASE-trifluoroacetate, which dissolved completely

during the TMAC assay, in contrast to others, which did not. The higher solubility of RASE-trifluoroacetate is due to a high content in anthocyanins, increasing the TMAC value. This result agrees with Barnes *et al*., who reported that TFA as an additive in the extraction solvent showed the highest peak at 520 nm, which correlated to anthocyanin content compared to other acids such as HCl, FA and AA. TFA, as a strong counterion for anthocyanin in a flavylium cationic form, provides better extraction efficiency.[10]

Meanwhile, anthocyanins produced by milder acids such as FA, AA, and OA (**Table 4.1**, **Entry 3-5**) ranged from 24.9 to 28.3 w/w % RASE. Longer chain aliphatic acids give a higher yield (OA > AA > FA). TMAC of AA was higher than FA, which agrees with the results reported in the literature.[10,149] RASE from all acid's extraction-purifications were then analysed and characterised by using various techniques.

4.2. Characterisation of RASE with Organic Counterions

Characterisation of RASE produced from the extraction-purification using various organic acids, including HCl, was carried out with a UV-Vis spectrophotometer, HPLC-DAD and ^{1}H-NMR spectroscopy. Individual anthocyanins such as Cy3gal, Cy3glc, Cy3ara, Cy3xyl and the aglycone; neutral polyphenols such as DHBA, nCA, CA, and Q; and polymeric proanthocyanidins have been identified and characterised in **Chapter 3**. In this section, the anthocyanin profiles from each RASE produced using the different acids are discussed, as well as the purity and physico-chemical properties of the anthocyanins.

4.2.1. UV-Vis studies

As various counterions were studied in this work, the addition of external counterions from acid used to acidify solvent in the analysis should be avoided to give as accurate as possible results. Solvents without the addition of any acids were used instead, making them slightly acidic to neutral. Consequently, a flavylium cationic form (**AH^{+}**) might not present as a predominant species and would be in equilibrium with the conjugate bases (**CB**) (see **Section 1.1.6, Scheme 1.12**).[151] In this study, the measurements were conducted in two different solvent systems: methanol and water (both without additional acid). Methanol can dissolve RASE completely regardless of anthocyanin counterions, especially RASE obtained from strong acids containing more anthocyanidin, neutral polyphenols and polymeric proanthocyanidins. These polymeric species were confirmed to have low solubility in water compared to other

polyphenols present in RASE. Anthocyanins as flavylium cationic forms display red colouring and have more monomer forms in protic solvents. The red colouring is favoured when the concentration of a flavylium cationic form increases.[6] The UV-Vis absorption spectra of anthocyanins from RASE were recorded between 200 and 800 nm with an Agilent double beam scanning UV-Vis spectrophotometer (**Figure 4.4**).

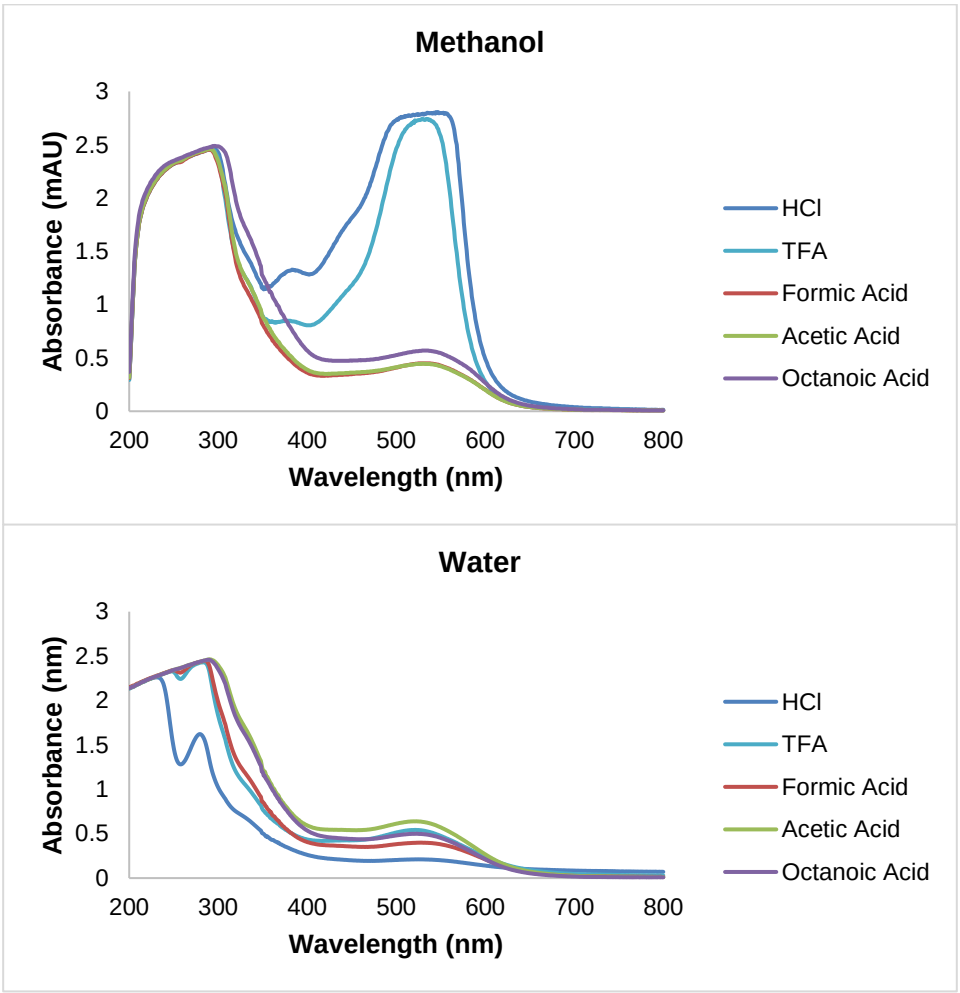

Figure 4.4 Effect of various acids on the absorbance of anthocyanins extracted from *Aronia* skin waste measured in methanol and water.

Figure 4.4 shows that the position and intensity of an absorption band shifted when the spectrum was recorded in different solvents. Two bands of maximum absorption in the UV-Vis spectrum were identified for both solvents: one band was found at 291-296 nm for water and 279-290 nm for methanol, indicating the presence of the phenolic aromatic ring. Brouillard reported that an absorbance at *ca*. 275 nm belonged to the colourless carbinol pseudobase or hemiketal form, which confirmed that in this slightly acidic to neutral pH, flavylium cationic forms equilibrate with other species.[151] Another band was identified at 521-528 nm for water, while for methanol,

the band was identified at 531-547 nm. These typical wavelengths of anthocyanins agree with the results reported by Pedro *et al*., who reported maximum absorptions at 274 nm and 524 nm in 50% ethanol solution, and 278 and 535 in absolute ethanol.[104]

According to the results discussed in **Section 2.1.1.1**, RASE from the extraction-purification using HCl showed a $\lambda_{vis\text{-}max}$ at 514 nm in buffer solution pH 1. In this study, RASE obtained using the same method showed a $\lambda_{vis\text{-}max}$ at 525 nm in pure water without acidification. This can be explained that the addition of acid is required to maximise the formation of flavylium cationic forms. Otherwise, an increase of pH to slightly acidic to neutral could change the equilibrium of anthocyanin itself (**AH^+** 514 nm → **A** 564 nm → **A^-** 590 nm). In this case, the quantity of flavylium cationic forms decreased while its conjugate bases increased, which contributed to the bathochromic shift of spectrum ($\lambda_{vis\text{-}max}$ 514 nm → 525 nm). The observed blue-shift of visible $\lambda_{max\text{-}vis}$ of anthocyanins with respect to pH increase is also observed by Fossen *et al*. who reported that $\lambda_{vis\text{-}max}$ and ε of Cy3glc (2.06×10^{-4}) were 510 nm and 20,000 M^{-1} cm^{-1} at pH 1; and 554 nm and 6,900 M^{-1} cm^{-1} at pH 7.[35] This finding agrees with the results reported by Ahmadiani *et al*., where a bathochromic shift occurred when acidified methanol was used compared to buffer solution pH 1.[128] There was a decrease in the maximum visible wavelength ($\lambda_{vis\text{-}max}$) measured in water compared to the maximum visible wavelength measured in methanol for all acids due to differences in the polarity and solubility (**Table 4.2**).

Table 4.2 $\lambda_{vis\text{-}max}$ of RASE measured in methanol and water.

Acid	**λ_{max} in methanol (nm)**		**λ_{max} in water (nm)**	
	1	2	1	2
Hydrochloric acid (HCl)	279	547	292	525
Trifluoroacetic acid (TFA)	283	534	291	521
Formic acid (FA)	284	531	291	528
Acetic acid (AA)	290	531	291	523
Octanoic acid (OA)	288	532	296	523

For strong acids such as HCl and TFA (**Table 4.2**, **Entries 1** and **2**), the difference between $\lambda_{vis\text{-}max}$ methanol and water were 49 and 13 nm for HCl and TFA, respectively. The formation of anthocyanidin might cause a hypsochromic shift of RASE in water compared to methanol due to the solubility and polarity of these

compounds. Meanwhile, for milder carboxylic acids such as FA, AA and OA, the difference of $\lambda_{vis\text{-}max}$ methanol and water was 3, 8 and 9 nm, respectively. FA, AA and OA (**Table 4.2**, **Entries 3-5**) showed slightly different absorbances in both solvent systems (0.05-0.19 unit). While TFA and HCl showed a significant increase in methanol absorbances compared to absorbances in water (2.6 and 2.2 unit, respectively). In terms of acid used in the extraction-purification, TFA and HCl resulted in the greatest RASE absorption measured in methanol. This result is in agreement with Giusti *et al*., who studied the effect of solvent on the absorption of anthocyanins.[133]

4.2.2. HPLC studies

The method used in this study followed the method discussed earlier in **Chapter 2**, **Section 2.2.2,** as this method has shown the best separation for anthocyanins from *Aronia* skin waste. The acid additive for the mobile phase in this separation was 0.5% TFA regardless of the acids used in producing RASE. HCl provides better extraction efficiency and chromatographic resolution at 520 nm (**Figure 4.5**). HCl and TFA as strong acids degrade anthocyanins through hydrolysis, forming its aglycone (cyanidin). Nevertheless, the intensity of cyanidin formed in the TFA chromatogram is much lower compared to that in the HCl chromatogram. On the other hand, it is notable that there was no aglycone formation observed in the chromatogram for the milder organic acids (FA, AA, OA) (**Figure 4.5**).

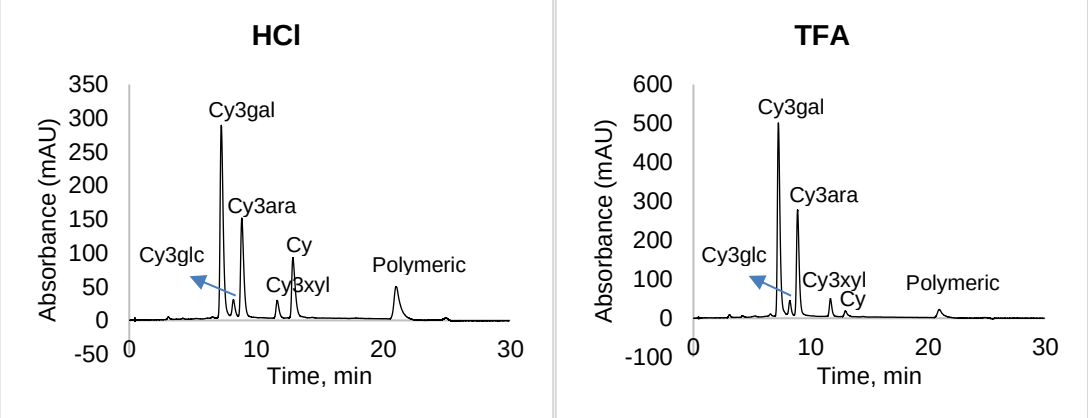

Figure 4.5 Anthocyanin profiles of RASE shown in HPLC chromatograms. Solvent A: H_2O/TFA (99.5:0.5); solvent B: acetonitrile. Detected by DAD at 520 nm.

To estimate the quantity of anthocyanins extracted from *Aronia* skin waste, the integration of Cy3gal peak from the crude extracts produced using different acids is compared. This is later discussed in **Section 4.3**.

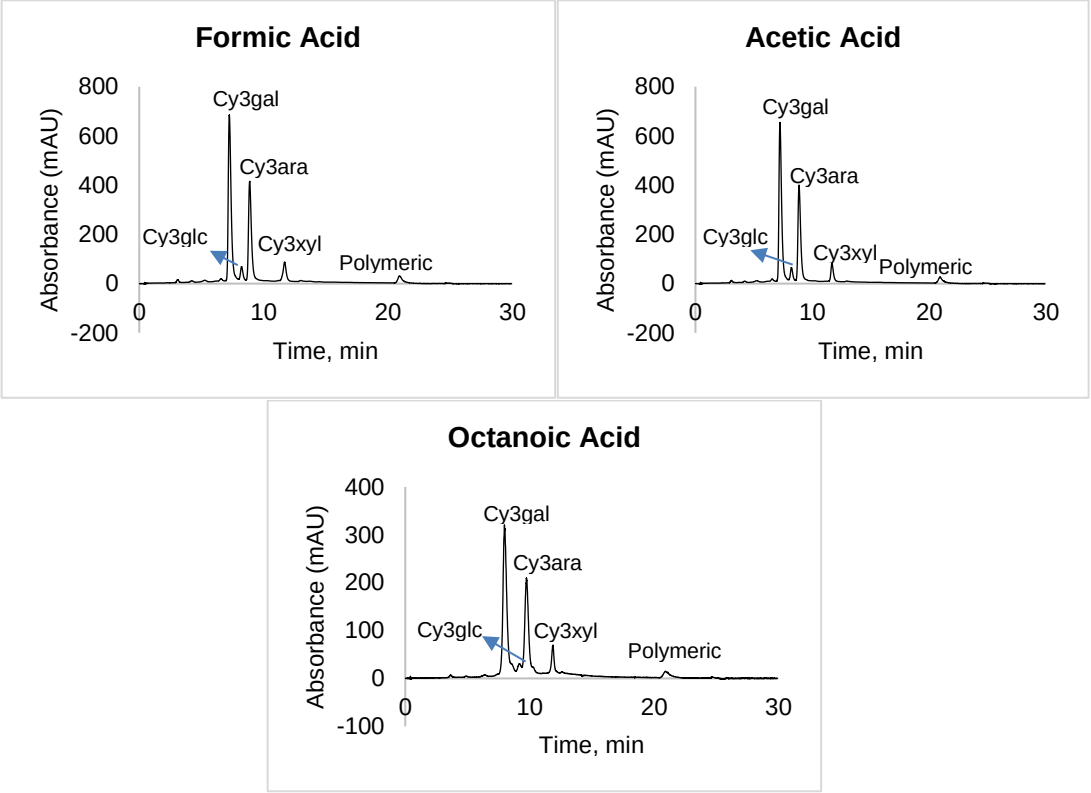

Figure 4.5. (continued).

The anthocyanins profile shown in HPLC chromatograms of various acids was similar as reported in RASE-chloride, where Cy3gal and Cy3gal were the major anthocyanins. However, there is a slight difference amongst acids used in the extraction-purification regarding the ratio of Cy3gal and Cy3ara (**Table 4.3**). The highest Cy3gal/Cy3ara ratios were found for TFA and HCl (1.86 and 1.85, respectively). Other weaker acids have ratios in the range of 1.62-1.76. The higher ratio of Cy3gal/Cy3ara implies that the concentration of Cy3gal in RASE is higher than Cy3ara. It suggests that Cy3ara, which contains five carbons of sugar, is easier to deglycosylate by the presence of strong acids forming its aglycone (Cyanidin), compared to Cy3gal, which contains six carbons of sugar (see **Chapter 2**, **Section 2.3.2**).

Table 4.3 The ratio of Cy3gal/Cy3ara based on HPLC chromatograms (520 nm).

Acid	Cy3gal/Cy3ara ratio
Hydrochloric acid (HCl)	1.86
Trifluoroacetic acid (TFA)	1.85
Octanoic acid (OA)	1.76
Formic acid (FA)	1.71
Acetic acid (AA)	1.62

Cyanidin aglycone is not present naturally in *Aronia* berries as anthocyanins are more stable with a sugar moiety(s) or occasionally, an acylated sugar moiety(s), see **Chapter 1**, **Section 1.1.1**. This compound is a product of deglycosylation during the SPE elution and concentration of anthocyanins. Additionally, RASE produced from the extraction-purification using HCl showed increasing cyanidin concentration during storage (see **Chapter 2**, **Section 2.2.2.2**). The relative percentage (%) of anthocyanins and its aglycone in RASE with various counterions is presented in **Figure 4.6**. This relative percentage (%) was calculated based on the HPLC chromatogram of each RASE.

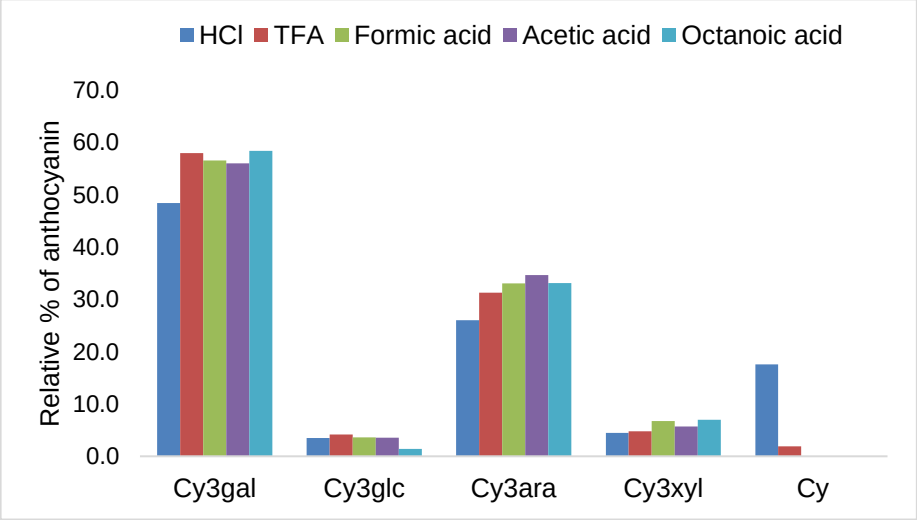

Figure 4.6 Relative percentage (%) of anthocyanins and its aglycone in RASE with various counterions.

Figure 4.6 shows that the concentration of Cy3gal and Cy3ara from the HCl extraction were 8.6 and 7.6 % lower than other acids, respectively. The difference was compensated by the presence of cyanidin aglycone (17.6%). It suggested that the formation of aglycone comes from the major anthocyanins in *Aronia* berries. The deglycosylation of anthocyanins has been discussed in **Chapter 2**, **Section 2.2.2.3**.

TFA was observed to produce about 2% of aglycone. Milder organic acids were observed to not produce any aglycone during the extraction-purification of anthocyanins or acidified ethanolic eluate concentration, which is an important finding. Cy3gal ranged from 48.5% (HCl) to 58.4% (OA). Cy3glc ranged from 1.4% (OA) to 4.2% (TFA). Cy3ara ranged from 26% (HCl) to 34.7% (AA). Cy3xyl ranged from 4.5% (HCl) to 7% (OA).

4.2.3. NMR studies

Dried RASE with various counterions were dissolved in deuterated methanol with or without the addition of TFA-d. The use of acidified methanol (CD_3OD/CF_3COOD 95:5) allowed characterisation wholly in their flavylium cationic forms. In the absence of additional TFA, the original acid used in the extraction is expected to allow the formation of the flavylium cation, which would be particularly favourable for strong acids such as HCl and TFA. On the other hand, RASE produced using weaker organic acids would be less likely to produce the flavylium forms but more likely to give the hemiketal or quinonoid species. The formation and chemical characterisation of hemiketal forms of anthocyanins from RASE will be further discussed in **Chapter 5**.

4.2.3.1. NMR studies of RASE in acidified methanol (CD_3OD/CF_3COOD 95:5)

The findings from the HPLC studies were confirmed by ^{1}H-NMR (**Figure 4.7**). The diagnostic anthocyanin protons (H-4, 8.50-9.10 ppm) have been previously assigned as Cy3gal, Cy3glc, Cy3ara, Cy3xyl (see **Chapter 3**). Its aglycone (cyanidin, Cy) was only observed in HCl and TFA extracts which appeared as a singlet in the region of 8.50-8.75 ppm, confirming the formation of aglycone via hydrolysis by strong acids (see **Chapter 2**, **Section 2.2.2.2**). Formate peak appears as a singlet at 8.06 ppm overlapping with H-2' peak of anthocyanins. Both acetate and octanoate appear at the aliphatic region. Acetate peak appears as a singlet at 1.97 ppm (CH_3). Peaks of octanoate were observed at 2.25, 1.57, 1.29 and 0.87 ppm, which belong to CH_2-α, CH_2-β, $(CH_2)_{4-7}$ and CH_3, respectively.

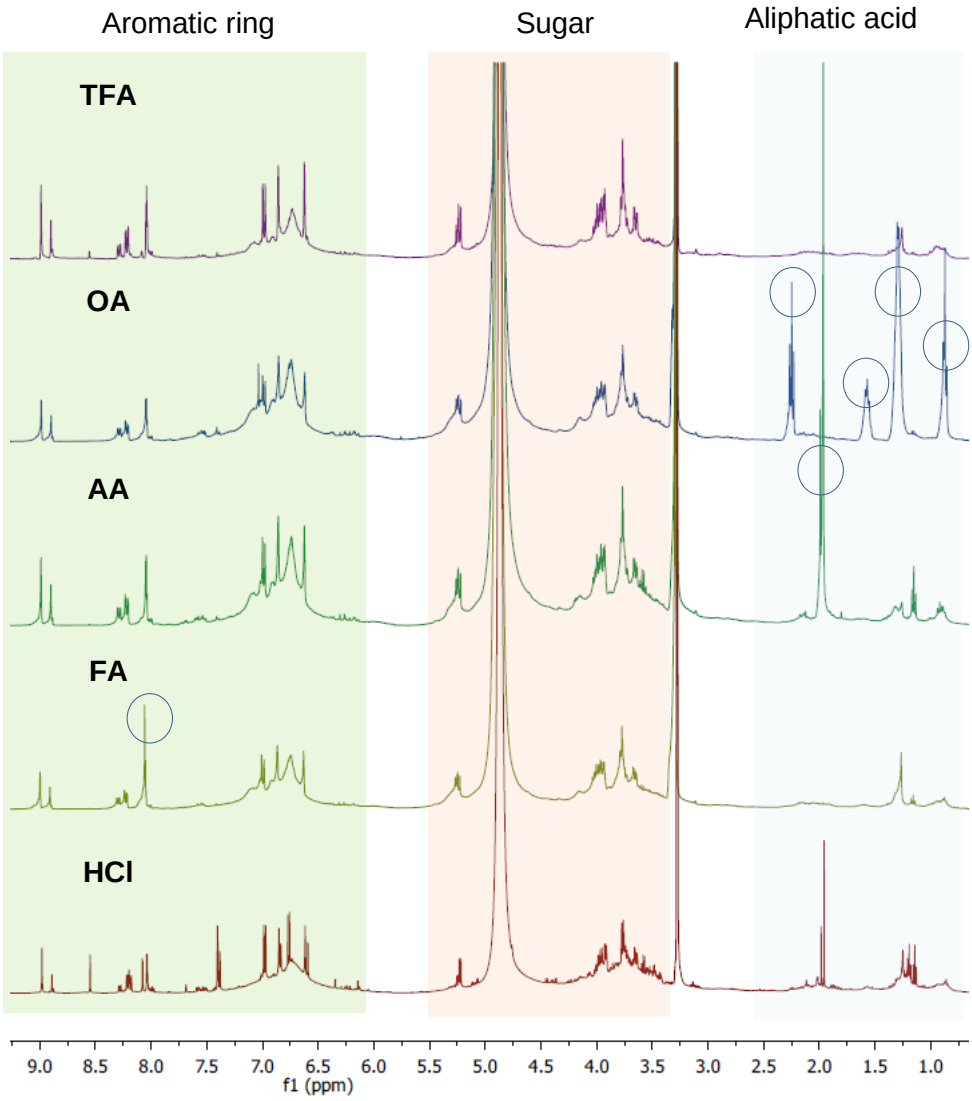

Figure 4.7 ^{1}H-NMR spectrum of RASE from different extractions using various acids in the extraction. 1) HCl, 2) FA, 3) AA, 4) OA, 5) TFA. Recorded at 500 MHz (25 °C). Solvent: CD_3OD/ CF_3COOD (95:5). Circles indicate protons from acid counterion where relevant.

The presence of organic counterions and/or excess acid in RASE can be calculated by comparing the integration of H-4 of anthocyanins in a flavylium cationic form which is present as a singlet, with the integration of acid protons in the ^{1}H-NMR spectra. As such, it also helps quantify the purity of RASE. The comparison of the integration of H-4 of anthocyanins (combination of Cy3gal, Cy3glc, Cy3ara and Cy3xyl) and integration of acid's protons are summarised in **Table 4.4**. Both formate and acetate show the ratio 1:1 to anthocyanins, suggesting the formation of anthocyanin salts with those organic counterions. Meanwhile, octanoate shows the ratio of 1:2 to anthocyanins, suggesting that the small quantity of octanoic acid may still be present

in RASE-octanoate. The higher the boiling point of acid, the more they were found in RASE as evaporation could not take them out completely.

Table 4.4 Comparison of integration of H-4 of anthocyanins with the integration of acid's proton. Solvent: CD_3OD at 25 ºC.

Acid	Ratio	
	Anthocyanin (H-4)	**Acid counterion**
FA	1	1
AA	1	1
OA	1	2

RASE produced by the extraction-purification using HCl shows the highest quantity of an aglycone compared to the extraction-purifications using other carboxylic acids. The backbone protons of cyanidin (Ring A and Ring B), H-6, H-8, H-2', H-5' and H-6', can be seen in the aromatic region of 6.50-8.30 ppm. Polymeric proanthocyanidins were observed as a broad peak in the region of 6.50-7.25 ppm overlapping with the aromatic peaks. Some of the aromatic peaks belonging to neutral polyphenols were obscured by the polymeric proanthocyanin broad peak. Based on the results described above, TFA and milder organic acids such as FA, AA and OA can be used as alternatives to HCl as these RASEs show a less complex profile of anthocyanins but with a good yield. These acids were also observed to extract less polyphenols such as 3,4-dihydroxybenzoic acid (DHBA), Quercetin (Q), Chlorogenic acid (CA) and Neochlorogenic acid (nCA) which were abundant in RASE-chloride (**Chapter 3**).

The expanded ^{1}H-NMR spectra of RASE are presented in **Figure 4.8**. As mentioned previously, HCl can also induce deglycosylation via hydrolysis producing its aglycone, hence an abundance of this species was found in this RASE. The use of milder acid during the extraction and SPE elution changed the proportion of polymeric species in RASE. Since the pK_a values of FA and AA are higher than the pH of the extraction solvent (**Table 4.1**, **Entries 2** and **3**), these acids were mostly present in the free acid HA forms. Additionally, these acids hardly deglycosylate anthocyanins via hydrolysis. In slightly acidic to neutral methanol, anthocyanins are mostly found in the hemiketal and quinonoid base forms.

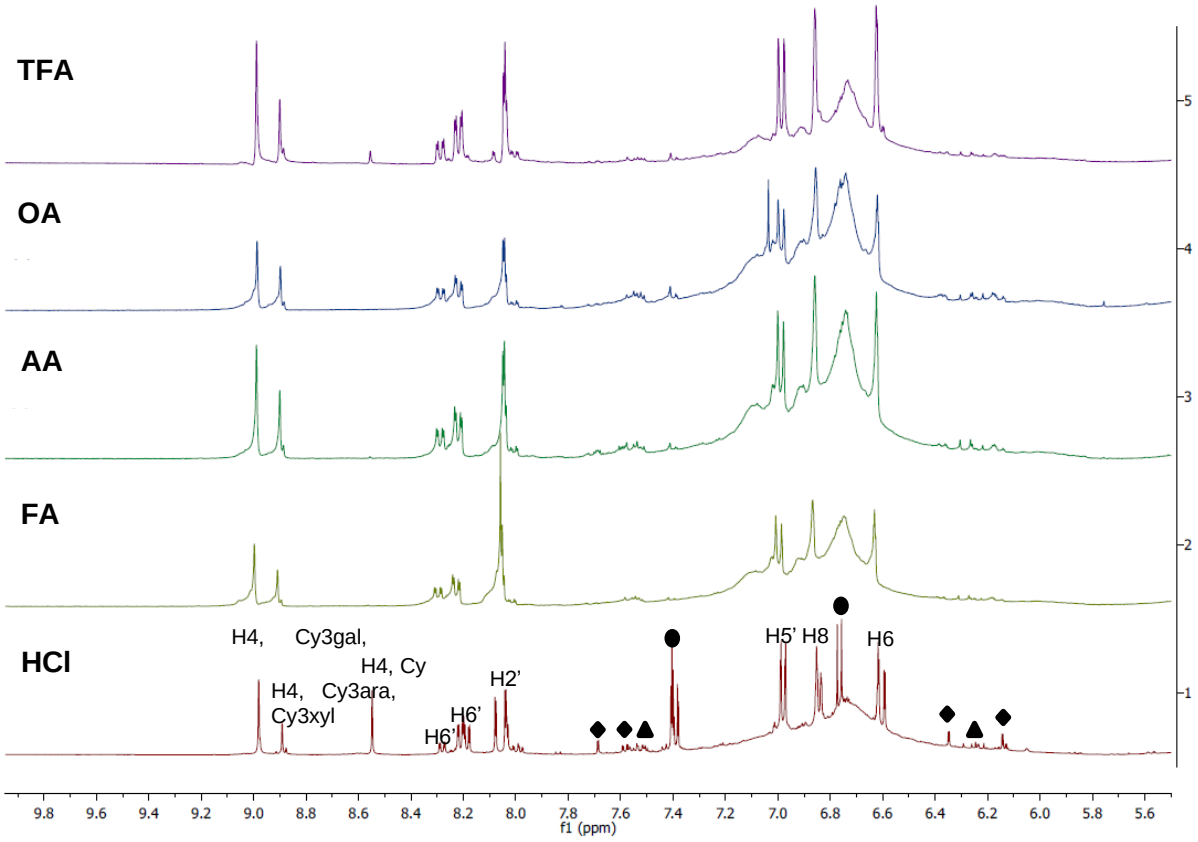

Figure 4.8 Expanded ^{1}H-NMR spectrum of RASE using various acids in the extraction (aromatic region). 1) HCl, 2) FA, 3) AA, 4) OA, 5) TFA. Recorded at 500 MHz (25 °C). Solvent: CD_3OD/ CF_3COOD (95:5).
(●) DHBA (♦) Q (▲) CA and nCA.

Because of the complexity of the extracts, especially in the sugar region (3.3-5.5 ppm), the signal assignment was successfully carried out for the anthocyanidin backbone (rings A, B and C), and the anomeric and H-2" protons of the sugar moiety. Other remaining sugar peaks were assigned as multiplets. The aglycone from HCl and TFA extracts are summarised in **Table 4.5**. Cyanidin-3-*O*-galactoside (**Cy3gal**) and cyanidin-3-*O*-glucoside (**Cy3glc**) peaks were overlapping and summarised in **Table 4.6**. Cyanidin-3-*O*-arabinoside (**Cy3ara**) and cyanidin-3-*O*-xyloside (**Cy3xyl**) were also overlapping and summarised in **Table 4.7**.

Following the chemical characterisation of anthocyanins from RASE as flavylium, cationic forms reported in **Chapter 3**, 2D NMR spectroscopy was carried to assist in assigning anthocyanin peaks, especially for those that overlap or appear under polymeric proanthocyanidins. In general, as already mentioned, the H-4 peaks of Cy3gal and Cy3glc from all acids appear as singlets in the region of 8.98-9.01 ppm.

Cy3ara and Cy3xyl appear as singlets in the region of 8.80-8.92 ppm. Meanwhile, H-4 peaks of Cy aglycone from HCl and TFA appear at 8.55 and 8.56 ppm, respectively. H-6' (8.21-8.25 ppm for Cy3gal and Cy3glc, 8.28-8.32 ppm for Cy3ara and Cy3xyl, 8.19-8.21 for Cy) peaks appear as doublet of doublets which correlate with H-2' (8.04-8.06 ppm for Cy3gal and Cy3glc, 8.03-8.06 ppm for Cy3ara and Cy3xyl, 8.08-8.10 ppm for Cy) and H-5' (6.98-7.00 ppm). Both H-2' and H-5' appeared as doublets. These peaks can be distinguished from each other because they have different coupling constants. Meanwhile, H-8 (6.85-6.87 ppm for anthocyanins, 6.84-6.86 ppm for Cy) peaks appeared as doublet and correlated with H-6 (6.62-6.64 ppm for anthocyanins, 6.59-6.61 ppm for Cy). It can be concluded that there is no significant difference in chemical shift amongst RASE with various counterions.

Table 4.5 ^{1}H-NMR spectrum of Cyanidin (**Cy, 2**) in CD_3OD/CF_3COOD (95:5, v/v). Recorded at 500 MHz (25 °C)**.**

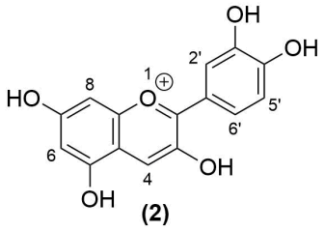

(2)

	HCl		TFA	
Aglycone	**δ^{1}H (ppm)**	**J (Hz)**	**δ^{1}H (ppm)**	**J (Hz)**
H-4	8.55	s	8.56	s
H-6'	8.19	dd, 8.5, 2.5	8.21	dd, 8.5, 2.0
H-2'	8.08	d, 2.0	8.10	d, 2.0
H-5'	6.98	d, 8.5	7.00	d, 8.5
H-8	6.84	d, 2.0	6.86	d, 2.0
H-6	6.59	d, 2.0	6.61	d, 2.0

Table 4.6 ^{1}H-NMR spectra of Cyanidin-3-*O*-galactoside (**Cy3gal, 27**) and Cyanidin-3-*O*-glucoside (**Cy3glc, 21**) in CD_3OD/CF_3COOD (95:5, v/v). Recorded at 500 MHz (25 °C).

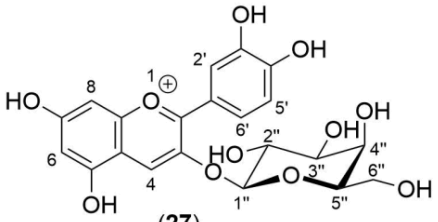

(**27**)

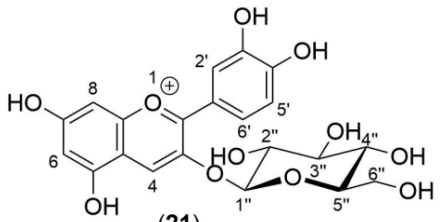

(**21**)

	HCl		**Formic acid**		**Acetic acid**		**Octanoic acid**		**TFA**	
Aglycone	**δ^{1}H (ppm)**	**J (Hz)**	**δ^{1}H (ppm)**	**J (Hz)**	**δ^{1}H (ppm)**	**J (Hz)**	**δ^{1}H (ppm)**	**J (Hz)**	**δ^{1}H (ppm)**	**J (Hz)**
H-4	8.98	s	9.00	s	8.99	s	8.99	s	9.01	s
H-6’	8.21	dd, 9.0, 2.5	8.24	dd, 8.5, 2.0	8.22	dd, 11.0, 3.0	8.22	dd, 11.0, 3.0	8.25	dd, 8.5, 2.0
H-2’	8.04	d, 2.0	8.06	d, 2.0	8.04	d, 3.0	8.05	d, 3.0	8.06	d, 2.5
H-5’	6.98	d, 9.0	7.00	d, 10.0	6.99	d, 10.5	6.99	d, 11.0	7.00	d, 8.5
H-8	6.85	d, 2.0	6.87	d, 2.0	6.86	d, 2.0	6.85	d, 2.0	6.87	d, 2.0
H-6	6.62	d, 2.0	6.64	d, 2.0	6.63	d, 2.0	6.62	d, 2.0	6.63	d, 2.0
Sugar										
H-1”	5.23	d, 7.5	5.24	d, 9.5	5.23	d, 9.5	5.23	d, 10.0	5.23	d, 10.0
H-2”	3.97	dd, 10.0, 8.0	3.99	dd, 10.0, 8.0	3.98	dd, 12.0, 9.5	3.98	dd, 12.0, 9.5	3.99	dd, 9.5, 7.5
H-3”, H-4”, H-5”, H-6”A/B	3.63-3.93	m	3.64-3.94	m	3.64-3.94	m	3.63-3.93	m	3.63-3.94	m

Table 4.7 ^{1}H-NMR spectra of Cyanidin-3-*O*-arabinoside (**Cy3ara, 28**) and Cyanidin-3-*O*-xyloside (**Cy3xyl, 29**) in CD_3OD/CF_3COOD (95:5, v/v). Recorded at 500 MHz (25 °C).

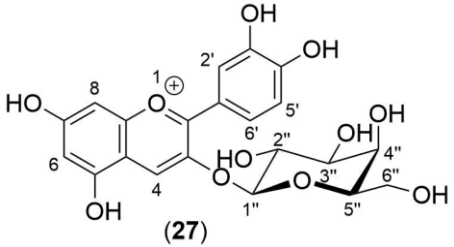

(**27**)

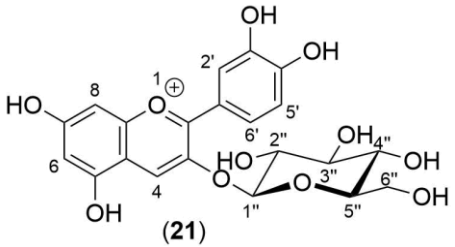

(**21**)

	HCl		Formic acid		Acetic acid		Octanoic acid		TFA	
Aglycone	**δ^1H (ppm)**	**J (Hz)**	**δ^1H (ppm)**	**J (Hz)**	**δ^1H (ppm)**	**J (Hz)**	**δ^1H (ppm)**	**J (Hz)**	**δ^1H (ppm)**	**J (Hz)**
H-4	8.89*/ 8.88**	s	8.92*/ 8.90**	s	8.90*/ 8.89**	s	8.90*/ 8.80**	s	8.91*/ 8.90**	s
H-6’	8.28	dd, 9.0, 2.5	8.31	dd, 9.0, 2.5	8.29	dd, 11.0, 2.5	8.29	dd, 11.0, 2.5	8.32	dd, 8.5, 2.0
H-2’	8.03	d, 2.5	8.06	d, 2.0	8.04	d, 3.0	8.03	d, 3.5	8.05	d, 2.5
H-5’	6.98	d, 9.0	7.00	d, 9.0	6.99	d, 10.5	6.99	d, 11.0	7.00	d, 8.5
H-8	6.85	d, 2.0	6.87	d, 2.0	6.86	d, 2.0	6.85	d, 2.0	6.87	d, 2.0
H-6	6.62	d, 2.0	6.64	d, 1.5	6.62	d, 2.0	6.62	d, 2.0	6.63	d, 2.0
Sugar										
H-1”	5.25	d, 6.0	5.27	d, 7.5	5.25	d, 8.0	5.25	d, 7.5	5.25	d, 8.0
H-2”	4.00	dd, 8.0, 6.0	4.02	dd, 8.0, 6.5	4.01	dd, 10.0, 7.5	4.00	d, 10.5. 8.0	4.03	dd, 8.0, 6.0
H-3”, H-4”, H-5”A/B	3.63-3.93	m	3.64-3.94	m	3.64-3.94	m	3.63-3.93	m	3.63-3.94	m

*Cy3ara, **Cy3xyl

4.2.3.2. NMR studies of RASE in neutral methanol (CD_3OD)

The comparison of ^{1}H-NMR spectra of RASE-chloride and RASE-trifluoroacetate in neutral methanol can be seen in **Figure 4.9**. Flavylium cation forms can still be observed in neutral methanol even without the usual TFA-d addition. The assignment for anthocyanins from RASE-chloride and RASE-trifluoroacetate dissolved in methanol are similar to the previous assignment summarised in **Table 4.8** for Cy3gal and Cy3glc and in **Table 4.9** for Cy3ara and Cy3xyl. There is no significant difference in chemical shift (ppm) of anthocyanins dissolved in methanol with/without the addition of acid.

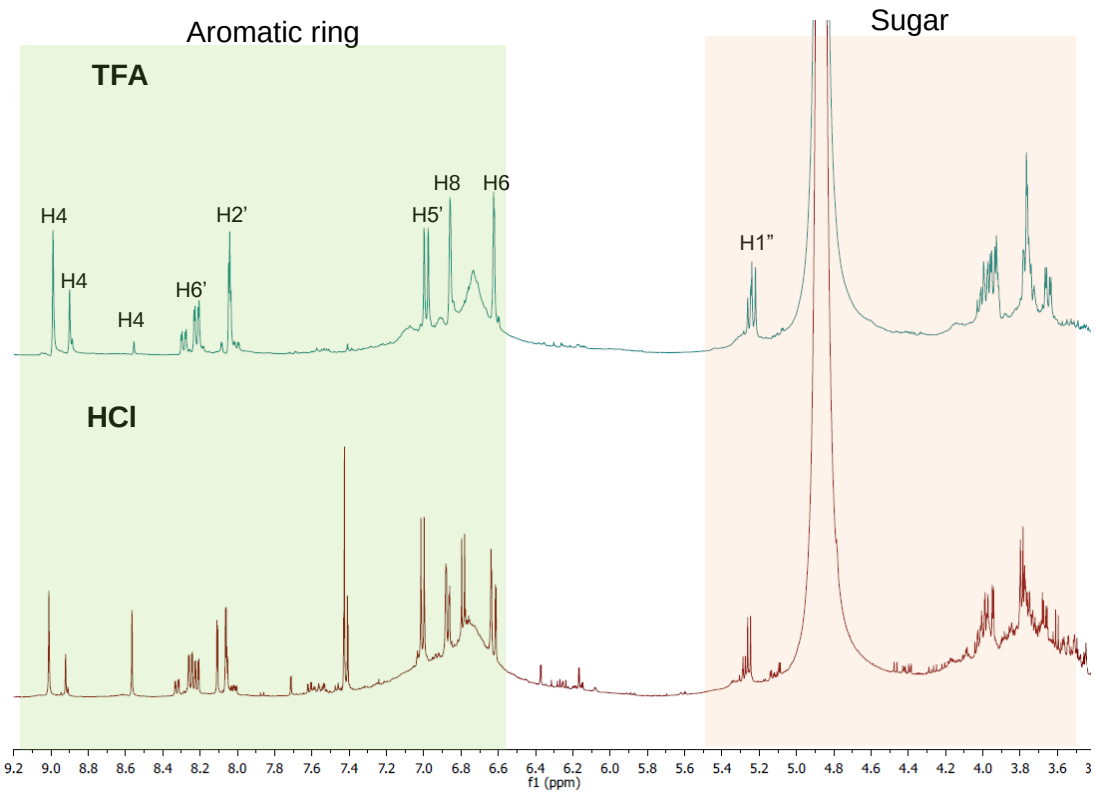

Figure 4.9 ^{1}H-NMR spectra of RASE from different extraction-purifications using HCl and TFA. Recorded at 500 MHz, 25 °C. Solvent: CD_3OD (no TFA added).

Interestingly, for RASE from milder organic acids, only hemiketal forms were observed in the NMR spectra, with no significant flavylium ion signals (**Figure 4.10**). Hemiketal forms of anthocyanins from RASE with milder organic acids can be formed in methanolic solvent without acid to produce a pH of slightly acidic to neutral (**Scheme 4.1**). The residual water from the solvent and/or solvent might promote the formation of hemiketal forms. Alternatively, anthocyanins could take water from the air as the sample vial is not vacuum sealed. Lee *at al*. reported that the hygroscopicity of anthocyanin standards ranged from 10-22%.[92] Hemiketal forms (**B**) of anthocyanins can be easily identified at this pH. The formation of hemiketal of

anthocyanins as a mixture alongside other species such as a flavylium cationic form and chalcone has been reported in literature.[112,132,152,153] Leydet *et al*. reported that at pH 5.5, there was an equilibrium between a flavylium cationic form (**AH$^+$**), hemiketal form (**B**) and chalcones (**$C_{E/Z}$**).[132] The experiment was carried out for delphinidin-3-*O*-glucoside (8 x 10^{-4} M). However, the only hemiketal forms of cyanidin-based anthocyanins from *Aronia* berries have not been reported in literature.

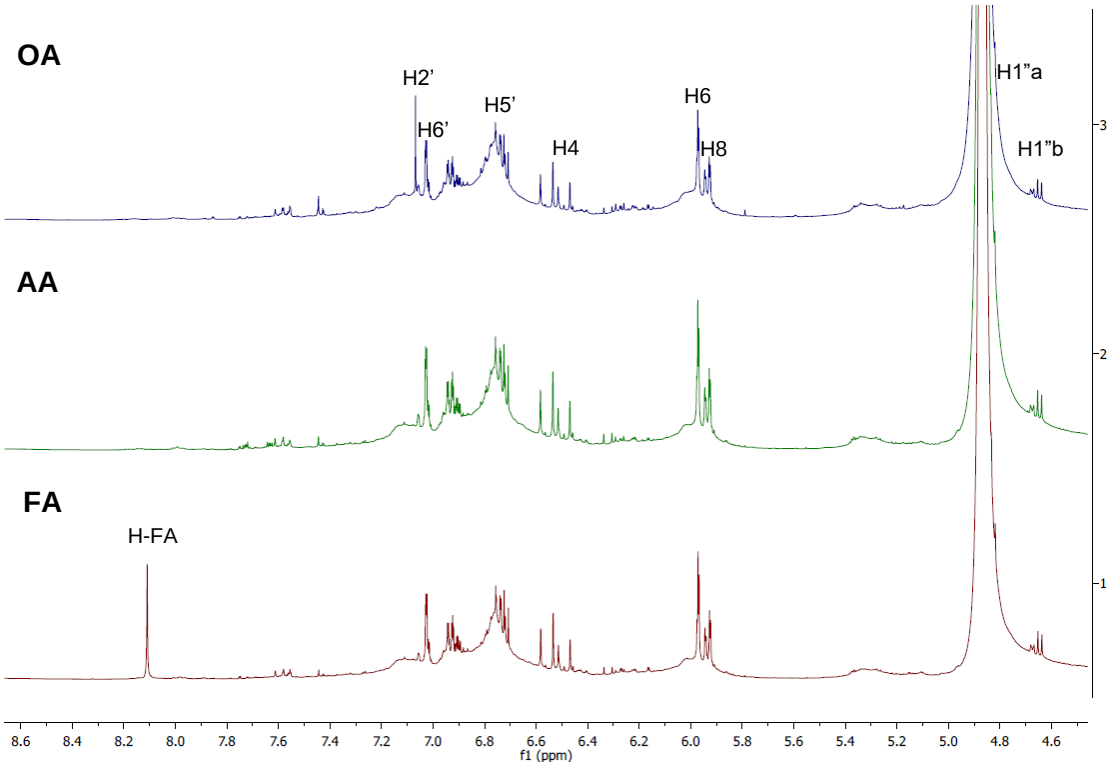

Figure 4.10 Extended ^{1}H-NMR spectra of RASE from different extraction-purifications using various acids 1) FA, 2) AA, 3) OA. Recorded at 500 MHz, 25 °C. Solvent: CD_3OD (no TFA added).

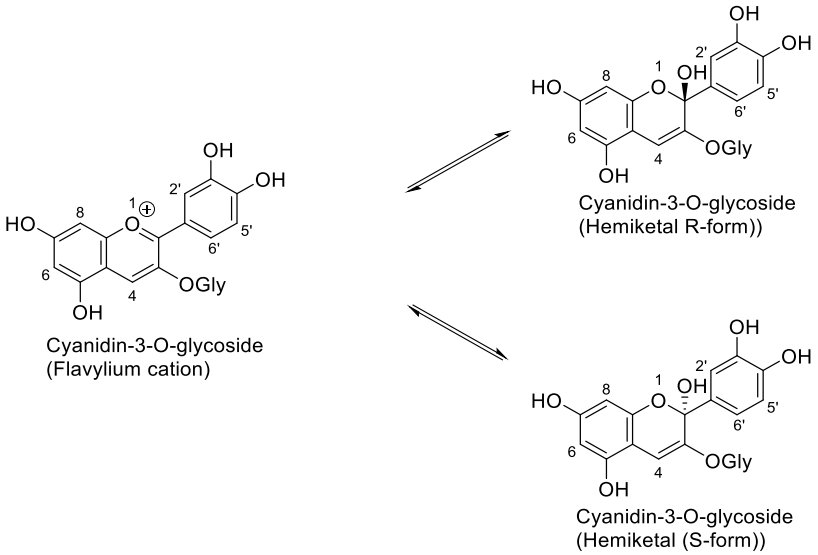

Scheme 4.1 The equilibrium of a flavylium cationic form and hemiketal forms of cyanidin-based anthocyanins (a, major and b, minor).[112]

Scheme 4.1 shows that the hemiketal form appears as two peaks (**a**, major and **b**, minor) which correlates to two epimers (R/S) at carbon position 2 (C-2) in the ring C. However, it cannot be determined which epimer is the minor or major. The uncontrolled stereocenter C-2 is formed by hydration at this position.[132] Fernandes *et al*. reported the formation of hemiketal form (**B**) of Cy3glc in D_2O at pD 3.9 by ^{1}H-NMR spectroscopy alongside flavylium cationic form (**AH$^+$**) and cis/trans chalcone (**C_Z/C_E**).[152] However, in our work, anthocyanins were observed only forming hemiketal forms, which is a notable new observation, and simplifies the ^{1}H NMR spectra considerably. The assignments of the hemiketal form of RASE from organic acids are summarised in **Table 4.8** and **Table 4.9**. The detailed characterisation of the hemiketal species is discussed further in **Chapter 5**.

Table 4.8 ^{1}H-NMR spectra of Cyanidin-3-*O*-galactoside (**Cy3gal, 25**) and Cyanidin-3-*O*-glucoside (**Cy3glc, 21**) in CD_3OD. Recorded at 500 MHz (25 °C).

	Formic acid				Acetic acid				Octanoic acid			
	Major		Minor		Major		Minor		Major		Minor	
Aglycone	**δ^1H (ppm)**	**J (Hz)**	**δ^1H (ppm)**	**J (Hz)**	**δ^1H (ppm)**	**J (Hz)**	**δ^1H (ppm)**	**J (Hz)**	**δ^1H (ppm)**	**J (Hz)**	**δ^1H (ppm)**	**J (Hz)**
H-4	6.53	s	6.58	s	6.53	s	6.58	s	6.53	s	6.58	s
H-6’	6.93	dd, 2.0, 8.5	6.91	dd, 2.0, 8.0	6.93	dd, 2.0, 8.5	6.92	dd, 2.0, 8.0	6.93	dd, 2.0, 8.5	6.91	dd, 2.0, 8.5
H-2’	7.03	d, 2.0	7.03	d, 2.0	7.03	d, 2.0	7.03	d, 2.0	7.03	d, 2.0	7.03	d, 2.0
H-5’	6.72	d, 8.0	6.75	d, 8.5	6.72	d, 8.0	6.75	d, 8.0	6.71	d, 8.5	6.75	d, 8.5
H-8	5.93	d, 2.0	5.94	d, 2.0	5.93	d, 2.5	5.94	d, 2.0	5.92	d, 2.0	5.94	d, 2.5
H-6	5.97	d, 2.0	5.97	d, 2.0	5.97	d, 2.0	5.97	d, 2.0	5.97	d, 2.5	5.97	d, 2.0
Sugar												
H-1”	4.83	d, 7.5	4.65	d, 8.0	4.83	d, 8.0	4.65	d, 8.0	4.83	d, 8.0	4.64	d, 7.5
H-2”												
H-3”, H-4”, H-5”, H-6”A/B	3.45-3.89	m	3.45-3.89	m	3.45-3.89	m	3.45-3.89	m	3.46-3.89	m	3.46-3.89	m

*****major: hemiketal a, minor: hemiketal b

Cy3gal and Cy3glc peaks were overlapping, and it is hard to clearly observe those compounds separately; hence they were assigned together. The same procedure was also applied to Cy3ara and Cy3xyl. In general, H-4 from major and minor products shifted to the upfield region as the C-ring's aromaticity decreased due to the addition of water at the carbon position 2 compared to a flavylium cationic form. Typically, the difference between the ^{1}H-NMR of these two species (H-4) was about

2.55 ppm upfield shift. These peaks appear as singlets at 6.47-6.58 ppm. Meanwhile, ^{13}C-NMR of these two species gave chemical shift differences of 60.9 and 38.5 ppm upfield shifts for C-2 and C-4, respectively.[112]

Table 4.9 ^{1}H NMR spectra of Cyanidin-3-*O*-arabinoside (**Cy3ara, 26**) and Cyanidin-3-*O*-xyloside (**Cy3xyl, 27**) in CD_3OD. Recorded at 500 MHz (25 °C).

	Formic acid				Acetic acid				Octanoic acid			
	Major		Minor		Major		Minor		Major		Minor	
Aglycone	**δ^{1}H (ppm)**	**J (Hz)**	**δ^{1}H (ppm)**	**J (Hz)**	**δ^{1}H (ppm)**	**J (Hz)**	**δ^{1}H (ppm)**	**J (Hz)**	**δ^{1}H (ppm)**	**J (Hz)**	**δ^{1}H (ppm)**	**J (Hz)**
H-4	6.47	s	6.51	s	6.47	s	6.51	s	6.47	s	6.51	s
H-6’	6.93	dd, 2.0, 8.5	6.90	dd, 2.0, 8.0	6.93	d, 2.0, 8.0	6.90	d, 2.0, 8.0	6.94	dd, 2.0, 8.0	6.90	dd, 2.0, 8.0
H-2’	7.03	d, 2.0	7.02	d, 2.5	7.03	d, 2.0	7.02	d, 2.5	7.03	d, 2.0	7.02	d, 2.5
H-5’	6.73	d, 8.5	6.75	d, 8.0	6.73	d, 8.5	6.74	d, 8.5	6.73	d, 8.5	6.74	d, 8.5
H-8	5.93	d, 2.0	5.94	d, 1.5	5.93	d, 2.5	5.94	d, 2.0	5.93	d, 2.0	5.94	d, 2.0
H-6	5.97	d, 2.0	5.97	d, 2.0	5.97	d, 2.0	5.97	d, 2.0	5.97	d, 2.5	5.97	d, 2.0
Sugar												
H-1”	*		4.67	d, 6.5	*		4.67	d, 6.5	*		4.67	d, 6.5
H-2”, H-3”, H-4”, H-5”, H-6”A/B	3.45-3.89	m	3.45-3.89	m	3.45-3.89	m	3.45-3.89	m	3.46-3.89	m	3.46-3.89	m

*H-1”a (major) of Cy3ara is under the solvent’s peak

In general, the anthocyanins' assignment in hemiketal form follows the same assignment as a flavylium cationic form. H-6’ peak appears as doublet of doublets which correlate to doublets of H-5’ and H-2’. H-5’ is *meta* coupled with H-6’ whereas H-2’ is *ortho* coupled. H-6’ for Cy3gal and Cy3glc appear at 6.91 ppm for hemiketal b and 6.92-6.93 ppm for hemiketal a with coupling constants of 2.0 and 8.0-8.5. H-2’ appears at 7.03 ppm regardless of acid or hemiketal form with coupling constants of 2.0-2.5. H-5’ appears at 6.71-6.75 ppm with coupling constants of 8.0-8.5. Both H-8 and H-6 appear as doublets that correlate to each other. These peaks appear at 5.92-5.97 ppm with coupling constants of 2.0-2.5.

For Cy3ara and Cy3xyl, H-6’ peak appears at 6.90 ppm for hemiketal b and 6.93-6.94 ppm for hemiketal a with coupling constants of 2.0 and 8.0-8.5. H-2’ appears at 7.02-7.03 ppm with coupling constants of 2.0-2.5. H-5’ appears at 6.73-6.75 ppm with coupling constants of 8.0-8.5. Both H-8 and H-6 appear as doublets that correlate to each other. These peaks appear at 5.93-5.97 ppm with coupling constants of 1.5-2.5.

The anomeric proton (H-1”) of sugar moieties in hemiketal forms showed an upfield shift with similar coupling constants as in flavylium cationic forms (6.5-8.0). These sugar moieties with coupling constants higher than 6.5 were assigned as β-D-glycopyranose.[154] Hemiketal a has more downfield chemical shift compared to hemiketal b. The chemical shift of H-1” proton of a flavylium cationic form and hemiketal forms are in this order (**AH**$^+$) > **B** (a, major) > **B** (b, minor). H-1”a (major) of Cy3ara is under the solvent peak and is hard to assign. The peaks which belong to the remaining sugar protons are assigned as multiplets at 3.45-3.89 ppm. The assignment is in agreement with the results reported in literature.[112,152] Information about the chemical characterisation of anthocyanins in hemiketal forms is limited in the literature as they were only as a mixture alongside other anthocyanin forms.[112,152]

Due to the presence of CD_3OD in large quantity as an NMR solvent, the formation of anthocyanins in ketal forms might also occur. However, the presence of CD_3 could not be confirmed by NMR spectroscopy. The mechanism is as follows: the hydroxyl group attached at the carbon position 2 of anthocyanins in hemiketal forms becomes protonated and is lost as water. Then, the carbocation that is formed is attacked by methanol, forming ketals. The ketal forms are highly unstable and can form back hemiketals as this reaction is reversible in the presence of by-product water from dehydration.[155]

In general, the formation of hemiketal forms of anthocyanins is preferable to the formation of ketals. The steric hindrance of methoxy when attached at the carbon position 2 is greater than hydroxyl as the size of water is much smaller than methanol. Furthermore, as the formation of ketals of anthocyanins requires harsher conditions (acidic environment) than what has been done in this research, this condition could lead to deglycosylation of anthocyanins, forming its aglycone (see **Scheme 2.3** and **2.4**). However, in our observation, their NMR spectra still show the protons of the sugar moiety of anthocyanins in hemiketal forms which suggests that ketal’s formation does not occur as there is no evidence of deglycosylation. According to the equilibrium of anthocyanins (see **Scheme 1.10**), hemiketal forms can transform back to a flavylium cationic form by protonation as these equilibriums are reversible depending on the pH of a solution. In conclusion, it is suggested that the ketal’s formation is less likely for anthocyanins compared to hemiketal’s formation.

4.3. Effect of Counterions on Deglycosylation of RASE.

It was observed that anthocyanins from *Aronia* skin waste could deglycosylate during the extraction-purification using SPE and concentration on a rotary evaporator. The presence of mineral acid such as HCl in RASE could also deglycosylate anthocyanin during the storage, even in the dark at room temperature (see **Chapter 2**, **Section 2.2.2.3**). In this study, RASE from the extraction-purification using organic acids were investigated to complete the anthocyanin deglycosylation study. A strong acid such as HCl could degrade anthocyanins, and milder acids were expected to limit deglycosylation. Preparation of stable anthocyanins is important as it can give benefits for further application.

The deglycosylation studies were carried out using HPLC-DAD, and the TFA, FA and AA were studied alongside HCl as a comparison. The composition was investigated at two different stages in the process; crude extract, and extract after SPE and concentration. An aliquot of crude extract prior to SPE purification, was analysed at different wavelengths to identify its polyphenol components. The identification of polyphenols was carried out at 285 nm for phenolic acids and proanthocyanidins (**Figure 4.11**), 350 nm for flavonols (**Figure 4.12**) and 520 nm for anthocyanins (**Figure 4.13**).[43,67,105] Regardless of the acids used, the anthocyanin profile shown in **Figure 4.12**-**4.14** were similar. Additionally, peaks which belong to other polyphenols were also similar. It suggests that regardless of the acid used, the crude extract always shows very similar chemical profile of polyphenols, with the only difference being the quantity of each polyphenol. These polyphenols agree with reported polyphenols in *Aronia* berries from the literature.[4,68,90,106]

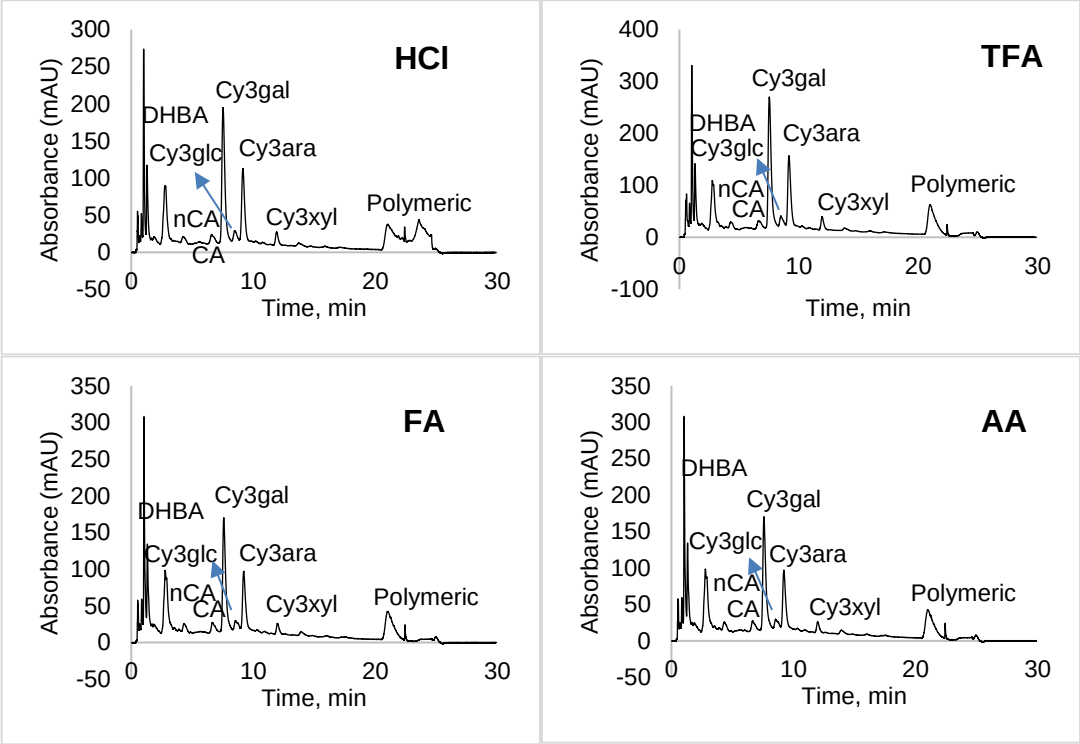

Figure 4.11 HPLC-DAD chromatogram of crude extract from HCl, TFA, FA and AA. Solvent A: H_2O/TFA (99.5:0.5); Solvent B: acetonitrile. Detected by DAD at 285 nm. The injection volume for all samples was same and all parameters were equivalent.

The quantity of anthocyanins in the crude extracts can be determined from the integration of Cy3gal peak at 520 nm (see **Figure 4.13**). The concentration of crude extract was the same. As the injection volume for all samples was same and all parameters were equivalent, the direct comparison of Cy3gal peak can show which the extraction method extracted more anthocyanins. According to **Figure 4.13**, it can be concluded that the extraction using acidified water with TFA 0.1% gives the highest anthocyanin content (420.450 mAU) followed by HCl 0.1% (305.353 mAU), FA 0.1% (267.689 mAU) and AA 0.1% (260.8954 mAU). This finding suggests that the extraction can be conducted using acidified water with TFA and HCl to obtain higher anthocyanin content. However, another aspect such as the susceptibility for the deglycosylation of anthocyanins during the elution, concentration or storage should also be considered.

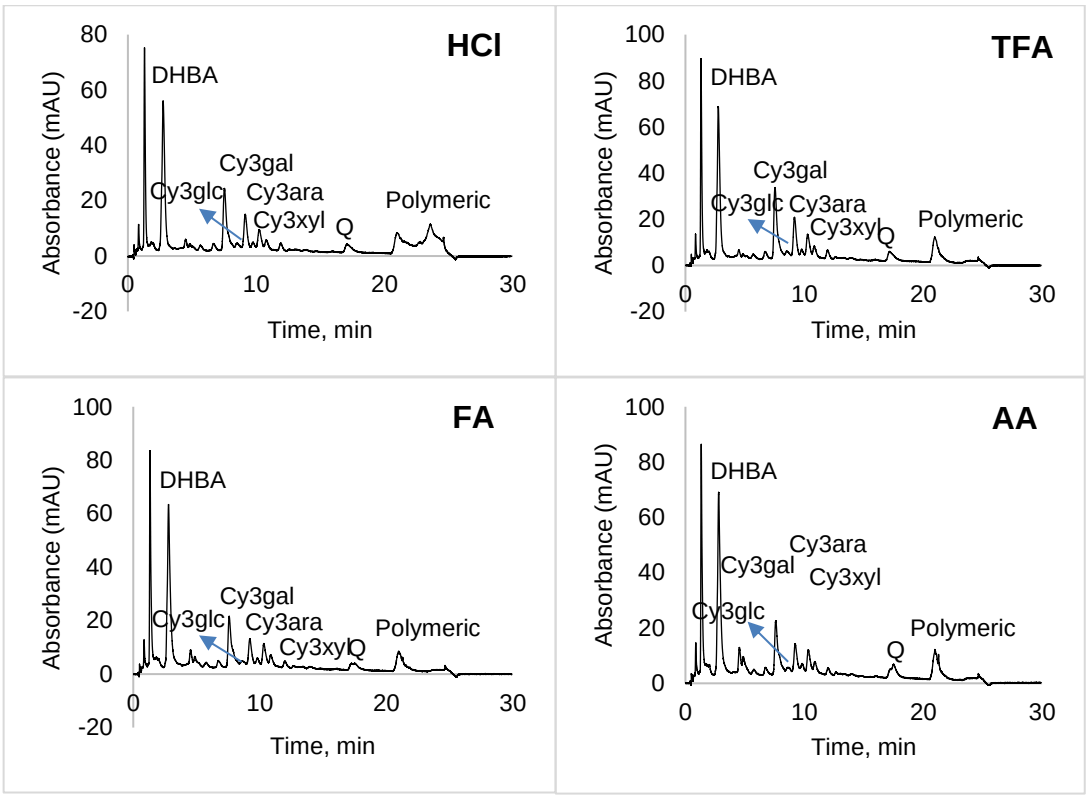

Figure 4.12 HPLC-DAD chromatogram of crude extract from HCl, TFA, FA and AA. Solvent A: H_2O/TFA (99.5:0.5); Solvent B: acetonitrile. Detected by DAD at 350 nm. The injection volume for all samples was same and all parameters were equivalent.

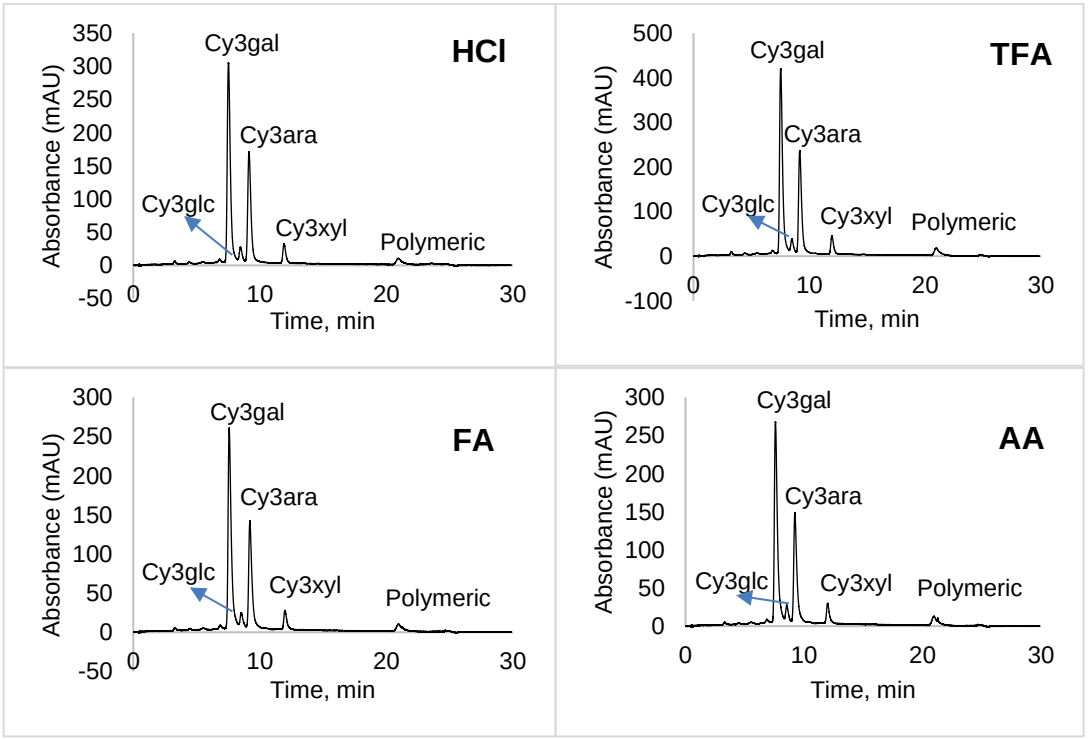

Figure 4.13 HPLC-DAD chromatogram of crude extract from HCl, TFA, FA and AA. Solvent A: H_2O/TFA (99.5:0.5); Solvent B: acetonitrile. Detected by DAD at 520 nm. The injection volume for all samples was same and all parameters were equivalent.

Furthermore, **Figure 4.13** shows that cyanidin (the product of anthocyanin deglycosylation) was not observed in any of the samples (520 nm), suggesting that deglycosylation of anthocyanins did not occur in the crude extract. In **Chapter 2**, **Section 2.2.2.2**, it has been discussed that the deglycosylation of anthocyanins was first observed during the SPE elution using acidified ethanol. Concentrating strong acid present in the ethanolic eluate during the evaporation in the rotary evaporator could also catalyse the deglycosylation. It was also observed that the concentration of polymeric proanthocyanidins increased during the SPE elution while the concentration of anthocyanins decreased. Aglycones from the deglycosylation of anthocyanins may react with each other forming the polymeric species. This result is in agreement with Ichinayagi *et al*., who reported that at higher TFA concentrations, the formed aglycones reacted successively with each other forming polymeric products.[111] The formation of anthocyanin dimers was also reported by other research groups.[156,157] Santos-buelga *et al*. also reported the formation of flavonol-anthocyanins condensation in red wines (F-A-A^+ trimers).[157] Further study is still required to confirm this finding.

The ethanol eluate from each acid's SPE desorption was evaporated to dryness to produce RASE with various counterions and analysed by HPLC-DAD. **Figure 4.5** in **Section 4.2.2** shows that RASE from HCl produced higher polymeric proanthocyanidins than milder acids. This finding was also to confirm the results discussed in **Section 4.1** where some solid of RASE from HCl were insoluble in water due to the high content of polymeric proanthocyanidins. Additionally, it also shows that TFA, FA and AA produced simpler polyphenols profile, which could be beneficial for further application as it alleviates starting material complexity.

To study the deglycosylation of anthocyanins with organic counterions versus storage time, RASE produced from the extraction-purification using HCl, FA, AA, and OA were reanalysed by HPLC-DAD after a certain time. RASE from HCl was reanalysed after the storage time of 24 months, FA was 21 months, AA was 17 months, whereas OA was stored for 18 months. RASE was stored in a closed vial where contamination of air or moisture was minimised, and in the dark at room temperature (**Figure 4.14**). Even though RASE from FA, AA and OA were stored in such conditions for a long time, they still show a similar anthocyanin profile to the initial RASE. The small peak of cyanidin was observed with low intensity after the

storage of 17 months. Aglycone formation was much slower than in RASE-HCl, where the concentration of cyanidin and polymeric proanthocyanidins increased significantly over time. This finding suggests that milder acids such as FA, AA, and OA could also prevent anthocyanins from deglycosylation, and the formation of the significantly less stable aglycone.

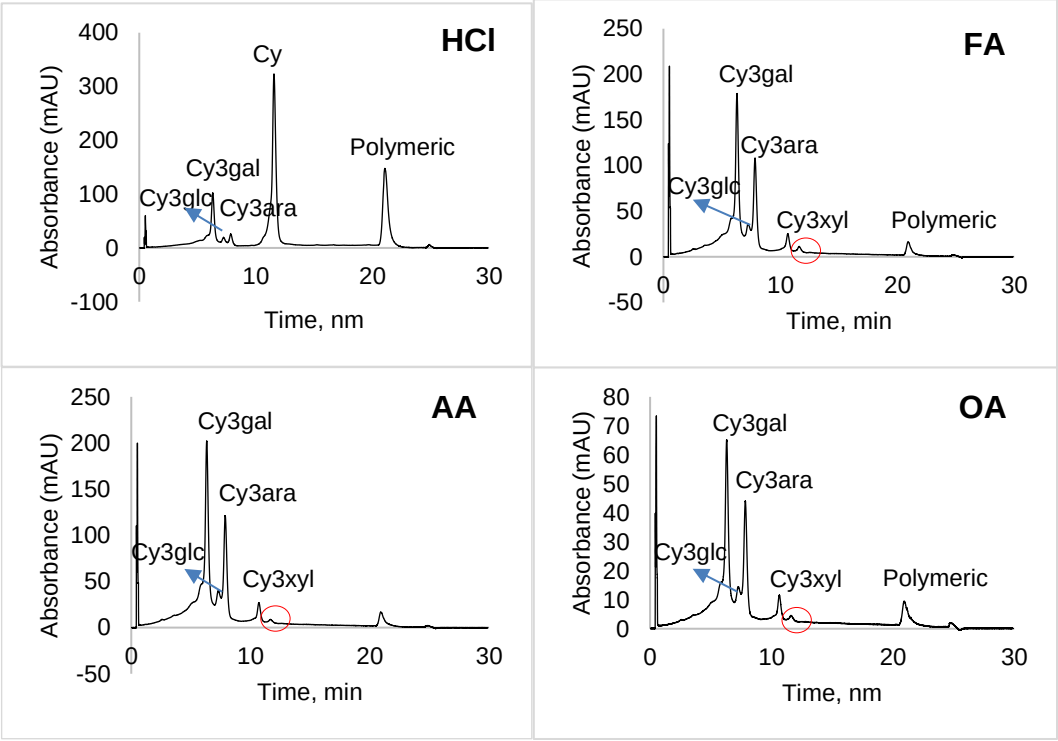

Figure 4.14 HPLC-DAD chromatogram of RASE from HCl, FA, AA and OA with the storage time of over 17 months in the dark at room temperature. The red circle shows the peak of cyanidin (Cy). Solvent A: H_2O/TFA (99.5:0.5); Solvent B: acetonitrile. Detected by DAD at 520 nm.

In future extractions, one suggestion when considering the high yield produced from the extraction-purification using HCl but with low stability of anthocyanins, is that the extraction could be carried out in acidified water (0.1% v/v, HCl). Then, organic acids are employed during the SPE elution. The use of organic acids instead of HCl during the SPE elution is expected to avoid anthocyanin deglycosylation during the SPE elution, concentration, or storage. Another conclusion from this finding was that anthocyanins are more stable at pH where hemiketal formed, and in a more hydrophobic environment. Hemiketal forms (**B**) were reported to be a thermodynamically stable form of anthocyanins and favoured at slightly acidic to neutral pH (**A** ⇌ **AH**$^+$ ⇌ **B**).[147,158]

4.4. Evaluation of the physico-chemical properties of RASE with Organic Counterions

To further understand potential applications of the new extracts developed, the physico-chemical properties such as total phenolic content (TPC), antioxidant capacity or DPPH radical scavenging activity (%RScA), and lipophilicity (Log P) of RASE produced from the extraction-purification using various acids were evaluated by adaptation of methods reported in the literature.[159–161]

4.4.1. Total Phenolic Content (TPC) of RASE

TPC of RASE was quantified to determine the extraction-purification process efficiency from various acids in extracting polyphenols. TPC in this study was determined using the Folin-Ciocalteu (F-C) method. This method's principle was through complexation of the F-C reagent (which contains a mixture of phosphomolybdate and phosphotungstate) by phenolic molecules which is achieved at a pH similar to their pK_a (*ca*. 10).[159] For this reason, sodium carbonate solution was employed to produce the required pH. At this basic pH, anthocyanins mostly exist as a quinonoid base (Cy3gal, pK_a 4.4) (see **Scheme 1.12**).[117] Phosphomolybdate reduction from Mo^{6+} to Mo^{5+} is observed as blue products with the detection wavelength of 765 nm.[159] A calibration curve was made using gallic acid at various concentrations. The absorbance of each concentration was then transformed as a graph showing concentration as x-axis and absorbance as the y-axis ($y = 0.44x + 0.75$, $R = 0.995$). TPC was expressed as gallic acid equivalent (mg/g of RASE, GAE) (**Table 4.10**).

Table 4.10 Total Phenolic Content (TPC) of RASE with various counterions.

RASE	TPC (mg/g of RASE (GAE))
Chloride	618.2
Trifluoroacetate	557.6
Formate	279.9
Acetate	377.8
Octanoate	448.2

In this study, the TPC ranged from 279.9 (FA) to 618.2 (HCl) mg/g of RASE, GAE. Based on the results shown in **Table 4.10**, TPC of RASE with different counterions

follows this order: HCl > TFA > OA > AA > FA. Application of various acids during the extraction-purification process caused changes of TPC in the obtaining RASE. The finding in this study indicates that HCl extracts a higher level of total polyphenolic compounds compared to other acids. It has been discussed in **Section 4.2.3** that HCl extracted more DHBA, Q, nCA, CA and polymeric proanthocyanidins compared to other acids, which contributed to the higher TPC value.

Overall, the TPC content in this study was higher than those reported by Denev *et al*., who had carried out the extraction using citric acid with a concentration of 1%, and reported that total polyphenols in *Aronia* chokeberry extract after SPE was 352 mg/g GAE.[81] Wangensteen *et al*. reported that total phenolic content of four cultivars of *Aronia* berries ranged from 98 to 148 mg GAE/g extract.[162] They did the extraction in methanol with 0.5% TFA. However, they used fruits instead of pomace, and it has been known that total polyphenols content in pomace is much higher than in the fruits.[4] All the studies also reported that polyphenols in *Aronia* chokeberry were higher than other berries.

4.4.2. DPPH Radical Scavenging Activity (%RScA) of RASE

Aronia skin waste contains polyphenols, which are well known for their antioxidant properties.[4,163] Antioxidants recovered from agro-industrial waste and by-products such as *Aronia* skin waste are worth exploring, as an alternative to synthetic antioxidants, and to reduce pollution due to waste disposal. Antioxidant properties of phenolic compounds are affected by the numbers and arrangement of OH groups.[163] These phenolic groups possess hydrogen donating capabilities to act as antioxidants.[164] The mechanism of antioxidant activity of anthocyanins as a flavylium cationic form is presented in **Chapter 1**, **Scheme 1.7**, while the antioxidant mechanism for other polyphenols present in RASE is presented in **Scheme 4.2**. The antioxidant activity of *Aronia* pomace was much higher than its fruits and juice.[4] This can be explained by the fact that the total phenolics, which are mostly predominated by polymeric proanthocyanidins in *Aronia* berries, were much higher in pomace than fruits or juice.[4]

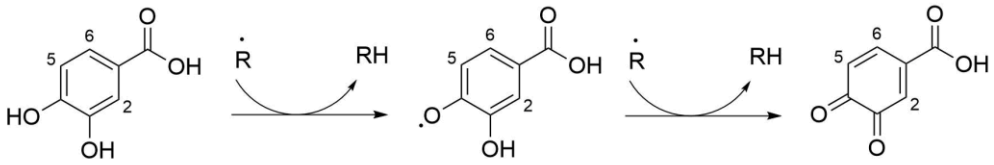

3,4-Dihydroxybenzoic acid
(**DHBA**)

Scheme 4.2 Mechanism reaction of antioxidant activity of DHBA as one of neutral polyphenols found in RASE.

The antioxidant activity of RASE in this study was determined using the DPPH (2,2-diphenyl-1-picrylhydrazyl) assay, as previously described by Guldbrandsen *et al*.[160] A solution of DPPH (0.14 mM) was prepared first, and then the solutions of samples in methanol, in a concentration range from 0.6 to 40 mg/L. The experiments were performed in triplicate, the absorbance was measured at 517 nm after incubation for 30 min in the dark. This assay determines the reduction of the purple stable DPPH radical to the yellow-coloured DPPH-H in the presence of a hydrogen-donating antioxidant (AH) (**Scheme 4.3**).

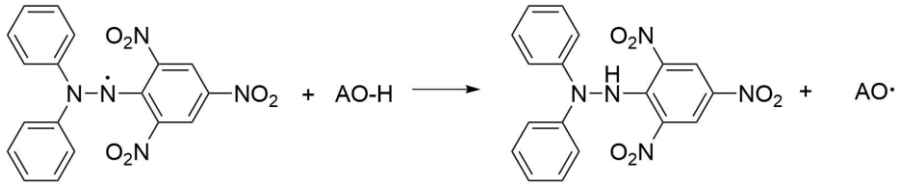

Scheme 4.3 DPPH and antioxidant reaction.[165]

The colour measurement is typically taken after *ca*. 30 minutes, although colour development begins as soon as the DPPH solution is added with the RASE solution. To study the wavelength shift of this reaction, Cy3gal and DPPH solutions were separately prepared in methanol and then analysed by a UV-visible spectrophotometer at 200-800 nm. Those solutions were then mixed and analysed by a UV-visible spectrophotometer at 200-800 nm. The colour development for 30 minutes at room temperature in the dark was performed. Afterwards, the mixture was analysed. All spectra were combined and presented in **Figure 4.15**. The maximum wavelength of the DPPH solution in methanol was 516 nm, similar to the maximum wavelength reported in the literature (517 nm). There was no significant difference between the measurement after 5 min and 30 min of Cy3gal-DPPH mixing and colour development in the dark. After a certain time, the remaining DPPH● was measured and responsible for the sample's radical scavenging activity.

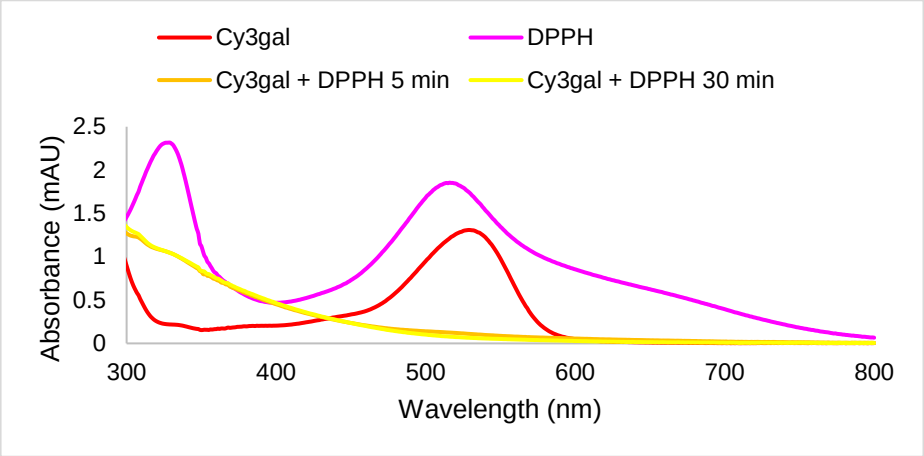

Figure 4.15 Colour development of the mixture solution of DPPH radical reaction with Cy3gal. Solvent: methanol.

Antioxidant activity (%RScA) value where the concentration of the sample is required to scavenge 50% of total free DPPH radicals is defined as the inhibitory concentration 50 or IC_{50}.[164] The lower IC_{50} value shows the higher antioxidant activity as it requires the lower concentration to inhibit the initial free radical concentration by 50%. IC_{50} of RASE with different counterions ranged from 4.8-5.7 mg/L following this order: HCl > AA = FA > TFA = OA (**Table 4.11**). It must be noted that this finding represents the antioxidant activity of polyphenols as a mixture, not a single compound. The chemical characterisation of polyphenols present in RASE can be found in **Chapter 3**.

Table 4.11 IC_{50} of RASE with various counterions

RASE-counterion	IC_{50} (mg/L)
Chloride	4.8
Trifluoroacetate	5.7
Formate	5.3
Acetate	5.3
Octanoate	5.7

The correlation between TPC and %RScA (IC_{50}) of RASE in this study is presented in **Figure 4.16**. Oszmianski and Wojdylo reported that pomace's antioxidant activity was higher than fruit and juice, which corresponds to its polyphenols content.[4] Hwang *et al*. also reported the correlation between TPC and antioxidant activity with a correlation coefficient of 0.9953.[49] However, in this study, there is no clear correlation between the total polyphenols and antioxidant activity. Bolling *et al*. also reported that DPPH IC_{50} values of *Aronia* juices did not correlate to polyphenols.[64]

According to the chemical composition of RASE (see **Section 4.2**), RASE from the extraction-purification using HCl produced more neutral polyphenols (DHBA, Q, nCA, CA) and anthocyanin aglycone compared to RASE from other acids. Li *et al*. reported that DHBA showed antioxidant activity with an IC_{50} of 1.88 mg/L.[166] Jakobek *et al*. found that small phenolic acids such as DHBA could react with DPPH radicals easier and faster than bigger polyphenols because of reduced steric hindrance.[67] Higher content of phenolic acids in wild chokeberries showed stronger antioxidant activity by DPPH assay.[67] Meanwhile, other minor polyphenols also contributed to antioxidant activity but have weaker radical scavenging potential against DPPH. IC_{50} of quercetin, chlorogenic acid and neochlorogenic acid were 8.5, 6.2 and 8.1 mg/L, respectively.[167,168] Meanwhile, RASE-trifluoroacetate showed slightly weaker antioxidant activity compared to HCl even though the anthocyanin content is higher, most likely due to the polymerisation of the anthocyanins resulting in higher molecular compounds which are less effective as radical scavengers.[67]

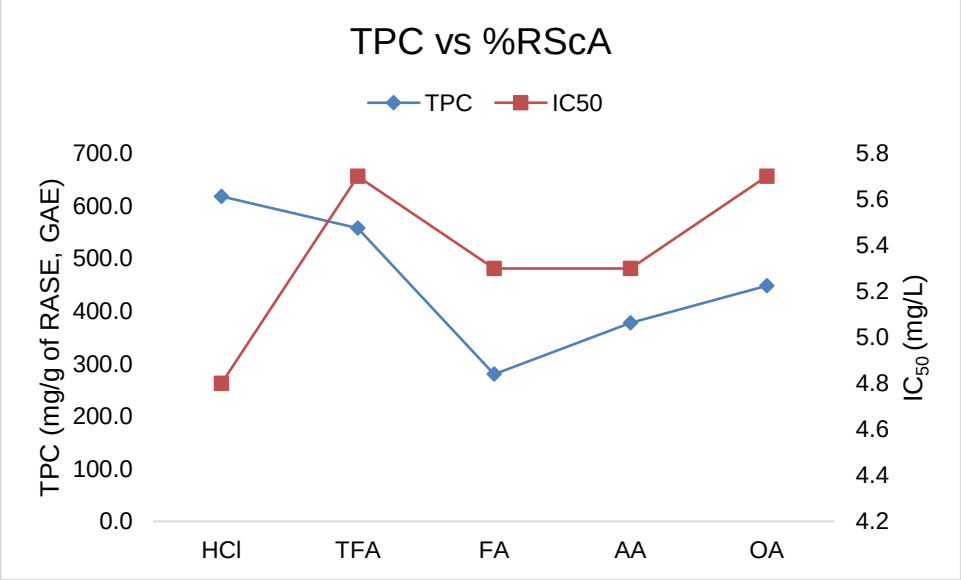

Figure 4.16 Antioxidant activity (%RScA) vs TPC of RASE with various counterions.

4.4.3. Lipophilicity (Log P)

The octanol/water partition coefficient (Log P) for a variety of RASE extracts was measured to understand the change in lipophilicity due to different acid counterions. The evaluation of Log P of RASE was carried out following the methods reported by Zhu *et al*. and Cruz *et al*. with slight modification.[161,169] For this purpose, n-octanol was saturated with acidified water (2% of HCl v/v) for > 24 h before use. Initially,

RASE was dissolved in a small quantity of methanol (100 µL) and then added with pre-saturated n-octanol. It was then partitioned with pre-saturated acidified water, and absorbance measurements performed at 520 nm.

Even though they bear a sugar moiety, anthocyanins may still have some hydrophobic character due to their aromatic rings.[150] However, anthocyanin lipophilicity is expected to be low as hydroxyl groups form the anthocyanin core and sugar moiety, and are polar enough to form extensive hydrogen bonding with water. Nevertheless, it was expected that the extraction-purification using acids with different polarity might affect the lipophilicity of RASE produced.

Log P's values of RASE salts obtained in this study were as follows 0.044 (FA), 0.048 (AA), 0.058 (OA), 0.068 (TFA) and 0.115 (HCl). Log P for all RASE were positive, which means that they are more hydrophilic than hydrophobic. RASE salts from strong acids such as HCl and TFA showed slightly higher Log P than RASE from weaker acids as cyanidin (which does not have the sugar moiety attached) was present in these RASE, so has significantly greater lipophilicity. Cyanidin in these RASE was generated as a deglycosylation product and only found in RASE-chloride and RASE-trifluoroacetate as already discussed earlier in **Section 4.2.2**. It is reported in the literature that cyanidin has a higher LogP value (3.05) compared to Cy3gal (0.24), Cy3glc (0.39), Cy3ara (1.06), and Cy3xyl (1.06); the higher the value of Log P, the molecules are less polar and therefore less soluble in the aqueous phase.[170] Polymeric proanthocyanidins were also higher in RASE-chloride, which makes this extract less water-soluble than RASE from other acids. The 7-month-sample of RASE-HCl, which is rich in cyanidin aglycone, was also assessed for its lipophilicity for comparison. The absence of sugar moiety on the cyanidin core make this compound more hydrophobic. It was observed that the cyanidin's octanol layer was redder than the other RASE octanol layer after partitioning for 24 h (**Figure 4.17**).

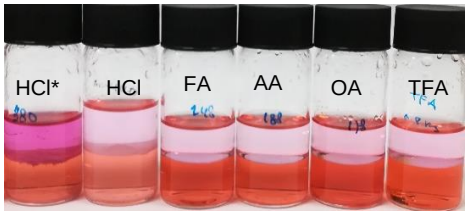

Figure 4.17 Lipophilicity assay of RASE in an octanol-water system. *Stored for 7 months.

The HPLC-DAD analysis was carried out for both aqueous and octanol layers to investigate the components which go to each layer. After partitioning for 24 h, an aliquot of each layer was taken and analysed by HPLC-DAD at 520 nm for anthocyanin monitoring. Most anthocyanins (Cy3gal, Cy3glc, Cy3ara and Cy3xyl) can be identified in an aqueous layer and only a small quantity found in the octanol layer (no more than 3 mAU). Cyanidin was only found in an octanol layer due to its lipophilicity. It can be concluded that a sugar moiety has an important role in driving the lipophilicity of anthocyanins (see **Section 2.2.2.2**). This finding also suggests a simple and inexpensive method to separate anthocyanins from their aglycone.

4.5. Conclusion

Anthocyanins from *Aronia* skin wastes have been extracted and purified in a batch method using the previous study's extraction parameters. Strong acids such as HCl and TFA, and milder organic acids such as FA, AA and OA were employed for the extraction-purification process to produce various anthocyanin salts. Cyanidin-3-*O*-galactoside (Cy3gal) and cyanidin-3-*O*-arabinoside (Cy3ara) were the major anthocyanins found in RASE regardless of acids used in the extraction-purification process, whereas cyanidin-3-*O*-glucoside (Cy3glc) and cyanidin-3-*O*-xyloside (Cy3xyl) were identified as minor anthocyanins (< 10%). HCl and TFA as strong acids could degrade anthocyanins through hydrolysis, forming its aglycone (cyanidin), but this did not occur with milder organic acids. However, the ratio of Cy3gal/Cy3ara varied amongst those acids. Strong acids gave a Cy3gal/Cy3ara ratio of 1.86, while milder acids ranged from 161-1.76. HCl extracted more neutral polyphenols and produced more polymeric proanthocyanidins compared to other acids. However, TFA, FA and AA can be an alternative to HCl as these acids showed a simpler profile but higher content of anthocyanins.

Anthocyanins produced from the extraction-purification using HCl and TFA were observed in the flavylium cationic form in MeOH, whereas milder organic acids gave a hemiketal form instead. Chloride and trifluoroacetate are strong counterions for anthocyanins. Milder acids are considered weak counterions for anthocyanins as they are less able to form the flavylium cation. Deglycosylation studies of RASE also showed that RASE produced by the addition of milder organic acids during the extraction-purification were relatively more stable than HCl. Preserving anthocyanins at least at milder pH with a more hydrophobic counterion is suggested, especially if

used for a longer period (months). This is advantageous for further application, such as chemical modification, because it can simplify the reaction and provide a reasonable quantity of anthocyanins to be present in the starting material (RASE).

RASE produced using strong acids showed higher TPC compared to RASE produced using milder acids. The highest TPC was found in RASE produced from the extraction-purification using HCl. The strong acids can penetrate and break the cellular membrane, leading to the higher polyphenols content present in RASE. This high content of polyphenols contributes to higher antioxidant activity. A small phenolic compound such as DHBA possibly has a more rapid interaction with the DPPH free radicals due to reduced steric hindrance.

On the other hand, RASE, which contains larger polyphenols and higher anthocyanins content, showed lower antioxidant capacities. The strong acids could also hydrolyse anthocyanins producing its aglycone. Consequently, RASE, which contains a higher amount of aglycone, is more lipophilic than RASE from milder acids where aglycone is limited. A sugar moiety affects the hydrophilicity of anthocyanins and polyphenols in general.

Chapter 5
New Methods for Preparation and Characterisation of Hemiketal Forms of Anthocyanins from *Aronia* Skin Waste

This chapter discusses the new methods for preparing and characterising anthocyanins from *Aronia* skin waste as their hemiketal forms (**Figure 5.1**). **Section 5.1** discusses the preparation of hemiketal forms of Cy3gal through nucleophilic addition of water. The formation of hemiketal a (major) and hemiketal b (minor) was observed, and both are characterised in this study. The hemiketal forms in a mixture alongside a flavylium cationic form were then analysed. **Section 5.2** discusses the preparation and characterisation of a flavylium-hemiketal mixture of Cy3gal, Cy3glc, Cy3ara and Cy3xyl. This study was carried out by performing the analysis in NMR tubes using deuterated methanol without TFA-d. The proportion of flavylium cationic and hemiketal forms was determined, alongside the proportion of major and minor hemiketals. **Section 5.3** discusses the production of RASE in hemiketal forms from the extraction-purification when the use of HCl was limited during the SPE elution. **Section 5.4** discusses a pH jump experiment for Cy3gal and RASE as an alternative method to prepare anthocyanins in their hemiketal forms.

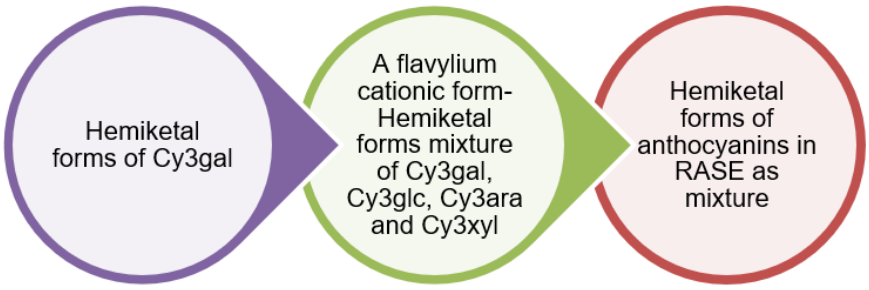

Figure 5.1 General scheme for preparing and characterising hemiketal forms of anthocyanins from RASE as an individual compound and mixture.

5.1. New Methods for Preparation and Characterisation of Hemiketal Forms of Cy3gal.

Due to the instability of anthocyanins, their production and characterisation, particularly in their hemiketal forms, remains challenging, and to the best of our knowledge, there are no literature reports of hemiketals being observed as a single species. The use of D_2O (without additional acid) for NMR analysis typically gives a mixture of flavylium cationic form (**AH^+**), hemiketal (**B**) and chalcone (**C_E/C_Z**) at pH 2.6.[153] The adjustment of pH can be made by adding NaOD or DCl.[153] Fernandes *et*

al. dissolved Cy3glc in D_2O and adjusted the pD to 3.9 by adding NaOD to give a mixture of anthocyanin species.[152] Additionally, Leydet *et al*. reported the formation of this mixture as observed by NMR. However, the analysis was performed in non-deuterated water. To adjust the pH of anthocyanin containing solution, HCl and NaOH were added.[132] Although water is a good solvent for anthocyanins, its presence will obscure peaks in the sugar region unless water suppression is performed.[171]

Alternatively, for the NMR analysis, anthocyanins were dissolved in deuterated methanolic solution with the presence of an acid, usually CF_3COOD or DCl.[172] The CD_3OD/CF_3COOD (95:5, v/v) solution is commonly applied to ensure acidic pH to maximise the formation of the flavylium cationic form (**AH^+**) and dissolve the sample completely, especially when it contains polymeric proanthocyanidins which have greater methanol solubility and lower solubility in water compared to anthocyanins.[26] Without the addition of deuterated acid in the solution, Jordheim *et al*. reported that a mixture of flavylium and hemiketal anthocyanins was observed and characterised when the pH of the solution was slightly acidic to neutral.[112]

To estimate the pH of the deuterated solution, the pH of the non-deuterated solvent was measured. The methanolic solution with the addition of TFA (CH_3OH/ CF_3COOH, 95:5) was prepared in the same manner as the deuterated solvent, and it is expected that the pD of the deuterated solution would be similar enough to pH for our purposes. McConnell *et al*. reported that in deuterium oxide, the pK_a of acetic acid-d_4 (4.65) was higher than non-deuterated acetic acid (4.63), suggesting that deuterium compound is less ionised than non-deuterated.[173] The pH of acidified methanol was 0.41 (acidic), which is sufficient to exclusively produce the flavylium cationic form. The pH of methanol itself was 7.21, and at this pH, anthocyanins were considered to present predominantly as hemiketal forms (see **Chapter 2**, **Section 2.2.1**).

An excess of trifluoroacetic acid from a semi-preparative HPLC was suggested to substantially decrease the pH of methanol to slightly acidic, resulting in the formation of the flavylium cationic form (**AH^+**) and hemiketal forms (**B**) as a mixture (**Scheme 5.1**).[147] This equilibrium was observed in the H-NMR, which is later discussed in **Section 5.2**. The limited literature on the hemiketal forms exists, and at present, it is not possible to stereochemically assign the two possible hemiketal epimers, the R- or S- forms present in unequal amounts as major (a) or the minor (b) forms.

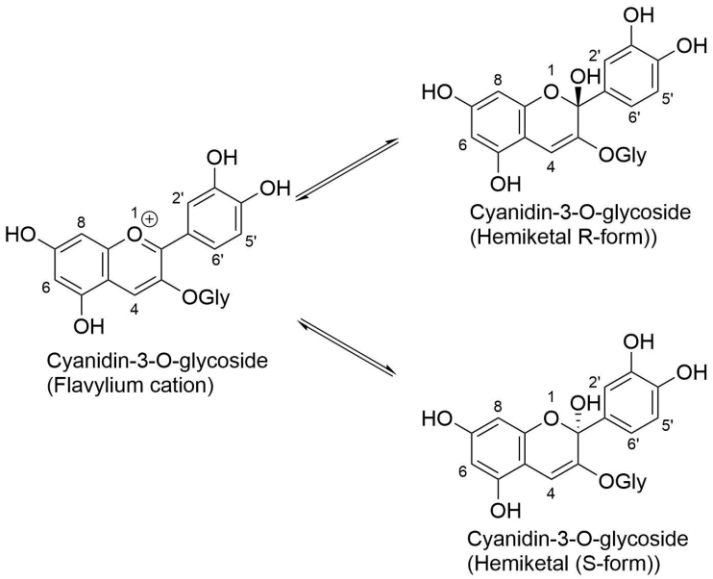

Scheme 5.1 An equilibrium between flavylium cation and hemiketal forms of cyanidin glycoside.[147]

The ^{19}F-NMR spectroscopy showed the presence of trifluoroacetic acid in the isolated samples. The ^{19}F-NMR spectrum of Cy3gal in CD_3OD without the addition of CF_3COOD still showed a fluorine peak that belonged to TFA. It appears as a singlet at -76.95 ppm ($CFCl_3$, 0 ppm as reference).

The characterisation of hemiketal forms of anthocyanins is important as it can complete the gap in this field. RASE contains 4 different anthocyanins, and each anthocyanin can form two different hemiketals. In total, theoretically, there are 12 different species of anthocyanins in RASE alongside its aglycone, neutral polyphenols and polymeric proanthocyanidins. To alleviate the complexity in characterising the mixture of RASE, the characterisation was done initially for a single anthocyanin for both a flavylium cationic form and hemiketal forms. Once the flavylium cationic form and hemiketal forms of all individual anthocyanins have been assigned, then the assignment for the mixture will be greatly simplified.

In this study, the pure hemiketal forms of Cy3gal were characterised successfully. *Aronia* berries only contain cyanidin-based anthocyanins, but with various monosaccharide glycosides. This enables Cy3gal in its hemiketal forms to be used as a basis for assigning other anthocyanins. These individual anthocyanins have been isolated from RASE using semi-preparative HPLC with relatively high purity (~97%). In this section, new methods for preparation and characterisation of hemiketal forms of Cy3gal were carried out.

5.1.1. Selective Formation of hemiketals of Cy3gal.

Direct NMR analysis of individual anthocyanins in neutral CD_3OD showed a mixture of flavylium-hemiketal forms (**Section 5.2**). This anthocyanin containing solution was evaporated in a rotary evaporator to dryness. The recovered anthocyanins were then re-dissolved in CD_3OD to give purplish-blue solution and slowly evaporated by an N_2 stream containing water vapour at room temperature, as shown in **Figure 5.2**. The remaining trifluoroacetic acid was expected to evaporate, bringing the pH of the solution slightly acidic to neutral. This process was repeated several times until hemiketal forms appeared as a major or exclusive component in the mixture.

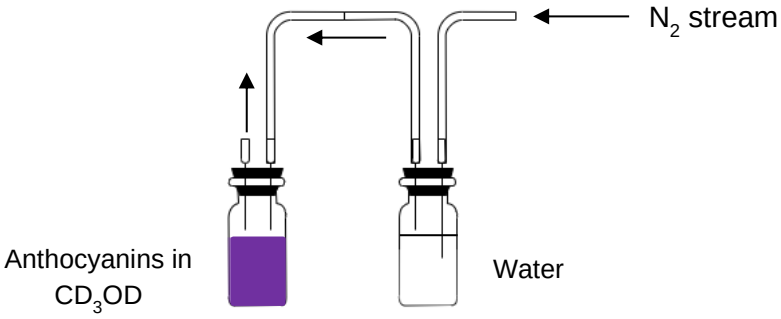

Figure 5.2 General preparation to produce hemiketal forms of anthocyanins. N_2 is passed through a vial containing water, and it goes to a vial containing anthocyanins in CD_3OD to dry the solvent out slowly.

According to this equilibrium, $\mathbf{AH^+} \overset{+H_2O}{\rightleftharpoons} \mathbf{B} + \mathbf{H^+}$, continuous nucleophilic addition of water with the removal of the acid on Cy3gal could lead to the formation of hemiketal forms, following Le Chatelier's principle.[174] It states that the equilibrium changes to the right when one of the products is removed as soon as it is formed. The equilibrium would keep on moving on the right if the acid is kept removed, turning this into a one-way reaction. One cycle consisted of dissolving the dried Cy3gal in CD_3OD, slowly evaporation to dryness, re-dissolving the dried Cy3gal in CD_3OD and analysed by NMR spectroscopy (**Figure 5.3**). The first cycle was referred to as Cycle 1. Cycle 2 means that the anthocyanin containing solution from Cycle 1 was subjected to the same procedure, and so on. Through this process, the concentration of a flavylium cationic form decreased while hemiketal concentration increased every time the experiment was repeated, and relatively pure hemiketals were produced after several cycles. This allowed the characterisation of this species using 1D and 2D ^{1}H-NMR spectra. ^{13}C-NMR was also carried out to get HSQC spectra to assign all carbons with protons attached, although the quality of ^{13}C-NMR was poor due to the small sample size. The remaining carbons of the hemiketal forms were determined from a ^{13}C-NMR spectrum of a flavylium-hemiketal mixture (**Section 5.1.2**).

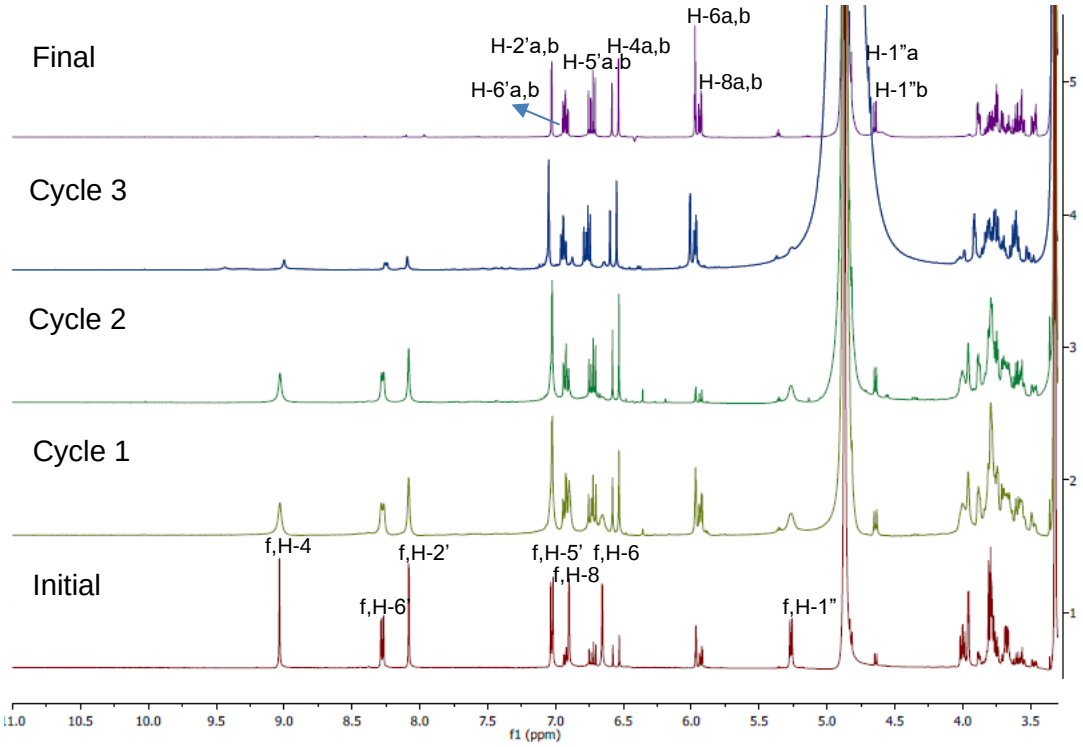

Figure 5.3 ^{1}H-NMR spectra (500 MHz, 25 °C) of Cy3gal showing the formation of hemiketal forms by nucleophilic addition of water experiment. f = flavylium cation; a = hemiketal a (major); b = hemiketal b (minor).

Hemiketal forms are expected to be essentially colourless species due to the interruption of the extensive conjugation between the anthocyanin aromatic rings.[147] Interestingly, in this study, even though the NMR spectra only showed the hemiketal forms, the colour of Cy3gal methanolic solution appeared as purplish blue in a neutral alcoholic solution, consistent with the presence of a quinonoid base. It is suggested that the small quantity of quinonoid base is still present in this solution to account for the colouration, despite not being detected in the NMR spectra (see **Figure 5.3**).

Forino *et al*. reported that increasing the pH from 3.06 to 3.99 resulted in a decrease of flavylium cation (Mal3glc) molar fraction *ca*. 10 fold.[171] The pH jump experiment from pH 1.0 to pH 5.3 decreased the absorbance of Cy3glc at 530 nm (flavylium cation), whereas the absorbance at 350 nm increased.[117] This indicates that the isomerisation process occurred, which led to colourless hemiketal forms.[117] Gómez-Alonso *et al*. reported that the addition of CF_3COOD (5-30% v/v) changed the flavylium-hemiketal mixture ratio. The hemiketal forms were observed when a minimum amount of CF_3COOD was added, and larger amounts resulted in enhanced flavylium cation concentration.[126]

Forino *et al*. also reported hemiketal forms at pH 6.96, which is slightly acidic to neutral pH.[171] As pure methanol-d_4 was used in this analysis, hemiketal forms were expected to dominate. Through this process, C-2 of Cy3gal was continuously attacked by water, forming hemiketal forms. It has been well known that tertiary carbocation is the most stable amongst other carbocations. Therefore, nucleophilic addition by water can occur at this position, forming hemiketal form (**B**).[175] The proposed mechanism of nucleophilic addition by water on anthocyanins via a flavylium cationic form is presented in **Scheme 5.2**.[147]

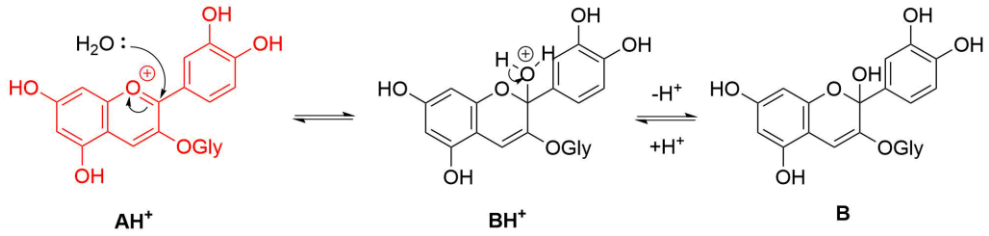

Scheme 5.2 Proposed mechanism of nucleophilic addition of water at carbon position 2 of a flavylium cationic form in general.[147]

5.1.2. Characterisation of Hemiketal Forms of Cy3gal

In the downfield region of the ^{1}H-NMR spectrum of Cy3gal dissolved in neutral CD_3OD, only peaks which belong to hemiketal forms were present (**Figure 5.4**). The flavylium cationic form peaks of Cy3gal were not observed, indicating that the sample is relatively pure. To the best of our knowledge, this is the first time single hemiketal forms (major and minor) have been prepared, which greatly helps the assignment of the different species present.

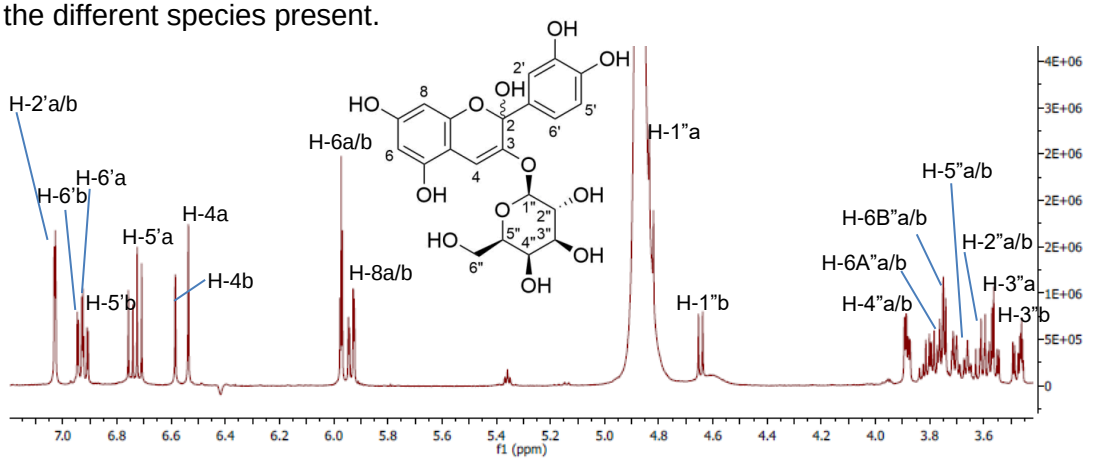

Figure 5.4 ^{1}H-NMR spectrum of Cy3gal hemiketals dissolved in neutral CD_3OD. Recorded at 500 MHz (25 ºC).

According to **Scheme 5.1**, there were two epimers of hemiketal observed in this study. The two stereoisomer hemiketal species found in this study cannot be stereochemically assigned but referred to as the major and minor hemiketals (R- and S-form) hemiketals. H-2'a and H-2'b peaks appear overlapping to each other at 7.03 ppm as doublets with a coupling constant of 2.0 Hz for both (see **Figure 5.4**). It can be distinguished easily in the pure hemiketal form, but appeared under H-5' of flavylium cationic form in the flavylium-hemiketal mixture (see **Section 5.2.1**). The same problem was apparent for H-6'a and H-6'b peaks; these peaks appear close to H-8 of the flavylium cationic form, making them hard to assign precisely. However, these peaks are easily assigned in these pure hemiketal forms as doublet of doublets at 6.94 ppm and 6.92 ppm with both coupling constants of 8.0 Hz and 2.0 Hz for H-6'a and H-6'b, respectively. H-5'a and H-5'b peaks appear as doublets at 6.72 ppm and 6.79 ppm with coupling constants of 8.0 Hz and 8.5 Hz, respectively.

Meanwhile, in the upfield region of the ^{1}H-NMR spectrum, a ^{1}H-^{1}H COSY spectrum was useful to assign sugar peaks as they sometimes appear overlapping to each other peaks (**Figure 5.5**). The two epimers of the hemiketal should give different chemical shifts for the sugar moiety. A doublet at 4.83 ppm with a coupling constant of 7.5 ($J_{ax\text{-}ax}$) is assigned as β anomeric sugar of H-1"a (anomeric proton for hemiketal major). The anomeric proton for hemiketal minor (H-1"b) appears as a doublet at 4.65 ppm with a coupling constant of 7.5, also assigned as a β anomeric sugar.

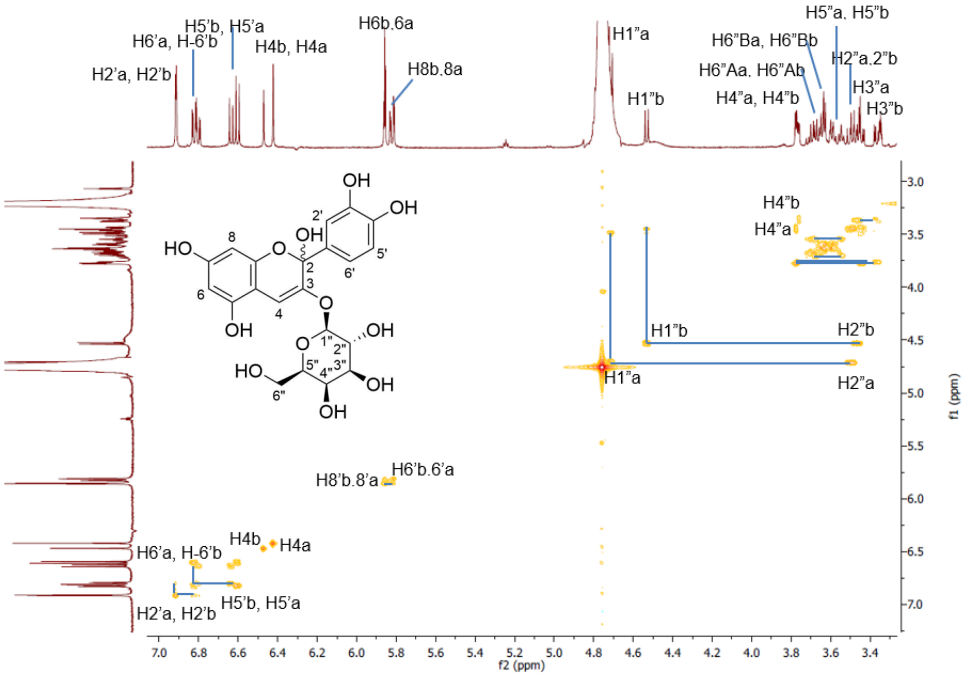

Figure 5.5 Expanded region of a COSY spectrum (500 MHz) of Cy3gal in CD_3OD at 25 °C. a = hemiketal a (major); b = hemiketal b (minor).

According to **Figure 5.5**, H-2” has a strong correlation with H-1”, therefore a doublet of doublets at 3.61 ppm with coupling constants of 7.5 Hz and 10.0 Hz is assigned as H-2”a. A doublet of doublets at 3.58 ppm with coupling constants of 7.5 Hz and 9.5 Hz is assigned as H-2”b. The same technique is used to distinguish H-3”, H-4”, H-5” and H6”A/B. H-3” is assigned because of a strong correlation with H-2” shown in the COSY spectrum. H-3”a appears as a doublet of doublets at 3.56 ppm with coupling constants of 3.0 Hz and 9.5 Hz. H-3”b appears as a doublet of doublets at 3.48 ppm with coupling constants of 3.5 Hz and 9.5 Hz. H-4” also shows a strong correlation with H-3” and H-5” as they are a neighbour proton to each other. H-4”a can be found at 3.89 ppm as a doublet with a coupling constant of 3.0 Hz. H-4”b can be found at 3.88 ppm as a doublet with a coupling constant of 3.5 Hz. These protons are found as doublets in literature.[112] To differentiate the peaks of H-5” and H-6”A/B, ^{1}H-^{13}C HSQC was carried out (**Figure 5.6**). These protons are found as multiplets at 3.66-3.83 ppm. This assignment has been confirmed with the reported literature.[112]

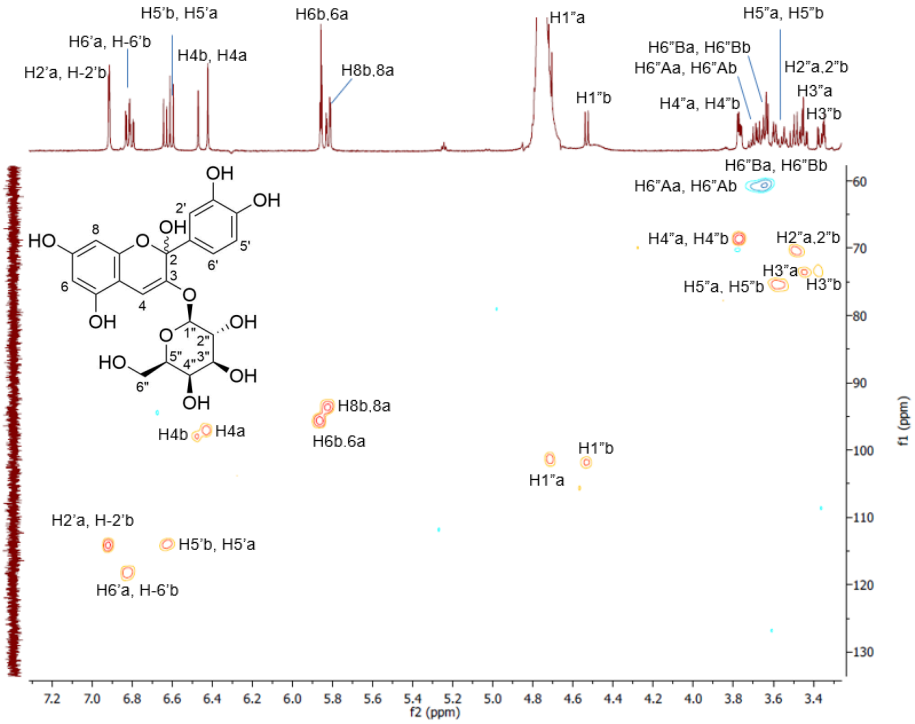

Figure 5.6 Expanded region of an HSQC spectrum (500 MHz) of Cy3gal in CD_3OD at 25 °C. a = hemiketal a (major); b = hemiketal b (minor).

The summary of the NMR data of major and minor hemiketal of Cy3gal is presented in **Table 5.1** and **Table 5.2**.

Table 5.1 ^{1}H (500 MHz) and ^{13}C (125 MHz) NMR Data for **Cy3gal** in CD_3OD at 25 °C (**hemiketal a, major**).

Aglycone	Cy3gal (major)			Cy3gal (literature*)[112]		
	$\delta^{1}H$ (ppm)	J (Hz)	$\delta^{13}C$(ppm)	$\delta^{1}H$ (ppm)	J (Hz)	$\delta^{13}C$(ppm)
H-4	6.54	d, 0.7	97.1	6.61	d, 0.7	98.6
H-6'	6.94	dd, 8.0, 2.0	118.2	7.01	dd, 8.3, 2.2	119.8
H-2'	7.03	d, 2.0	114.1	7.11	d, 2.2	95.1
H-5'	6.72	d, 8.0	114.1	6.79	d, 8.3	115.4
H-8	5.94	d, 2.0	93.6	6.00	dd, 2.2, 0.7	95.1
H-6	5.97	d, 2.0	95.6	6.04	d, 2.2	97.1
Sugar						
H-1"	4.83	d, 7.5	101.4	4.90	d, 7.7	102.7
H-2"	3.61	dd,10.0, 7.5	70.5	3.69	dd, 9.8, 7.7	71.9
H-3"	3.56	dd, 9.5, 3.0	73.5	3.64	dd, 9.8, 3.4	74.8
H-4"	3.89	d, 3.0	68.7	3.97	dd, 3.4, 1.1	70.0
H-5"	3.66-3.83	m	75.6	3.78	m	76.8
H-6"A		m	60.9	3.84	m	62.2
H-6"B		m	60.9	3.80	m	62.2

*it is a mixture alongside its flavylium cation

Table 5.2 ^{1}H (500 MHz) and ^{13}C (125 MHz) NMR Data for **Cy3gal** in CD_3OD at 25 °C **(hemiketal b, minor)**.

Aglycone	Cy3gal (minor)			Cy3gal (literature*)[112]		
	$\delta^{1}H$ (ppm)	J (Hz)	$\delta^{13}C$(ppm)	$\delta^{1}H$ (ppm)	J (Hz)	$\delta^{13}C$(ppm)
H-4	6.58	s	98.0	6.66	d, 0.7	99.6
H-6'	6.92	dd, 8.0, 2.0	118.2	7.00	dd, 8.3, 2.2	119.7
H-2'	7.03	d, 2.0	114.3	7.11	d, 2.2	115.5
H-5'	6.79	d, 8.5	114.2	6.83	d, 8.3	115.5
H-8	5.93	d, 2.0	93.7	6.02	dd, 2.2, 0.7	95.3
H-6	5.97	d, 2.5	95.8	6.05	d, 2.2	97.1
Sugar						
H-1"	4.65	d, 7.5	101.9	4.72	d, 7.7	103.4
H-2"	3.58	dd, 9.5, 7.5	72.8	3.66	dd, 9.8, 7.7	71.9
H-3"	3.48	dd, 9.5, 3.5	69.2	3.56	dd, 9.8, 3.4	74.5
H-4"	3.88	d, 3.5	68.8	3.95	dd, 3.5, 1.1	70.0
H-5"	3.66-3.83	m	75.4	3.74	m	77.0
H-6"A		m	60.9	3.89	m	62.3
H-6"B		m	60.9	3.86	m	62.3

*it is a mixture alongside its flavylium cation

The proportion between hemiketal a and hemiketal b was 61% and 39%, respectively. This result is similar to the result reported by Jordheim *et al*. They also reported the proportion between hemiketal epimers from other anthocyanins with different aglycones, ranging from 56-60% and 40-44%.[112]

5.2. Preparation and Characterisation of Flavylium-Hemiketal mixture of Individual Anthocyanins from RASE

To investigate the formation of a flavylium-hemiketal mixture, the individual dried Cy3gal, Cy3glc, Cy3ara, Cy3xyl, which have been isolated through semi-preparative HPLC, were dissolved in CD_3OD with or without the addition of CF_3COOD (95:5, v/v) and then immediately analysed by an NMR spectroscopy. In the acidified solvent, a flavylium cationic form was the only species of anthocyanins observed, as expected (**Chapter 3**), and was used as a reference in characterising the flavylium-hemiketal mixture. For spectra obtained in CD_3OD without the addition of CF_3COOD, not only was the flavylium cation observed but also new peaks which have been confirmed from the previous experiment (see **Section 5.1.2**) as hemiketal forms. The mixture of a flavylium cation and hemiketal forms have been previously reported in the literature.[112,153,176] However, the finding of this study can reduce the complexity in characterising the mixture of several forms of anthocyanins from RASE in the NMR spectra. Understanding the chemical properties of hemiketal forms can contribute to the characterisation of further chemically modified products and improve the use of anthocyanins as natural colorants in much wider applications at higher pHs.

5.2.1. NMR Studies to Produce Flavylium-Hemiketal Mixtures

5.2.2. Characterisation of Flavylium-Hemiketal Forms of Cy3gal

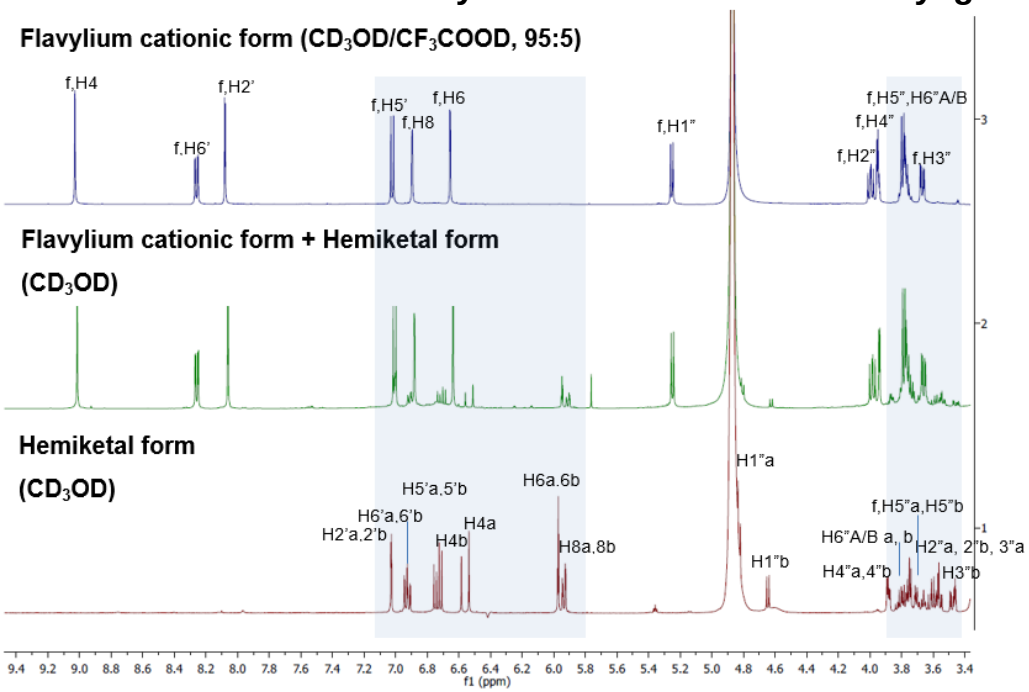

Figure 5.7 ^{1}H-NMR spectra (500 MHz) of Cy3gal in different conditions at 25 °C. Flavylium (top), a mixture of flavylium-hemiketal (middle) and hemiketal (bottom). f = flavylium; a = hemiketal a (major); b = hemiketal b (minor).

Figure 5.7 shows that in the downfield region of the ^{1}H-NMR spectrum of Cy3gal dissolved in neutral CD_3OD; more than sixteen aromatic proton signals of a mixture of flavylium cationic form and hemiketal form were present. Six of these had similar chemical shift values and coupling constants to the six aromatic proton signals representing the flavylium cationic form (f) of Cy3gal in CD_3OD/ CF_3COOD (95:5, v/v). The chemical assignment of Cy3gal in a flavylium cationic form can be seen in **Chapter 3**. The chemical assignment of Cy3gal in hemiketal forms can be seen in **Section 5.1.2**.

Jordheim *et al*. reported that the observed positive exchange cross-peaks confirmed the equilibrium between each of the two epimeric hemiketals and the corresponding flavylium cation in the 2D ^{1}H-1H NOESY spectra (**Scheme 5.1**).[112] In this study, the NOESY spectrum of Cy3gal in the downfield region revealed exchange cross-peaks at δ 9.02/6.51 (f, H-4/H-4a) and δ 9.02/6.56 (f,H-4/H-4b) between the characteristic peak of anthocyanins in the flavylium cationic form and two other H-4 peaks from a hemiketal form (**Figure 5.8**). In the upfield region, it was reported in the literature that in the NOESY NMR spectra, negative exchange cross-*peaks* between the flavylium cationic form (f, H-1" anomeric) and the hemiketal forms H-1"a (major) and H-1"b (minor), indicating that the two epimeric hemiketal forms are in equilibrium with the same flavylium cation.[112]

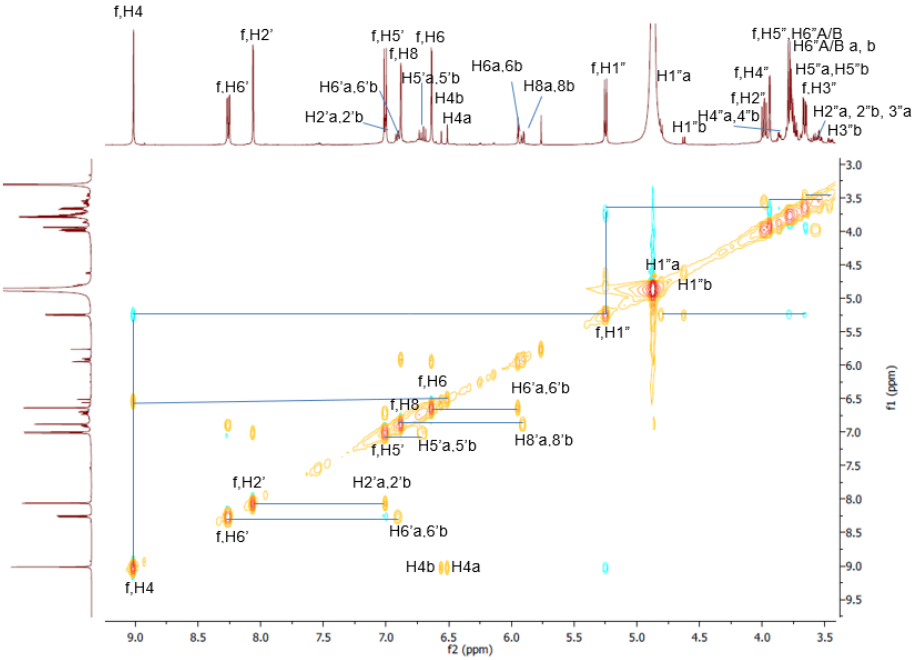

Figure 5.8 Expanded region of a NOESY spectrum (500 MHz) of Cy3gal in CD_3OD at 25 °C. f = flavylium; a = hemiketal a (major); b = hemiketal b (minor).

The same technique was used to determine other protons attached to the aglycone (Ring A and Ring C). Cross peaks at 8.26/6.91 (f, H-6'/H-6'a), 8.26/6.89 (f, H-6'/H-6'b), 8.08/7.00 (f, H-2'/H-2'a), 8.08/7.00 (f, H-2'/H-2'b), 7.02/6.69 (f, H-5'/H-5'a), 7.02/6.73 (f, H-5'/H-5'b), 6.66/5.94 (f, H-6/H-6a), 6.66/5.95 (f, H-6/H-6b), 6.90/5.90 (f, H-8/H-8a) and 6.90/5.92 (f, H-8/H-8b) are assigned for H-6'a, H-6'b, H-2'a, H-2'b, H-5'a, H-5'b, H-6a, H-6b, H-8a and H-8b.Cross peaks at 3.99/3.59 (f, H-2"/H-2"a), 3.99/3.56 (f, H-2"/H-2"b), 3.67/3.54 (f, H-3"/H-3"a), 3.67/3.46 (f, H-3"/H-3"b), 3.94/3.87 (f, H-4"/H-4"a), 3.94/3.86 (f, H-4"/H-4"b) are assigned for H-2"a, H-2"b, H-3"a, H-3"b, H-4"a and H-4"b. H-6"Aa, H-6"Ab, H-6"Ba and H-6"Bb peaks are under f, H-6"A/B peaks which appear as multiplets. Meanwhile, H-5"a and H-5"b peaks are under f, H-3" peak which appear as a doublet of doublets.

5.2.3. Characterisation of Flavylium-Hemiketal Forms of Cy3glc, Cy3ara and Cy3xyl

The remaining anthocyanins (Cy3glc, Cy3ara and Cy3xyl) were similarly treated as Cy3gal in order to achieve anthocyanins in hemiketal forms. This experiment was also carried out for the cyanidin aglycone but without success, as it only showed the flavylium cationic form in the H-NMR spectra, suggesting that the formation of hemiketal forms is favoured with glycoside anthocyanidins. Because of small sample sizes, it was decided to focus analysis on the mixture of the flavylium cation and hemiketal forms for the respected anthocyanins, using methods developed for Cy3gal (see **Section 5.2.1**). The relationship between the signals of the flavylium cationic form and the two stereoisomer hemiketals of these anthocyanins followed the exchange cross-peaks in the respective 2D ^{1}H-^{1}H NOESY spectrum of Cy3gal as they share the same flavan nucleus. The hemiketal forms for these anthocyanins share the same pattern for its signals corresponding to cyanidin backbone in hemiketal forms regardless of the sugar moieties attached. The summary of ^{1}H and ^{13}C NMR data for Cy3glc, Cy3ara and Cy3xyl are presented in **Table 5.3-5.5**.

Table 5.3 ^{1}H (500 MHz) and ^{13}C (125 MHz) NMR data for **Cy3glc** in CD_3OD at 25 °C as the hemiketal forms a (major) and b (minor). *under solvent peak

Aglycone	Cy3glc (major)			Cy3glc (minor)		
	$\delta^{1}H$ (ppm)	J (Hz)	$\delta^{13}C$(ppm)	$\delta^{1}H$ (ppm)	J (Hz)	$\delta^{13}C$(ppm)
H-4	6.51	s	96.9	6.57	s	98.2
H-6'	6.94	dd, 8.5, 2.0	118.5	6.92	dd, 8.5, 2.5	118.5
H-2'	7.04	d, 2.0	114.2	7.02	d, 2.5	114.2
H-5'	6.73	d, 8.5	114.3	6.75	d, 8.5	114.3
H-8	5.93	d, 2.0	93.7	5.95	d, 2.0	93.7
H-6	5.97	d, 2.0	95.7	5.98	d, 2.0	95.5
Sugar						
H-1"	4.85	*	101.5	4.68	d, 7.5	101.5
H-2"	3.29	dd, 9.5, 7.5	73.3	3.25	dd, 9.5, 7.5	74.9
H-3"	3.38	dd, 9.5, 9.0	76.7	3.35	dd, 9.5, 8.5	76.7
H-4"	3.26-3.55	m	76.6	3.26-3.55	m	76.6
H-5"		m	76.9		m	76.9
H-6"A	3.91	dd, 12.0, 2.0	61.1	3.93	dd,12.0, 2.0	61.1
H-6"B	3.71	dd, 12.0, 4.0	61.1	3.72	dd,12.0, 4.5	61.1

Table 5.4 ^{1}H (500 MHz) and ^{13}C (125 MHz) NMR data for **Cy3ara** in CD_3OD at 25 °C as the hemiketal a (major) and hemiketal b (minor).

Aglycone	Cy3ara (major)			Cy3ara (minor)		
	$\delta^{1}H$ (ppm)	J (Hz)	$\delta^{13}C$(ppm)	$\delta^{1}H$ (ppm)	J (Hz)	$\delta^{13}C$(ppm)
H-4	6.47	s	97.5	6.52	s	97.0
H-6'	6.93	dd, 8.5, 2.5	118.4	6.91	dd, 8.0, 2.0	118.4
H-2'	7.03	d, 2.5	113.9	7.03	d, 2.0	113.9
H-5'	6.73	d, 8.5	114.3	6.75	d, 8.5	114.3
H-8	5.92	d, 2.0	93.7	5.94	d, 2.0	93.7
H-6	5.97	d, 2.0	95.7	5.97	d, 2.5	95.7
Sugar						
H-1"	4.85	d, 6.0	100.4	4.68	d, 6.0	100.9
H-2"	3.66	dd, 8.0, 6.0	70.6	3.58	dd, 8.0, 6.0	70.3
H-4"	3.57-3.62	m	72.0	3.57-3.62	m	72.0
H-5"A	3.81	dd,12.0, 3.5	64.7	3.81	dd,12.0, 3.5	64.7
H-3"	(3.84-3.87)	m	67.3	(3.84-3.87)	m	67.3
H-5"B	3.68	dd,12.5, 2.0	64.7	3.68	dd,12.5, 2.0	64.7

Table 5.5 ^{1}H (500 MHz) and ^{13}C (125 MHz) NMR Data for **Cy3xyl** in CD_3OD at 25 °C as the hemiketal a (major) and hemiketal b (minor).

Aglycone	Cy3xyl (major)			Cy3xyl (minor)		
	$\delta^{1}H$ (ppm)	J (Hz)	$\delta^{13}C$(ppm)	$\delta^{1}H$ (ppm)	J (Hz)	$\delta^{13}C$(ppm)
H-4	6.46	s	96.8	6.49	s	97.7
H-6'	6.92	dd, 8.5, 2.0	118.2	6.88	dd, 8.5, 2.0	118.2
H-2'	7.02	d, 2.0	114.1	7.01	d, 2.0	114.1
H-5'	6.73	d, 8.5	114.3	6.74	d, 8.5	114.3
H-8	5.92	d, 2.0	93.7	5.93	d, 2.0	93.7
H-6	5.97	d, 2.0	95.6	5.97	d, 2.0	95.6
Sugar						
H-1"	4.85	d, 7.0	101.1	4.66	d, 7.0	101.6
H-2"	3.28	dd, 9.0, 7.0	72.8	3.23	dd, 9.0, 7.0	72.8
H-4"	3.59	ddd, 9.5, 8.5, 5.0	70.5	3.59	ddd, 9.5, 8.5, 5.0	70.5
H-5"A	3.86	dd,11.5, 4.5	65.6	3.96	dd,11.0, 5.0	65.6
H-3"	3.38-3.42	m	75.8	3.38-3.42	m	75.8
H-5"B	3.38	dd,12.0, 9.5	65.6	3.36	dd,11.5, 9.5	65.6

The proportion of the flavylium-hemiketal mixture varies depending on the acidity of a solution, which is governed by the percentage of trifluoroacetic acid in the solution.[126] The proportion of flavylium and hemiketal form can determine the direction of equilibrium of this mixture. The flavylium cationic form is dominating in the more acidic solution. Even though the treatment for all solids was the same, the proportions varied, most likely because the remaining trifluoroacetic acid content from the semi-prep HPLC fraction in the freeze-dried solid varied depending on the quality of evaporation in the freeze dryer. The proportions in percentage (%) of hemiketal a (major) and hemiketal b (minor) of Cy3gal, Cy3glc, Cy3ara and Cy3xyl can be quantified by comparing the integration of H-4 in the ^{1}H-NMR spectrum. The ratio of hemiketal a and hemiketal b for hexose (Cy3gal and Cy3glc) and pentose (Cy3ara and Cy3xyl) were similar. The ratio of hemiketal a and hemiketal b were 56-60% and 40-44%, respectively. The proportions of hemiketal forms in this study agree with the data reported by Jordheim *et al*., which showed 60% of hemiketal a (major) and 40% of hemiketal b (minor).[112]

5.3. Extraction-Purification of Anthocyanins to Produce RASE in Hemiketal Forms

The extraction-purification using organic acids such as formic acid, acetic acid and octanoic acid successfully produced anthocyanins in hemiketal forms (see **Chapter 4, Section 4.2.3.2**). Limiting the use of strong acid such as HCl during the desorption of anthocyanins from Amberlite XAD-7HP adsorbent was studied to investigate this

effect on the production of anthocyanins as their hemiketal forms. In this study, there were three different methods for the SPE elution. They were normal elution as described in **Chapter 2**, using reduced amounts of acid during the anthocyanin desorption, and neutral SPE elution. Normal elution followed the batch method previously discussed, which included acidified water wash (0.1% v/v HCl), ethyl acetate wash and acidified ethanol wash (0.1% v/v HCl).[108] Reduced acid during the anthocyanin desorption followed the normal elution method, but the difference was that non-acidified ethanol was employed in recovering anthocyanins. Neutral SPE elution was done as follows: the SPE column was washed with acidified water (0.1% v/v HCl), further copious amounts of water, then ethyl acetate and finally non-acidified ethanol.

The water wash of the SPE column was performed to remove the excess HCl from the SPE column from the previous acidified water wash. This wash also allows the SPE column to be close to neutral pH to maximise the formation of hemiketal forms (**B**) instead of a flavylium cationic form ($\mathbf{AH^+}$). It was also visually observed during the water wash without acid addition (pH 5-6). Amberlite XAD-7HP resin changed from red to bluish red (**Figure 5.9**). Hence, anthocyanins in this stage were initially identified to be present as a quinonoid base because of the colour appearances ($\lambda_{max\text{-}vis}$ 564 nm, see **Chapter 2**, **Figure 2.6**).

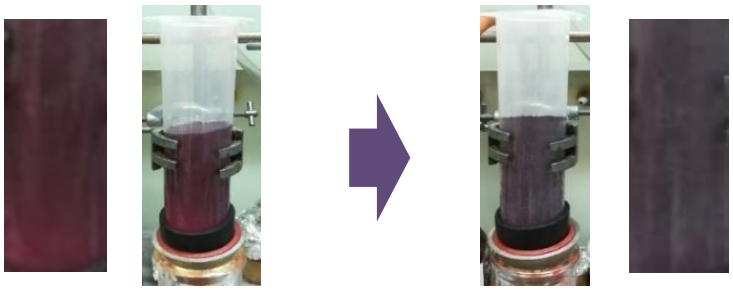

Figure 5.9 The appearance of Amberlite XAD-7HP resin on the left after elution with acidified wash (red) and on the right after elution with a copious amount of water (bluish-red).

The loaded SPE column was eluted with ethanol or acidified ethanol to recover anthocyanins. Anthocyanins in hemiketal forms might be formed on release from the SPE column under the neutral conditions. The resulting ethanol eluates from three different SPE experiments were then separately evaporated to dryness under reduced pressure on a rotary evaporator without neutralisation. RASE produced from these experiments were then analysed by NMR spectroscopy. Neutral methanol deuterium was applied in the NMR analysis to maximise the formation of hemiketal forms (**Figure 5.10**).

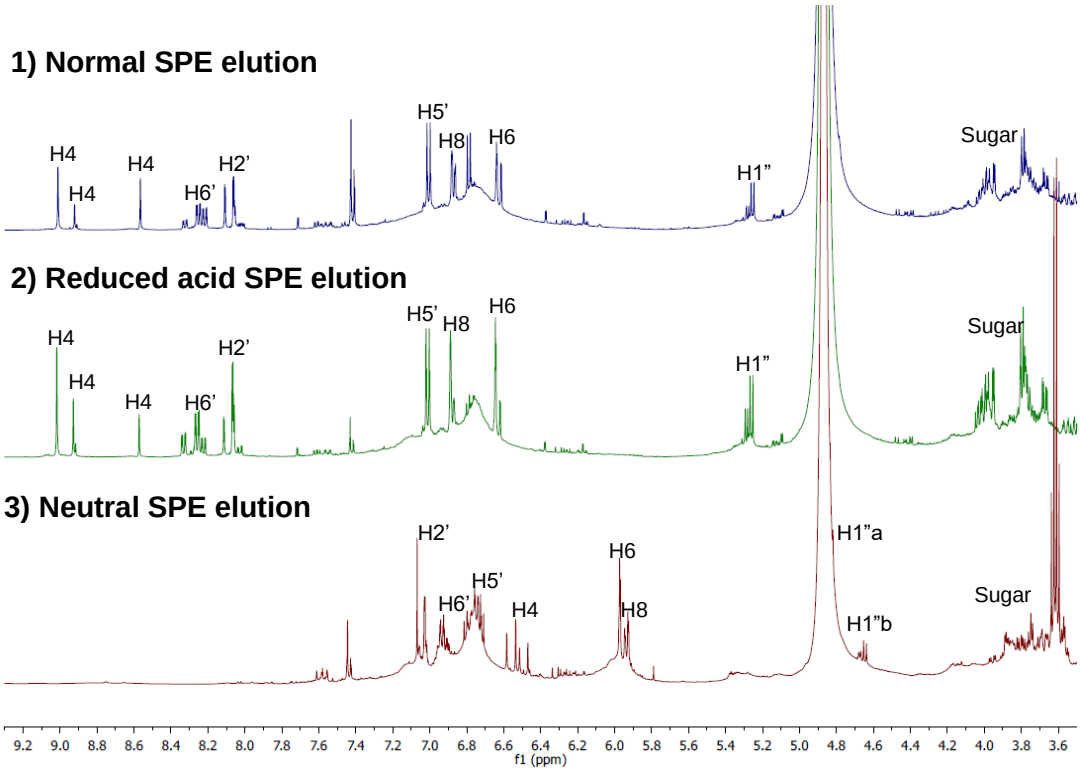

Figure 5.10 ^{1}H-NMR spectra of RASE from different SPE elution experiments (HCl) recorded at 500 MHz (25 °C). Solvent: CD_3OD.

In **Figure 5.10**, the normal and reduced acid SPE elution experiment for HCl show anthocyanins exclusively in the flavylium cationic form. Because HCl is such a strong acid, the excess may not be needed for flavylium cation formation, however a small quantity of excess of HCl may also be present and could further enhance the formation of the flavylium cation. Furthermore, when a neutral SPE elution experiment was carried out, anthocyanins were found to be present as their hemiketal forms. The characterisation of hemiketal forms of RASE from a neutral SPE elution follows the characterisation discussed in **Section 5.2**.

5.4. pH jump to Alkaline pH

A rapid method to form hemiketals was through a pH jump to an alkaline pH experiment.[177] It has been known that increasing the pH can transform anthocyanins into various species (see **Chapter 1**, **Section 1.1.6**).[37,38] The characterisation of individual flavylium cationic form, hemiketal forms and both as a mixture have been discussed in an earlier section. To obtain hemiketal forms using the pH jump experiment, initially, Cy3gal from semi-preparative HPLC was dissolved in acidified deuterated methanol (CD_3OD/CF_3COOD 95:5) and then added with NaOD 5% solution (100 µl) to neutralise the solution. The equilibrium between a hemiketal form and a quinonoid form of Cy3gal was observed in **Figure 5.11, c**.

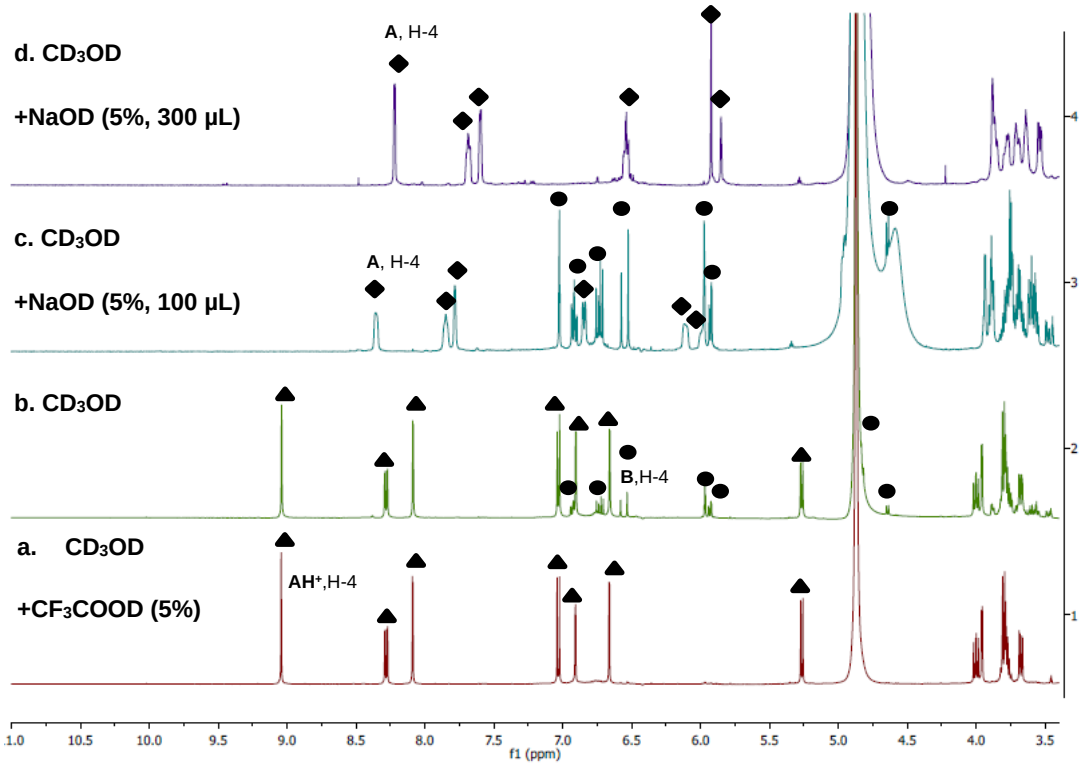

Figure 5.11 ^{1}H-NMR spectra of Cy3gal after addition of NaOD 5%. The ^{1}H-NMR spectra were recorded at 500 MHz (25 °C). Solvent: CD_3OD. (▲) Flavylium catanionic form, (●) Hemiketal form, (♦) quinonoid base.

According to **Figure 5.11**, it suggests that when anthocyanins were present as a neutral quinonoid base **A** or an anionic quinonoid form $\mathbf{A}^-$, it will share a similar pattern (coupling constant, *J* and splitting) for Ring A (H-6 and H-8), ring B (H-2', H-5' and H-6') and ring C (H-4) in the pyran nucleus as a flavylium cationic form $\mathbf{AH}^+$. At higher pH (basic, pH > 7), anthocyanins will be deprotonated, forming its anionic quinonoid $\mathbf{A}^-$ form (pK_{a2} ~7). It is difficult to characterise anthocyanins in a quinonoid base form because, at this form, it is unstable and rapidly transforms into different forms. The transformation of this form into different forms was recorded by the appearance of board peaks in the NMR spectrum. These peaks were tentatively assigned as a quinonoid form of Cy3gal. After a few hours, the colour of the solution turned yellow, suggesting the formation of a chalcone.[37,38] However, chalcone's formation was not observed in this study.

To replicate the results from a pH jump experiment for Cy3gal, the same manner was applied for RASE. A pH jump experiment was initially performed from an acidic solution, CD_3OD/CF_3COOD (95:5, v/v) (**Figure 5.12**). The predominantly flavylium cationic form ($\mathbf{AH}^+$) was observed as expected. The methanolic containing anthocyanin solution in an NMR tube was added with a NaOD solution (5% v/v in D_2O, 100 µl) to reach a neutral pH. An addition of NaOD into a solution formed

different species of anthocyanins, which are the quinonoid base (**A**) and hemiketal (**B**) in equilibrium because the pH of the solution was higher than the pK'_a, pK_a and pK_h of anthocyanins (Cy3glc, 2.8, 3.7, 2.9 respectively).[117]

Meanwhile, at basic pH, where the pH is higher than pK_{a1} (4.0) and pK_{a2} (7.0) values of anthocyanins, an anionic quinonoid form is dominating as products of deprotonation.[20] It can be observed by colour changes during the pH jump from acidic to basic (red to bluish). Carbita *et al.* also reported colour changes when increasing the pH of the solution from acidic to neutral pH (Cy3glc, 510 nm → 554 nm). This bathochromic shift suggested the formation of a quinonoid form.[35]

Alonso *at al*. reported that a strong basic solution with the pH ranged from 10.0 to 12.0, the neutral quinonoid base **A** should be deprotonated, forming an anionic quinonoid base $\mathbf{A}^-$. At higher pH (13.0), the maximum absorbance wavelength shifted to 360 nm, causing the solution turned light yellow, indicating a chalcone form $\mathbf{C_{E/Z}}$.[126] This finding was in good agreement with the results in this study. However, the reacidification could bring back anthocyanins into the flavylium cationic form ($\mathbf{AH^+}$).

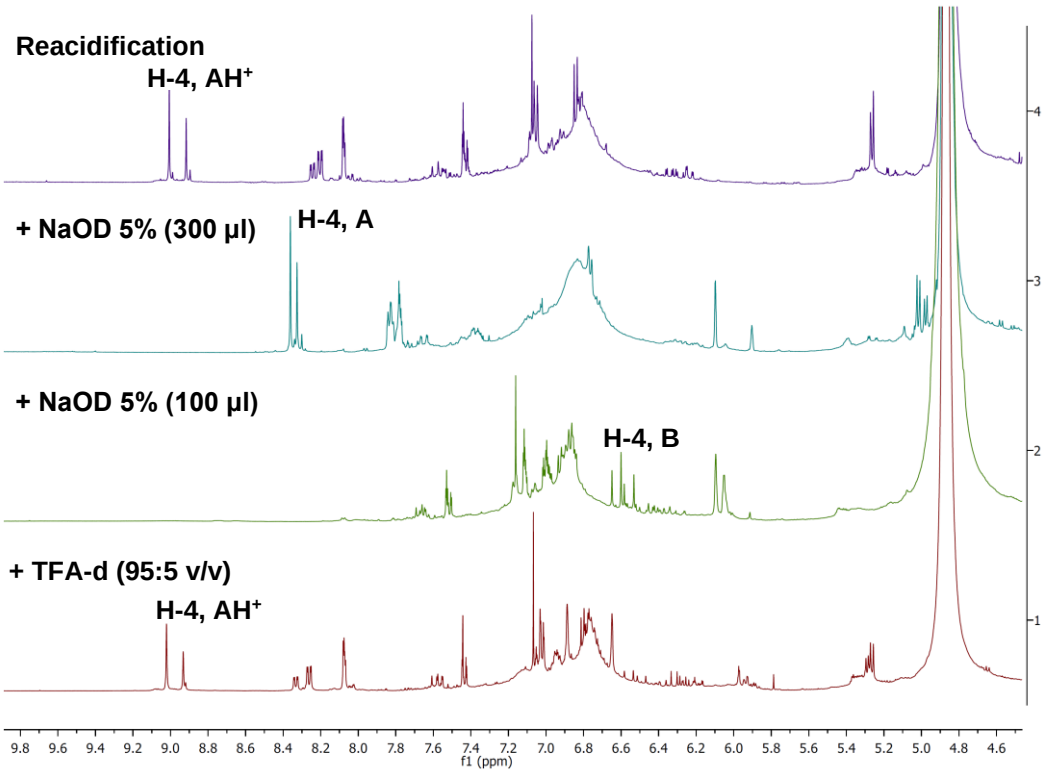

Figure 5.12 The ^{1}H-NMR spectra were recorded at 500 MHz (25 °C). Solvent: CD_3OD. $\mathbf{AH^+}$: Flavylium cationic form, **B**: Hemiketal form, **A**: Quinonoid form.

The formation of a quinonoid base form was confirmed by the NMR spectrum (**Figure 5.12**) when an excess of NaOD (5% v/v in D_2O, 300 µl) was added into a methanolic containing anthocyanin solution. **Figure 5.12**, **NaOD 5% 300 µl,** shows new peaks which have a similar pattern for H-4 (s), H-6' (dd), H-2' (d), H-5' (d), H-8 (s/d) and H-6 (s/d) in a flavylium cationic form as both share the same conjugated double bond core, a flavan nucleus. However, a quinonoid base is a kinetic product and the transformation to form this species is fast.[158] The peaks shown in the NMR spectrum were broad, suggesting that this species' transformation into different species was in equilibrium. The competition amongst flavylium-quinonoid base equilibrium, hemiketal-quinonoid base equilibrium and chalcone-quinonoid equilibrium remained unclear. Further investigation is required to resolve this problem.

5.5. Conclusion

Anthocyanins can transform into various forms depending on the pH of the solution. Many researchers in literature have well documented the characterisation of anthocyanins in a flavylium cationic form. However, literature reporting anthocyanins' characterisation in other forms is limited because of anthocyanins' reactivity and instability. In this study, hemiketal forms of Cy3gal have been characterised as a single compound through slow evaporation of acid through equilibration. The characterisation of flavylium-hemiketal forms mixture for Cy3gal, Cy3glc, Cy3ara and Cy3xyl were obtained by dissolving these anthocyanins in methanol-d_4 and analysed by an NMR spectroscopy. Cyanidin aglycone was treated the same but without success. The proportion between a flavylium cationic form and hemiketal forms depends on the solution's acidity. In this case, it was affected by the percentage of TFA remained in the dried anthocyanin samples from the semi-preparative HPLC experiment. Even though the proportions of the flavylium cationic form/hemiketal a/hemiketal b were varying, the ratio of hemiketal a (major) and hemiketal b (minor) for hexose (Cy3gal and Cy3glc) and pentose (Cy3ara and Cy3xyl) were similar. The ratio of hemiketal a and hemiketal b were 56-60% and 40-44%, respectively.

For HCl, hemiketal forms in RASE can be obtained from the extraction-purification process through an acid removal in the SPE column by washing it with a copious amount of water before removing other neutral polyphenols and recovering anthocyanins. Limiting the use of strong acid during an SPE wash could also avoid deglycosylation of anthocyanins. Milder organic acids such as FA, AA, and OA

always gave hemiketal forms in RASE even though these acids were applied during the SPE elution.

A rapid pH jump can also give hemiketal forms. The equilibrium between hemiketal forms and a quinonoid form was observed in the NMR spectrum when NaOD 5% was added to bring the pH of the alkaline solution. However, a quinonoid form's structural characterisation is still challenging because this species is the kinetic product that can transform into other species quickly. As such, they appeared as broad peaks. The formation of hemiketal forms (**B**) can be achieved through a flavylium cationic form ($\mathbf{AH^+}$) or a quinonoid base (**A**) routes. However, the competition between those two routes is unclear.

Chapter 6
Chemical Modification of Anthocyanins from *Aronia* Skin Waste, Structural Characterisation and Determination of Physico-chemical Properties

Anthocyanins are water-soluble compounds, and therefore the application of anthocyanins in more lipophilic environments such as fats, oils, lipid-based food or cosmetic formulas and emulsions, as well as biological environments, are limited.[145] The stability of anthocyanins is also another issue that requires to be resolved. Temperature, light, pH, metals, enzymes, oxygen, ascorbic acid, sugars, *etc*., can all affect anthocyanin stability. As such, a new method to alleviate those problems is required to increase the potential application of anthocyanins. The utilisation of anthocyanin-rich food waste could add a value and help contribute to a sustainable circular economy.

The colours displayed by anthocyanins are appealing and attractive for consumers, and represents an added value for cosmetic, textiles and food companies in the development of product enriched with these compounds. A potential solution to improving the hydrophobic nature of anthocyanins is the acylation of hydroxyl groups with hydrophobic acyl donors. However, only a few investigations on the acylation of anthocyanins have been reported, due to the reactivity of the flavylium cation itself, which is chemically labile and difficult to handle. Anthocyanins in the most stable form are positively charged and have only low solubility in organic solvents and are also unstable under neutral and basic conditions.

The instability of anthocyanins under certain conditions has already been discussed (see **Chapter 1**, **Section 1.1.5**), and chemical modification can be performed to help alleviate some of these problems. Modifying the physico-chemical properties of anthocyanins can be achieved through the acylation of hydroxyl groups of anthocyanin glycosides with aliphatic or aromatic acids.[23] Acylation of anthocyanins is reported to enhance their resistance towards colour fading with increasing pH.[95,178] Moreover, chemical modification of hydrophilic anthocyanins to more lipophilic compounds can be achieved by acylation with fatty acids (**Scheme 6.1**). Their miscibility with lipophilic media can be improved through this reaction, which can lead to an enhancement of their application in food matrices, textiles, medicinal and cosmetic products.[145,179] Cruz *et al*. reported that the acylation of anthocyanin glycosides occurred preferentially at the hydroxyl groups of the glucose moiety,

instead of any phenolic groups in the flavylium core. This current literature approach produces a mixture of mono-, di- and tri-stearic ester derivatives of malvidin-3-*O*-glucoside, and the separation to given individual compounds could not be achieved. NMR characterisation was only possible for protons of the fatty acid's residue attached to a sugar moiety. In contrast, the protons of a flavylium cation were unresolved and with very low intensity, and hence their chemical shifts and coupling constants could not be accurately measured.[179] A similar chemical lipophilisation was also reported by Grajeda-Iglesias *et al*., by acylation of anthocyanins from *Hisbiscus sabdariffa* flowers using octanoyl chloride. The delphinidin aglycone was reported to be mono esterified, suggesting that the acylation could occur in both the sugar moiety and the aglycone unit. The formation of an esterified anthocyanin was confirmed by HPLC-ESI-MS. However, the determination of the chemical structure of the esters by NMR was not carried out.[144]

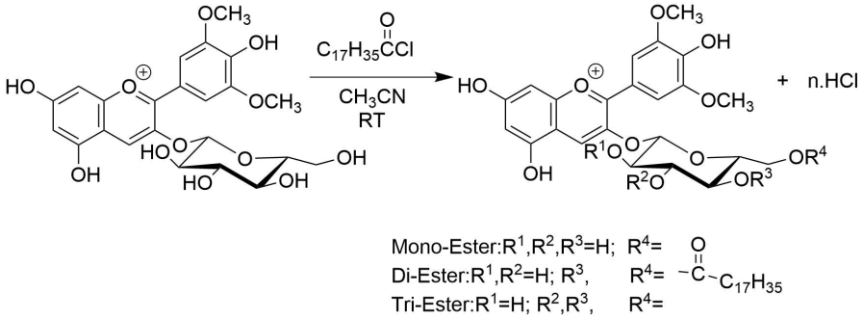

Scheme 6.1 Synthesis of malvidin-3-*O*-glucoside-stearic acid conjugates from malvidin-3-glucoside and stearoyl chloride.[179]

In order to achieve a more selective reaction to form the monoester, an enzyme (lipase B) mediated acylation has been utilised in the lipophilisation of malvidin-3-*O*-glucoside with oleic acid (**Scheme 6.2**). The highest conversion yield of 21% was achieved when the reaction was conducted for 48 h.[145] The monoester anthocyanin shows the characteristic red-violet colour and retains antioxidant activity. As the yield from this method was still quite low (80% of material is left unreacted), new methods are required to increase both the selectivity and yield of products. Cruz *et al.* reported that the lipophilicity of esterified anthocyanins increased with the fatty acid chain length attached to a sugar moiety.[169] Enzymatic lipophilisation of anthocyanins using lauric acid increased lipophilicity, thermostability, the capacity to inhibit lipid peroxidation and antioxidant capacity.[57,58,180]

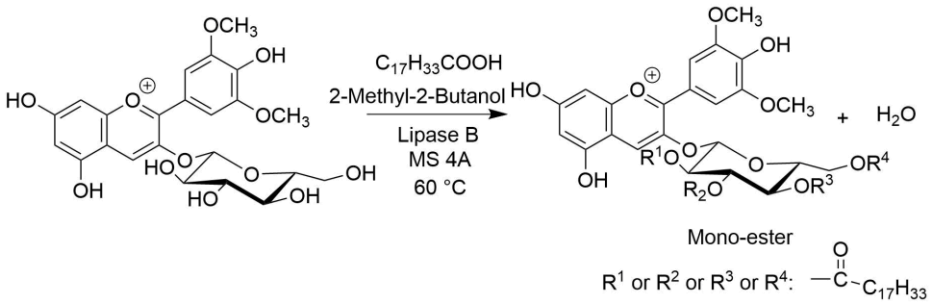

Scheme 6.2 Synthesis of malvidin-3-*O*-glucoside-oleic acid conjugates from malvidin-3-glucoside and oleic acid under enzymatic catalysis acylation.[145]

This chapter discusses the chemical modification of anthocyanins from *Aronia* skin waste, the structural characterisation and evaluation of physio-chemical properties of novel lipophilic anthocyanin derivatives. **Section 6.1** describes the preliminary studies on the acylation of selected commercially available polyphenols to develop the method which could be potentially applied for anthocyanins. **Section 6.2** discusses an acylation of anthocyanins from RASE, with different acylating agents (acetyl chloride C2, butanoyl chloride C4, and octanoyl chloride C8). The structural characterisation and physio-chemical properties of novel acylated anthocyanins were determined and are also discussed in this section. **Section 6.3** discusses a new method of acetonation of anthocyanins to alternatively produce anthocyanin derivatives. Even though this method's results were promising, the optimisation of reaction parameters and purification techniques are still required.

6.1. Preliminary Studies on the Acylation of Selected Polyphenols

Preliminary studies on the acylation of commercially available phenolic compounds such as resveratrol and quercetin were performed to find the suitable method for the acylation of anthocyanins extracted from *Aronia* skin waste. Resveratrol and quercetin were selected for preliminary studies as these chemicals are simple phenolic compounds and commercially available as a single compound with high purity (>97%), and they do not contain a sugar unit. As such, they can reduce the complexity of the reaction, and any interference from impurities is limited. An acylation was accomplished by reacting the selected commercially available polyphenols with an acylating agent (acetyl chloride) in DCM with a presence of pyridine as a catalyst.[181] The synthesis of ester derivatives of resveratrol and quercetin was conducted using two different conditions.[182,183] For **Method 1**, a reaction was conducted at -78 °C for 3 h and then continued for another 1 h at room

temperature. For **Method 2**, a reaction was conducted at room temperature for 3 h. The results were then compared. The ester derivatives of resveratrol and quercetin were characterised by UV-Vis, IR, melting point, HRMS, ^{1}H-NMR and ^{13}C-NMR.

6.1.1. Synthesis of *trans*-3,4',5-triacetyl resveratrol

The acylation of resveratrol is a good start for a simple acylation of polyphenols as it only contains three hydroxyl groups. Acylation of all three hydroxyl groups of resveratrol (**41**) with six equivalents of acetyl chloride was performed by slightly modifying published procedures to obtain *trans*-3,4',5-triacetyl resveratrol (**42**) (**Scheme 6.3**).[182,183]

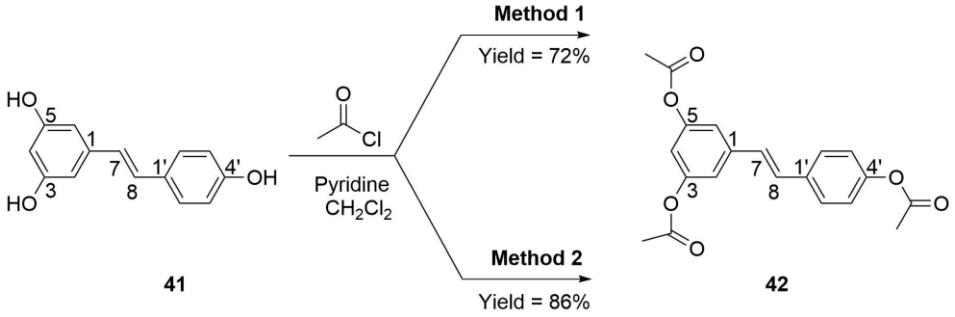

Scheme 6.3 Synthesis of *trans*-3,4',5-triacetyl resveratrol (**42**).

Triacetate **42** was obtained in 86% isolated yield from the reaction with six equivalents of acetyl chloride using **Method 2**, whereas 72% yield was obtained using **Method 1**. The product is assigned as *trans*-3,4',5-triacetylresveratrol (**42)** based on ^{1}H-NMR analysis (**Table 6.1**). This assignment is in agreement with the result reported by Jungong and Novikov.[184]

Table 6.1 Complete assignments of the NMR data of **42** measured in $CDCl_3$. ^{1}H NMR was recorded at 400 MHz. Concentration: 6.3 x 10^{-2} M.

Assignment	**42 (experimental)**		**42 (literature)**[184]	
	δ^{1}H (ppm)	J (Hz)	δ^{1}H (ppm)	J (Hz)
H-2/6	7.12	d, 2.0	7.12	d, 2.0
H-4	6.83	t, 2.0	6.83	t, 2.0
H-7	7.06	d, 16.3	7.07	d, 16.0
H-8	6.97	d, 16.3	6.97	d, 16.0
H-2'/6'	7.48	d, 8.6	7.50	d, 8.5
H-3'/5'	7.09	d, 8.6	7.10	d, 8.5
3, 4', 5-OAc	2.30	s (9H)	2.32	s (9H)

Data from literature was also recorded in the same solvent system, $CDCl_3$

As shown in **Table 6.1**, the ^{1}H-NMR chemical shift of *trans* isomer was observed (J ^{1}H-^{1}H = 16.3 Hz). Koh *et al*. reported that the ^{1}H chemical shift of *trans* isomers were more downfield shifted than *cis* isomers.[185] The doublet at 7.12 ppm, which integrated

to two protons, was assigned to two protons (H-2/6). The triplet at 6.83 ppm was assigned to H-4. The doublet at 7.48 ppm, which integrated to two protons, was assigned to H-2'/6'. The doublet at 7.09 ppm, which also integrated to two protons, was assigned to H-3'/5'. The ^{1}H-NMR signal of the methyl group appeared as a singlet at 2.30 ppm, which integrated to nine protons (3 x CH_3). ^{1}H-^{1}H COSY NMR was performed to confirm the structure of **42**. The triplet signal, which belongs to H-4, correlated with H-2/6. The doublet signal of H-7 correlated with H-8. The doublet signal, which belongs to H-3'/5', correlated with H-2'/6'.

Triacetate **42** can be distinguished from its precursor (**41**) by IR spectroscopy. A broad -OH band is observed in the 3000-3500 cm^{-1} region in the spectra of **41**. The absence of hydroxyl groups in **42** is observed, indicating that all hydroxyl groups of **41** were acylated. A new peak is present at 1753 cm^{-1} in the spectra of **42**, suggesting the presence of ester groups. Liu reported that the melting point of **42** was 116-118 °C with a molecular mass HRMS-ESI: $[M]^+$ of 354.1118 whereas the melting point of obtained product (**42**) from this study was 118-121 °C with molecular mass HRMS-ESI:$[M+Na]^+$ of 377.0997, calculated for $[M+Na]^+$ of 377.1001 (error mass of 1.1 ppm).[186] The recrystallisation was carried out in methanol. Both **41** and **42** are colourless solids. **Figure 6.1** shows a hypsochromic shift of absorption to a shorter wavelength (12 nm of reduction) of maximum wavelength (λ_{max}) due to the substitution effect. The maximum wavelength (λ_{max}) of **42** (315 nm) was shorter than the precursor (327 nm).

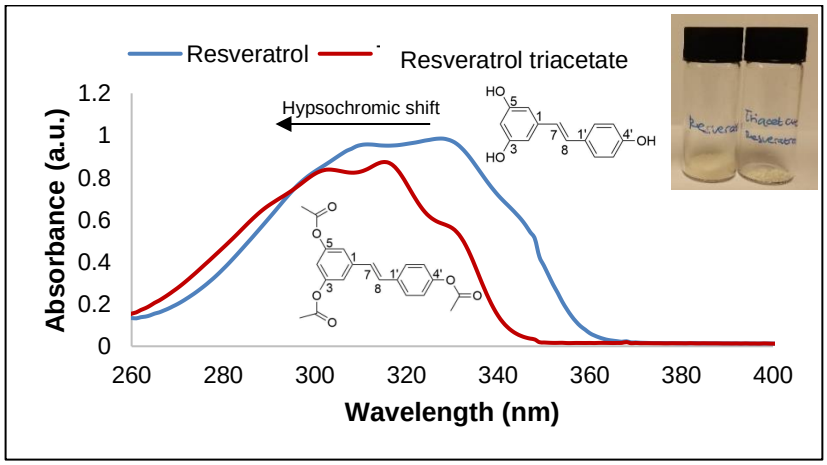

Figure 6.1 UV spectra of 41 (blue) and 42 (red). The UV spectra were measured in DMSO.

6.1.2. Synthesis of 3,3',4',5,7-pentaacetyl quercetin

After successfully synthesising **42** using two different methods with relatively high yields, the same methods were also applied for the acylation of quercetin (**40**). This

polyphenol has a greater number of hydroxyl groups. Even though quercetin has different reactivity and property compared to anthocyanins, it is a good example to understand side reactions, and that acylation of phenols is possible. Acylation of all five hydroxyl groups of **40** with eight equivalents of acetyl chloride was also performed by modifying published procedures to obtain 3,3',4',5,7-pentaacetyl quercetin (**43**) (**Scheme 6.4**).[182,183]

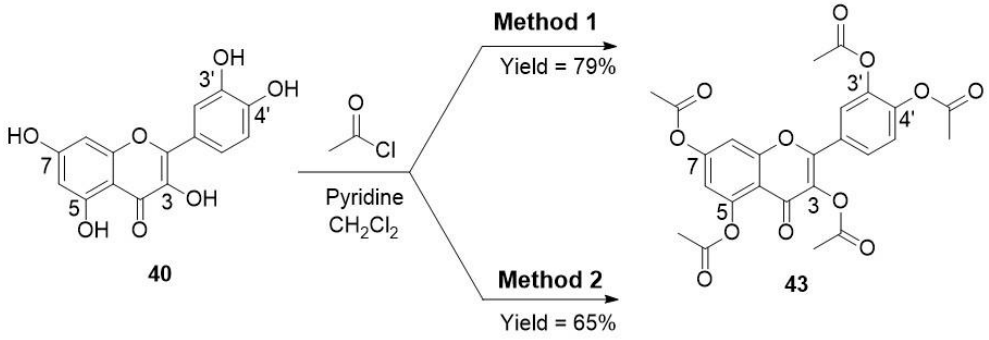

Scheme 6.4 Synthesis of 3,3',4',5,7-pentaacetyl quercetin (43).

Pentaacetate **43** was obtained in 79% isolated yield from the reaction mixture with eight equivalents of acetyl chloride using **Method 1** whereas 65% yield was obtained using **Method 2**. The product is assigned as 3, 3', 4', 5, 7-pentaacetyl quercetin (**43**) based on ^{1}H-NMR (**Table 6.2**). This assignment is consistent with the work carried out by Ren *et al*., where the ^{1}H-NMR data was recorded at 400 MHz in $CDCl_3$.[187]

Table 6.2 Complete assignments of the NMR data of **43** measured in $CDCl_3$. ^{1}H-NMR was recorded at 400 MHz. Concentration: 4.2 x 10^{-2} M.

Assignment	**43 (experimental)**		**43 (literature)**[187]	
	δ^1H (ppm)	**J (Hz)**	**δ^1H (ppm)**	**J (Hz)**
H-6	6.87	d, 2.2	6.88	d, 2.0
H-8	7.33	d, 2.2	7.34	d, 2.0
H-2'	7.69	d, 2.1	7.69	d, 2.0
H-5'	7.35	d, 8.5	7.35	d, 8.8
H-6'	7.72	dd, 8.5, 2.1	7.72	dd, 14.0, 2.2
3-OAc	2.43	s	2.44	s
3', 4', 5, 7-OAc	2.33	s	2.33, 2.34, 2.35	s, s, s

Data from literature was also recorded in the same solvent system, $CDCl_3$

The two meta-coupled protons (H-6/8) on the A-ring were assigned as doublets. The doublet of doublet at 7.72 ppm was assigned to H-6'. The doublet at 7.69 ppm was assigned to H-2', and the doublet at 7.35 ppm was assigned to H-5'. The ^{1}H signal of methyl groups appeared as singlets. The methyl group attached at the 3 position of the C-ring showed a signal at 2.43 ppm, which integrated to 3 protons. The methyl groups attached at the 3', 4', 5' and 7 position showed a signal at 2.33 ppm, which integrated to 12 protons. ^{1}H-^{1}H COSY NMR was performed to confirm the structure

of **43**. The doublet signal, which belongs to H-6, correlated with H-8. The doublet signal, which belongs to H-5', correlated with H-2'. The ^{13}C-NMR characterisation of **43** is consistent with the result reported by Ren *et al*., who analysed the ^{13}C-NMR spectra at 101 MHz in $CDCl_3$.[187]

A successful acylation of five hydroxyl groups of **43** can be determined by the absence of the hydroxyl group in the IR spectra. A broad -OH band is observed in the 3000-3500 cm^{-1} region in quercetin spectra. The absence of hydroxyl groups in **43** is observed, indicating that all hydroxyl groups were acylated. A new peak is present at 1762-1773 cm^{-1} in the spectra of **40**, suggesting the presence of ester groups. Ren *et al.* reported that the melting point of **43** was 194-195 °C with a molecular mass HRMS-ESI: $[M+H]^+$ of 513.3 whereas the melting point of obtained product (**43**) from this study was 197-200 °C with molecular mass HRMS-ESI$^+$:$[M+H]^+$ of 513.1027, calculated for $[M+H]^+$ of 513.1033 (error mass of 1.2 ppm).[187] The recrystallisation was carried out in methanol. Quercetin **43** is a yellow solid, while **43** is a colourless solid and shows quite a significant hypsochromic shift of 77 nm compared to **40** (**Figure 6.2**). The maximum wavelength (λ_{max}) of **43** was lower than the precursor.

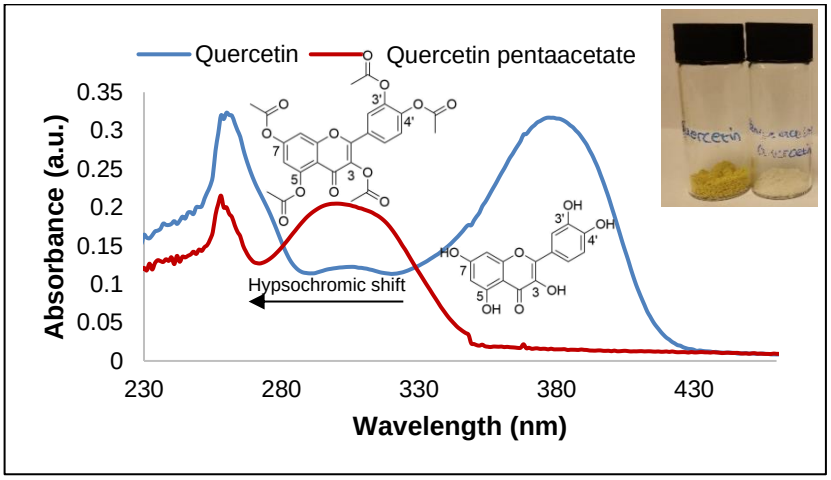

Figure 6.2 The UV spectra of **40** (blue) and **43** (red). The UV spectra were measured in DMSO.

The successful acylation for resveratrol and quercetin shows the potential application of the same acylation method for anthocyanins. It should be noted that some modification of processes may be required as those compounds have different reactivity and stability, mainly due to glycosylation.

6.2. Chemical Modification of Anthocyanins from *Aronia* Skin Waste to Produce Novel Lipophilic Derivatives

6.2.1. Method Development for Lipophilisation of Anthocyanins

Lipophilisation of anthocyanins from *Aronia* skin waste followed the acylation methods for resveratrol and quercetin from the preliminary studies described in **Section 6.1**. An acylating agent was expected to react with the hydroxyl group(s) of Cy3gal and Cy3ara as the major anthocyanins in RASE. The presence of other impurities might also compete with anthocyanins during the acylation reaction. However, the competition amongst anthocyanins in RASE to react with an acylating agent; and the reaction between an acylating agent with other polyphenols may also occur but was not studied in this research.

Improving anthocyanin content in the starting material can be performed by further purification such as prep-HPLC, liquid-liquid extraction, and Biotage flash purification (see **Chapter 3**). To find the suitable starting materials for the acylation of anthocyanins, RASE produced from the extraction-purification using organic acids (see **Chapter 4**) were reacted with acylating agents. The mono acylated anthocyanins have been reported on the primary alcohol of the sugar moiety due to its greater reactivity.[58,145,169,180,188] Further acylation on other secondary hydroxyl groups is possible in the chemical acylation as this reaction typically produces multiacylated products, especially in the presence of excess acylating agent. Further study on this reaction is still required to understand better the acylation of anthocyanins extracted from *Aronia* skin waste. As such, the effect of solvent, including biphasic solvents system, type of RASE, reaction temperature, and reaction time on the relative distribution of anthocyanins and their acylated anthocyanins, were studied.

6.2.1.1. Effect of Solvent

The solubility of anthocyanins in the reaction media is a fundamental requirement to perform the acylation reaction because it could affect the conversion yield. As such, some organic solvents such as acetonitrile, DMSO, DCM and chloroform were selected to find the compatible solvent for the chemical modification of anthocyanins (**Table 6.3**).[57] Anthocyanins were completely soluble in DMSO and only partially soluble in acetonitrile. The higher solubility of anthocyanins in the reaction medium could give a higher chance for the reaction with acylating agents. Neither DCM nor chloroform showed any sign of dissolving anthocyanins. However, the ability to remove the solvent after the reaction finished was also taken into consideration.

The purified anthocyanin starting materials were obtained from a Biotage flash purification. The dried fraction, mostly Cy3gal (89.6%, see **Chapter 3**), was reacted with selected acylating agents. All reactions were carried out at room temperature and monitored for 24 h. To avoid the degradation of anthocyanins by light, the reaction flask was covered with aluminium foil. An aliquot (10 µL) was taken periodically and diluted with DMSO up to 100 µL. Afterwards, the solution was analysed by LC-MS. The product's formation was assigned based on the expected acylated anthocyanins' molecular mass (see **Table 6.3**). The distribution of anthocyanins and their ester derivatives were calculated by comparing their peak intensities which appeared in LC-MS chromatograms.

Table 6.3 Effect of solvent on the formation of acylated anthocyanins.

No.	Acylating agent	Pyridine	Solvent	Distribution of ANC & their ester derivatives (%)
1.	Acetyl chloride	No	Chloroform-d	No reaction. Starting material remained.
2.	Acetyl chloride	No	DMSO-d	No reaction. Starting material remained.
3.	Acetyl chloride	Yes	DMSO-d	Cy3gal (89.3), Cy3gal diacetate (10.7) in 5 h. It formed back Cy3gal after 24 h.
4.	Octanoyl chloride	Yes	DCM	Cy3gal (0.8), Cy3gal monooctanoate (13.5), Cy3gal dioctanoate (31.6), Cy3gal trioctanoate (54.1)
5.	Acetyl chloride	No	Acetonitrile-d	Cy3gal monoacetate (25), Cy3gal diacetate (62.5), Cy3gal triacetate (12.5)
6.	Acetyl chloride	No	Acetonitrile anhydrous	Cy3gal monoacetate (17.4), Cy3gal diacetate (60.9), Cy3gal triacetate (21.7)
7.	Acetyl chloride	No	Acetonitrile	Cy3gal (7), Cy3gal monoacetate (23.2), Cy3gal diacetate (52.8) Cy3gal triacetate (17)
8.	Octanoyl chloride	No	Acetonitrile-d	Cy3gal monooctanoate (56.8), Cy3gal dioctanoate (43.2)
9.	Octanoyl chloride	No	Acetonitrile anhydrous	Cy3gal (9.3), Cy3gal monooctanoate (44.6), Cy3gal dioctanoate (46.1)
10.	Octanoyl chloride	No	Acetonitrile	Cy3gal monooctanoate (9.9), Cy3gal dioctanoate (64.2), Cy3gal trioctanoate (25.9)

*The reaction was carried out for 24 h at room temperature. Entry 9 was carried out for 2 h. The acylating agents were 3 eq relative to Cy3gal. Entry 7 and 10 were 4 eq, and entry 9 was 1 eq relative to Cy3gal, respectively. All starting materials were obtained from Biotage purification. ANC: anthocyanins.

Pyridine was added to assist the acylation reaction of anthocyanins as a catalyst. **Table 6.3** shows that the presence of pyridine in DMSO and DCM could produce acylated anthocyanins in the first 5 h, but curiously appeared to give precursors back

over 24 h. On the other hand, the absence of pyridine in DMSO and chloroform did not produce acylated anthocyanins, and only starting material remained. However, anthocyanins tend to degrade at alkaline pH.[35,189] Additionally, to remove pyridine from the reaction products, acidified water or water is usually used, which might cause hydrolysis on the acylated anthocyanins. As such, the acylation in other solvents was performed without pyridine.

The acylation reaction in acetonitrile could produce acylated anthocyanins even without the addition of a catalyst. This result suggested that anthocyanins could directly react with acylating agents in acetonitrile. After 24 h, the reaction of anthocyanins and acetyl chloride in acetonitrile produced Cy3gal monoacetate (17.4-25%), Cy3gal diacetate (52.8-62.5%) and Cy3gal triacetate (12.5-21.7%). The selective production of acylated anthocyanins might be possible by controlling the reaction time and quantity of acylating agents, which is discussed later. Cruz *et al*. also reported the synthesis of malvidin-3-glucoside stearic acid derivatives in anhydrous acetonitrile at room temperature overnight under an argon atmosphere.[179]

Acetonitrile-d was used for the NMR studies to monitor the formation of acylated anthocyanins. Anhydrous acetonitrile was taken from the dry solvent system. Alternatively, acetonitrile was freshly taken from the closed solvent bottle. For practical reasons, acetonitrile from the closed solvent bottle was used in this study. This method was repeated with different reaction parameters to find the better yield of acylated anthocyanins.

6.2.1.2. Effect of a Biphasic Solvent System

There is a significant challenge when attempting to react a highly hydrophilic anthocyanin with a hydrophobic acylating agent due to their very different solubility properties. One option is to investigate a biphasic solvent approach, in this case using two immiscible solvents, acetonitrile/hexane, 1:1. The acylation reaction mechanism in this medium should follow a typical acylation reaction. A biphasic solvent was intended to selectively extract the acylated anthocyanins formed during the acylation reaction from the interphase layer to the hexane layer (**Figure 6.3**). However, the hexane layer remained uncoloured even after the reaction finished, suggesting that the mono- and diacylated anthocyanins (acetate and octanoate derivatives) if formed, are still too polar to move to the hexane layer.

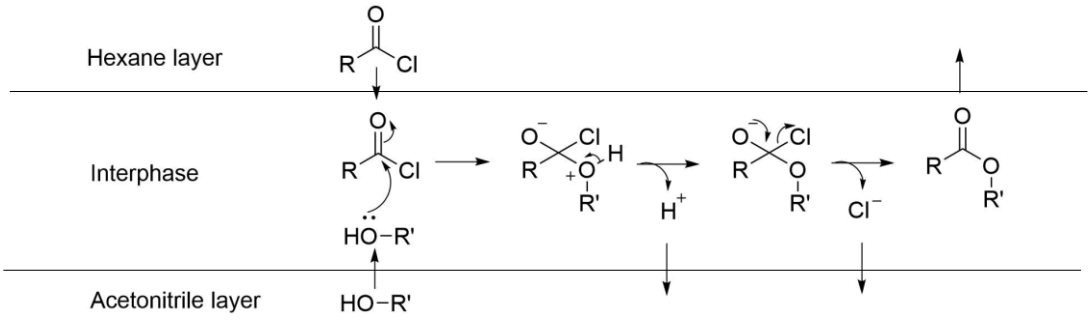

Figure 6.3 Acylation reaction in a biphasic solvent system.

The starting material was obtained from RASE with trifluoroacetate as a counterion. It was selected amongst other RASE with different counterions due to anthocyanins' high content (42.2 w/w % RASE, see **Chapter 4**). Anthocyanins were reacted with 4 equivalents of octanoyl chloride at 40 ºC for 7 h. The results are summarised in **Table 6.4**.

Table 6.4 Comparison of biphasic (acetonitrile/hexane, 1:1) and monophasic approaches for the formation of acylated anthocyanins.

Entry	Acylating agent	Biphasic	Distribution of ANC & their ester derivatives (%)
1.	Octanoyl chloride	Yes	Cy (17.3), Cy3gal (3.2), Cy3ara (7.6), Cy3gal monooctanoate (59.5), Cy3gal dioctanoate (12.4)
2.	Octanoyl chloride	No	Cy (21.1), Cy3gal monooctanoate (10.3), Cy3ara monooctanoate (7.5), Cy3gal dioctanoate (61)

The reaction was carried out at 40 ºC for 7 h. Biphasic solvents contain acetonitrile/hexane, 1:1). Monophasic solvent is acetonitrile. The acylating agent was 4 eq relative to Cy3gal. The counterion of RASE was trifluoroacetate (CH_3COO^-).

The acylation reaction conducted in a biphasic solvent produced higher Cy3gal monooctanoate (59.5%) than in a one-phase solvent, acetonitrile (7.5%). On the other hand, Cy3gal dioctanoate was observed higher (61%) when the acylation reaction conducted in acetonitrile than in a biphasic solvent (12.4%). Approximately 10.8% of anthocyanins remained unreacted in a biphasic solvent reaction, whereas all anthocyanins reacted with octanoyl chloride in a monophasic solvent. Octanoyl chloride in a biphasic solvent might react with Cy3gal gradually, whereas it reacted quickly in acetonitrile as all the reagents were in the same phase. These results suggest that a particular acylated anthocyanin production can be driven by controlling the reaction medium, although there is much scope for further optimisation. The combination of acetonitrile with other immiscible solvents might need to be further

studied to find a suitable solvent system that could produce acylated anthocyanins with a higher yield.

6.2.1.3. Effect of RASE counterions on acylation efficiency.

Solubility is a key factor in the reactions of anthocyanins, and the anionic counterion associated with an anthocyanin could have a significant influence on this. RASE with various counterions (see **Chapter 4**) were separately reacted with 4 equivalents of acylating agents. The reaction was carried out in a biphasic solvent system (acetonitrile/hexane, 1:1) at 40 ºC for 7h. The results are summarised in **Table 6.5**, the percentage of Cy3gal in each RASE is also given.

Table 6.5 The effect of RASE counterion on the formation of acylated anthocyanins.

Entry	Starting material-counterion	Acylating agent	Distribution of ANC & their ester derivatives (%)
1.	RASE-chloride (Cy3gal 48.5%)	Acetyl chloride	No reaction. Starting material remained.
2.	RASE-chloride	Octanoyl chloride	No reaction. Starting material remained.
3.	RASE-no chloride* (Cy3gal 51.4%)	Acetyl chloride	Cy (11.3), Cy3gal (21.7), Cy3ara (7.5), Cy3gal monoacetate (19.8), Cy3gal diacetate (39.6)
4.	RASE-no chloride*	Octanoyl chloride	Cy3gal (16), Cy3ara (34), Cy (6), Cy3gal monooctanoate (32), Cy3gal dioctanoate (12)
5.	RASE-trifluoroacetate (Cy3gal 58%)	Acetyl chloride	Cy (29.3), Cy3gal (10.7), Cy3gal monoacetate (8), Cy3gal diacetate (45.3), Cy3gal triacetate (6.7)
6.	RASE-trifluoroacetate	Octanoyl chloride	Cy3gal (3.2), Cy3ara (7.6), Cy (17.3), Cy3gal monooctanoate (59.5), Cy3gal dioctanoate (12.4)
7.	RASE-trifluoroacetate from Biotage (Cy3gal 89.6%)	Octanoyl chloride	Cy3gal (18.1), Cy3gal monooctanoate (75.4), Cy3gal dioctanoate (6.5)
8.	RASE-formate (Cy3gal 56.6%)	Octanoyl chloride	Cy3gal (4.2), Cy3ara (6.3), Cy (23.9), Cy3gal monooctanoate (16.7), Cy3ara monooctanoate (10.4), Cy3gal dioctanoate (38.5)
9.	RASE-acetate (Cy3gal 56%)	Octanoyl chloride	Cy3gal (4.3), Cy3ara (8.6), Cy (18.3), Cy3gal monooctanoate (22.6), Cy3ara monooctanoate (12.9), Cy3gal dioctanoate (33.3)

The reactions were carried out in a biphasic solvent (acetonitrile/hexane, 1:1) at 40 ºC for 7 h. The acylating agents were 4 eq relative to Cy3gal. *RASE-no chloride was obtained from the extraction-purification where the use of acid is limited during the SPE elution (see **Chapter 5**). The SPE elution was done as follows: the SPE column was washed with acidified water (0.1% v/v HCl), further copious amounts of water, then ethyl acetate and finally non-acidified ethanol.

Figure 6.3 in **Section 6.2.1.2** suggests that the reaction between anthocyanins and acylating agents occur at the interphase region between acetonitrile and hexane. For RASE with chloride as counterion, anthocyanins remain strictly in the acetonitrile layer due to this anion polarity and hydrophilicity. On the other hand, RASE with no chloride from neutral SPE elution (see **Chapter 5**) began to show some reaction, possibly inferring the presence of some less polar species, such as a hemiketal form. Additionally, formate, acetate and trifluoroacetate encouragingly also showed an enhanced reaction. RASE-no chloride produced higher Cy3gal monoacetate (19.8%) than RASE-trifluoroacetate (8%). Meanwhile, Cy3gal diacetate was higher in RASE-trifluoroacetate (45.3%) than RASE-no chloride (39.6%). Cy3gal diester in both RASE was dominating. Cy3gal triacetate was only observed in RASE-trifluoroacetate. The unreacted anthocyanins and their aglycone after the reaction ranged from 18.1 (RASE-trifluoroacetate from Biotage) to 56% (RASE-no chloride).

Overall, the percentage of octanoate derivatives of anthocyanins produced in this study followed this order, Cy3gal monooctanoate: RASE-trifluoroacetate (Biotage) (75.4%) > RASE-trifluoroacetate (59.5%) > RASE-no chloride (32%) > RASE-acetate (22.6%) > RASE-formate (16.7%). Meanwhile, for Cy3gal dioctanoate, the order are as follows: RASE-formate (38.5%) > RASE-acetate (33.3%) > RASE-trifluoroacetate (12.4%) > RASE-no chloride (12%) > RASE-trifluoroacetate (Biotage) (6.5%). It should be noted that monoacylated Cy3gal can be further acylated to produce diacylated Cy3gal and so on. It was observed that the acylation of RASE-trifluoroacetate and RASE-no chloride with octanoyl chloride in a biphasic-solvent produced more monoacylated anthocyanins than diacylated anthocyanins. On the other hand, RASE-formate and RASE-acetate produced more Cy3gal diester than Cy3gal monoester. According to the results discussed in **Chapter 4**, anthocyanins in RASE-formate and RASE-acetate were mostly found as their hemiketal forms which are less polar species. As such, it suggests that anthocyanins in those RASE tend to react more with octanoyl chloride at the interphase region between acetonitrile and hexane, resulting higher percentage of Cy3gal diester. The acylation of these RASE with selected acylating agents in a monophasic solvent system is required for comparison. It is also suggested that the acylation reaction of longer chain length acylating agents may more suitable being carried out in a biphasic solvent system due to higher lipophilicity.

6.2.1.4. Effect of Reaction Temperature

Anthocyanins are sensitive to temperature changes and can degrade at high temperatures.[190,191] Hence, the reaction temperature should be controlled to avoid

anthocyanin's degradation. Two different temperatures, room temperature and 40 °C, were employed in this reaction. The starting material was RASE-trifluoroacetate and reacted with 4 equivalents of octanoyl chloride. The reaction was carried out in acetonitrile for 7 h. This reaction was carried out in a monophasic solvent to investigate the effect of reaction temperature on the formation of multiacylated anthocyanins, not limited to the production of mono- and diesters. The distribution of anthocyanins and their ester derivatives are summarised in **Table 6.6**.

Table 6.6 The effect of reaction temperature on the formation of acylated anthocyanins.

Entry	Starting material-counterion	Acylating agent	T (°C)	Distribution of ANC & their ester derivatives (%)
1.	RASE-trifluoroacetate	Octanoyl chloride	RT	Cy (26.1), Cy3gal monooctanoate (26.1), Cy3ara monooctanoate (13), Cy3gal dioctanoate (34.8)
2.	RASE-trifluoroacetate	Octanoyl chloride	40	Cy (21.1), Cy3gal monooctanoate (10.3), Cy3ara monooctanoate (7.5), Cy3gal dioctanoate (61)

The reaction was carried out in acetonitrile at different temperatures for 7 h. The acylating agent was 4 eq relative to Cy3gal. ANC: anthocyanins.

Table 6.6 shows that Cy3gal monooctanoate was higher when the acylation reaction was carried out at RT (26.1%) than at 40 ºC (10.3%). On the other hand, the percentage of Cy3gal dioctanoate was higher when the acylation reaction was carried out at 40 ºC (61%) than at RT (34.8%). The fundamental kinetic theory states that the activation energy (E_a) is directly proportional to temperature ($k=Ae^{-E_a/RT}$).[192] An increase in reaction temperature typically increases the reaction rate in which the average kinetic energy of the reactants also increases. It is suggested that the higher yield of multiacylated anthocyanins can be achieved by conducting the reaction at 40 ºC (or potentially higher, provided degradation is not observed).

6.2.1.5. Effect of Reaction Time

To investigate the effect of reaction time on the distribution of anthocyanins and their derivatives, a starting material from Biotage flash purification (Cy3gal, 89.6%) was reacted with 4 equivalents of acetyl chloride in acetonitrile at room temperature, and the reaction was monitored for 24 h (**Figure 6.4**).

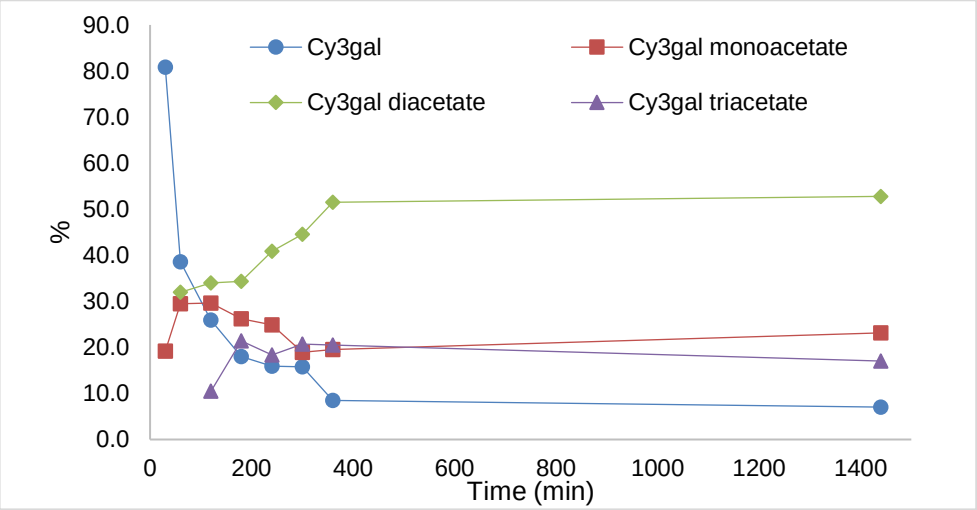

Figure 6.4 Distribution of Cy3gal and its ester derivatives (%) in acetonitrile at room temperature for 24 h. The starting material was obtained from the Biotage experiment. The acylating agent was 4 equivalents relative to Cy3gal.

Figure 6.4 shows that the concentration of Cy3gal as starting material decreased rapidly whilst the concentration of acylated Cy3gal increased over time. The formation of Cy3gal diacetate dominated (52.8%), followed by Cy3gal monoacetate (23.2%) and Cy3gal triacetate (17%) after the reaction for 24 h, although reaction appeared to be essentially complete after 400 mins. Cy3gal monooctanoate dominated in the first 3 h of the reaction and decreased over time. Meanwhile, the concentration of Cy3gal triacetate was found to be at its highest after 5 h. It should be noted that in this study, the acylation reaction does not use an enzyme as the catalyst, and therefore multiacylation on anthocyanin's hydroxyl groups may occur. As such, the distribution of acylated anthocyanins might vary depending on the percentage of anthocyanins present in the starting material and also the quantity of acylating agents used in the reaction. The longer reaction time leads to further acylation of free hydroxyl groups as long as excess acylating agent is present.

6.2.2. Synthesis and Chemical Characterisation of Novel Acylated Anthocyanins

Anthocyanins from *Aronia* skin waste were obtained from the extraction-purification using TFA (RASE-trifluoroacetate), and were separately reacted with 4 equivalents of acetyl chloride (C_2), butanoyl chloride (C_4), and octanoyl chloride (C_8) to obtain acylated anthocyanins with the respective acylating agents. The reaction was carried out in acetonitrile at room temperature for 3h. These reaction parameters were selected to sustain monoacylated anthocyanins while producing a higher number of acylation products. To produce acylated anthocyanins with a higher acylation number

(>4 acylation), RASE-trifluoroacetate was reacted with 20 equivalents of acetyl chloride at 40 ºC for 2 days. The reaction products were purified and isolated by semi-preparative HPLC-DAD. The collected fractions were freeze dried and stored in the freezer until further use. Acylated anthocyanins in a flavylium cationic form are expected to be encountered by trifluoroacetate from the semi-preparative HPLC.

Cy3gal represents 24.5% of total polyphenols present in RASE-trifluoroacetate (see **Chapter 4**). The yield of acylated anthocyanins was calculated as Cy3gal equivalent (CGE) and ranged from 2.1 to 15.4%. Due to the limited amount of acylated anthocyanins produced through this reaction, the chemical characterisation was only carried out for the major components, the Cy3gal derivatives. The products were obtained as red amorphous powders with a purity ranged from 42.4 to 92.9 % based on the comparison of peak areas at 520 nm by HPLC-DAD analysis. The confirmation of the acylated anthocyanin structure was determined by 1D and 2D NMR spectroscopy using $(CD_3)_2SO/CF_3COOD$ (95:5, v/v). The flavylium cationic form of acylated Cy3gal derivatives is countered by trifluoroacetate. The molecular mass of acylated Cy3gal derivatives was determined by HRMS.

Overall, the chemical characterisation of Cy3gal derivatives follows the chemical characterisation of its precursor, Cy3gal (See **Chapter 3**). The changes in the chemical shift by comparing upfield and downfield shifts between acylated anthocyanins and their precursors can be used to determine the acylation site on the hydroxyl group(s). Multiacylation is unavoidable in this system; hence, acylation occurs on both the primary and secondary hydroxyl(s) of sugar moiety and, after prolonged reaction times, hydroxyl(s) of the aromatic ring (**Table 6.7**). The order of acylation site on anthocyanins, and hence selectivity, is discussed later.

Table 6.7 List of possible acylated anthocyanins with different acylating agents and number of acylation (C_2, acetate; C_4, butanoate; and C_8, octanoate).*

Cy3gal derivative	Number of acylation	$[M]^+$ -Acetate	$[M]^+$ -Butanoate	$[M]^+$ -Octanoate
Cy3gal-monoester	1	491.12	519.15	575.21
Cy3gal-diester	2	533.13	589.19	701.32
Cy3gal-triester	3	575.14	659.23	827.42
Cy3gal-tetraester	4	617.15	729.28	953.53
Cy3gal-pentaester	5	659.16	799.32	1079.63
Cy3gal-hexaester	6	701.17	869.36	1205.73
Cy3gal-heptaester	7	743.18	939.40	1331.84
Cy3gal-octaester	8	785.19	1009.44	1457.94

*Molecular mass is calculated using ChemDraw Prime 16.0.

6.2.2.1. Acylation of anthocyanins with Acetyl Chloride (C_2)

6.2.2.1.1. Cy3gal monoacetate (Cyanidin-3-β-*O*-(6”-acetylgalactoside)) trifluoroacetate

Cyanidin-3-β-*O*-(6”-acetylgalactoside) trifluoroacetate, **44**, was confirmed by the molecular mass [M^+] m/z of 491.1196, calculated for [M^+]: 491.1184 (mass error of 2.4 ppm) with a purity of 89.7%. The reaction yield was 7.1% CGE. The first acylation site occurred on the primary hydroxyl of the sugar moiety. The primary hydroxyl group's reactivity has been reported to be greater than that of a secondary hydroxyl group.[193] The ^{1}H chemical shift of H-6”A/B changes to downfield from 3.50-3.60 ppm to 4.13-4.21 ppm. The ^{13}C chemical shift of C-6”A/B shifted from 61.4 ppm to 64.5 ppm. Meanwhile, the chemical shifts of other peaks are rather similar. This finding is in agreement with the results from other researchers who did the enzymatic acylation of anthocyanins, they also reported the mono acylation on the primary hydroxyl of a sugar moiety (6”-OH).[58,145,169,180,188] A peak of the acetate moiety was observed in the ^{1}H-NMR at 2.00 ppm as a singlet. The ^{13}C-NMR confirmed the acyl moiety and carbonyl group at 20.6 and 170.6 ppm. The chemical characterisation of this compound (^{1}H and ^{13}C) is summarised in **Table 6.8**, with the NMR data of Cy3gal also given for comparison.

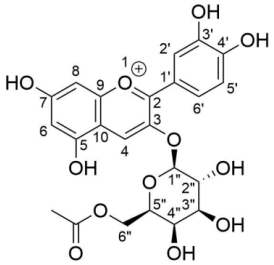

Table 6.8 ^{1}H (500 MHz) and ^{13}C (125 MHz) NMR Data for **44** in $(CD_3)_2SO$ /CF_3COOD (95:5, v/v) at 25 °C.

Aglycone	**Cy3gal (27)**			**44**		
	δ^{1}H (ppm)	J (Hz)	δ^{13}C(ppm)	δ^{1}H (ppm)	J (Hz)	δ^{13}C(ppm)
H-4	8.87	s	135.6	8.80	s	134.2
H-6’	8.24	dd, 8.5, 2.5	128.1	8.25	dd, 8.5, 2.5	127.4
H-2’	7.99	d, 2.5	118.5	7.99	d, 2.5	117.0
H-5’	7.03	d, 8.5	117.8	7.03	d, 9.0	116.5
H-8	6.90	d, 1.0	95.2	6.90	d, 2.0	94.4
H-6	6.69	d, 1.0	103.3	6.71	d, 2.0	102.4
Sugar						
H-1”	5.27	d, 7.5	103.7	5.30	d, 7.5	102.5
H-2”	3.82	dd, 9.0, 7.5	71.2	3.83	9.5, 8.0	70.0
H-4”	3.74	d, 3.5	69.1	3.76	d, 3.5	68.8
H-5”	4.56	t, 6.5	77.3	4.06	dd, 8.0, 3.0	73.7
H-6”A	(3.55-3.60)	m	61.4	(4.13-4.21)	m	64.5
H-3”	(3.50-3.53)	m	74.2	3.54	dd, 9.5, 3.5	72.9
H-6”B	(3.50-3.53)	m	61.4	(4.13-4.21)	m	64.5
Acyl						
CH_3	-	-	-	2.00	s	20.9
C=O	-	-	-	-	-	170.8

6.2.2.1.2. Cy3gal diacetate (Cyanidin-3-β-*O*-(3",6"-diacetylgalactoside)) trifluoroacetate

Once the primary hydroxyl group in the sugar moiety has been acylated, the second acylation occurred on the sugar moiety's secondary hydroxyl. The chemical shift of H-3" changes drastically from 3.54 to 4.78 ppm. The ^{13}C-NMR shows the changes of the chemical shift from 72.9 ppm to 75.9 ppm. The ^{1}H chemical shift of H-2" and H-4" as adjacent protons change to upfield from 3.83 ppm to 4.08 ppm and from 3.76 ppm to 3.96 ppm respectively. The ^{13}C chemical shift of C-2" shifted from 70.0 ppm to 67.4 ppm and C-4" shifted from 68.8 ppm to 65.9 ppm. This compound was confirmed as cyanidin-3-β-*O*-(3",6"-diacetylgalactoside) trifluoroacetate, **45**, by the molecular mass [M^{+}] m/z of 533.1292, calculated for [M^{+}]: 533.1290 (mass error of 0.4 ppm) with the purity of 92.9%. The reaction yield was 6.5% CGE. The chemical characterisation of this compound (^{1}H and ^{13}C) is summarised in **Table 6.9**. This result is in agreement with Chebil *et al*., who reported that the second acylation of isoquercetin occurred on the secondary hydroxyl group of a sugar moiety (6"-OH and 3"-OH), producing isoquercetin 3",6"-diacetate.[194] It suggested that acylation occurs on the 3"-OH due to minimum steric hindrance.

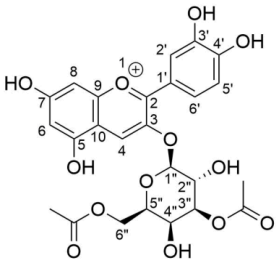

Table 6.9 ^{1}H (500 MHz) and ^{13}C (125 MHz) NMR Data for **45** in $(CD_3)_2SO$ /CF_3COOD (95:5, v/v) at 25 °C.

Aglycone	**45**		
	δ^{1}H (ppm)	J (Hz)	δ^{13}C(ppm)
H-4	8.81	s	134.2
H-6'	8.23	dd, 8.5, 2.5	127.4
H-2'	7.98	d, 2.5	117.7
H-5'	7.03	d, 9.0	117.0
H-8	6.91	d, 2.0	94.5
H-6	6.72	d, 2.0	101.9
Sugar			
H-1"	5.49	d, 7.5	102.5
H-2"	4.08	dd,10.0, 7.5	67.4
H-4"	3.97	d, 3.5	65.9
H-5"	(4.15-4.22)	m	73.2
H-6"A	(4.15-4.22)	m	64.0
H-3"	4.78	dd, 10.5, 3.5	75.9
H-6"B	(4.15-4.22)	m	64.0
Acyl			
CH_3 (a)	2.01	s	21.4
CH_3 (b)	2.10	s	20.9
C=O (a)	-	-	170.8
C=O (b)	-	-	170.6

6.2.2.1.3. Cy3gal triacetate (Cyanidin-3-β-*O*-(3",4",6"-triacetylgalactoside)) trifluoroacetate

The third acylation occurred on the 4"-OH of the sugar moiety, as evidenced by the changes of the ^{1}H-NMR chemical shift to downfield, from 3.97 ppm to 5.34 ppm. The ^{13}C-NMR shows the changes of the chemical shift from 65.9 ppm to 67.4 ppm. The ^{1}H chemical shift of H-3" and H-5" as adjacent protons change to upfield from 4.78 ppm to 5.05 ppm and from 4.15-4.22 ppm to 4.52 ppm, respectively. The ^{13}C chemical shift of C-3" shifted from 75.9 ppm to 72.5 ppm and C-5" shifted from 73.7 ppm to 73.2 ppm. This compound was confirmed as cyanidin-3-β-*O*-(3",4",6"-triacetylgalactoside), **46**, by the molecular mass [M^+] m/z of 575.1413, calculated for [M^+]: 575.1395 (mass error of 3.1 ppm) with the purity of 76.2%. The reaction yield was 8.4% CGE. The broad peak at 6.2-7.2 ppm belongs to polymeric proanthocyanidins. The polymeric proanthocyanins tend to co-elute with triacylated Cy3gal because they have similar retention time. The chemical characterisation of this compound (^{1}H and ^{13}C) is summarised in **Table 6.10**.

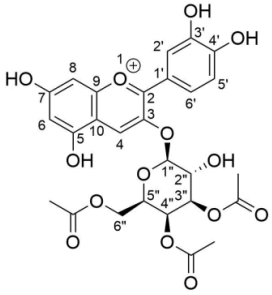

Table 6.10 ^{1}H (500 MHz) and ^{13}C (125 MHz) NMR Data for **46** in $(CD_3)_2SO$ /CF_3COOD (95:5, v/v) at 25 °C.

Aglycone	**46**		
	δ^{1}H (ppm)	J (Hz)	δ^{13}C(ppm)
H-4	8.81	s	134.4
H-6'	8.22	dd, 8.5, 2.0	127.5
H-2'	7.97	d, 2.0	117.5
H-5'	7.04	d, 9.0	116.3
H-8	6.92	d, 2.0	94.4
H-6	6.72	d, 2.0	102.5
Sugar			
H-1"	5.63	d, 8.0	101.7
H-2"	4.00	dd,10.5, 8.0	67.4
H-4"	5.34	d, 4.0	67.4
H-3"	5.05	dd, 10.0, 3.5	72.5
H-5"	4.52	dd,8.5, 4.0	73.2
H-6"A	4.12	dd,11.5, 4.0	63.2
H-6"B	4.04	dd, 11.0, 8.0	63.2
Acyl			
CH_3 (a)	2.05	s	20.6
CH_3 (b)	2.00	s	20.6
CH_3 (c)	1.90	s	20.6
C=O (b)	-	-	170.2

However, Chebil *et al*. reported that the third acylation occurred on the C-2” hydroxyl, producing isoquercetin 2”,3”,6”-triacetate.[194] It should be noted that isoquercetin is a glucoside, whereas, in this study, we have a galactoside linked to the core of anthocyanin. These monosaccharides differ on the orientation of OH at C-4” within the sugar ring. It is axial for galactoside and equatorial for glucoside and hence will have quite different acylation reactivity. The hydrogen bond between a carbonyl from acetyl attached at C-3” with OH at C-2” may avoid the acylation on this site. As such, the 4”-OH is preferred for the third acylation reaction.

6.2.2.1.4. Cy3gal tetraacetate (Cyanidin-3-β-*O*-(2”,3”,4”,6”-tetraacetylgalactoside))

Further acylation on the sugar moiety occurred on the hydroxyl group at the C-2”. The ^{1}H-NMR chemical shift of H-2” changes from 4.00 ppm to 5.41 ppm. The ^{13}C-NMR chemical shift of C-2” changes from 67.4 ppm to 68.6 ppm. The ^{1}H chemical shift of H-1” and H-3” as adjacent protons change to upfield from 5.63 ppm to 5.87 ppm and from 5.05 to 5.28 ppm, respectively. The ^{13}C chemical shift of C-1” shifted from 101.7 ppm to 98.8 ppm and C-3” shifted from 72.5 ppm to 73.4 ppm. This compound was confirmed as cyanidin-3-β-*O*-(2”,3”,4”,6”-tetraacetylgalactoside) trifluoroacetate, **47**, by the molecular mass [M^{+}] m/z of 617.1518, calculated for [M^{+}]: 617.1501 (mass error of 2.7 ppm) with the purity of 42.4%. It mixed with later confirmed as Cy3gal pentaacetate. The reaction yield was 13.5% CGE. According to HRMS, cyanidin-3-β-*Oc*-(4’,2”,3”,4”,6”-pentaacetylgalactoside), **48** was also observed in this sample. Development of separation and purification of this ester mixture is still required. The chemical characterisation of this compound (^{1}H and ^{13}C) is summarised in **Table 6.11**.

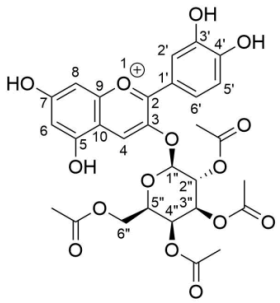

Table 6.11 ^{1}H (500 MHz) and ^{13}C (125 MHz) NMR Data for 48 in $(CD_3)_2SO$ /CF_3COOD (95:5, v/v) at 25 °C.

	47		
	δ^{1}H (ppm)	J (Hz)	δ^{13}C(ppm)
H-4	8.82	s	134.6
H-6’	7.88	dd, 8.5, 2.5	127.2
H-2’	7.78	d, 2.0	117.4
H-5’	6.95	d, 8.5	115.3
H-8	6.92	d, 2.0	94.3
H-6	6.73	d, 2.0	102.7

	47		
	δ^{1}H (ppm)	J (Hz)	δ^{13}C(ppm)
Sugar			
H-1”	5.87	d, 8.0	98.8
H-2”	5.41	dd,10.5, 8.0	68.6
H-4”	5.43	d, 3.5	65.8
H-5”	4.61	dd,9.0, 3.5	71.7
H-6”A	4.12	dd,11.5, 8.5	63.2
H-3”	5.28	dd, 10.5, 3.5	73.4
H-6”B	4.15-4.17	m	63.2
Acyl			
CH_3 (a)	2.16	s	20.8
CH_3 (b)	2.02	s	20.8
CH_3 (c)	1.94	s	20.8
CH_3 (d)	1.86	s	20.8
C=O (b)	-	-	170.3

6.2.2.1.5. Cy3gal pentaacetate (Cyanidin-3-β-*O*-(4’,2”,3”,4”,6”-pentaacetylgalactoside)) trifluoroacetate

Once all hydroxyl groups on the sugar moiety have been acylated, further acylation occurred on the aglycone's hydroxyl group(s). The first hydroxyl group on the anthocyanin core that has been acylated is located at the C-4’. The ^{1}H-NMR chemical shift of H-5’ as adjacent proton changes from 6.95 ppm to 7.18 ppm. The ^{13}C-NMR chemical shift of C-5’ changes from 115.3 ppm to 122.5 ppm. Chebil *et al*. also reported that the first acylation of quercetin occurred on the hydroxyl group at C-4’.[194] This compound was confirmed as cyanidin-3-β-*O*-(4’,2”,3”,4”,6”-pentaacetyl galactoside) trifluoroacetate, **48**, by the molecular mass [M^{+}] m/z of 659.1620, calculated for [M^{+}]: 659.1607 (mass error of 2 ppm) with the purity of 77.9%. The reaction yield was 14.1% CGE. The chemical characterisation of this compound (^{1}H and ^{13}C) is summarised in **Table 6.12**.

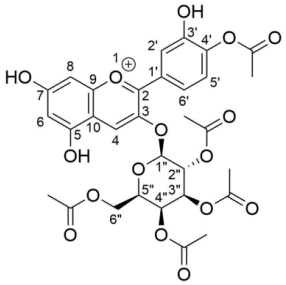

Table 6.12 ^{1}H (500 MHz) and ^{13}C (125 MHz) NMR Data for **48** in $(CD_3)_2SO$ /CF_3COOD (95:5, v/v) at 25 °C.

	48		
	δ^{1}H (ppm)	J (Hz)	δ^{13}C(ppm)
H-4	8.87	s	134.9
H-6’	8.24	dd, 9.0, 2.5	131.6
H-2’	8.10	d, 2.5	126.9
H-5’	7.18	d, 8.5	122.5
H-8	7.02	d, 1.0	116.8
H-6	6.76	d, 1.0	115.7

	48		
	δ^{1}H (ppm)	J (Hz)	δ^{13}C(ppm)
Sugar			
H-1”	6.01	d, 8.0	98.6
H-2”	5.42	d,10.5, 8.0	68.4
H-4”	5.44	d, 4.0	67.5
H-5”	4.65	dd, 8.5, 3.5	71.6
H-6”A	4.16	dd, 11.5, 3.5	62.6
H-3”	5.30	dd, 10.0, 3.5	70.6
H-6”B	4.06	dd, 11.5, 8.5	62.6
Acyl			
CH_3	2.16	s	20.4
CH_3	2.01	s	20.4
CH_3	1.96	s	20.4
CH_3	1.93	s	20.4
CH_3	1.89	s	20.4
C=O	-	-	170.1

6.2.2.1.6. Cy3gal hexaacetate (Cyanidin-3-β-*O*-(4’,7,2”,3”,4”,6”-hexaacetylgalactoside)) trifluoroacetate

The second hydroxyl group on the aglycone was located at the C-7. The ^{1}H-NMR chemical shift of H-6 as adjacent proton changed from 6.76 ppm to 6.85 ppm. The ^{13}C-NMR chemical shift of C-8 as adjacent carbon changed from 116.8 ppm to 121.3 ppm. Chebil *et al*. reported that the second acylation of quercetin occurred on the hydroxyl group at C-3’.[194] Due to the steric hindrance from the acyl group attached at the C-4’, the next acylation is suggested to occur at the C7-OH. According to the equilibrium of anthocyanins (see **Chapter 1**), the hydroxyl groups at the C-7 and C-4’ are the most acidic, allowing the acylation with acylating agents. This compound was confirmed as cyanidin-3-β-*O*-(4’,7,2”,3”,4”,6”-hexaacetylgalactoside) trifluoroacetate, **49**, by the molecular mass [M^{+}] m/z of 701.1724, calculated for [M^{+}]: 701.1712 (mass error of 1.7 ppm) with the purity of 71.1 %. The reaction yield was 6.9% CGE. The chemical characterisation of this compound (^{1}H and ^{13}C) is summarised in **Table 6.13**.

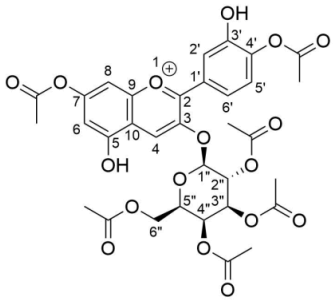

Table 6.13 ^{1}H (500 MHz) and ^{13}C (125 MHz) NMR Data for **49** in $(CD_3)_2SO$ /CF_3COOD (95:5, v/v) at 25 °C.

	49		
	δ^{1}H (ppm)	J (Hz)	δ^{13}C(ppm)
H-4	9.07	s	134.9

	49		
	δ^{1}H (ppm)	J (Hz)	δ^{13}C(ppm)
H-6'	8.25	dd, 8.5, 2.0	131.6
H-2'	8.16	d, 2.0	126.9
H-5'	7.20	d, 8.5	122.9
H-8	7.01	d, 2.5	121.3
H-6	6.85	d, 2.0	115.9
Sugar			
H-1"	6.03	d, 7.5	98.6
H-2"	5.40	d,10.0, 7.5	68.4
H-4"	5.45	d, 3.5	67.5
H-5"	4.40	dd, 8.0, 3.5	71.6
H-6"A	4.11	dd, 12, 4.0	62.6
H-3"	5.27	dd, 10.5, 3.5	70.6
H-6"B	4.06	dd, 12, 8.5	62.6
Acyl			
CH_3	2.33	s	20.7
CH_3	2.16	s	20.7
CH_3	2.01	s	20.7
CH_3	1.96	s	20.7
CH_3	1.91	s	20.7
CH_3	1.87	s	20.7
C=O	-	-	170.4

In summary, the acylation of anthocyanins started from the most reactive hydroxyl group, the primary hydroxyl group in the sugar moiety at the C-6" followed by the secondary hydroxyl groups, 3"-OH, 4"-OH, and 2"-OH. Once all hydroxyl groups from sugar moiety have been acylated, further acylation occurred on the aglycone. The first acylation on the aromatic anthocyanin core occurred on the 4'-OH, followed by the 7-OH. It is suggested that the next acylation is on the 3'-OH due to the steric hindrance. Lastly, the acylation is suggested to occur on the 5-OH. Further research is required to confirm this finding. The summary of the order of acylation site of anthocyanins is presented in **Table 6.14**.

Table 6.14 Summary of the order of acylation site on Cy3gal.

Number of acylation	**Acylation site in the sugar moiety**			
	6"-OH	**3"-OH**	**4"-OH**	**2"-OH**
1	✓	-	-	-
2	✓	✓	-	-
3	✓	✓	✓	-
4	✓	✓	✓	✓
Number of acylation	**Acylation site in the aromatic ring**			
	4'-OH	**7-OH**	**3'-OH**	**5-OH**
5	✓	-	-	-
6	✓	✓	-	-
7	✓	✓	✓	-
8	✓	✓	✓	✓

The same order of acylation should also apply to the acylation using different acylating agents. To study the effect of acylating agents on acylated anthocyanins' physio-chemical properties, anthocyanins' acylation with butanoyl chloride and octanoyl chloride was carried out. However, the characterisation was performed only for mono- and diesters of the respective acylating agents.

6.2.2.2. Acylation of anthocyanins with Butanoyl Chloride (C_4)

RASE-trifluoroacetate (200 mg, 0.44 mmol, 1 equivalent relative to Cy3gal as the major anthocyanin) was dissolved in acetonitrile (8 mL to give a concentration of 25 g/L). Butyryl chloride (182.1 µL, 1.76 mmol, 4 eq.) was added dropwise. The reaction was performed at 25 ºC for 3 h and covered from light. The reaction mixture was evaporated and purified using semi-preparative HPLC-DAD. The collected fractions were freeze-dried, and dried acylated anthocyanins were stored in the freezer until further use. The acylated anthocyanins were analysed by UV-Vis, HPLC-DAD, HRMS and NMR spectroscopy.

6.2.2.2.1. Cy3gal monobutanoate (Cyanidin-3-β-*O*-(6”-butyrylgalactoside)) trifluoroacetate

Cyanidin-3-β-*O*-(6”-butyrylgalactoside) trifluoroacetate, **50**, was confirmed by the molecular mass [M^+] m/z of 519.1514, calculated for [M^+]: 519.1497 (mass error of 3.3 ppm) with the purity of 71.2%. The reaction yield was 11.8% CGE. The chemical characterisation of this compound (^{1}H and ^{13}C) is summarised in **Table 6.15**. New peaks of the butyryl group were observed at 2.24, 1.45 and 0.77 ppm, which belong to CH_2-α, CH_2-β and CH_3.

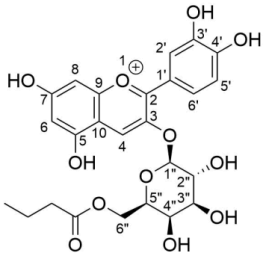

Table 6.15 ^{1}H (500 MHz) and ^{13}C (125 MHz) NMR Data for **50** in $(CD_3)_2SO$ /CF_3COOD (95:5, v/v) at 25 °C.

	50		
	δ^{1}H (ppm)	J (Hz)	δ^{13}C(ppm)
H-4	8.79	s	134.2
H-6’	8.24	dd, 9.0, 2.5	127.4
H-2’	7.98	d, 2.5	117.7
H-5’	7.03	d, 9.0	117.0
H-8	6.90	d, 2.0	94.4
H-6	6.72	d, 2.0	102.5
Sugar			

	50		
	δ^{1}H (ppm)	J (Hz)	δ^{13}C(ppm)
H-1”	5.33	d, 8.0	102.2
H-2”	3.83	9.5, 7.5	70.1
H-4”	3.76	d, 3.0	68.8
H-5”	(4.05-4.08)	m	73.7
H-6”A	4.22	dd, 11.5, 3.0	64.2
H-3”	3.55	dd, 9.5, 3.0	72.9
H-6”B	4.13	dd, 12.0, 9.0	64.2
Acyl moiety			
CH_2-α	2.24	dt, 7.5, 5.5	35.5
CH_2-β	1.45	ddd, 14.5, 7.0, 5.0	18.3
CH_3	0.77	t, 7.0	13.7
C=O	-	-	173.2

6.2.2.2.2. Cy3gal dibutanoate (Cyanidin-3-β-*O*-(3”,6”-dibutyrylgalactoside)) trifluoroacetate

Cyanidin-3-β-*O*-(3”,6”-dibutyrylgalactoside) trifluoroacetate, **51**, was confirmed by the molecular mass [M^+] m/z of 589.1922, calculated for [M^+]: 589.1916 (mass error of 1 ppm) with the purity of 82.2%. The reaction yield was 15.4% CGE. The chemical characterisation of this compound (^{1}H and ^{13}C) is summarised in **Table 6.16**. New peaks of the second butyryl were observed at 2.33-2.38, 1.58-1.62 and 0.93 ppm, which belong to CH_2-α, CH_2-β and CH_3.

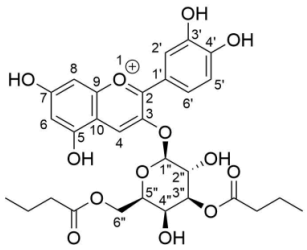

Table 6.16 ^{1}H (500 MHz) and ^{13}C (125 MHz) NMR Data for **51** in $(CD_3)_2SO$ /CF_3COOD (95:5, v/v) at 25 °C.

	51		
	δ^{1}H (ppm)	J (Hz)	δ^{13}C(ppm)
H-4	8.81	s	134.2
H-6’	8.22	dd, 8.5, 2.0	127.4
H-2’	7.97	d, 2.5	117.7
H-5’	7.03	d, 8.5	117.0
H-8	6.91	d, 1.0	102.5
H-6	6.73	d, 1.5	94.4
Sugar			
H-1”	5.52	d, 7.5	102.2
H-2”	4.08	10.5, 7.5	70.1
H-4”	3.96	d, 3.5	68.8
H-5”	(4.12-4.22)	m	73.7
H-6”A	(4.12-4.22)	m	64.2
H-3”	4.81	dd, 10.5, 3.5	72.9
H-6”B	(4.12-4.22)	m	64.2
Acyl moiety			

	51		
	δ^{1}H (ppm)	J (Hz)	δ^{13}C(ppm)
CH_2-α (a)	2.33-2.38	m	35.5
CH_2-β (a)	1.58-1.62	m	18.3
CH_3 (a)	0.93	t, 7.5	13.7
CH_2-α (b)	2.22-2.28	m	35.5
CH_2-β (b)	1.41-1.47	m	18.3
CH_3 (b)	0.78	t, 7.5	13.7
C=O (a)	-	-	173.2
C=O (b)	-	-	173.0

6.2.2.3. Acylation of anthocyanins with Octanoyl Chloride (C_8)

RASE-trifluoroacetate (200 mg, 0.44 mmol, 1 equivalent relative to Cy3gal as the major anthocyanin) was dissolved in acetonitrile (8 mL to give a concentration of 25 g/L). Caprylyl chloride (300.4 µL, 1.76 mmol, 4 eq.) was added dropwise. The reaction was performed at 25 ºC for 3 h and covered from light. The reaction mixture was evaporated and purified using semi-preparative HPLC-DAD. The collected fractions were freeze-dried, and dried acylated anthocyanins were stored in the freezer until further use. The acylated anthocyanins were analysed by UV-Vis, HPLC-DAD, HRMS and NMR spectroscopy.

6.2.2.3.1. Cy3gal monooctanoate (Cyanidin-3-β-O-(6''-caprylylgalactoside)) trifluoroacetate

Cyanidin-3-β-O-(6"-caprylylgalactoside) trifluoroacetate, **52**, was confirmed by the molecular mass [M^+] m/z of 575.2127, calculated for [M^+]: 575.2123 (mass error of 0.7 ppm) with the purity of 81.5%. The reaction yield was 8.5% CGE. The chemical characterisation of this compound (^{1}H and ^{13}C) is summarised in **Table 6.17**. New peaks of caprylyl were observed at 2.17, 1.48, 1.26 and 0.84 ppm, which belong to CH_2-α, CH_2-β, $(CH_2)_{4\text{-}7}$ and CH_3.

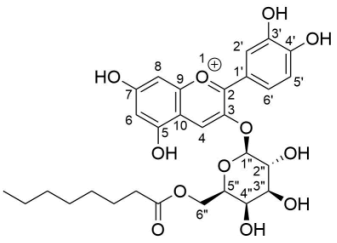

Table 6.17 ^{1}H (500 MHz) and ^{13}C (125 MHz) NMR Data for **52** in $(CD_3)_2SO$ /CF_3COOD (95:5, v/v) at 25 °C.

	52		
	δ^{1}H (ppm)	J (Hz)	δ^{13}C(ppm)
H-4	8.78	s	134.3
H-6'	8.24	dd, 9.0, 2.5	127.3
H-2'	7.99	d, 2.5	117.5
H-5'	7.03	d, 8.5	116.8
H-8	6.91	d, 1.0	94.0
H-6	6.71	d,1.5	102.4

	52		
	δ^{1}H (ppm)	J (Hz)	δ^{13}C(ppm)
Sugar			
H-1”	5.34	d, 8.0	102.4
H-2”	3.83	9.5, 8.0	69.9
H-4”	3.76	d, 3.5	68.5
H-5”	(4.05-4.10)	m	73.6
H-6”A	4.26	dd, 11.5, 8.5	63.7
H-3”	3.55	dd, 9.5, 3.5	72.8
H-6”B	(4.05-4.10)	m	63.7
Acyl moiety			
CH_2-α	2.17	t, 7.5	33.9
CH_2-β	1.48	m	24.9
CH_2 (4-7)	1.26	m	22.4
CH_3	0.84	t, 7.5	14.2

6.2.2.3.2. Cy3gal dioctanoate (Cyanidin-3-β-O-(3”,6”-dicaprylylgalactoside)) trifluoroacetate

Cyanidin-3-β-O-(3”,6”-dicaprylylgalactoside) trifluoroacetate, **53**, was confirmed by the molecular mass [M^+] m/z of 701.3171, calculated for [M^+]: 701.3168 (mass error of 0.4 ppm) with the purity of 80.4%. The reaction yield was 2.1% CGE. The chemical characterisation of this compound (^{1}H and ^{13}C) is summarised in **Table 6.18**. New peaks of the second caprylyl group were observed at 2.25, 1.57, 1.26 and 0.78 ppm, which belong to CH_2-α, CH_2-β, $(CH_2)_{4\text{-}7}$ and CH_3.

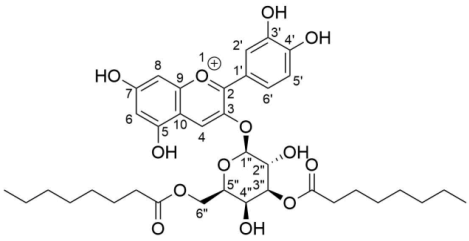

Table 6.18 ^{1}H (500 MHz) and ^{13}C (125 MHz) NMR Data for **53** in $(CD_3)_2SO$ /CF_3COOD (95:5, v/v) at 25 °C.

	53		
	δ^{1}H (ppm)	J (Hz)	δ^{13}C(ppm)
H-4	8.80	s	135.2
H-6’	8.21	dd, 8.5, 2.5	128.6
H-2’	7.97	d, 2.5	118.8
H-5’	7.03	d, 8.5	117.8
H-8	6.91	d, 2.0	95.5
H-6	6.72	d, 2.0	103.5
Sugar			
H-1”	5.52	d, 8.0	102.7
H-2”	4.08	10.0, 7.5	68.3
H-4”	3.95	d, 3.5	66.8
H-5”	4.19	dd, 8.5, 3.0	73.9
H-6”A	4.25	dd, 11.0, 9.0	64.1
H-3”	4.81	dd, 10.0, 3.5	76.4
H-6”B	4.10	dd, 11.0, 3.0	64.1
Acyl moiety			
CH_2-α a	2.25	m	34.5

		53	
	$\delta^{1}H$ (ppm)	J (Hz)	$\delta^{13}C$(ppm)
CH_2-β b	1.57	m	25.8
CH_2-α a	2.17	m	34.5
CH_2-β b	1.38	m	25.8
CH_2 (4-7) a,b	1.25	m	29.6
CH_3 a	0.84	t, 7.0	15.1
CH_3 b	0.78	t, 7.5	15.1

It can be concluded that the acylation order follows the proposed acylation order presented in **Table 6.14** regardless of the acyl chain length. Salem *et al*. reported that the same regioselectivity of the acylation reaction did not depend on the acyl chain length.[195]

6.2.3. Determination of Physico-chemical Properties of Novel Acylated Anthocyanins

The physio-chemical properties of novel acylated anthocyanins from the chemical acylation of anthocyanins from *Aronia* skin waste were determined to evaluate these derivatives compared to their precursors, Cy3gal. For this reason, the lipophilicity (Log P), UV-Vis absorbance property, thermostability in lipophilic medium, and DPPH antioxidant activity of novel acylated anthocyanins and Cy3gal were studied.

6.2.3.1. Lipophilicity

The lipophilicity of the acylated derivatives of Cy3gal with trifluoroacetate as counterion was evaluated by the octanol-water partition coefficient (Log P), adopting the methods reported by Zhu *et al*. and Cruz *et al*.[161,169] In general, the higher the log P values indicate, the better the lipophilicity. **Table 6.19** shows that the acylation on hydroxyl groups increases anthocyanin derivative lipophilicity. The calculated Log P is also given for comparison and determined using http://www.vcclab.org/lab/alogps/.

Table 6.19 Log P of Cy3gal and its derivatives.

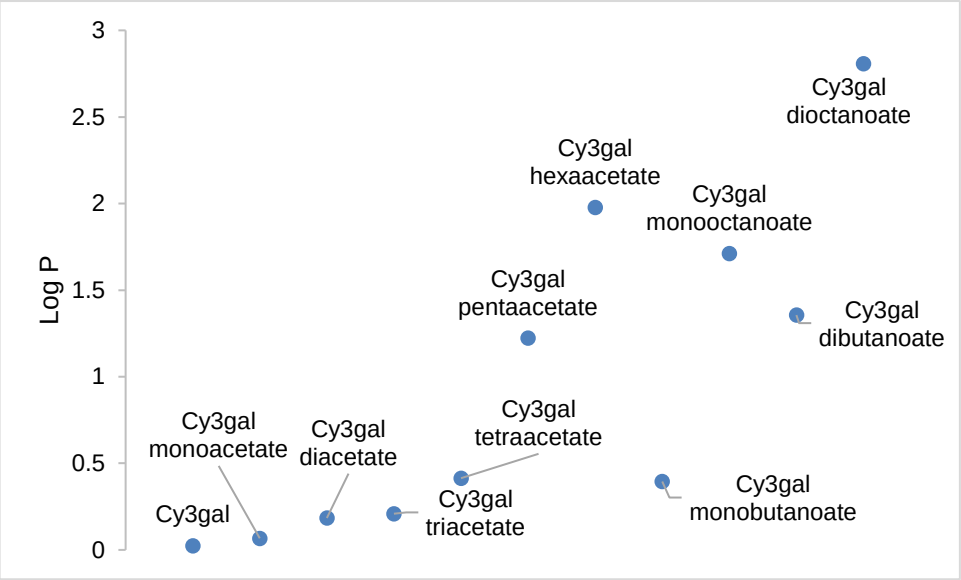

Compound	Experimental	Calculated*
Cy3gal	0.024	-0.06 (± 1.21)
Cy3gal monoacetate	0.067	0.38 (±1.26)
Cy3gal diacetate	0.184	0.86 (±1.43)
Cy3gal triacetate	0.209	1.42 (±1.44)
Cy3gal tetraacetate	0.414	1.93 (±1.38)
Cy3gal pentaacetate	1.223	2.22 (±1.29)
Cy3gal hexaacetate	1.978	2.44 (±1.10)
Cy3gal monobutanoate	0.395	1.18 (±1.40)
Cy3gal dibutanoate	1.356	2.40 (±1.66)
Cy3gal monooctanoate	1.711	3.05 (±1.32)
Cy3gal dioctanoate	2.808	5.95 (±2.02)

*Calculated Log P was determined using http://www.vcclab.org/lab/alogps/

The higher degree of acylation and longer acyl chain moiety increased the lipophilicity of anthocyanins. Log P of Cy3gal monooctanoate (1.711) is higher than Cy3gal monobutanoate (0.395) and Cy3gal monoacetate (0.067). It was also observed that the colour of octanol layer becomes more intense with longer aliphatic chain length of acyl moiety, suggesting it has greater affinity for octanol than water. Cruz *et al*. reported the increased lipophilicity of malvidin-3-*O*-glucoside derivatives due to the increased chain length of acyl moieties.[169] Other research groups also reported similar results.[58,196] The enhanced lipophilic properties of acylated anthocyanins could contribute to penetration into lipid matrices or lipophilic media and expand the

scope of anthocyanins' application as colorants from aqueous to fat-rich food matrices, cosmetics or textiles.[180]

6.2.3.2. UV-Vis Absorbance

The UV-Vis absorbance spectra were recorded to compare the λ_{max} of Cy3gal and its derivatives with trifluoroacetate as the counterion. Because of the low solubility of acylated Cy3gal in water, the samples were recorded in methanol. In general, the UV-Vis absorbance spectra of mono- and diacylated Cy3gal showed a similarity with the UV-Vis absorbance spectra of Cy3gal, and hence maintain the attractive colour of the precursor (**Figure 6.5**).

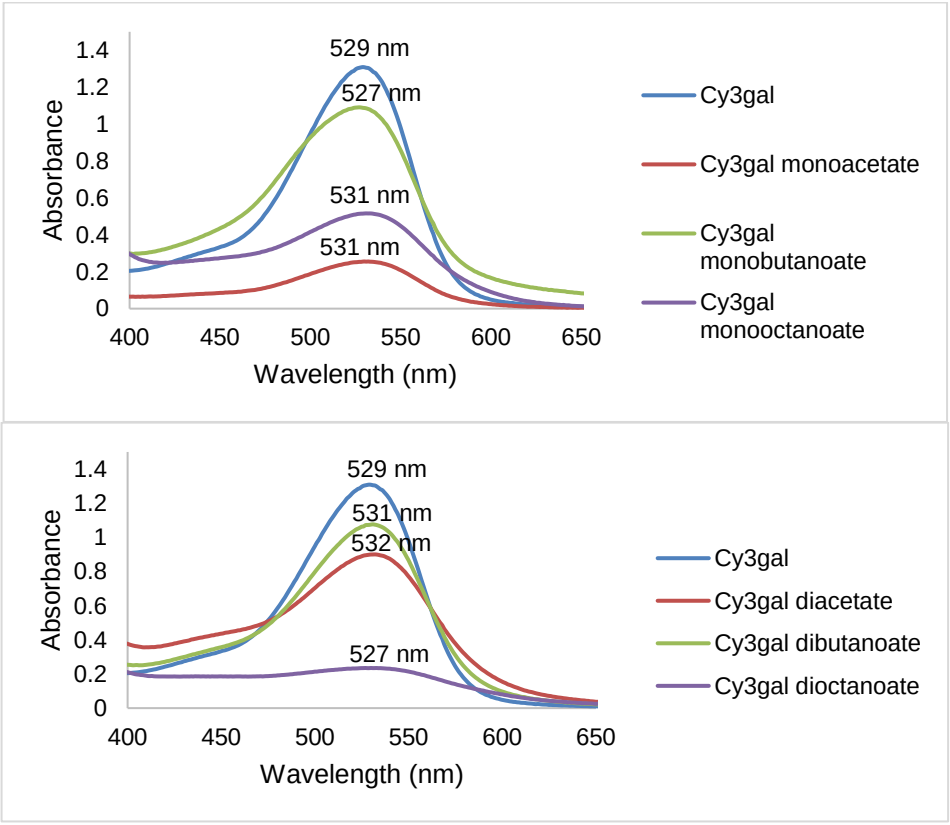

Figure 6.5 UV-Vis spectra of Cy3gal and its derivatives in methanol.

However, other researchers observed a bathochromic shift in the acylated anthocyanins compared to their precursors. Yang *et al*. reported that Cy3gal dodecanoate showed a small bathochromic shift of the absorption maximum (λ_{max}) from 517 nm to 525 nm.[180] The similar results were also reported by Guimarães *et al*., who did the enzymatic acylation of cyanidin-3-*O*-glucoside (Cy3glc) with a different chain length of fatty acids.[197] The maximum wavelength (λ_{max}) of Cy3glc (519 nm) shifted to 520 nm (Cy3glc-butanoate) and 525 nm (Cy3glc-octanoate). Both researchers carried out the experiment in an aqueous medium which is different from the solvent used in this study.

6.2.3.3. Thermostability in Lipophilic Medium

Anthocyanins are labile and start degrading at high temperatures, whereas acylated anthocyanins have been reported to have stability at such condition. To investigate the thermostability of novel acylated anthocyanins produced in this study, a thermostability assay was carried out. The flavylium cationic form of Cy3gal and its derivatives are countered with trifluoroacetate. Most esterified anthocyanin thermostability assays were carried out in acidified aqueous solvent at high temperatures (65-95 ºC).[58,180,196] It should be noted that these conditions could lead to acidic hydrolysis, which could reverse back the acylation products and promote anthocyanin deglycosylation. Additionally, potential applications of acylated anthocyanins are in lipophilic medium. Therefore, the thermostability assay in this study was performed in octanol, as a representative lipophilic medium. As Cy3gal and some acylated Cy3gal do not dissolve completely in octanol, methanol (100 µL) was added to assist the solubilisation of these compounds in octanol. Afterwards, the maximum absorbance in octanol was measured. The result showed that the maximum absorbance of Cy3gal in octanol was observed at 546 nm. Samples of other acylated anthocyanins and blank solution were prepared in the same manner to maintain consistency in the measurement. The solution containing anthocyanin and acylated anthocyanins in separate vials were set up at 25, 40 and 60 ºC for 22 h, and the absorbance was monitored at 546 nm periodically.

The logarithms of Cy3gal [$\ln(A/A_0)$] and its ester derivatives [$\ln(A/A_0)$] were plotted versus time of heat treatment (t) incubated at 25, 40 and 60 °C, respectively, which all showed linear relationships [$\ln(C/C_0) = \ln(A/A_0)$, where A_0 is the initial absorbance at 546 nm, A is the absorbance at 546 nm after heating at selected temperatures, C_0 is the initial concentration of samples, and C is the concentration of samples after heating at selected temperatures. The rate constant (k) and half-life time ($t_{1/2}$) were calculated by the equation as follows: [198]

$$\ln(C/C_0) = -kt \qquad \textbf{Equation 6.1}$$

$$(t_{1/2}) = -\ln(_{1/2})k - 1 \qquad \textbf{Equation 6.2}$$

Overall, the results showed that the degradation processes of Cy3gal and its ester derivatives followed the first-order reaction kinetics and were consistent with the previous studies.[58,180,196] The kinetic parameters are summarised in **Table 6.20**. Diacylated anthocyanins showed higher thermostability than monoacylated anthocyanins regardless of the chain length of acyl groups. The $t_{1/2}$ of Cy3gal derivatives at 60 ºC were higher than its precursor, suggesting that Cy3gal derivatives

have higher stability towards heating than the precursor. This is in agreement with those of previous investigations, acylated anthocyanins showed higher thermostability compared to non-acylated anthocyanins.[58,180,196] The higher thermostability might be due to the acylation on the OH group(s) of the sugar moiety, which allows the intramolecular or intermolecular co-pigmentation and self-association reactions.[95] However, at a lower temperature, 25 ºC, Cy3gal showed better thermostability than Cy3gal monoacetate. It suggested that Cy3gal monoacetate is unsuitable for the application at this temperature, but it is suitable for the application at higher temperatures such as 40 and 60 ºC. The lifetime of Cy3gal dibutanoate (purity 82.2%) showed 5 times higher than Cy3gal.

Table 6.20 Kinetic parameters of thermal degradation at different temperatures.

Compound	k (h^{-1})			$t_{1/2}$ (h)		
	25 °C	40 °C	60 °C	25 °C	40 °C	60 °C
Cy3gal	0.022 (0.939)	0.021 (0.913)	0.026 (0.884)	32.1	33.5	27.1
Cy3gal monoacetate	0.027 (0.965)	0.019 (0.911)	0.022 (0.902)	26.2	37.1	31.4
Cy3gal diacetate	0.008 (0.913)	0.015 (0.939)	0.019 (0.907)	87.7	45.9	35.7
Cy3gal monobutanoate	0.012 (0.953)	0.016 (0.947)	0.024 (0.936)	59.2	43.0	29.1
Cy3gal dibutanoate	0.004 (0.948)	0.006 (0.907)	0.005 (0.923)	182.4	117.5	135.9
Cy3gal monooctanoate	0.017 (0.882)	0.021 (0.865)	0.015 (0.855)	41.0	33.8	31.5
Cy3gal dioctanoate	0.016 (0.893)	0.018 (0.871)	0.015 (0.855)	43.3	39.4	46.8

Cy3gal is cyanidin-3-*O*-galactoside. Numbers in the bracket are the correlation coefficient (R).

6.2.3.4. DPPH Antioxidant Activity (IC_{50})

Anthocyanins from *Aronia* berries have been reported to exhibit antioxidant activity.[43,49,50] The antioxidant activity of anthocyanins is mainly governed by hydroxyl groups in the phenolic groups. Acylation of anthocyanins on the sugar moiety may not change the antioxidant activity but can affect the availability of antioxidant sites. The antioxidant activity of Cy3gal and its derivatives were assessed through DPPH assay and expressed as IC_{50}, adopting the method reported by Guldbrandsen *et al*. (**Table 6.21**).[160] The measurement was carried out in triplicate. The reduction in the

DPPH radical scavenging activity (IC_{50}) by acylation to produce Cy3gal derivatives was likely caused by the increase in the acylated anthocyanin size and structural complexity.[180] Steric hindrance and long-chain acyl moiety(s) might block the phenolic hydroxyl groups of anthocyanins, preventing the acylated anthocyanins from reacting with the active site of DPPH. Lue *et al*. reported decreased acylated rutin's antioxidant activity compared to its precursor due to the decreased inductive electron effect from the acyl moiety, steric hindrance from bond rotation and twisting of acyl chain moiety.[199] The acyl moiety is attached to rutinose. Similar results were also reported in a variety of acylated anthocyanins with long-chain fatty acids.[145,180] Nevertheless, these novel lipophilic antioxidants can be potentially applied in food matrices and cosmetics.

Table 6.21 DPPH antioxidant activity (IC_{50}) of Cy3gal and its derivatives.

Compound	IC_{50} (µg/L)	IC_{50} (µmol/L)
Cy3gal	18.8	3.3×10^{-2}
Cy3gal monoacetate	21.0	3.5×10^{-2}
Cy3gal diacetate	15.6	2.4×10^{-2}
Cy3gal monobutanoate	33.9	5.4×10^{-2}
Cy3gal dibutanoate	56.8	8.1×10^{-2}
Cy3gal monooctanoate	36.4	5.3×10^{-2}
Cy3gal dioctanoate	54.6	6.6×10^{-2}

The counterion is trifluoroacetate (CF_3COO^-) and included in the calculation.

6.3. New Potential Approach for Anthocyanin Modification

Although ester formation was successful and showed that lipophilicity and stability of anthocyanins could be enhanced, we also wished to see if alternative derivatives could be prepared based on quite different chemistry. Anthocyanins can potentially be modified through acetonation of the sugar moiety to form the corresponding *O*-isopropylidene derivatives (acetonides). This reaction involves acetone (or its equivalent) reacting with two hydroxyl groups of the sugar unit in the presence of a catalyst under anhydrous and/or dehydrating reaction conditions.[200] Acetonation reactions have been widely employed in carbohydrate chemistry to protect the hydroxyl groups of carbohydrates[201–204] and to enhance the solubility in organic solvents. Isopropylidene derivatives of anthocyanins can be directly applied in lipophilic medium.

Additionally, these groups are also well established as intermediates in the synthesis of complex saccharides.[202] Another potential application of these isopropylidene derivatives is as intermediates to produce selected acylation of anthocyanins, mostly on the secondary hydroxyls of sugar moieties (**Scheme 6.5**).[201] These partially acylated anthocyanins still bear hydroxyl groups on the sugar moieties, which could be further acylated or reacted with other reagents,[205,206] forming the desired compounds.

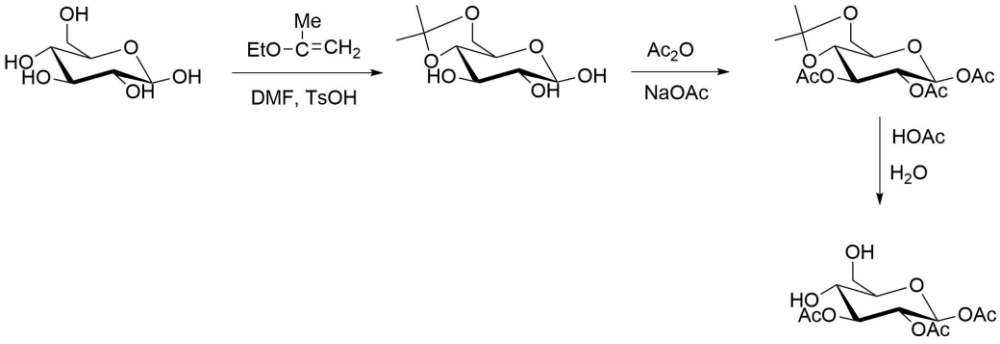

Scheme 6.5 Transformation of D-glucose to β-D-glucopyranose triacetate via isopropylidene intermediate.[201]

Wolfrom *et al*. reported the formation of the pyranoid 4,6-*O*-isopropylidene acetal of D-glucose under kinetic control, which favoured the initial attack at the sugar's primary alcohol.[201] Nishida and Thiem also reported the formation of 4,6-*O*-propylidene derivative from galactose and allyl alcohol with Amberlyst^{R}15.[207] D-Arabinose, which does not have the primary hydroxyl group, gave mainly the pyranoid 3,4-*O*-isopropylidene acetal.[204] As such, an acetonation reaction could be adapted to derivatise the sugar moiety of cyanidin-3-*O*-galactoside (Cy3gal) and cyanidin-3-*O*-arabinoside (Cy3ara) as the major anthocyanins found in *Aronia* skin waste. The proposed reaction mechanism of acetonation is presented in **Scheme 6.6**. It has been reported in literature that anthocyanins can react with acetone to form pyranoanthocyanins for longer periods.[27] The reaction occurs with the phenolic groups, not the sugar moiety. To the best of our knowledge, this reaction has not been carried out on the sugar moiety of anthocyanins.

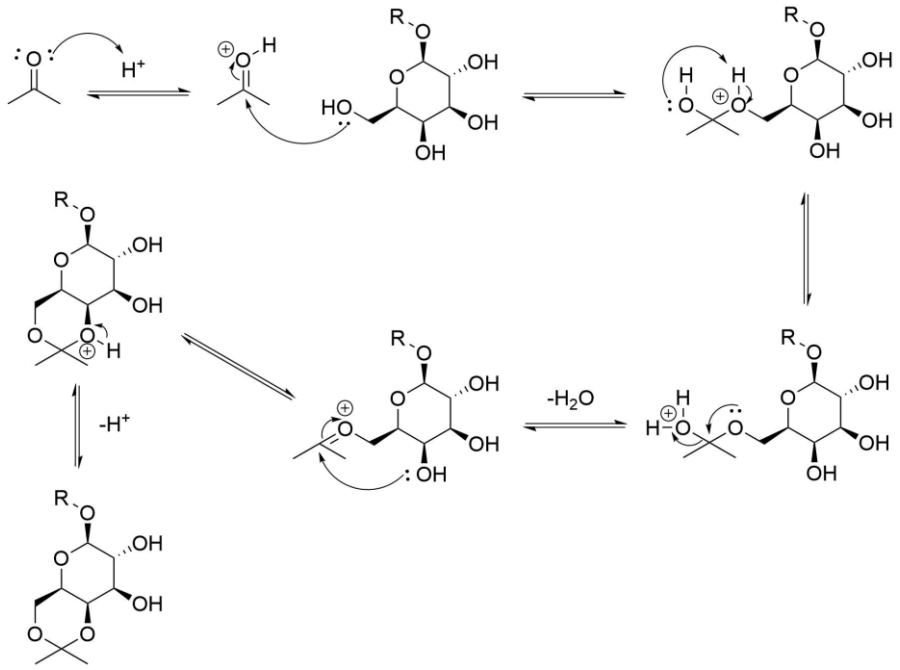

Scheme 6.6 Proposed reaction mechanism of acetonation of anthocyanins. Galactoside structure is used as an example. R = Cyanidin aglycone.

Initial attempts to prepare isopropylidene derivatives of anthocyanins were by condensation of anthocyanins extracted from *Aronia* skin waste (**Scheme 6.7**) with an excess of anhydrous acetone in the presence of TFA as catalyst. The anhydrous acetone served both as the solvent and the reagent. The reaction was performed at 40 °C, and it was complete in 3 hours as determined by LCMS. The presence of acid and water generated from this reaction could hydrolyse the isopropylidene derivatives of anthocyanins back to their precursors as part of the reaction equilibria. To adsorb the water produced during the reaction, the activated SiO_2 was added to a reaction flask. Neutralisation of the reaction mixture was carried out to remove the excess acid by adding solid $NaHCO_3$. In this study, reaction parameters such as concentration of reagents, type and quantity of solvent, reaction time and temperature were not optimised.

An aliquot (100 µL) of the reaction mixture was taken every hour and diluted up to 1 mL with DMSO to monitor the reaction and analysed by HRMS. The HRMS chromatograms (**Figure 6.6**) showed the m/z [M^+] of 489.1391 and 459.1284, calculated [M^+] 489.1391 and 459.1286 (mass error of 0 ppm and 0.4 ppm, respectively), consistent with isopropylidene derivatives of Cy3gal (**55**) and Cy3ara (**56**). However, these acetonides were not detected after attempted isolation and

evaporation, with only the original anthocyanins being observed. As such, H-NMR analysis of the isopropylidene derivatives of anthocyanins was unsuccessful.

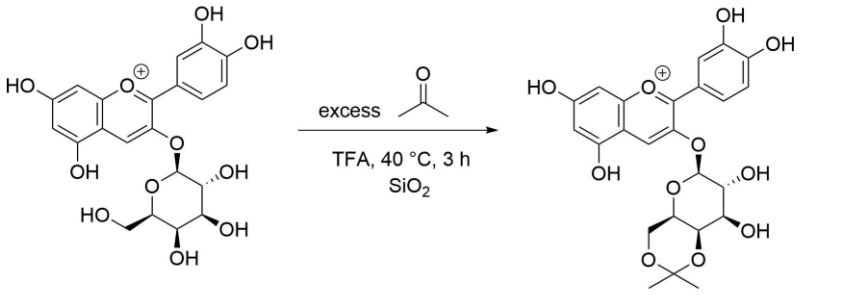

Cyanidin-3-O-galactoside, **27** (m/z 449.14)

Cyanidin-3-O-4,6-O-isopropylidine-galactoside, **55** (m/z 489.14)

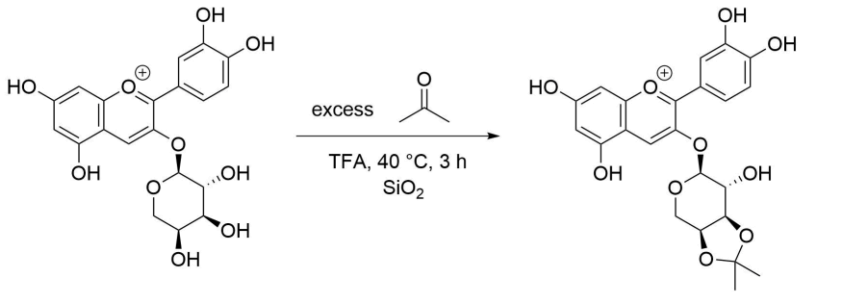

Cyanidin-3-O-arabinoside, **28** (m/z 419.13)

Cyanidin-3-O-4,6-O-isopropylidine-arabinoside, **56** (m/z 459.13)

Scheme 6.7 Proposed acetonation reaction of Cy3gal and Cy3ara as the major anthocyanins in *Aronia* skin waste.

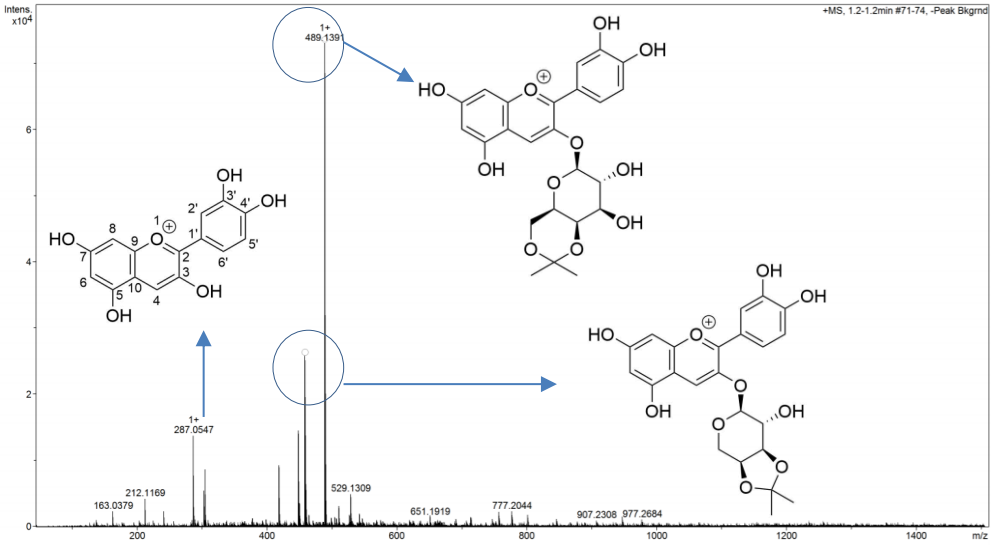

Figure 6.6 HRMS chromatogram of isopropylidene derivatives of Cy3gal (m/z 489.1391) and Cy3ara (m/z 459.1284).

To provide further confirmation of the formation of isopropylidene derivatives of anthocyanins, the reaction was also carried out in deuterated acetone (CD_3COCD_3)

and deuterated TFA (CF_3COOD) in the same manner as described in **Scheme 6.8**. An aliquot was taken and analysed directly by HRMS. Interestingly, the HRMS chromatograms also showed peaks at m/z [M^+] 495.1787 and 465.1676, calculated [M^+] 495.1768 and 465.1662 (mass error of 3.8 ppm and 2.8 ppm respectively), consistent with deuterated isopropylidene derivatives of Cy3gal and Cy3ara (**Scheme 6.9**). This result suggested that acetonide of anthocyanins could be formed through this method (**Figure 6.7**).

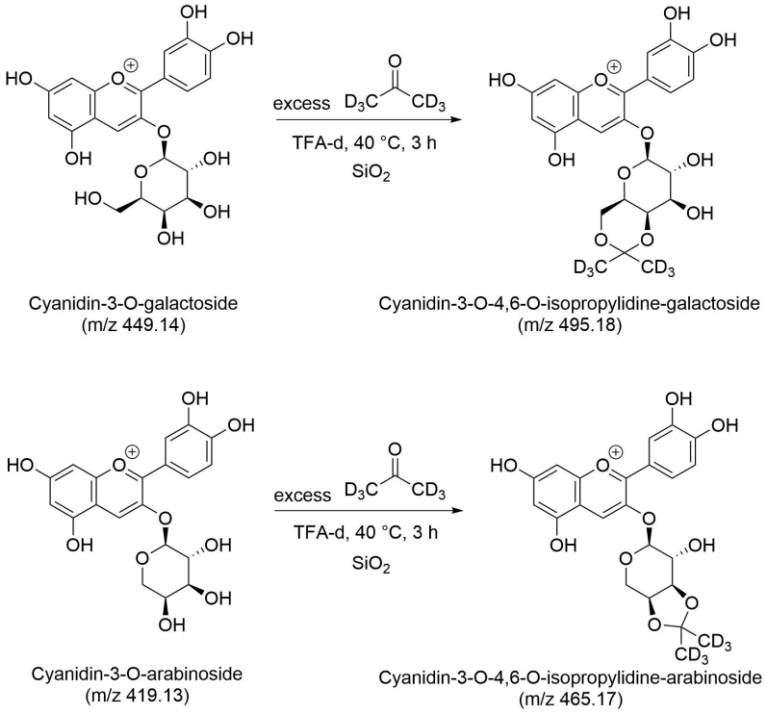

Scheme 6.8 Proposed acetonation reaction of Cy3gal and Cy3ara using deuterated reagents.

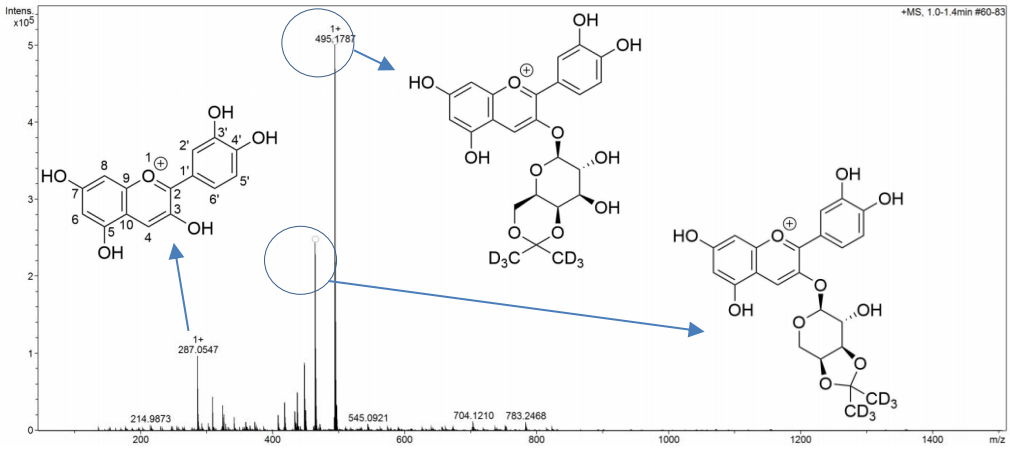

Figure 6.7 HRMS chromatogram of deuterated isopropylidene derivatives of Cy3gal (m/z 495.1787) and Cy3ara (m/z 465.1676).

As this reaction was carried out in the deuterated solvent, the crude reaction mixture can be directly analysed by ^{1}H-NMR spectroscopy. Cy3gal trifluoroacetate isolated

from a semi-preparative HPLC was dissolved in CD_3COCD_3/CF_3COOD, 95:5 and analysed by ^{1}H-NMR spectroscopy to characterise this species as a flavylium cationic form in such solvent system (**Figure 6.8**). Then peak of Cy3gal in such solvent was then compared to peaks of cyanidin-3-*O*-4,6-*O*-isopropylidene-β-galactoside**, 56**, from acetonation reaction of RASE. Interestingly, Cy3gal in acidified acetone-d showed the peaks of isopropylidene derivative of Cy3gal alongside its precursor. Therefore, the characterisation of **56** can be carried out.

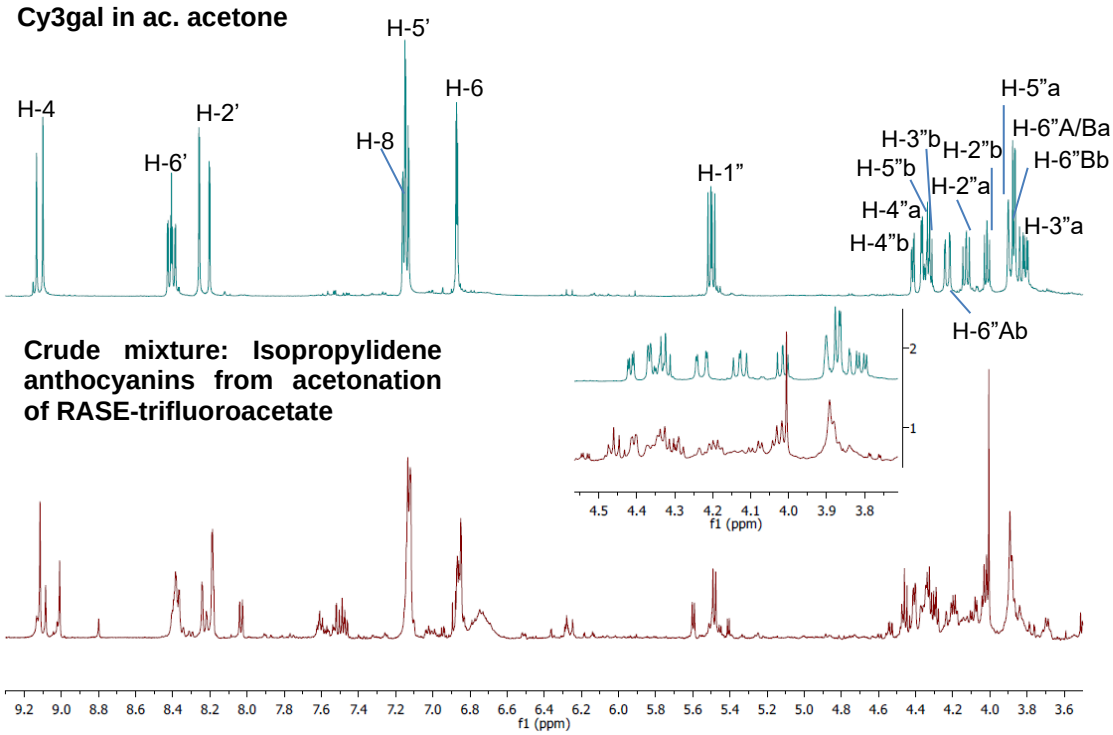

Figure 6.8 ^{1}H-NMR spectra of Cy3gal and crude isopropylidene derivatives of anthocyanins from RASE-trifluoroacetate in CD_3COCD_3/CF_3COOD, 95:5. Protons labelled with a: Cy3gal, b: Cyanidin-3-*O*-4,6-*O*-isopropylidene-β-galactoside, **56**.

It can be observed that chemical shifts of H-6"A/B and H-4" of a sugar moiety changed to downfield. The adjacent protons, H-5" and H-3", also shifted downfield. This finding simplifies the characterisation of isopropylidene derivatives of anthocyanins in a crude mixture. ^{1}H-NMR cannot characterise the methyl groups of acetonide from acetone-d6 as this species is present as CD_3 and not detected in NMR. The chemical characterisation of this derivative and its precursor is summarised in **Table 6.22**. However, the purification steps still did not give satisfactory results. Further research on this study is still required to understand the reaction better.

Table 6.22 ^{1}H (500 MHz) NMR Data for Cy3gal, **27**, and Cyanidin-3-*O*-4,6-*O*-isopropylidene-β-galactoside, **56**, in CD_3COCD_3/CF_3COOD (95:5, v/v) at 25 °C

Aglycone	**Cy3gal (27)**		**56**	
	δ^1H (ppm)	J (Hz)	δ^1H (ppm)	J (Hz)
H-4	9.10	s	9.13	s
H-6'	8.42	dd, 9.0, 2.5	8.40	dd, 8.5, 2.0
H-2'	8.26	d, 2.5	8.20	d, 2.5
H-8	7.16	d, 2.0	7.15	d, 2.5
H-5'	7.15	d, 9.0	7.13	d, 8.5
H-6	6.87	d, 2.0	6.87	d, 2.0
Sugar				
H-1"	5.51	d, 7.5	5.49	d, 7.5
H-2"	4.13	dd, 9.5, 7.5	4.02	dd, 7.0, 6.5
H-3"	3.81	dd, 9.5, 3.5	4.32	t, 6.5
H-4"	4.37	d, 3.0	4.42	dd, 5.5, 2.0
H-5"	(3.86-3.90)	m	4.34	dd, 6.0, 2.5
H-6"A	(3.86-3.90)	m	4.23	dd, 13.0, 2.0
H-6"B	(3.86-3.90)	m	3.85	dd, 13.5, 2.0

6.4. Conclusion and Future Work

6.4.1. Conclusion

This study reports the chemical modification of anthocyanins from *Aronia* skin waste to obtain novel lipophilic colorants. Successful acylation on resveratrol and quercetin was carried out to produce *trans*-3,4',5-triacetyl resveratrol and 3,3',4',5,7-pentaacetyl quercetin. However, the same methods require some modification for the acylation of anthocyanins. The effect of the reaction medium, type of RASE, reaction temperature and reaction time on the anthocyanin distribution and its ester derivatives were investigated. These factors gave significant control over the acylation of anthocyanins, and higher degrees of acylation could be achieved by increasing the acylating agent equivalent, reaction temperature and reaction time, in some cases, with reasonable levels of selectivity.

Cy3gal was the most abundant anthocyanin in RASE and chemically reacted with saturated acylating agents (acetyl chloride, C_2; butanoyl chloride, C_4; and octanoyl chloride, C_8). The first acylation occurred on the primary hydroxyl group in the sugar moiety at the C-6" which is the most reactive hydroxyl group, followed by the secondary hydroxyl groups, 3"-OH, 4"-OH, and 2"-OH. Further acylation could be achieved on the phenolic groups of the aglycone. The first acylation on the aglycone occurred on the 4'-OH, followed by the 7-OH. It is suggested that the further acylation is on the 3'OH due to the steric hindrance and then on the 5-OH. The order of

acylation should also apply to other anthocyanins, especially cyanidin-based anthocyanins. The regioselectivity of the acylation reaction appeared to be independent of the acyl chain length.

Overall, the results indicate that structural modification of anthocyanins could enhance the physio-chemical properties of anthocyanins whilst retaining antioxidant activity. Mono and diacylated anthocyanins could maintain the original colour of their precursor. Additionally, acylated anthocyanins showed higher thermostability at higher temperatures (40 and 60 ºC) than their precursor. Due to their lipophilic properties, acylated derivatives of anthocyanins from *Aronia* skin waste have enhanced potential to be incorporated into lipid-based foods, textiles, cosmetic formulations, and pharmaceutical products than the parent precursor. The results from this study open new potential research areas in the lipophilisation of anthocyanins with great potential.

Alternatively, anthocyanins could be modified through an acetonation reaction. Initial results indicate the potential chemical modification of anthocyanins can be achieved to produce novel lipophilic derivatives through this method. Furthermore, these isopropylidene derivatives of anthocyanins (acetonides) can be applied as intermediates of further reaction to control regioselectivity in acylation reactions.

6.4.2. Future Work

This study has demonstrated the potential of anthocyanins extracted from *Aronia* skin waste and their derivatives as natural and semisynthetic colorants. Most studies in this work were carried out for Cy3gal derivatives as the major anthocyanins found in *Aronia* skin waste. For future work, the acylation reaction could be extended to other anthocyanins found in this material, at least for Cy3ara, which is the second most anthocyanin (*ca*. 30% of total anthocyanins) and does not have primary alcohol on the sugar moiety. It is also interesting to study the acylation reaction of anthocyanins from various sources, which have different type of sugar moieties and anthocyanidin cores. This chemical modification of anthocyanins from various sources could provide wide ranges of novel acylated anthocyanins with exciting physio-chemical properties. Additionally, longer chain acylating agents (C_{12}, C_{16}, C_{18}), presence of double bond in the acylating agents (oleoyl chloride) and aromatic acylating agents

(benzoyl chloride and its derivatives bearing donor or withdrawing electron groups) could be studied to enrich the library of novel acylated anthocyanins.

The production of anthocyanins and their novel lipophilic anthocyanins could be scaled up for their application. The structural transformations of anthocyanins to more lipophilic derivatives have the main advantage of improving the technological application potential in lipophilic systems such as cosmetics, textiles, food colorants and pharmaceuticals. For example, in producing anthocyanin-based lipstick, anthocyanins or novel acylated anthocyanins could be incorporated into cosmetic formulation as colorants by combining with other components. The lipstick formulations are then evaluated and compared to reference samples of commercially available lipsticks and cosmetic colorants. The UV-protection and antiaging activity of these products could also be studied. Another example for the application of these compounds is for dyeing fabrics. The colour and colourfastness of dyed fabrics are evaluated. The application of novel lipophilic compounds in those fields could promote the zero-waste lifestyle.

Chapter 7
Experimental

7.1. General Methods

Nuclear magnetic resonance (NMR) spectra were recorded for ^{1}H at 400 MHz or 500 MHz, and ^{13}C at 101 or 125 MHz on a Bruker AV3HD 400 spectrometer or AV-NEO 500 spectrometer. ^{19}F NMR was performed at 376 MHz on a Bruker AV3HD 400 spectrometer. All NMR datasets were acquired at 298 K unless otherwise stated. Chemical shifts are reported in parts per million (ppm) downfield of tetramethylsilane (TMS, singlet at 0 ppm) for proton resonances. Signals are reported as s (singlet), d (doublet), t (triplet), dd (doublet of doublet) and m (multiplet). Coupling constants are reported in Hertz (Hz). To aid characterisation of polyphenols from *Aronia* skin waste and anthocyanin derivatives, DEPT-135 and two-dimensional nuclear magnetic resonance spectroscopy (2D-NMR) such as Correlation Spectroscopy (COSY), Heteronuclear Single-Quantum Correlation Spectroscopy (HSQC), Heteronuclear Multiple-Bond Correlation spectroscopy (HMBC) and Nuclear Overhauser Effect Spectroscopy (NOESY) pulse sequences were carried out.

HPLC analysis was carried out at 25 ºC using an Eclipse XDB C18 column with 5 µm particle size, 150 x 2.1 mm internal diameter column, which was equipped with a guard column. The analysis was carried out on Agilent 1200 UHPLC binary pump system with online degasser and photo diode-array detection (DAD). Two solvents were used: solvent A: water (HPLC grade, with acid); solvent B: acetonitrile (HPLC grade, with acid). Formic acid (0.1% v/v), phosphoric acid (0.1%) and TFA (0.1 and 0.5%) were added to the solvent A as an additive to find the best separation for anthocyanins. The best separation was obtained by use of 0.5% TFA as an additive in Solvent A hence was used predominantly. A linear gradient programme was applied of 0 minutes 5% B; 0-20 minutes linear increase to 20% B; 20-23 minutes linear increase to 100% B; 23-24 minutes hold at 100% B; 24-25 minutes linear decrease to 5% B; 25-30 minutes hold at 5% B. The flow rate was 1.0 ml/min, and peaks were detected at 254, 285, 325, 350 and 520 nm.

LC-MS analysis was carried out using a Thermo Scientific Ultimate 3000 HPLC system (Thermo Fisher Scientific, Waltham, MA, USA), interfaced with a mass spectrometer equipped with an electrospray-ionisation source operated in the positive mode (Bruker amaZon Speed, Bruker Daltonik GmbH, Billerica, MA, United States). Chromatographic separations were performed using a Kinetex C18 (2.1×50

mm i.d., 2.6 µm particle size; Phenomenex, Torrance, CA, USA) at a column temperature of 40 ℃. The mobile phases were (A) 0.1 % Formic acid in water and (B) 0.1 % Formic acid in acetonitrile. A gradient was used starting at 98 % of A and 2 % of B over 1.2 minutes, ending with 2 % A and 98 % B at a flow rate of 1.3 mL/min. The electrospray ionisation (ESI) parameters for the positive ionisation (PI) mode were as follows: spray voltage: 4000 V; dry gas flow rate: 10 dm^3 min^{-1}; dry gas temperature: 365 °C; capillary: 60 nA; nebulising pressure: 65 psi; nebulising gas: N_2. The positive mode was more sensitive for anthocyanins, whereas neutral polyphenols were more sensitive in the negative mode.

High resolution mass spectra (HRMS) were performed on a Bruker MaXis Impact spectrometer using electron spray ionisation (ESI); m/z values are reported in Daltons to four decimal places. UV/Vis analysis was carried out using either a Jenway 6300 spectrophotometer or an Agilent Cary 100 UV-Vis spectrophotometer. Infrared spectra were recorded on a Bruker Alpha Platinum ATR. Samples were analysed in the solid phase, and absorption maxima (ν_{max}) are given in wavenumbers (cm^{-1}) to the nearest whole wavenumber. Chloride content analysis was carried out by Elemental Microanalysis, Sheffield Analytical and Scientific Services. Melting point determination was carried out on a Reichert hot stage apparatus. The pH of solutions was measured using Hanna instrument pH meters which has been calibrated using Buffer solutions pH 4.01 and 7.01. Solvents were removed under reduced pressure using a Buchi rotary evaporator at 20 mbar, followed by further drying under a high vacuum at 0.5 mmHg.

7.2. Chemical and Materials

Seedless black chokeberry [*A. melanocarpa* (Michx.) Elliott] pomace was provided by GreenField s.c., Warsaw, Poland, and had been dried in a drum dryer at 75 °C for 15 min. All solvents and reagents were purchased from Alfa Aesar (UK), Fisher Chemicals (UK), Merck (UK), SLS (UK) and VWR Chemicals (UK); solvents were high-performance liquid chromatography (HPLC) and analytical grade and were used without further purification. Amberlite XAD-7 resin (Dow Chemical Company, USA) was used as the SPE adsorbent, which is a moderately polar nonionic macro reticular acrylic resin that adsorbs and releases ionic species through hydrophobic and polar interactions. Ultrapure water was prepared using an Elga Purelab, and resistivity was measured at 18.2 MΩ. Knitted polyester for making extraction bags was provided by The School of Design, University of Leeds. Flash silica chromatography was carried out using silica gel (230-400 mesh) supplied by E.M. Merck. Thin-layer

chromatography was performed using Merck aluminium TLC sheets (silica gel 60 F_{254}). Visualisation of the TLC plates was carried out using a UV lamp (245 nm).

7.3. Sequential Batch Extraction – adsorption Method

The initial extraction-purification was carried out using HCl to study the sequential batch extraction-adsorption method for the production of anthocyanins from *Aronia* skin waste. The extraction conditions were modified to obtain the higher extraction yield and anthocyanin content in RASE. Those parameters were varied as follows: extraction temperature (25, 40, 60 and 70 °C), extraction time (3, 6, 24 and 48 h), acid additive (0.1% v/v, HCl and no addition of acid), biomass-solvent ratio (1:8 and 1:16) and biomass-SPE resin ratio (1:1 and 1:2). The results were then compared to find the best extraction parameters in producing the highest yield of anthocyanins from *Aronia* skin waste (**Section 7.3.1** to **Section 7.3.5**). The extraction-purification methods for other acids were carried out following the best method using HCl.

Dried *Aronia* skin waste (31.25 g) was extracted with acidified water (500 mL, 0.1% v/v acid, see **Table 7.1**) at 60 °C for 3 h. Afterwards, the extraction liquor was filtered, cooled down and loaded into an SPE column containing Amberlite XAD-7 (31.25 g DW, pre-soaking).[85,99] Previously, Amberlite XAD-7 was prepared by soaking in deionised water for 1 h at room temperature to remove any salts; the resin quantity was a 1:1 ratio by mass of *Aronia* skin waste. The resin was then applied to the column, washed with ethanol to activate the resin, and finally washed with acidified water to have a similar environment as the extraction liquor.

Table 7.1 Concentration of acid used in the extraction-purification 0.1% v/v

Acid	Concentration (M)	pH
Hydrochloric acid (HCl)	3.3×10^{-2}	2.3
Trifluoroacetic acid (TFA)	1.3×10^{-2}	2.2
Formic acid (FA)	2.6×10^{-2}	2.7
Acetic acid (AA)	1.7×10^{-2}	3.3
Octanoic acid (OA)	6.3×10^{-3}	3.7

The loaded SPE resin was washed with acidified water (500 mL, 0.1% v/v acid) to remove free sugars. The resin was then eluted with ethyl acetate (250 mL) to get the first fraction which contains non-anthocyanin polyphenols. Finally, the resin was eluted with acidified ethanol (250 mL, 0.1% v/v acid) to recover anthocyanins. The ethanol eluates were then evaporated to dryness under reduced pressure on a rotary

evaporator. Afterwards, these residues were further dried under a high vacuum overnight to remove trace solvents, yielding a dark red amorphous solid which could be powdered by grinding. The dried ethanol residues are referred to as Refined *Aronia* Skin Waste Extract (RASE) throughout the thesis. To characterise individual anthocyanins present in RASE, further purification was carried out using semi-preparative HPLC (**Section 7.6**).

The excess of volatile acids such as TFA, FA and AA could be removed from RASE through high vacuum evaporation overnight. However, excess OA is not sufficiently volatile and is quite challenging to remove. As such, it cannot be removed from the acidified ethanolic eluate through the rotary evaporator, so an alternative procedure was developed. After an SPE elution using acidified ethanol (0.1% v/v of OA), the ethanolic solution was evaporated. The remaining liquid RASE, which contained an excess of OA, was added with methanol (30 mL) and then extracted several times with hexane (3 x 30 mL) in a separating funnel. As the highly coloured anthocyanin does not dissolve in a non-polar solvent such as n-hexane (which remained colourless during the extraction process), it remains in methanol fraction while the excess of OA is extracted into the hexane fraction. The methanol fraction was then evaporated to dryness under reduced pressure on a rotary evaporator followed by evaporation under a high vacuum overnight to produce RASE octanoate.

The resulting solids were then weighed to determine the extraction yield. To analyse the polyphenols component in the dried residues, RASE was dissolved in acidified H_2O/C_2H_5OH (9:1, v/v for ethanol residues, and 0.1% v/v HCl was added to bring the sample to a flavylium cationic form) for HPLC and LC-MS analyses. Characterisation of anthocyanins by ^{1}H-NMR and ^{13}C-NMR were conducted in CD_3OD/CF_3COOD (95:5). A stock solution of NMR solvents was prepared as follows: CF_3COOD (0.5 mL) was added into CD_3OD (10 mL). To determine the effect of acids used in the extraction-purification experiment to produce various anthocyanin counterions, RASE produced from these acids and neutral polyphenols were analysed in neutral CD_3OD.

7.3.1. Effect of extraction temperature on the extraction yield

The extraction was conducted at various temperatures (25, 40, 60 and 70 °C) using the same manner described in **Section 7.3**. The extraction yield of RASE from each extraction temperatures is presented in **Table 7.2**.

Table 7.2 The extraction yields of *Aronia* skin waste after SPE and evaporation.

Extraction temperature (°C)	Extraction yield (g)		Extraction yield (mg/g DW)	
	Ethanol wash	Ethyl acetate wash	Ethanol wash	Ethyl acetate wash
25	0.11	0.04	3.39	1.29
40	0.13	0.06	4.28	2.07
60	0.31	0.11	10.04	3.38
70	0.14	0.02	4.54	0.82

7.3.2. Effect of extraction time on the extraction yield

The extraction was conducted at 60 °C for various extraction times (3, 6, 24 and 48 h) using the same manner as already described in **Section 7.3**. The extraction yield of RASE from each extraction time is presented in **Table 7.3**.

Table 7.3 The extraction yields of *Aronia* skin waste after SPE and evaporation.

Extraction time (h)	Extraction yield (g)		Extraction yield (mg/g DW)	
	Ethanol wash	Ethyl acetate wash	Ethanol wash	Ethyl acetate wash
3	0.16	0.04	5.25	1.39
6	0.22	0.04	7.03	1.19
24	0.31	0.11	10.04	3.38
48	0.12	0.03	3.79	1.08

7.3.3. Effect of extraction pH on the extraction yield

The extraction was conducted at 60 °C for 24 h using the same manner as already described in **Section 7.3**. The extraction yield of RASE from each of the extraction pHs was calculated is presented in **Table 7.4**.

Table 7.4 The extraction yields of *Aronia* skin waste after SPE and evaporation.

pH	Extraction yield (g)		Extraction yield (mg/g DW)	
	Ethanol wash	Ethyl acetate wash	Ethanol wash	Ethyl acetate wash
2.4	0.31	0.11	10.04	3.38
5.2*	0.21	0.01	6.81	0.19

*without the addition of HCl

7.3.4. Effect of the biomass-solvent ratio on the extraction yield

The extraction was conducted at 60 °C for 6 h using the same manner as already described in **Section 7.3**. Two different biomass-solvent ratios were carried out. Those were the biomass-solvent ratio of 1:8 (62.5 g of *Aronia* skin waste in 500 mL

of extraction solvent) and 1:16 (31.25 g of *Aronia* skin waste in 500 mL of extraction solvent). The extraction yield of RASE from each biomass-solvent ratio is presented in **Table 7.5**.

Table 7.5 The extraction yields of *Aronia* skin waste after SPE and evaporation.

Biomass-solvent ratio	Extraction yield (g)		Extraction yield (mg/g DW)	
	Ethanol wash	Ethyl acetate wash	Ethanol wash	Ethyl acetate wash
1:8	0.27	0.07	4.27	1.11
1:16	0.22	0.04	7.03	1.19

7.3.5. Effect of the biomass-SPE resin ratio on the extraction yield

The extraction was conducted at 60 °C for 6 h using the same manner as already described in **Section 7.3**. Two different biomass-SPE resin ratios were carried out. Those were biomass-SPE resin ratio of 1:1 (each 31.25 g) and 1:2 (31.25 g of *Aronia* skin wastes and 62.5 g of Amberlite XAD-7). The extraction yield of RASE from each biomass-SPE resin ratio is presented in **Table 7.6**.

Table 7.6 The extraction yields of *Aronia* skin waste after SPE and evaporation.

Biomass-SPE resin ratio	Extraction yield (g)		Extraction yield (mg/g DW)	
	Ethanol wash	Ethyl acetate wash	Ethanol wash	Ethyl acetate wash
1:1	0.22	0.04	7.03	1.19
1:2	0.24	0.04	7.77	1.57

7.4. Integrated Extraction – adsorption Method

The experimental set-up for the integrated extraction-adsorption experiment is presented in **Chapter 2**, **Figure 2.5**.[85,100] The extraction solution was circulated using a peristaltic pump in a closed-loop the 1 L round bottom flask and the packed adsorption column. The experiment was carried out using the optimum conditions obtained from a batch method, namely extraction temperature of 60 °C, extraction time of 3 h, acid additive (0.1% v/v, HCl), the biomass-solvent ratio of 1:16 and biomass-SPE resin ratio of 1:1. This study's extraction parameters were varied as follows: cooling process during sample loading (yes or no) and flow rate of sample loading (0.6, 1.0, 1.3 mL/min). After the end of the integrated extraction-adsorption process, the SPE column elution followed the method described in **Section 7.3**.

7.4.1. Effect of the cooling process during sample loading on the extraction yield

An integrated extraction-adsorption was carried out using the same manner as already described in **Section 7.4**. An ice bath cooler was added to the system between the extractor and an SPE column to maintain the temperature of extraction liquor at ca. 25 °C before loaded into Amberlite XAD-7 resin in the SPE column. The extraction yield of RASE is presented in **Table 7.7**.

Table 7.7 The extraction yields of *Aronia* skin waste after SPE and evaporation.

Cooling		Extraction yield (g)		Extraction yield (mg/g DW)	
		Ethanol wash	Ethyl acetate wash	Ethanol wash	Ethyl acetate wash
3 h	Yes	0.25	0.16	8.07	5.22
	No	0.29	0.04	9.14	1.40
24 h	Yes	0.33	0.06	10.66	1.99
	No	0.62	0.17	19.98	5.48

7.4.2. Effect of flow rate of sample loading on the extraction yield

An integrated extraction-adsorption without cooling was carried out using the same manner as already described in **Section 7.4**. Three different flow rates, namely 0.6, 1.0 and 1.3 mL/s during sample loading into the SPE column was studied. The extraction yield of RASE is presented in **Table 7.8**.

Table 7.8 The extraction yields of *Aronia* skin waste after SPE and evaporation.

Flow rate of sample loading (mL/s)	Extraction yield (g)		Extraction yield (mg/g DW)	
	Ethanol wash	Ethyl acetate wash	Ethanol wash	Ethyl acetate wash
0.6	0.24	0.07	7.80	2.37
1.0	0.29	0.04	9.14	1.40
1.3	0.45	0.13	14.40	4.29

7.5. Determination of UV-Vis Properties

7.5.1. Determination of λ_{max}

RASE (1 mg) was dissolved in either water or methanol to give a concentration of 0.2 g/L. The maximum wavelength in these two solvents was recorded. To measure the maximum wavelength of ester derivatives of resveratrol and quercetin, these compounds (1 mg) were dissolved in DMSO (2 mL, to give a concentration of 0.5

g/L). An aliquot (100 µL, 0.5 g/L) was diluted up to 10 mL. The maximum wavelength of acylated anthocyanins (0.5 mg) was determined in methanol. Agilent Cary 100 UV-Vis spectrophotometer was used to measure absorbances from 200 to 800 nm. To study anthocyanins' absorbance in various pHs, RASE (1 mg) was dissolved in acidified water (0.1% v/v, HCl to give a concentration of 1 g/L). An aliquot (250 µL, 1 g/L) was then diluted up to 10 mL using various buffer solutions. Buffer solutions of 11 different pH values were prepared, as shown in **Table 7.9**. The pH for each buffer solution was measured and adjusted using a HANNA pH instrument.

Table 7.9 Solvent proportions (v/v) of the 11 different buffer solutions applied in the pH region of 1-12.[35,92]

pH	KCl 0.2 M	KHphthalate 0.1 M	KH_2PO_4 0.1 M	NaOAc 0.2 M	$Na_2B_4O_7$ 0.025 M	$NaHCO_3$ 0.05 M	HCl 0.2 M	HCl 0.1 M	AcOH 0.2 M	NaOH 0.1 M	NaOH 0.2 M
1	50						134				
2	50						13				
3		100						44.6			
4.5				43					69		
5		100								45.2	
6			100							11.2	
7			100							58.2	
9					100			9.2			
10						100				21.4	
11						100				45.4	
12	50										12

7.5.2. Determination of Molar Absorptivity of Cy3gal

Cy3gal-trifluoroacetate isolated from semi-preparative HPLC was dissolved in 2 mL of buffer solution pH 1 to make a stock solution with a concentration of 6.5 x 10^{-1} g/L. An exact aliquot of the stock solution was diluted in buffer solution pH 1 to give concentrations of 2.3 x 10^{-6} - 2.3 x 10^{-5} M, Mr Cy3gal trifluoroacetate: 562.41 g/mol. Molar absorptivity of Cy3gal (ε) was calculated using Beer-Lambert law: $A = \varepsilon \times c \times l$; where A = absorbance, ε = molar absorptivity, c = concentration, and l = pathlength (1 cm).[129] Each concentration was then measured its absorbance at 520 nm. Each concentration was then plotted with respective absorbance at 520 nm to give a slope of 16,519 L mol^{-1} cm^{-1}. The slope of the equation determined the molar absorptivity. Cy3gal in buffer solution pH 1 with various concentrations were monitored its absorbance at 520 nm for 4 consecutive days. The solutions were kept in the dark at the refrigerator's temperature (4 ºC) for the next absorption measurement (**Table 7.10**).

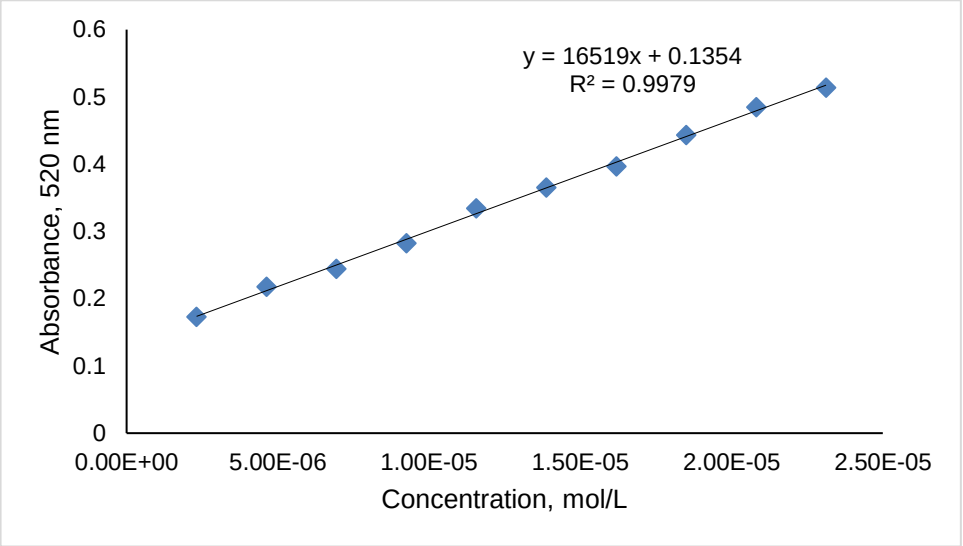

Table 7.10 ε of Cy3gal in Buffer Solution pH 1 for 4 consecutive days

Conc. (M)	Day 0	Day 1	Day 2	Day 3
	A (520 nm)	A (520 nm)	A (520 nm)	A (520 nm)
2.31×10^{-6}	0.1731	0.175	0.1717	0.1809
4.62×10^{-6}	0.2178	0.2194	0.215	0.2231
6.94×10^{-6}	0.2442	0.2454	0.2412	0.2518
9.25×10^{-6}	0.2825	0.2830	0.2790	0.2881
1.16×10^{-5}	0.3343	0.3352	0.3324	0.3405
1.39×10^{-5}	0.365	0.3636	0.3606	0.3701
1.62×10^{-5}	0.3965	0.3972	0.3942	0.4032
1.85×10^{-5}	0.4434	0.4432	0.4407	0.4504
2.08×10^{-5}	0.4846	0.4842	0.4812	0.4929
2.31×10^{-5}	0.5138	0.5136	0.5109	0.5204

7.5.3. Determination of p*K'*$_a$ of Cy3gal

Cy3gal-trifluoroacetate (Mr 562.41 g/mol) isolated from semi-preparative HPLC (3.2 mg) was dissolved in water (90 mL), and the pH of the solution was measured. The aliquot (2 mL) was taken and placed into a cuvette. The pH was brought to acidic by adding concentrated HCl dropwise. With each addition of HCl, the pH was measured, and the aliquot was taken. The solution of each pH was analysed by UV-Vis spectrophotometer. The p*K'*$_a$ calculation followed the method reported in literature.[131,132] The value of p*K'*$_a$ shows the pH where, at thermal equilibrium, half of the flavylium cationic form (**AH**$^+$) has been transformed into its conjugated base (**CB**).[39,131] The absorption band is measured at 511 nm as this is the maximum wavelength for Cy3gal in a flavylium cationic form (**Table 7.11**).

Table 7.11 Absorbance of Cy3gal at various pH (511 nm).

pH	**4.46**	**4.21**	**4.06**	**3.92**	**3.86**	**3.79**	**3.74**	**3.68**	**3.59**	**3.54**
A (511 nm)	0.149	0.208	0.262	0.317	0.361	0.403	0.440	0.485	0.561	0.608
	3.47	**3.41**	**3.24**	**3.15**	**3.06**	**2.96**	**2.9**	**2.85**	**2.77**	**2.72**
	0.657	0.727	0.877	0.951	1.036	1.097	1.122	1.156	1.196	1.220
	2.66	**2.59**	**2.5**	**2.42**	**2.34**	**2.27**	**2.18**	**2.05**	**1.97**	**1.63**
	1.246	1.268	1.300	1.323	1.337	1.349	1.368	1.379	1.392	1.397

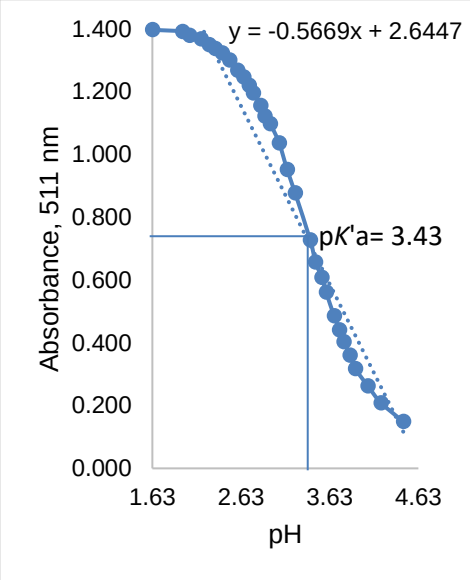

K'_a = [A] + [B] + [C_{trans}] + [C_{cis}]

½ A_0 = ½ x 1.397 = 0.698

y = -0.5669x + 2.6447

x = (2.6447-y)/0.5669

y (½ A_0) = 0.698 → x = (2.6447-0.698)/0.5669

= 3.43 (pK'_a)

7.6. Purification of anthocyanins and acylated anthocyanins by semi-preparative HPLC-DAD

RASE (30 mg) or reaction mixture (200 mg) was redissolved either in H_2O/EtOH 1:1 (0.1% v/v, HCl) or DMSO to give a concentration of 10 g/L. The analysis was carried out at 25 ºC on an Agilent 1200 UHPLC binary pump system with an online degasser and photo diode-array detection (DAD). The samples were loaded on an XBridge Prep C18 column, 10 x 50 mm, 5 µm in 300-900 µL injections and eluted using gradient solvent system. The binary solvent system consisted of solvent A: water (HPLC grade) with an additive (TFA, 0.5%); solvent B: acetonitrile (HPLC grade). A linear gradient programme was applied of 0 minutes 5% B; 0-30 minutes linear increase to 20% B; 30-33 minutes linear increase to 100% B; 33-34 minutes hold at 100% B; 34-35 minutes linear decrease to 5% B; 35-40 minutes hold at 5% B. The flow rate was 5 mL/min. The peaks were monitored at 254, 285, 325, 350 and 520 nm. The fraction collection was carried out at 520 nm. All the collected fractions were freeze-dried and stored in the freezer until further use. The characterisation of

individual anthocyanins is presented in **Section 7.15,** whereas the characterisation of acylated anthocyanins is presented in **Section 7.19**.

7.7. Purification of Anthocyanins by Liquid-liquid Extraction (LLE)

RASE-chloride (60 mg) was redissolved in acidified water (100 mL, 0.1% v/v conc. HCl, to give a concentration of 0.6 g/L). This solution was then partitioned against isopropyl acetate (1 x 100 mL) and ethyl acetate (3 x 100 mL) sequentially.[99] Insoluble solid was removed by filtration. Both organic layers were dried under reduced pressure to give isopropyl acetate extract, which contains DHBA and quercetin (yellow amorphous solid, 9.1 mg) and ethyl acetate extract, which contains DHBA, chlorogenic acid and neochlorogenic acid (red amorphous solid, 9.3 mg), whereas the aqueous layer was freeze-dried to afford a red amorphous solid and stored in the freezer until further use (27.4 mg). The characterisation of these neutral polyphenols can be seen in **Section 7.16**.

7.8. Purification of Anthocyanins by Biotage Flash Purification

RASE (30-300 mg) was dissolved either in H_2O/EtOH 1:1 (0.1% v/v, HCl) or DMSO to give a concentration of 10-100 g/L. The samples were loaded on a RediSep Rf Gold® reversed-phase C18-Aq cartridge (50 g). The analysis was carried out at 25 ºC. The binary solvent system consisted of solvent A: water (HPLC grade) with an additive (TFA, 0.5%); solvent B: acetonitrile (HPLC grade). A linear gradient programme was applied of 1 CV 5% B; 7 CV linear increase to 20% B; 3 CV linear increase to 100% B; 2 CV hold at 100% B. The peaks were monitored at 280 nm. The fraction collection was carried out at 520 nm. All the collected fractions were freeze-dried and stored in the freezer until further use.

7.9. Total monomeric anthocyanin content (TMAC) Assay

TMAC experiments were conducted according to the pH-differential method.[92] The basic concept of determining anthocyanins' content in the material is by measuring the change in absorbance at two different pH values (pH 1 and 4.5). Monomeric anthocyanins undergo reversible structural transformations with a pH change (coloured oxonium form at pH 1 and colourless hemiketal form at pH 4.5). Then, the

difference in absorbance at $\lambda_{vis\text{-}max}$ (ca. 520 nm) of the coloured compound is proportional to the concentration of the coloured compound. Absorbance at 700 nm was carried out to correct for haze RASE (1 mg) was dissolved separately in buffer solution pH 1 and pH 4.5. Buffer solutions were made following the method presented in **Table 7.9**. The absorbance at 520 nm and 700 nm at each pH were recorded. Results are expressed as cyanidin-3-glucoside equivalents (**Table 7.12**-**Table 7.19**) using an equation as follows:

$$\text{Anthocyanin content } \left(\frac{mg}{L}\right) = \frac{A \times MW \times DF \times 10^3}{\varepsilon \times l} \qquad \textbf{Equation 7.1}$$

Where A (absorbance) = $(A_{520nm}\text{-}A_{700nm})_{pH\ 1} - (A_{520m}\text{-}A_{700nm})_{pH\ 4.5}$; MW (molecular weight) = 484.7 g/mol for cyanidin-3-*O*-glucoside with chloride as counterion; MW for other counterions depend on the type of counterions; DF = dilution factor; l = pathlength in cm; ε = 26,900 molar extinction coefficient, in L x mol^{-1} x cm^{-1}, for cyanidin-3-*O*-glucoside as reported in literature and 10^3 = factor for conversion from g to mg.

Table 7.12 TMAC of RASE obtained from the effect of extraction temperature on the anthocyanin content experiments

Temp. (°C)	Conc. (mg/mL)	pH 1		pH 4.5		pH 1	pH 4.5	A	Anthocyanin content (mg/mL)	% Content (w/w)
		$A_{520\ nm}$	$A_{700\ nm}$	$A_{520\ nm}$	$A_{700\ nm}$	A_{520nm}-A_{700nm}	A_{520nm}-A_{700nm}			
25	1.00	0.133	0.005	0.017	0.009	0.128	0.008	0.12	0.22	21.6
	1.00	0.135	0.006	0.017	0.009	0.129	0.008	0.121	0.22	21.8
	1.00	0.137	0.007	0.017	0.009	0.13	0.008	0.122	0.22	22.0
40	1.10	0.328	0.006	0.042	0.013	0.322	0.029	0.293	0.26	24.0
	1.10	0.328	0.006	0.042	0.014	0.322	0.028	0.294	0.26	24.1
	1.10	0.328	0.005	0.042	0.013	0.323	0.029	0.294	0.26	24.1
60	1.00	0.062	0.004	0.004	0.002	0.058	0.002	0.056	0.10	10.1
	1.00	0.06	0.002	0.004	0.002	0.058	0.002	0.056	0.10	10.1
	1.00	0.062	0.003	0.004	0.003	0.059	0.001	0.058	0.10	10.5
70	1.00	0.009	0.003	0.005	0.004	0.006	0.001	0.005	0.01	0.9
	1.00	0.008	0.003	0.004	0.004	0.005	0.000	0.005	0.01	0.9
	1.00	0.01	0.004	0.006	0.004	0.006	0.002	0.004	0.01	0.7

Table 7.13 TMAC of RASE obtained from the effect of extraction time on the anthocyanin content experiments

Time (h)	Conc. (mg/mL)	pH 1		pH 4.5		pH 1	pH 4.5	A	Anthocyanin content (mg/mL)	% Content (w/w)
		$A_{520\ nm}$	$A_{700\ nm}$	$A_{520\ nm}$	$A_{700\ nm}$	A_{520nm}-A_{700nm}	A_{520nm}-A_{700nm}			
3	1.00	0.125	0.004	0.022	0.01	0.121	0.012	0.109	0.20	19.6
	1.00	0.126	0.004	0.021	0.01	0.122	0.011	0.111	0.20	20.0
	1.00	0.127	0.004	0.023	0.011	0.123	0.012	0.111	0.20	20.0

Time (h)	Conc. (mg/mL)	pH 1		pH 4.5		pH 1	pH 4.5	A	Anthocyanin content (mg/mL)	% Content (w/w)
		$A_{520\ nm}$	$A_{700\ nm}$	$A_{520\ nm}$	$A_{700\ nm}$	A_{520nm}-A_{700nm}	A_{520nm}-A_{700nm}			
6	1.00	0.113	0.005	0.019	0.009	0.108	0.01	0.098	0.18	17.7
	1.00	0.113	0.004	0.02	0.009	0.109	0.011	0.098	0.18	17.7
	1.00	0.114	0.004	0.018	0.008	0.110	0.010	0.100	0.18	18.0
24	1.00	0.062	0.004	0.004	0.002	0.058	0.002	0.056	0.10	10.1
	1.00	0.06	0.002	0.004	0.002	0.058	0.002	0.056	0.10	10.1
	1.00	0.062	0.003	0.004	0.003	0.059	0.001	0.058	0.10	10.5
48	1.00	0.08	0.011	0.024	0.006	0.069	0.018	0.051	0.09	9.2
	1.00	0.08	0.01	0.026	0.007	0.07	0.019	0.051	0.09	9.2
	1.00	0.079	0.01	0.023	0.023	0.069	0.000	0.069	0.12	12.4

Table 7.14 TMAC of RASE obtained from the effect of pH on the anthocyanin content experiments

pH	Conc. (mg/mL)	pH 1		pH 4.5		pH 1	pH 4.5	A	Anthocyanin content (mg/mL)	% Content (w/w)
		$A_{520\ nm}$	$A_{700\ nm}$	$A_{520\ nm}$	$A_{700\ nm}$	A_{520nm}-A_{700nm}	A_{520nm}-A_{700nm}			
2.5	1	0.062	0.004	0.004	0.002	0.058	0.002	0.056	0.10	10.1
	1	0.06	0.002	0.004	0.002	0.058	0.002	0.056	0.10	10.1
	1	0.062	0.003	0.004	0.003	0.059	0.001	0.058	0.10	10.5
5.2	1	0.097	0.009	0.028	0.01	0.088	0.018	0.07	0.13	12.6
	1	0.097	0.008	0.028	0.01	0.089	0.018	0.071	0.13	12.8
	1	0.097	0.008	0.027	0.01	0.089	0.017	0.072	0.13	13.0

Table 7.15 TMAC of RASE obtained from the effect of biomass-solvent ratio on the anthocyanin content experiments

Ratio	Conc. (mg/mL)	pH 1		pH 4.5		pH 1	pH 4.5	A	Anthocyanin content (mg/mL)	% Content (w/w)
		$A_{520\ nm}$	$A_{700\ nm}$	$A_{520\ nm}$	$A_{700\ nm}$	A_{520nm}-A_{700nm}	A_{520nm}-A_{700nm}			
1:8	1.00	0.118	0.011	0.034	0.012	0.107	0.022	0.085	0.15	15.3
	1.00	0.118	0.012	0.033	0.013	0.106	0.020	0.086	0.16	15.5
	1.00	0.118	0.011	0.033	0.013	0.107	0.020	0.087	0.16	15.7
1:16	1.00	0.113	0.005	0.019	0.009	0.108	0.010	0.098	0.18	17.7
	1.00	0.113	0.004	0.020	0.009	0.109	0.011	0.098	0.18	17.7
	1.00	0.114	0.004	0.018	0.008	0.110	0.010	0.100	0.18	18.0

Table 7.16 TMAC of RASE obtained from the effect of biomass-SPE resin ratio on the anthocyanin content experiments

Ratio	Conc. (mg/mL)	pH 1		pH 4.5		pH 1	pH 4.5	A	Anthocyanin content (mg/mL)	% Content (w/w)
		$A_{520\ nm}$	$A_{700\ nm}$	$A_{520\ nm}$	$A_{700\ nm}$	A_{520nm}-A_{700nm}	A_{520nm}-A_{700nm}			
1:1	1.00	0.113	0.005	0.019	0.009	0.108	0.01	0.098	0.18	17.7
	1.00	0.113	0.004	0.02	0.009	0.109	0.011	0.098	0.18	17.7
	1.00	0.114	0.004	0.018	0.008	0.11	0.01	0.1	0.18	18.0
1:2	1.00	0.123	0.001	0.022	0.004	0.122	0.018	0.104	0.19	18.7
	1.00	0.124	0.001	0.021	0.003	0.123	0.018	0.105	0.19	18.9
	1.00	0.123	0.001	0.022	0.003	0.122	0.019	0.103	0.19	18.6

Table 7.17 TMAC of RASE obtained from the effect of a cooling process during sample loading on the anthocyanin content experiments

	Conc. (mg/mL)	pH 1		pH 4.5		pH 1	pH 4.5	A	Anthocyanin content (mg/mL)	% Content (w/w)
		$A_{520\ nm}$	$A_{700\ nm}$	$A_{520\ nm}$	$A_{700\ nm}$	A_{520nm}-A_{700nm}	A_{520nm}-A_{700nm}			
Without cooling	1.05	0.143	0.003	0.032	0.006	0.14	0.026	0.114	0.21	19.6
60 °C, 3h	1.05	0.143	0.003	0.032	0.006	0.14	0.026	0.114	0.21	19.6
	1.05	0.144	0.003	0.032	0.007	0.141	0.025	0.116	0.21	19.9
with cooling	1.10	0.156	0.005	0.032	0.007	0.151	0.025	0.126	0.23	20.6
60 °C, 3h	1.10	0.156	0.005	0.032	0.008	0.151	0.024	0.127	0.23	20.8
	1.10	0.158	0.006	0.031	0.008	0.152	0.023	0.129	0.23	21.1
Without cooling	1.15	0.065	0.013	0.027	0.013	0.052	0.014	0.038	0.07	6.0
60 °C, 24h	1.15	0.064	0.012	0.027	0.012	0.052	0.015	0.037	0.07	5.8
	1.15	0.065	0.012	0.025	0.013	0.053	0.012	0.041	0.07	6.4
with cooling	1.05	0.062	-0.002	0.009	-0.002	0.064	0.011	0.053	0.10	9.1
60 °C, 24h	1.05	0.061	-0.003	0.008	-0.004	0.064	0.012	0.052	0.09	8.9
	1.05	0.061	-0.004	0.009	-0.002	0.065	0.011	0.054	0.10	9.3

Table 7.18 TMAC of RASE obtained from the effect of sample loading flow rate on the anthocyanin content experiments

Flow rate (mL/s)	Conc. (mg/mL)	pH 1		pH 4.5		pH 1	pH 4.5	A	Anthocyanin content (mg/mL)	% Content (w/w)
		$A_{520\ nm}$	$A_{700\ nm}$	$A_{520\ nm}$	$A_{700\ nm}$	A_{520nm}-A_{700nm}	A_{520nm}-A_{700nm}			
0.6	1.10	0.129	0.002	0.02	-0.005	0.127	0.025	0.102	0.18	16.7
	1.10	0.129	0.002	0.02	-0.006	0.127	0.026	0.101	0.18	16.5
	1.10	0.123	-0.007	0.02	-0.005	0.13	0.025	0.105	0.19	17.2
1	1.05	0.143	0.003	0.032	0.006	0.14	0.026	0.114	0.21	19.6
	1.05	0.143	0.003	0.032	0.006	0.14	0.026	0.114	0.21	19.6
	1.05	0.144	0.003	0.032	0.007	0.141	0.025	0.116	0.21	19.9

1.3	1.10	0.235	0.011	0.051	0.017	0.224	0.034	0.19	0.17	15.6
	1.10	0.235	0.009	0.052	0.018	0.226	0.034	0.192	0.17	15.7
	1.10	0.236	0.011	0.051	0.019	0.225	0.032	0.193	0.17	15.8

Table 7.19 Comparison of Batch and Integrated method

	Conc. (mg/mL)	**pH 1**		**pH 4.5**		**pH 1**	**pH 4.5**	**A**	**Anthocyanin content (mg/mL)**	**% Content (w/w)**
		$A_{520\ nm}$	**$A_{700\ nm}$**	**$A_{520\ nm}$**	**$A_{700\ nm}$**	**A_{520nm}-A_{700nm}**	**A_{520nm}-A_{700nm}**			
Batch	1.00	0.125	0.004	0.022	0.01	0.121	0.012	0.109	0.20	19.6
	1.00	0.126	0.004	0.021	0.01	0.122	0.011	0.111	0.20	20.0
	1.00	0.127	0.004	0.023	0.011	0.123	0.012	0.111	0.20	20.0
Integrated	1.15	0.231	0.023	0.054	0.025	0.208	0.029	0.179	0.32	28.1
	1.15	0.233	0.023	0.053	0.026	0.210	0.027	0.183	0.33	28.7
	1.15	0.232	0.024	0.053	0.026	0.208	0.027	0.181	0.33	28.4

Table 7.20 Comparison of Extraction-Purification in A Batch Method with Various Acids

Acid	**Conc. (mg/mL)**	**pH 1**		**pH 4.5**		**pH 1**	**pH 4.5**	**A**	**Anthocyanin content (mg/ml)**	**% Content (w/w)**
		$A_{520\ nm}$	**$A_{700\ nm}$**	**$A_{520\ nm}$**	**$A_{700\ nm}$**	**A_{520nm}-A_{700nm}**	**A_{520nm}-A_{700nm}**			
HCl	0.85	0.131	0.001	0.029	0.002	0.130	0.027	0.103	0.17	20.2
	0.85	0.131	0.001	0.027	0.001	0.130	0.026	0.104	0.17	20.4
	0.85	0.132	0.002	0.029	0.002	0.130	0.027	0.103	0.17	20.2
TFA	1.20	0.315	0.002	0.079	0.008	0.313	0.071	0.242	0.40	33.7
	1.20	0.315	0.002	0.079	0.008	0.313	0.071	0.242	0.40	33.7
	1.20	0.315	0.002	0.079	0.008	0.313	0.071	0.242	0.40	33.7

Acid	Conc. (mg/mL)	pH 1		pH 4.5		pH 1	pH 4.5	A	Anthocyanin content (mg/ml)	% Content (w/w)
		$A_{520\ nm}$	$A_{700\ nm}$	$A_{520\ nm}$	$A_{700\ nm}$	A_{520nm}-A_{700nm}	A_{520nm}-A_{700nm}			
FA	1.60	0.304	0.002	0.08	0.006	0.302	0.074	0.228	0.38	23.8
	1.60	0.304	0.002	0.08	0.007	0.302	0.073	0.229	0.38	23.9
	1.60	0.304	0.003	0.08	0.006	0.301	0.074	0.227	0.38	23.7
AA	1.40	0.272	0.001	0.066	0.004	0.271	0.062	0.209	0.35	24.9
	1.40	0.273	0.001	0.066	0.004	0.272	0.062	0.210	0.35	25.0
	1.40	0.272	0.001	0.066	0.005	0.271	0.061	0.210	0.35	25.0
OA	1.30	0.197	0.003	0.051	0.005	0.194	0.046	0.148	0.25	19.0
	1.30	0.197	0.003	0.051	0.005	0.194	0.046	0.148	0.25	19.0
	1.30	0.196	0.003	0.053	0.005	0.193	0.048	0.145	0.24	18.6

*Mr 449.2 g/mol excluding the counterions. ε = 26,900 L/mol.cm

Table 7.21 Comparison of Extraction-Purification in A Batch Method with Various Acids

Acid	Conc. (mg/mL)	pH 1		pH 4.5		pH 1	pH 4.5	A	Anthocyanin content (mg/ml)	% Content (w/w)
		$A_{520\ nm}$	$A_{700\ nm}$	$A_{520\ nm}$	$A_{700\ nm}$	A_{520nm}-A_{700nm}	A_{520nm}-A_{700nm}			
HCl	0.85	0.131	0.001	0.029	0.002	0.130	0.027	0.103	0.30	35.6
	0.85	0.131	0.001	0.027	0.001	0.130	0.026	0.104	0.31	35.9
	0.85	0.132	0.002	0.029	0.002	0.130	0.027	0.103	0.30	35.6
TFA	1.20	0.315	0.002	0.079	0.008	0.313	0.071	0.242	0.82	68.7
	1.20	0.315	0.002	0.079	0.008	0.313	0.071	0.242	0.82	68.7
	1.20	0.315	0.002	0.079	0.008	0.313	0.071	0.242	0.82	68.7

Acid	Conc. (mg/mL)	pH 1		pH 4.5		pH 1	pH 4.5	A	Anthocyanin content (mg/ml)	% Content (w/w)
		$A_{520\ nm}$	$A_{700\ nm}$	$A_{520\ nm}$	$A_{700\ nm}$	A_{520nm}-A_{700nm}	A_{520nm}-A_{700nm}			
FA	1.60	0.304	0.002	0.08	0.006	0.302	0.074	0.228	0.68	42.7
	1.60	0.304	0.002	0.08	0.007	0.302	0.073	0.229	0.69	42.8
	1.60	0.304	0.003	0.08	0.006	0.301	0.074	0.227	0.68	42.5
AA	1.40	0.272	0.001	0.066	0.004	0.271	0.062	0.209	0.64	45.9
	1.40	0.273	0.001	0.066	0.004	0.272	0.062	0.210	0.65	46.2
	1.40	0.272	0.001	0.066	0.005	0.271	0.061	0.210	0.65	46.2
OA	1.30	0.197	0.003	0.051	0.005	0.194	0.046	0.148	0.53	40.9
	1.30	0.197	0.003	0.051	0.005	0.194	0.046	0.148	0.53	40.9
	1.30	0.196	0.003	0.053	0.005	0.193	0.048	0.145	0.52	40.1

*Including the molecular mass of respective counterions. Mr $Cy3glc^{+}.Cl^{-}$, 484.8 g/mol, $Cy3glc^{+}.CF_3COO^{-}$, 562.2 g/mol, Mr $Cy3glc^{+}.HCOO^{-}$, 494.4 g/mol, Mr $Cy3glc^{+}.CH_3COO^{-}$, 508.4 g/mol, Mr $Cy3glc^{+}.CH_3(CH_2)_6COO^{-}$, 593.4 g/mol. ε = 26,900 L/mol.cm from literature. This TMAC was used to calculate the yield of anthocyanins.

7.10. Total Phenolic Content (TPC) Assay

The TPC of RASE was measured colourimetrically using the Folin–Ciocalteu (F-C) method.[159] Gallic acid (10 mg) was dissolved in a 1:1 water and ethanol mixture (5 mL) to produce a 2 g/L solution. This solution was further diluted with the same solvent to make solutions at 1000, 500, 250, 125, and 62.5 mg/L. RASE (1 mg) was dissolved in a 1:1 water and ethanol mixture (2mL) to produce a 500 mg/L solution. Then the aliquot (100 µL) of each solution was transferred into a cuvette and then mixed thoroughly with 100 µL of F-C reagent (2N). After 5 min, 2.0 ml of sodium carbonate (2M) was added and mixed thoroughly. The mixtures were then allowed to stand for 30 min in the dark for colour development. The absorbance was measured at 765 nm against the blank, containing solvent (water/ethanol, 1:1), F-C solution, and Na_2CO_3 solution in a single beam UV–Vis spectrophotometer. The TPC values were expressed in mg gallic acid equivalent (GAE)/g on a dried RASE basis.

Table 7.22 Gallic acid standard.

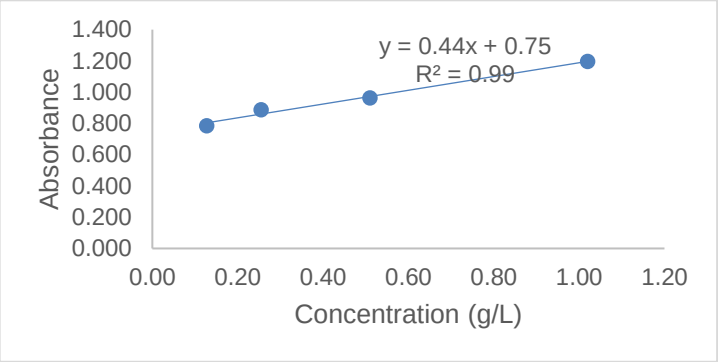

Conc. (g/L)	Absorbance			Absorbance Average
	1	2	3	
1.02	1.203	1.198	1.190	1.197
0.51	0.971	0.961	0.957	0.963
0.26	0.895	0.878	0.890	0.888
0.13	0.786	0.792	0.779	0.786

Table 7.23 TPC of RASE with different counterions

RASE	C (g/L)	Absorbance			Average	x (g/L GAE)	TPC (mg/g GAE)
		1	2	3			
Chloride	0.50	0.884	0.888	0.886	0.886	0.3091	618.2
Trifluoroacetate	0.50	0.878	0.870	0.87	0.873	0.279	557.6
Formate	0.95	0.870	0.854	0.877	0.867	0.2659	279.9
Acetate	0.75	0.883	0.883	0.858	0.875	0.283	377.8
Octanoate	0.60	0.864	0.870	0.871	0.868	0.269	448.2

7.11. Lipophilicity (Log P) Assay

The lipophilicity of RASE and the acylated derivatives was evaluated by determining the octanol/water partition coefficient (Log P).[161,169] Briefly, acidified water (2% HCl) and n-octanol were mutually saturated with each other (1:1, v/v) for 24 h. The samples were initially dissolved in methanol (100 µL), and then n-octanol (5 mL) saturated with acidified water was added, and the absorbance (A_0) at 520 nm was determined. Afterwards, 5 mL of acidified water (2% HCl) saturated with n-octanol was added, and the mixtures were vortex shaken for 1 min and allowed to stand for 24 h for separation. Absorbance (A_x) of n-octanol in the upper layer was measured at 520 nm. The octanol/water partition coefficient was calculated using the equation as follows:

$$\text{Log P} = \text{Log}\,[A_x/(A_0 - A_x)] \qquad \textbf{Equation 7.2}$$

Table 7.24 Log P of RASE with different counterions

RASE-counterion	A_0			Average	A_x			Average	A_0-A_x	$A_0/(A_0-A_x)$	Log $A_0/(A_0-A_x)$
	1	2	3		1	2	3				
Formate	1.058	1.049	1.061	1.056	0.100	0.099	0.107	0.102	0.954	1.107	0.044
Acetate	1.023	1.025	0.984	1.011	0.107	0.107	0.104	0.106	0.905	1.117	0.048
Octanoate	1.123	1.125	1.094	1.114	0.147	0.135	0.138	0.140	0.974	1.144	0.058
Trifluoroacetate	1.584	1.574	1.560	1.573	0.227	0.238	0.223	0.229	1.343	1.171	0.068
Chloride	0.998	0.998	1.000	0.999	0.230	0.221	0.246	0.232	0.766	1.303	0.115

Table 7.25 Log P of Cy3gal and its ester derivatives

Compound	A_0			Average	A_x			Average	A_0-A_x	$A_0/(A_0-A_x)$	Log $A_0/(A_0-A_x)$
	1	2	3		1	2	3				
Cy3gal	1.789	1.791	1.797	1.792	0.094	0.096	0.095	0.095	1.697	1.06	0.024
Cy3gal monoacetate	1.548	1.558	1.556	1.554	0.221	0.222	0.222	0.222	1.332	1.17	0.067
Cy3gal diacetate	1.724	1.725	1.634	1.694	0.587	0.587	0.583	0.586	1.109	1.53	0.184
Cy3gal triacetate	1.045	1.043	1.043	1.044	0.396	0.397	0.401	0.398	0.646	1.62	0.209
Cy3gal tetraacetate	1.179	1.175	1.177	1.177	0.729	0.717	0.723	0.723	0.454	2.59	0.414
Cy3gal pentaacetate	0.293	0.298	0.294	0.295	0.276	0.280	0.276	0.277	0.018	16.70	1.223
Cy3gal hexaacetate	0.030	0.032	0.033	0.032	0.030	0.032	0.032	0.031	0.000	95	1.978
Cy3gal monobutanoate	1.215	1.238	1.196	1.216	0.731	0.725	0.722	0.726	0.490	2.48	0.395
Cy3gal dibutanoate	1.959	1.888	1.914	1.920	1.808	1.824	1.875	1.836	0.085	22.68	1.356
Cy3gal monooctanoate	0.651	0.651	0.651	0.651	0.642	0.640	0.633	0.638	0.013	51.39	1.711
Cy3gal dioctanoate	0.427	0.43	0.427	0.428	0.422	0.431	0.429	0.427	0.001	642	2.808

7.12. Radical Scavenging Activity (RScA) Assay

The antioxidant activity was determined using 2,2-diphenyl-1-picrylhyrazyl (DPPH) radical scavenging capacity assay, following a protocol described by Guldbrandsen *et al*.[160] A solution of DPPH (16.5 mg in 300 mL ethanol) was prepared first. Afterwards, the solutions of samples in methanol, in a concentration range from 0.6 to 40 mg/L were prepared. The experiments were carried out in triplicate, the absorbance of four different solutions was measured at 517 nm after incubation for 30 min in the dark, and the activity was calculated using the equation as follows:

$$\%RScA = \{[(A-B)-(C-D)]/(A-B)\} \times 100 \qquad \textbf{Equation 7.3}$$

where A is a mixture of 1.0 mL of DPPH solution and 1.0 mL of methanol (blank without sample nor DPPH), B is a mixture of 1.0 mL of ethanol and 1.0 mL of methanol, C is a mixture of 1.0 mL of DPPH solution and 1.0 mL of test compound solution, and D is a mixture of 1.0 mL of ethanol and 1.0 mL of test compound solution (blank without DPPH).

Table 7.26 %RScA of RASE with different counterions

		1	2	3	Average		1	2	3	Average
	A	0.678	0.671	0.705	0.685	**A***	0.702	0.705	0.742	0.716
	B	0.049	0.050	0.048	0.049	**B***	0.048	0.050	0.050	0.049
			C					**D**		
	Conc. (g/L)	**1**	**2**	**3**	**Average**	**1**	**2**	**3**	**Average**	**%RScA**
RASE-formate	0.052000	0.111	0.111	0.111	0.111	0.099	0.103	0.101	0.101	98.43
	0.026000	0.091	0.09	0.09	0.090	0.071	0.072	0.07	0.071	96.96
	0.013000	0.090	0.088	0.088	0.089	0.059	0.066	0.059	0.061	95.70
	0.006500	0.267	0.243	0.236	0.249	0.05	0.052	0.052	0.051	68.96
	0.003250	0.430	0.442	0.434	0.435	0.049	0.049	0.049	0.049	39.22
	0.001625	0.556	0.564	0.511	0.544	0.05	0.047	0.047	0.048	22.02
	0.000813	0.587	0.586	0.604	0.592	0.048	0.047	0.047	0.047	14.26
RASE-acetate	0.044000	0.099	0.099	0.099	0.099	0.086	0.08	0.084	0.083	97.54
	0.022000	0.089	0.089	0.088	0.089	0.067	0.066	0.066	0.066	96.49
	0.011000	0.108	0.095	0.096	0.100	0.058	0.057	0.057	0.057	93.34
	0.005500	0.314	0.386	0.307	0.336	0.053	0.053	0.053	0.053	55.53
	0.002750	0.471	0.481	0.461	0.471	0.049	0.051	0.051	0.050	33.82
	0.001375	0.572	0.567	0.568	0.569	0.050	0.049	0.049	0.049	18.25
	0.000688	0.640	0.626	0.628	0.631	0.049	0.049	0.05	0.049	8.44
RASE-octanoate	0.040000	0.092	0.094	0.092	0.093	0.073	0.072	0.073	0.073	96.85
	0.020000	0.087	0.088	0.086	0.087	0.060	0.060	0.060	0.060	95.75
	0.010000	0.170	0.173	0.168	0.170	0.055	0.054	0.055	0.055	81.80
	0.005000	0.400	0.399	0.383	0.394	0.051	0.051	0.051	0.051	46.04
	0.002500	0.523	0.531	0.496	0.517	0.050	0.050	0.050	0.050	26.59
	0.001250	0.589	0.589	0.595	0.591	0.049	0.050	0.049	0.049	14.79

		C				D				
	Conc. (g/L)	1	2	3	Average	1	2	3	Average	%RScA
RASE-chloride	0.040000	0.193	0.180	0.177	0.183	0.196	0.189	0.193	0.193	101.47
	0.020000	0.124	0.123	0.118	0.122	0.095	0.091	0.094	0.093	95.54
	0.010000	0.141	0.136	0.124	0.134	0.059	0.059	0.059	0.059	88.25
	0.005000	0.301	0.346	0.333	0.327	0.053	0.054	0.055	0.054	57.11
	0.001250	0.554	0.556	0.557	0.556	0.050	0.052	0.051	0.051	20.61
	0.000625	0.596	0.605	0.618	0.606	0.049	0.049	0.051	0.050	12.43
RASE-trifluoroacetate*	0.056000	0.241	0.249	0.248	0.246	0.259	0.264	0.262	0.262	102.35
	0.028000	0.159	0.152	0.152	0.154	0.088	0.078	0.078	0.081	89.06
	0.014000	0.201	0.194	0.203	0.199	0.084	0.062	0.062	0.069	80.51
	0.007000	0.317	0.324	0.322	0.321	0.054	0.055	0.052	0.054	59.92
	0.003500	0.490	0.484	0.489	0.488	0.051	0.050	0.050	0.050	34.43
	0.001750	0.572	0.588	0.590	0.583	0.050	0.049	0.051	0.050	20.04
	0.000875	0.643	0.649	0.651	0.648	0.049	0.05	0.05	0.050	10.34

Table 7.27 %RScA of Cy3gal and its ester derivatives

	1	2	3	Average		1	2	3	Average
A	0.887	0.899	0.906	0.897	**A***	0.852	0.841	0.811	0.835
B	0.052	0.052	0.052	0.052	**B***	0.050	0.050	0.051	0.050

		C				D				
	Conc. (g/L)	1	2	3	Average	1	2	3	Average	%RScA
Cy3gal Monoacetate	0.028000	0.231	0.235	0.231	0.232	0.255	0.255	0.251	0.254	102.52
	0.014000	0.415	0.414	0.405	0.411	0.11	0.11	0.11	0.110	64.35
	0.007000	0.608	0.606	0.594	0.603	0.06	0.06	0.072	0.064	36.28

			C				D			
	Conc. (g/L)	1	2	3	Average	1	2	3	Average	%RScA
	0.003500	0.691	0.685	0.683	0.686	0.055	0.056	0.058	0.056	25.47
	0.001750	0.774	0.775	0.766	0.772	0.056	0.056	0.057	0.056	15.38
	0.000875	0.826	0.846	0.840	0.837	0.053	0.057	0.054	0.055	7.41
	0.000438	0.838	0.849	0.855	0.847	0.053	0.053	0.057	0.054	6.19
Cy3gal Diacetate	0.032000	0.193	0.193	0.189	0.192	0.162	0.16	0.16	0.161	96.33
	0.016000	0.348	0.344	0.334	0.342	0.085	0.084	0.083	0.084	69.48
	0.008000	0.489	0.488	0.473	0.483	0.063	0.064	0.064	0.064	50.35
	0.004000	0.572	0.585	0.59	0.582	0.057	0.057	0.058	0.057	37.89
	0.002000	0.704	0.715	0.718	0.712	0.056	0.057	0.058	0.057	22.48
	0.001000	0.791	0.793	0.797	0.794	0.058	0.054	0.056	0.056	12.74
	0.000500	0.836	0.832	0.824	0.831	0.056	0.053	0.057	0.055	8.28
Cy3gal Dibutanoate*	0.036000	0.386	0.379	0.409	0.391	0.098	0.100	0.100	0.099	62.77
	0.018000	0.606	0.552	0.566	0.575	0.058	0.057	0.058	0.058	34.08
	0.009000	0.644	0.658	0.716	0.673	0.054	0.055	0.054	0.054	21.16
	0.004500	0.793	0.742	0.746	0.760	0.053	0.056	0.054	0.054	9.99
	0.002250	0.839	0.791	0.783	0.804	0.057	0.054	0.053	0.055	4.42
	0.001125	0.86	0.815	0.805	0.827	0.059	0.055	0.056	0.057	1.83
	0.000563	0.861	0.821	0.804	0.829	0.055	0.052	0.052	0.053	1.10
Cy3gal Monooctanoate	0.028000	0.385	0.381	0.374	0.380	0.061	0.06	0.058	0.060	62.11
	0.014000	0.561	0.564	0.559	0.561	0.057	0.058	0.057	0.057	40.38
	0.007000	0.707	0.71	0.699	0.705	0.055	0.054	0.055	0.055	23.03
	0.003500	0.786	0.791	0.778	0.785	0.053	0.055	0.055	0.054	13.56
	0.001750	0.822	0.828	0.814	0.821	0.052	0.054	0.054	0.053	9.15
	0.000875	0.842	0.843	0.836	0.840	0.055	0.054	0.054	0.054	7.02
	0.000438	0.85	0.855	0.849	0.851	0.054	0.053	0.053	0.053	5.60

		C				D			
Conc. (g/L)	1	2	3	Average	1	2	3	Average	%RScA
0.016000	0.632	0.64	0.649	0.640	0.056	0.056	0.056	0.056	25.50
0.004000	0.761	0.781	0.778	0.773	0.051	0.053	0.052	0.052	8.03
0.002000	0.824	0.831	0.826	0.827	0.052	0.053	0.052	0.052	1.23
0.001000	0.856	0.858	0.848	0.854	0.055	0.051	0.051	0.052	-2.21
0.000500	0.871	0.875	0.868	0.871	0.054	0.052	0.053	0.053	-4.33

7.13. Thermal Stability Assay

The thermal stability of Cy3gal isolated from semi-preparative HPLC and its derivatives (counterion: trifluoroacetate) are measured in the lipophilic medium, octanol. The maximum absorbance of Cy3gal in octanol was observed at 546 nm. Test compounds (0.5 mg) are dissolved in 100 µL of methanol. The solution was then added with 9 mL of octanol, and the absorbance (A_0) was read at 546 nm. The solution was diluted if it is too concentrated. A blank with no sample was prepared with the same manner. Afterwards, the solution was divided into three different vials. The effect of temperature on the colour stability of anthocyanin solution was investigated at 25, 40, and 60 °C. After 2, 4, 6, and 22 h of each treatment, change in colour intensity was determined with a Jenway 6300 UV/vis spectrophotometer by measuring the Absorbance of the upper phase (A_x) at 546 nm.[198] The first-order reaction rate constant (k) and half-life time ($t_{1/2}$) were calculated by the following equations:[198]

$$\ln (C_x/C_0) = - k \times t \qquad \textbf{Equation 7.4}$$

$$t_{1/2} = - \ln (1/2) \times k^{-1} \text{ or } t_{1/2} = 0.693/k \qquad \textbf{Equation 7.5}$$

According to Beer-Lambert law: $A = \varepsilon \times l \times C$. In which A = absorbance, ε = molar absorptivity, C=concentration, and l =pathlength (1 cm). At the constant ε and l, A equals to C, where C_0 is the initial anthocyanin content, C_x is the anthocyanin content after t min of heating at a given temperature.

Table 7.28 Thermostability of Cy3gal and its ester derivatives

	Absorbance												
25 °C	**Time (h)**					**A_x/A_0**				**ln (A_x/A_0)**			
Compound	**0**	**2**	**4**	**6**	**22**	**2**	**4**	**6**	**22**	**2**	**4**	**6**	**22**
Cy3gal	0.587	0.565	0.499	0.440	0.386	0.963	0.850	0.750	0.658	-0.038	-0.162	-0.288	-0.419
Cy3gal monoacetate	0.395	0.390	0.330	0.294	0.231	0.987	0.835	0.744	0.585	-0.013	-0.180	-0.295	-0.536
Cy3gal diacetate	0.372	0.363	0.345	0.333	0.321	0.976	0.927	0.895	0.863	-0.024	-0.075	-0.111	-0.147
Cy3gal monobutanoate	0.991	0.963	0.900	0.866	0.788	0.972	0.908	0.874	0.795	-0.029	-0.096	-0.135	-0.229
Cy3gal dibutanoate	1.092	1.085	1.055	1.045	1.013	0.994	0.966	0.957	0.928	-0.006	-0.034	-0.044	-0.075
Cy3gal monooctanoate	0.361	0.337	0.301	0.278	0.266	0.934	0.834	0.770	0.737	-0.069	-0.182	-0.261	-0.305
Cy3gal dioctanoate	0.264	0.253	0.226	0.206	0.197	0.958	0.856	0.780	0.746	-0.043	-0.155	-0.248	-0.293
40 °C													
Cy3gal	0.587	0.524	0.478	0.448	0.399	0.893	0.814	0.763	0.680	-0.114	-0.205	-0.270	-0.386
Cy3gal monoacetate	0.395	0.367	0.330	0.304	0.279	0.929	0.835	0.770	0.706	-0.074	-0.180	-0.262	-0.348
Cy3gal diacetate	0.328	0.315	0.292	0.269	0.245	0.960	0.890	0.820	0.747	-0.040	-0.116	-0.198	-0.292
Cy3gal monobutanoate	0.991	0.928	0.861	0.824	0.724	0.936	0.869	0.831	0.731	-0.066	-0.141	-0.185	-0.314
Cy3gal dibutanoate	1.092	1.054	1.021	1.018	0.978	0.965	0.935	0.932	0.896	-0.035	-0.067	-0.070	-0.110
Cy3gal monooctanoate	0.361	0.311	0.288	0.264	0.251	0.861	0.798	0.731	0.695	-0.149	-0.226	-0.313	-0.363
Cy3gal dioctanoate	0.264	0.241	0.219	0.199	0.193	0.913	0.830	0.754	0.731	-0.091	-0.187	-0.283	-0.313
60 °C													
Cy3gal	0.587	0.475	0.451	0.411	0.367	0.809	0.768	0.700	0.625	-0.212	-0.264	-0.356	-0.470
Cy3gal monoacetate	0.395	0.349	0.317	0.291	0.263	0.884	0.803	0.737	0.666	-0.124	-0.220	-0.306	-0.407
Cy3gal diacetate	0.328	0.297	0.274	0.249	0.229	0.905	0.835	0.759	0.698	-0.099	-0.180	-0.276	-0.359
Cy3gal monobutanoate	0.991	0.882	0.806	0.742	0.628	0.890	0.813	0.749	0.634	-0.117	-0.207	-0.289	-0.456
Cy3gal dibutanoate	1.092	1.056	1.041	1.029	0.992	0.967	0.953	0.942	0.908	-0.034	-0.048	-0.059	-0.096
Cy3gal monooctanoate	0.361	0.303	0.272	0.257	0.247	0.839	0.753	0.712	0.684	-0.175	-0.283	-0.340	-0.379
Cy3gal dioctanoate	0.240	0.214	0.199	0.194	0.185	0.194	0.892	0.829	0.808	0.771	0.808	-0.115	-0.187

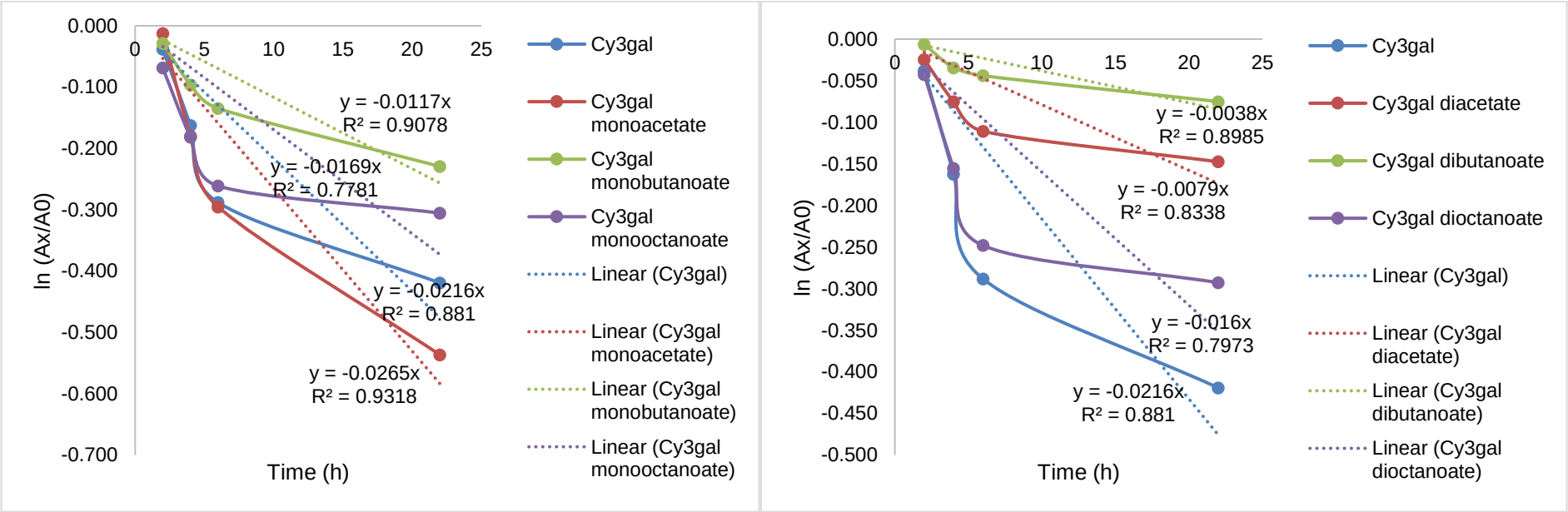

Figure 7.1. Thermal stability of Cy3gal and its derivatives at 25 °C

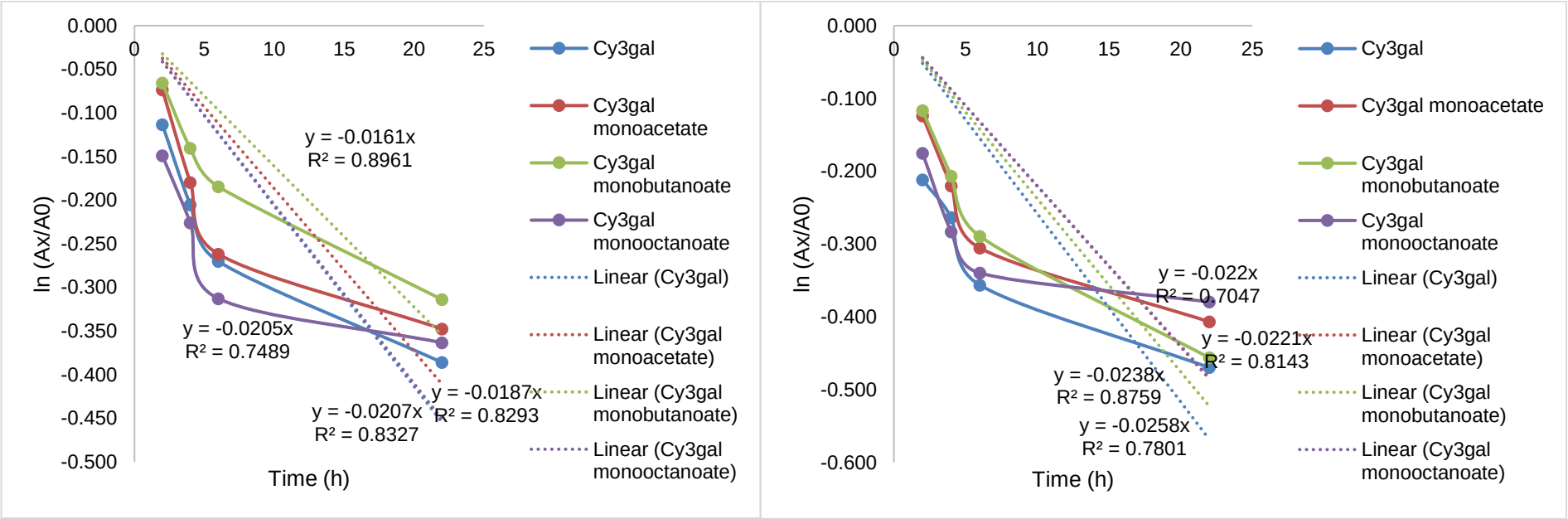

Figure 7.2. Thermal stability of Cy3gal and its derivatives at 40 °C

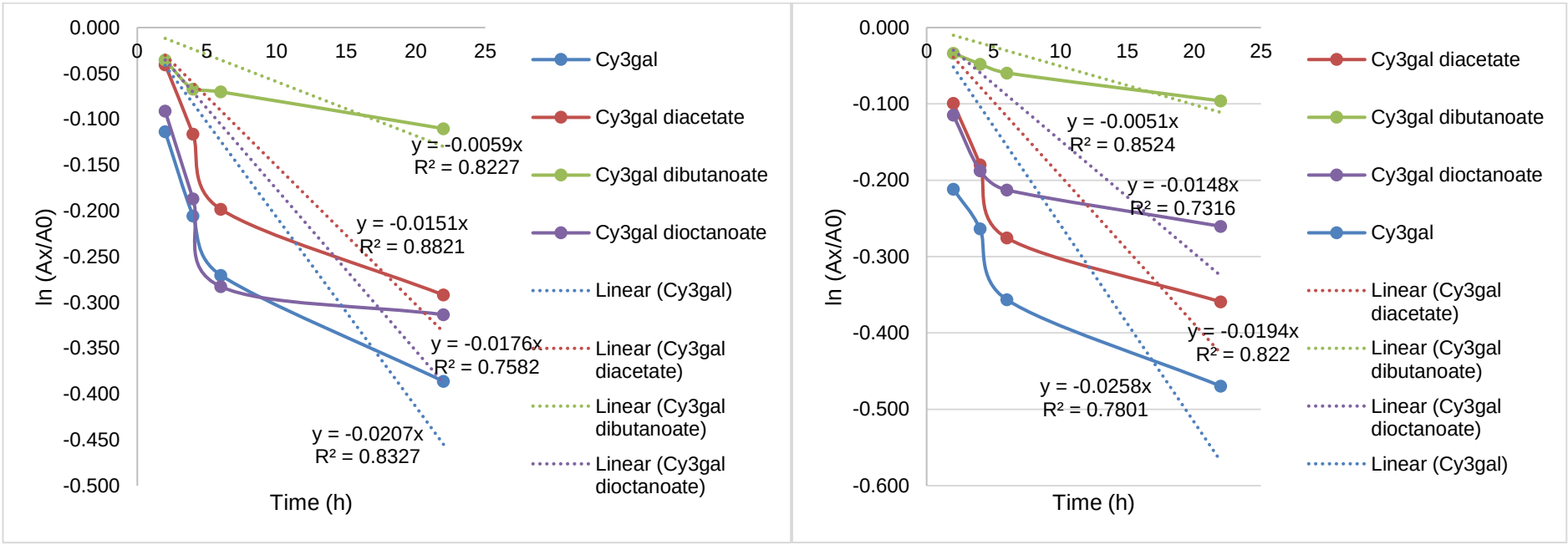

Figure 7.3. Thermal stability of Cy3gal and its derivatives at 60 °C

7.15. Chemical Characterisation of anthocyanins extracted from *Aronia* skin waste.

RASE was obtained from the extraction using HCl, followed by a neutral SPE. The isolation of anthocyanins follows the method described in **Section 7.6**. Anthocyanins isolated from RASE were successfully characterised in their flavylium cation and hemiketal forms. In a flavylium cationic form, trifluoroacetate is the counterion.

7.15.1. Flavylium cationic form (AH^+)

Cyanidin-3-*O*-β-galactoside (Cy3gal), 27

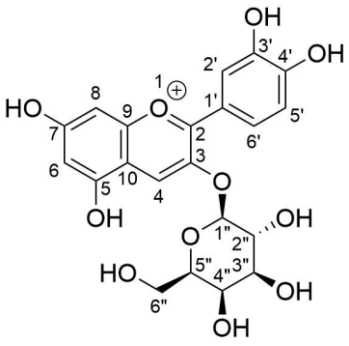

It was isolated from RASE using method described in **Section 7.6** (red solid, 4.0 mg, 10.8%). **^{1}H-NMR (500 MHz, CD_3OD/CF_3COOD 95:5)** δ 9.03 (s, 1H, H-4), 8.26 (dd, *J* = 8.5, 2.5 Hz, 1H, H-6'), 8.08 (d, *J* = 2.5 Hz, 1H, H-2'), 7.02 (d, *J* = 8.5 Hz, 1H, H-5'), 6.90 (d, *J* = 1.5 Hz, 1H, H-8), 6.66 (d, *J* = 1.5 Hz, 1H, H-6), 5.25 (d, *J* = 7.5 Hz, 1H, anomeric H-1''), 3.99 (dd, *J* = 9.5, 7.5 Hz, 1H, H-2''), 3.94 (d, 3.5 Hz, 1H, H-4''), 3.73-3.82 (m, 3H, H-5'', H-6A'', H-6B''), 3.67 (dd, *J* = 9.5, 3.5 Hz, 1H, H-3''). **^{13}C-NMR (125 MHz, CD_3OD/CF_3COOD 95:5)** δ169.0 (C7), 163.1 (C2), 157.9 (C5), 156.3 (C9), 154.4 (C4'), 146.0 (C3'), 144.3 (C3), 135.6 (C4), 126.8 (C6'), 119.8 (C1'), 117.1 (C2'), 116.0 (C5'), 112.0 (C10), 103.0 (C1"), 102.0 (C6), 93.7 (C8), 76.4 (C5"), 73.5 (C3"), 70.7 (C2"), 68.7 (C4"), 60.9 (C6"A/B). **^{1}H-NMR (500 MHz, $(CD_3)_2SO/CF_3COOD$ 95:5)** δ 8.87 (s, 1H, H-4), 8.24 (dd, *J* = 8.5, 2.5 Hz, 1H, H-6'), 7.99 (d, *J* = 2.5 Hz, 1H, H-2'), 7.03 (d, *J* = 8.5 Hz, 1H, H-5'), 6.90 (d, *J* = 1.0 Hz, 1H, H-8), 6.69 (d, *J* = 1.0 Hz, 1H, H-6), 5.27 (d, *J* = 7.5 Hz, 1H, anomeric H-1''), 3.81 (dd, *J* = 9.0, 7.5 Hz, 1H, H-2''), 3.75 (d, 3.5 Hz, 1H, H-4''), 3.58 (dd, *J* = 11.0, 6.0 Hz, 1H, H-6"A), 3.49-3.52 (m, 3H, H-3'', H-5'', H-6"B). **^{13}C-NMR (125 MHz, $(CD_3)_2SO$ /CF_3COOD 95:5)** δ169.2 (C7), 162.9 (C2), 159.3 (C5), 156.9 (C9), 155.4 (C4'), 147.2 (C3'), 145.5 (C3), 135.6 (C4), 128.1 (C6'), 120.8 (C1'), 118.5 (C2'), 117.8 (C5'), 112.9 (C10), 103.7 (C1"), 103.3 (C6), 95.2 (C8), 77.3 (C5"), 74.2 (C3"), 71.2 (C2"), 69.1 (C4"), 61.4 (C6"A/B). **^{1}H-NMR (500 MHz, CD_3COCD_3/CF_3COOD 95:5)** δ 9.10 (s, 1H, H-4), 8.42 (dd, *J* = 9.0, 2.5 Hz, 1H, H-6'), 8.26 (d, *J* = 2.5 Hz, 1H, H-2'), 7.16 (d, *J* = 2.0 Hz, 1H, H-8), 7.15 (d, *J* = 9.0 Hz, 1H, H-5'), 6.87 (d, *J* = 2.0 Hz, 1H, H-6), 5.51 (d, *J* = 7.5 Hz, 1H, anomeric H-1''), 4.37 (d, 3.0 Hz, 1H, H-4''), 4.13 (dd, *J* = 9.5, 7.5 Hz, 1H, H-2''), 3.86-3.90 (m, 3H, H-5'', H-6''A/B), 3.81 (dd, 9.5, 3.5 Hz, 1H, H-3''). Prep-HPLC-DAD (520 nm) retention time, 30 min run: 11.14 min. UV-Vis λ_{max} (Buffer solution pH 1): 511 nm. UV-Vis λ_{max}

(methanol): 529 nm. HRMS: m/z (ESI$^+$) calculated for [M$^+$]: 449.1078; found [M$^+$]: 449.1072. The ^{1}H and ^{13}C NMR data in the current work are in agreement with data published in literature.[106]

Cyanidin-3-*O*-β-glucoside (Cy3glc), 21

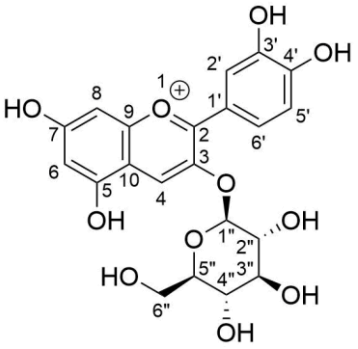

It was isolated from RASE using method described in **Section 7.6** (red solid, 2.8 mg, 7.5%). **^{1}H-NMR (500 MHz, CD_3OD/CF_3COOD 95:5)** δ 9.02 (s, 1H, H-4), 8.25 (dd, *J* = 8.5, 2.5 Hz, 1H, H-6'), 8.04 (d, *J* = 2.5 Hz, 1H, H-2'), 7.02 (d, *J* = 8.5 Hz, 1H, H-5'), 6.89 (d, *J* = 1.5 Hz, 1H, H-8), 6.65 (d, *J* = 1.5 Hz, 1H, H-6), 5.28 (d, *J* = 8.0 Hz, 1H, anomeric H-1''), 3.67 (dd, *J* = 9.5, 8.0 Hz, 1H, H-2''), 3.55 (dd, 9.5, 9.0 Hz, 1H, H-3''), 3.42 (dd, 9.5, 9.0 Hz, 1H, H-4''), 3.53 (ddd, 9.5, 6.0, 2.0 Hz, 1H, H-5''), 3.90 (dd, *J* = 12.0, 2.5 Hz, 1H, H-6''A), 3.69 (dd, *J* = 12.0, 6.0 Hz, 1H, H-6''B). **^{13}C-NMR (125 MHz, CD_3OD/CF_3COOD 95:5)** δ135.8 (C4), 126.9 (C6'), 102.3 (C1"), 101.7 (C6), 93.6 (C8), 77.5 (C5"), 76.7 (C3"), 73.3 (C2"), 69.6 (C4"), 60.6 (C6"A/B). HPLC-DAD (520 nm) retention time: 12.24 min. UV-Vis λ_{max} (methanol): 531 nm. HRMS: m/z (ESI$^+$) calculated for [M$^+$]: 449.1078; found [M$^+$]: 449.1072. The ^{1}H and ^{13}C NMR data in the current work are in agreement with data published in literature.[106]

Cyanidin-3-*O*-β-arabinoside (Cy3ara), 28

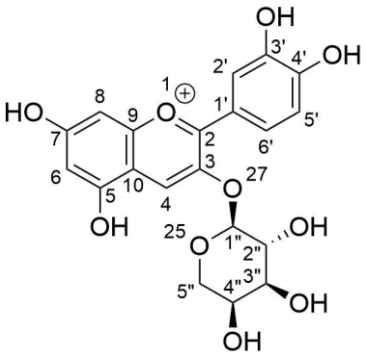

It was isolated from RASE using method described in **Section 7.6** (red solid, 4.4 mg, 11.8%). **^{1}H-NMR (500 MHz, CD_3OD/CF_3COOD 95:5)** δ 8.84 (s, 1H, H-4), 8.24 (dd, J = 9.0, 2.0 Hz, 1H, H-6'), 7.97 (d, J = 2.0 Hz, 1H, H-2'), 6.92 (d, J = 9.0 Hz, 1H, H-5'), 6.80 (d, J = 1.0 Hz, 1H, H-8), 6.55 (d, J = 1.5 Hz, 1H, H-6), 5.19 (d, J = 6.0 Hz, 1H, anomeric H-1''), 3.93 (dd, *J* = 8.0, 6.0 Hz, 1H, H-2''), 3.86-3.91 (m, 2H, H-4'', H-5''A), 3.65-3.68 (m, 2H, H-3", H-5''B). **^{13}C-NMR (125 MHz, CD_3OD/CF_3COOD 95:5)** δ168.9 (C7), 163.2 (C2), 158.1 (C9), 156.3 (C5), 154.5 (C4'), 146.1 (C1'), 144.2 (C3), 134.8 (C4), 127.2 (C6'), 119.8 (C3'), 116.9 (C2'), 116.0 (C5'), 111.8 (C10), 102.6 (C1"), 101.8 (C6), 93.7 (C8), 72.2 (C3"), 70.6 (C2"), 67.3 (C4"), 65.3 (C5"A/B). **^{1}H-NMR (500 MHz, $(CD_3)_2SO/CF_3COOD$ 95:5)** δ 8.80 (s, 1H, H-4), 8.23 (dd, J = 9.0, 2.5 Hz, 1H, H-6'), 7.98 (d, J = 2.5 Hz, 1H, H-2'), 7.02 (d, J = 9.0 Hz, 1H, H-5'), 6.91 (d, J = 1.0 Hz, 1H, H-8), 6.71 (d, J = 1.5 Hz, 1H, H-6), 5.36 (d, J = 7.5 Hz, 1H, anomeric H-1''), 3.85 (dd, *J* = 10.5, 4.5 Hz, 1H, H-4''), 3.51 (dd, *J* = 9.0, 7.5 Hz, 1H, H-2''), 3.85 (dd, *J*

= 9.0, 4.5 Hz, 1H, H-3''), 3.39 (t, *J* = 10.5 Hz, 1H, H-5''A), 3.35 (t, *J* = 8.5 Hz, 1H, H-5''B). HPLC-DAD (520 nm) retention time: 13.15 min. UV-Vis λ_{max} (Buffer solution pH 1): 508 nm. HRMS: m/z (ESI^+) calculated for [M^+]: 419.0973; found [M^+]: 419.0967. The ^1H and ^{13}C NMR data in the current work are in agreement with data published in literature.[106]

Cyanidin-3-*O*-β-xyloside (Cy3xyl), 29

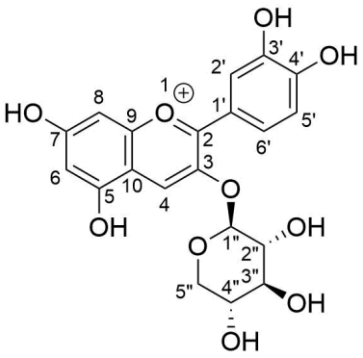

It was isolated from RASE using method described in **Section 7.6** (red solid, 2.4 mg, 6.4%). **^{1}H NMR (500 MHz, CD_3OD/CF_3COOD 95:5)** δ 8.92 (s, 1H, H-4), 8.27 (dd, *J* = 9.0, 2.5 Hz, 1H, H-6'), 8.01 (d, *J* = 2.5 Hz, 1H, H-2'), 7.00 (d, *J* = 9.0 Hz, 1H, H-5'), 6.89 (d, J = 1.0 Hz, 1H, H-8), 6.65 (d, *J* = 1.0 Hz, 1H, H-6), 5.24 (d, *J* = 7.0 Hz, 1H, anomeric H-1''), 4.00 (dd, *J* = 11.5, 5.0 Hz, 1H, H-5''A), 3.66 (dd, *J* = 9.0, 7.0 Hz, 1H, H-2''), 3.63 (ddd, *J* = 9.5, 8.5, 5.0 Hz, 1H, H-4"), 3.51 (dd, *J* = 9.0, 8.5 Hz, 1H, H-3''), 3.44 (dd, *J* = 11.5, 9.5 Hz, 1H, H-5''B). **^{13}C-NMR (125 MHz, CD_3OD/CF_3COOD 95:5)** δ135.4 (C4), 127.1 (C6'), 117.1 (C2'), 116.1 (C5'), 103.3 (C1"), 101.8 (C6), 93.5 (C8), 75.5 (C3"), 72.8 (C2"), 73.7 (C4"), 65.6 (C5"A/B). HPLC-DAD (520 nm) retention time: 15.64 min. UV-Vis λ_{max} (methanol): 531 nm. HRMS: m/z (ESI^+) calculated for [M^+]: 419.0973; found [M^+]: 419.0967. The ^1H and ^{13}C NMR data in the current work are in agreement with data published in literature.[106]

Cyanidin (Cy), 2

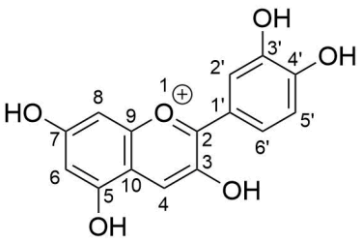

It was isolated from RASE-chloride using method described in **Section 7.6** (red solid, 2.3 mg, 7.6%). **^{1}H-NMR (500 MHz, CD_3OD/CF_3COOD 95:5)** δ 8.59 (s, 1H, H-4), 8.23 (dd, J = 8.5, 2.0 Hz, 1H, H-6'), 8.12 (d, J = 2.5 Hz, 1H, H-2'), 7.02 (d, J = 8.5 Hz, 1H, H-5'), 6.87 (d, J = 2.0 Hz, 1H, H-8), 6.63 (d, J = 2.0 Hz, 1H, H-6). **^{13}C-NMR (125 MHz, CD_3OD/CF_3COOD 95:5)** δ167.6 (C7), 160.8 (C2), 156.7 (C5), 155.7 (C9), 153.8 (C4'), 146.0 (C3'), 145.3 (C3), 132.7 (C4), 125.8 (C6'), 120.6 (C1'), 116.6 (C2'), 115.9 (C5'), 112.3 (C10), 101.7 (C6), 93.4 (C8). **^{1}H-NMR (500 MHz, $(CD_3)_2SO/CF_3COOD$ 95:5)** δ 8.54 (s, 1H, H-4), 8.15 (dd, J = 8.5, 2.0 Hz, 1H, H-6'), 8.07 (d, J = 2.5 Hz, 1H, H-2'), 7.04 (d, J = 8.5 Hz, 1H, H-5'), 6.88 (d, J = 2.0 Hz, 1H, H-8), 6.67 (d, J = 2.0 Hz, 1H, H-6). **^{13}C-NMR (125 MHz, $(CD_3)_2SO/CF_3COOD$ 95:5)** δ168.0 (C7), 160.0 (C2), 157.6 (C5), 156.4 (C9), 154.7 (C4'), 147.2 (C3'), 146.4 (C3), 134.2 (C4), 126.6 (C6'), 121.5 (C1'), 118.2 (C2'), 117.8 (C5'), 113.3 (C10),

103.2 (C6), 95.0 (C8). HPLC-DAD (520 nm) retention time: 18.58 min. UV-Vis λ_{max} (methanol): 540 nm. HRMS: m/z (ESI^+) calculated for [M^+]: 287.0550; found [M^+]: 287.0549. NMR data was not found in literature.

7.15.2. Hemiketal form (B)

Anthocyanins isolated from semi-preparative HPLC purification were dissolved in CD_3OD and analysed by NMR spectroscopy to give a mixture of flavylium cationic form and hemiketal form. A single hemiketal form of Cy3gal can be achieved by slow hydration and evaporation by nitrogen stream, which was carried simultaneously.

Cyanidin-3-*O*-β-galactoside (Cy3gal)

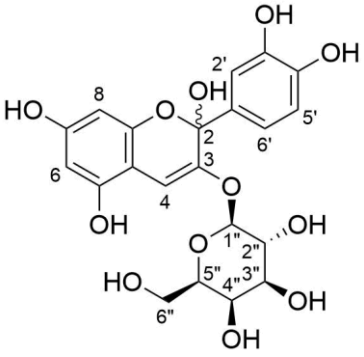

Hemiketal a, major

It was isolated from RASE using method described in **Section 7.6** (red solid, 4.0 mg, 10.8%). **^{1}H-NMR (500 MHz, CD_3OD)** δ 7.03 (d, *J* = 2.0 Hz, 1H, H-2'), 6.94 (dd, *J* = 8.0, 2.0 Hz, 1H, H-6'), 6.72 (d, *J* = 8.0 Hz, 1H, H-5'), 6.54 (s, 1H, H-4), 5.97 (d, *J* = 2.0 Hz, 1H, H-6), 5.94 (d, *J* = 2.0, 1H, H-8), 4.83 (d, *J* = 7.5 Hz, 1H, H-1'' Anomeric), 3.89 (d, 3.0 Hz, 1H, H-4''), 3.66-3.83 (m, 3H, H-5'', H-6"A, H-6''B), 3.61 (dd, *J* = 10.0, 7.5 Hz, 1H, H-2''), 3.56 (dd, *J* = 9.5, 3.0 Hz, 1H, H-3''). **^{13}C-NMR (125 MHz, CD_3OD)** δ118.2 (C6'), 114.1 (C5'), 114.1 (C2'), 101.4 (C1"), 97.1 (C4), 95.6 (C6), 93.6 (C8), 75.6 (C5"), 73.5 (C3"), 70.5 (C2"), 68.7 (C4"), 60.9 (C6"A/B).

Hemiketal b, minor

^{1}H-NMR (500 MHz, CD_3OD) δ 7.03 (d, *J* = 2.0 Hz, 1H, H-2'), 6.92 (dd, *J* = 8.0, 2.0 Hz, 1H, H-6'), 6.79 (d, *J* = 8.5 Hz, 1H, H-5'), 6.58 (s, 1H, H-4), 5.97 (d, *J* = 2.5 Hz, 1H, H-6), 5.93 (d, *J* = 2.0, 1H, H-8), 4.65 (d, *J* = 7.5 Hz, 1H, H-1'' Anomeric), 3.88 (d, 3.5 Hz, 1H, H-4''), 3.66-3.83 (m, 3H, H-5'', H-6"A, H-6''B), 3.58 (dd, *J* = 9.5, 7.5 Hz, 1H, H-2''), 3.48 (dd, *J* = 9.5, 3.5 Hz, 1H, H-3''). **^{13}C-NMR (125 MHz, CD_3OD)** δ118.2 (C6'), 114.2 (C5'), 114.3 (C2'), 101.9 (C1"), 98.0 (C4), 95.8 (C6), 93.7 (C8), 75.4 (C5"), 73.5 (C3"), 70.6 (C2"), 68.8 (C4"), 60.9 (C6"A/B).

Cyanidin-3-*O*-β-glucoside

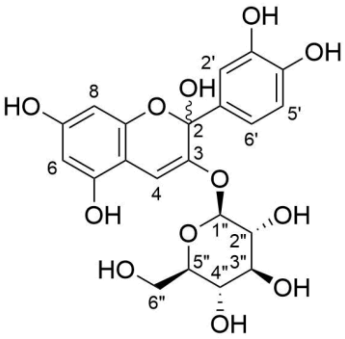

Hemiketal a, major

It was isolated from RASE using method described in **Section 7.6** (red solid, 2.8 mg, 7.5%). **^{1}H-NMR (500 MHz, CD_3OD)** δ 7.04 1 (d, *J* = 2.0 Hz, 1H, H-2'), 6.94 (dd, *J* = 8.5, 2.0 Hz, 1H, H-6'), 6.73 (d, *J* = 8.5 Hz, 1H, H-5'), 6.51 (s, 1H, H-4), 5.97 (d, *J* = 2.0 Hz, 1H, H-6), 5.93 (d, *J* = 2.0 Hz, 1H, H-8), 4.85 (under solvent's peak, H-1'' Anomeric), 3.91 (dd, *J* = 12.0, 2.0 Hz, 1H, H-6"A), 3.71 (dd, *J* = 12.0, 4.0 Hz, 1H, H-6''B), 3.26-3.55 (m, 2H, H-4'', H-5''), 3.38 (dd, *J* = 9.5, 9.0 Hz, 1H, H-3''), 3.29 (dd, *J* = 9.5, 7.5 Hz, 1H, H-2''). **^{13}C-NMR (125 MHz, CD_3OD)** δ118.5 (C6'), 114.3 (C5'), 114.2 (C2'), 101.5 (C1"), 96.9 (C4), 95.7 (C6), 93.7 (C8), 76.9 (C5"), 76.7 (C3"), 73.3 (C2"), 76.6 (C4"), 61.1 (C6"A/B).

Hemiketal b, minor

^{1}H-NMR (500 MHz, CD_3OD) δ 7.02 1 (d, *J* = 2.5 Hz, 1H, H-2'), 6.92 (dd, *J* = 8.5, 2.5 Hz, 1H, H-6'), 6.75 (d, *J* = 8.5 Hz, 1H, H-5'), 6.57 (s, 1H, H-4), 5.98 (d, *J* = 2.0 Hz, 1H, H-6), 5.93 (d, *J* = 2.0 Hz, 1H, H-8), 4.68 (d, *J* = 7.5 Hz, H-1'' Anomeric), 3.93 (dd, *J* = 12.0, 2.0 Hz, 1H, H-6"A), 3.72 (dd, *J* = 12.0, 4.5 Hz, 1H, H-6''B), 3.26-3.55 (m, 2H, H-4'', H-5''), 3.35 (dd, *J* = 9.5, 8.5 Hz, 1H, H-3''), 3.29 (dd, *J* = 9.5, 7.5 Hz, 1H, H-2''). **^{13}C-NMR (125 MHz, CD_3OD)** δ118.5 (C6'), 114.3 (C5'), 114.2 (C2'), 101.5 (C1"), 98.2 (C4), 95.5 (C6), 93.7 (C8), 76.9 (C5"), 76.7 (C3"), 74.9 (C2"), 76.6 (C4"), 61.1 (C6"A/B).

Cyanidin-3-*O*-β-arabinoside (Cy3ara)

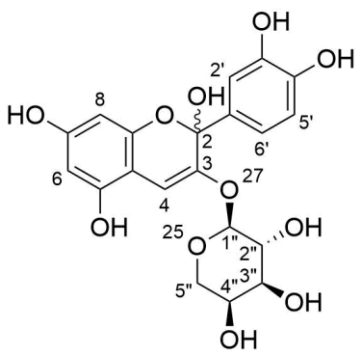

Hemiketal a, major

It was isolated from RASE using method described in **Section 7.6** (red solid, 4.4 mg, 11.8%). **^{1}H-NMR (500 MHz, CD_3OD)** δ 7.03 (d, *J* = 2.5 Hz, 1H, H-2'), 6.93 (dd, *J* = 8.5, 2.5 Hz, 1H, H-6'), 6.73 (d, *J* = 8.5 Hz, 1H, H-5'), 6.47 (s, 1H, H-4), 5.97 (d, *J* = 2.0 Hz, 1H, H-6), 5.92 (d, *J* = 2.0, 1H, H-8), 4.85 (d, *J* = 7.5 Hz, 1H, H-1'' Anomeric), 3.84-3.87 (m, 1H, H-3''), 3.81 (dd, *J* = 12.0, 3.5 Hz, 1H, H-5"A), 3.68 (dd, *J* = 12.5, 2.0 Hz, 1H, H-5''B), 3.66 (dd, *J* = 8.0, 6.0 Hz, 1H, H-2''), 3.57-3.62 (m, 1H, H-4''). **^{13}C-NMR (125 MHz, CD_3OD)** δ118.4 (C6'), 114.3 (C5'), 113.9 (C2'), 100.4 (C1"), 97.5 (C4), 95.7 (C6), 93.7 (C8), 67.3 (C3"), 70.6 (C2"), 72.0 (C4"), 64.7 (C5"A/B).

Hemiketal b, minor

^{1}H-NMR (500 MHz, CD_3OD) δ 7.03 (d, *J* = 2.0 Hz, 1H, H-2'), 6.91 (dd, *J* = 8.0, 2.0 Hz, 1H, H-6'), 6.75 (d, *J* = 8.5 Hz, 1H, H-5'), 6.52 (s, 1H, H-4), 5.97 (d, *J* = 2.5 Hz, 1H, H-6), 5.94 (d, *J* = 2.0, 1H, H-8), 4.68 (d, *J* = 6.0 Hz, 1H, H-1'' Anomeric), 3.84-3.87 (m, 1H, H-3''), 3.81 (dd, *J* = 12.0, 3.5 Hz, 1H, H-5"A), 3.68 (dd, *J* = 12.5, 2.0 Hz, 1H, H-5''B), 3.58 (dd, *J* = 8.0, 6.0 Hz, 1H, H-2''), 3.57-3.62 (m, 1H, H-4''). **^{13}C-NMR (125 MHz, CD_3OD)** δ118.4 (C6'), 114.3 (C5'), 113.9 (C2'), 100.9 (C1"), 97.0 (C4), 95.7 (C6), 93.7 (C8), 67.3 (C3"), 70.3 (C2"), 72.0 (C4"), 64.7 (C5"A/B).

Cyanidin-3-*O*-β-xyloside (Cy3xyl)

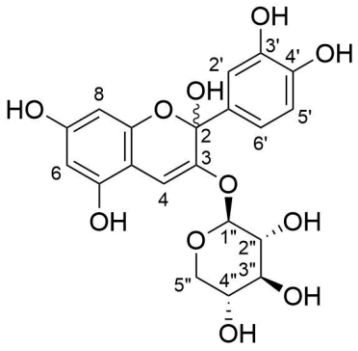

Hemiketal a, major

It was isolated from RASE using method described in **Section 7.6** (red solid, 2.4 mg, 6.4%). **^{1}H-NMR (500 MHz, CD_3OD)** δ 7.02 (d, *J* = 2.0 Hz, 1H, H-2'), 6.92 (dd, *J* = 8.5, 2.0 Hz, 1H, H-6'), 6.73 (d, *J* = 8.5 Hz, 1H, H-5'), 6.46 (s, 1H, H-4), 5.97 (d, *J* = 2.0 Hz, 1H, H-6), 5.92 (d, *J* = 2.0, 1H, H-8), 4.85 (d, *J* = 7.0 Hz, 1H, H-1'' Anomeric), 3.86 (dd, *J* = 11.5, 4.5 Hz, 1H, H-5''A), 3.28 (dd, *J* = 9.0, 7.0 Hz, 1H, H-2''), 3.59 (ddd, *J* = 9.5, 8.5, 5.0 Hz, 1H, H-4"), 3.38-3.42 (m, 1H, H-3"), 3.38 (dd, *J* = 12.0, 9.5 Hz, 1H, H-5''B). **^{13}C-NMR (125 MHz, CD_3OD)** δ118.2 (C6'), 114.3 (C5'), 114.1 (C2'), 101.1 (C1"), 96.8 (C4), 95.6 (C6), 93.7 (C8), 75.8 (C3"), 72.8 (C2"), 70.5 (C4"), 65.8 (C5"A/B).

Hemiketal b, minor

^{1}H-NMR (500 MHz, CD_3OD) δ 7.01 (d, *J* = 2.0 Hz, 1H, H-2'), 6.88 (dd, *J* = 8.5, 2.0 Hz, 1H, H-6'), 6.74 (d, *J* = 8.5 Hz, 1H, H-5'), 6.49 (s, 1H, H-4), 5.97 (d, *J* = 2.0 Hz, 1H, H-6), 5.93 (d, *J* = 2.0, 1H, H-8), 4.66 (d, *J* = 7.0 Hz, 1H, H-1'' Anomeric), 3.96 (dd, *J* = 11.5, 4.5 Hz, 1H, H-5''A), 3.23 (dd, *J* = 9.0, 7.0 Hz, 1H, H-2''), 3.59 (ddd, *J* = 9.5, 8.5, 5.0 Hz, 1H, H-4"), 3.38-3.42 (m, 1H, H-3"), 3.36 (dd, *J* = 12.0, 9.5 Hz, 1H, H-5''B). **^{13}C-NMR (125 MHz, CD_3OD)** δ118.2 (C6'), 114.3 (C5'), 114.1 (C2'), 101.6 (C1"), 97.7 (C4), 95.6 (C6), 93.7 (C8), 75.8 (C3"), 72.8 (C2"), 70.5 (C4"), 65.6 (C5"A/B).

7.16. Characterisation of Neutral Polyphenols in RASE

3,4-Dihydroxybenzoic acid (DHBA), 39

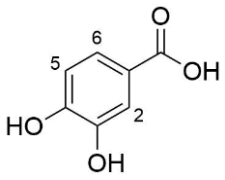

It was found in both *i*propyl acetate and ethyl acetate layer using method described in **Section 7.7** (yellow solid, 9.1 mg, 7.1%). **^{1}H-NMR (500 MHz, CD_3OD)** δ 7.44 (d, *J* = 2.0 Hz, 1H, H-2), 7.43 (dd, *J* = 8.5, 2.0 Hz, 1H, H-6), 6.80 (d, *J* = 8.5 Hz, 1H, H-5). **^{13}C-NMR (125 MHz, CD_3OD)** δ122.5 (C6), 116.4 (C2), 114.3 (C5), 168.8 (C=O). HRMS: calculated for $[M-H]^-$: 153.0193; found m/z of 153.0186 $[M-H]^-$; fragment m/z of 109.0283 $[M-H-CO_2]^-$. The ^{1}H and ^{13}C NMR data in the current work are in agreement with data published in literature.[106]

Quercetin (Q), 40

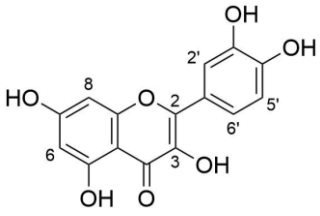

It was found in *i*propyl acetate layer using method described in **Section 7.7** (yellow solid, 3.1 mg, 2.4%). **^{1}H-NMR (500 MHz, CD_3OD)** δ 7.75 (d, *J* = 2.0 Hz, 1H, H-2'), 7.65 (dd, *J* = 8.5, 2.0 Hz, 1H, H-6'), 6.90 (d, *J* = 8.5 Hz, 1H, H-5'), 6.40 (d, *J* = 2.0 Hz, 1H, H-8), 6.20 (d, *J* = 2.0, 1H, H-6). **^{13}C-NMR (125 MHz, CD_3OD)** δ120.2 (C6'), 114.9 (C5'), 114.6 (C2'), 97.9 (C6), 93.2 (C8). HRMS: calculated for $[M-H]^-$: 301.0354; found m/z of 301.0352 $[M-H]^-$. The ^{1}H and ^{13}C NMR data in the current work are in agreement with data published in literature.[125]

Neochlorogenic acid (nCA), 31

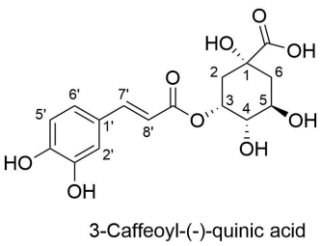

3-Caffeoyl-(-)-quinic acid

It was found in ethyl acetate layer using method described in **Section 7.7** (reddish orange solid, 3.1 mg, 2.4%). **^{1}H-NMR (500 MHz, CD_3OD)** δ 7.60 (d, *J* = 16.0 Hz, 1H, H-7'), 7.06 (dd, *J* = 2.0 Hz, 1H, H-2'), 6.96 (d, *J* = 8.0, 2.0 Hz, 1H, H-6'), 6.80 (d, *J* = 8.0, 1H, H-5'), 6.32 (d, *J* = 16.0 Hz, 1H, H-8'), 5.34-5.37 (m, 1H, H-3), 5.73-5.76 (m, 1H, H-4), 4.10-4.16 (m, 1H, H-5), 2.11-2.23 (m, 2H, H-2A/B), 2.11-2.23 (m, 2H, H-6A/B). **^{13}C-NMR (125 MHz, CD_3OD)** δ145.5 (C7'), 121.6 (C6'), 113.7 (C2'), 115.1 (C5'), 114.6 (C8'), 71.5 (C4), 70.3 (C3), 70.2 (C5), 36.7 (C6), 36.2 (C2). HRMS: calculated for $[M-H]^-$: 353.0878; found m/z of 353.0872 $[M-H]^-$; fragment m/z of 191.0552. The ^{1}H and ^{13}C NMR data in the current work are in agreement with data published in literature.[106]

Chlorogenic acid (CA), 32

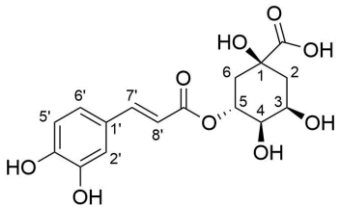

5-Caffeoyl-(-)-quinic acid

It was found in ethyl acetate layer using method described in **Section 7.7** (reddish orange solid, 3.1 mg, 2.4%). **^{1}H-NMR (500 MHz, CD_3OD)** δ 7.57 (d, *J* = 15.5 Hz, 1H, H-7'), 7.06 (dd, *J* = 2.5 Hz, 1H, H-2'), 6.97 (d, *J* = 8.0, 2.5 Hz, 1H, H-6'), 6.79 (d, *J* = 8.0, 1H, H-5'), 6.28 (d, *J* = 15.5 Hz, 1H, H-8'), 4.10-4.16 (m, 1H, H-3), 3.73-3.76 (m, 1H, H-4), 5.26-5.29 (m, 1H, H-5), 2.06-2.19 (m, 2H, H-2A/B), 2.06-2.19 (m, 2H, H-6A/B). **^{13}C-NMR (125 MHz, CD_3OD)** δ145.5 (C7'), 121.6 (C6'), 113.7 (C2'), 115.1 (C5'), 114.6 (C8'), 71.5 (C4), 70.1 (C3), 70.2 (C5), 36.7 (C6), 36.2 (C2). HRMS: calculated for $[M-H]^-$: 353.0878; found m/z of 353.0872 $[M-H]^-$; fragment m/z of 191.0552. The ^{1}H and ^{13}C NMR data in the current work are in agreement with data published in literature.[106]

7.19. Synthesis of ester derivatives of selected polyphenols

The synthesis of ester derivatives of resveratrol and quercetin was conducted by modifying esterification methods in literature.[182,183]

7.19.1. *trans*-3,4',5'-Triacetyl resveratrol, 42

Method 1

Resveratrol (100 mg, 0.44 mmol, 1 eq.) was dissolved in dichloromethane (CH_2Cl_2) (2 ml) and pyridine (0.50 ml, 6.2 mmol, 14 eq.). Acetyl chloride (0.20 ml, 2.8 mmol, 6 eq.) was added dropwise. The reaction mixture was stirred for 3 h at room temperature. Afterwards, the reaction mixture was diluted with CH_2Cl_2 (15 ml) and washed with 3M aq. HCl (3 x 10 ml). The organic layer was dried over $MgSO_4$ and filtered. The solvent was evaporated under reduced pressure, and the residue was purified by silica gel column chromatography (10 g SiO_2, eluent hexane/ethyl acetate 2:1, R_f = 0.37) to obtain a colourless solid *trans*-3,4',5'-triacetyl resveratrol (135 mg, 86% yield).

Method 2

The chemicals and the amount of chemicals used in this method were the same as **Method 1**. The reaction mixture was carried out at -78 °C for 3 h and continued at room temperature for 1 h. Liquid-liquid extraction was carried out using water (2 x 15 mL) and brine (2 x 15 mL), respectively. Na_2SO_4 was used as a drying agent. The solvent was evaporated under reduced pressure, and the residue was purified by

silica gel column chromatography (10 g SiO_2, eluent hexane/ethyl acetate 2:1, Rf = 0.4) to obtain a colourless solid *trans*-3,4',5'-triacetyl resveratrol (112 mg, 72% yield).

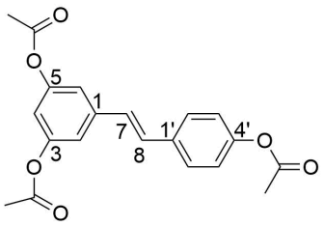

^{1}H NMR (400 MHz, $CDCl_3$) δ 7.48 (d, *J* = 8.6 Hz, 2H, H-2'/6'), 7.12 (d, *J* = 2.1 Hz, 2H, H-2/6), 7.09 (d, *J* = 8.6 Hz, 2H, H-3'/5'), 7.06 (d, *J* = 16.5 Hz, 1H, H-8), 6.97 (d, *J* = 16.3 Hz, 1H, H-7), 6.83 (t, *J* = 2.0 Hz, 1H, H-4), 2.30 (s, 9H, 3 x CH_3). **^{13}C NMR (101 MHz, $CDCl_3$)** δ 169.4, 169.00, 151.3, 150.4, 139.5, 134.4, 129.6, 127.67, 127.2, 121.9, 116.9, 114.42. λ_{max} in DMSO: 315 nm. IR (ATR), v/cm^{-1}: 3073, 1753, 1611, 1578, 1289 cm^{-1}. Melting point: 119-121 °C. HRMS: m/z (ESI+) calculated for $[M+Na]^+$: 377.1001; found $[M+Na]^+$: 377.0997. The ^{1}H and ^{13}C NMR data in the current work are in agreement with data published in literature.[184]

7.19.2. 3,3',4',5,7-Pentaacetyl quercetin, 43

Method 1

Quercetin (100 mg, 0.33 mmol, 1 eq.) was dissolved in dichloromethane (CH_2Cl_2) (2 ml) and pyridine (0.5 ml, 6.2 mmol, 18 eq.). Acetyl chloride (0.2 ml, 2.8 mmol, 8 eq.) was added dropwise. The reaction mixture was stirred for 3 h at room temperature. Afterwards, the reaction mixture was diluted with CH_2Cl_2 (15 ml) and washed with 3M aq. HCl (3 x 10 ml). The organic layer was dried over $MgSO_4$ and filtered. The solvent was evaporated under reduced pressure, and the residue was purified by silica gel column chromatography (eluent CH_2Cl_2/hexane/ethyl acetate 9:2:1, R_f = 0.34) to obtain a colourless solid 3,3',4',5,7-pentaacetyl quercetin (110 mg, 65% yield).

Method 2

The chemicals and the amount of chemicals used in this method were the same as **Method 1**. The reaction mixture was carried out at -78 °C for 3 h and continued at room temperature for 1 h. Liquid-liquid extraction was carried out using water (2 x 15 mL) and brine (2 x 15 mL), respectively. Na_2SO_4 was used as a drying agent. The solvent was evaporated under reduced pressure, and the residue was purified by silica gel column chromatography (10 g SiO_2, eluent hexane/ethyl acetate 1:1, R_f = 0.33) to obtain a colourless solid 3,3',4',5,7-pentaacetyl quercetin (133 mg, 79% yield).

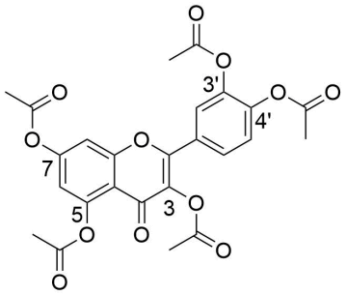

^{1}H NMR (400 MHz, $CDCl_3$) δ 7.72 (dd, *J* = 8.5, 2.1 Hz, 1H, H-6'), 7.69 (d, *J* = 2.1 Hz, 1H, H-2'), 7.35 (d, *J* = 8.5 Hz, 1H, H-5'), 7.33 (d, *J* = 2.2 Hz, 1H, H-8), 6.87 (d, *J* = 2.2 Hz, 1H, H-6), 2.43 (s, 3H, CH_3), 2.33 (s, 12H, 4 x CH_3). **^{13}C NMR (101 MHz, $CDCl_3$)** δ 171.0, 170.2, 168.8, 168.8, 168.7, 168.7, 157.8, 155.2, 154.7, 151.4, 145.3, 143.2, 135.0, 128.7, 127.4, 124.9, 124.8, 115.7, 114.8, 109.9, 22.1, 22.0, 21.6, 21.4. λ_{max} in DMSO: 258 and 300 nm. IR (ATR), v/cm^{-1}: 3086, 1773, 1760, 1644, 1627, 1627, 1177 cm^{-1}. Melting point: 198-200 °C. HRMS: m/z (ESI+) calculated for $[M+H]^+$: 513.1033; found $[M+H]^+$: 513.1027. The ^{1}H and ^{13}C NMR data in the current work are in agreement with data published in literature.[187]

7.20. Lipophilisation of anthocyanins from *Aronia* skin waste

RASE-trifluoroacetate (200 mg, 0.44 mmol, 1 equivalent relative to Cy3gal as the major anthocyanin) was dissolved in acetonitrile (8 mL to give a concentration of 25 g/L). Acylating agents (acetyl chloride, 116.1 µL, 1.76 mmol, 4 eq.), (butyryl chloride, 182.1 µL, 1.76 mmol, 4 eq.) or (caprylyl chloride, 300.4 µL, 1.76 mmol, 4 eq.) were added dropwise. The reaction was performed at 25 ºC for 3 h and covered from light. To produce acylated anthocyanins with a higher acylation number, RASE-trifluoroacetate was reacted with 20 equivalents of acetyl chloride at 40 ºC for 2 days. The completion of the reaction was checked by LC-MS. An aliquot of the reaction mixture (100 µL) was diluted up to 1 mL with DMSO. The reaction mixture was evaporated and purified using semi-preparative HPLC-DAD (see **Section 7.6**). The collected fractions were freeze-dried, and dried acylated anthocyanins were stored in the freezer until further use. The acylated anthocyanins were analysed by UV-Vis, HPLC-DAD, HRMS and NMR spectroscopy.

7.21. Characterisation of acylated anthocyanins

Cy3gal monoacetate (Cyanidin-3-β-*O*-(6''-acetylgalactoside)), 44

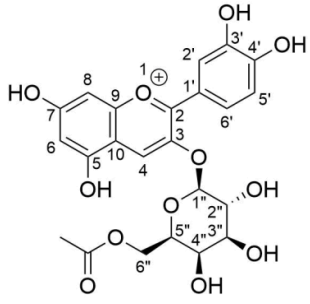

^{1}H-NMR (500 MHz, $(CD_3)_2SO/CF_3COOD$ 95:5) δ 8.80 (s, 1H, H-4), 8.25 (dd, *J* = 8.5, 2.5 Hz, 1H, H-6'), 7.99 (d, *J* = 2.5 Hz, 1H, H-2'), 7.03 (d, *J* = 8.5 Hz, 1H, H-5'), 6.90 (d, *J* = 2.0 Hz, 1H, H-8), 6.71 (d, *J* = 2.0 Hz, 1H, H-6), 5.30 (d, *J* = 8.0 Hz, 1H, anomeric H-1''), 4.13-4.21 (m, 2H, H-6''A, H-6''B), 4.06 (dd, *J* = 8.0, 3.0 Hz, 1H, H-5''), 3.83 (dd, *J* = 9.0, 7.5 Hz, 1H, H-2''), 3.76 (d, 3.5 Hz, 1H, H-4''), 3.54

(dd, 9.5, 3.5 Hz, 1H, H-3''), 2.00 (s, 3H, -CH_3). **^{13}C-NMR (125 MHz, $(CD_3)_2SO$ /CF_3COOD 95:5)** δ170.8 (C=O), δ168.3 (C7), 162.1 (C2), 159.1 (C9), 156.1 (C5), 154.6 (C4'), 146.4 (C1'), 144.8 (C3), 134.2 (C4), 127.4 (C6'), 119.9 (C3'), 117.0 (C2'), 116.5 (C5'), 111.9 (C10), 102.4 (C1"), 102.4 (C6), 94.4 (C8), 73.7 (C5"), 72.9 (C3"), 70.0 (C2"), 68.8 (C4"), 64.5 (C6"A/B), 20.9 (CH_3). UV-Vis λ_{max} (methanol): 530 nm. HRMS: m/z (ESI$^+$) calculated for [M$^+$]: 491.1184; found [M$^+$]: 491.1196. Purity: 89.7%. Yield: 7.1% CGE.

Cy3gal diacetate (Cyanidin-3-β-*O*-(3'',6''-diacetylgalactoside)), 45

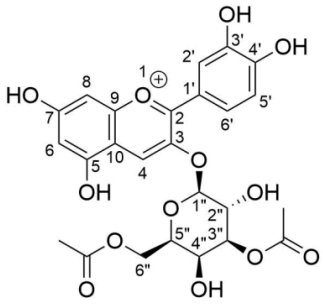

^{1}H-NMR (500 MHz, $(CD_3)_2SO/CF_3COOD$ 95:5) δ 8.81 (s, 1H, H-4), 8.23 (dd, *J* = 8.5, 2.5 Hz, 1H, H-6'), 7.98 (d, *J* = 2.5 Hz, 1H, H-2'), 7.03 (d, *J* = 9.0 Hz, 1H, H-5'), 6.91 (d, *J* = 2.0 Hz, 1H, H-8), 6.72 (d, *J* = 2.0 Hz, 1H, H-6), 5.49 (d, *J* = 7.5 Hz, 1H, anomeric H-1''), 4.78 (dd, 10.5, 3.5 Hz, 1H, H-3''), 4.15-4.22 (m, 3H, H-5'',H-6''A, H-6''B), 4.08 (dd, *J* = 10.0, 7.5 Hz, 1H, H-2''), 3.97 (d, 3.5 Hz, 1H, H-4''), 2.10 (s, 3H, -CH_3 b), 2.00 (s, 3H, -CH_3 a). **^{13}C-NMR (125 MHz, $(CD_3)_2SO$ /CF_3COOD 95:5)** δ170.8 (C=O, a), δ170.6 (C=O, b), δ168.4 (C7), 162.2 (C2), 159.2 (C9), 156.2 (C5), 154.7 (C4'), 146.5 (C1'), 144.5 (C3), 134.2 (C4), 127.4 (C6'), 119.9 (C3'), 117.7 (C2'), 117.0 (C5'), 111.9 (C10), 102.5 (C1"), 101.9 (C6), 94.5 (C8), 75.9 (C5"), 73.2 (C3"), 67.4 (C2"), 65.9 (C4"), 64.0 (C6"A/B), 21.4 (CH_3), 20.9 (CH_3). UV-Vis λ_{max} (methanol): 532 nm. HRMS: m/z (ESI$^+$) calculated for [M$^+$]: 533.1290; found [M$^+$]: 533.1292. Purity: 81.5%. Yield: 6.5% CGE.

Cy3gal triacetate (Cyanidin-3-β-*O*-(3'',4'',6''-triacetylgalactoside)), 46

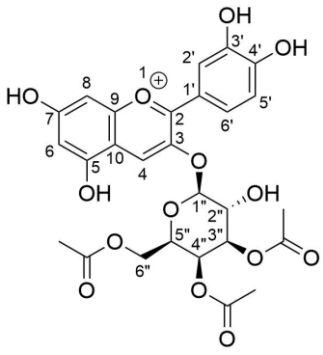

^{1}H-NMR (500 MHz, $(CD_3)_2SO/CF_3COOD$ 95:5) δ 8.81 (s, 1H, H-4), 8.22 (dd, *J* = 8.5, 2.0 Hz, 1H, H-6'), 7.97 (d, *J* = 2.0 Hz, 1H, H-2'), 7.04 (d, *J* = 9.0 Hz, 1H, H-5'), 6.92 (d, *J* = 2.0 Hz, 1H, H-8), 6.72 (d, *J* = 2.0 Hz, 1H, H-6), 5.63 (d, *J* = 7.5 Hz, 1H, anomeric H-1''), 5.34 (d, 4.0 Hz, 1H, H-4''), 5.05 (dd, 10.0, 3.5 Hz, 1H, H-3''), 4.52 (dd, 8.5, 4.0 Hz, 1H, H-5''), 4.12 (dd, 11.5, 4.0 Hz, 1H, H-6''A), 4.04 (dd, 11.0, 8.0 Hz, 1H, H-6''B), 4.00 (dd, *J* = 10.5, 8.0 Hz, 1H, H-2''), 2.05 (s, 3H, -CH_3 c), 2.00 (s, 3H, -CH_3 b), 1.90 (s, 3H, -CH_3 a). **^{13}C-NMR (125 MHz, $(CD_3)_2SO$ /CF_3COOD 95:5)** δ170.2 (C=O), 134.4 (C4), 127.5 (C6'), 117.5 (C2'), 101.7 (C1"), 102.5 (C6), 94.4 (C8), 73.2 (C5"), 72.5 (C3"), 67.4 (C2"), 67.4(C4"), 63.2 (C6"A/B), 20.6 (CH_3). UV-Vis λ_{max} (methanol): 529 nm. HRMS: m/z

(ESI$^+$) calculated for [M$^+$]: 575.1395; found [M$^+$]: 575.1413. Purity: 76.2%. Yield: 8.4% CGE.

Cy3gal tetraacetate (Cyanidin-3-β-*O*-(2”,3”,4”,6”-tetraacetylgalactoside)), 47

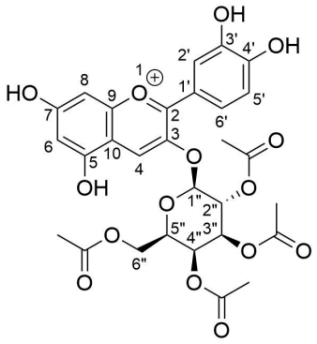

^{1}H-NMR (500 MHz, $(CD_3)_2SO/CF_3COOD$ 95:5) δ 8.82 (s, 1H, H-4), 7.88 (dd, *J* = 8.5, 2.5 Hz, 1H, H-6’), 7.78 (d, *J* = 2.0 Hz, 1H, H-2’), 6.95 (d, *J* = 8.5 Hz, 1H, H-5’), 6.92 (d, *J* = 2.0 Hz, 1H, H-8), 6.73 (d, *J* = 2.0 Hz, 1H, H-6), 5.87 (d, *J* = 8.0 Hz, 1H, anomeric H-1’’), 5.43 (d, 3.5 Hz, 1H, H-4’’), 5.41 (dd, *J* = 10.5, 8.0 Hz, 1H, H-2’’), 5.28 (dd, 10.5, 3.5 Hz, 1H, H-3’’), 4.61 (dd, 9.0, 3.5 Hz, 1H, H-5’’), 4.15-4.17 (m, 1H, H-6’’A), 4.12 (dd, 11.5, 8.5 Hz, 1H, H-6’’B), 2.16 (s, 3H, -CH_3 d), 2.02 (s, 3H, -CH_3 c), 1.94 (s, 3H, -CH_3 b), 1.86 (s, 3H, -CH_3 a). **^{13}C-NMR (125 MHz, $(CD_3)_2SO$ /CF_3COOD 95:5)** δ170.3 (C=O), 134.6 (C4), 127.2 (C6’), 117.4 (C2’), 98.8 (C1”), 102.7 (C6), 94.3 (C8), 65.8 (C5”), 73.4 (C3”), 68.6 (C2”), 65.8 (C4”), 63.2 (C6”A/B), 20.8 (CH_3). UV-Vis λ_{max} (methanol): 521 nm. HRMS: m/z (ESI$^+$) calculated for [M$^+$]: 617.1501; found [M$^+$]: 617.1518. Purity: 65.4%. Yield: 13.5% CGE.

Cy3gal pentaacetate (Cyanidin-3-β-*O*-(4’,2”,3”,4”,6”-pentaacetylgalactoside)), 48

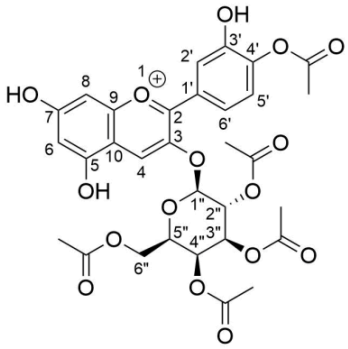

^{1}H-NMR (500 MHz, $(CD_3)_2SO/CF_3COOD$ 95:5) δ 8.87 (s, 1H, H-4), 8.24 (dd, *J* = 9.0, 2.5 Hz, 1H, H-6’), 8.10 (d, *J* = 2.0 Hz, 1H, H-2’), 7.18 (d, *J* = 8.5 Hz, 1H, H-5’), 7.02 (d, *J* = 1.0 Hz, 1H, H-8), 6.76 (d, *J* = 1.0 Hz, 1H, H-6), 6.01 (d, *J* = 8.0 Hz, 1H, anomeric H-1’’), 5.44 (d, 4.0 Hz, 1H, H-4’’), 5.42 (dd, *J* = 10.5, 8.0 Hz, 1H, H-2’’), 5.30 (dd, 10.0, 3.5 Hz, 1H, H-3’’), 4.65 (dd, 8.5, 3.5 Hz, 1H, H-5’’), 4.16 (dd, 11.5, 3.5 Hz, 1H, H-6’’A), 4.06 (dd, 11.5, 8.5 Hz, 1H, H-6’’B), 2.16 (s, 3H, -CH_3 e), 2.01 (s, 3H, -CH_3 d), 1.96 (s, 3H, -CH_3 c), 1.93 (s, 3H, -CH_3 b), 1.89 (s, 3H, -CH_3 a). **^{13}C-NMR (125 MHz, $(CD_3)_2SO$ /CF_3COOD 95:5)** δ170.1 (C=O), 134.9 (C4), 131.6 (C6’), 126.9 (C2’), 98.6 (C1”), 115.7 (C6), 116.8 (C8), 71.6 (C5”), 70.6 (C3”), 68.4 (C2”), 67.5 (C4”), 62.6 (C6”A/B), 20.4 (CH_3). UV-Vis λ_{max} (methanol): 516 nm. HRMS: m/z (ESI$^+$) calculated for [M$^+$]: 659.1607; found [M$^+$]: 659.1620. Purity: 77.9%. Yield: 14.1% CGE.

Cy3gal hexaacetate (Cyanidin-3-β-*O*-(4',7,2'',3'',4'',6''-hexaacetylgalactoside)), 49

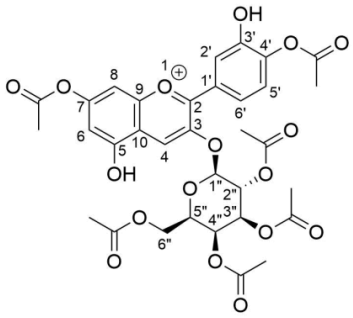

^{1}H-NMR (500 MHz, $(CD_3)_2SO/CF_3COOD$ 95:5) δ 9.07 (s, 1H, H-4), 8.25 (dd, *J* = 8.5, 2.0 Hz, 1H, H-6'), 8.16 (d, *J* = 2.0 Hz, 1H, H-2'), 7.20 (d, *J* = 8.5 Hz, 1H, H-5'), 7.01 (d, *J* = 2.5 Hz, 1H, H-8), 6.85 (d, *J* = 2.0 Hz, 1H, H-6), 6.03 (d, *J* = 7.5 Hz, 1H, anomeric H-1''), 5.45 (d, 4.0 Hz, 1H, H-4''), 5.40 (dd, *J* = 10.0, 7.5 Hz, 1H, H-2''), 5.27 (dd, 10.5, 3.5 Hz, 1H, H-3''), 4.40 (dd, 8.0, 3.5 Hz, 1H, H-5''), 4.11 (dd, 12.0, 4.0 Hz, 1H, H-6''A), 4.06 (dd, 12.0, 8.5 Hz, 1H, H-6''B), 2.33 (s, 3H, -CH_3 f), 2.16 (s, 3H, -CH_3 e), 2.01 (s, 3H, -CH_3 d), 1.96 (s, 3H, -CH_3 c), 1.91 (s, 3H, -CH_3 b), 1.87 (s, 3H, -CH_3 a). **^{13}C-NMR (125 MHz, $(CD_3)_2SO$ /CF_3COOD 95:5)** δ170.4 (C=O), 134.9 (C4), 131.6 (C6'), 126.9 (C2'), 98.6 (C1"), 115.9 (C6), 121.3 (C8), 71.6 (C5"), 70.6 (C3"), 68.4 (C2"), 67.5 (C4"), 62.6 (C6"A/B), 20.7 (CH_3). HRMS: m/z (ESI^+) calculated for [M^+]: 701.1712; found [M^+]: 701.1724. Purity: 71.1%. Yield: 6.9% CGE.

Cy3gal monobutanoate (Cyanidin-3-β-*O*-(6''-butyrylgalactoside)), 50

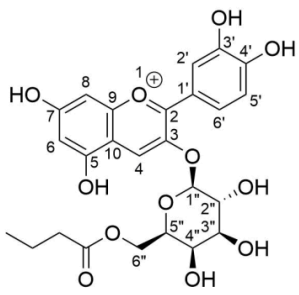

^{1}H-NMR (500 MHz, $(CD_3)_2SO/CF_3COOD$ 95:5) δ 8.79 (s, 1H, H-4), 8.24 (dd, *J* = 9.0, 2.5 Hz, 1H, H-6'), 7.98 (d, *J* = 2.5 Hz, 1H, H-2'), 7.03 (d, *J* = 9.0 Hz, 1H, H-5'), 6.90 (d, *J* = 2.0 Hz, 1H, H-8), 6.72 (d, *J* = 2.0 Hz, 1H, H-6), 5.33 (d, *J* = 8.0 Hz, 1H, anomeric H-1''), 4.22 (dd, 11.5, 3.0 Hz, 1H, H-6''A), 4.13 (dd, 12.0, 9.0 Hz, 1H, H-6"B), 4.05-4.08 (m, 1H, H-5''), 3.83 (dd, *J* = 9.5, 7.5 Hz, 1H, H-2''), 3.76 (d, 3.0 Hz, 1H, H-4''), 3.55 (dd, 9.5, 3.0 Hz, 1H, H-3''), 2.24 (dt, 7.5, 5.5 Hz, 2H, CH_2-α), 1.45 (ddd, 14.5, 7.0, 5.0 Hz, 2H, CH_2-β), 0.77 (s, 3H, -CH_3). **^{13}C-NMR (125 MHz, $(CD_3)_2SO$ /CF_3COOD 95:5)** δ173.2 (C=O), δ168.4 (C7), 162.1 (C2), 159.3 (C9), 156.1 (C5), 154.6 (C4'), 146.4 (C1'), 144.6 (C3), 134.2 (C4), 127.4 (C6'), 119.9 (C3'), 117.7 (C2'), 117.0 (C5'), 111.9 (C10), 102.5 (C1"), 102.2 (C6), 94.4 (C8), 73.7 (C5"), 72.9 (C3"), 70.1(C2"), 68.8 (C4"), 64.2 (C6"A/B), 35.5 (CH_2-α), 18.3 (CH_2-β), 13.7 (CH_3). UV-Vis λ_{max} (methanol): 527 nm. HRMS: m/z (ESI^+) calculated for [M^+]: 519.1497; found [M^+]: 519.1514. Purity: 71.2%. Yield: 11.8% CGE.

Cy3gal dibutanoate (Cyanidin-3-β-*O*-(3'',6''- dibutyrylgalactoside)), 51

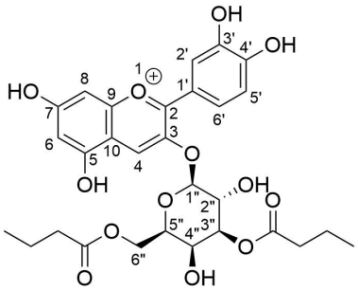

^{1}H-NMR (500 MHz, $(CD_3)_2SO/CF_3COOD$ 95:5) δ 8.81 (s, 1H, H-4), 8.22 (dd, *J* = 8.5, 2.0 Hz, 1H, H-6'), 7.97 (d, *J* = 2.5 Hz, 1H, H-2'), 7.03 (d, *J* = 8.5 Hz, 1H, H-5'), 6.91 (d, *J* = 1.0 Hz, 1H, H-8), 6.73 (d, *J* = 1.5 Hz, 1H, H-6), 5.52 (d, *J* = 7.5 Hz, 1H, anomeric H-1''), 4.81 (dd, 10.5, 3.5 Hz, 1H, H-3''), 4.12-4.22 (m, 3H, H-6''A, H-6"B, H-5''), 4.08 (dd, *J* = 10.5, 7.5 Hz, 1H, H-2''), 3.96 (d, 3.5 Hz, 1H, H-4''), 2.33-2.38 (m, 2H, CH_2-α a), 2.22-2.28 (m, 2H, CH_2-α b), 1.58-1.62 (m, 2H, CH_2-β a), 1.41-1.47 (m, 2H, CH_2-β b), 0.93 (s, 3H, -CH_3 a), 0.78 (s, 3H, -CH_3 b). **^{13}C-NMR (125 MHz, $(CD_3)_2SO$ /CF_3COOD 95:5)** δ173.2 (C=O a), δ173.2 (C=O b), 134.2 (C4), 127.4 (C6'), 117.7 (C2'), 102.2 (C1"), 102.5 (C6), 94.4 (C8), 73.7 (C5"), 72.9 (C3"), 70.1(C2"), 68.8 (C4"), 64.2 (C6"A/B), 35.5 (CH_2-α), 18.3 (CH_2-β), 13.7 (CH_3). UV-Vis λ_{max} (methanol): 531 nm. HRMS: m/z (ESI^+) calculated for [M^+]: 589.1916; found [M^+]: 589.1922. Purity: 82.2%. Yield: 15.4% CGE.

Cy3gal monooctanoate (Cyanidin-3-β-*O*-(6''- caprylylgalactoside)), 52

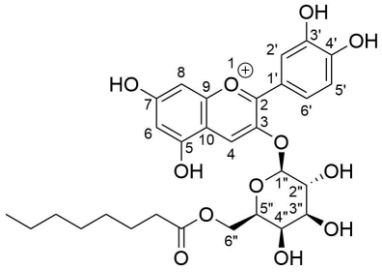

^{1}H-NMR (500 MHz, $(CD_3)_2SO/CF_3COOD$ 95:5) δ 8.78 (s, 1H, H-4), 8.24 (dd, *J* = 9.0, 2.5 Hz, 1H, H-6'), 7.99 (d, *J* = 2.5 Hz, 1H, H-2'), 7.03 (d, *J* = 8.5 Hz, 1H, H-5'), 6.91 (d, *J* = 1.0 Hz, 1H, H-8), 6.71 (d, *J* = 1.5 Hz, 1H, H-6), 5.34 (d, *J* = 8.0 Hz, 1H, anomeric H-1''), 4.26 (dd, 11.5, 8.5 Hz, 1H, H-6''A), 4.05-4.10 (m, 2H, H-5'', H-6"B), 3.83 (dd, *J* = 9.5, 8.0 Hz, 1H, H-2''), 3.76 (d, 3.5 Hz, 1H, H-4''), 3.55 (dd, 9.5, 3.5 Hz, 1H, H-3''), 2.17 (t, 7.5 Hz, 2H, CH_2-α), 1.48 (m, 2H, CH_2-β), 1.26 (m, 7.5 Hz, 2H, $(CH_2)_{4-7}$), 0.84 (t, 7.5 Hz, 3H, -CH_3). **^{13}C-NMR (125 MHz, $(CD_3)_2SO$ /CF_3COOD 95:5)** 134.3 (C4), 127.3 (C6'), 117.5 (C2'), 116.8 (C5'), 102.4 (C1"), 102.4 (C6), 94.0 (C8), 73.6 (C5"), 72.8 (C3"), 69.9 (C2"), 68.5 (C4"), 63.7 (C6"A/B), 33.9 (CH_2-α), 24.9 (CH_2-β), 22.4 (CH_2)4-7, 14.2 (CH_3). UV-Vis λ_{max} (methanol): 531 nm. HRMS: m/z (ESI^+) calculated for [M^+]: 575.2123; found [M^+]: 575.2127. Purity: 81.5%. Yield: 8.5% CGE.

Cy3gal dioctanoate (Cyanidin-3-β-*O*-(3'',6''- dibutyrylgalactoside)), 53

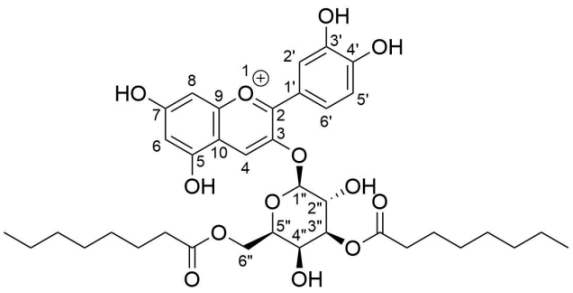

^{1}H-NMR (500 MHz, $(CD_3)_2SO/CF_3COOD$ 95:5) δ 8.80 (s, 1H, H-4), 8.21 (dd, *J* = 8.5, 2.5 Hz, 1H, H-6'), 7.97 (d, *J* = 2.5 Hz, 1H, H-2'), 7.03 (d, *J* = 8.5 Hz, 1H, H-5'), 6.91 (d, *J* = 2.0 Hz, 1H, H-8), 6.72 (d, *J* = 2.0 Hz, 1H, H-6), 5.52 (d, *J* = 8.0 Hz, 1H, anomeric H-1''), 4.81 (dd, 10.0, 3.5 Hz, 1H, H-3''), 4.25 (dd, 11.0, 9.0 Hz, 1H, H-6''A), 4.19 (dd, 8.5, 3.0, 1H, H-5''), 4.10 (dd, 11.0, 3.0 Hz, 1H, H-6"B), 4.08 (dd, *J* = 10.0, 7.5 Hz, 1H, H-2''), 3.95 (d, 3.5 Hz, 1H, H-4''), Acyl moiety 1: 2.25 (m, 2H, CH_2-α), 2.17 (m, 2H, CH_2-β), 1.25 (m, 2H, $(CH_2)_{4-7}$), 0.78 (s, 3H, $-CH_3$), Acyl moiety 2: 1.57 (m, 2H, CH_2-α), 1.38 (m, 2H, CH_2-β), 1.25 (m, 2H, $(CH_2)_{4-7}$), 0.84 (s, 3H, $-CH_3$). **^{13}C-NMR (125 MHz, $(CD_3)_2SO$ /CF_3COOD 95:5)** 135.2 (C4), 128.6 (C6'), 118.8 (C2'), 102.7 (C1"), 103.5 (C6), 95.5 (C8), 73.9 (C5"), 76.4 (C3"), 68.3 (C2"), 66.8 (C4"), 64.1 (C6"A/B), 34.5 (CH_2-α), 25.8 (CH_2-β), 29.6 (CH_2)4-7, 15.1 (CH_3). UV-Vis λ_{max} (methanol): 527 nm. HRMS: m/z (ESI$^+$) calculated for [M$^+$]: 701.3168; found [M$^+$]: 701.3171. Purity: 80.4%. Yield: 2.1% CGE.

7.22. Acetonation of Anthocyanins

Isopropylidene derivatives of anthocyanins were obtained by condensation of anthocyanins extracted from *Aronia* skin waste (20 mg, 0.044 mmol, 1 eq) which were initially dissolved in dry acetone (2.33 ml) in the presence of TFA (1% v/v of solvent, 0.02 mL) as the catalysts. The anhydrous acetone serves both as the solvent and the reagent. Activated SiO_2 (60 mg) was added as a drying agent to absorb water as the acidic wet condition could hydrolyse the products. The reaction is performed at 40 °C, and it is completed in 3 hours under N_2 stream. The reaction mixture was filtered off to remove SiO_2 and unreacted anthocyanins by gravity filtration. The filtrate was neutralised by adding $NaHCO_3$ solid before the evaporation. The completion of the reaction was determined by HRMS. After the reaction was complete, an aliquot (10 µl) was diluted with DMSO up to 100 µl and analysed by HRMS. Every step was checked by HRMS. The HRMS chromatograms showed the m/z [M$^+$] of 489.1391 and 459.1248, calculated [M$^+$] 489.1391 and 459.1286, which belong to

isopropylidene derivatives of Cy3gal and Cy3ara. The reaction was also carried out in deuterated acetone (CD_3COCD_3) and deuterated TFA (CF_3COOD) in the same manner. Through this reaction, the characterisation of isopropylidene derivatives of Cy3gal is possible.

Cyanidin-3-*O*-4,6-*O*-isopropylidene-β-galactoside, 54

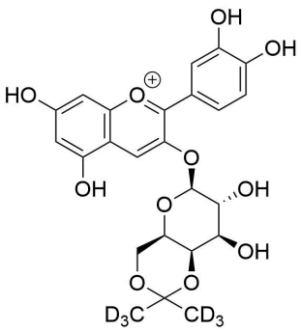

^{1}H-NMR (500 MHz, CD_3COCD_3/CF_3COOD 95:5) δ 9.13 (s, 1H, H-4), 8.40 (dd, *J* = 8.5, 2.0 Hz, 1H, H-6'), 8.20 (d, *J* = 2.5 Hz, 1H, H-2'), 7.15 (d, *J* = 2.5 Hz, 1H, H-8), 7.13 (d, *J* = 8.5 Hz, 1H, H-5'), 6.87 (d, *J* = 2.0 Hz, 1H, H-6), 5.49 (d, *J* = 7.5 Hz, 1H, anomeric H-1''), 4.42 (dd, 5.5, 2.0 Hz, 1H, H-4''), 4.34 (dd, 6.0, 2.5, 1H, H-5''), 4.32 (t, 6.5 Hz, 1H, H-3''), 4.23 (dd, 13.0, 2.0 Hz, 1H, H-6''A), 4.02 (dd, *J* = 7.0, 6.5 Hz, 1H, H-2''), 3.85 (dd, 13.5, 2.0 Hz, 1H, H-6"B). C$\underline{D}_3$ signals were not recorded. HRMS: m/z (ESI$^+$) calculated for [M$^+$]: 495.1768; found [M$^+$]: 495.1787.

List of References

1 N. Martins and I. C. F. R. Ferreira, *Trends Food Sci. Technol.*, 2017, **62**, 33–48.

2 N. Kryževičiute, P. Kraujalis and P. R. Venskutonis, *J. Supercrit. Fluids*, 2016, **108**, 61–68.

3 L. Grunovaite, M. Pukalskiene, A. Pukalskas and P. R. Venskutonis, *J. Funct. Foods*, 2016, **24**, 85–96.

4 J. Oszmianski and A. Wojdylo, *Eur. Food Res. Technol.*, 2005, **221**, 809–813.

5 J. M. Kong, L. S. Chia, N. K. Goh, T. F. Chia and R. Brouillard, *Phytochemistry*, 2003, **64**, 923–933.

6 A. Castañeda-Ovando, M. de L. Pacheco-Hernández, M. E. Páez-Hernández, J. A. Rodríguez and C. A. Galán-Vidal, *Food Chem.*, 2009, **113**, 859–871.

7 I. Ignat, I. Volf and V. I. Popa, *Food Chem.*, 2011, **126**, 1021–1035.

8 G. T. Sigurdson, R. J. Robbins, T. M. Collins and M. M. Giusti, *Food Chem.*, 2017, **221**, 1088–1095.

9 A. De Villiers, P. Venter and H. Pasch, *J. Chromatogr. A*, 2015, **1430**, 16–78.

10 J. S. Barnes, H. P. Nguyen, S. Shen and K. A. Schug, *J. Chromatogr. A*, 2009, **1216**, 4728–4735.

11 F. C. Stintzing and R. Carle, *Trends Food Sci. Technol.*, 2004, **15**, 19–38.

12 H. S. Lee and V. Hong, *J. Chromatogr.*, 1992, **624**, 221–234.

13 C. Adaku, I. Skaar, H. Berland, R. Byamukama, M. Jordheim and Ø. M. Andersen, *Phytochem. Lett.*, 2019, **29**, 225–230.

14 Y. Tanaka, N. Sasaki and A. Ohmiya, *Plant J.*, 2008, **54**, 733–749.

15 L. Cabrita, T. Fossen and O. M. Andersen, *Food Chem.*, 2000, **68**, 101–107.

16 Z. Y. Ju and L. R. Howard, *J. Agric. Food Chem.*, 2003, **51**, 5207–5213.

17 K. Springob, J. Nakajima, M. Yamazaki and K. Saito, *Nat. Prod. Rep.*, 2003, **20**, 288–303.

18 F. He, L. Mu, G. L. Yan, N. N. Liang, Q. H. Pan, J. Wang, M. J. Reeves and C. Q. Duan, *Molecules*, 2010, **15**, 9057–9091.

19 H. Du, J. Wu, K. X. Ji, Q. Y. Zeng, M. W. Bhuiya, S. Su, Q. Y. Shu, H. X. Ren, Z. A. Liu and L. S. Wang, *J. Exp. Bot.*, 2015, **66**, 6563–6577.

20 O. Dangles and J.-A. Fenger, *Molecules*, 2018, **23**, 1–23.

21 J. E. Farr, G. T. Sigurdson and M. M. Giusti, *Food Chem.*, 2019, **278**, 443–451.

22 V. de Freitas and N. Mateus, *Environ. Chem. Lett.*, 2006, **4**, 175–183.

23 C. L. Zhao, Y. Q. Yu, Z. J. Chen, G. S. Wen, F. G. Wei, Q. Zheng, C. De Wang and X. L. Xiao, *Food Chem.*, 2017, **214**, 119–128.

24 F. Heidarizadeh and F. Abadast, *Orient. J. Chem.*, 2011, **27**, 1421–1436.

25 F. Pina, *J. Agric. Food Chem.*, 2014, **62**, 6885–6897.

26 B. Berké, C. Chèze, J. Vercauteren and G. Deffieux, *Tetrahedron Lett.*, 1998, **39**, 5771–5774.

27 Y. Lu and L. Y. Foo, *Tetrahedron Lett.*, 2001, **42**, 1371–1373.

28 M. Schwarz and P. Winterhalter, *Tetrahedron Lett.*, 2003, **44**, 7583–7587.

29 P. Trouillas, J. C. Sancho-García, V. De Freitas, J. Gierschner, M. Otyepka and O. Dangles, *Chem. Rev.*, 2016, **116**, 4937–4982.

30 K. Yoshida, M. Mori and T. Kondo, *Nat. Prod. Rep.*, 2009, **26**, 884–915.

31 S. Asen, R. N. Stewart and K. H. Norris, *Phytochemistry*, 1972, **11**, 1139–1144.

32 F. L. Han and Y. Xu, *South African J. Enol. Vitic.*, 2015, **36**, 105–116.

33 D. G. Coffey, F. M. Clydesdale, F. J. Francis and R. A. Damon, *J. Food Prot.*, 1981, **44**, 516–523.

34 L. Estévez, N. Otero and R. A. Mosquera, *Theor. Chem. Acc.*, 2011, **128**, 485–495.

35 T. Fossen, L. Cabrita and O. M. Andersen, *Food Chem.*, 1998, **63**, 435–440.

36 F. Nave, V. Petrov, F. Pina, N. Teixeira, N. Mateus and V. De Freitas, *J. Phys. Chem. B*, 2010, **114**, 13487–13496.

37 V. O. Silva, A. A. Freitas, A. L. Maçanita and F. H. Quina, *J. Phys. Org. Chem.*, 2016, **29**, 594–599.

38 F. Pina, J. Oliveira and V. De Freitas, *Tetrahedron*, 2015, **71**, 3107–3114.

39 J. Oliveira, N. F. Brás, M. A. Da Silva, N. Mateus, A. J. Parola and V. De Freitas, *Phytochemistry*, 2014, **105**, 178–185.

40 J. Fleschhut, F. Kratzer, G. Rechkemmer and S. E. Kulling, *Eur. J. Nutr.*, 2006, **45**, 7–18.

41 K. Trošt, A. Golc-Wondra, M. Prošek and L. Milivojevič, *J. Food Sci.*, 2008, **73**, 405–411.

42 C. Malien-Aubert, O. Dangles and M. J. Amiot, *J. Agric. Food Chem.*, 2000, **49**, 170–176.

43 L. Jakobek, M. Šeruga, M. Medvidović-Kosanović and I. Novak, *Dtsch. Leb.*, 2007, **103**, 58–64.

44 L. Jakobek, M. Seruga, I. Novak and M. Medvidovic-Kosanovic, *Deutshce Leb.*, 2007, **103**, 369–378.

45 M. J. Bermúdez-Soto, F. A. Tomás-Barberán and M. T. García-Conesa, *Food Chem.*, 2007, **102**, 865–874.

46 D. Zapolska-Downar, D. Bryk, M. Małecki, K. Hajdukiewicz and D. Sitkiewicz, *Eur. J. Nutr.*, 2012, **51**, 563–572.

47 D. A. Martin, R. Taheri, M. H. Brand, A. Draghi, F. A. Sylvester and B. W. Bolling, *J. Funct. Foods*, 2014, **8**, 68–75.

48 K. Appel, P. Meiser, E. Millán, J. A. Collado, T. Rose, C. C. Gras, R. Carle and E. Muñoz, *Fitoterapia*, 2015, **105**, 73–82.

49 S. J. Hwang, W. B. Yoon, O. H. Lee, S. J. Cha and J. D. Kim, *Food Chem.*, 2014, **146**, 71–77.

50 D. Rugină, Z. Sconţa, L. Leopold, A. Pintea, A. Bunea and C. Socaciu, *J. Med. Food*, 2012, **15**, 700–6.

51 K. Gąsiorowski, K. Szyba, B. Brokos, B. Kołaczyńska, M. Jankowiak-Włodarczyk and J. Oszmiański, *Cancer Lett.*, 1997, **119**, 37–46.

52 L. Sueiro, G. G. Yousef, D. Seigler, E. G. De Mejia, M. H. Grace and M. A. Lila, *J. Food Sci.*, 2006, **71**, 480–488.

53 M. Bräunlich, R. Slimestad, H. Wangensteen, C. Brede, K. E. Malterud and H. Barsett, *Nutrients*, 2013, **5**, 663–678.

54 V. Sivakumar, J. Vijaeeswarri and J. L. Anna, *Ind. Crops Prod.*, 2011, **33**, 116–122.

55 P. Velmurugan, J. I. Kim, K. Kim, J. H. Park, K. J. Lee, W. S. Chang, Y. J. Park, M. Cho and B. T. Oh, *J. Photochem. Photobiol. B Biol.*, 2017, **173**, 571–579.

56 B. A. Cevallos-Casals and L. Cisneros-Zevallos, *Food Chem.*, 2004, **86**, 69–77.

57 F. Fernandez-Aulis, A. Torres, E. Sanchez-Mendoza, L. Cruz and A. Navarro-Ocana, *Food Chem.*, 2019, **309**, 1–8.

58 W. Yang, M. Kortesniemi, X. Ma, J. Zheng and B. Yang, *Food Chem.*, 2019, **281**, 189–196.

59 A. Kokotkiewicz, Z. Jaremicz and M. Luczkiewicz, *J. Med. Food*, 2010, **13**, 255–269.

60 M. H. Brand, *Arnoldia*, 2010, **67**, 14–25.

61 J. Bussières, S. Boudreau, G. Clément-Mathieu, B. Dansereau and L. Rochefort, *HortScience*, 2008, **43**, 494–499.

62 T. Hirvi and E. Honkanen, *J. Sci. Food Agric.*, 1985, **36**, 808–810.

63 B. Strik, C. Finn and R. Wrolstad, *Acta Hortic.*, 2003, **626**, 447–451.

64 B. W. Bolling, R. Taheri, R. Pei, S. Kranz, M. Yu, S. N. Durocher and M. H. Brand, *Food Chem.*, 2015, **187**, 189–196.

65 J. Oszmianski and J. C. Sapis, *J. Food Sci.*, 1988, **53**, 1241–1242.

66 N. Kardum, M. Takić, K. Šavikin, M. Zec, G. Zdunić, S. Spasić and A. Konić-Ristić, *J. Funct. Foods*, 2014, **9**, 89–97.

67 L. Jakobek, M. Drenjančević, V. Jukić and M. Šeruga, *Sci. Hortic. (Amsterdam).*, 2012, **147**, 56–63.

68 M. Sójka, K. Kołodziejczyk and J. Milala, *Ind. Crops Prod.*, 2013, **51**, 77–86.

69 R. Taheri, B. A. Connolly, M. H. Brand and B. W. Bolling, *J. Agric. Food Chem.*, 2013, **61**, 8581–8588.

70 M. Vagiri and M. Jensen, *Food Chem.*, 2017, **217**, 409–417.

71 F. Bucar, A. Wube and M. Schmid, *Nat. Prod. Rep.*, 2013, **30**, 525–545.

72 S. Sasidharan, Y. Chen, D. Saravanan, K. M. Sundram and L. Yoga Latha, *African J. Tradit. Complement. Altern. Med.*, 2011, **8**, 1–10.

73 S. S. Handa, S. P. S. Khanuja, G. Longo and D. D. Rakesh, *Extraction Technologies for Medicinal and Aromatic Plants*, Italy, 2008, vol. 5.

74 M. Naczk and F. Shahidi, *J. Chromatogr. A*, 2004, **1054**, 95–111.

75 L. Galvan D'Alessandro, K. Kriaa, I. Nikov and K. Dimitrov, *Sep. Purif. Technol.*, 2012, **93**, 42–47.

76 M. Ramić, S. Vidović, Z. Zeković, J. Vladić, A. Cvejin and B. Pavlić, *Ultrason. Sonochem.*, 2015, **23**, 360–368.

77 Y. Xu, Y. Qiu, H. Ren, D. Ju and H. Jia, *Prep. Biochem. Biotechnol.*, 2016, **47**, 312–321.

78 E. Espada-Bellido, M. Ferreiro-González, C. Carrera, M. Palma, C. G. Barroso and G. F. Barbero, *Food Chem.*, 2017, **219**, 23–32.

79 N. Ćujić, K. Šavikin, T. Janković, D. Pljevljakušić, G. Zdunić and S. Ibrić, *Food Chem.*, 2016, **194**, 135–142.

80 J. Heinonen, H. Farahmandazad, A. Vuorinen, H. Kallio, B. Yang and T. Sainio, *Food Bioprod. Process.*, 2016, **99**, 136–146.

81 P. Denev, M. Ciz, G. Ambrozova, A. Lojek, I. Yanakieva and M. Kratchanova, *Food Chem.*, 2010, **123**, 1055–1061.

82 J. Chandrasekhar, M. C. Madhusudhan and K. S. M. S. Raghavarao, *Food Bioprod. Process.*, 2012, **90**, 615–623.

83 A. Kraemer-Schafhalter, H. Fuchs and W. Pfannhauser, *J. Sci. Food Agric.*, 1998, **78**, 435–440.

84 E. M. Silva, D. R. Pompeu, Y. Larondelle and H. Rogez, *Sep. Purif. Technol.*, 2007, **53**, 274–280.

85 L. Galván D'Alessandro, P. Vauchel, R. Przybylski, G. Chataigné, I. Nikov and K. Dimitrov, *Sep. Purif. Technol.*, 2013, **120**, 92–101.

86 V. Camel, *Specrochimica Acta Part B*, 2005, **58**, 1177–1233.

87 C. Erger and T. C. Schmidt, *TrAC - Trends Anal. Chem.*, 2014, **61**, 74–82.

88 A. Andrade-Eiroa, M. Canle, V. Leroy-Cancellieri and V. Cerda, *TrAC - Trends Anal. Chem.*, 2016, **80**, 641–654.

89 M. M. Giusti, L. E. Rodríguez-Saona, D. Griffin and R. E. Wrolstad, *J. Agric. Food Chem.*, 1999, **47**, 4657–4664.

90 K. R. Määttä-Riihinen, A. Kamal-Eldin, P. H. Mattila, A. M. González-Paramás and R. Törrönen, *J. Agric. Food Chem.*, 2004, **52**, 4477–4486.

91 N. Gao, Y. Wang, X. Jiao, S. Chou, E. Li and B. Li, *Molecules*, 2018, **23**, 1–14.

92 J. Lee, R. W. Durst and R. E. Wrolstad, *J. AOAC Int.*, 2005, **88**, 1269–1278.

93 C. Qin, Y. Li, W. Niu, Y. Ding, R. Zhang and X. Shang, *Czech J. Food Sci.*, 2010, **28**, 117–126.

94 L. Ekici, Z. Simsek, I. Ozturk, O. Sagdic and H. Yetim, *Food Anal. Methods*, 2014, **7**, 1328–1336.

95 M. M. Giusti and R. E. Wrolstad, *Biochem. Eng. J.*, 2003, **14**, 217–225.

96 L. Galván D'Alessandro, K. Dimitrov, P. Vauchel and I. Nikov, *Chem. Eng. Res. Des.*, 2014, **92**, 1818–1826.

97 K. N. Prasad, E. Yang, C. Yi, M. Zhao and Y. Jiang, *Innov. Food Sci. Emerg. Technol.*, 2009, **10**, 155–159.

98 G. L. Liu, H. H. Guo and Y. M. Sun, *Int. J. Mol. Sci.*, 2012, **13**, 6292–6302.

99 S. Farooque, P. M. Rose, M. Benohoud, R. S. Blackburn and C. M. Rayner, *J. Agric. Food Chem.*, 2018, **66**, 12265–12273.

100 N. Beaumont, Master Thesis, University of Leeds, 2015.

101 X. Qiu, N. Li, X. Ma, S. Yang, Q. Xu, H. Li and J. Lu, *J. Environ. Chem. Eng.*, 2014, **2**, 745–751.

102 P. Atkins and J. de Paula, *Atkin's Physical Chemistry*, Oxford: Oxford Universoty Press, 10th editi., 2014.

103 X. Liu, Z. Xu, Y. Gao, B. Yang, J. Zhao and L. Wang, *Int. J. Food Eng.*, 2007, **3**, 1–16.

104 A. C. Pedro, D. Granato and N. D. Rosso, *Food Chem.*, 2016, **191**, 12–20.

105 A. Chandra, J. Rana and Y. Li, *J. Agric. Food Chem.*, 2001, **49**, 3515–3521.

106 T. Esatbeyoglu, M. Rodríguez-Werner and P. Winterhalter, *Eur. Food Res. Technol.*, 2017, **243**, 1261–1275.

107 R. Edelman, I. Kusner, R. Kisiliak, S. Srebnik and Y. D. Livney, *Food Hydrocoll.*, 2015, **48**, 27–37.

108 M. H. Wathon, N. Beaumont, M. Benohoud, R. S. Blackburn and C. M. Rayner, *Color. Technol.*, 2019, **135**, 5–16.

109 M. Monagas, B. Bartolomé and C. Gómez-Cordovés, *Crit. Rev. Food Sci. Nutr.*, 2005, **45**, 85–118.

110 U. Takahama, R. Yamauchi and S. Hirota, *Food Chem.*, 2013, **141**, 282–288.

111 T. Ichiyanagi, K. Oikawa, C. Tateyama and T. Konishi, *Chem. Pharm. Bull*, 2001, **49**, 114–117.

112 M. Jordheim, T. Fossen and Ø. Y. M. Andersen, *J. Agric. Food Chem.*, 2006, **54**, 9340–9346.

113 C. Gauche, E. D. Malagoli and M. T. B. Luiz, *Sci. Agric.*, 2010, **67**, 41–46.

114 M. M. Giusti, L. E. Rodríguez-Saona and R. E. Wrolstad, *J. Agric. Food Chem.*, 1999, **47**, 4631–4637.

115 C. R. Welcha, Q. Wub and J. E. Simonb, *Curr. Anal. Chem.*, 2008, **4**, 75–101.

116 R. Myjavcová, P. Marhol, V. Křen, V. Šimánek, J. Ulrichová, I. Palíková, B. Papoušková, K. Lemr and P. Bednář, *J. Chromatogr. A*, 2010, **1217**, 7932–7941.

117 A. Fernandes, A. Sousa, J. Azevedo, N. Mateus and V. De Freitas, *Food Res. Int.*, 2013, **51**, 748–755.

118 M. Jordheim, K. Aaby, T. Fossen, G. Skrede and Ø. M. Andersen, *J. Agric. Food Chem.*, 2007, **55**, 10591–10598.

119 B. Inaki, J. I. Santos, G. del Campo and J. I. Miranda, *Talanta*, 2003, **61**, 139–145.

120 J. Ramirez-Perez, C. Maria and C. P. Santacruz, *Renewables Wind. Water, Sol.*, 2019, **6**, 1–15.

121 J. Nti-Gyabaah, K. Gbewonyo and Y. C. Chiew, *J. Chem. Eng. Data*, 2010, **55**, 3356–3363.

122 K. Ramluckan, K. G. Moodley and F. Bux, *Fuel*, 2014, **116**, 103–108.

123 M. H. Abraham, H. S. Chadha, G. S. Whiting and R. C. Mitchell, *J. Pharm. Sci.*, 1994, **83**, 1085–1100.

124 C. D. Stalikas, *J. Sep. Sci.*, 2007, **30**, 3268–3295.

125 J. Penso, K. C. F. A. Cordeiro, C. R. M. da Cunha, P. F. da S. Castro, D. R. Martins, L. M. Lião, M. L. Rocha and V. de Oliveira, *Eur. J. Pharmacol.*, 2014, **733**, 75–80.

126 S. Gómez-Alonso, D. Blanco-Vega, M. V. Gómez and I. Hermosín-Gutiérrez, *J. Agric. Food Chem.*, 2012, **60**, 12210–12223.

127 J. Lee, C. Rennaker and R. E. Wrolstad, *Food Chem.*, 2008, **110**, 782–786.

128 N. Ahmadiani, R. J. Robbins, T. M. Collins and M. M. Giusti, *Food Chem.*, 2016, **197**, 900–906.

129 G. T. Sigurdson, R. J. Robbins, T. M. Collins and M. Mónica Giusti, *Food Chem.*, 2018, **271**, 497–504.

130 K. Torskangerpoll and Ø. M. Andersen, *Food Chem.*, 2005, **89**, 427–440.

131 C. Grajeda-Iglesias, M. C. Figueroa-Espinoza, N. Barouh, B. Barea, A. Fernandes, V. De Freitas and E. Salas, *J. Nat. Prod.*, 2016, **79**, 1709–1718.

132 Y. Leydet, R. Gavara, V. Petrov, A. M. Diniz, A. Jorge Parola, J. C. Lima and F. Pina, *Phytochemistry*, 2012, **83**, 125–135.

133 M. M. Giusti, L. E. Rodriguez-Saona and R. E. Wrolstad, *J. Agric. Food Chem.*, 1999, **47**, 4631–4637.

134 E. Revilla, J. M. Ryan and G. Martín-Ortega, *J. Agric. Food Chem.*, 1998, **46**, 4592–4597.

135 S. Sipahli, V. Mohanlall and J. J. Mellem, *Food Sci. Technol.*, 2017, **37**, 209–215.

136 W. Wiczkowski, D. Szawara-nowak and J. Topolska, *Food Res. Int.*, 2013, **51**, 303–309.

137 R. Slimestad, K. Torskangerpoll, H. S. Nateland, T. Johannessen and N. H. Giske, *J. Food Compos. Anal.*, 2005, **18**, 61–68.

138 J. K. Monrad, L. R. Howard, J. W. King, K. Srinivas and A. Mauromoustakos, *J. Agric. Food Chem.*, 2010, **58**, 2862–2868.

139 A. Trummal, L. Lipping, I. Kaljurand, I. A. Koppel and I. Leito, *J. Phys. Chem. A*, 2016, **120**, 3663–3669.

140 M. D. Liptak and G. C. Shields, *Int. J. Quantum Chem.*, 2001, **85**, 727–741.

141 B. A. Wellen, E. A. Lach and H. C. Allen, *Phys. Chem. Chem. Phys.*, 2017, **19**, 26551–26558.

142 D. Mazzarella, G. E. M. Crisenza and P. Melchiorre, *J. Am. Chem. Soc.*, 2018, **140**, 8439–8443.

143 M. Danihelová, J. Viskupičová and E. Šturdík, *Acta Chim. Slovaca*, 2012, **5**, 59–69.

144 C. Grajeda-Iglesias, E. Salas, N. Barouh, B. Baréa and M. C. Figueroa-Espinoza, *Food Chem.*, 2017, **230**, 189–194.

145 L. Cruz, I. Fernandes, M. Guimarães, V. de Freitas and N. Mateus, *Food*

Funct., 2016, **7**, 2754–2762.

146 N. S. Mosier, C. M. Ladisch and M. R. Ladisch, *Biotechnol. Bioeng.*, 2002, **79**, 610–618.

147 R. Brouillard and J. Dubois, *J. Am. Chem. Soc.*, 1977, **99**, 1359–1364.

148 G. C. Cretu and G. E. Morlock, *Food Chem.*, 2014, **146**, 104–112.

149 H. T. Hong, M. E. Netzel and T. J. O'Hare, *Food Chem.*, 2020, **319**, 126515.

150 S. Hosseini, M. Gharachorloo, B. Ghiassi-Tarzi and M. Ghavami, *Polish J. Food Nutr. Sci.*, 2016, **66**, 261–269.

151 R. Brouillard, *Phytochemistry*, 1983, **22**, 1311–1323.

152 A. Fernandes, G. Ivanova, N. F. Brás, N. Mateus, M. J. Ramos, M. Rangel and V. De Freitas, *Carbohydr. Polym.*, 2014, **102**, 269–277.

153 H. Santos, D. L. Turner, J. C. Lima, P. Figueiredo, F. S. Pina, A. L. Maçanita, N. Terahara, H. Suzuki, K. Toki, H. Kuwano, N. Saito and T. Honda, *J. Nat. Prod.*, 1993, **56**, 335–340.

154 C. A. Glass, *Can. J. Chem.*, 1965, **43**, 2652–2659.

155 J. L. Dong, L. S. H. Yu and J. W. Xie, *ACS Omega*, 2018, **3**, 4974–4985.

156 S. Pati, M. T. Liberatore, G. Gambacorta, D. Antonacci and E. La Notte, *J. Chromatogr. A*, 2009, **1216**, 3864–3868.

157 C. Alcalde-eon, Mar´ıa Teresa Escribano-Bail ´on, C. Santos-buelga and Juli ´an C. Rivas-Gonzalo, *J. Mass Spectrosc.*, 2007, **42**, 735–748.

158 R. Brouillard and B. Delaporte, *J. Am. Chem. Soc.*, 1977, **99**, 8461–8468.

159 V. L. Singleton, R. Orthofer and R. M. Lamuela-Raventós, *Methods Enzymol.*, 1999, **299**, 152–178.

160 N. Guldbrandsen, M. De Mieri, M. Gupta, E. Liakou, H. Pratsinis, D. Kletsas, E. Chaita, N. Aligiannis, A. L. Skaltsounis and M. Hamburger, *Sci. Pharm.*, 2015, **83**, 177–190.

161 S. Zhu, Y. Li, Z. Li, C. Ma, Z. Lou, W. Yokoyama and H. Wang, *Food Res. Int.*, 2014, **56**, 279–286.

162 H. Wangensteen, M. Bräunlich, V. Nikolic, K. E. Malterud, R. Slimestad and H. Barsett, *J. Funct. Foods*, 2014, **7**, 746–752.

163 P. Denev, M. Číž, M. Kratchanova and D. Blazheva, *Food Chem.*, 2019, **284**, 108–117.

164 S. J. Hossain, S. Sultana, M. A. Taleb, M. H. Basar, M. G. Sarower and A. Hossain, *Int. J. Food Prop.*, 2014, **17**, 2089–2099.

165 S. Benvenuti, F. Pellati, M. Melegari and D. Bertelli, *J. Food Sci.*, 2004, **69**, 164–169.

166 X. Li, X. Wang, D. Chen and S. Chen, *Funct. Foods Heal. Dis. 2011,* 2011, **1**, 232–244.

167 M. Majewska, M. Skrzycki, M. Podsiad and H. Czeczot, *Acta Pol. Pharm. - Drug Res.*, 2011, **68**, 611–615.

168 J. Gong, B. Chu, L. Gong, Z. Fang, X. Zhang, S. Qiu, J. Wang, Y. Xiang, G. Xiao, H. Yuan and F. Zheng, *Antioxidants*, 2019, **8**, 8–12.

169 L. Cruz, M. Guimarães, P. Araújo, A. Évora, V. de Freitas and N. Mateus, *J. Agric. Food Chem.*, 2017, **65**, 6513–6518.

170 F. J. Olivas-Aguirre, J. Rodrigo-García, N. D. R. Martínez-Ruiz, A. I. Cárdenas-Robles, S. O. Mendoza-Díaz, E. Álvarez-Parrilla, G. A. González-Aguilar, L. A. De La Rosa, A. Ramos-Jiménez and A. Wall-Medrano, *Molecules*, 2016, **21**, 1–30.

171 M. Forino, A. Gambuti, P. Luciano and L. Moio, *J. Agric. Food Chem.*, 2019, **67**, 1222–1229.

172 I. Fernandes, F. Marques, V. De Freitas and N. Mateus, *Food Chem.*, 2013, **141**, 2923–2933.

173 R. M. McConnell, W. E. Godwin, B. Stanley and M. Shane Green, *J. Ark. Acad. Sci.*, 1997, **51**, 135–140.

174 N. Basílio and F. Pina, *Molecules*, 2016, **21**, 1–25.

175 L. Jurd, *J. Org. Chem.*, 1963, **28**, 987–991.

176 A. Fernandes, G. Ivanova, N. F. Brás, N. Mateus, M. J. Ramos, M. Rangel and V. De Freitas, *Carbohydr. Polym.*, 2014, **102**, 269–277.

177 R. Brouillard, B. Delaporte and J. E. Dubois, *J. Am. Chem. Soc.*, 1978, **100**, 6202–6205.

178 A. Bakowska-Barczak, *Pol. J. Food Nutr. Sci*, 2005, **1455**, 107–116.

179 L. Cruz, V. C. Fernandes, P. Araújo, N. Mateus and V. De Freitas, *Food Chem.*, 2015, **174**, 480–486.

180 W. Yang, M. Kortesniemi, B. Yang and J. Zheng, *J. Agric. Food Chem.*, 2018, **66**, 2909–2916.

181 P. a. Procopiou, S. P. D. Baugh, S. S. Flack and G. G. a. Inglis, *J. Org. Chem.*, 1998, **63**, 2342–2347.

182 A. Mattarei, L. Biasutto, F. Rastrelli, S. Garbisa, E. Marotta, M. Zoratti and C. Paradisi, *Molecules*, 2010, **15**, 4722–4736.

183 K. Ishihara, H. Kurihara and H. Yamamoto, *J. Org. Chem.*, 1993, **58**, 3791–3793.

184 C. S. Jungong and A. V Novikov, *Synthesis (Stuttg).*, 2012, **42**, 3589–3597.

185 D. Koh, K. H. Park, J. Jung, H. Yang, K. H. Mok and Y. Lim, *Magn. Reson. Chem.*, 2001, **39**, 768–770.

186 J. Liu, PhD Thesis, Brigham Young University, 2007.

187 X. Ren, L. Shen, O. Muraoka and M. Cheng, *J. Carbohydr. Chem.*, 2011, **30**, 119–131.

188 L. Cruz, M. Benohoud, C. M. Rayner, N. Mateus, V. de Freitas and R. S. Blackburn, *Food Chem.*, 2018, **266**, 415–419.

189 Y. Liu, Y. Liu, C. Tao, M. Liu, Y. Pan and Z. Lv, *J. Food Meas. Charact.*, 2018, **12**, 1744–1753.

190 E. Sadilova, F. C. Stintzing and R. Carle, *J. Food Sci.*, 2006, **71**, 504–512.

191 Z. Zori, V. Dragovi, S. Pedisi and I. E. Garofuli, *Food Technol. Biotechnol.*, 2014, **52**, 101–108.

192 Z. Hou, P. Qin, Y. Zhang, S. Cui and G. Ren, *Food Res. Int.*, 2013, **50**, 691–

697.

193 J. M. Sugihara, *Adv. Carbohydr. Chem.*, 1953, **8**, 1–44.

194 L. Chebil, J. Anthoni, C. Humeau, C. Gerardin, J. M. Engasser and M. Ghoul, *J. Agric. Food Chem.*, 2007, **55**, 9496–9502.

195 J. H. Salem, C. Humeau, I. Chevalot, C. Harscoat-Schiavo, R. Vanderesse, F. Blanchard and M. Fick, *Process Biochem.*, 2010, **45**, 382–389.

196 P. Zhang, S. Liu, Z. Zhao, L. You, M. D. Harrison and Z. Zhang, *Food Chem.*, 2020, **343**, 128482.

197 M. Guimarães, N. Mateus, V. de Freitas and L. Cruz, *J. Agric. Food Chem.*, 2018, **66**, 10003–10010.

198 Z. Yan, C. Li, L. Zhang, Q. Liu, S. Ou and Z. Xiaoxiong, *J. Agric. Food Chem.*, 2016, **64**, 1137–1143.

199 B. M. Lue, N. S. Nielsen, C. Jacobsen, L. Hellgren, Z. Guo and X. Xu, *Food Chem.*, 2010, **123**, 221–230.

200 J. J. Forsman and R. Leino, *Carbohydr. Res.*, 2010, **345**, 1548–1554.

201 M. L. Wolfrom, A. B. Diwadkar, J. Gelas and D. Horton, *Carbohydr. Res.*, 1974, **35**, 87–96.

202 J. Gelas and D. Horton, *Carbohydr. Res.*, 1979, **71**, 103–121.

203 J. Gelas and D. Horton, *Carbohydr. Res.*, 1978, **67**, 371–387.

204 J. Gelas and D. Horton, *Carbohydr. Res.*, 1975, **45**, 181–195.

205 M. Koruyucu, F. Saltan, G. Kök, H. Akat and Y. Salman, *Iran. Polym. J. (English Ed.*, 2016, **25**, 455–463.

206 A. M. Pană, L. M. Ştefan, G. Bandur, P. Sfîrloagă, V. Gherman, M. Silion, M. Popa and L. M. Rusnac, *J. Polym. Environ.*, 2013, **21**, 981–994.

207 Y. Nishida and J. Thiem, *J. Carbohydr. Chem.*, 1994, **13**, 1059–1063.

Appendix A

A.1 Chapter 4

A.1.1 HPLC Chromatograms of the Octanol Layers after partitioning from Log P Experiment for RASE

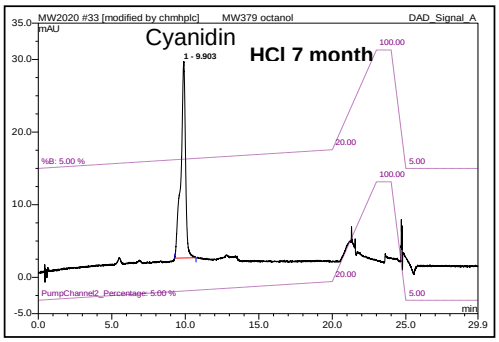

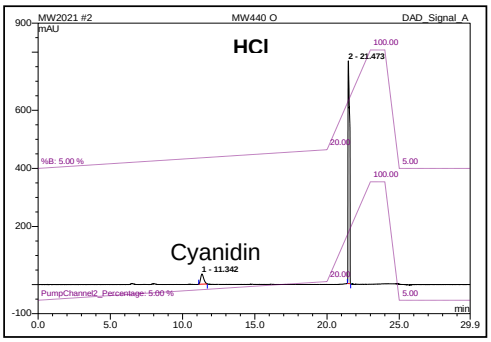

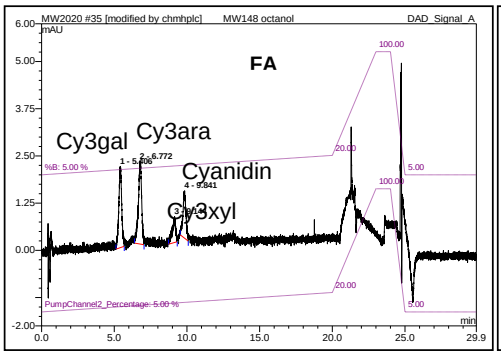

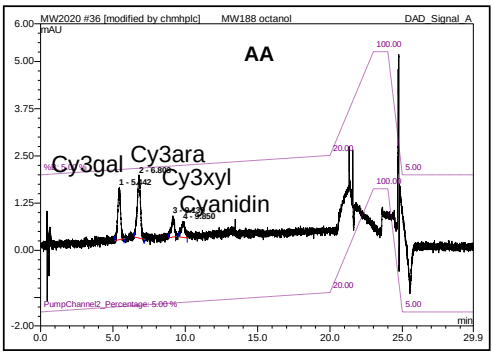

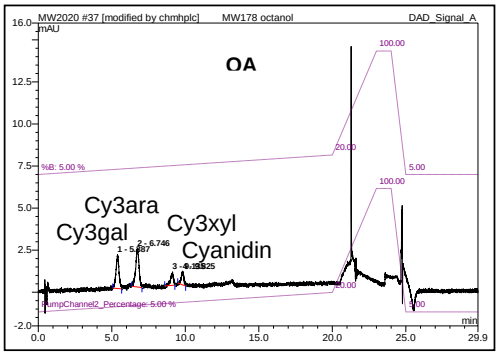

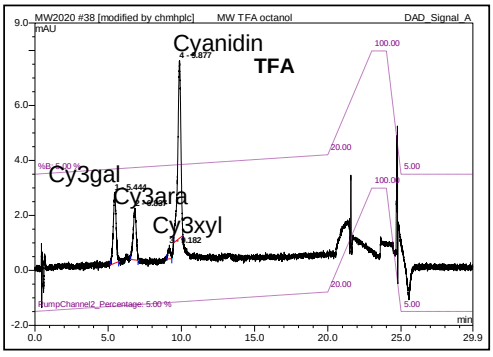

A.1.2 HPLC Chromatograms of the water Layers after partitioning from Log P Experiment for RASE

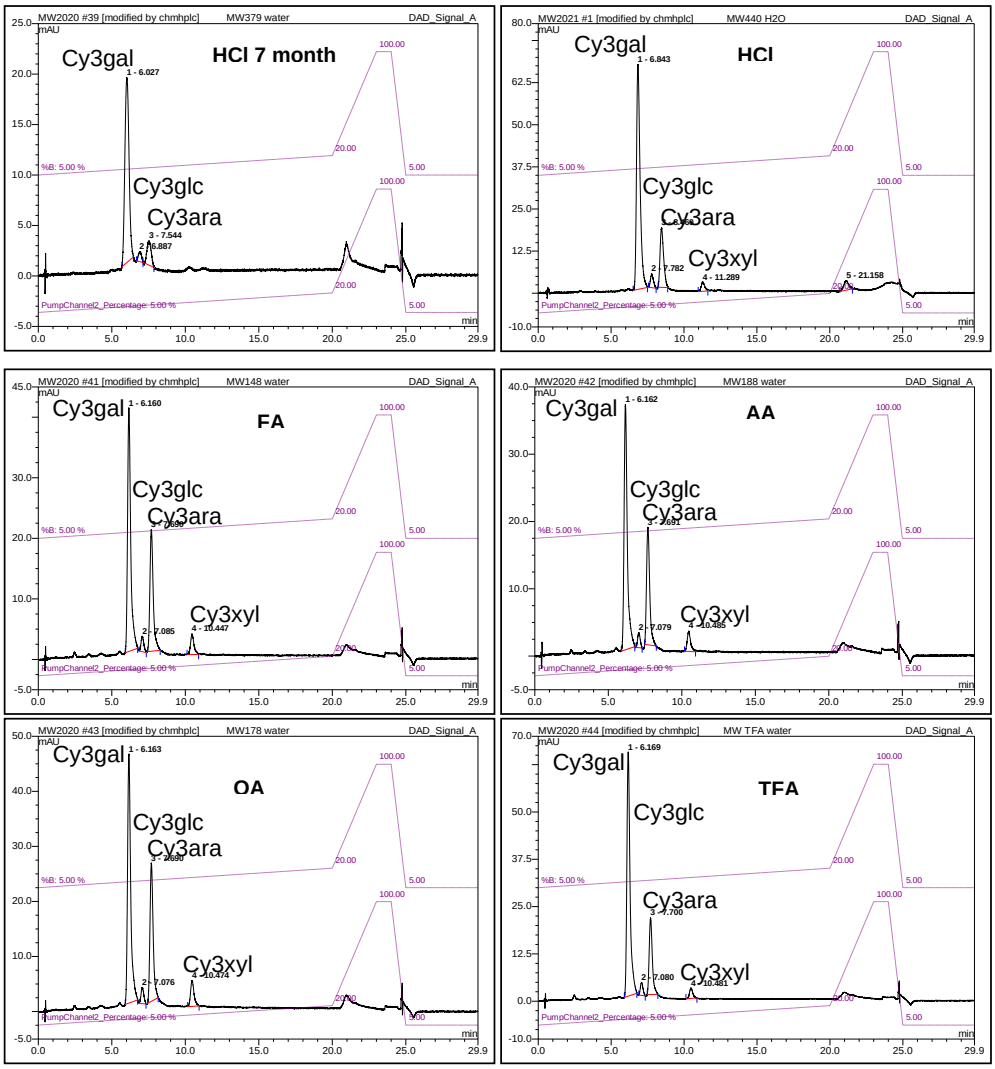

A.2 Chapter 5

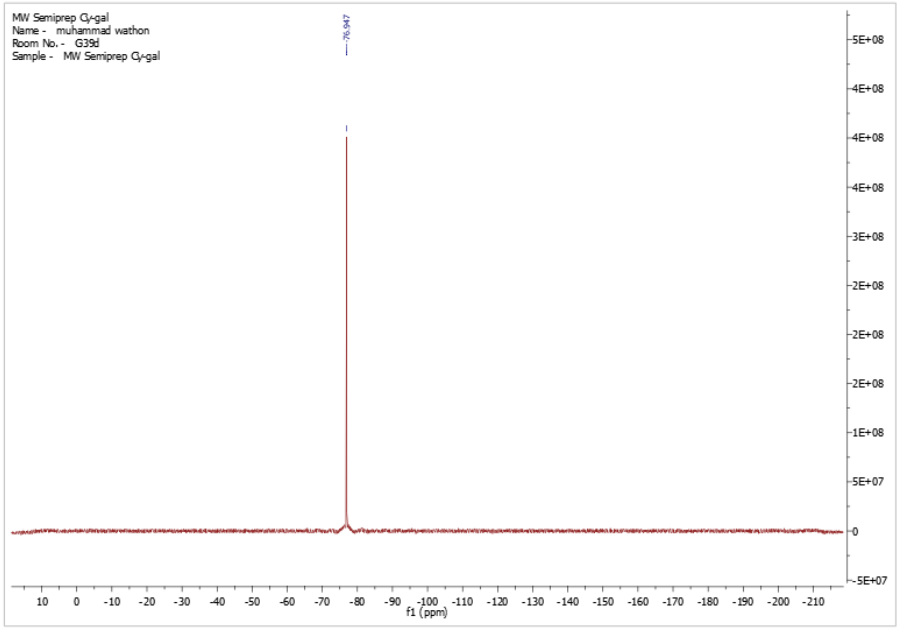

^{19}F-NMR spectrum of Cy3gal dissolved in CD_3OD. Recorded at 400 MHz (25 ºC).

A.3 Chapter 6

A.3.1 *trans*-3,4',5-triacetyl resveratrol, 42

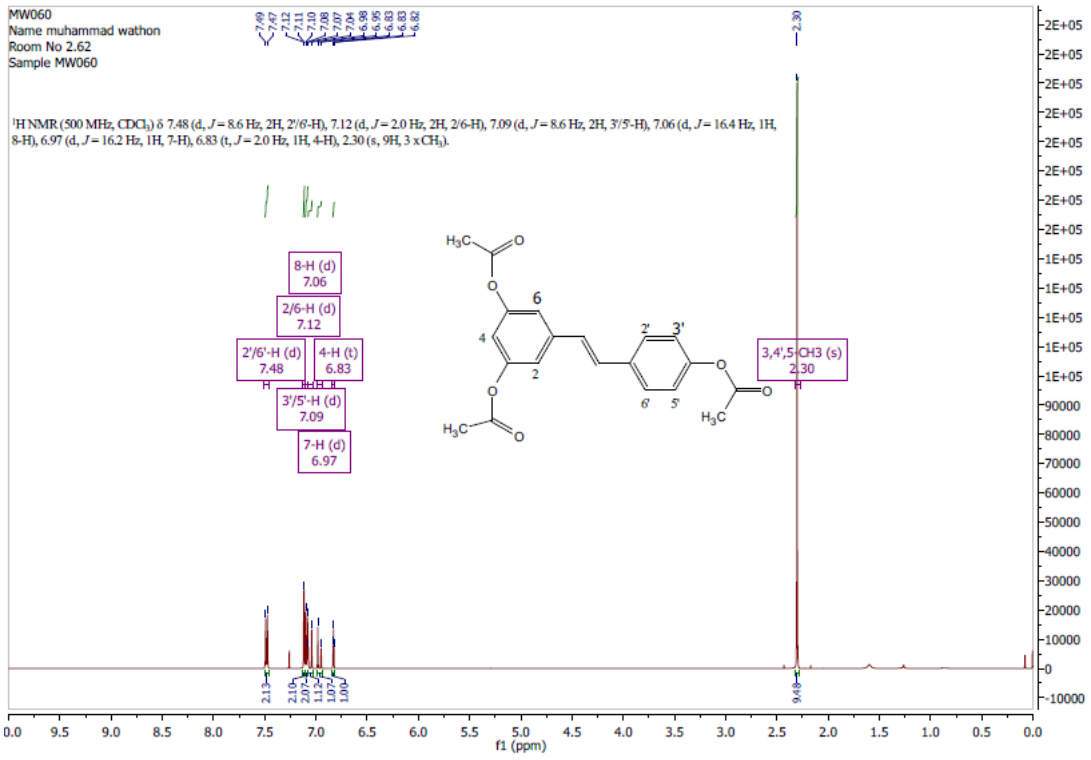

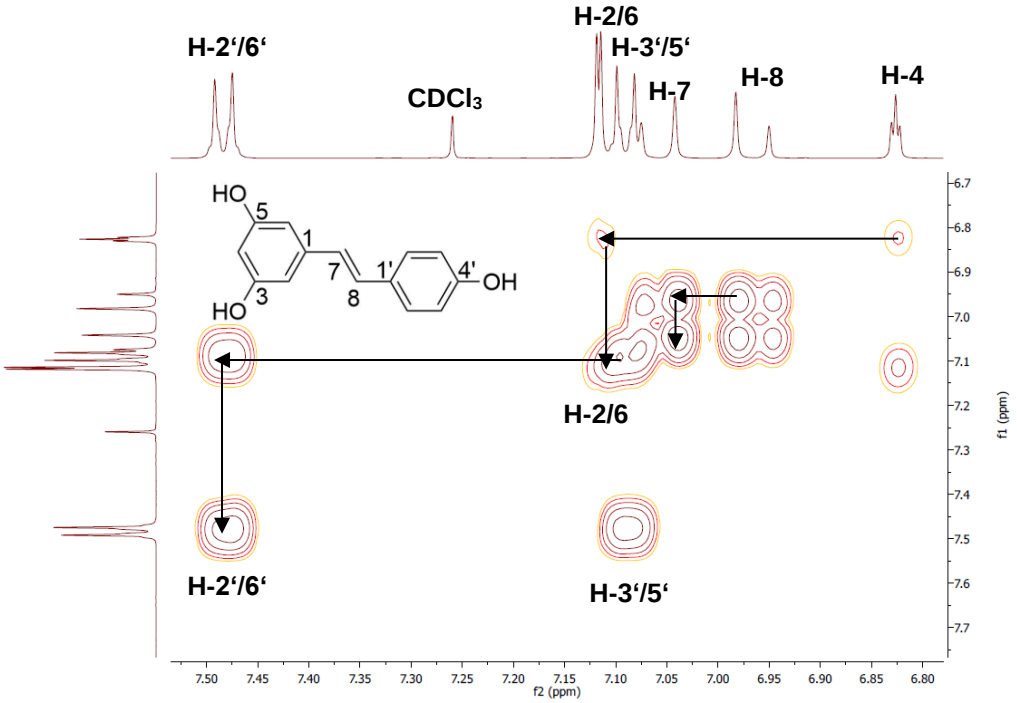

^{1}H-^{1}H COSY spectra of **42** between 6.75-7.75ppm.

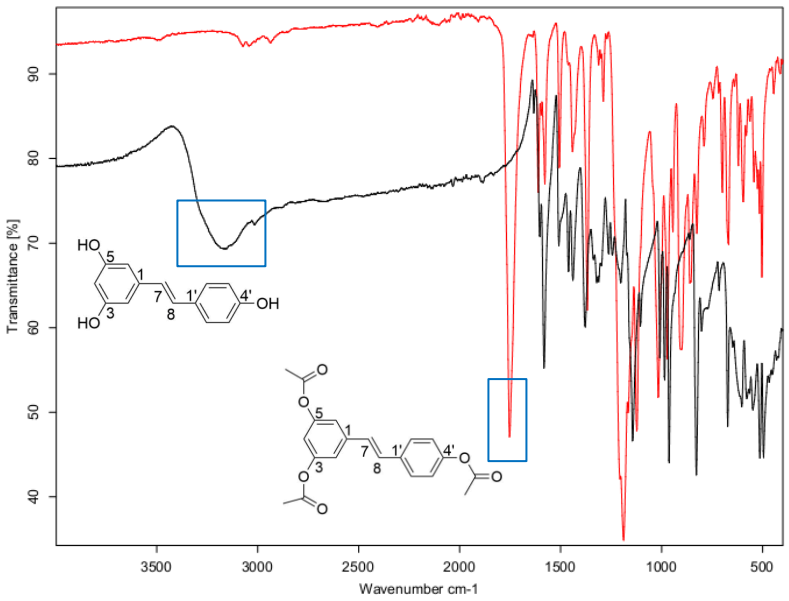

Infrared spectrum of **41** (black) and **42** (red).

A.3.2 3,3',4',5,7-pentaacetyl quercetin, 43

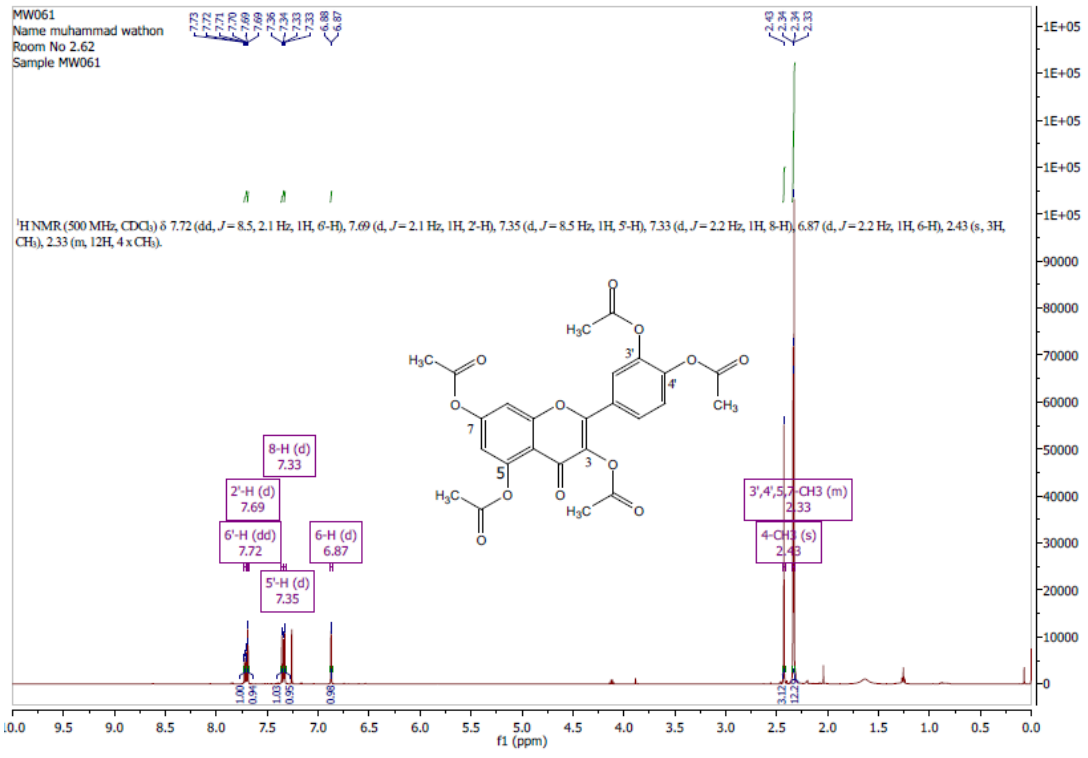

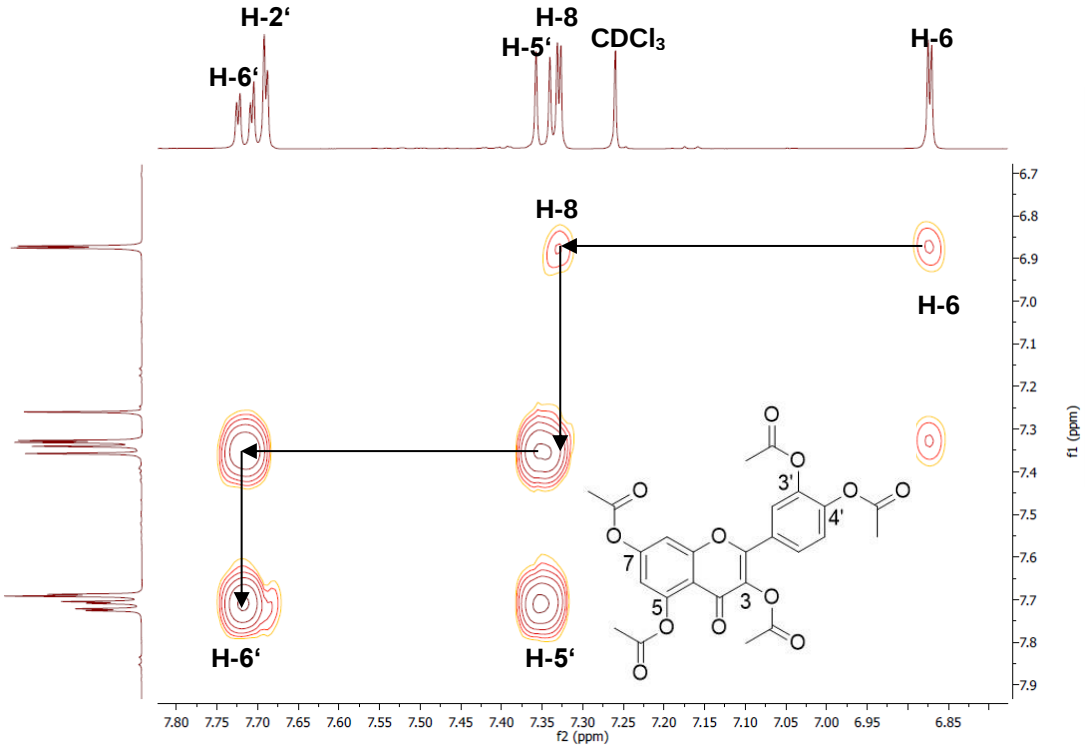

^{1}H-^{1}H COSY spectra of **43** between 6.7-7.8 ppm showing protons in aromatic regions.

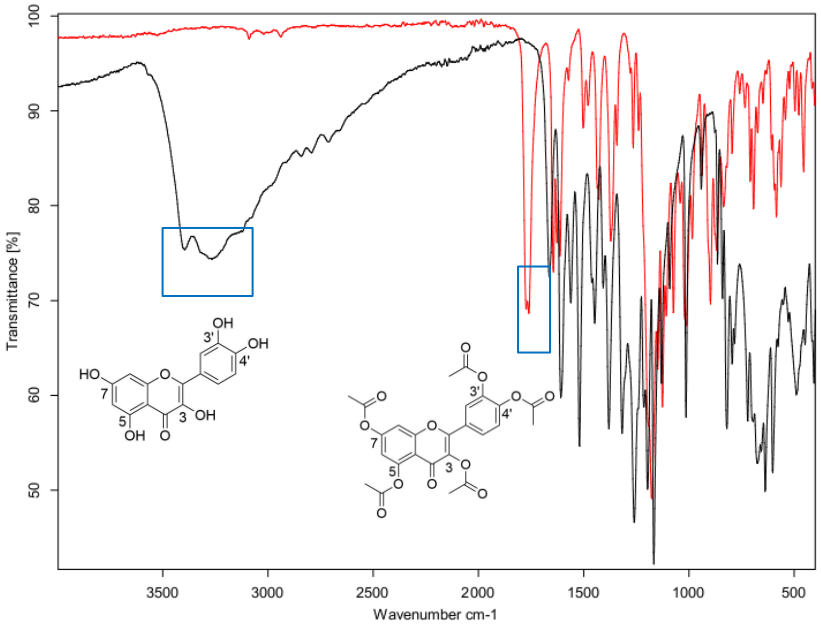

Infrared spectrum of **40** (black) and **43** (red).

A.3.3 Cyanidin-3-β-*O*-(6”-acetylgalactoside) trifluoroacetate, 44

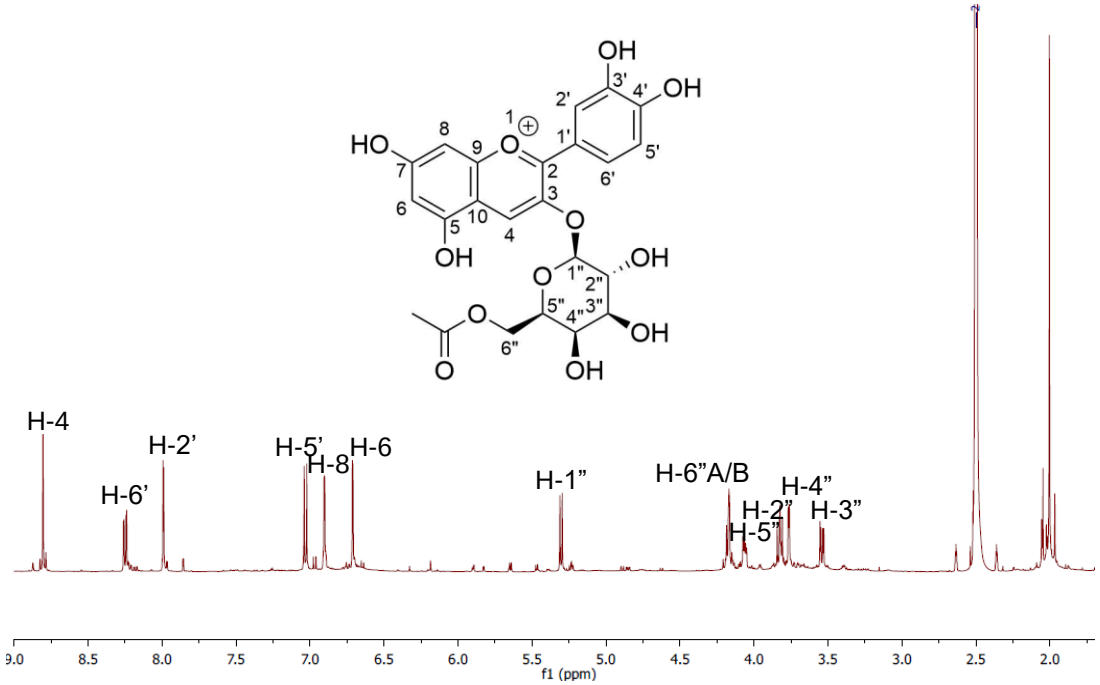

^{1}H-NMR spectrum (500 MHz) of **44** in $(CD_3)_2SO/CF_3COOD$ (95:5, v/v) recorded at 25 °C. Concentration of 10.4 mM.

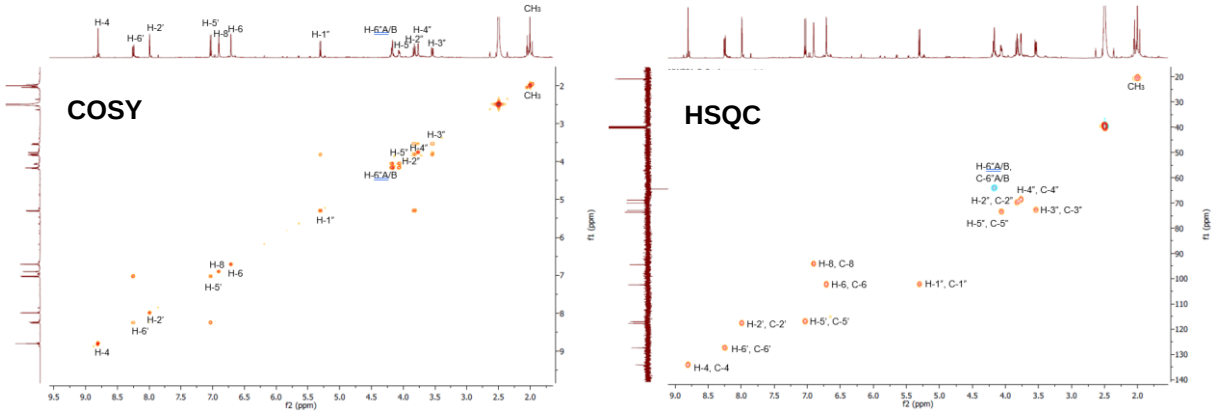

Expanded region of a ^{1}H-^{1}H COSY and ^{1}H-^{13}C HSQC spectrum (500 MHz) of **44** in $(CD_3)_2SO/CF_3COOD$ (95:5), 25 °C.

A.3.4 Cyanidin-3-β-*O*-(3”,6”-diacetylgalactoside), 45

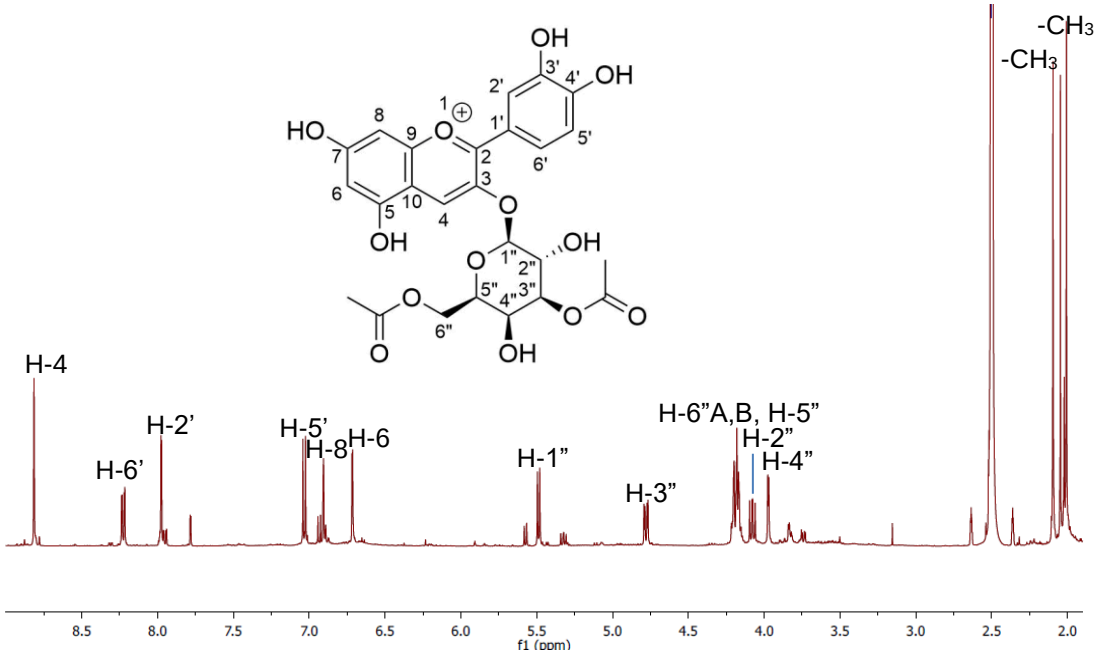

^{1}H-NMR spectrum (500 MHz) of **45** in $(CD_3)_2SO/CF_3COOD$ (95:5, v/v) recorded at 25 °C. Concentration of 9.8 mM.

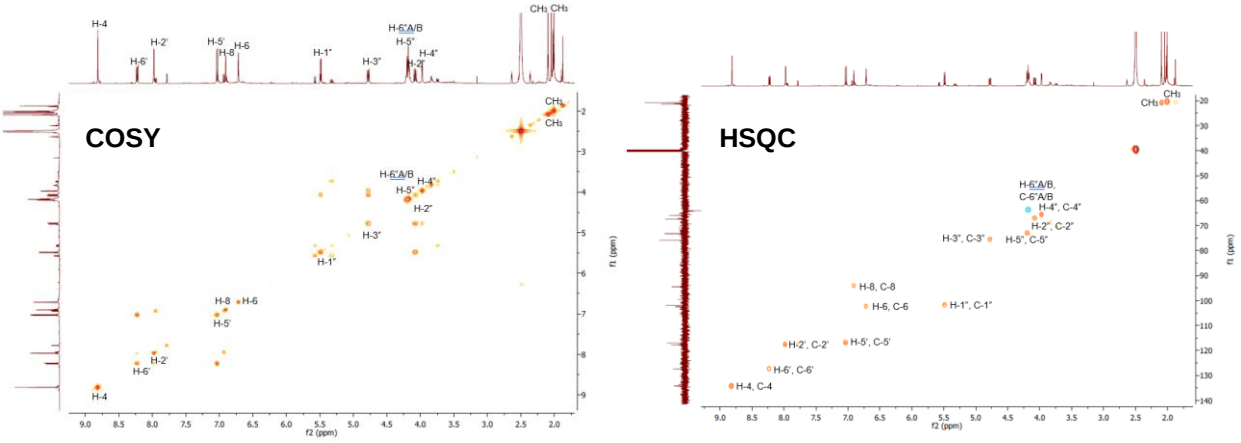

Expanded region of a ^{1}H-^{1}H COSY and ^{1}H-^{13}C HSQC spectrum (500 MHz) of **45** in $(CD_3)_2SO/CF_3COOD$ (95:5), 25 °C. Concentration of 9.8 mM.

A.3.5 Cyanidin-3-β-*O*-(3”,4”,6”-triacetylgalactoside), 46

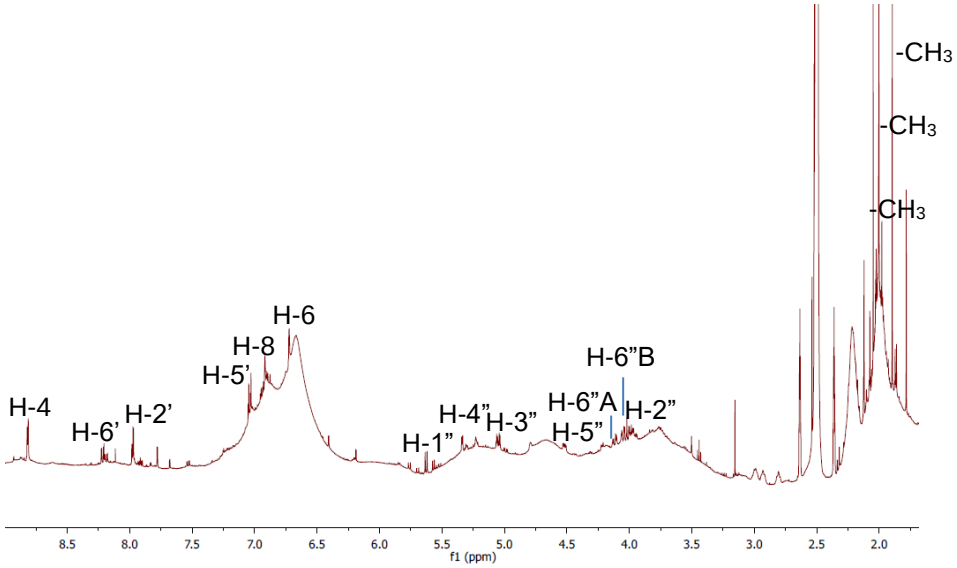

^{1}H-NMR spectrum (500 MHz) of **46** in $(CD_3)_2SO/CF_3COOD$ (95:5, v/v) recorded at 25 °C. Concentration of 4.4 mM.

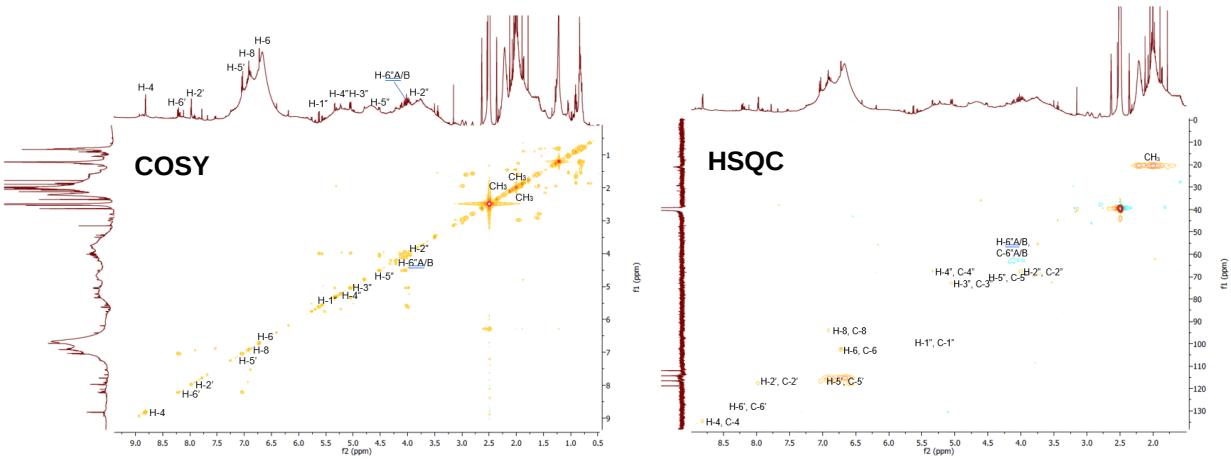

Expanded region of a ^{1}H-^{1}H COSY and ^{1}H-^{13}C HSQC spectrum (500 MHz) of **46** in $(CD_3)_2SO/CF_3COOD$ (95:5), 25 °C. Concentration of 4.4 mM.

A.3.6 Cyanidin-3-β-*O*-(2”,3”,4”,6”-tetraacetylgalactoside), 47

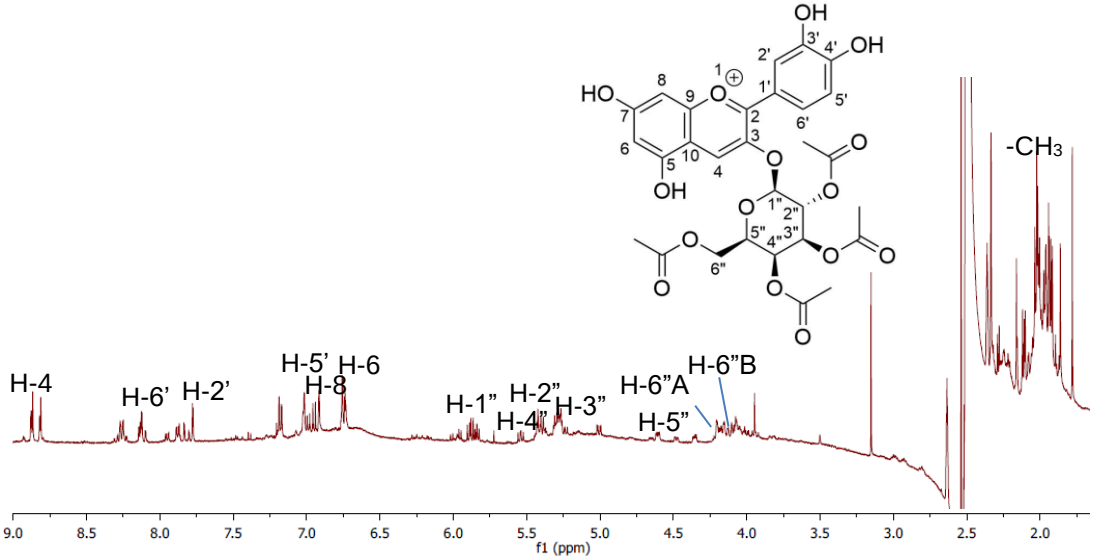

^{1}H-NMR spectrum (500 MHz) of **47** in $(CD_3)_2SO/CF_3COOD$ (95:5, v/v) recorded at 25 °C. Concentration of 6.6 mM.

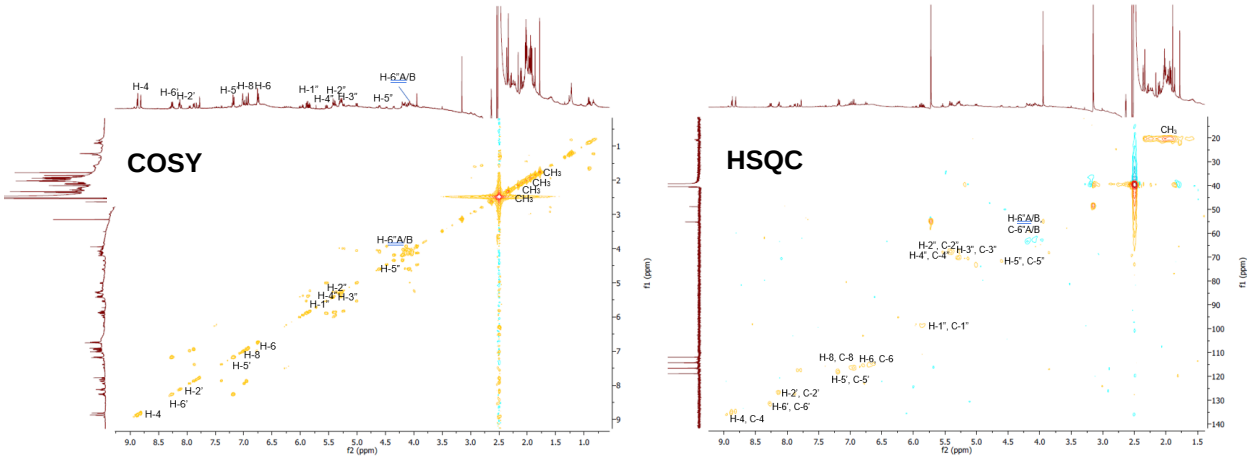

Expanded region of a ^{1}H-^{1}H COSY and ^{1}H-^{13}C HSQC spectrum (500 MHz) of **47** in $(CD_3)_2SO/CF_3COOD$ (95:5, v/v) recorded at 25 °C. Concentration of 6.6 mM.

A.3.7 Cyanidin-3-β-*O*-(4',2",3",4",6"-pentaacetyl galactoside), 48

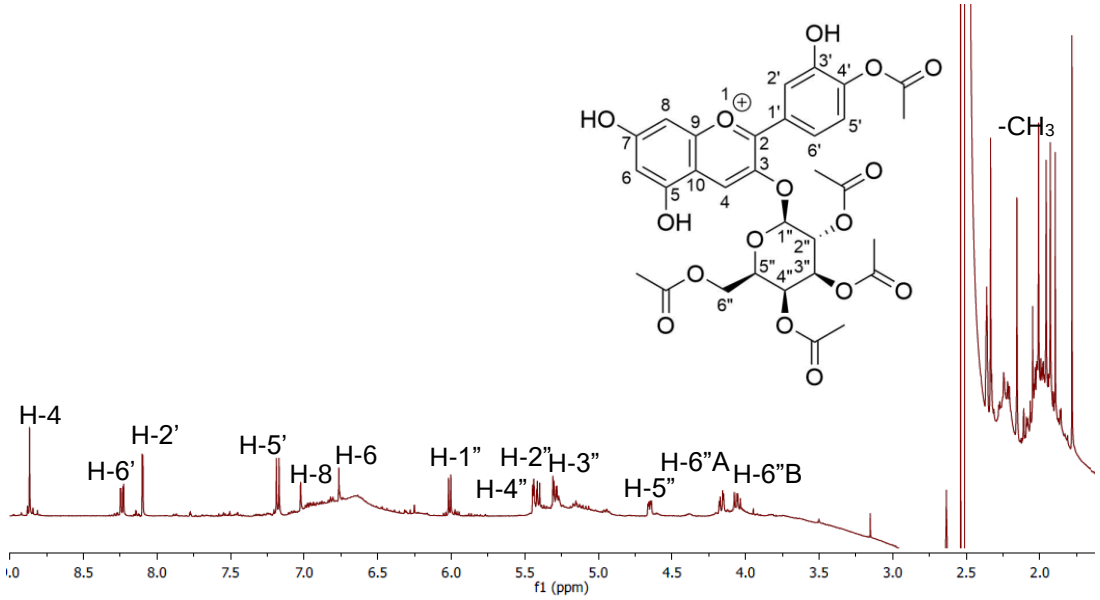

^{1}H-NMR spectrum (500 MHz) of Cyanidin-3-β-*O*-(4',2",3",4",6"-pentaacetylgalactoside) **48** in $(CD_3)_2SO/CF_3COOD$ (95:5, v/v) recorded at 25 °C. Concentration of 6.0 mM.

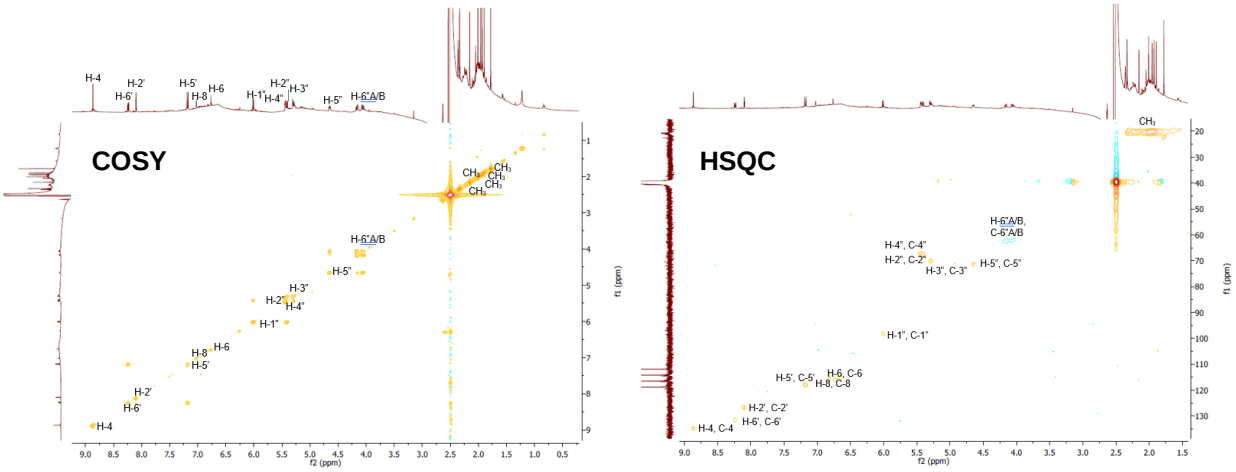

Expanded region of a ^{1}H-^{1}H COSY and ^{1}H-^{13}C HSQC spectrum (500 MHz) of **48** in $(CD_3)_2SO/CF_3COOD$ (95:5, v/v) recorded at 25 °C. Concentration of 6.0 mM.

A.3.8 Cyanidin-3-β-*O*-(4',7,2",3",4",6"-hexaacetylgalactoside), 49

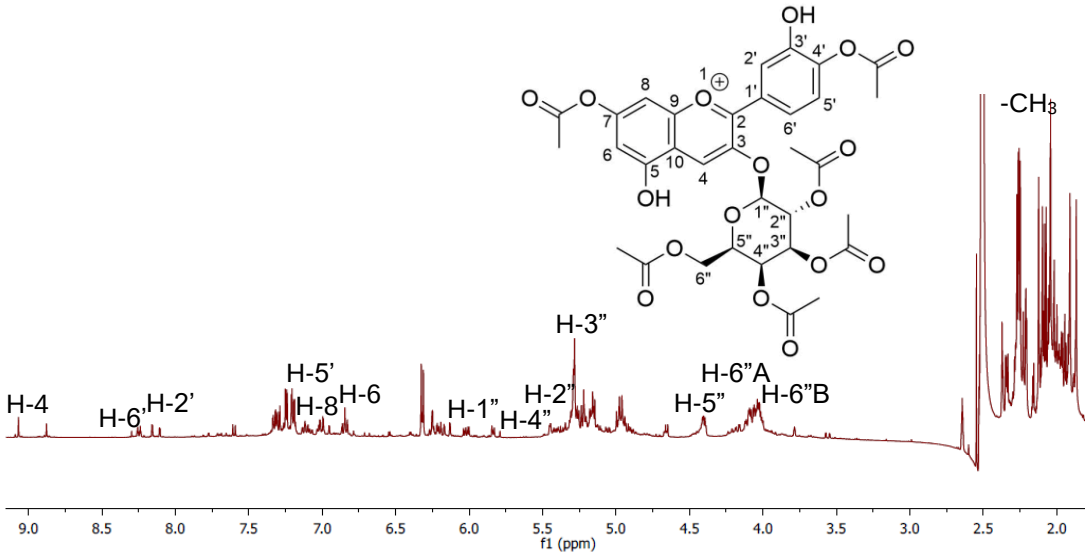

^{1}H-NMR spectrum (500 MHz) of **49** in $(CD_3)_2SO/CF_3COOD$ (95:5, v/v) recorded at 25 °C. Concentration of 5.7 mM.

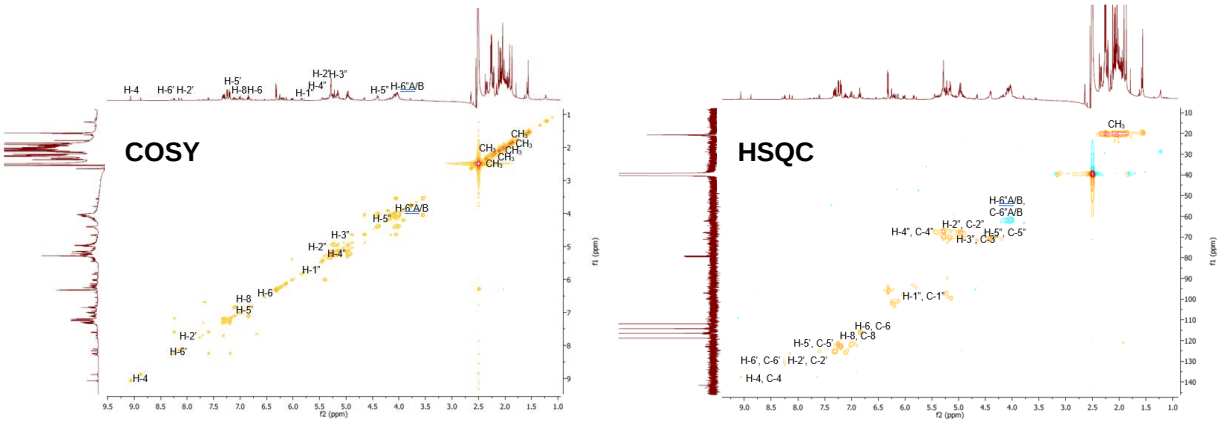

Expanded region of a ^{1}H-^{1}H COSY and ^{1}H-^{13}C HSQC spectrum (500 MHz) of **49** in $(CD_3)_2SO/CF_3COOD$ (95:5, v/v) recorded at 25 °C. Concentration of 5.7 mM.

A.3.9 Cyanidin-3-β-*O*-(6”-butyrylgalactoside), 50

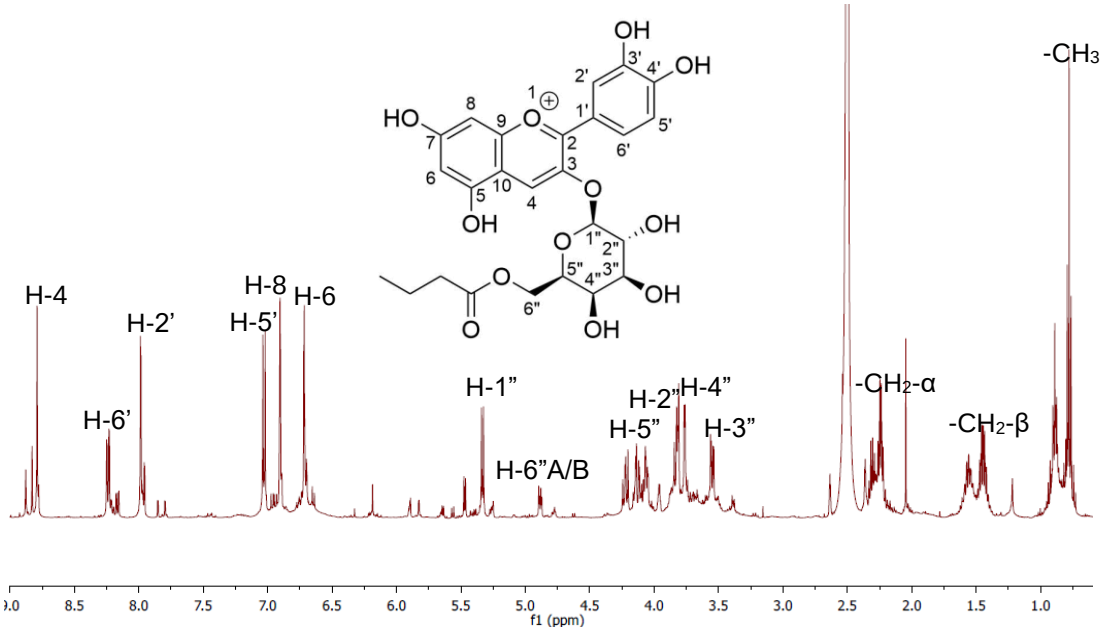

^{1}H-NMR spectrum (500 MHz) of **50** in $(CD_3)_2SO/CF_3COOD$ (95:5, v/v) recorded at 25 °C. Concentration of 17.7 mM.

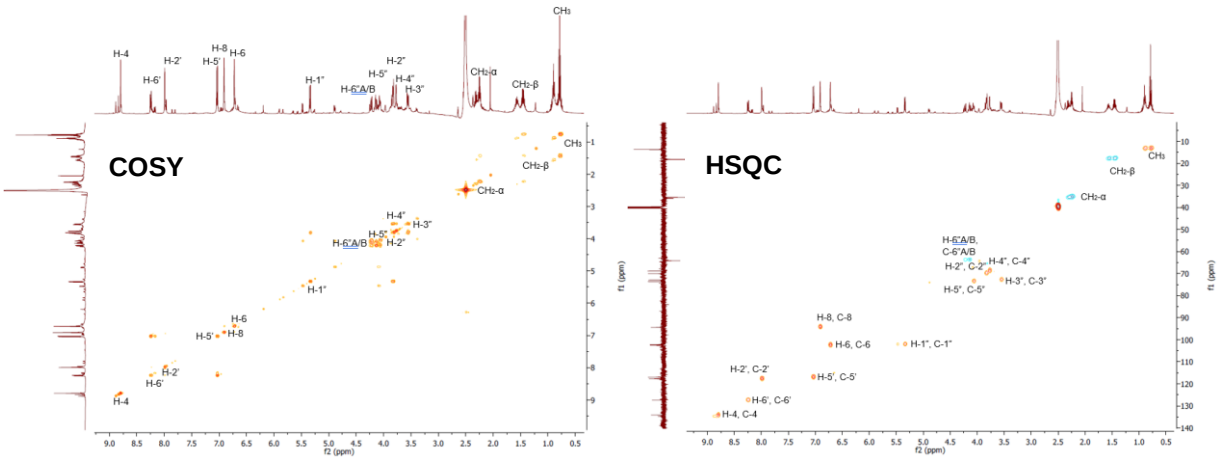

Expanded region of a ^{1}H-^{1}H COSY and ^{1}H-^{13}C HSQC spectrum (500 MHz) of **50** in $(CD_3)_2SO/CF_3COOD$ (95:5, v/v) recorded at 25 °C. Concentration of 17.7 mM.

A.3.10 Cyanidin-3-β-*O*-(3”,6”-dibutyrylgalactoside), 51

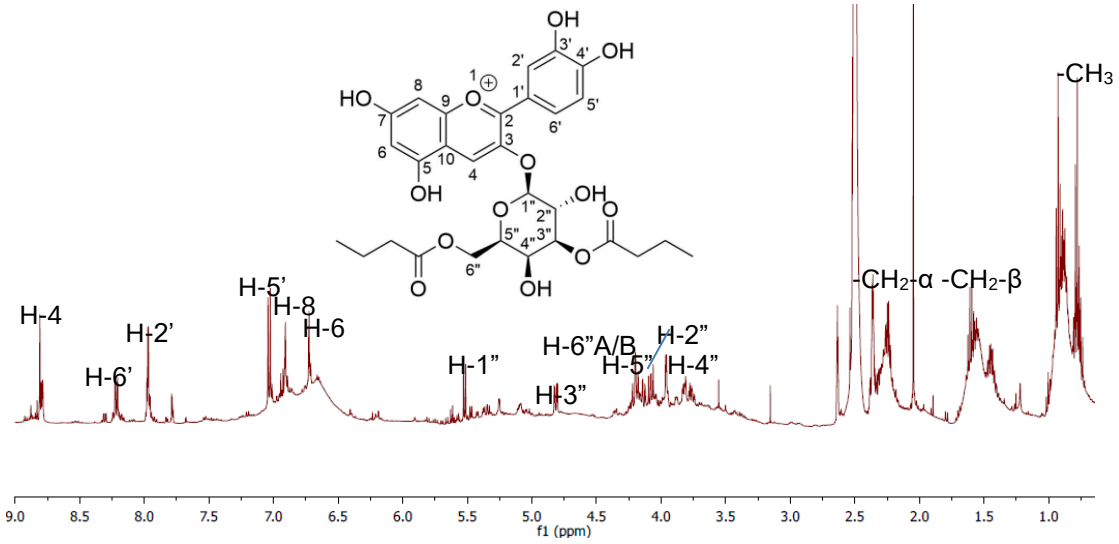

^{1}H-NMR spectrum (500 MHz) of **51** in $(CD_3)_2SO/CF_3COOD$ (95:5, v/v) recorded at 25 °C. Concentration of 12.6 mM.

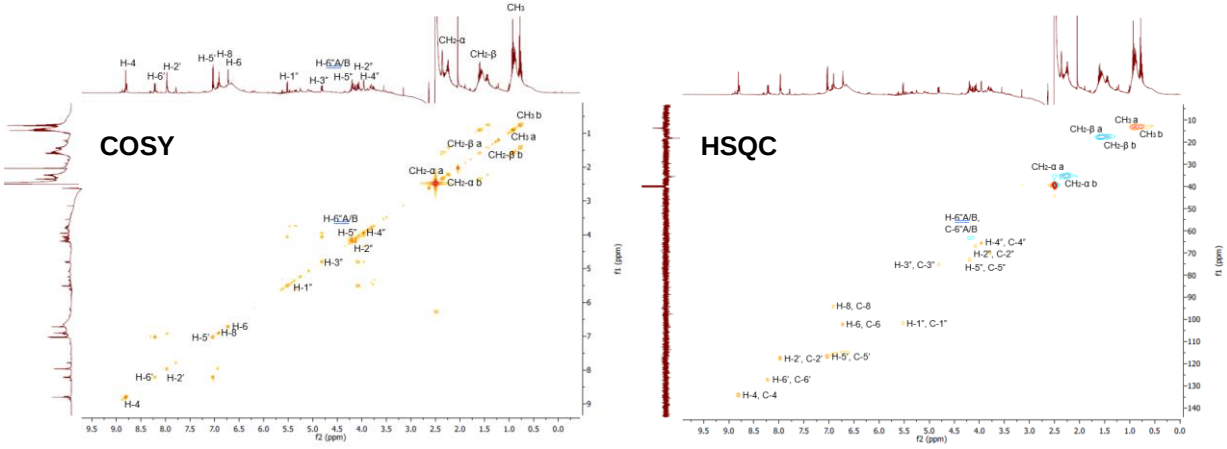

Expanded region of a ^{1}H-^{1}H COSY and ^{1}H-^{13}C HSQC spectrum (500 MHz) of **51** in $(CD_3)_2SO/CF_3COOD$ (95:5, v/v) recorded at 25 °C. Concentration of 12.6 mM.

A.3.11 Cyanidin-3-β-O-(6”-caprylylgalactoside), 52

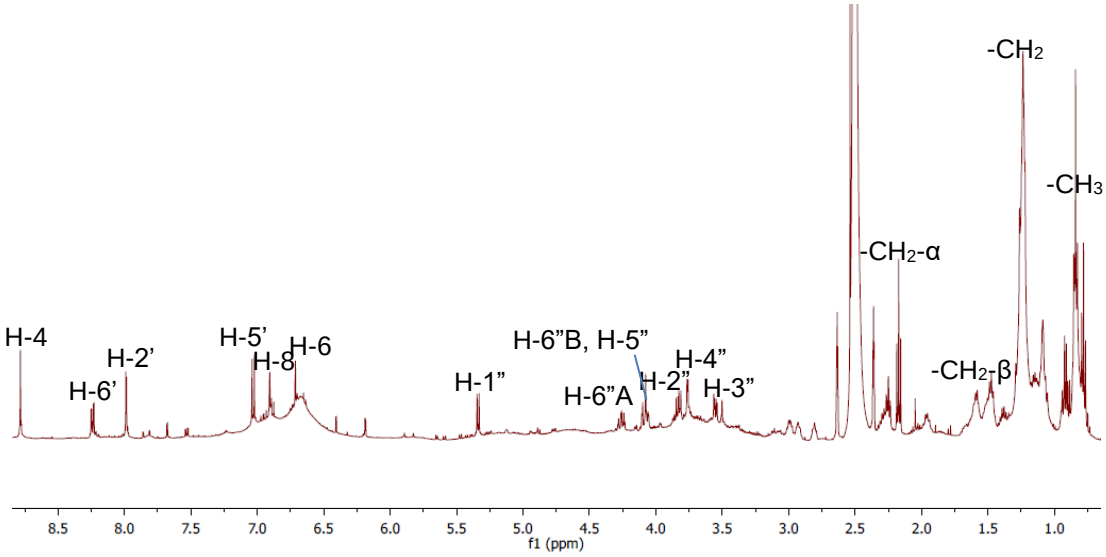

^{1}H-NMR spectrum (500 MHz) of **52** in $(CD_3)_2SO/CF_3COOD$ (95:5, v/v) recorded at 25 °C. Concentration of 5.8 mM.

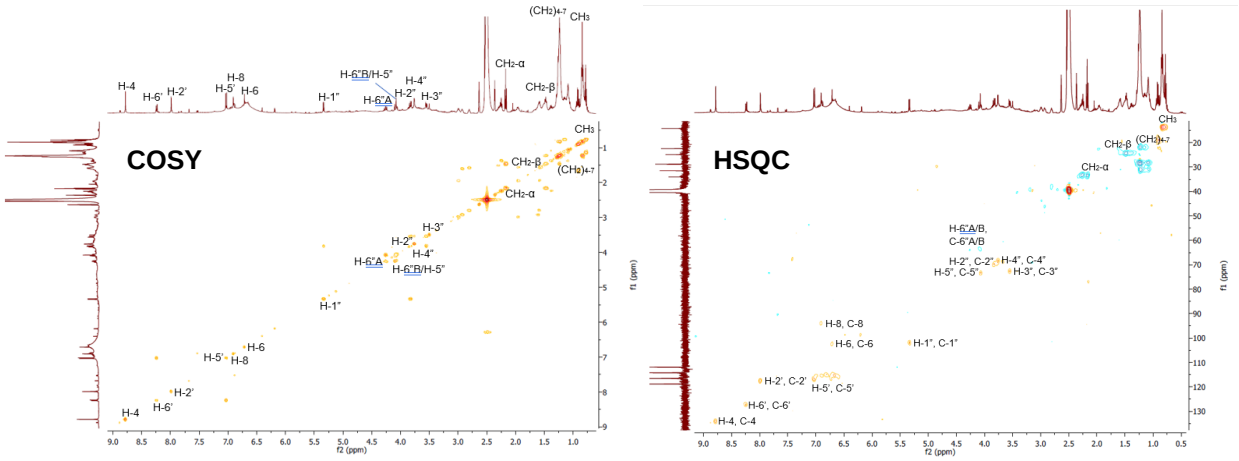

Expanded region of a ^{1}H-^{1}H COSY and ^{1}H-^{13}C HSQC spectrum (500 MHz) of **52** in $(CD_3)_2SO/CF_3COOD$ (95:5, v/v) recorded at 25 °C. Concentration of 5.8 mM.

A.3.12 Cyanidin-3-β-O-(3”,6”-dicaprylylgalactoside), 53

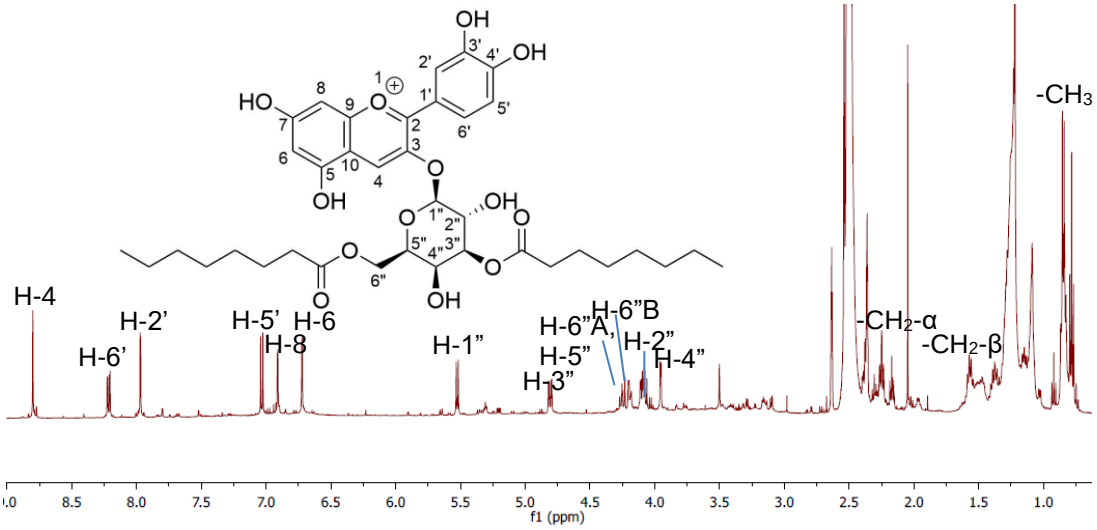

^{1}H-NMR spectrum (500 MHz) of **53** in $(CD_3)_2SO/CF_3COOD$ (95:5, v/v) recorded at 25 °C. Concentration of 5.8 mM.

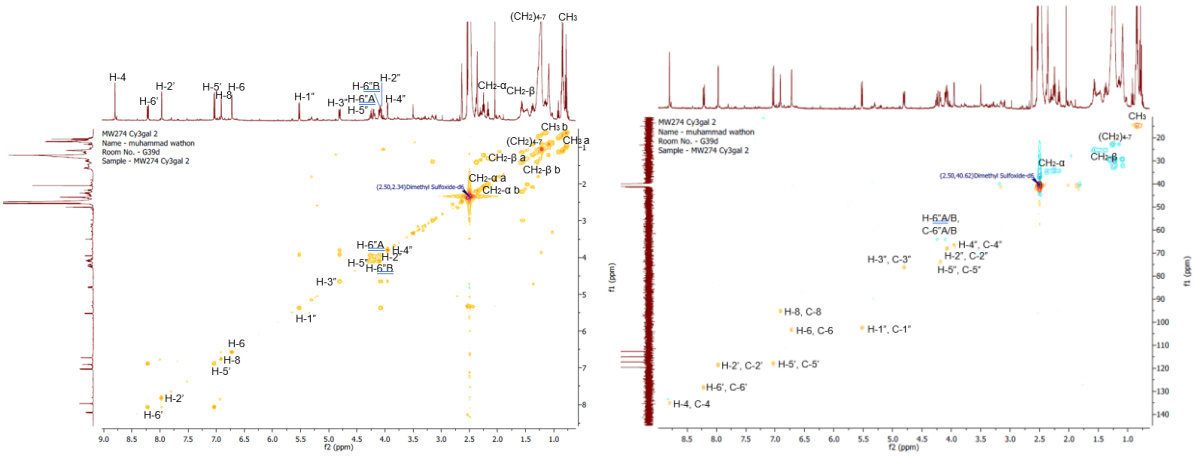

Expanded region of a ^{1}H-^{1}H COSY and ^{1}H-^{13}C HSQC spectrum (500 MHz) of **53** in $(CD_3)_2SO/CF_3COOD$ (95:5, v/v) recorded at 25 °C. Concentration of 5.8 mM.